

DEVELOPMENT OF NI-CATALYZED ASYMMETRIC REDUCTIVE CROSS-  
COUPLING REACTIONS

Thesis by  
Nathaniel Thomas Kadunce

In Partial Fulfillment of the Requirements  
for the Degree of  
Doctor of Philosophy

CALIFORNIA INSTITUTE OF TECHNOLOGY

Pasadena, California

2016

(Defended May 24, 2016)

© 2016

Nathaniel Thomas Kadunce

All Rights Reserved

*To my family*

## ACKNOWLEDGEMENTS

My time at Caltech has been one of the most fortunate and formative times of my life, and it is a place I will fondly remember. The close-knit community of brilliant and supportive students, staff, and faculty makes the challenging work of chemistry possible. I have made many excellent friends here and grown close to tremendous colleagues I look forward to knowing and working with in the future. Caltech is a special place that fosters these relationships and I am lucky to have developed as a scientist here.

First, I must enthusiastically thank my advisor, Prof. Sarah Reisman, for her guidance, mentorship, and the opportunity to work and learn in her group. It has been a privilege to learn from someone who so earnestly cares for her students. Whether it is our scientific development, health and well-being, or futures and careers, Sarah has been constantly helpful, patient, and encouraging to all in the lab. Over the last five years the group has nearly doubled in size, contributed an immense amount of research, and become a leader in our field. It is not lost on me, or any of us, what a feat that is, and how fortunate we are to enjoy our place in it.

I am also grateful to the members of my thesis committee, Profs. Jonas Peters and Brian Stoltz, and chairman, Prof. Gregory Fu. In yearly meetings, not least of all candidacy and proposals, all of my committee members have taken valuable time to mentor and educate me. The organometallic perspective and knowledge contributed by Jonas and Greg has added greatly to the understanding we have of the research described in this thesis and my own learning. I would like to thank Prof. Stoltz in particular for his constant dedication to our groups' success and to our division. Brian's cheerful demeanor and insightful contributions add greatly to our joint group meetings and the experience of

working on our floor. The collaborative dialogue between the Stoltz and Reisman groups is a special part of the research we do, whether it concerns friendship, chemicals, or, most often, both.

The staff and facilities at Caltech are a critical part of all the successful research we do there. In particular, Dr. David Vander Velde and Dr. Scott Virgil have been instrumental to my work at every turn. Dave has constantly maintained and updated our NMR facility, ensuring that whole screens of data could be easily gathered at any time. Scott has worked tirelessly at the Caltech Center for Catalysis and Chemical Synthesis, keeping up an always-rotating cast of instruments and tools. His care for the SFC, glovebox, cooling wells, and rotary stir plates has been key to the success of each and every project I have pursued here. Even more importantly, his patience and mentorship is an essential part of every third-floor graduate student's learning, teaching us how the instruments we rely on work and how to perform routine maintenance ourselves with confidence.

Most importantly to the experience of working over the last five years have been the people of the Reisman lab. It has been an honor to work alongside some of the most driven, curious, and brilliant people I have known. I joined the group in Sarah's fourth class, being fortunate to overlap with all of her first students and to gain from their experience of the lab's roots. Over the years, it has been both challenging and lovely to see people move on to their future endeavors and to welcome new students in their place. The lab has developed to a bigger, more dynamic place, but at each stage along the way it has kept the same friendly, supportive, encouraging atmosphere that defines it.

In my second year, Sarah asked me to join (now Dr.) Alan Cherney on a new project doing Ni catalysis. At that time, I knew next to nothing about Ni, and was still learning the ropes about everything else. Alan has been one of the most supportive and patient colleagues I have had, and become a great friend as well. The experience of working with him has been foundational to my experience at Caltech, putting my research on its track and brightening every day with his dry wit and straight-ahead determination. As the Ni project has matured and developed I have had the opportunity to work with many new and excellent graduate students and post-docs. Dr. Leah Cleary was a great friend and coworker, whether it meant talking about science or going to see punk shows. I've been very fortunate to transition roles in the last two years to mentor new members of Team Ni. Julie Hofstra has made remarkable headway toward a mechanistic understanding of the reactions we develop. Kelsey Poremba has been a phenomenal project partner, bay-mate, and friend. I feel very lucky and confident leaving the future of the Ni project in their capable hands.

Graduate school is not an easy endeavor, and I owe a debt of gratitude to all the friends and institutions that have made the journey possible. While there are too many to name, I would like to especially thank Lauren Chapman, Jane Ni, Guy Edouard, Matt Hesse, Nick Cowper, Jordan Beck, Denise Grünenfelder, Ingmar Saberi, Ian Finneran, and Laura Rios for their camaraderie and support over the years and for all the fun that we've had (and will have). I must also thank Blake Daniels in particular for not only being a tremendous friend and colleague, but also for being the surprise witness at our wedding. I am looking forward to lots of adventures in the Bay very soon (you too, Matt).

As I could not have gotten through Caltech without the people above, I could never have gotten there in the first place without the following: my teachers and family. My first real contact with chemistry was Steve Witowich's AP Chemistry class. His outsized and ridiculous love of teaching, science, and his students was a huge inspiration and he is dearly missed. Moving on to Oberlin College, I was fortunate to work with several instrumental advisors and teachers in a great department. I would like to especially thank Prof. Albert Matlin and Prof. Jason Belitsky. Working alongside them was my first experience with hands-on research and it lit the fire that led me to graduate school. I must thank Jason in particular for sparking my interests in both metal catalysis and Caltech, two things that have shaped my life since.

Finally, and most importantly, I would like to thank all of my family who have loved and supported me my whole life. My parents, who always showed me the importance of learning and gave me the freedom to explore what I loved, have been my greatest cheerleaders. I am endlessly grateful for their love, patience, and encouragement. More recently, I have been given the gift of great parents-in-law as well. Mindy and Brett have not only been welcoming and generous, but have shown me great love and have made our stay in Los Angeles all the better. Most of all, I thank my wife Julia, who made the leap of faith to the best coast with me to begin this adventure. Exploring LA, music, food, and life with you has been the anchor that makes this all worthwhile. Your boundless love and support at every turn has made this journey the best time in my life, and our wedding is the best memory of them all. I could not have done it without you and I can't wait to adventure in our new home. Last but not least, Winchester and Sugarbeet.

## ABSTRACT

Over the last half century, the development of metal-catalyzed cross-coupling reactions has transformed the toolkit of transformations available to synthetic chemists. From the very beginning of this effort, researchers have studied the application of these reactions to afford enantioenriched products via asymmetric catalysis. A great deal of success has been achieved in this arena, giving rise to an ever-growing number of chiral catalysts for a wide range of transformations. Despite these efforts, inherent difficulties in the reactivity of C(sp<sup>3</sup>) electrophiles with the most common noble metal catalysts have limited the development of these substrates until more recently. A resurgence of interest in Ni-catalysis has enabled the stereoconvergent cross-coupling of C(sp<sup>3</sup>) electrophiles with many partners, opening doors to access these challenging chiral products.

Reductive cross-coupling, involving the union of two different electrophiles, has emerged still more recently, and had previously not been employed asymmetrically. Herein we describe our efforts to develop the first Ni-catalyzed asymmetric reductive cross-couplings of C(sp<sup>3</sup>) halides to afford highly enantioenriched products. In the first such reaction, the coupling of acyl chlorides with benzylic chlorides affords acyclic  $\alpha$ -tertiary ketone products. Following this, we describe the coupling of new C(sp<sup>3</sup>) partners,  $\alpha$ -chloronitriles, with challenging Lewis-basic heteroaryl iodides, enabled by the development of a novel PHOX ligand scaffold. Finally, we report the extension of a more general dioxane/TMSCl solvent condition to new asymmetric reductive couplings, including that of heteroaryl iodides with benzylic chlorides, as well as additional preliminary results with new substrate classes.

## PUBLISHED CONTENT AND CONTRIBUTIONS

Cherney, A. H.; Kadunce, N. T.; and Reisman, S. E. “Enantioselective and Enantiospecific Transition-Metal-Catalyzed Cross-Coupling Reactions of Organometallic Reagents to Construct C–C Bonds.” *Chem. Rev.* **2015**, *115*, 9587. DOI: 10.1021/acs.chemrev.5b00162.

N.T.K. participated in conception of the review scope and coverage, compilation of the review bibliography, and the writing of the manuscript.

Cherney, A. H.; Kadunce, N. T.; and Reisman, S. E. “Catalytic Asymmetric Reductive Acyl Cross-Coupling: Synthesis of Enantioenriched Acyclic  $\alpha,\alpha$ -Disubstituted Ketones.” *J. Am. Chem. Soc.* **2013**, *135*, 7442. DOI: 10.1021/ja402922w.

N.T.K. participated in reaction development and screening, compilation of data, preparation and evaluation of substrates, and characterization of products.

Kadunce, N. T. and Reisman, S. E. “Nickel-Catalyzed Asymmetric Reductive Cross-Coupling Between Heteroaryl Iodides and  $\alpha$ -Chloronitriles.” *J. Am. Chem. Soc.* **2015**, *137*, 10480. DOI: 10.1021/jacs.5b06466.

N.T.K. conducted all reaction development and screening, compilation of data, preparation and evaluation of substrates, and characterization of products. N.T.K. participated in the conception of the project and the writing of the manuscript.

## TABLE OF CONTENTS

<b>CHAPTER 1</b>	<b>1</b>
<i>Nickel Catalysis in Cross-Coupling: A Review of Applications in Asymmetric Catalysis and the Rise of Reductive Cross-Coupling</i>	
<b>1.1 INTRODUCTION.....</b>	<b>1</b>
<b>1.2 REACTIONS OF SECONDARY ALKYL ORGANOMETALLIC REAGENTS .....</b>	<b>5</b>
1.2.1 Organomagnesium Reagents.....	6
1.2.2 Organozinc Reagents.....	12
1.2.3 Organoboron Reagents .....	14
<b>1.3 REACTIONS OF SECONDARY ALKYL ELECTROPHILES .....</b>	<b>15</b>
1.3.1 With Organomagnesium Reagents .....	16
1.3.2 With Organozinc Reagents .....	17
1.3.3 With Organoboron Reagents.....	24
1.3.4 With Organosilicon Reagents.....	29
1.3.5 With Organozirconium Reagents .....	30
1.3.6 With Organoindium Reagents.....	31
<b>1.4 TRANSITION METAL-CATALYZED DESYMMETRIZATION REACTIONS.....</b>	<b>31</b>
1.4.1 With Organozinc Reagents .....	32
<b>1.5 CROSS-ELECTROPHILE COUPLING .....</b>	<b>34</b>
<b>1.5 CONCLUDING REMARKS .....</b>	<b>38</b>
<b>1.6 NOTES AND REFERENCES .....</b>	<b>40</b>

<b>CHAPTER 2</b>	<b>46</b>
<i>Catalytic Asymmetric Reductive Acyl Cross-Coupling: Synthesis of Enantioenriched Acyclic <math>\alpha,\alpha</math>-Disubstituted Ketones</i>	
<b>2.1 INTRODUCTION.....</b>	<b>46</b>
<b>2.2 REACTION DEVELOPMENT.....</b>	<b>53</b>
<b>2.3 SUBSTRATE SCOPE.....</b>	<b>65</b>
<b>2.4 CONCLUDING REMARKS .....</b>	<b>70</b>
<b>2.5 EXPERIMENTAL SECTION.....</b>	<b>71</b>
2.5.1 Materials and Methods.....	71
2.5.2 Substrate Synthesis.....	72
2.5.3 Enantioselective Reductive Cross-Coupling.....	74
2.5.4 SFC Traces of Racemic and Enantioenriched Ketone Products .....	93
<b>2.6 NOTES AND REFERENCES .....</b>	<b>114</b>
<b>APPENDIX 1</b>	<b>116</b>
Spectra Relevant to Chapter 2	
<b>CHAPTER 3</b>	<b>169</b>
<i>Nickel-Catalyzed Asymmetric Reductive Cross-Coupling Between Heteroaryl Iodides and <math>\alpha</math>-Chloronitriles</i>	
<b>3.1 INTRODUCTION.....</b>	<b>169</b>
<b>3.2 REACTION DEVELOPMENT.....</b>	<b>173</b>
<b>3.3 SUBSTRATE SCOPE.....</b>	<b>182</b>
<b>3.4 MECHANISTIC STUDIES.....</b>	<b>197</b>
<b>3.5 CONCLUDING REMARKS .....</b>	<b>199</b>

<b>3.6 EXPERIMENTAL SECTION.....</b>	<b>200</b>
3.6.1 Materials and Methods.....	200
3.6.2 Ligand and Substrate Preparation .....	201
3.6.3 Enantioselective Reductive Cross-Coupling.....	212
3.6.4 Derivatization of Enantioenriched Nitrile Products.....	233
3.6.5 SFC Traces of Racemic and Enantioenriched Ketone Products .....	237
<b>3.7 NOTES AND REFERENCES .....</b>	<b>263</b>
<b>APPENDIX 2</b>	<b>265</b>
Spectra Relevant to Chapter 3	
<b>CHAPTER 4</b>	<b>354</b>
<i>Nickel-Catalyzed Asymmetric Reductive Cross-Coupling to Access 1,1-Di(hetero)arylalkanes</i>	
<b>4.1 INTRODUCTION.....</b>	<b>354</b>
4.1.1 Background and Catalytic Asymmetric Approaches .....	354
4.1.2 Reductive Cross-Coupling Approaches and Preliminary Investigations .....	356
4.1.3 Reaction Design: Substrate and Condition Considerations .....	359
<b>4.2 REACTION DEVELOPMENT.....</b>	<b>361</b>
4.2.1 Ligand Exploration and Condition Optimization .....	361
4.2.2 Substrate Scope and Disconnection Strategy .....	368
<b>4.3 MECHANISTIC INVESTIGATIONS.....</b>	<b>372</b>
<b>4.4 CONCLUDING REMARKS .....</b>	<b>376</b>
<b>4.5 EXPERIMENTAL SECTION.....</b>	<b>376</b>
4.5.1 Materials and Methods.....	376
4.5.2 Ligand Preparation.....	378

4.5.3 Substrate Preparation .....	383
4.5.4 Enantioselective Reductive Cross-Coupling.....	386
4.5.5 Mechanistic Experiments .....	402
<b>4.5 NOTES AND REFERENCES .....</b>	<b>406</b>
<b>APPENDIX 3</b>	<b>408</b>
Spectra Relevant to Chapter 4	
<b>CHAPTER 5</b>	<b>456</b>
<i>Preliminary Results Toward Novel Ni-Catalyzed Asymmetric Reductive Cross-Couplings</i>	
<b>5.1 INTRODUCTION.....</b>	<b>456</b>
<b>5.2 VINYLATION OF CHLORONITRILES .....</b>	<b>459</b>
<b>5.3 COUPLING OF BENZYL CHLORIDES WITH CHLOROPHOSPHINES.....</b>	<b>462</b>
<b>5.4 COUPLING OF (HETERO)ARYL IODIDES AND CHLOROESTERS .....</b>	<b>465</b>
<b>5.5 CONCLUDING REMARKS .....</b>	<b>468</b>
<b>5.6 EXPERIMENTAL SECTION.....</b>	<b>469</b>
5.6.1 Materials and Methods.....	469
5.6.2 Vinyl iodide/ $\alpha$ -Chloronitrile Cross-Coupling .....	470
5.6.3 Chlorophosphine/Benzyl Chloride Cross-Coupling .....	470
5.6.4 (Hetero)aryl Iodide/ $\alpha$ -Chloroester Cross-Coupling .....	471
<b>5.7 NOTES AND REFERENCES .....</b>	<b>472</b>
<b>ABOUT THE AUTHOR.....</b>	<b>473</b>

**LIST OF ABBREVIATIONS**

$[\alpha]_D$	angle of optical rotation of plane-polarized light
Å	angstrom(s)
Ac	acetyl
acac	acetylacetonate
<sup>t</sup> Am	<i>tert</i> -amyl
APCI	atmospheric pressure chemical ionization
app	apparent
aq	aqueous
Ar	aryl group
bathophen	bathophenanthroline
BBN	borabicyclo[3.3.1]nonane
BHT	2,6-di- <i>tert</i> -butyl-4-methylphenol (“ <u>butylated hydroxytoluene</u> ”)
Biox	bi(oxazoline)
BINAP	2,2'-bis(diphenylphosphino)-1,1'-binaphthyl
BINOL	1,1'-bi(2-naphthol)
Bn	benzyl
Boc	<i>tert</i> -butoxycarbonyl
Box	bis(oxazoline)
bp	boiling point
BPPFA	<i>N,N</i> -dimethyl-1-[1',2-bis(diphenylphosphino)ferrocenyl]ethylamine
br	broad

Bu	butyl
<sup>i</sup> Bu	<i>iso</i> -butyl
<sup>n</sup> Bu	butyl or <i>norm</i> -butyl
<sup>s</sup> Bu	<i>sec</i> -butyl
<sup>t</sup> Bu	<i>tert</i> -butyl
Bz	benzoyl
<i>c</i>	concentration of sample for measurement of optical rotation
°C	degrees Celsius
calc'd	calculated
CAM	cerium ammonium molybdate
cm <sup>-1</sup>	wavenumber(s)
cod	1,5-cyclooctadiene
conc.	concentrated
Cp	cyclopentadienyl
Cy	cyclohexyl
Cyp	cyclopentyl
d	doublet
<i>d</i>	dextrorotatory
D	deuterium
dba	dibenzylideneacetone
DFT	density functional theory
DIOP	2,3- <i>O</i> -isopropylidene-2,3-dihydroxy-1,4-bis(diphenylphosphino)butane

DKR	dynamic kinetic resolution
DMA	<i>N,N</i> -dimethylacetamide
DMBA	2,6-dimethylbenzoic acid
DME	1,2-dimethoxyethane
DMF	<i>N,N</i> -dimethylformamide
DMI	1,3-dimethyl-2-imidazolidinone
DMPU	<i>N,N'</i> -dimethylpropylene urea
DMSO	dimethylsulfoxide
dppb	1,4-bis(diphenylphosphino)butane
dppbz	1,2-bis(diphenylphosphino)benzene
dppf	1,1'-bis(diphenylphosphino)ferrocene
dppe	1,2-bis(diphenylphosphino)ethane
dr	diastereomeric ratio
dtbpy	4,4'-di- <i>tert</i> -butyl-2,2'-bipyridine
DYKAT	dynamic kinetic asymmetric transformation
<i>E</i>	trans (entgegen) olefin geometry
ee	enantiomeric excess
EI	electron impact
EPPF	1-diphenylphosphino-2-ethylferrocene
ESI	electrospray ionization
Et	ethyl
FAB	fast atom bombardment
FcPN	1-dimethylaminomethyl-2-diphenyl-phosphinoferrocene

g	gram(s)
GC	gas chromatography
h	hour(s)
$^1\text{H}$	proton
hex	hexyl
HMDS	hexamethyldisilazane
$h\nu$	light
HPLC	high performance liquid chromatography
HRMS	high resolution mass spectrometry
Hz	hertz
IPA	isopropanol
IR	infrared spectroscopy
$J$	coupling constant
$k$	rate constant
L	liter or neutral ligand
$l$	levorotatory
LED	light-emitting diode
m	multiplet or meter(s)
M	molar or molecular ion
$m$	meta
Me	methyl
mg	milligram(s)
MHz	megahertz

min	minute(s)
mL	milliliter(s)
MM	mixed method
mol	mole(s)
MOP	2-(diphenylphosphino)-2'-methoxy-1,1'-binaphthyl
mp	melting point
Ms	methanesulfonyl (mesyl)
MS	molecular sieves or mass spectrometry
$m/z$	mass-to-charge ratio
naph	naphthyl
Naphos	2,2'-bis(diphenylphosphinomethyl)-1,1'-binaphthyl
nbd	norbornadiene
NBS	<i>N</i> -bromosuccinimide
NMDPP	neomenthyl diphenylphosphine
NMP	<i>N</i> -methyl-2-pyrrolidone
NMR	nuclear magnetic resonance
Norphos	2,3-bis(diphenylphosphino)-bicyclo[2.2.1]hept-5-ene
<i>o</i>	ortho
<i>p</i>	para
Pc	phthalocyanine
Ph	phenyl
pH	hydrogen ion concentration in aqueous solution
phen	1,10-phenanthroline

PHOX	phosphinooxazoline
pin	pinacol
Piv	pivaloyl
$pK_a$	acid dissociation constant
PPFA	<i>N,N</i> -dimethyl-1-[2-(diphenylphosphino)ferrocenyl]ethylamine
Pr	propyl
<sup>i</sup> Pr	isopropyl
<sup>n</sup> Pr	propyl or <i>norm</i> -propyl
Prophos	1,2-bis(diphenylphosphino)propane
py	pyridine
PyBox	pyridine-bis(oxazoline)
PyOx	pyridine-oxazoline
pyphos	(2-diphenylphosphino)ethylpyridine
q	quartet
Quinox	quinoline-oxazoline
R	alkyl group
<i>R</i>	rectus
ref	reference
$R_f$	retention factor
rt	room temperature
s	singlet or seconds
<i>S</i>	sinister
sat.	saturated

SET	single-electron transfer
SFC	supercritical fluid chromatography
t	triplet
TADDOL	$\alpha,\alpha,\alpha,\alpha$ -tetraaryl-1,3-dioxolane-4,5-dimethanol
TBAB	tetra- <i>n</i> -butylammonium bromide
TBAI	tetra- <i>n</i> -butylammonium iodide
TBAT	tetra- <i>n</i> -butylammonium difluorotriphenylsilicate
TBS	<i>tert</i> -butyldimethylsilyl
TDAE	tetrakis(dimethylamino)ethylene
TFA	trifluoroacetic acid
temp	temperature
terpy	2,2':6',2''-terpyridine
THF	tetrahydrofuran
TIPS	triisopropylsilyl
TLC	thin layer chromatography
TMEDA	<i>N,N,N',N'</i> -tetramethylethylenediamine
TMS	trimethylsilyl
TOF	time-of-flight
tol	toluene
UV	ultraviolet
v/v	volume per volume
X	anionic ligand or halide
Z	cis (zusammen) olefin geometry

## **Chapter 1**

### *Nickel Catalysis in Cross-Coupling: A Review of Applications in Asymmetric Catalysis and the Rise of Reductive Cross-Coupling<sup>∘</sup>*

#### **1.1 INTRODUCTION**

The stereocontrolled construction of C–C bonds remains one of the foremost challenges in organic synthesis. At the heart of any chemical synthesis of a natural product or designed small molecule is the need to carefully orchestrate a series of chemical reactions to prepare and functionalize a carbon framework. Transition metal catalysis, most notably by Pd, has transformed the palette of tools available to the synthetic chemist, enabling new disconnections and streamlining access to complex scaffolds. While the incredible versatility and reliable predictability of Pd-mediated reactions has made them a mainstay of synthetic organic chemistry (and earned their inventors a Nobel prize), the unique reactivity of Ni and other base metals has brought

---

<sup>∘</sup> Portions of this chapter have been reproduced from a published review coauthored with Prof. Sarah E. Reisman and Dr. Alan H. Cherney (see reference 1).

about a resurgence of interest in these catalysts as well, particularly to effect stereoselective transformations.

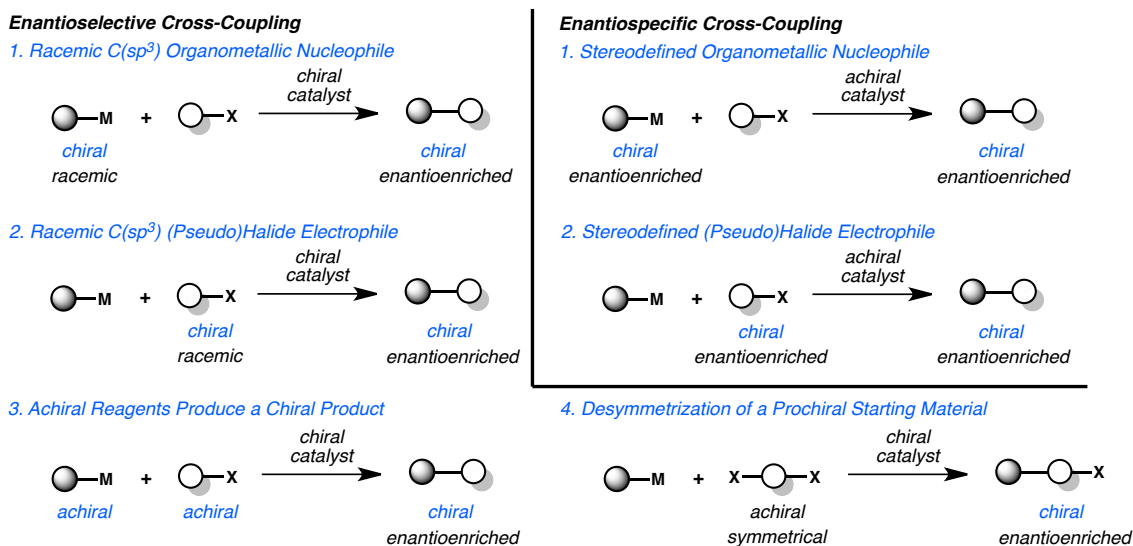
The potential of using transition metal-catalyzed C–C bond formation to prepare enantioenriched molecules was immediately recognized by the synthetic chemistry community. Indeed, the first forays into enantioselective cross-coupling reactions occurred contemporaneously with the development of the transition metal-catalyzed reactions themselves. Though some of the earliest and most foundational studies in cross-coupling (including asymmetric reactions, *vide infra*) were conducted using Ni catalysis, much of this field has been dominated by precious metals until recently. Below we have collected the Ni-catalyzed asymmetric cross-coupling reactions reported over the last five decades, highlighting the utility of this base metal in catalysis and underscoring its role in the history of asymmetric cross-coupling. Here we define *Ni-catalyzed cross-coupling reactions* as C–C bond forming reactions between an organic electrophile (typically an organic halide or pseudo halide, such as alcohols, amines, and their derivatives) and an organometallic reagent, mediated by a nickel catalyst.

Enantio-controlled Ni-catalyzed cross-coupling reactions to form C–C bonds, in which the stereogenic unit is defined by the C–C bond forming event, can be organized into two general categories. The first group comprises *enantioselective* Ni-catalyzed cross-coupling reactions, which we define as *reactions in which there is selective formation of one enantiomer over the other as defined by a non-racemic chiral Ni catalyst*. There are several different types of enantioselective cross-coupling reactions: those in which (a) racemic, C(sp)<sup>3</sup> organometallic reagents are stereoconvergently coupled to organic electrophiles; (b) racemic, C(sp)<sup>3</sup> organic electrophiles are

stereoconvergently coupled to organometallic reagents; (c) achiral organic electrophiles are coupled to achiral organometallic reagents to produce chiral, non-racemic products; and (d) a prochiral starting material (either the organic electrophile or organometallic reagent) is desymmetrized. These reactions are schematically represented in **Figure 1.1**. These types of enantioselective reactions have been used to prepare molecules exhibiting centro, axial, and planar chirality. Our discussion here will encompass enantioselective Ni-catalyzed cross-coupling reactions of organic electrophiles and organometallic reagents, covering the literature published through the end of the year 2014.<sup>1</sup>

Although not discussed further in this chapter, it is important to note that the second group comprises *enantiospecific* Ni-catalyzed alkyl cross-coupling reactions, which we define as *chirality exchange reactions in which the stereochemistry of a chiral, enantioenriched substrate defines the stereochemistry of the product*. These reactions can be further categorized into those which involve the cross-coupling of (a) a stereodefined organometallic reagent with an electrophile, or (b) a stereodefined electrophile with an organometallic reagent. While much of this field has been dominated by the stereospecific coupling of enantioenriched organometallic reagents by Pd, Ni has received significant recent attention for its ability to stereospecifically cross-couple pseudohalide electrophiles such as benzylic ethers, carbamates, esters, and ammonium salts.<sup>2</sup> These reactions are an area of substantial current interest and represent a valuable alternative approach to access chiral products.

**Figure 1.1.** Strategies for enantiocontrolled cross-coupling.

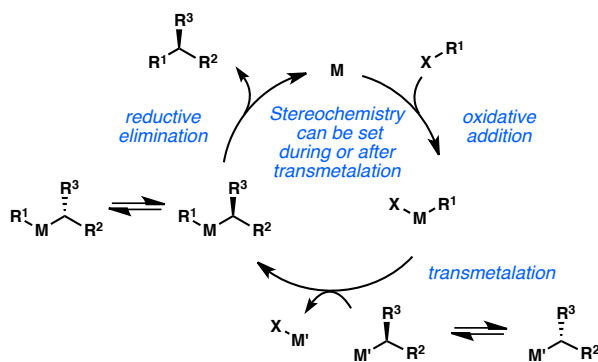


Despite promising initial reports, highly enantioselective transition metal-catalyzed alkyl cross-coupling reactions were slow to develop, in part because of the general challenges encountered in Pd-catalyzed alkyl cross-coupling reactions. For Pd and other metals that react by polar, two-electron mechanisms, *sec*-alkyl organometallic reagents are typically slower than their *n*-alkyl or C(sp<sup>2</sup>) hybridized counterparts to undergo transmetalation.<sup>3</sup> Similarly, *sec*-alkyl electrophiles are frequently slow to undergo oxidative addition to Pd.<sup>4</sup> Moreover, in either case, the resulting *sec*-alkyl transition metal complexes can suffer from rapid, non-productive β-hydride elimination. Thus, the successful realization of enantioselective transition metal-catalyzed alkyl cross-coupling reactions has resulted from fundamental studies of the factors, especially ligands, which control and influence the efficiency of these transformations. In particular, a renewed interest in Ni catalysts, which can engage with *sec*-alkyl halides through single electron oxidative addition mechanisms, has resulted in a rapidly increasing number of enantioselective alkyl cross-coupling reactions.

## 1.2 REACTIONS OF SECONDARY ALKYL ORGANOMETALLIC REAGENTS

Early efforts to develop enantioselective transition metal-catalyzed alkyl cross-coupling reactions focused primarily on the use of configurationally labile *sec*-alkyl organometallic species such as organomagnesium and organozinc reagents. In general, the configurational stability of an organometallic reagent correlates to the electronegativity of the metal, with less electronegative metals resulting in more configurationally labile *sec*-alkyl reagents.<sup>5</sup> For example, *sec*-alkyl magnesium reagents have been shown to racemize above  $-10\text{ }^{\circ}\text{C}$ , while the corresponding *sec*-alkyl boron reagents are configurationally stable indefinitely at room temperature.<sup>6</sup> In principle, fast equilibration between the two enantiomers of a *sec*-alkyl organometallic reagent or between two diastereomers of a chiral transition metal complex could enable enantioselective cross-coupling through a dynamic kinetic asymmetric transformation (DYKAT), in which the newly formed stereogenic center is controlled by the chirality of the metal catalyst (**Figure 1.2**).

**Figure 1.2.** Stereochemical outcome of cross-coupling with secondary nucleophiles.



Enantioselective reactions of configurationally stable *sec*-alkyl organometallic reagents can arise from catalyst-controlled kinetic resolution processes, wherein the

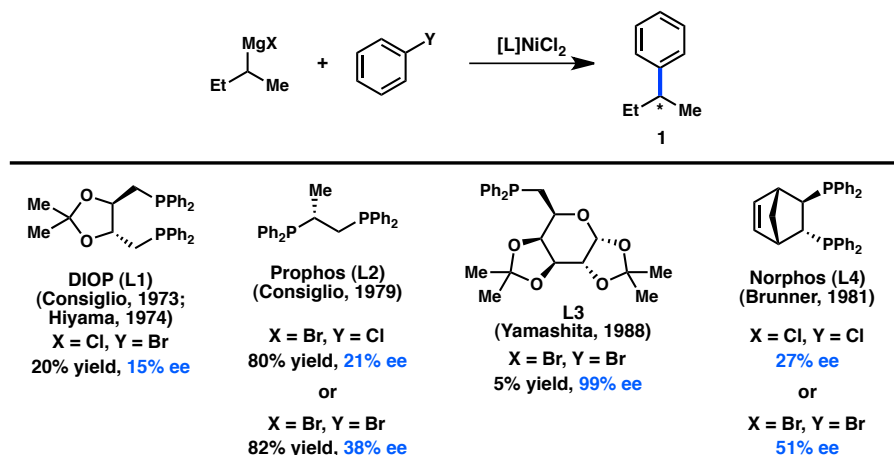
relative rates of transmetalation for the two enantiomers of the chiral organometallic reagent are substantially different. In this case, an excess of the organometallic reagent must be used to obtain the cross-coupled product in good yield. A third possibility involves a stereoablative mechanism, in which the initial configuration of the starting material is destroyed and then reset by the chiral catalyst during the reaction.

### 1.2.1 Organomagnesium Reagents

In 1972 Corriu and Kumada independently reported the Ni-catalyzed cross-coupling between alkyl organomagnesium halides and aryl or vinyl halides;<sup>7</sup> shortly thereafter the first studies aimed at utilizing chiral transition metal complexes to catalyze these reactions enantioselectively were reported.<sup>8</sup> In 1973 and 1974, respectively, Consiglio and Kumada independently reported that the complex generated from Ni-halide salts and the chiral bidentate phosphine ligand DIOP (**L1**) catalyzes the reaction between *sec*-butylmagnesium bromide or chloride and bromo- or chlorobenzene to give product **1** with promising enantioinduction (**Figure 1.3**).<sup>9</sup> These results were an important proof of concept for the area of enantioselective cross-coupling; however, since low yields of product were obtained, it remains ambiguous whether these reactions proceed by kinetic resolution of the *sec*-alkylmagnesium reagent or through a DYKAT. It was subsequently reported that Prophos (**L2**) provides improved enantioinduction and higher yields of **1**.<sup>10</sup> The identity of the halogen on both the organic halide and the organometallic reagent was shown to significantly influence the absolute configuration and the ee of **1**. Further improvements were observed when Norphos (**L4**) was employed as the chiral ligand,

providing **1** in 50% ee.<sup>11</sup> A carbohydrate-derived chiral ligand (**L3**) was also reported to deliver **1** in good ee, although with poor yields.<sup>12</sup>

**Figure 1.3.** Stereoconvergent arylation of *sec*Bu Grignard reagents.



Concurrent to their efforts to develop enantioselective cross-coupling reactions of *sec*-butyl Grignard reagents, Kumada and coworkers investigated the Ni-catalyzed enantioselective coupling between  $\alpha$ -methylbenzyl Grignard reagents and vinyl halides (Figure 1.4). DIOP (**L1**) and the axially chiral Naphos (**L6**) ligand systems provided the product with low enantioinduction.<sup>9b,13</sup> Following up on Kumada's studies, Brunner and coworkers reported that Norphos (**L4**) furnished **2** in 95% yield and 67% ee.<sup>14</sup>

**Figure 1.4.** Stereoconvergent vinylation of benzylic Grignard reagents.

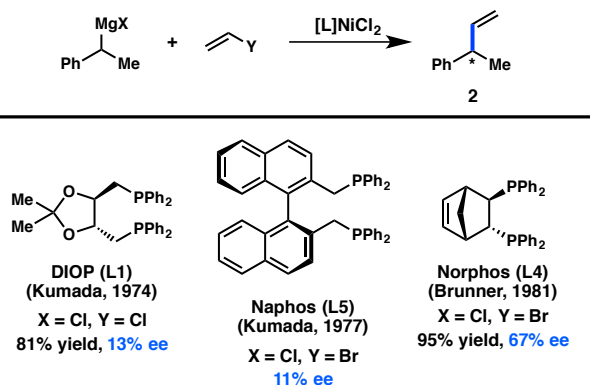
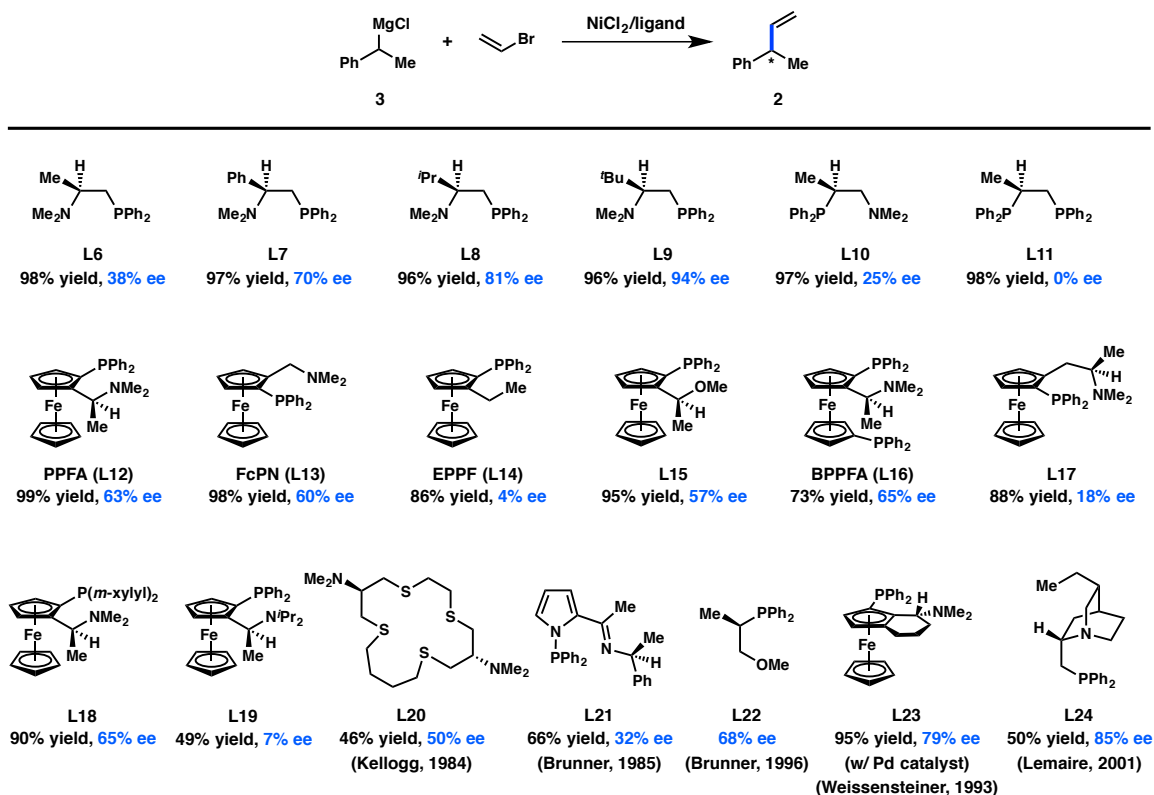


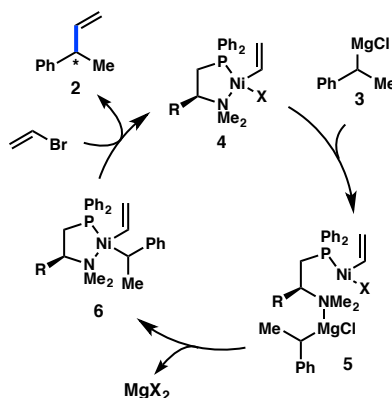
**Figure 1.5.** Chiral ligands developed for the enantioselective cross-coupling of  $\alpha$ -methylbenzyl Grignard reagents.



Since Kumada's initial report, the majority of studies have focused on identifying new ligands to improve the selectivity in the coupling between  $\alpha$ -methylbenzyl Grignard reagents (**3**) and vinyl bromide. Whereas the early studies focused on the use of bidentate bis-phosphine ligands, which delivered modest levels of enantioinduction, later efforts turned to chiral P,N ligands. Kumada, Hayashi, and coworkers reported that chiral ( $\beta$ -aminoalkyl)phosphines—easily prepared from enantiopure amino acids—delivered exceptionally high yields for the cross-coupling between **3** and vinyl bromide (**Figure 1.5**).<sup>15</sup> Interestingly, whereas the alkyl substitution on the ligand backbone exhibited little influence on the yield of the reaction, it dramatically impacted the enantioselectivity: increasing the steric profile of the ligand raised the ee from 38% when the chiral tertiary

substituent was Me (**L6**) to 94% when this group was <sup>t</sup>Bu (**L9**). In order to probe the origin of asymmetric induction, the isomeric P,N-ligand **L10** was designed. Under the same reaction conditions, **L10** delivered **4** in only 25% ee. Moreover, the analogous bisphosphine **L11** provided no enantioinduction, suggesting a critical role for the amino group. A proposed catalytic cycle for this reaction is shown in **Figure 1.6** and involves precoordination between Grignard reagent **3** and the amino group of the ligand to give complex **5**. The authors hypothesize that this coordination could selectively direct the transmetalation of a single enantiomer of the organometallic reagent, although the importance of this interaction has been debated.<sup>16</sup>

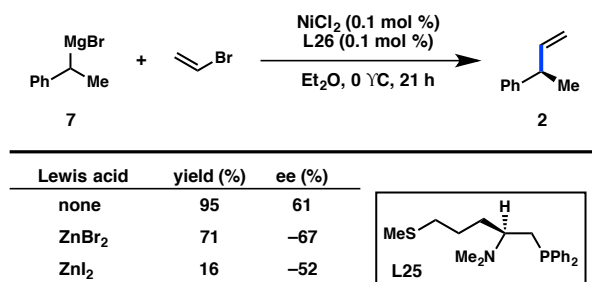
**Figure 1.6.** Proposed catalytic cycle for the enantioselective coupling of  $\alpha$ -methylbenzyl Grignard reagents.



Elaborating on this concept, Kellogg and coworkers investigated the use of ( $\beta$ -aminoalkyl)phosphine ligands bearing pendant heteroatoms, such as those derived from lysine or methionine.<sup>17</sup> The authors reported a reversal of the stereochemical outcome in the presence of exogenous zinc halide salts (**Figure 1.7**). Control experiments using pre-generated  $\alpha$ -methylbenzylzinc bromide did not support the intermediacy of an organozinc species; instead it is possible that coordination between the Lewis acidic zinc halide and

the sidechain heteroatom could alter or disrupt the ability of the amino group to direct the transmetalation event.

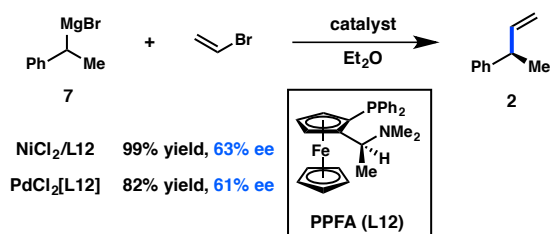
**Figure 1.7.** Addition of exogenous zinc halide salts reverses the sense of enantioinduction when sulfur-containing ligand **L25** is used.



The importance of an amino directing group on the chiral ligand was also reported by Kumada, Hayashi, and coworkers, during their investigations of ferrocenyl phosphines in the Ni-catalyzed coupling between  $\alpha$ -methylbenzyl Grignard reagent **3** and vinyl bromide (**Figure 1.5**). These bidentate P,N ligands possess both centrochirality at carbon as well as planar chirality. The ligand PPFA (**L12**), furnished **2** in an excellent 99% yield and 63% ee.<sup>18</sup> The ee of the product was determined to remain roughly constant over the course of the reaction.<sup>19</sup> A structure-activity relationship study revealed that FcPN (**L13**), while lacking centrochirality but maintaining planar chirality, gave **2** in 60% ee, demonstrating the dominant role of planar chirality in this system. EPPF (**L14**), which possesses neither centrochirality nor the dimethylamino group, delivered **2** in only 4% ee, validating the importance of the amino group and supporting a role for pre-coordination as proposed in **Figure 1.6**. Further evidence for the significance of a coordinating group comes from **L15**, which possesses a methoxy moiety instead of a dimethylamino group and provides **2** in 57% ee. Diphosphine BPPFA (**L16**), which could potentially coordinate through phosphorus in a bidentate fashion, also provides **2** in 65% ee. The

similarity of the ee data obtained with **L14** and **L16** suggests that they both coordinate the metal in the same fashion, likely through a P-N mode. Consistent with this observation, changing the steric bulk on the amine of **L12** gives a range of ee values for **2** (see **L19**), while changing the steric environment of the phosphine does not significantly perturb the selectivity (see **L18**). Homologated ligand **L17** delivers **2** in poor ee.<sup>20</sup> Pd catalysts were also investigated and were shown to give comparable results to Ni (**Figure 1.8**).<sup>18c</sup>

**Figure 1.8.** The use of the P-N ligand PPFA provides similar results in both Ni- and Pd-catalyzed transformations.

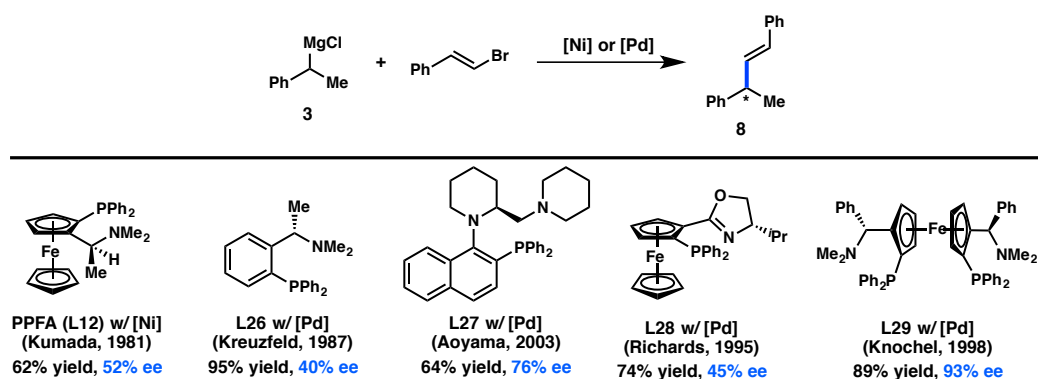


Several other ligand families have been developed for the enantioselective preparation of **2** (**Figure 1.5**). Catalysts generated from macrocyclic sulfides (**L20**) and nickel salts have been shown to impart moderate enantioselectivity, possibly through a simple kinetic resolution.<sup>21</sup> The use of pyrrole-containing P,N ligand **L21** or phosphine **L22** delivers **2** in 32% ee and 68% ee, respectively, under Ni catalysis.<sup>22,23</sup> Using Pd catalysis, the P,N ligand **L23**, which contains both planar and centrochirality, gives improved results with respect to PPFA (**L12**).<sup>24</sup> High ee can also be achieved with phosphine-quinoridine **L24**.<sup>25</sup>

Despite the advances made through ligand tuning when vinyl bromide is used as an electrophile, the scope of the asymmetric alkyl cross-coupling is poor. Disubstituted alkenes were typically found to be less enantioselective; for example, the reaction of *E*-

bromostyrene using PPFA (**L12**) as the ligand delivered **8** in only 52% ee and moderate yield (**Figure 1.9**).<sup>18c,26</sup> While the yield could be improved using the simpler aminophosphine **L26**, the ee of **8** decreased.<sup>27</sup> **L27**, designed to induce axial chirality upon coordination to a transition metal, was able to induce 76% ee for **8**.<sup>28</sup> Moderate ee could also be attained with phosphine-oxazoline ligand **L28**.<sup>29</sup> Knochel and coworkers reported *C*<sub>2</sub>-symmetric ferrocenyl phosphine **L29** as being capable of delivering excellent ee for the coupling of bromostyrene, although the reaction scope is still limited.<sup>30</sup>

**Figure 1.9.** Asymmetric Kumada–Corriu cross-coupling of bromostyrene.

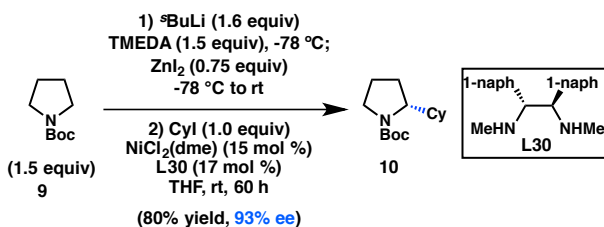


## 1.2.2 Organozinc Reagents

The pioneering studies of enantioselective transition metal-catalyzed alkyl cross-coupling reactions were initially performed using Ni catalysts and organomagnesium reagents—a species expected to exhibit configurational lability. Advances in the development of the Negishi cross-coupling subsequently enabled the use of organozinc reagents in asymmetric alkyl cross-coupling reactions, with Hayashi, Kumada, and coworkers reporting the first examples in 1983.<sup>31</sup> Preliminary studies investigated the coupling of the organozinc chloride prepared from transmetalation of **3** with ZnCl<sub>2</sub>; however, Ni catalysts were determined to be poorly reactive. On the other hand, the

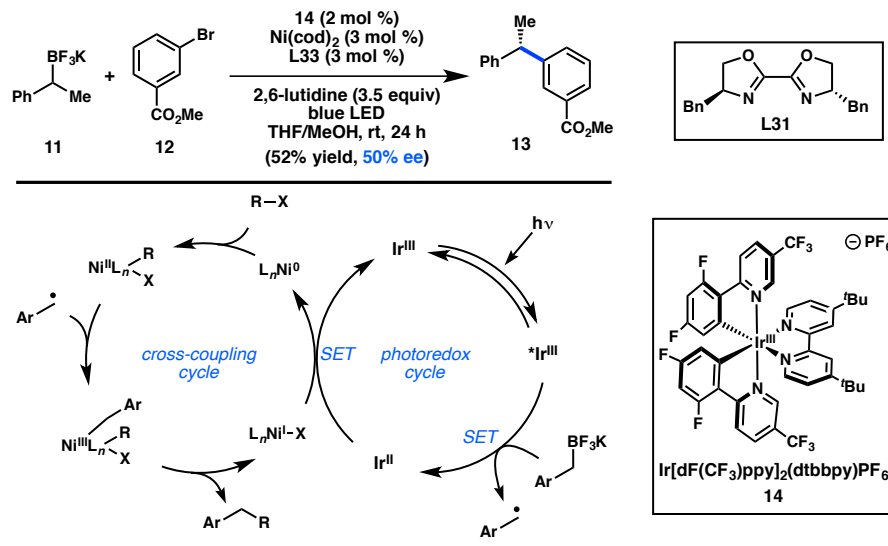
combination of Pd and PPFA (**L12**) delivered **2** in 85% ee. Despite a growing interest in the enantioselective Ni-catalyzed cross-coupling reactions of organozinc reagents over the past three decades, successful efforts to further expand upon the enantioselective alkyl Negishi cross-coupling have been limited.

**Scheme 1.1.** Enantioselective functionalization of pyrrolidine.



However, in a seminal 2013 report, Fu reinvestigated the Negishi cross-coupling of  $\alpha$ -zincated *N*-Boc-pyrrolidine, which Campos and coworkers had previously shown can undergo stereospecific Pd-catalyzed cross-coupling to deliver enantioenriched  $\alpha$ -arylpyrrolidine products.<sup>32</sup> Under Ni catalysis, in the absence of a chiral ligand, coupling of the stereodefined organozinc reagent with cyclohexyl iodide produced the coupled product in almost racemic form. Alternatively, when the chiral Ni/**L30** complex was used as the catalyst, coupling of racemic **9** with cyclohexyl iodide furnished **10** with high ee in a stereoconvergent fashion, representing the first enantioconvergent alkyl-alkyl coupling of a racemic organometallic reagent (**Scheme 1.1**).<sup>33</sup> Mechanistic studies have determined that this stereoconvergence does not arise from a series of  $\beta$ -hydride elimination/alkene insertion processes of the organometallic reagent.

**Figure 1.10.** Dual catalysis approach to asymmetric cross-coupling.

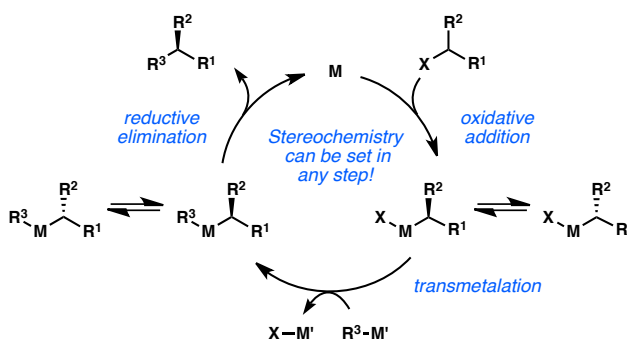


### 1.2.3 Organoboron Reagents

Trifluoroborate salts are often used in the Suzuki–Miyaura cross-coupling due to their improved stability with respect to boronic acids and esters. The two-electron mechanism of transmetalation typically believed to be operative in Suzuki–Miyaura reactions innately favors transmetalation in a stereospecific manner. However, Molander and coworkers hypothesized that transmetalation through a single electron pathway could favor transfer of a C(sp<sup>3</sup>)-hybridized alkyl fragment via a stereoconvergent, radical process. In order to generate a radical from an organoboron reagent (**11**), the authors envisaged a dual catalysis mechanism in which Ni-catalyzed cross-coupling and Ir-catalyzed photoredox events occur synergistically (**Figure 1.10**).<sup>34</sup> In an important proof of concept, chiral bioxazoline (BiOX) **L31** was used to furnish **13** in 50% ee. Electron transfer to an excited state \*Ir<sup>III</sup> complex from an organoboron species would generate an alkyl radical. The alkyl radical can then combine with a chiral Ni<sup>II</sup> complex to form a Ni<sup>III</sup>

species that can reductively eliminate the desired product. The resulting  $\text{Ni}^{\text{I}}$  can be reduced by  $\text{Ir}^{\text{II}}$  to complete both catalytic cycles. Additional investigations toward asymmetric catalysis would be valuable.

**Figure 1.11.** Stereochemical outcome of cross-coupling with 2° electrophiles.

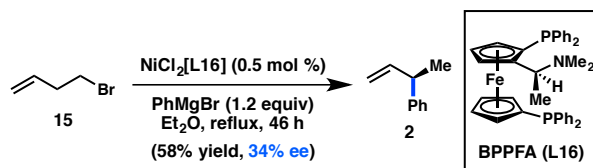


### 1.3 REACTIONS OF SECONDARY ALKYL ELECTROPHILES

The challenges associated with oxidative addition of *sec*-alkyl electrophiles, as well as the propensity for alkyl transition metal complexes to undergo rapid  $\beta$ -hydride elimination, conspired to make the cross-coupling of these electrophiles difficult to realize using Pd, which had emerged as the metal of choice for cross-coupling in the 1980s. In the early 2000's, researchers began re-investigating first-row transition metals for the cross-coupling of *sec*-alkyl halides and organometallic reagents.<sup>4</sup> Following the first reports of alkyl cross-coupling to form stereogenic  $\text{C}(\text{sp}^3)$  centers, the systematic examination of asymmetric induction in these processes became a chief objective. In these systems, catalysts that favor a single-electron oxidative addition mechanism may undergo a stereoconvergent oxidative addition to set the ultimate stereochemistry of the product. Alternatively, rapidly equilibrating mixtures of diastereomeric transition metal

complexes can result in preferential transmetalation or reductive elimination of one diastereomer over the other (**Figure 1.11**).

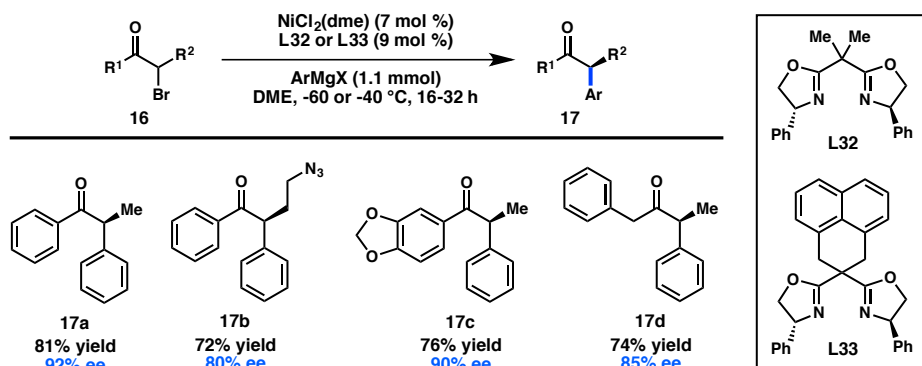
**Scheme 1.2.** Primary-to-secondary isomerization in asymmetric cross-coupling.



### 1.3.1 With Organomagnesium Reagents

The earliest example of an enantioselective transition metal-catalyzed cross-coupling reaction between an alkyl electrophile and an organomagnesium reagent was disclosed by Kumada and coworkers in 1977, the result of a surprising alkyl group isomerization observed during the coupling between homoallylic halide **15** and  $\text{PhMgBr}$  (**Scheme 1.2**).<sup>35</sup> In the presence of the chiral catalyst  $\text{NiCl}_2[\text{BPPFA}]$ , **2** was formed in 34% ee. While the isomerization of secondary organometallic reagents to primary species is a well-known side reaction in cross-coupling chemistry, the inverse isomerization is much more rarely observed.<sup>36</sup> Although this preliminary result was not developed further by Kumada and coworkers, it presaged the explosion of asymmetric cross-couplings of *sec*-alkyl electrophiles that would emerge in the literature nearly two decades later.

**Figure 1.12.** Stereoconvergent Kumada–Corriu coupling of  $\alpha$ -haloketones.



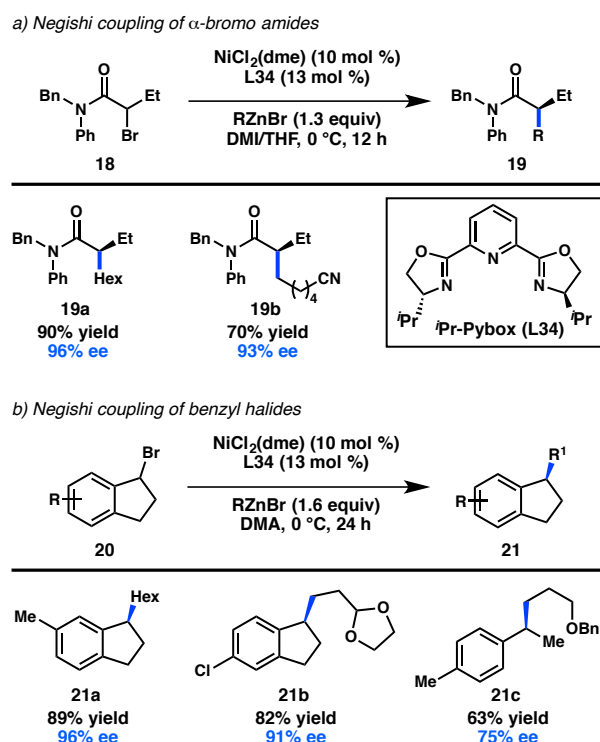
The first synthetically useful enantioselective, stereoconvergent cross-coupling between a *sec*-alkyl electrophile and a Grignard reagent was developed by Fu and coworkers in 2010. In this seminal report, the combination of NiCl<sub>2</sub>(dme) and bidentate bis(oxazoline) ligand **L32** or **L33** was found to promote the coupling of  $\alpha$ -haloketones **16** and arylmagnesium halides to give  $\alpha$ -aryl ketones **17** (**Figure 1.12**).<sup>37</sup> Notably, the reaction can be run at some of the lowest temperatures reported for the cross-coupling of alkyl electrophiles (–60 °C); the low temperature prevents the racemization of ketone product **17** through enolization by the Brønsted basic Grignard reagent. Both alkyl and aryl ketones can be prepared by this method, and these products can be diastereoselectively derivatized to access chiral alcohols and amines.<sup>38</sup>

### 1.3.2 With Organozinc Reagents

In 2005, two reports from the Fu laboratory demonstrated the first utilization of secondary alkyl electrophiles in highly enantioselective cross-coupling reactions. In one example, treatment of  $\alpha$ -bromo amide **18** with an alkylzinc reagent and a Ni/**L34** catalyst delivered **19** in good yield and high ee (**Figure 1.13, a**).<sup>39</sup> The identity of the amide substituents played a key role in achieving high enantioselectivity. When the organozinc reagent is used as a limiting reagent, the  $\alpha$ -bromo amide is recovered as a racemate, suggesting that the reaction does not proceed by a kinetic resolution. In a second example by Fu and coworkers, the Ni/**L34**-catalyzed coupling of 1-bromoindanes and alkyl halides produced chiral indane **20** in good yield and high ee (**Figure 1.13, b**).<sup>40</sup> The use of acyclic 1-(1-bromoethyl)-4-methylbenzene furnished **21c** with more modest enantioselectivity. In both cases, only primary organozinc reagents were compatible with

the reaction conditions. A computational investigation by Lin and coworkers proposed that a Ni<sup>I</sup>/Ni<sup>III</sup> mechanism consisting of transmetalation/oxidative addition/reductive elimination is more energetically favorable than a Ni<sup>0</sup>/Ni<sup>II</sup> mechanism.<sup>41</sup> The enantioselectivity of the reaction was also correlated to the difference in free energy between the two transition states for reductive elimination.

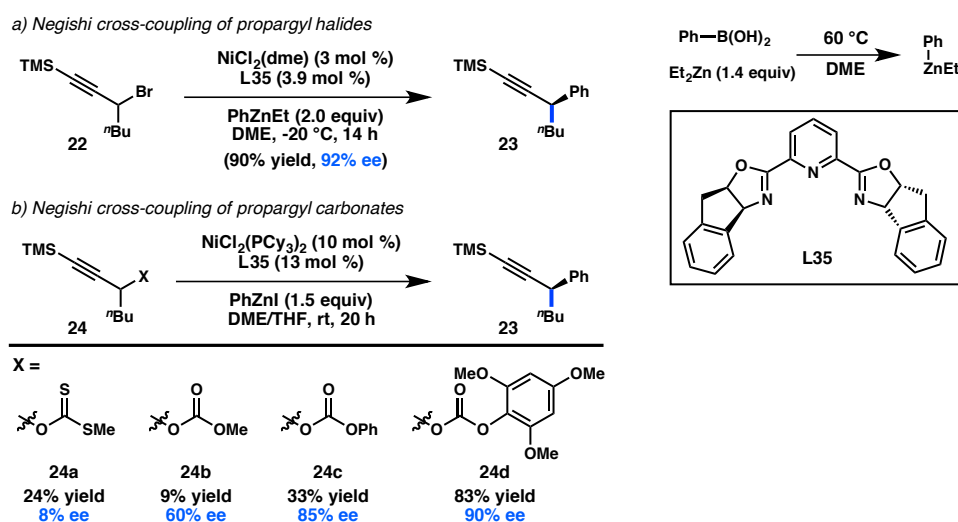
**Figure 1.13.** Seminal stereoconvergent cross-couplings of secondary alkyl halides.



In spite of Fu's promising results for the asymmetric, stereoconvergent Negishi cross-coupling of *alkylzinc* reagents, the extension to *arylzinc* species proved challenging. After a lengthy investigation, it was discovered that Ni/L35 complexes catalyze the cross-coupling between propargyl halide **22** and Ph<sub>2</sub>Zn to furnish **23** in a high yield and ee (Figure 1.14, a).<sup>42</sup> Since relatively few diarylzinc reagents are commercially available, the group sought to identify other arylzinc reagents that were effective for this transformation. Unfortunately, the use of arylzinc halides or *in situ*-

prepared diarylzincs, generated from transmetalation of the corresponding organolithium or –magnesium reagent, was unsuccessful. However, the group determined that  $\text{ArZnEt}$ , prepared from  $\text{ArB(OH)}_2$  and  $\text{Et}_2\text{Zn}$ , could react to provide comparable results. In contrast to the stereospecific Pd-catalyzed coupling of propargyl halides, no allene formation arising from  $\text{S}_{\text{N}}2'$  oxidative addition was observed.<sup>43</sup> Fu and coworkers reported a detailed mechanistic study of this transformation in 2014, showing that the oxidative addition of the propargylic electrophile proceeds via a radical chain pathway, with the stabilized prochiral radical intermediate facilitating enantioconvergence.<sup>44</sup>

**Figure 1.14.** Stereoconvergent Negishi cross-coupling of propargylic electrophiles.

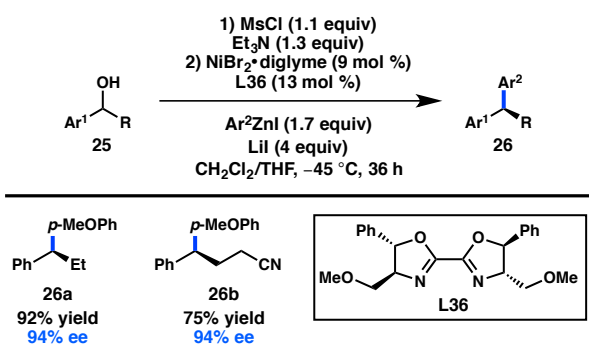


Organic halides are frequently prepared from the corresponding alcohols, and for certain substrates this functional group interconversion can be low yielding. Recognizing the synthetic advantage of using oxygen-based electrophiles directly in cross-coupling reactions, Fu and colleagues turned their attention to the asymmetric cross-coupling of propargylic alcohol derivatives. Hypothesizing that the reaction would proceed through a radical-based oxidative addition to Ni, a xanthate was chosen as a potential leaving group, due to its propensity toward radical cleavage in Barton-McCombie-type

transformations. However, these substrates performed poorly, producing **23** in low yield and ee (**Figure 1.14, b**).<sup>45</sup> On the other hand, simple carbonate **24b** underwent cross-coupling with improved enantioselectivity. Further investigation revealed that both the yield and ee could be improved by use of aryl-substituted carbonates, with **24d** delivering **23** in 83% yield and 90% ee. The optimized reaction conditions proved to be general not just for propargyl carbonates, but also for the coupling of propargyl halides.

In 2013, Fu and coworkers published a stereoconvergent Negishi coupling of benzylic mesylates that could be prepared from the corresponding alcohols immediately prior to the coupling and used without purification (**Figure 1.15**).<sup>46</sup> Bi-oxazoline **L36** was identified as the optimal ligand, with more traditional Pybox and Box ligands delivering poor enantioselectivity. LiI was employed to allow *in situ* displacement of the mesylate to form a reactive benzylic iodide. A wide substrate scope was demonstrated for the cross-coupling; a slight erosion of ee is observed when R = Me. Although several stereospecific routes to diarylalkanes have been developed to date,<sup>47</sup> this reaction provides a complementary approach.

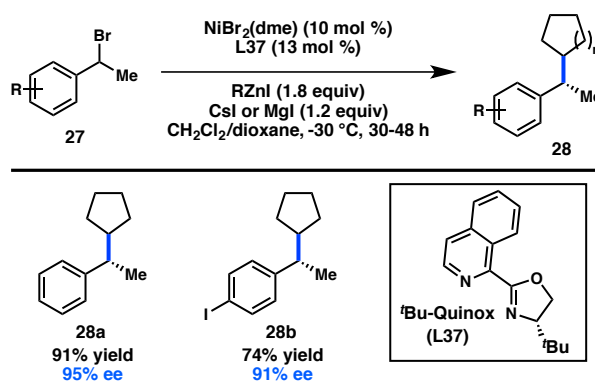
**Figure 1.15.** Stereoconvergent Negishi cross-coupling of benzyl alcohol derivatives.



A long-term objective in the area of enantioselective alkyl cross-coupling is to couple *sec*-alkyl electrophiles with *sec*-alkyl organometallic reagents. The Fu laboratory

made a significant advance toward this objective in 2012 when they reported the asymmetric Negishi cross-coupling between benzylic bromide **27** and cyclic organozinc halides (Figure 1.16).<sup>36</sup> Isoquinoline-oxazoline ligand **L37** delivered the products in high yields and ee's, in contrast to the more commonly employed PyBox and Box ligands. Acyclic secondary organozinc halides resulted in a mixture of branched and linear products; surprisingly, primary organozinc halides also resulted in a mixture of branched and linear products.

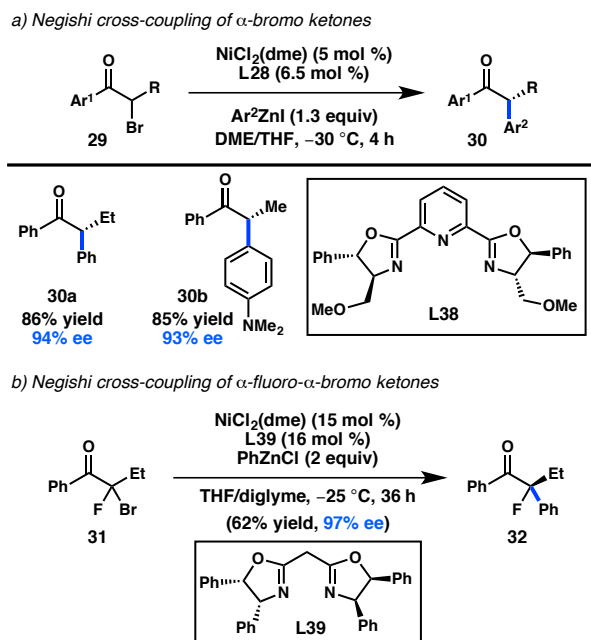
**Figure 1.16.** Enantioconvergent Negishi cross-coupling of secondary organozinc reagents.



Prior to their disclosure of the enantioselective cross-coupling between  $\alpha$ -bromoketones and aryl Grignard reagents (see Figure 1.13), the Fu laboratory developed a Ni/**L38**-catalyzed asymmetric cross-coupling of  $\alpha$ -bromoketones and arylzinc reagents (Figure 1.17, a).<sup>38</sup> The low basicity of the organozinc reagent, as well as a reduced reaction temperature, accounts for the configurational stability of the potentially sensitive tertiary stereocenter in **30**. The synthesis of dialkyl ketones proceeded with lower enantioinduction; however, this substrate limitation is addressed by their subsequently developed Kumada–Corriu conditions.<sup>37</sup> A recent modification of the reaction conditions

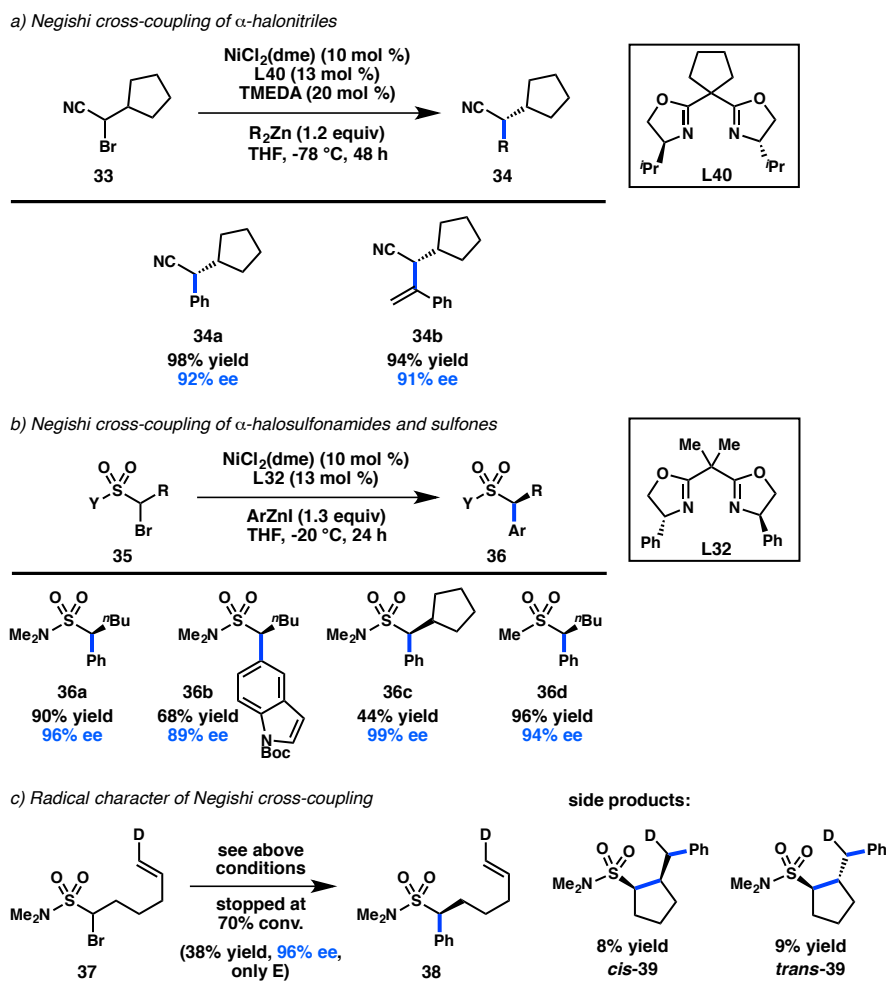
has permitted the use of  $\alpha$ -halo- $\alpha$ -fluoroketones **31**, enabling the asymmetric formation of tertiary fluorides **32** (**Figure 1.17, b**).<sup>48</sup>

**Figure 1.17.** Asymmetric Negishi cross-coupling of  $\alpha$ -halo ketones.



The Fu group has further expanded the scope of alkyl electrophiles amenable to Ni-catalyzed stereoconvergent Negishi cross-coupling to include  $\alpha$ -bromonitriles.<sup>49</sup> Coupling of  $\alpha$ -bromonitrile **33** and  $\text{R}_2\text{Zn}$  in the presence of  $\text{NiCl}_2(\text{dme})$  and **L40** at  $-78\text{ }^\circ\text{C}$  furnishes **34** in high yield and ee (**Figure 1.18, a**).<sup>50</sup> For the first time, alkenylzinc reagents were suitable coupling partners, delivering **34b** in 94% yield and 91% ee. Somewhat unexpectedly, a variant of **34** containing a pendant alkene failed to cyclize under the reaction conditions, in contrast to what was observed in the related coupling of simple unactivated halide electrophiles.<sup>51</sup> A more comprehensive mechanistic analysis is thus required to elucidate the mechanism of oxidative addition for the given transformation.

**Figure 1.18.** Other directing groups in asymmetric Ni-catalyzed Negishi cross-coupling.



The previous examples of Ni-catalyzed stereoconvergent Negishi cross-coupling reactions from the Fu laboratory have focused on the use of activated secondary electrophiles; in 2014, they reported the coupling between  $\alpha$ -halosulfonamides (**35**) and arylzinc reagents (**Figure 1.18, b**).<sup>52</sup> Since sulfonyl groups do not significantly stabilize  $\alpha$ -radicals, **35** can be considered as an unactivated electrophile. Investigations of the substrate scope revealed that sulfones are also suitable substrates without any change in the reaction conditions, furnishing **36d** in high yield and ee. Subjection of radical clock

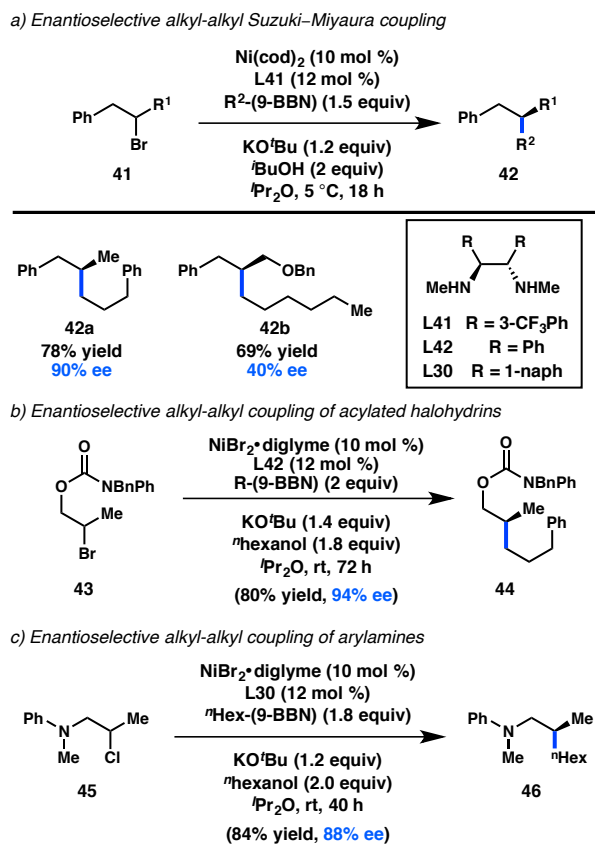
substrate **37** to the reaction conditions provided a mixture of **38**, *cis*-**39** and *trans*-**39**; the ratio of uncyclized product to cyclized product was found to increase linearly with increased Ni loading (**Figure 1.18, c**). These data could suggest that the reaction proceeds through a noncaged radical species, and also illustrates the dichotomy between the coupling of electrophiles **33** and **35**.

### 1.3.3 With Organoboron Reagents

Seminal contributions to the transition metal-catalyzed enantioselective cross-coupling of *sec*-alkyl electrophiles with organoboron reagents have been made by the Fu laboratory. Shortly after disclosing the Ni-catalyzed cross-coupling of *sec*-alkyl electrophiles with alkylboranes to prepare racemic products,<sup>53</sup> Fu and coworkers reported that use of catalytic Ni(cod)<sub>2</sub> in conjunction with chiral 1,2-diamine ligand **L41** enabled the enantioselective coupling of homobenzylic bromides (**41**) with organoboranes (**Figure 1.19, a**).<sup>54</sup> The Ni catalyst was proposed to engage in a secondary interaction with the benzylic substituent on **41**, allowing for differentiation between the two alkyl groups of the starting material. While a variety of homobenzylic bromides were tolerated, poor enantioselectivity was attained in the formation of **42b**. Fu hypothesized that the ether might also interact with the Ni catalyst, leading to poor asymmetric induction. Based on this hypothesis, the group subsequently reported that carbamate-protected halohydrins (**43**) can also be coupled with alkylboranes in high enantioselectivity using a chiral 1,2-diamine **L42** (**Figure 1.19, b**).<sup>55</sup> Modified conditions permitted the enantioselective coupling of a homologated halohydrin. Further expansion of the substrate scope determined that halides (**45**) bearing proximal arylamines as directing groups can be

coupled with alkylboranes in high enantioselectivity as well (**Figure 1.19, c**).<sup>56</sup> The reaction was found to be directed by the nitrogen atom of the arylamine group.

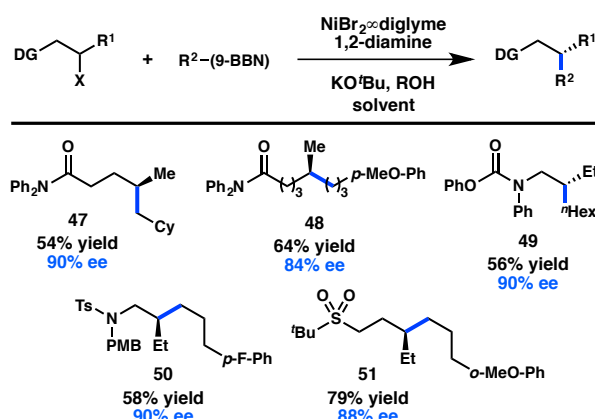
**Figure 1.19.** Enantioconvergent Ni-catalyzed alkyl-alkyl Suzuki–Miyaura coupling.



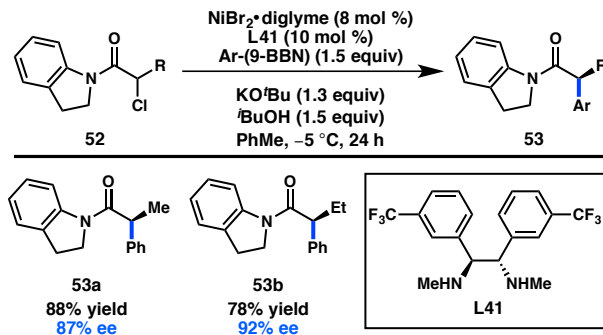
The early examples of enantioconvergent alkyl-alkyl Suzuki–Miyaura couplings all involved alkyl halide substrates with a directing group capable of coordinating the Ni center. Subsequent efforts turned to identifying new directing groups and to exploring how far removed the directing group could be from the reacting C–halide bond. Illustrating that distal functional groups are still capable of directing highly enantioselective reactions, both  $\gamma$ - and  $\delta$ -chloroamides were shown to undergo Suzuki–Miyaura cross-coupling with good asymmetric induction to form **47** and **48**, respectively (**Figure 1.20**).<sup>57</sup> Various halides proximal to protected amines, such as carbamates or

sulfonamides, were also optimized toward enantioconvergent cross-coupling.<sup>58</sup> After confirming that the oxygen of the sulfonamide was the key directing atom, Fu and coworkers examined sulfone-containing electrophiles and reported that good enantioselectivity can still be maintained for these substrates.<sup>58a</sup>

**Figure 1.20.** Examples of directing groups for the enantioconvergent Suzuki–Miyaura coupling.

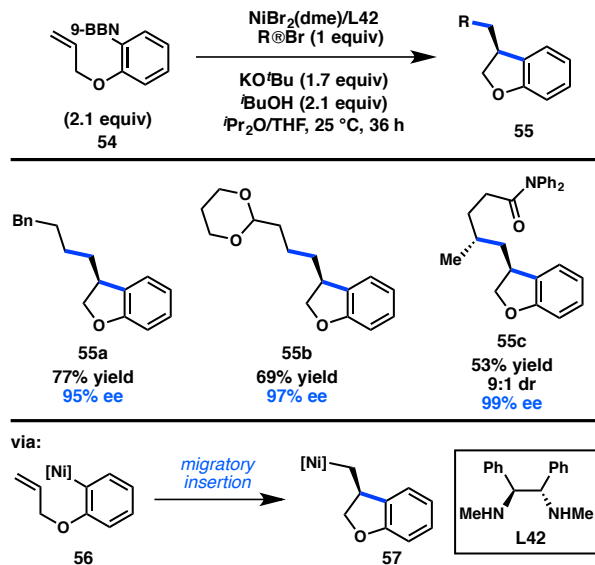


In addition to the Ni-catalyzed cross-coupling of organomagnesium and organozinc reagents to  $\alpha$ -halocarbonyl compounds, the Fu laboratory has identified conditions for the enantioselective coupling between  $\alpha$ -haloamides and arylboron reagents. After first investigating several different amides, it was found that the combination of  $\text{NiBr}_2 \cdot \text{diglyme}$  and **L41** catalyzed the coupling between  $\alpha$ -chloroamides (**52**) and Ar-(9-BBN) reagents to furnish **53** in good yields and high ee's (**Figure 1.21**).<sup>59</sup> The identity of the amide substituents was important for good enantioinduction: diphenyl amides and Weinreb amides delivered nearly racemic products. In contrast to previous stereoconvergent couplings of secondary electrophiles, a modest kinetic resolution of **52** was observed. Further studies confirmed an irreversible oxidative addition step.  $\gamma$ -Haloamides can also be arylated with Ph-(9-BBN) in good ee but only moderate yield.<sup>57</sup>

**Figure 1.21.** Asymmetric Suzuki–Miyaura coupling of  $\alpha$ -haloamides.

Building off their growing mechanistic understanding of Ni-catalyzed stereoconvergent alkyl cross-coupling reactions, Fu and coworkers have developed a cascade cyclization/cross-coupling to forge two C–C bonds in one step with both excellent ee and high dr (**Figure 1.22**).<sup>60</sup> Key to this transformation was the insight that a “transmetalation first” mechanism could be operative, and that organonickel complex **56** might undergo migratory insertion faster than oxidative addition of the alkyl halide electrophile. This theory was validated in the Ni-catalyzed asymmetric cascade cyclization/cross-coupling reaction between arylborane **54** and several simple alkyl bromides, in which heterocyclic products **55** were obtained in excellent ee. Realizing the compatibility of their reaction conditions with those previously optimized for coupling of  $\gamma$ -haloamides (see **Figure 1.20**), a  $\gamma$ -haloamide was also used as an electrophile.<sup>57</sup> Remarkably, a single Ni complex controls the stereochemical outcome of two distinct C–C bond forming processes, giving product **55c** in good yield, good dr, and excellent ee.

**Figure 1.22.** Asymmetric cascade cyclization/cross-coupling.



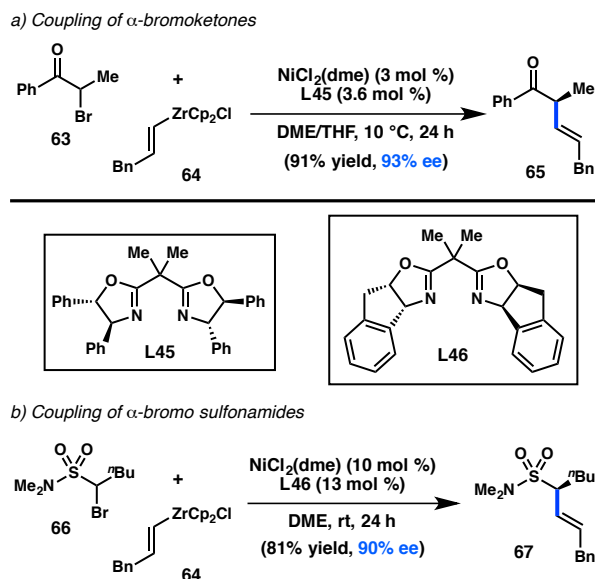
The Doyle laboratory has focused on expanding the scope of electrophiles suitable for transition metal catalysis, investigating the cross-coupling reactions of acetals and *N,O*-acetals. These efforts led to the discovery that  $\text{Ni}(\text{cod})_2$  catalyzes the addition of various aryl boroxines to *N,O*-acetal **58**, presumably via the intermediacy of quinolinium ion **60**.<sup>61</sup> When chiral phosphoramidite **L43** is used as a supporting ligand, **59** is formed in 52% ee (**Figure 1.23**). A unique oxidative addition mechanism, in which the Lewis acidic boroxine promotes ionization of the leaving group and results in an  $\text{S}_{\text{N}}1$ -type addition of  $\text{Ni}^0$ , was discovered for this coupling.<sup>62</sup> A wider survey of ligands showed that improved ee could be realized with TADDOL-based phosphonite **L44**.<sup>63</sup> In an extension, the addition of arylzinc reagents into pyridinium ions was subsequently reported.<sup>64</sup>



### 1.3.5 With Organozirconium Reagents

Alkenylzirconium complexes are attractive vinyl organometallic species for use in organic synthesis because they can be easily prepared from Schwartz's reagent and an alkyne. While Fu has disclosed a remarkable variety of stereoconvergent arylation reactions, most of the reaction conditions could not easily be extended to the cross-coupling of alkenyl metal species, with alkenyl silicon<sup>65</sup> and zinc<sup>50</sup> reagents being the most promising. In 2010, Fu and coworkers published the Ni/L45-catalyzed asymmetric cross-coupling of alkenylzirconium reagents and  $\alpha$ -bromoketones, allowing access to **65** in 93% ee (**Figure 1.25, a**).<sup>66</sup> The versatility of this approach has been exemplified by the efficient coupling of both aryl-alkyl ketones and dialkyl ketones under the same conditions. Alkenylzirconium complexes have also been shown to react with  $\alpha$ -bromosulfonamides **66** in high yield and ee (**Figure 1.25, b**).<sup>52</sup>

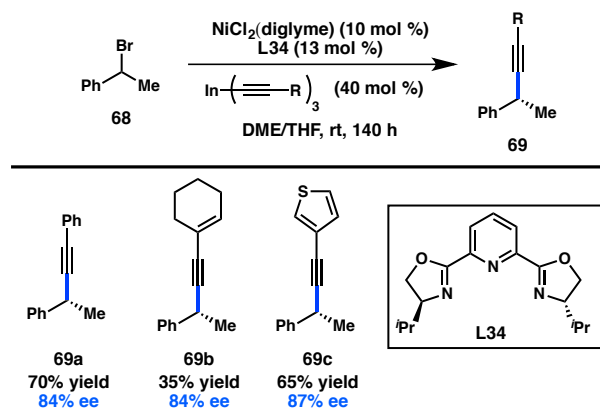
**Figure 1.25.** Stereoconvergent coupling of alkenylzirconium reagents.



### 1.3.6 With Organoindium Reagents

Shortly after the publication of Fu's seminal examples of Ni-catalyzed stereoconvergent cross-coupling reactions between *sec*-alkyl electrophiles and either C(sp<sup>3</sup>)- or C(sp<sup>2</sup>)-hybridized organometallic reagents,<sup>39-40</sup> Sestelo, Sarandeses, and coworkers investigated the asymmetric coupling between C(sp)-hybridized organometallic reagents and benzylic bromides. Alkynylindium reagents exhibited clean cross-coupling under Ni-catalysis, and were selected for further study. Pybox ligand **L34** was optimal, delivering cross-coupled product **69** in up to 87% ee for several different alkynes (Figure 1.26).<sup>67</sup> Further work on the asymmetric coupling of C(sp) organometallic reagents has not been disclosed.

**Figure 1.26.** Alkynyl organometallic reagents in stereoconvergent cross-coupling.

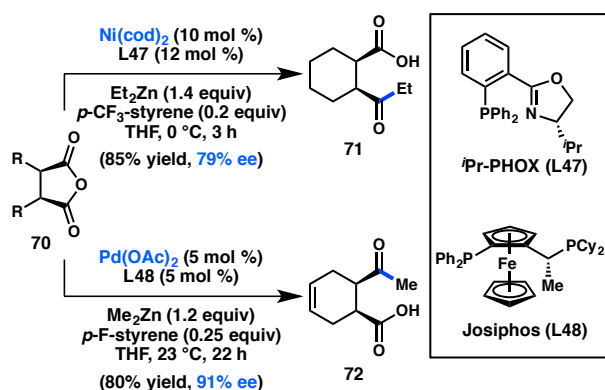


## 1.4 NICKEL-CATALYZED DESYMMETRIZATION REACTIONS

One approach to generating enantioenriched products through transition metal-catalyzed alkyl cross-coupling reactions is to perform desymmetrization reactions of *meso* compounds. In this case, the C(sp<sup>3</sup>)-hybridized carbon at the site of C–C bond formation is not necessarily stereogenic; instead, the C–C bond formation is used to break

symmetry through a catalyst-controlled process, giving rise to a molecule with centrochirality. Most of the work in this area has focused on the desymmetrization of *meso* electrophiles; however, some researchers have investigated the desymmetrization of *meso* bis-organometallic reagents or processes that involve desymmetrization by C-H functionalization.

**Scheme 1.3.** Alkylative desymmetrization of *meso*-anhydrides.

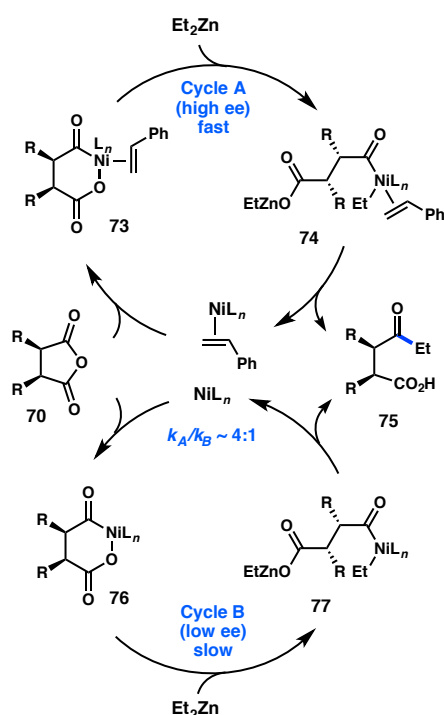


### 1.4.1 Organozinc Reagents

The desymmetrization of *meso*-anhydrides has emerged as a robust method for the synthesis of enantiopure products.<sup>68</sup> Rovis and coworkers<sup>69</sup> have developed a monofunctionalization of cyclic anhydrides through a Ni-catalyzed Negishi coupling with  $\text{Et}_2\text{Zn}$ .<sup>70</sup> The transformation was sensitive to the bite angle of the ligand and required an electron-deficient styrene additive, which has been demonstrated by Knochel to accelerate reductive elimination over  $\beta$ -hydride elimination.<sup>71</sup> Based on these initial findings, the authors sought to develop a desymmetrizing Negishi reaction of *meso*-cyclic anhydride **70**, and determined that the catalyst prepared from  $\text{Ni}(\text{cod})_2$  and *i*Pr-PHOX (**L47**) furnished **71** in 79% ee (**Scheme 1.3**).<sup>72</sup> Surprisingly, omission of the *p*- $\text{CF}_3$ -

styrene additive reduced the ee to 4%, prompting Rovis and coworkers to more closely examine the mechanism of the reaction.

**Figure 1.27.** Competing mechanisms in the Ni-catalyzed desymmetrization of meso-anhydrides.



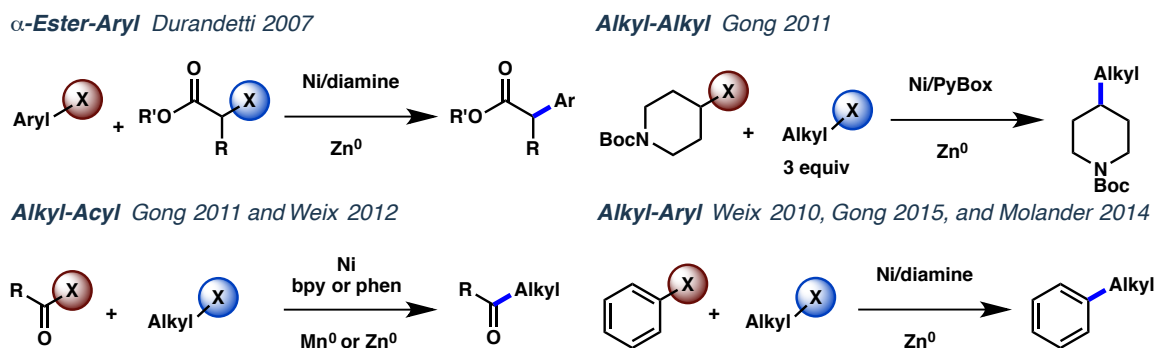
Kinetic analysis of the reaction revealed two competing mechanisms for the formation of **75** (Figure 1.27).<sup>73</sup> One occurred in the absence of styrene and proceeded with low enantioselectivity (cycle B). The other involved coordination of styrene and provided **75** in high ee (cycle A). For both reactions, the rate-determining step was realized to be oxidative addition. However, in contrast to the initial proposal that *p*-CF<sub>3</sub>-styrene would accelerate reductive elimination, it was instead shown to increase the rate of oxidative addition. While the origin of this rate enhancement is unclear, it was hypothesized that *p*-CF<sub>3</sub>-styrene might coordinate to Ni and facilitate deligation of cod, providing a three-coordinate Ni complex capable of undergoing oxidative addition. The

kinetic analysis determined that cycle A proceeds approximately four times faster than cycle B and is roughly consistent with the somewhat modest enantioselectivities obtained under these conditions.

## 1.5 CROSS-ELECTROPHILE COUPLING

The methodologies discussed above are limited to enantioselective cross-couplings of electrophiles (halides and pseudohalides) with organometallic reagents. Indeed, until very recently, all examples of Ni-catalyzed asymmetric cross-coupling fell into this category of redox-neutral transformations. However, our group realized that mechanisms at play in the stereoconvergent redox-neutral couplings described in the previous sections could also be leveraged toward the development of asymmetric reductive cross-couplings between two electrophilic partners. Indeed, recent work by our laboratory has led to the development of cross-electrophile coupling reactions that afford the products in excellent enantioselectivity. These efforts will be the focus of subsequent chapters of this thesis. However a brief introduction to the precedents and mechanistic hypotheses underlying these campaigns will be provided here.

**Scheme 1.4.** Selected examples of Ni-catalyzed reductive cross-couplings.

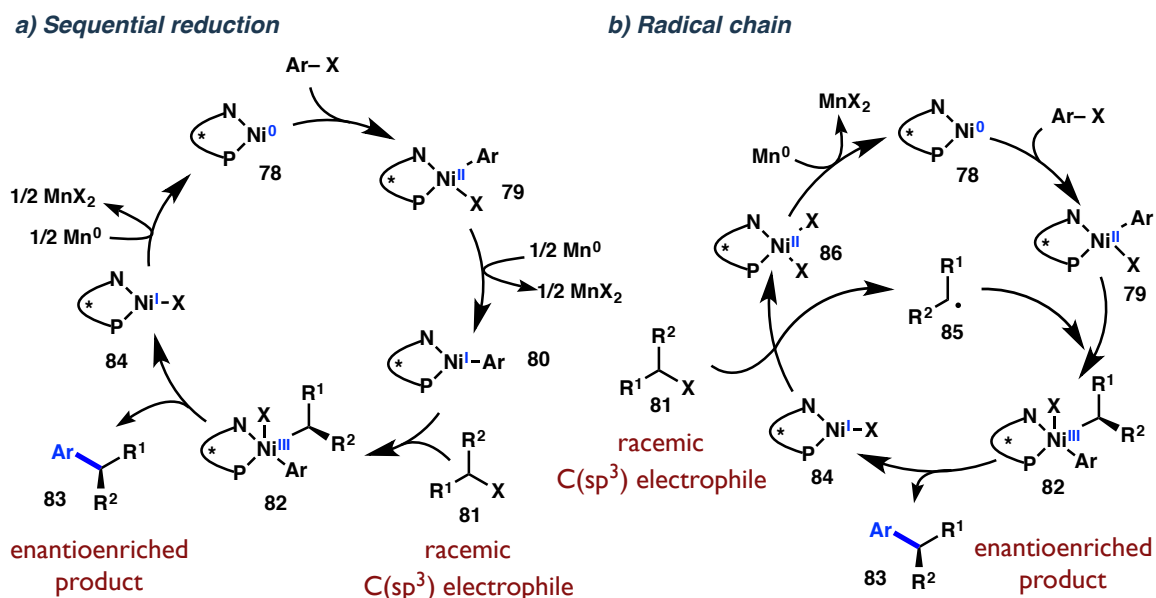


While the first disclosure of Ni-mediated reductive homocoupling of halide electrophiles was by Semmelhack and coworkers in 1971, renewed interest has seen the development of many reductive catalytic cross-couplings over the last ten years.<sup>74</sup> Reductive cross-coupling to form C–C bonds under Ni catalysis and employing chemical reductants debuted in 2007, with a seminal report by Durandetti and coworkers.<sup>75</sup> Employing aryl halides and  $\alpha$ -haloesters, the cross-coupling is effected by a catalytic Ni<sup>II</sup> source and stoichiometric Zn metal. This archetypal transformation has been expounded upon by the Weix, Gong, and Molander labs, with new couplings employing many C(sp<sup>2</sup>) (aryl, vinyl, acyl) and C(sp<sup>3</sup>) (activated and unactivated alkyl) partners (**Scheme 1.4**).<sup>76</sup> These reactions benefit from their exceedingly mild conditions and from the lack of organometallic functionality. As a result, excellent functional group tolerance is routinely observed in these reports, which would be incompatible with conventional organometallic preparations. It is also worth noting that many organometallic reagents are generated from the corresponding halides, in which case reductive cross-coupling offers a shorter, streamlined disconnection.

However a key challenge in the development of reductive cross-couplings, especially in contrast to conventional redox-neutral couplings, is the need to achieve cross-selectivity.<sup>77</sup> Employing two electrophilic partners, some means of differentiation between the partners must be identified in order to avoid a statistical mixture of homo- and cross-coupled products. While a simple solution to this challenge is to manipulate the stoichiometry of the reagents, this does not circumvent the formation of dimers and requires an undesirable excess of one coupling partner.<sup>76c</sup> A preferable means of distinguishing the electrophilic partners relies instead on their hybridization. If differently

hybridized halides can selectively react with different oxidation states of Ni, then a sequencing of oxidative addition events can be envisioned that affords cross-selectivity.

**Scheme 1.5.** Two hypothetical mechanisms for asymmetric reductive cross-couplings (shown with aryl halide as the C(sp<sup>2</sup>) electrophile for clarity).



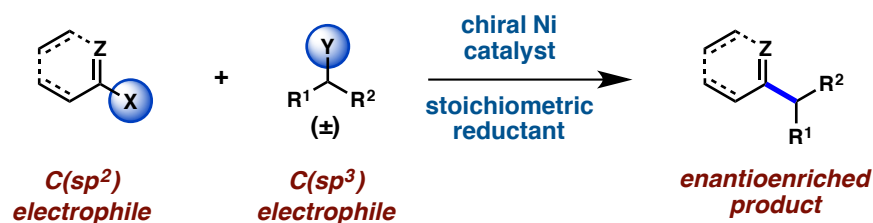
Computational studies and experimental mechanistic investigations by the Weix, Gong, and Reisman groups have led to coalescence about two related mechanistic hypotheses for these transformations (Scheme 1.5).<sup>76a,78</sup> A sequential reduction mechanism can be proposed in which a C(sp<sup>2</sup>) halide undergoes concerted oxidative addition to a Ni<sup>0</sup> center (**78**) (or a primary alkyl halide capable of undergoing an S<sub>N</sub>2-type oxidative addition). Reduction to Ni<sup>I</sup> **80** then facilitates halide abstraction from the C(sp<sup>3</sup>) electrophile (**81**) to generate a solvent-caged alkyl radical. Recombination of this prochiral radical with the Ni<sup>II</sup> center generates a Ni<sup>III</sup> complex (**82**). Reductive elimination then affords the cross-coupled product (**83**) and subsequent reduction of the resulting Ni<sup>I</sup> halide **84** regenerates Ni<sup>0</sup> **80** to reenter the catalytic cycle. If the radical generated by halide abstraction is sufficiently long-lived to escape the solvent cage (**85**),



In either of the pathways described above, it is the single electron processes involved that we hypothesize enable asymmetric Ni-catalyzed reductive cross-couplings. Radical intermediates are planar, prochiral species and have been generated via halide abstraction (as above),<sup>76a</sup> decarboxylation,<sup>81-82</sup> or fragmentation of suitable nucleophiles<sup>83</sup> (**Figure 1.28**). In all of these cases, an appropriate chiral ligand has been shown to successfully direct its combination with a Ni center to afford a thermodynamically preferred diastereomer of the resulting complex that can reductively eliminate the enantioenriched product. In this process, the enantiodetermining step may be radical combination with the Ni<sup>II</sup> center followed by fast reductive elimination. However, if radical combination is reversible, then reductive elimination may be enantiodetermining via a Curtin-Hammett-type mechanism.<sup>84</sup> This stereoconvergent process has been exploited in redox-neutral conventional couplings as described above (Fu), photoredox-enabled couplings (Molander, Kozłowski, MacMillan/Fu),<sup>84-85</sup> and, as detailed in the following chapters, reductive cross-electrophile couplings (Reisman).<sup>86</sup>

## 1.6 CONCLUDING REMARKS

**Figure 1.29.** General disconnection for asymmetric reductive cross-couplings.



The history of asymmetric cross-coupling is rich in examples of stereoselective reactivity being uniquely promoted by Ni and other base metals. Besides being earth-abundant and inexpensive, Ni has the advantage of accessible odd-electron oxidation

states. This enables Ni to perform radical chemistry not easily replicated by Pd or its noble metal cousins, promoting stereoconvergent reactions of C(sp<sup>3</sup>) electrophiles. More recently, a surge of Ni-catalyzed cross-electrophile couplings has been disclosed. These reactions obviate the need for organometallic reagents and occur under uncommonly mild conditions. However the synthesis of these fields remained unknown until the work described herein. We are delighted here to report the successful development of a series of Ni-catalyzed asymmetric reductive cross-couplings (**Figure 1.29**).

## 1.7 NOTES AND REFERENCES

- (1) Cherney, A. H.; Kadunce, N. T.; Reisman, S. E. *Chem. Rev.* **2015**, *115*, 9587.
- (2) (a) Tollefson, E. J.; Hanna, L. E.; Jarvo, E. R. *Acc. Chem. Res.* **2015**, *48*, 2344; (b) Srinivas, H. D.; Zhou, Q.; Watson, M. P. *Org. Lett.* **2014**, *16*, 3596; (c) Shacklady-McAtee, D. M.; Roberts, K. M.; Basch, C. H.; Song, Y. G.; Watson, M. P. *Tetrahedron* **2014**, *70*, 4257; (d) Zhou, Q.; Srinivas, H. D.; Dasgupta, S.; Watson, M. P. *J. Am. Chem. Soc.* **2013**, *135*, 3307; (e) Maity, P.; Shacklady-McAtee, D. M.; Yap, G. P.; Sirianni, E. R.; Watson, M. P. *J. Am. Chem. Soc.* **2013**, *135*, 280.
- (3) Jana, R.; Pathak, T. P.; Sigman, M. S. *Chem. Rev.* **2011**, *111*, 1417.
- (4) Rudolph, A.; Lautens, M. *Angew. Chem., Int. Ed.* **2009**, *48*, 2656.
- (5) (a) Whitesides, G. M.; Roberts, J. D. *J. Am. Chem. Soc.* **1965**, *87*, 4878; (b) Whitesides, G. M.; Witanowski, M.; Roberts, J. D. *J. Am. Chem. Soc.* **1965**, *87*, 2854; (c) Witanowski, M.; Roberts, J. D. *J. Am. Chem. Soc.* **1966**, *88*, 737.
- (6) Hoffmann, R. W.; Hölzer, B.; Knopff, O.; Harms, K. *Angew. Chem., Int. Ed.* **2000**, *39*, 3072.
- (7) (a) Corriu, R. J. P.; Masse, J. P. *J. Chem. Soc., Chem. Commun.* **1972**, 144; (b) Tamao, K.; Sumitani, K.; Kumada, M. *J. Am. Chem. Soc.* **1972**, *94*, 4374; (c) Tamao, K. *J. Organomet. Chem.* **2002**, *653*, 23.
- (8) Hayashi, T. *J. Organomet. Chem.* **2002**, *653*, 41.
- (9) (a) Consiglio, G.; Botteghi, C. *Helv. Chim. Acta* **1973**, *56*, 460; (b) Kiso, Y.; Tamao, K.; Miyake, N.; Yamamoto, K.; Kumada, M. *Tetrahedron Lett.* **1974**, 3.
- (10) Consiglio, G.; Piccolo, O. *J. Organomet. Chem.* **1979**, *177*, C13.
- (11) (a) Consiglio, G.; Morandini, F.; Piccolo, O. *Tetrahedron* **1983**, *39*, 2699; (b) Consiglio, G.; Indolese, A. *J. Organomet. Chem.* **1991**, *417*, C36.
- (12) Iida, A.; Yamashita, M. *Bull. Chem. Soc. Jpn.* **1988**, *61*, 2365.
- (13) Tamao, K.; Yamamoto, H.; Matsumoto, H.; Miyake, N.; Hayashi, T.; Kumada, M. *Tetrahedron Lett.* **1977**, *18*, 1389.
- (14) Brunner, H.; Pröbster, M. *J. Organomet. Chem.* **1981**, *209*, C1.
- (15) (a) Hayashi, T.; Fukushima, M.; Konishi, M.; Kumada, M. *Tetrahedron Lett.* **1980**, *21*, 79; (b) Hayashi, T.; Nagashima, N.; Kumada, M. *Tetrahedron Lett.*

- 1980**, 21, 4623; (c) Hayashi, T.; Konishi, M.; Fukushima, M.; Kanehira, K.; Hioki, T.; Kumada, M. *J. Org. Chem.* **1983**, 48, 2195.
- (16) Baker, K. V.; Brown, J. M.; Cooley, N. A.; Hughes, G. D.; Taylor, R. J. *J. Organomet. Chem.* **1989**, 370, 397.
- (17) (a) Cross, G. A.; Kellogg, R. M. *J. Chem. Soc., Chem. Commun.* **1987**, 1746; (b) Cross, G.; Vriesema, B. K.; Boven, G.; Kellogg, R. M.; van Bolhuis, F. *J. Organomet. Chem.* **1989**, 370, 357.
- (18) (a) Hayashi, T.; Tajika, M.; Tamao, K.; Kumada, M. *J. Am. Chem. Soc.* **1976**, 98, 3718; (b) Tamao, K.; Hayashi, T.; Matsumoto, H.; Yamamoto, H.; Kumada, M. *Tetrahedron Lett.* **1979**, 2155; (c) Hayashi, T.; Konishi, M.; Fukushima, M.; Mise, T.; Kagotani, M.; Tajika, M.; Kumada, M. *J. Am. Chem. Soc.* **1982**, 104, 180; (d) Hayashi, T.; Kumada, M. *Acc. Chem. Res.* **1982**, 15, 395.
- (19) Indolese, A.; Consiglio, G. *J. Organomet. Chem.* **1993**, 463, 23.
- (20) Hayashi, T.; Konishi, M.; Hioki, T.; Kumada, M.; Ratajczak, A.; Niedbala, H. *Bull. Chem. Soc. Jpn.* **1981**, 54, 3615.
- (21) (a) Lemaire, M.; Buter, J.; Vriesema, B. K.; Kellogg, R. M. *J. Chem. Soc., Chem. Commun.* **1984**, 309; (b) Vriesema, B. K.; Lemaire, M.; Buter, J.; Kellogg, R. M. *J. Org. Chem.* **1986**, 51, 5169.
- (22) Brunner, H.; Li, W.; Weber, H. *J. Organomet. Chem.* **1985**, 288, 359.
- (23) Terfort, A.; Brunner, H. *J. Chem. Soc., Perkin Trans. 1* **1996**, 1467.
- (24) Jedlicka, B.; Kratky, C.; Weissensteiner, W.; Widhalm, M. *J. Chem. Soc., Chem. Commun.* **1993**, 1329.
- (25) Pellet-Rostaing, S.; Saluzzo, C.; Halle, R. T.; Breuzard, J.; Vial, L.; Le Guyader, F.; Lemaire, M. *Tetrahedron: Asymmetry* **2001**, 12, 1983.
- (26) (a) Hayashi, M.; Takaoki, K.; Hashimoto, Y.; Saigo, K. *Enantiomer* **1997**, 2, 293; (b) Yamago, S.; Yanagawa, M.; Nakamura, E. *J. Chem. Soc., Chem. Commun.* **1994**, 2093; (c) Yamago, S.; Yanagawa, M.; Mukai, H.; Nakamura, E. *Tetrahedron* **1996**, 52, 5091.
- (27) (a) Kreuzfeld, H. J.; Döbler, C.; Abicht, H. P. *J. Organomet. Chem.* **1987**, 336, 287; (b) Döbler, C.; Kreuzfeld, H. J. *J. Organomet. Chem.* **1988**, 344, 249.
- (28) (a) Horibe, H.; Kazuta, K.; Kotoku, M.; Kondo, K.; Okuno, H.; Murakami, Y.; Aoyama, T. *Synlett* **2003**, 2047; (b) Hideo, H.; Fukuda, Y.; Kondo, K.; Okuno, H.; Murakami, Y.; Aoyama, T. *Tetrahedron* **2004**, 60, 10701.

- (29) (a) Richards, C. J.; Hibbs, D. E.; Hursthouse, M. B. *Tetrahedron Lett.* **1995**, *36*, 3745; (b) Lloyd-Jones, G. C.; Butts, C. P. *Tetrahedron* **1998**, *54*, 901.
- (30) Schwink, L.; Knochel, P. *Chem. Eur. J.* **1998**, *4*, 950.
- (31) Hayashi, T.; Hagihara, T.; Katsuro, Y.; Kumada, M. *Bull. Chem. Soc. Jpn.* **1983**, *56*, 363.
- (32) Campos, K. R.; Klapars, A.; Waldman, J. H.; Dormer, P. G.; Chen, C.-y. *J. Am. Chem. Soc.* **2006**, *128*, 3538.
- (33) Cordier, C. J.; Lundgren, R. J.; Fu, G. C. *J. Am. Chem. Soc.* **2013**, *135*, 10946.
- (34) Tellis, J. C.; Primer, D. N.; Molander, G. A. *Science* **2014**, *345*, 433.
- (35) Zembayashi, M.; Tamao, K.; Hayashi, T.; Mise, T.; Kumada, M. *Tetrahedron Lett.* **1977**, *18*, 1799.
- (36) Binder, J. T.; Cordier, C. J.; Fu, G. C. *J. Am. Chem. Soc.* **2012**, *134*, 17003.
- (37) Lou, S.; Fu, G. C. *J. Am. Chem. Soc.* **2010**, *132*, 1264.
- (38) Lundin, P. M.; Esquivias, J.; Fu, G. C. *Angew. Chem., Int. Ed.* **2009**, *48*, 154.
- (39) Fischer, C.; Fu, G. C. *J. Am. Chem. Soc.* **2005**, *127*, 4594.
- (40) Arp, F. O.; Fu, G. C. *J. Am. Chem. Soc.* **2005**, *127*, 10482.
- (41) Lin, X.; Sun, J.; Xi, Y.; Lin, D. *Organometallics* **2011**, *30*, 3284.
- (42) Smith, S. W.; Fu, G. C. *J. Am. Chem. Soc.* **2008**, *130*, 12645.
- (43) Partridge, B. M.; Chausset-Boissarie, L.; Burns, M.; Pulis, A. P.; Aggarwal, V. K. *Angew. Chem., Int. Ed.* **2012**, *51*, 11795.
- (44) Schley, N. D.; Fu, G. C. *J. Am. Chem. Soc.* **2014**, *136*, 16588.
- (45) Oelke, A. J.; Sun, J.; Fu, G. C. *J. Am. Chem. Soc.* **2012**, *134*, 2966.
- (46) Do, H.-Q.; Chandrashekar, E. R. R.; Fu, G. C. *J. Am. Chem. Soc.* **2013**, *135*, 16288.
- (47) (a) Imao, D.; Glasspoole, B. W.; Laberge, V. S.; Crudden, C. M. *J. Am. Chem. Soc.* **2009**, *131*, 5024; (b) Taylor, B. L. H.; Swift, E. C.; Waetzig, J. D.; Jarvo, E. R. *J. Am. Chem. Soc.* **2011**, *133*, 389; (c) Greene, M. A.; Yonova, I. M.; Williams,

- F. J.; Jarvo, E. R. *Org. Lett.* **2012**, *14*, 4293; (d) Yonova, I. M.; Johnson, A. G.; Osborne, C. A.; Moore, C. E.; Morrisette, N. S.; Jarvo, E. R. *Angew. Chem., Int. Ed.* **2014**, *53*, 2422; (e) Zhou, Q.; Srinivas, H. D.; Dasgupta, S.; Watson, M. P. *J. Am. Chem. Soc.* **2013**, *135*, 3307; (f) Maity, P.; Shacklady-McAtee, D. M.; Yap, G. P. A.; Sirianni, E. R.; Watson, M. P. *J. Am. Chem. Soc.* **2013**, *135*, 280; (g) Shacklady-McAtee, D. M.; Roberts, K. M.; Basch, C. H.; Song, Y.-G.; Watson, M. P. *Tetrahedron* **2014**, *70*, 4257.
- (48) Liang, Y.; Fu, G. C. *J. Am. Chem. Soc.* **2014**, *136*, 5520.
- (49) He, A.; Falck, J. R. *J. Am. Chem. Soc.* **2010**, *132*, 2524.
- (50) Choi, J.; Fu, G. C. *J. Am. Chem. Soc.* **2012**, *134*, 9102.
- (51) (a) Powell, D. A.; Maki, T.; Fu, G. C. *J. Am. Chem. Soc.* **2005**, *127*, 510; (b) Gonzalez-Bobes, F.; Fu, G. C. *J. Am. Chem. Soc.* **2006**, *128*, 5360.
- (52) Choi, J.; Martín-Gago, P.; Fu, G. C. *J. Am. Chem. Soc.* **2014**, *136*, 12161.
- (53) Saito, B.; Fu, G. C. *J. Am. Chem. Soc.* **2007**, *129*, 9602.
- (54) Saito, B.; Fu, G. C. *J. Am. Chem. Soc.* **2008**, *130*, 6694.
- (55) Owston, N. A.; Fu, G. C. *J. Am. Chem. Soc.* **2010**, *132*, 11908.
- (56) Lu, Z.; Wilsily, A.; Fu, G. C. *J. Am. Chem. Soc.* **2011**, *133*, 8154.
- (57) Zultanski, S. L.; Fu, G. C. *J. Am. Chem. Soc.* **2011**, *133*, 15362.
- (58) (a) Wilsily, A.; Tramutola, F.; Owston, N. A.; Fu, G. C. *J. Am. Chem. Soc.* **2012**, *134*, 5794; (b) Jiang, X.; Sakthivel, S.; Kulbitski, K.; Nisnevich, G.; Gandelman, M. *J. Am. Chem. Soc.* **2014**, *136*, 9548.
- (59) Lundin, P. M.; Fu, G. C. *J. Am. Chem. Soc.* **2010**, *132*, 11027.
- (60) Cong, H.; Fu, G. C. *J. Am. Chem. Soc.* **2014**, *136*, 3788.
- (61) Graham, T. J. A.; Shields, J. D.; Doyle, A. G. *Chem. Sci.* **2011**, *2*, 980.
- (62) Sylvester, K. T.; Wu, K.; Doyle, A. G. *J. Am. Chem. Soc.* **2012**, *134*, 16967.
- (63) Shields, J. D.; Ahneman, D. T.; Graham, T. J. A.; Doyle, A. G. *Org. Lett.* **2014**, *16*, 142.
- (64) Chau, S. T.; Lutz, J. P.; Wu, K.; Doyle, A. G. *Angew. Chem., Int. Ed.* **2013**, *52*, 9153.

- (65) Dai, X.; Strotman, N. A.; Fu, G. C. *J. Am. Chem. Soc.* **2008**, *130*, 3302.
- (66) Lou, S.; Fu, G. C. *J. Am. Chem. Soc.* **2010**, *132*, 5010.
- (67) Caeiro, J.; Pérez Sestelo, J.; Sarandeses, L. A. *Chem. Eur. J.* **2008**, *14*, 741.
- (68) (a) Willis, M. C. *J. Chem. Soc., Perkin Trans. 1* **1999**, 1765; (b) Chen, Y.; McDaid, P.; Deng, L. *Chem. Rev.* **2003**, *103*, 2965; (c) Díaz de Villegas, M. D.; Gálvez, J. A.; Etayo, P.; Badorrey, R.; López-Ram-de-Víu, P. *Chem. Soc. Rev.* **2011**, *40*, 5564.
- (69) Johnson, J. B.; Rovis, T. *Acc. Chem. Res.* **2008**, *41*, 327.
- (70) Bercot, E. A.; Rovis, T. *J. Am. Chem. Soc.* **2005**, *127*, 247.
- (71) (a) Giovannini, R.; Stüdemann, T.; Dussin, G.; Knochel, P. *Angew. Chem., Int. Ed.* **1998**, *37*, 2387; (b) Giovannini, R.; Stüdemann, T.; Devasagayaraj, A.; Dussin, G.; Knochel, P. *J. Org. Chem.* **1999**, *64*, 3544.
- (72) Bercot, E. A.; Rovis, T. *J. Am. Chem. Soc.* **2002**, *124*, 174.
- (73) Johnson, J. B.; Bercot, E. A.; Rowley, J. M.; Coates, G. W.; Rovis, T. *J. Am. Chem. Soc.* **2007**, *129*, 2718.
- (74) Semmelhack, M. F.; Helquist, P. M.; Jones, L. D. *J. Am. Chem. Soc.* **1971**, *93*, 5908.
- (75) Durandetti, M.; Gosmini, C.; Périchon, J. *Tetrahedron* **2007**, *63*, 1146.
- (76) (a) Weix, D. J. *Acc. Chem. Res.* **2015**, *48*, 1767; (b) Knappke, C. E.; Grupe, S.; Gartner, D.; Corpet, M.; Gosmini, C.; Jacobi von Wangelin, A. *Chem. Eur. J.* **2014**, *20*, 6828; (c) Gu, J.; Wang, X.; Xue, W.; Gong, H. *Org. Chem. Front.* **2015**, *2*, 1411.
- (77) (a) Everson, D. A.; Jones, B. A.; Weix, D. J. *J. Am. Chem. Soc.* **2012**, *134*, 6146; (b) Everson, D. A.; Weix, D. J. *J. Org. Chem.* **2014**, *79*, 4793.
- (78) Ren, Q.; Jiang, F.; Gong, H. *J. Organomet. Chem.* **2014**, *770*, 130.
- (79) Biswas, S.; Weix, D. J. *J. Am. Chem. Soc.* **2013**, *135*, 16192.
- (80) (a) Jones, G. D.; Martin, J. L.; McFarland, C.; Allen, O. R.; Hall, R. E.; Haley, A. D.; Brandon, R. J.; Konovalova, T.; Desrochers, P. J.; Pulay, P.; Vivic, D. A. *J. Am. Chem. Soc.* **2006**, *128*, 13175; (b) Anderson, T. J.; Jones, G. D.; Vivic, D. A. *J. Am. Chem. Soc.* **2004**, *126*, 8100.

- (81) (a) Cornella, J.; Edwards, J. T.; Qin, T.; Kawamura, S.; Wang, J.; Pan, C. M.; Gianatassio, R.; Schmidt, M.; Eastgate, M. D.; Baran, P. S. *J. Am. Chem. Soc.* **2016**; (b) Qin, T.; Cornella, J.; Li, C.; Malins, L. R.; Edwards, J. T.; Kawamura, S.; Maxwell, B. D.; Eastgate, M. D.; Baran, P. S. *Science* **2016**.
- (82) Zuo, Z.; Ahneman, D. T.; Chu, L.; Terrett, J. A.; Doyle, A. G.; MacMillan, D. W. *Science* **2014**, *345*, 437.
- (83) (a) Tellis, J. C.; Primer, D. N.; Molander, G. A. *Science* **2014**, *345*, 433; (b) Primer, D. N.; Karakaya, I.; Tellis, J. C.; Molander, G. A. *J. Am. Chem. Soc.* **2015**, *137*, 2195; (c) Jouffroy, M.; Primer, D. N.; Molander, G. A. *J. Am. Chem. Soc.* **2016**, *138*, 475.
- (84) Gutierrez, O.; Tellis, J. C.; Primer, D. N.; Molander, G. A.; Kozlowski, M. C. *J. Am. Chem. Soc.* **2015**, *137*, 4896.
- (85) Zuo, Z.; Cong, H.; Li, W.; Choi, J.; Fu, G. C.; MacMillan, D. W. *J. Am. Chem. Soc.* **2016**, *138*, 1832.
- (86) (a) Cherney, A. H.; Kadunce, N. T.; Reisman, S. E. *J. Am. Chem. Soc.* **2013**, *135*, 7442; (b) Cherney, A. H.; Reisman, S. E. *J. Am. Chem. Soc.* **2014**, *136*, 14365; (c) Kadunce, N. T.; Reisman, S. E. *J. Am. Chem. Soc.* **2015**, *137*, 10480.

## Chapter 2

### *Catalytic Asymmetric Reductive Acyl Cross-Coupling: Synthesis of Enantioenriched Acyclic $\alpha,\alpha$ -Disubstituted Ketones<sup>o</sup>*

#### 2.1. INTRODUCTION

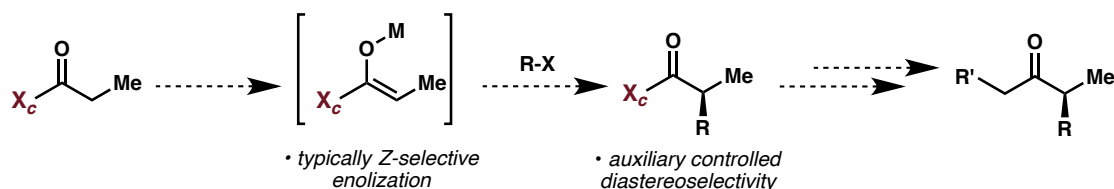
Enantioenriched  $\alpha,\alpha$ -disubstituted carbonyl compounds are versatile intermediates in the synthesis of natural products and pharmaceuticals. As such, their preparation has received ample attention from the organic chemistry community, leading to the development of a rich palette of transformations. With respect to acyclic systems, these largely fall into two categories: the chiral-auxiliary directed  $\alpha$ -functionalization of amides,<sup>1</sup> and the more recently-developed direct  $\alpha$ -functionalization of carbonyl compounds,<sup>2</sup> frequently via organocatalysis.

---

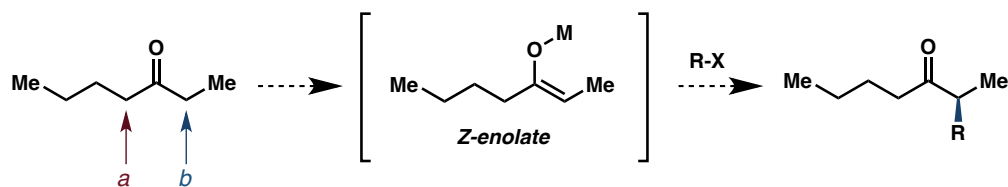
<sup>o</sup> Portions of this chapter have been reproduced from published studies (see reference **16**) and the supporting information found therein. The research presented in this chapter was completed in collaboration with Alan H. Cherney, Ph.D., then a graduate student in the Reisman group.

A significant majority of these methods, especially those most widely employed in synthesis, proceed via enolate intermediates. Chiral auxiliaries enable the diastereoselective alkylation of an enolate by controlling the facial selectivity of electrophile approach (**Scheme 2.1**). These methods offer a well-established and robust route to stereogenic carbonyl compounds. However they also require synthetic manipulations to append and cleave the auxiliary. Moreover, ketone products in particular require additional transformations to access following the alkylation event. While organocatalytic methodologies obviate the need to append and cleave auxiliaries, these methods suffer from similar issues of elaboration to ketone products. Neither of these well-established methods provides a direct route to  $\alpha$ -stereogenic acyclic ketone products.

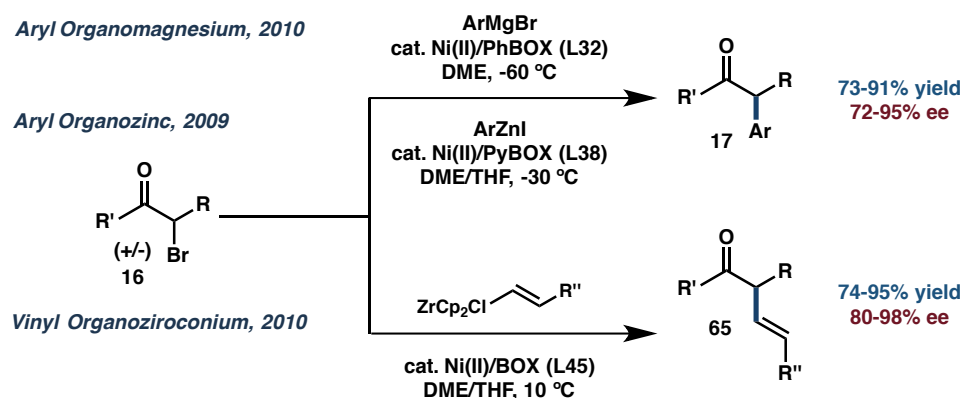
**Scheme 2.1.** Chiral auxiliary-directed alkylation methodologies.



An ideal solution relying on these principles would be the enantioselective alkylation of an acyclic ketone-derived enolate. To obtain a single desired product from such a route would require i) the regioselective generation of the correct enolate (site a vs. b), ii) the stereoselective generation of the *E* or *Z* enolate, and iii) the facially-selective approach of the electrophile (**Scheme 2.2**). Finally, all of this must be accomplished while avoiding racemization of the ketone product under the reaction conditions. While this has been demonstrated in some cyclic systems (eliminating the *E/Z* control requirement), no such method exists for the alkylation of acyclic ketones.

**Scheme 2.2.** Elements of control in ketone enolate alkylation.

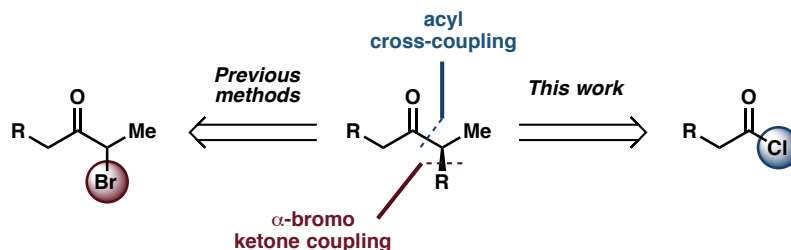
Metal-catalyzed, asymmetric cross-coupling has recently emerged as a viable strategy to access  $\alpha,\alpha$ -disubstituted enantioenriched ketones. While Pd-catalyzed  $\alpha$ -allylations have been known for some time,<sup>3</sup> the only catalytic asymmetric methods for broader  $\alpha$ -functionalization of acyclic ketones currently available are the Ni-catalyzed reactions developed by Fu and coworkers. These transformations involve the cross-coupling of  $\alpha$ -bromoketones (**16**) with vinylzirconium reagents, aryl Grignard reagents, and aryl organozinc reagents (**Scheme 2.3**).<sup>4</sup> This technology represents a major practical and strategic advance in the stereoselective preparation of  $\alpha$ -acyl tertiary centers. However these methods still require the preparation of unsymmetrical  $\alpha$ -bromoketones, sometimes a nontrivial synthetic operation.

**Scheme 2.3.** Fu's catalytic asymmetric ketone  $\alpha$ -functionalizations.

In considering a solution to this problem, we envisioned an alternative disconnection: acyl-alkyl cross-coupling (**Figure 2.1**).<sup>5</sup> This approach avoids the

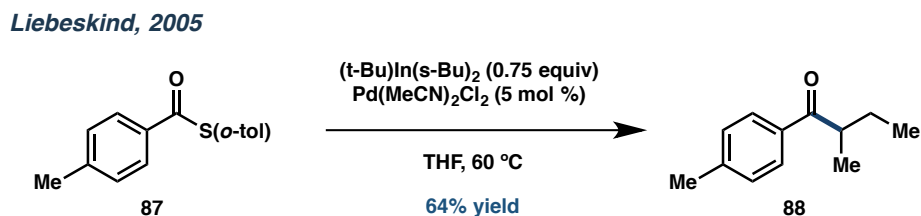
difficulties innate to enolate intermediates and resolves the issue of differentiating the  $\alpha$ -positions of a ketone substrate before or during the reaction.

**Figure 2.1.** Cross-coupling disconnections to access chiral  $\alpha$ -tertiary ketones.



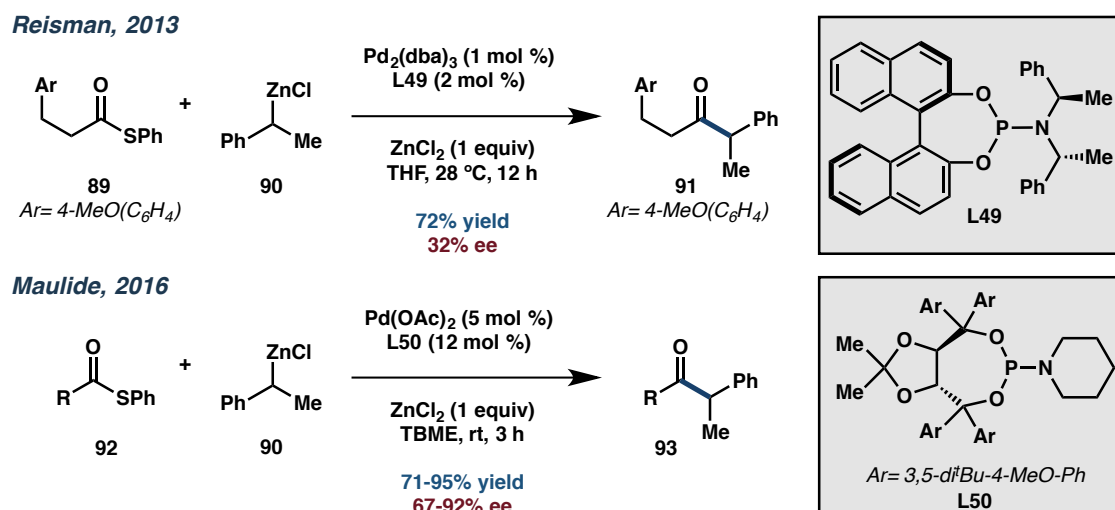
At the time of our research in this area, acyl cross-coupling reactions using secondary organometallic reagents were preceded using only simple nucleophiles.<sup>6</sup> While a variety of acyl electrophiles had been utilized, including carboxylates, thioesters, acyl halides, and anhydrides, only one example had been reported in which the secondary organometallic partner was non-symmetrical.<sup>7</sup> Liebeskind and coworkers reported the selective transfer of a *sec*-butyl group from  $(t\text{-Bu})(s\text{-Bu})_2\text{In}$  via Pd catalysis to form ketone **88** (Scheme 2.4). This dearth of examples reflects the challenge of coupling secondary organometallic reagents. These substrates are prone to  $\beta$ -hydride elimination and rearrangement, leading to a mixture of products. They are also frequently pyrophoric and unstable to long-term storage, making the development of methodology that avoids preformed organometallics a desirable aim.

**Scheme 2.4.** Acyl cross-coupling of unsymmetrical nucleophile.



At this juncture, it is important to note that following the publication of the work described here, two cross-coupling methods employing acyl electrophiles and unsymmetrical secondary organozinc reagents were reported (**Scheme 2.5**). The first, describing earlier work in our laboratory to access this class of products, achieves only a modest 32% ee with the optimal substrate, but affords a wider range of racemic  $\alpha$ -tertiary ketones in good to excellent yields.<sup>8</sup> The second, reported in 2016 by the Maulide group, achieves excellent enantioselectivities but employs only one organozinc substrate (**90**), significantly limiting the accessible range of products.<sup>9</sup> These efforts further illustrate the difficulty of cross-coupling secondary organozinc reagents to access highly enantioenriched ketone products.

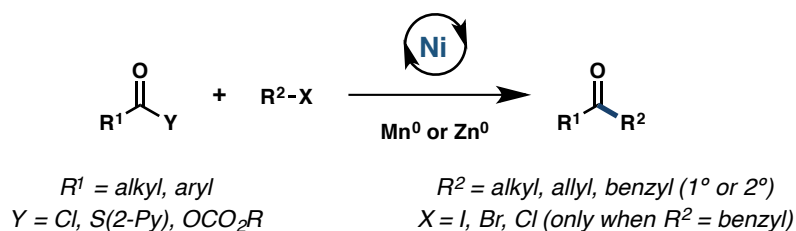
**Scheme 2.5.** Asymmetric Negishi couplings of acyl electrophiles.



With the challenges encountered in the development of asymmetric Fukuyama-type cross-coupling in mind, we turned to recent reports of nickel-catalyzed reductive cross-coupling (see **Chapter 1**). These methodologies couple two electrophiles in the presence of a stoichiometric reductant to turn over the Ni catalyst, obviating the need for organometallic reagents.<sup>10</sup> Specifically, Weix and Gong have reported the racemic

reductive cross-coupling of acyl electrophiles, as shown in **Scheme 2.6**.<sup>11</sup> These reactions show excellent functional-group tolerance due to their mild conditions and demonstrate the feasibility of employing hindered unsymmetrical secondary alkyl electrophiles in cross-coupling to afford ketone products. The absence of base in these reactions is particularly encouraging for asymmetric catalysis, as it minimizes risk of epimerization of the ketone products.

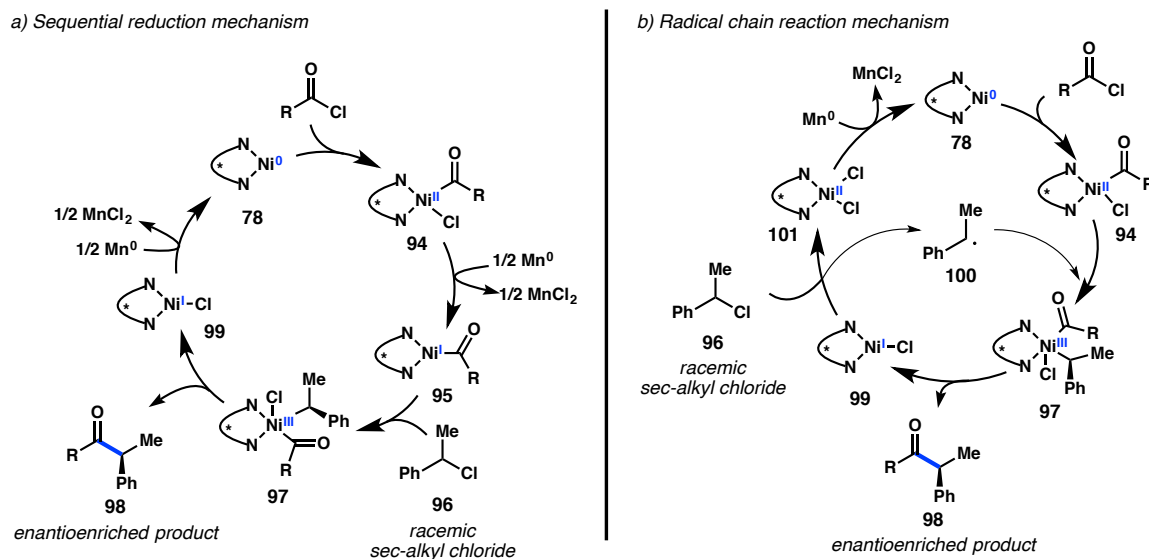
**Scheme 2.6.** Racemic Reductive Cross-Coupling of Acyl Electrophiles.



Although several mechanisms have been proposed for these reactions, two limiting cases will be considered here.<sup>12</sup> First, in a sequential reduction mechanism, concerted oxidative addition of the acyl chloride to Ni<sup>0</sup> **78** could generate Ni<sup>II</sup>-acyl complex **94**, which could be reduced by Mn<sup>0</sup> to afford Ni<sup>I</sup>-acyl species **95** (**Figure 2.2**). Single-electron oxidative addition of benzyl chloride **96** via a radical rebound process would then generate Ni<sup>III</sup> complex **97**, converging both enantiomers of **96** to a single diastereomer of **97**. Reductive elimination of ketone **98** from **97** followed by reduction of Ni<sup>I</sup>-chloride **99** would close the catalytic cycle. The basis for high cross-selectivity arises from the different rates of oxidative addition of the C(sp<sup>2</sup>) and C(sp<sup>3</sup>)-hybridized electrophiles with Ni<sup>0</sup> and Ni<sup>II</sup>, respectively, while the single-electron reaction of **96** affords an entry to stereoconvergence.<sup>13</sup>

An alternative proposal is a radical chain mechanism, wherein  $\text{Ni}^{\text{II}}$ -acyl complex **94**, formed by reaction of  $\text{Ni}^0$  with an acyl chloride, combines with free benzylic radical **100** to produce  $\text{Ni}^{\text{III}}$  complex **97**. Reductive elimination delivers ketone **98** and  $\text{Ni}^{\text{I}}$ -chloride **99**, which can abstract the benzylic halide from **96**, resulting in chain propagation. Reduction of  $\text{Ni}^{\text{II}}$ -dichloride **101** by  $\text{Mn}^0$  to reform  $\text{Ni}^0$  complex **78** closes the catalytic cycle. The key mechanistic difference between these two proposed cycles is the lifetime of benzylic radical **100**: If **100** recombines with the Ni center that generated it, then the sequential reduction mechanism is operative, whereas if **100** undergoes solvent cage escape to combine with another Ni center, then the radical chain mechanism is operative. Recent studies by Weix and coworkers support a radical chain mechanism for the related reductive coupling of aryl and alkyl halides.<sup>12b</sup>

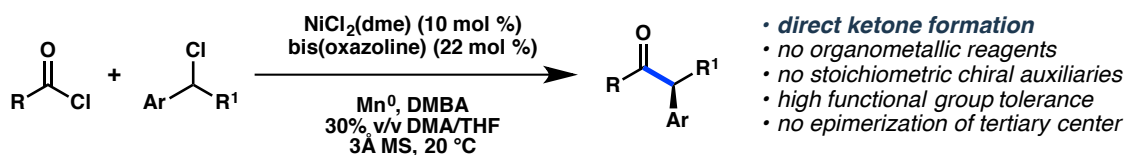
**Figure 2.2.** Two potential mechanisms for Ni-catalyzed reductive cross-coupling.



Regardless of which mechanism is operative under our reaction conditions, we hypothesized that an appropriate chiral catalyst could promote a stereoconvergent cross-coupling of benzyl chloride **96**. Halide abstraction by  $\text{Ni}^{\text{I}}$  in either cycle would generate

the stabilized prochiral radical **100**, facilitating stereoconvergence. Indeed, Fu and coworkers have demonstrated that chiral Ni catalysts can promote stereoconvergent cross-couplings of racemic secondary electrophiles with organometallic reagents under similar reaction conditions.<sup>14</sup> While a stereoconvergent oxidative addition is one possible mechanism of enantioinduction, Molander and Kozlowski have also recently established the feasibility of a stereochemistry-determining reductive elimination.<sup>13b</sup> Based on this mechanistic reasoning, we asked whether the use of a chiral Ni catalyst could enable the stereoconvergent synthesis of enantioenriched  $\alpha,\alpha$ -disubstituted ketones from racemic alkyl halides. Herein we report the successful realization of this strategy, leading to the development of the first enantioselective Ni-catalyzed reductive cross-coupling reaction between halide electrophiles (**Scheme 2.7**).

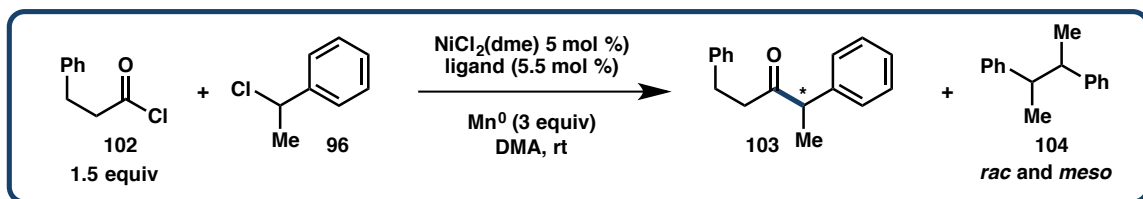
**Scheme 2.7.** *This work: Asymmetric reductive acyl cross-coupling.*



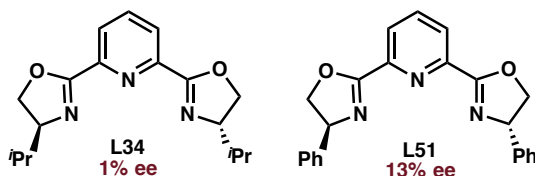
## 2.2 REACTION DEVELOPMENT

We began our study employing the racemic conditions reported by Weix *et al.* (**Figure 6, entry 3**) and conducting a chiral ligand screen. We selected as our model substrates 3-phenylpropionyl chloride (**55**) as the acyl chloride component and (1-chloroethyl)benzene (**96**) as the C(sp<sup>3</sup>) partner. Utilizing 5 mol % NiCl<sub>2</sub>(dme), 3 equivalents of Mn<sup>0</sup> as the terminal reductant, and DMA as solvent, we evaluated a variety of ligand architectures for enantioinduction (**Scheme 2.8**).

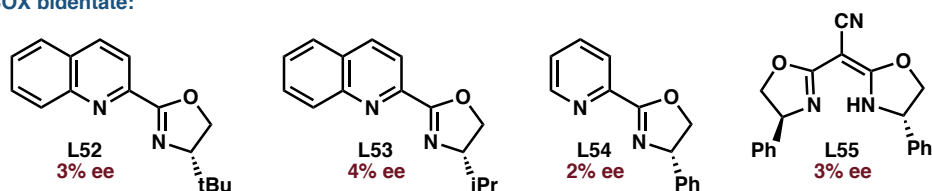
**Scheme 2.8.** Initial evaluation of chiral ligands.



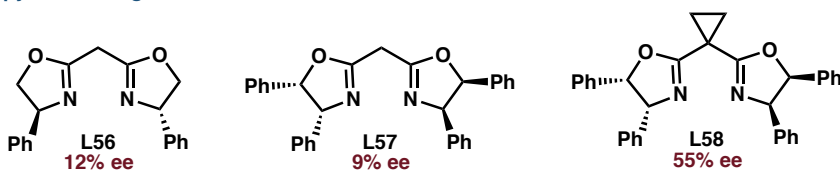
**PyBOX tridentate:**



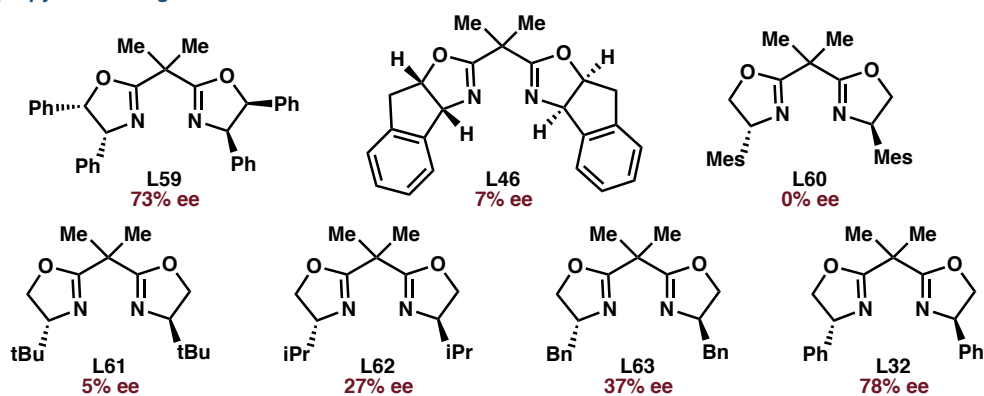
**Non-BOX bidentate:**



**Non-isopropylidene-bridged BOX:**



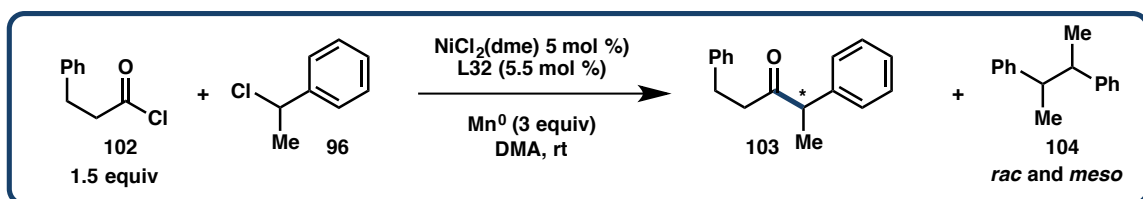
**Isopropylidene-bridged BOX:**



Tridentate PyBOX scaffolds employed in some reductive couplings of alkyl electrophiles were found to give low ee (**L34** and **L51**).<sup>12a</sup> Moving to bidentate ligands, semicorrin (**L55**) and Quin/PyOx ligands (**L52-54**) also gave low enantioinduction. The best ligand family was found to be the bisoxazoline (BOX) ligands, with the

isopropylidene-bridged entries generally giving the highest ee's. Cyclopropylidene (**L58**) and methylenidene bridged (**L56-57**) BOX ligands afforded poor results. We were delighted to find that one ligand, PhBOX (**L32**), afforded **103** in an encouraging 78% ee, but only trace yield. The major product of this reaction was observed to be homocoupling of the benzylic chloride partner to afford bibenzyl **104** as a 1:1 mixture of the *rac* and *meso* compounds (45% yield).

**Table 2.1.** Solvent and reductant screens.



**a) Solvent screen:**

Entry	Solvent	ee (%)
1	DMPU	37
2	DMF	50
3	DMA	66
4	DME	72
5	EtOAc	82
6	THF	92

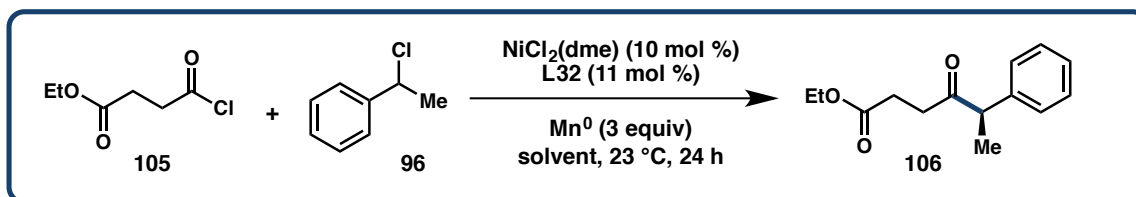
**b) Reductant screen in THF:**

Entry	Reductant	Conversion (%)	Yield (%)	ee (%)
1	Mn <sup>0</sup>	43	19	92
2	Zn <sup>0</sup>	100	10	88
3	Mg <sup>0</sup>	100	trace	20
4	Co <sup>0</sup>	0	0	--
5	Fe <sup>0</sup>	0	0	--
6	CoCp <sub>2</sub>	0	0	--

To address the issue of chemoselectivity as well as enantioselectivity, we began a systematic exploration of the other reaction parameters. Beginning with solvent, we explored a range of polar solvents common to reductive cross-couplings (DMPU and DMF shown, **Table 2.1a**, entries 1 and 2). None of these were found to improve ee or reduce side-product formation. Moving to a broader solvent screen, we noted an improvement in ee with decreasing solvent polarity, with THF affording **103** in 92% ee. However, **103** was still produced in only 19% yield due to poor conversion, with

competitive dimerization of the benzylic partner being the major product (**104**). Other ethereal solvents such as *tert*-butyl methyl ether, cyclopentyl methyl ether, and diethyl ether gave no product and failed to suspend the powdered  $\text{Mn}^0$  throughout the reaction.

At this stage, control experiments run in the absence of Ni showed that Mn could facilitate the homocoupling side-reaction. Therefore, we investigated other terminal reductants that have been employed in reductive cross-coupling, as well as less commonly used entries (selected results shown in **Table 2.1b**). Soluble reductants were sought especially due to the difficulties inherent in maintaining the heterogeneous Mn suspension. These included tetrakis(dimethylamino)ethylene (TDAE), cobaltocene, chromium dichloride, and  $\text{Ru}(\text{bpy})_3/\text{h}\nu$ . Unfortunately none of the homogeneous reductants gave more than trace product in the reaction. Additional heterogeneous reductants screened included zinc, magnesium, gallium, indium, aluminum, and iron. Of all reductants, only Zn was shown to furnish product, albeit in decreased yield (10%) and ee (88%) relative to Mn.

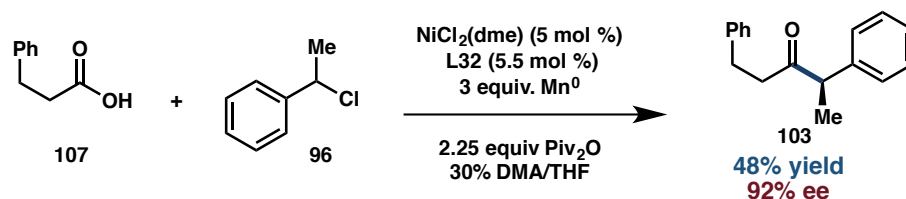
**Table 2.2.** Evaluation of binary solvent conditions.

Entry	Solvent	Conversion (%)	Yield (%)	ee (%)
1	THF	72	24	86
2	10% DMA in THF	45	46	87
3	20% DMA in THF	57	47	87
4	30% DMA in THF	90	62	86
5	40% DMA in THF	87	36	82
6	50% DMA in THF	100	43	74
7	75% DMA in THF	100	52	64
8	DMA	100	59	73

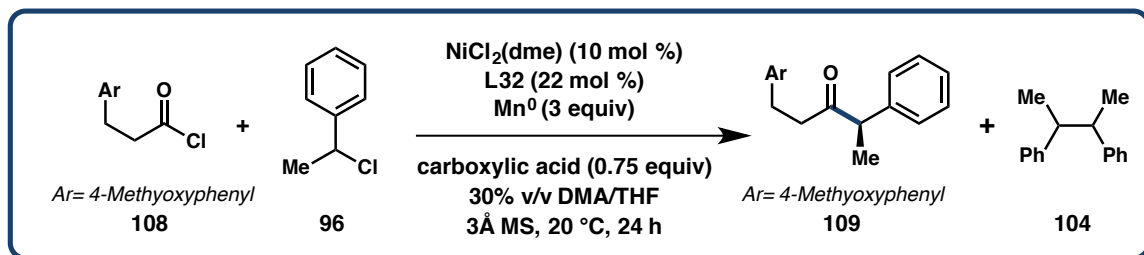
With Mn conclusively identified as the optimal reductant, we returned to investigating the solvent system for this reaction. While DMA and other amide solvents had afforded full conversion of the starting materials, these solvents afforded large amounts of homocoupling and lower enantioselectivity. THF afforded **106** in slightly higher yields and excellent ee, but with sluggish reactivity and lower conversions. This led us to hypothesize that a mixed solvent system may be optimal, with polar amide solvents being critical for reactivity and THF being necessary for good enantioinduction. To evaluate this, screens of amide cosolvents (DMF, DMA, N,N-diethylacetamide and N,N-diisopropylacetamide) in a gradient with THF showed that DMA was the optimal amide, with 30% DMA in THF as the best ratio (**Table 2.2**). This combination afforded 62% yield of **106** while maintaining a high 86% ee. The improved reactivity with DMA may suggest that a higher dielectric solvent is required to achieve optimal rates of

electron transfer events, or it may reflect some solvation of key Ni intermediates and aggregation states.

**Scheme 2.9.** Reductive cross-coupling of anhydride acyl electrophiles.

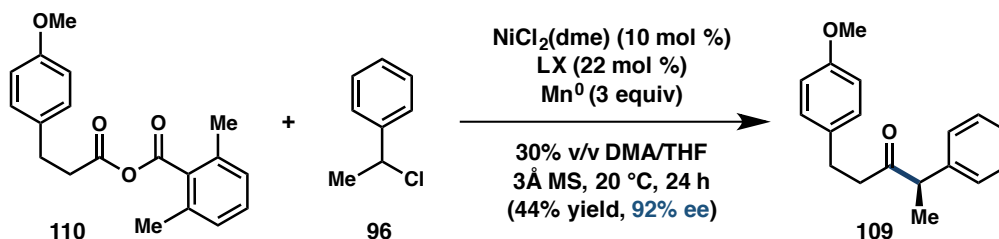


The use of a binary solvent system led to a significantly improved reaction profile, with modest yields and excellent ee. In an effort to further improve yields, we decided to explore other acyl electrophiles positing that a more reactive acyl partner might outcompete side-reactions such as homocoupling. Carboxylic acids have been shown to undergo reductive cross-couplings in the presence of super-stoichiometric amounts of pivalic anhydride via the intermediacy of mixed anhydrides.<sup>15</sup> Therefore, we explored this cross-coupling under analogous conditions, employing hydrocinnamic acid (107), and 2.25 equivalents of pivalic anhydride (Scheme 2.9). A similar result in terms of yield and enantioselectivity was observed with this substrate. However the yield based on recovered starting material was substantially improved and less bibenzyl 104 was formed. While it was unclear what led to this improvement, we hypothesized that the presence of carboxylic acid (either starting material or pivalic acid generated as a byproduct) in these reactions may be responsible for this change in reactivity.

**Table 2.3.** Evaluation of carboxylic acid additives.

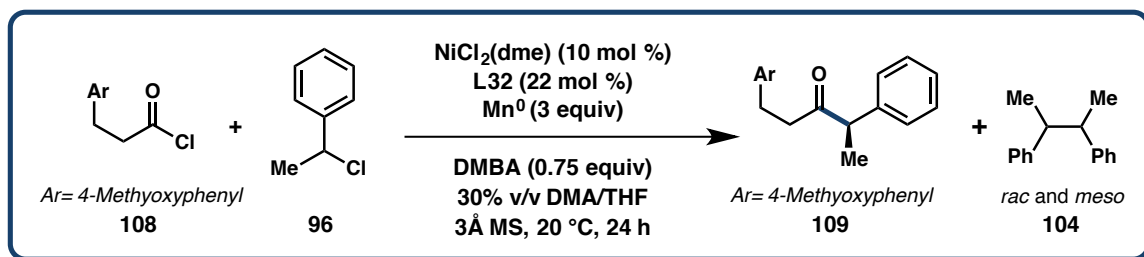
Entry	Acid	Yield <b>104</b> (%)	Yield <b>109</b> (%)	ee <b>109</b> (%)
1	--	22	52	94
2	AcOH	17	65	92
3	BzOH	14	40	92
4	DMBA	4	85	93

A screen of carboxylic acid additives was therefore conducted to evaluate their role in attenuating formation of dimer **104**. As an initial control, 1 equivalent of HCl was added to determine if unselective protonation by the carboxylic acid was solely responsible for the observed effects. This resulted in complete decomposition with no observed product formation. From here we turned our attention to carboxylic acid additives exclusively. It became clear that aryl carboxylic acids were the most effective at inhibiting the homocoupling reaction, with benzoic acid emerging as an early lead. More extensive screening indicated that electron-rich benzoic acids gave the best improvements in reactivity. Of these, 2,6-dimethylbenzoic acid (DMBA) provided the best yields. Further optimization of the reaction concentration, the ligand-to-metal ratio, and addition of 3Å molecular sieves permitted ketone **109** to be obtained in 85% yield and 93% ee, with only a 4% yield of homodimer (**Table 2.3**, entry 4). It was also observed that these additives led to slower rates overall, with the reaction of some substrates stalling at incomplete conversion.

**Scheme 2.10.** Reaction of a preformed mixed DMBA anhydride.

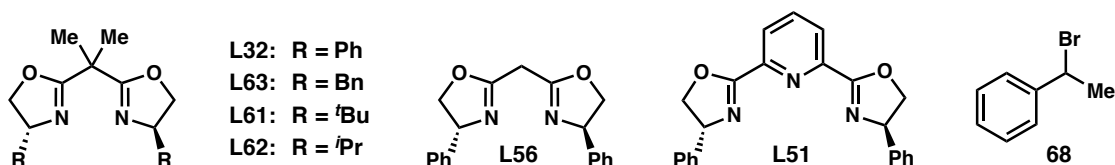
We imagined that a mixed anhydride generated *in situ* from acyl chloride **108** and DMBA may be the active acyl electrophile in this transformation, potentially explaining the change in reaction profile. To explore this, we prepared anhydride **110** and subjected it to the reaction conditions (**Scheme 2.10**). As expected, **110** is a competent electrophile in the reductive cross-coupling. The reaction afforded **109** in identical ee, suggesting that it may intercept the same productive catalytic cycle. However the yield obtained was significantly lower than that observed using exogenous DMBA, indicating that the mixed anhydride is likely not the sole active acyl electrophile.

A mixture of acyl chloride **108** and DMBA under the reaction conditions in the absence of Ni or benzyl chloride does not lead to the formation of **110**, and **110** is not observed during the reaction, leading us to believe the role of DMBA is not simple anhydride formation. Rather, it may coordinate to Ni at some point in the catalytic cycle, altering the relative rates of key steps. It is interesting to note that DMBA exerts the greatest influence over product distribution in neat THF, while it leads to minimal change in neat DMA. This may be explained by DMBA's decreased relative coordination ability in a polar medium, in which it must compete with the amide solvent for coordination of Ni intermediates. However, further investigations are required to determine the role of DMBA in the catalytic reaction.

**Table 2.4.** Control experiments for optimized reaction conditions.

Entry <sup>a</sup>	Deviation from conditions	Conv. 96 <sup>b</sup>	Yield 104 <sup>b</sup>	Yield 109 <sup>b</sup>	ee <sup>c</sup> 109	Entry <sup>a</sup>	Deviation from conditions	Conv. 96 <sup>b</sup>	Yield 104 <sup>b</sup>	Yield 109 <sup>b</sup>	ee <sup>c</sup> 109
1	none	90	4	85	92	12	L63, no L32	61	24	22	45
2	no $\text{Mn}^0$	0	0	0	--	13	L56, no L32	15	1	10	0
3	no $\text{NiCl}_2(\text{dme})$	35	35	0	--	14	L51, no L32	99	53	4	9
4	no L32	73	5	8	--	15	11 mol % L32	82	3	72	92
5	no DMBA	100	22	52	94	16	neat DMA	99	43	30	88
6	No 3 Å MS	100	7	76	90	17	neat THF	25	<1	26	94
7	$\text{Zn}^0$ , no $\text{Mn}^0$	85	26	31	88	18	neat MeCN	28	4	16	45
8	$\text{Ni}(\text{cod})_2$ , no $\text{NiCl}_2(\text{dme})$	98	18	68	92	19	AcOH, no DMBA	96	17	65	92
9	$\text{CoCl}_2$ , no $\text{NiCl}_2(\text{dme})$	73	24	0	--	20	PivOH, no DMBA	97	51	33	92
10	L61, no L32	98	62	14	2	21	BzOH, no DMBA	73	14	40	92
11	L62, no L32	89	52	40	69	22	BnBr 68, no 96	100	42	58	92

<sup>a</sup> Reactions conducted on 0.2 mmol scale under an  $\text{N}_2$  atmosphere in a glovebox. <sup>b</sup> Determined by GC versus an internal standard. <sup>c</sup> Determined by SFC using a chiral stationary phase.



With the conditions described above in hand, we conducted a series of control experiments to confirm the necessity of all the identified reaction components (**Table 2.4**).<sup>16</sup> As expected, Ni and Mn are required for the cross-coupling to proceed (**Entries 2 and 3**). However, Mn alone is capable of mediating homocoupling of the benzylic partner (**Entry 3**). The desired reaction appears to be ligand-dependent, with the ligand free conditions affording significant decomposition (**Entry 4**). 2,6-DMBA provides a

marked decrease in homocoupling, while other acid additives are less effective (**Entry 5 vs. entries 19-21**).  $\text{NiCl}_2(\text{dme})$  was still shown to be the optimal Ni source, although the use of  $\text{Ni}(\text{cod})_2$  instead demonstrates that  $\text{Ni}^0$  is capable of entering the catalytic cycle (**Entry 8**). In contrast,  $\text{CoCl}_2$  gave none of the desired **109** (**Entry 9**). A follow-up ligand screen returned the same results as the initial investigation, with phenyl substitution (**L32**) being optimal and the isopropylidene bridge proving necessary for high ee (**Entries 10-15**). The solvent effects determined in the initial evaluation were unchanged by optimization, with DMA being required for reactivity and THF needed for high enantioinduction (**Entries 16-18**). Finally, the benzylic bromide substrate **68** did not lead to an improvement in reactivity, being more prone to homocoupling and affording a lower yield of **109**, albeit in the same ee (**Entry 22**).

#### **Additional variables explored**

Over the course of the extensive optimization process, many additional variables and additives were studied that did not generate any productive impact on the reaction. However some of these gave insight into the reaction nonetheless; these are summarized below.

**Lewis acid additives:** It was hypothesized that activation of the acid chloride partner via Lewis acid coordination could increase its reactivity relative the benzyl chloride partner, reducing homocoupling. Strong Lewis acids such as  $\text{TiCl}_4$  were found to erode ee and yield while milder ones had no effect.  $\text{LiCl}$  was singularly found to decrease ee to 3% without significantly impacting yield.

**Bases:** The Weix group has noted in some of their reductive cross-coupling methodologies that addition of pyridine leads to increased yields and improved

reproducibility.<sup>17</sup> They postulate that pyridine may act to stabilize Ni<sup>III</sup> intermediates in the catalytic cycle, promoting the desired pathway. To investigate this, coordinating and noncoordinating amine bases as well as inorganic bases were added to the reaction. The addition of K<sub>2</sub>CO<sub>3</sub>, 2,6-di-*t*-Bu-pyridine, pyridine, and DIPEA did not significantly impact the reaction. It is notable that these are tolerated in that they do not lead to racemization of the products or intermediates, nor do they inhibit the reaction via undesirable coordination.

**$\pi$ -Acids:** The addition of  $\pi$ -acids to catalytic cross-coupling reactions has been shown to facilitate reductive elimination, improving turnover and reaction yields in some cases.<sup>18</sup> While there does not appear to be an issue in this step of the desired catalytic cycle, we conducted the simple experiment of adding maleic anhydride as well as *p*-fluorostyrene to the reaction. These additives served only to promote homocoupling, improving turnover of the undesired pathway with no observed increase in cross-coupled yield.

**Halide additives:** The Weix and Reisman groups have noted in some of their reductive cross-coupling methods that the addition of sub-stoichiometric NaI leads to an increase in yield.<sup>19</sup> Suggested explanations for this include assistance in electron transport in the catalyst turnover steps, formation of more reactive alkyl iodides *in situ*, or the formation of nickelate complexes. Therefore we screened the addition of catalytic NaI and TBAI as well as TBAB and TBAC as halide sources. None of these significantly impacted the reaction.

**Metal-surface activators:** Contrary to findings by Durandetti,<sup>20</sup> Weix,<sup>21</sup> and later work by our laboratory (see Chapters 3-5),<sup>22</sup> treatment of the stoichiometric metal reductant

with activating agents such as TMSCl, Brønsted acids, and 1,2-dibromoethane had no effect.

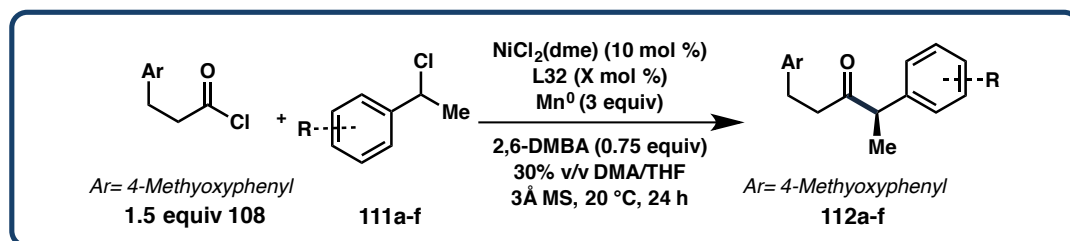
**Nickel sources:** Most Ni<sup>II</sup> sources give yields within 10% of NiCl<sub>2</sub>(dme) (NiCl<sub>2</sub>, NiBr<sub>2</sub>•xH<sub>2</sub>O, Ni(BF<sub>4</sub>)<sub>2</sub>, Ni(acac)<sub>2</sub>, Ni(hfacac)<sub>2</sub>). Ni(cod)<sub>2</sub>, the only Ni<sup>0</sup> source explored, gave a modest yield, identical ee, and increased homocoupling even in the presence of DMBA. Therefore NiCl<sub>2</sub>(dme) was used as the Ni source in all substrate screening.

**Prestir time:** We examined a prestir interval of Ni, ligand, and Mn prior to the addition of substrates. This variable was periodically explored throughout the optimization. Optimized systems showed a decrease in yield with longer prestir time, with no prestir being the optimal condition. We tentatively attribute this effect to catalyst dimerization, with the prestir generating Ni<sup>I</sup> halides that can then dimerize in the absence of reactants. No prestir was used in subsequent substrate evaluation.

## 2.3 SUBSTRATE SCOPE

With optimized conditions in hand, we sought to explore the substrate scope of the reaction with respect to both partners. Beginning with the benzyl chloride component, we examined substitution about the ring as well as the effect of  $\alpha$ -substitution.

**Table 2.5.** Electron-rich benzyl chloride substrate scope.



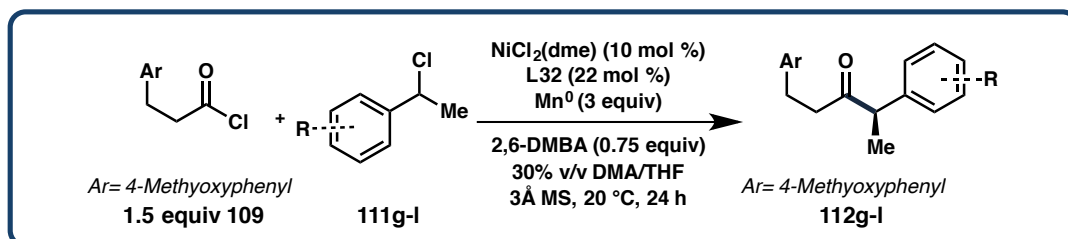
R	Product	L:M	Conversion 111 <sup>a</sup>	Yield 112 <sup>b</sup>	ee 112 <sup>c</sup>
H	112a	2.2: 1	>90	79	93
		3.3: 1	100	80	93
2-Me	112b	2.2: 1	100	35	72
3-Me	112c	2.2: 1	72	51	94
		3.3: 1	81	75	91
4-Me	112d	2.2: 1	77	64	93
		3.3: 1	78	72	93
4-OMe	112e	2.2: 1	69	48	89
		3.3: 1	64	56	86
2-Nap	112f	2.2: 1	74	50	92
		3.3: 1	100	65	91

<sup>a</sup> Determined by GC versus an internal standard. <sup>b</sup> Isolated yield, reactions conducted on 0.2 mmol scale under an N<sub>2</sub> atmosphere in a glovebox. <sup>c</sup> Determined by SFC using a chiral stationary phase.

Electronic perturbations to the benzyl chloride partner were found to exert a significant impact on the reaction. Electron-donating substituents on the phenyl ring generally led to slower reaction rates, with the reactions not reaching full conversion (**Table 2.5**). However the yields and ee's were high for these substrates, with the lowest being for the strongly donating *p*-methoxy substrate (**112e**). Yields for these substrates were found to increase with higher ligand to metal ratios, with 3.3:1 being optimal for all of the substrates. This may simply be the result of the slow reaction rate necessitating

higher ligand loadings to prevent catalyst death over the increased reaction time. *Ortho*-substitution is poorly tolerated (**112b**), leading to only modest ee's and poor yields.

**Table 2.6.** Electron-poor benzyl chloride substrate scope.



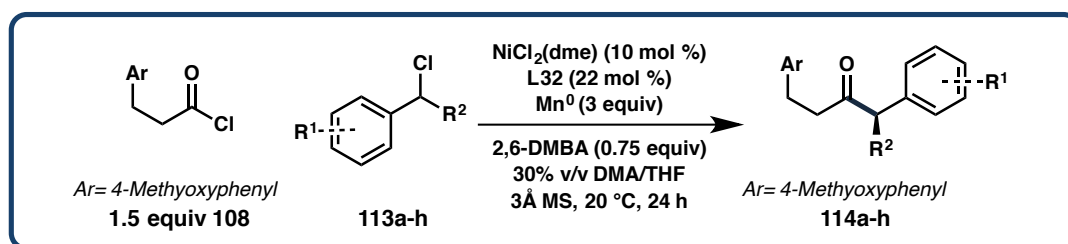
R	Product	Conversion 110 <sup>a</sup>	Yield 112	ee 112 <sup>c</sup>
4-CN	112g	100	44 <sup>a</sup>	66
4-CF <sub>3</sub> <sup>d</sup>	112h	100	64 <sup>b</sup>	82
4-Cl	112i	100	76 <sup>b</sup>	91
4-Br <sup>e</sup>	112j	100	73 <sup>b</sup>	86
4-CO <sub>2</sub> Et	112k	100	25 <sup>a</sup>	70
4-B(pin)	112l	100	52 <sup>a</sup>	74

<sup>a</sup> Determined by GC versus an internal standard. <sup>b</sup> Isolated yield, reactions conducted on 0.2 mmol scale under an  $\text{N}_2$  atmosphere in a glovebox. <sup>c</sup> Determined by SFC using a chiral stationary phase. <sup>d</sup> Run in 20% v/v DMA/THF. <sup>e</sup> Run with 1.25 equiv DMBA.

Substrates bearing electron-withdrawing substituents on the aryl ring behave rather differently, with conversion occurring more quickly and reaching completion in all cases (**Table 2.6**). Additionally, these reactions did not require or benefit from increased ligand loading. At a 2.2: 1 ligand: metal ratio, many of these substrates gave good yields and ee's. However, these numbers began to decline as strongly withdrawing substituents were introduced, with *p*-trifluoromethyl **112h** giving 86% ee and *p*-boronic acid pinacol ester **112l** giving 75% ee. We were pleased to find that the reaction is completely orthogonal to aryl halides, with the *p*-bromo (**111j**) and *p*-chloro (**111i**) substrates coupling chemoselectively. These substrates provide useful handles for further derivatization of the cross-coupled products.

Unfortunately, benzylic halides bearing conjugated electron-withdrawing groups were not well tolerated. The *p*-carboxaldehyde, *p*-acetyl, and ethyl *p*-carboxylate **111k** substrates produced very messy reactions with only trace to low yields of product obtained. Sufficient *p*-acetyl product was isolated, although not cleanly, to obtain an ee value of 60% for this substrate. Finally, benzonitrile substrate **111g** gave only moderate yield and selectivity. We hypothesize that stabilized radical intermediates generated from these substrates may be sufficiently long-lived to escape the solvent cage and participate in side reactions. These non-inner sphere side reactions may generate racemic product, deteriorating ee, while unproductive side reactions would explain the low yields and messy crude spectra obtained for these substrates.

**Table 2.7.**  $\alpha$ -Substituted benzyl chloride substrate scope.



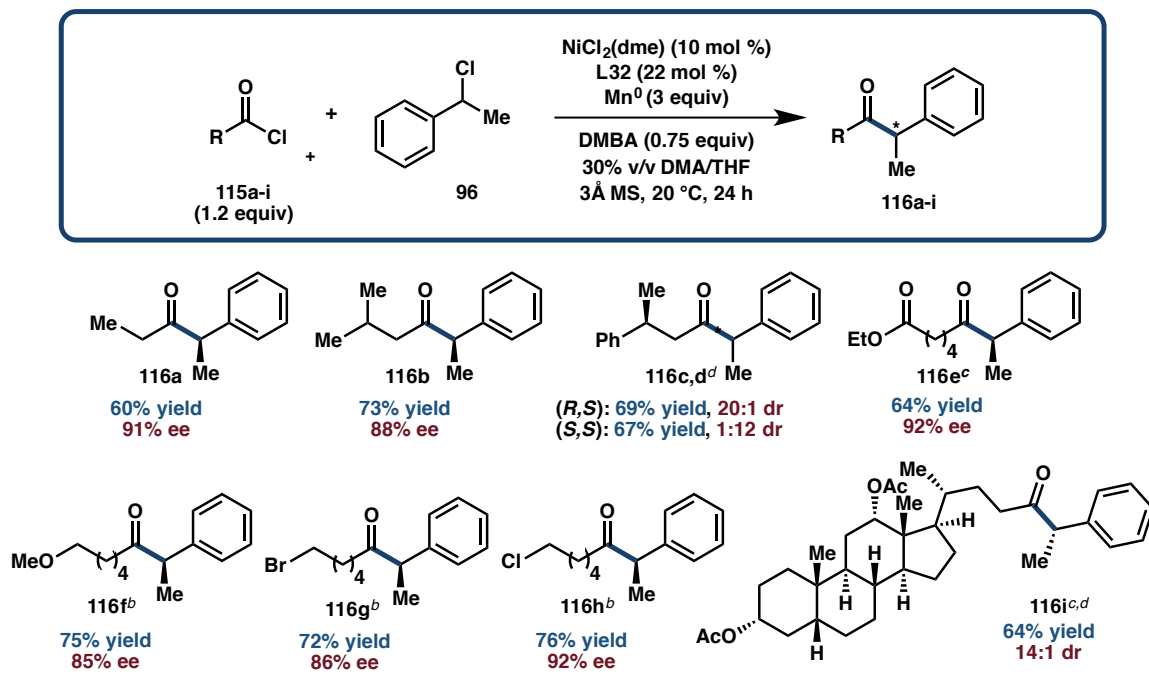
R <sup>1</sup>	R <sup>2</sup>	Product	Conversion 113 <sup>a</sup>	Yield 114 <sup>b</sup>	ee 114 <sup>c</sup>
H	Et	114a	72	50	94
H	Bn	114b	100	79	92
H	CH <sub>2</sub> OTBS	114c <sup>f</sup>	60	51	89
H	<i>i</i> Pr	114d	low	trace <sup>a</sup>	82
H	4-pentenyl	114e	100	38	92
H	CO <sub>2</sub> Ph	114f	65	38 <sup>a</sup>	89
4-Cl	Et	114g	70	65	90
2,3-dihydro-1H-inden-1-yl		114h	100	68	78

<sup>a</sup> Determined by GC versus an internal standard. <sup>b</sup> Isolated yield, reactions conducted on 0.2 mmol scale under an N<sub>2</sub> atmosphere in a glovebox. <sup>c</sup> Determined by SFC using a chiral stationary phase. <sup>d</sup> Run in 50% v/v THF/DMA.

Lastly, substrates bearing substituents at the benzylic  $\alpha$ -position were also shown to cross-couple smoothly, providing the ketone products in good to excellent ee's (**Table**

**2.7**). These substrates generally reacted more slowly and did not reach full conversion. The exception to this is the anomalously well-performing deoxybenzoin-derived substrate **113b**, bearing an  $\alpha$ -benzyl group. Synthetically valuable substrates such as  $\beta$ -silyloxy **113c** and the  $\alpha$ -benzoate-substituted **113f** coupled with high ee and no observed elimination under the reaction conditions. The yield of **114c** was improved further by increasing the DMA loading to 50%, although no benefit was obtained beyond that. Increasing the bulk of the  $\alpha$ -substituent to an isopropyl group (**113d**) was not tolerated, affording only a trace of detectable **114d**. Finally, a cyclic benzylic chloride, the indanyl **113h**, provided the ketone in more modest selectivity but still high yield.

It is worth noting that the reaction was also conducted employing benzylic bromides. The *p*-fluoro-,  $\alpha$ -ethyl-, and unsubstituted model substrates were prepared and explored alongside the chlorides. It was found that while these substrates undergo the cross-coupling with nearly identical enantioselectivity, they afford lower yields of the desired product and undergo homocoupling more readily (see **Table 2.4, entry 22**). Manipulation of DMBA loading and solvent ratio were not found to effectively mitigate this and the benzyl bromides were not pursued further.

**Scheme 2.11.** Acid chloride substrate scope.

<sup>a</sup> Isolated yield, reactions conducted on 0.2 mmol scale under an  $\text{N}_2$  atmosphere in a glovebox. % ee determined by SFC using a chiral stationary phase. <sup>b</sup> Run in 20% v/v DMA/THF. <sup>c</sup> Run in 10% v/v DMA/THF. <sup>d</sup> Run with *ent*-L32.

We then turned our attention to the substrate scope of the acid chloride coupling partner (**115a-i**) (Scheme 2.11). It was quickly determined that increased steric bulk at the  $\alpha$ -carbon resulted in poor reactivity, with cyclohexanecarbonyl chloride and *t*-butylacetyl chloride giving only poor ee's and yields (not shown). Interestingly, aryl chlorides and aryl acetyl chlorides did not afford any cross-coupled products under the reaction conditions. Finally, substrates capable of forming 4- and 5-membered chelates upon oxidative addition to Ni (methoxyacetyl, 3-phenoxyprionyl, and methyl malonyl chloride) were found to be unsuccessful substrates. With these exceptions however, the reaction was found to be functional group- and branching-tolerant. 6-Chloro- (**115h**) and 6-bromohexanoyl chloride (**115g**) behaved well, demonstrating perfect chemoselectivity of the reaction in the presence of unactivated alkyl halides. These, as well as the ester-

containing adipoyl substrate (**115e**), are notable because their products are not directly accessible by chiral auxiliary-directed alkylation followed by Weinreb ketone synthesis. Reaction with either enantiomer of 3-phenylbutyryl chloride (**115c,d**) gave excellent catalyst-controlled diastereoselectivity and good yields. The more highly functionalized steroidal acyl chloride derived from deoxycholic acid (**115i**) also delivered high yields and excellent dr.

## 2.4 CONCLUSION

A new method has been developed for the direct enantioselective preparation of acyclic  $\alpha,\alpha$ -disubstituted ketones. This reaction is the first reported example of a catalytic asymmetric reductive cross-coupling of halide substrates. This approach presents nucleophile-free cross-coupling as a viable alternative to traditional methods of accessing chiral products. It does not require the use of stoichiometric chiral auxiliaries or pregenerated organometallic reagents, marking an advance in both usability and efficiency. The acyl chloride and benzylic chloride substrates are commercially available or easily prepared from carboxylic acids and benzylic alcohols respectively and are bench-stable, enabling the rapid assembly of stereogenic acyclic ketones from accessible materials. The further development and application of this reaction, as well as study of the mechanism, is the focus of ongoing research in our laboratory.

## 2.5 EXPERIMENTAL SECTION

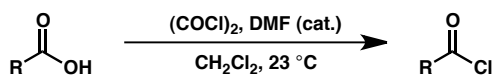
### 2.5.1 Materials and Methods

Unless otherwise stated, reactions were performed under a nitrogen atmosphere using freshly dried solvents. Tetrahydrofuran (THF), methylene chloride ( $\text{CH}_2\text{Cl}_2$ ), and acetonitrile (MeCN) were dried by passing through activated alumina columns. Anhydrous dimethylacetamide (DMA) was purchased from Aldrich and stored under inert atmosphere. Manganese powder (-325 mesh, 99.3%) was purchased from Alfa Aesar. Unless otherwise stated, chemicals and reagents were used as received. All reactions were monitored by thin-layer chromatography using EMD/Merck silica gel 60 F254 pre-coated plates (0.25 mm) and were visualized by UV, *p*-anisaldehyde, or  $\text{KMnO}_4$  staining. Flash column chromatography was performed as described by Still et al. using silica gel (partical size 0.032-0.063) purchased from Silicycle. Optical rotations were measured on a Jasco P-2000 polarimeter using a 100 mm path-length cell at 589 nm.  $^1\text{H}$  and  $^{13}\text{C}$  NMR spectra were recorded on a Varian 400 MR (at 400 MHz and 101 MHz, respectively) or a Varian Inova 500 (at 500 MHz and 126 MHz, respectively), and are reported relative to internal  $\text{CHCl}_3$  ( $^1\text{H}$ ,  $\delta = 7.26$ ) or acetone ( $^1\text{H}$ ,  $\delta = 2.05$ ), and  $\text{CDCl}_3$  ( $^{13}\text{C}$ ,  $\delta = 77.0$ ) or acetone ( $^{13}\text{C}$ ,  $\delta = 29.8$ ). Data for  $^1\text{H}$  NMR spectra are reported as follows: chemical shift ( $\delta$  ppm) (multiplicity, coupling constant (Hz), integration). Multiplicity and qualifier abbreviations are as follows: s = singlet, d = doublet, t = triplet, q = quartet, m = multiplet, br = broad, app = apparent. IR spectra were recorded on a Perkin Elmer Paragon 1000 spectrometer and are reported in frequency of absorption ( $\text{cm}^{-1}$ ). HRMS were acquired using an Agilent 6200 Series TOF with an Agilent G1978A Multimode source in electrospray ionization (ESI) or mixed (MM) ionization mode, or

obtained from the Caltech Mass Spectral Facility in fast-atom bombardment mode (FAB). Analytical SFC was performed with a Mettler SFC supercritical CO<sub>2</sub> analytical chromatography system with Chiralcel AD-H, OD-H, AS-H, OB-H, and OJ-H columns (4.6 mm x 25 cm) with visualization at 210 nm. Analytical achiral GC was performed with an Agilent 6850 GC utilizing an Agilent DB-WAX (30.0 m x 0.25 mm) column (1.0 mL/min He carrier gas flow).

### 2.5.2 Substrate Synthesis

#### General Procedure 1: Acid Chloride Synthesis (115)



A flask was charged with the appropriate carboxylic acid (1.0 equiv) and CH<sub>2</sub>Cl<sub>2</sub> (0.5 M). Two drops of DMF and oxalyl chloride (1.2 equiv) were added dropwise. The solution was stirred at 23 °C for 3 h and then concentrated. The crude acid chloride was used without any further purification.

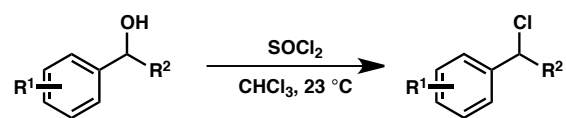
#### 3-(4-methoxyphenyl)Propanoic 2,6-dimethylbenzoic anhydride (110)



A flame-dried flask was charged with 2,6-dimethylbenzoic acid (1.0 mmol, 1 equiv) and CH<sub>2</sub>Cl<sub>2</sub> (0.33 M). To the solution was added NaH (60% dispersion in oil, 1.05 mmol, 1.05 equiv) and the reaction was allowed to stir for 3 h. 3-(4-methoxyphenyl)propanoyl chloride (**108**, 1.0 mmol, 1 equiv) was added dropwise to the reaction mixture and the

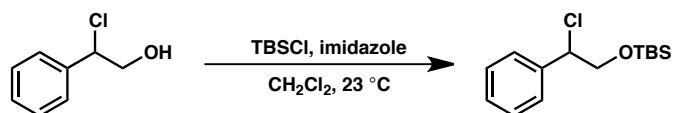
reaction was stirred overnight. The crude mixture was filtered through a small plug of celite with  $\text{CH}_2\text{Cl}_2$  and concentrated to afford **110** as a light yellow oil (291.1 mg, 93% yield).  $^1\text{H}$  NMR (500 MHz,  $\text{CDCl}_3$ )  $\delta$  7.24 (t,  $J = 7.7$  Hz, 1H), 7.13 (d,  $J = 8.7$  Hz, 2H), 7.06 (d,  $J = 7.5$  Hz, 2H), 6.84 (d,  $J = 8.7$  Hz, 4H), 3.79 (s, 3H), 2.97 (t,  $J = 7.6$  Hz, 2H), 2.82 (dd,  $J = 4879.7, 7.5$  Hz, 4H), 2.37 (d,  $J = 0.7$  Hz, 6H);  $^{13}\text{C}$  NMR (126 MHz,  $\text{CDCl}_3$ )  $\delta$  168.5, 165.1, 158.2, 135.8, 131.7, 131.6, 130.4, 129.3, 127.9, 114.0, 55.3, 37.5, 29.4, 20.0; FTIR (NaCl, thin film): 2955, 2931, 2836, 1811, 1740, 1612, 1595, 1584, 1513, 1466, 1301, 1248, 1179, 1124, 1079, 1036, 990, 827, 775  $\text{cm}^{-1}$ ; LRMS (ESI) calc'd for  $[\text{M}+\text{Na}]^+$  335.1, found 335.1.

### General Procedure 2: Benzyl Chloride Synthesis (111 and 113)



A flask was charged with the appropriate benzyl alcohol (1.0 equiv) and  $\text{CHCl}_3$  (1.5 M). Thionyl chloride (1.05 equiv) was added dropwise. Evolved gas was quenched via cannula into aqueous  $\text{NaHCO}_3$ . The solution was stirred at  $23\text{ }^\circ\text{C}$  for 12 h and then concentrated to afford a yellow oil. The crude residue was purified by Kugelrohr distillation to isolate a clear oil. Spectral data for all compounds matched those reported in the literature.

### [1-chloro-2-(*t*-butyldimethylsiloxy)ethyl]benzene (113c).



To a flask was added 2-chloro-2-phenylethanol (8.5 mmol, 1.0 equiv) and  $\text{CH}_2\text{Cl}_2$  (18 mL, 0.5 M) followed by imidazole (10.2 mmol, 1.2 equiv) and *tert*-butyldimethylsilyl chloride (10.2 mmol, 1.2 equiv). The reaction was stirred at 23 °C for 24 h and then quenched by pouring into water (40 mL). The aqueous and organic layers were separated and the aqueous layer was extracted with  $\text{CH}_2\text{Cl}_2$  (2 X 20 mL). The combined organic layers were washed with brine (1 X 20 mL) and dried ( $\text{Na}_2\text{SO}_4$ ), filtered, and concentrated. The crude residue was filtered through a thick pad of silica with hexanes and concentrated to afford a clear oil (2.21 g, 96% yield).  $^1\text{H}$  NMR (500 MHz,  $\text{CDCl}_3$ )  $\delta$  7.43 – 7.27 (m, 5H), 4.87 (t,  $J = 6.6$  Hz, 1H), 4.00 (dd,  $J = 10.7, 6.8$  Hz, 1H), 3.92 (dd,  $J = 10.7, 6.5$  Hz, 1H), 0.85 (s, 9H), 0.01 (s, 3H),  $-0.04$  (s, 3H);  $^{13}\text{C}$  NMR (126 MHz,  $\text{CDCl}_3$ )  $\delta$  139.0, 128.39, 128.37, 127.6, 68.5, 63.3, 25.7,  $-5.4, -5.5$ ; FTIR (NaCl, thin film): 2955, 2928, 2884, 2856, 1494, 1472, 1361, 1257, 1123, 1080, 837, 778  $\text{cm}^{-1}$ ; HRMS (FAB) calc'd for  $[\text{M}+\text{H}]^+$  271.1279, found 271.1290.

### 2.5.3 Enantioselective Reductive Cross-Coupling

#### General Procedure 3 (Variable Screening)

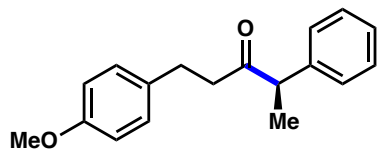
On a bench-top, to a 1/2 dram vial was added the appropriate ligand (0.044 mmol, 22 mol %), carboxylic acid (0.15 mmol, 0.75 equiv), 3 Å mol sieves (30 mg/0.2 mmol benzyl chloride), powdered metal reductant (0.6 mmol, 3 equiv), and nickel source (0.02 mmol, 10 mol %). Under an inert atmosphere in a glovebox, the vial was charged with the appropriate solvent (0.53 mL, 0.38 M) followed by benzyl chloride (0.2 mmol, 1 equiv), acid chloride (0.24 mmol, 1.2 equiv), and dodecane (internal standard). The mixture was stirred at 240 rpm, ensuring that the reductant was uniformly suspended. Stirring

continued at 20 °C under inert atmosphere for 24 h. The black slurry was transferred to a separatory funnel using 1 M HCl (5 mL) and diethyl ether (10 mL). The mixture was diluted with H<sub>2</sub>O (10 mL) and the aqueous and organic layers were separated. The aqueous layer was extracted with diethyl ether (2 × 10 mL) and the combined organic layers were washed with brine (1 × 15 mL) and dried (MgSO<sub>4</sub>), filtered, and concentrated. The crude residue was analyzed by GC.

#### **General Procedure 4: Enantioselective Reductive Coupling of Benzyl Chlorides and Acid Chlorides**

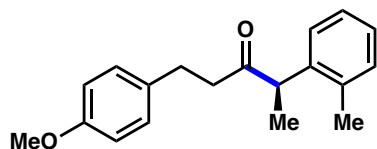
On a bench-top, to a 1/2 dram vial was added (*R,R*)-**L32** (0.044 mmol, 22 mol %), 2,6-DMBA (0.15 mmol, 0.75 equiv), 3 Å mol sieves (30 mg/0.2 mmol benzyl chloride), manganese powder (0.6 mmol, 3 equiv), and NiCl<sub>2</sub>(dme) (0.02 mmol, 10 mol %). Under an inert atmosphere in a glovebox, the vial was charged with 30% v/v DMA/THF (0.53 mL, 0.38 M) followed by benzyl chloride (**111** or **113**, 0.2 mmol, 1 equiv) and acid chloride (**108**, Table 2.5-2.7: 0.3 mmol, 1.5 equiv; **115**, Scheme 2.11: 0.24 mmol, 1.2 equiv). The mixture was stirred at 240 rpm, ensuring that the manganese powder was uniformly suspended. Stirring continued at 20 °C under inert atmosphere for 24 h. The black slurry was transferred to a separatory funnel using 1 M HCl (5 mL) and diethyl ether (10 mL). The mixture was diluted with H<sub>2</sub>O (10 mL) and the aqueous and organic layers were separated. The aqueous layer was extracted with diethyl ether (2 × 10 mL) and the combined organic layers were washed with brine (1 × 15 mL) and dried (MgSO<sub>4</sub>), filtered, and concentrated. The crude residue was purified by flash chromatography.

**(R)-1-(4-methoxyphenyl)-4-Phenylpentan-3-one (112a or 109)**



Prepared from (1-chloroethyl)benzene (**96** or **111a**, 0.20 mmol) and 3-(4-methoxyphenyl)propanoyl chloride (**108**, 0.30 mmol) according to General Procedure 4. The crude residue was purified by silica gel chromatography (5% ethyl acetate/hexanes) to yield **112a** (42.3 mg, 79% yield) in 93% ee as a clear oil. The enantiomeric excess was determined by chiral SFC analysis (OD-H, 2.5 mL/min, 5% IPA in CO<sub>2</sub>,  $\lambda = 210$  nm):  $t_R$  (minor) = 9.2 min,  $t_R$  (major) = 9.8 min.  $[\alpha]_D^{25} = -102.3^\circ$  ( $c = 1.10$ , CHCl<sub>3</sub>); <sup>1</sup>H NMR (500 MHz, CDCl<sub>3</sub>)  $\delta$  7.37 – 7.21 (m, 3H), 7.22 – 7.14 (m, 2H), 7.05 – 6.96 (m, 2H), 6.84 – 6.75 (m, 2H), 3.79 (s, 3H), 3.72 (q,  $J = 7.0$  Hz, 1H), 2.88 – 2.57 (m, 4H), 1.39 (d,  $J = 7.0$  Hz, 3H); <sup>13</sup>C NMR (126 MHz, CDCl<sub>3</sub>)  $\delta$  210.0, 157.8, 140.4, 133.0, 129.2, 128.9, 127.8, 127.1, 113.7, 55.2, 53.2, 42.8, 29.1, 17.3; FTIR (NaCl, thin film): 3060, 3027, 2973, 2931, 2834, 1713, 1611, 1513, 1493, 1452, 1300, 1247 cm<sup>-1</sup>; HRMS (MM) calc'd for [M-H]<sup>-</sup> 267.1391, found 267.1391.

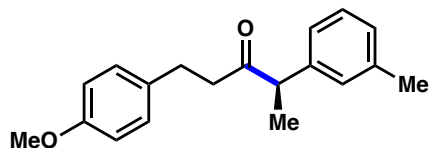
**(R)-1-(4-methoxyphenyl)-4-(*o*-tolyl)Pentan-3-one (112b)**



Prepared from 1-(1-chloroethyl)-2-methylbenzene (**111b**, 0.20 mmol) and 3-(4-methoxyphenyl)propanoyl chloride (**108**, 0.30 mmol) according to General Procedure 4 except using 33 mol % (*R,R*)-**L32** (0.066 mmol). The crude residue was purified by silica gel chromatography (5% ethyl acetate/hexanes) to yield **112b** (19.8 mg, 35% yield) in 72% ee as a clear oil. The enantiomeric excess was determined by chiral SFC analysis (OD-H, 2.5 mL/min, 10% IPA in CO<sub>2</sub>,  $\lambda = 210$  nm):  $t_R$  (minor) = 5.3 min,  $t_R$  (major) = 5.7 min.

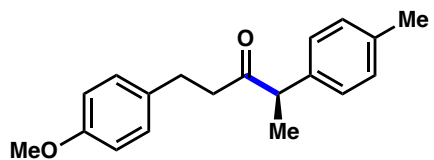
$[\alpha]_D^{25} = -72.3^\circ$  ( $c = 0.56$ ,  $\text{CHCl}_3$ );  $^1\text{H NMR}$  (500 MHz,  $\text{CDCl}_3$ )  $\delta$  7.21 – 7.09 (m, 3H), 7.02 – 6.92 (m, 3H), 6.77 (d,  $J = 8.6$  Hz, 2H), 3.87 (q,  $J = 6.9$  Hz, 1H), 3.76 (s, 3H), 2.85 – 2.68 (m, 2H), 2.64 – 2.47 (m, 2H), 2.33 (s, 3H), 1.32 (d,  $J = 6.9$  Hz, 3H);  $^{13}\text{C NMR}$  (126 MHz,  $\text{CDCl}_3$ )  $\delta$  210.4, 157.9, 140.0, 135.7, 133.1, 130.8, 129.2, 127.0, 126.6, 113.8, 55.2, 49.2, 42.8, 29.2, 19.7, 16.7; FTIR (NaCl, thin film): 2931, 2834, 1712, 1611, 1513, 1491, 1463, 1300, 1246, 1171, 1036, 828  $\text{cm}^{-1}$ ; HRMS (MM) calc'd for  $\text{M}^+$  282.1614, found 282.1543.

**(R)-1-(4-methoxyphenyl)-4-(*m*-tolyl)Pentan-3-one (112c)**

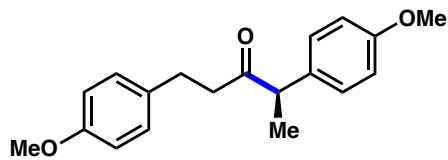


Prepared from 1-(1-chloroethyl)-3-methylbenzene (**111c**, 0.20 mmol) and 3-(4-methoxyphenyl)propanoyl chloride (**108**, 0.30 mmol)

according to General Procedure 4 except using 33 mol % (*R,R*)-**L32** (0.066 mmol). The crude residue was purified by silica gel chromatography (5% ethyl acetate/hexanes) to yield **111c** (42.5 mg, 75% yield) in 93% ee as a clear oil. The enantiomeric excess was determined by chiral SFC analysis (OD-H, 2.5 mL/min, 5% IPA in  $\text{CO}_2$ ,  $\lambda = 210$  nm):  $t_R$  (minor) = 9.1 min,  $t_R$  (major) = 9.9 min.  $[\alpha]_D^{25} = -90.4^\circ$  ( $c = 1.46$ ,  $\text{CHCl}_3$ );  $^1\text{H NMR}$  (500 MHz,  $\text{CDCl}_3$ )  $\delta$  7.19 (t,  $J = 7.5$  Hz, 1H), 7.09 – 7.01 (m, 1H), 7.02 – 6.92 (m, 4H), 6.77 (d,  $J = 8.5$  Hz, 2H), 3.77 (s, 3H), 3.66 (q,  $J = 6.9$  Hz, 1H), 2.84 – 2.56 (m, 4H), 2.31 (s, 3H), 1.36 (d,  $J = 6.9$  Hz, 3H);  $^{13}\text{C NMR}$  (126 MHz,  $\text{CDCl}_3$ )  $\delta$  210.1, 157.8, 140.4, 138.6, 133.1, 129.2, 128.8, 128.6, 127.9, 125.0, 113.8, 55.2, 53.1, 42.8, 29.1, 21.4, 17.3; FTIR (NaCl, thin film): 2931, 2834, 1714, 1611, 1584, 1513, 1453, 1300, 1246, 1178, 1036, 825  $\text{cm}^{-1}$ ; HRMS (MM) calc'd for  $[\text{M}+\text{H}]^+$  283.1693, found 283.1557.

**(R)-1-(4-methoxyphenyl)-4-(p-tolyl)Pentan-3-one (112d)**

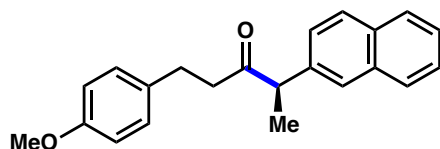
Prepared from 1-(1-chloroethyl)-4-methylbenzene (**111d**, 0.20 mmol) and 3-(4-methoxyphenyl)propanoyl chloride (**108**, 0.30 mmol) according to General Procedure 4 except using 33 mol % (*R,R*)-**L32** (0.066 mmol). The crude residue was purified by silica gel chromatography (5% ethyl acetate/hexanes) to yield **112d** (41.8 mg, 74% yield) in 93% ee as a clear oil. The enantiomeric excess was determined by chiral SFC analysis (OD-H, 2.5 mL/min, 5% IPA in CO<sub>2</sub>,  $\lambda = 210$  nm):  $t_R$  (minor) = 9.0 min,  $t_R$  (major) = 9.8 min.  $[\alpha]_D^{25} = -84.9^\circ$  (c = 1.37, CHCl<sub>3</sub>); <sup>1</sup>H NMR (500 MHz, CDCl<sub>3</sub>)  $\delta$  7.11 (d,  $J = 7.9$  Hz, 2H), 7.05 (d,  $J = 7.9$  Hz, 2H), 6.99 (d,  $J = 9.0$  Hz, 2H), 6.77 (d,  $J = 8.6$  Hz, 2H), 3.77 (s, 3H), 3.66 (q,  $J = 6.9$  Hz, 1H), 2.84 – 2.55 (m, 4H), 2.33 (s, 3H), 1.35 (d,  $J = 7.0$  Hz, 3H); <sup>13</sup>C NMR (126 MHz, CDCl<sub>3</sub>)  $\delta$  210.2, 157.8, 137.4, 136.7, 133.1, 129.6, 129.2, 127.7, 113.8, 55.2, 52.8, 42.8, 29.1, 21.0, 17.3; FTIR (NaCl, thin film): 2930, 2834, 1713, 1612, 1584, 1513, 1454, 1300, 1246, 1178, 1036, 824 cm<sup>-1</sup>; HRMS (MM) calc'd for [M+H]<sup>+</sup> 283.1647, found 283.1693.

**(R)-1,4-bis(4-methoxyphenyl)Pentan-3-one (112e)**

Prepared from 1-(1-chloroethyl)-4-methoxybenzene (**111e**, 0.20 mmol) and 3-(4-methoxyphenyl)propanoyl chloride (**108**, 0.30 mmol) according to General Procedure 4 except using 33 mol % (*R,R*)-**L32** (0.066 mmol). The crude residue was purified by silica gel chromatography (5% ethyl acetate/hexanes) to yield **112e** (33.4 mg, 56% yield) in 86% ee as a clear oil. The

enantiomeric excess was determined by chiral SFC analysis (OB-H, 2.5 mL/min, 10% IPA in CO<sub>2</sub>,  $\lambda = 210$  nm):  $t_R$  (minor) = 6.8 min,  $t_R$  (major) = 7.4 min.  $[\alpha]_D^{25} = -77.2^\circ$  (c = 1.22, CHCl<sub>3</sub>); <sup>1</sup>H NMR (500 MHz, CDCl<sub>3</sub>)  $\delta$  7.10 (d,  $J = 8.3$  Hz, 2H), 6.98 (d,  $J = 8.0$  Hz, 2H), 6.83 (d,  $J = 9.0$  Hz, 2H), 6.76 (d,  $J = 9.0$  Hz, 2H), 3.79 (s, 3H), 3.77 (s, 3H), 3.64 (q,  $J = 6.9$  Hz, 1H), 2.83 – 2.54 (m, 4H), 1.34 (d,  $J = 7.0$  Hz, 3H); <sup>13</sup>C NMR (126 MHz, CDCl<sub>3</sub>)  $\delta$  210.3, 158.7, 157.9, 133.1, 132.4, 129.2, 128.9, 114.3, 113.8, 55.24, 55.23, 52.3, 42.7, 29.1, 17.3 ; FTIR (NaCl, thin film): 2930, 2834, 1710, 1611, 1582, 1512, 1463, 1301, 1246, 1177, 1034, 827 cm<sup>-1</sup>; HRMS (MM) calc'd for M<sup>+</sup> 298.1563, found 298.1622.

**(R)-1-(4-methoxyphenyl)-4-(naphthalen-2-yl)Pentan-3-one (112f)**

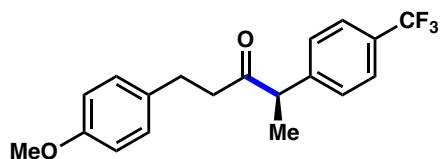


Prepared from 2-(1-chloroethyl)naphthalene (**111f**, 0.20 mmol) and 3-(4-methoxyphenyl)propanoyl chloride (**108**, 0.30 mmol) according to General

Procedure 4 except using 33 mol % (*R,R*)-**L32** (0.066 mmol). The crude residue was purified by silica gel chromatography (5% ethyl acetate/hexanes) to yield **112f** (41.7 mg, 65% yield) in 91% ee as a clear oil. The enantiomeric excess was determined by chiral SFC analysis (AS-H, 2.5 mL/min, 5% IPA in CO<sub>2</sub>,  $\lambda = 210$  nm):  $t_R$  (minor) = 10.7 min,  $t_R$  (major) = 11.3 min.  $[\alpha]_D^{25} = -100.4^\circ$  (c = 1.00, CHCl<sub>3</sub>); <sup>1</sup>H NMR (500 MHz, CDCl<sub>3</sub>)  $\delta$  7.85 – 7.73 (m, 3H), 7.59 (s, 1H), 7.52 – 7.42 (m, 2H), 7.29 – 7.23 (m, 1H), 6.95 (d,  $J = 8.8$  Hz, 2H), 6.71 (d,  $J = 8.8$  Hz, 2H), 3.86 (q,  $J = 6.9$  Hz, 1H), 3.73 (s, 3H), 2.85 – 2.60 (m, 4H), 1.46 (d,  $J = 6.9$  Hz, 3H); <sup>13</sup>C NMR (126 MHz, CDCl<sub>3</sub>)  $\delta$  210.0, 157.8, 137.9, 133.6, 132.9, 132.5, 129.2, 128.7, 127.7, 127.6, 126.6, 126.2, 125.9, 113.7, 55.2, 53.3,

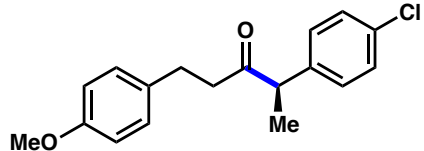
42.9, 29.0, 17.3; FTIR (NaCl, thin film): 3055, 2972, 2931, 2834, 1713, 1611, 1583, 1511, 1455, 1374, 1300, 1245, 1178, 1035, 822, 750  $\text{cm}^{-1}$ ; LRMS (ESI) calc'd for  $[\text{M}+\text{H}]^+$  319.2, found 319.2.

**(R)-1-(4-methoxyphenyl)-4-(4-(trifluoromethyl)phenyl)Pentan-3-one (112h)**



Prepared from 1-(1-chloroethyl)-4-(trifluoromethyl)benzene (**11h**, 0.20 mmol) and 3-(4-methoxyphenyl)propanoyl chloride (**108**, 0.30 mmol) according to General Procedure 4 except using 20% v/v DMA/THF. The crude residue was purified by silica gel chromatography (5% ethyl acetate/hexanes) to yield **112h** (42.8 mg, 64% yield) in 82% ee as a clear oil. The enantiomeric excess was determined by chiral SFC analysis (OJ-H, 2.5 mL/min, 5% IPA in  $\text{CO}_2$ ,  $\lambda = 210$  nm):  $t_R$  (major) = 6.0 min,  $t_R$  (minor) = 7.3 min.  $[\alpha]_D^{25} = -50.8^\circ$  ( $c = 1.01$ ,  $\text{CHCl}_3$ );  $^1\text{H}$  NMR (500 MHz,  $\text{CDCl}_3$ )  $\delta$  7.53 (d,  $J = 7.8$  Hz, 2H), 7.25 (d,  $J = 7.7$  Hz, 2H), 6.97 (d,  $J = 8.8$  Hz, 2H), 6.80 (d,  $J = 9.0$  Hz, 2H), 3.80 – 3.74 (m, 4H), 2.85 – 2.60 (m, 4H), 1.38 (d,  $J = 7.0$  Hz, 3H);  $^{13}\text{C}$  NMR (126 MHz,  $\text{CDCl}_3$ )  $\delta$  209.0, 158.0, 144.2, 132.7, 129.3, 129.2, 128.2, 125.8, 113.9, 113.8, 55.2, 53.0, 43.1, 28.9, 17.3; FTIR (NaCl, thin film): 2934, 2837, 1717, 1616, 1584, 1513, 1419, 1326, 1247, 1165, 1124, 1070, 1036, 825  $\text{cm}^{-1}$ ; HRMS (MM) calc'd for  $\text{M}^+$  336.1332, found 336.1342.

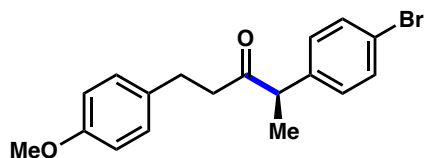
**(R)-4-(4-chlorophenyl)-1-(4-methoxyphenyl)Pentan-3-one (112i)**



Prepared from 1-chloro-4-(1-chloroethyl)benzene (**111i**, 0.20 mmol) and 3-(4-methoxyphenyl)propanoyl chloride (**108**, 0.30 mmol) according to General

Procedure 4. The crude residue was purified by silica gel chromatography (5% ethyl acetate/hexanes) to yield **112i** (45.9 mg, 76% yield) in 91% ee as a clear oil. The enantiomeric excess was determined by chiral SFC analysis (OD-H, 2.5 mL/min, 3% IPA in CO<sub>2</sub>,  $\lambda = 210$  nm):  $t_R$  (minor) = 19.6 min,  $t_R$  (major) = 20.6 min.  $[\alpha]_D^{25} = -64.1^\circ$  ( $c = 0.79$ , CHCl<sub>3</sub>); <sup>1</sup>H NMR (500 MHz, CDCl<sub>3</sub>)  $\delta$  7.25 (d,  $J = 8.8$  Hz, 2H), 7.06 (d,  $J = 8.8$  Hz, 2H), 6.97 (d,  $J = 8.8$  Hz, 2H), 6.76 (d,  $J = 8.4$  Hz, 2H), 3.77 (s, 3H), 3.67 (q,  $J = 7.0$  Hz, 1H), 2.83 – 2.55 (m, 4H), 1.34 (d,  $J = 7.0$  Hz, 3H); <sup>13</sup>C NMR (126 MHz, CDCl<sub>3</sub>)  $\delta$  209.4, 157.9, 138.8, 133.0, 132.8, 129.2, 129.0, 113.8, 55.2, 52.5, 42.9, 29.0, 17.3; FTIR (NaCl, thin film): 2932, 1713, 1611, 1513, 1491, 1300, 1247, 1178, 1093, 1036, 1014, 825 cm<sup>-1</sup>; HRMS (MM) calc'd for M<sup>+</sup> 302.1068, found 302.1001.

**(R)-4-(4-bromophenyl)-1-(4-methoxyphenyl)Pentan-3-one (112j)**

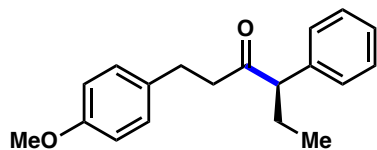


Prepared from 1-bromo-4-(1-chloroethyl)benzene (**111j**, 0.20 mmol) and 3-(4-methoxyphenyl)propanoyl chloride (**108**, 0.30 mmol) according to General

Procedure 4 except using 1.25 equiv 2,6-DMBA (0.25 mmol). The crude residue was purified by silica gel chromatography (5% ethyl acetate/hexanes) to yield **112j** (51.0 mg, 73% yield) in 86% ee as a clear oil. The enantiomeric excess was determined by chiral SFC analysis (OD-H, 2.5 mL/min, 5% IPA in CO<sub>2</sub>,  $\lambda = 210$  nm):  $t_R$  (minor) = 25.4 min,  $t_R$

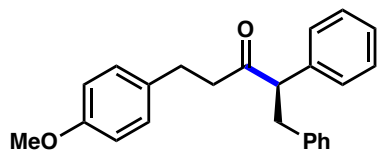
(major) = 27.0 min.  $[\alpha]_D^{25} = -53.5^\circ$  (c = 1.44,  $\text{CHCl}_3$ );  $^1\text{H NMR}$  (500 MHz,  $\text{CDCl}_3$ )  $\delta$  7.41 (d,  $J = 8.6$  Hz, 2H), 7.01 (d,  $J = 8.4$  Hz, 2H), 6.97 (d,  $J = 8.6$  Hz, 2H), 6.76 (d,  $J = 9.2$  Hz, 2H), 3.77 (s, 3H), 3.65 (q,  $J = 7.0$  Hz, 1H), 2.83 – 2.55 (m, 4H), 1.34 (d,  $J = 7.0$  Hz, 3H);  $^{13}\text{C NMR}$  (126 MHz,  $\text{CDCl}_3$ )  $\delta$  209.3, 157.9, 139.3, 132.8, 132.0, 129.6, 129.2, 121.1, 113.8, 55.2, 52.6, 42.9, 29.0, 17.3; FTIR (NaCl, thin film): 2932, 2834, 1714, 1611, 1513, 1487, 1453, 1300, 1247, 1178, 1036, 1010, 825  $\text{cm}^{-1}$ ; HRMS (MM) calc'd for  $\text{M}^+$  346.0563, found 346.0463.

**(R)-1-(4-methoxyphenyl)-4-Phenylhexan-3-one (114a)**



Prepared from (1-chloropropyl)benzene (**113a**, 0.20 mmol) and 3-(4-methoxyphenyl)propanoyl chloride (**108**, 0.30 mmol) according to General Procedure 4. The crude residue was purified by silica gel chromatography (5% ethyl acetate/hexanes) to yield **114a** (28.1 mg, 50% yield) in 94% ee as a clear oil. The enantiomeric excess was determined by chiral SFC analysis (OB-H, 2.5 mL/min, 5% IPA in  $\text{CO}_2$ ,  $\lambda = 210$  nm):  $t_R$  (minor) = 6.2 min,  $t_R$  (major) = 6.9 min.  $[\alpha]_D^{25} = -97.9^\circ$  (c = 0.96,  $\text{CHCl}_3$ );  $^1\text{H NMR}$  (500 MHz,  $\text{CDCl}_3$ )  $\delta$  7.33 – 7.20 (m, 3H), 7.19 – 7.12 (m, 2H), 6.98 (d,  $J = 8.8$  Hz, 2H), 6.76 (d,  $J = 8.5$  Hz, 2H), 3.76 (s, 3H), 3.48 (t,  $J = 7.4$  Hz, 1H), 2.84 – 2.56 (m, 4H), 2.11 – 1.99 (m, 1H), 1.77 – 1.64 (m, 1H), 0.80 (t,  $J = 7.4$  Hz, 3H);  $^{13}\text{C NMR}$  (126 MHz,  $\text{CDCl}_3$ )  $\delta$  209.7, 157.8, 138.8, 133.1, 129.2, 128.8, 128.3, 127.1, 113.8, 61.0, 55.2, 43.6, 29.0, 25.1, 12.1; FTIR (NaCl, thin film): 2961, 2932, 1711, 1611, 1513, 1492, 1453, 1300, 1247, 1178, 1036, 821  $\text{cm}^{-1}$ ; HRMS (MM) calc'd for  $\text{M}^+$  282.1614, found 282.1631.

**(R)-5-(4-methoxyphenyl)-1,2-Diphenylpentan-3-one (114b)**

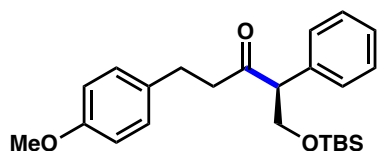


Prepared from (1-chloroethane-1,2-diyl)dibenzene (**113b**, 0.20 mmol) and 3-(4-methoxyphenyl)propanoyl chloride (**108**, 0.30 mmol) according to General Procedure 4. The

crude residue was purified by silica gel chromatography (5% ethyl acetate/hexanes) to yield **114b** (54.6 mg, 79% yield) in 92% ee as a clear oil. The enantiomeric excess was determined by chiral SFC analysis (AS-H, 2.5 mL/min, 10% IPA in CO<sub>2</sub>,  $\lambda = 210$  nm):  $t_R$  (major) = 4.5 min,  $t_R$  (minor) = 5.3 min.  $[\alpha]_D^{25} = -166.8^\circ$  (c = 0.85, CHCl<sub>3</sub>); <sup>1</sup>H NMR (500 MHz, CDCl<sub>3</sub>)  $\delta$  7.32 – 7.08 (m, 8H), 7.06 – 6.96 (m, 2H), 6.92 (d,  $J = 8.3$  Hz, 2H), 6.74 (d,  $J = 8.3$  Hz, 2H), 3.87 (t,  $J = 7.4$  Hz, 1H), 3.77 (s, 3H), 3.42 (dd,  $J = 13.7, 7.7$  Hz, 1H), 2.90 (dd,  $J = 13.7, 7.0$  Hz, 1H), 2.80 – 2.59 (m, 3H), 2.58 – 2.45 (m, 1H); <sup>13</sup>C NMR (126 MHz, CDCl<sub>3</sub>)  $\delta$  209.0, 157.8, 139.7, 138.3, 132.9, 129.1, 129.0, 128.9, 128.4, 128.2, 127.3, 126.1, 113.8, 61.1, 55.2, 44.1, 38.6, 28.9; FTIR (NaCl, thin film): 3027, 2930, 2834, 1712, 1611, 1583, 1513, 1495, 1453, 1300, 1247, 1178, 1035, 824 cm<sup>-1</sup>; HRMS (MM) calc'd for [M+H]<sup>+</sup> 345.1849, found 345.1831.

**(S)-1-((tert-butyldimethylsilyloxy)-5-(4-methoxyphenyl)-2-Phenylpentan-3-one**

**(114c)**

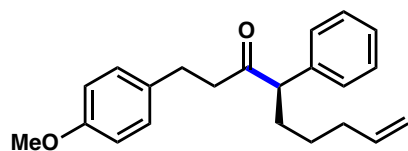


Prepared from [1-chloro-2-(*t*-butyldimethylsilyloxy)ethyl]benzene (**113c**, 0.20 mmol) and 3-(4-methoxyphenyl)propanoyl chloride (**108**, 0.30 mmol)

according to General Procedure 4 except using 50% v/v DMA/THF. The crude residue was purified by silica gel chromatography (5% ethyl acetate/hexanes) to yield **114c** (40.4

mg, 51% yield) in 89% ee as a clear oil. The enantiomeric excess was determined by chiral SFC analysis (AS-H, 2.5 mL/min, 5% IPA in CO<sub>2</sub>,  $\lambda$  = 210 nm):  $t_R$  (major) = 3.3 min,  $t_R$  (minor) = 3.8 min.  $[\alpha]_D^{25} = -50.0^\circ$  (c = 0.90, CHCl<sub>3</sub>); <sup>1</sup>H NMR (500 MHz, CDCl<sub>3</sub>)  $\delta$  7.33 – 7.23 (m, 3H), 7.20 (dd,  $J$  = 8.1, 1.6 Hz, 2H), 7.01 (d,  $J$  = 8.8 Hz, 2H), 6.77 (d,  $J$  = 8.8 Hz, 2H), 4.23 (dd,  $J$  = 9.7, 8.5 Hz, 1H), 3.92 (dd,  $J$  = 8.5, 5.7 Hz, 1H), 3.77 (s, 3H), 3.73 (dd,  $J$  = 9.7, 5.7 Hz, 1H), 2.88 – 2.68 (m, 4H), 0.84 (s, 9H), –0.01 (s, 3H), –0.03 (s, 3H); <sup>13</sup>C NMR (126 MHz, CDCl<sub>3</sub>)  $\delta$  208.8, 157.8, 135.9, 133.1, 129.2, 128.7, 128.5, 127.5, 113.8, 65.0, 61.0, 55.2, 45.1, 28.6, 25.8, 18.2, –5.57, –5.60; FTIR (NaCl, thin film): 2953, 2928, 2855, 1718, 1612, 1583, 1513, 1463, 1361, 1248, 1099, 835 cm<sup>-1</sup>; HRMS (MM) calc'd for [M+H]<sup>+</sup> 399.2350, found 399.2198.

**(R)-1-(4-methoxyphenyl)-4-Phenylnon-8-en-3-one (114e)**

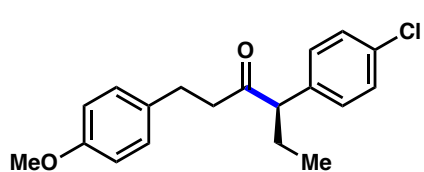


Prepared from (1-chlorohex-5-en-1-yl)benzene (**113e**, 0.20 mmol) and 3-(4-methoxyphenyl)propanoyl chloride (**108**, 0.30 mmol) according to General

Procedure 4. The crude residue was purified by silica gel chromatography (5% ethyl acetate/hexanes) to yield **114e** (24.6 mg, 38% yield) in 92% ee as a clear oil. The enantiomeric excess was determined by chiral SFC analysis (AD-H, 2.5 mL/min, 5% IPA in CO<sub>2</sub>,  $\lambda$  = 210 nm):  $t_R$  (major) = 10.9 min,  $t_R$  (minor) = 11.9 min.  $[\alpha]_D^{25} = -90.9^\circ$  (c = 0.47, CHCl<sub>3</sub>); <sup>1</sup>H NMR (500 MHz, CDCl<sub>3</sub>)  $\delta$  7.35 – 7.20 (m, 3H), 7.18 – 7.11 (m, 2H), 6.98 (d,  $J$  = 8.4 Hz, 2H), 6.76 (d,  $J$  = 8.9 Hz, 2H), 5.73 (ddt,  $J$  = 16.9, 10.2, 6.7 Hz, 1H), 5.02 – 4.88 (m, 2H), 3.76 (s, 3H), 3.55 (t,  $J$  = 7.4 Hz, 1H), 2.84 – 2.54 (m, 4H), 2.09 – 1.93 (m, 3H), 1.74 – 1.63 (m, 1H), 1.37 – 1.15 (m, 2H); <sup>13</sup>C NMR (126 MHz, CDCl<sub>3</sub>)  $\delta$

209.6, 157.9, 138.8, 138.4, 133.0, 129.2, 128.9, 128.3, 127.2, 114.7, 113.8, 59.1, 55.2, 43.6, 33.6, 31.4, 29.0, 26.7; FTIR (NaCl, thin film): 2930, 1712, 1640, 1611, 1583, 1513, 1453, 1300, 1247, 1177, 1036, 824  $\text{cm}^{-1}$ ; HRMS (MM) calc'd for  $[\text{M}+\text{H}]^+$  323.2006, found 323.1945.

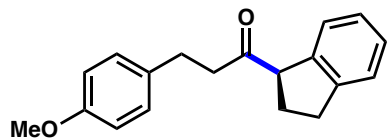
**(R)-4-(4-chlorophenyl)-1-(4-methoxyphenyl)Hexan-3-one (114g)**



Prepared from 1-chloro-4-(1-chloropropyl)benzene (**113g**, 0.20 mmol) and 3-(4-methoxyphenyl)propanoyl chloride (**108**, 0.30 mmol) according to General

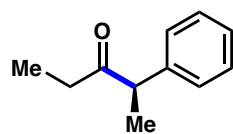
Procedure 4. The crude residue was purified by silica gel chromatography (5% ethyl acetate/hexanes) to yield **114g** (41.2 mg, 65% yield) in 91% ee as a clear oil. The enantiomeric excess was determined by chiral SFC analysis (OD-H, 2.5 mL/min, 3% IPA in  $\text{CO}_2$ ,  $\lambda = 210$  nm):  $t_R$  (minor) = 18.1 min,  $t_R$  (major) = 19.4 min.  $[\alpha]_D^{25} = -79.7^\circ$  ( $c = 1.85$ ,  $\text{CHCl}_3$ );  $^1\text{H}$  NMR (500 MHz,  $\text{CDCl}_3$ )  $\delta$  7.24 (d,  $J = 8.6$  Hz, 2H), 7.06 (d,  $J = 8.9$  Hz, 2H), 6.97 (d,  $J = 9.1$  Hz, 2H), 6.76 (d,  $J = 8.6$  Hz, 2H), 3.77 (s, 3H), 3.48 – 3.41 (m, 1H), 2.83 – 2.55 (m, 4H), 2.01 (dp,  $J = 14.4, 7.3$  Hz, 1H), 1.72 – 1.62 (m, 1H), 0.78 (t,  $J = 7.4$  Hz, 3H);  $^{13}\text{C}$  NMR (126 MHz,  $\text{CDCl}_3$ )  $\delta$  209.2, 157.9, 137.1, 133.0, 132.8, 129.6, 129.2, 128.9, 113.7, 60.3, 55.2, 43.7, 28.9, 25.1, 12.0; FTIR (NaCl, thin film): 2962, 2932, 2834, 1711, 1611, 1583, 1512, 1490, 1463, 1300, 1246, 1178, 1092, 1036, 1014, 819  $\text{cm}^{-1}$ ; LRMS (ESI) calc'd for  $[\text{M}+\text{H}]^+$  317.1, found 317.1.

**(R)-1-(2,3-dihydro-1H-inden-1-yl)-3-(4-methoxyphenyl)Propan-1-one (114h)**



Prepared from 1-chloro-2,3-dihydro-1H-indene (**113h**, 0.20 mmol) and 3-(4-methoxyphenyl)propanoyl chloride (**108**, 0.30 mmol) according to General Procedure 4. The crude residue was purified by silica gel chromatography (5% ethyl acetate/hexanes) to yield **114h** (38.3 mg, 68% yield) in 78% ee as a clear oil. The enantiomeric excess was determined by chiral SFC analysis (AD-H, 2.5 mL/min, 10% IPA in CO<sub>2</sub>,  $\lambda = 210$  nm):  $t_R$  (minor) = 7.9 min,  $t_R$  (major) = 8.9 min.  $[\alpha]_D^{25} = 11.3^\circ$  ( $c = 0.179$ , CHCl<sub>3</sub>); <sup>1</sup>H NMR (500 MHz, CDCl<sub>3</sub>)  $\delta$  7.30 – 7.10 (m, 4H), 7.07 (d,  $J = 8.9$  Hz, 2H), 6.83 (d,  $J = 8.7$  Hz, 3H), 4.08 (t,  $J = 7.1$  Hz, 1H), 3.78 (s, 3H), 3.05 (d,  $J = 7.9$  Hz, 1H), 2.98 – 2.67 (m, 5H), 2.37 – 2.18 (m, 2H); <sup>13</sup>C NMR (126 MHz, CDCl<sub>3</sub>)  $\delta$  210.0, 157.9, 144.6, 140.8, 133.2, 129.3, 127.5, 124.9, 124.8, 113.9, 113.8, 58.4, 55.3, 42.4, 31.9, 28.9, 28.5; FTIR (NaCl, thin film): 2932, 2849, 1709, 1611, 1583, 1513, 1458, 1300, 1247, 1178, 1036, 826, 755 cm<sup>-1</sup>; LRMS (ESI) calc'd for [M+H]<sup>+</sup> 281.2, found 281.1.

**(R)-2-Phenylpentan-3-one (116a)**

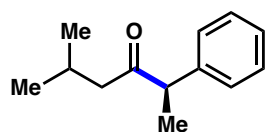


Prepared from (1-chloroethyl)benzene (**96**, 0.20 mmol) and propionyl chloride (**115a**, 0.24 mmol) according to General Procedure 4 except using 20% v/v DMA/THF. The crude residue was purified by silica gel chromatography (2% ethyl acetate/hexanes) to yield **116a** (19.5 mg, 60% yield) in 91% ee as a clear oil. The enantiomeric excess was determined by chiral SFC analysis (AS-H, 2.5 mL/min, 1% IPA in CO<sub>2</sub>,  $\lambda = 210$  nm):  $t_R$  (minor) = 1.8 min,  $t_R$  (major) = 2.0 min.  $[\alpha]_D^{25} = -225.9^\circ$  ( $c = 0.57$ , CHCl<sub>3</sub>); <sup>1</sup>H NMR (500 MHz, CDCl<sub>3</sub>)  $\delta$  7.36 – 7.29 (m, 2H), 7.28 – 7.23 (m, 1H),

7.23 – 7.19 (m, 2H), 3.76 (q,  $J = 7.0$  Hz, 1H), 2.42 – 2.33 (m, 2H), 1.39 (d,  $J = 7.0$  Hz, 3H), 0.97 (t,  $J = 7.3$  Hz, 3H);  $^{13}\text{C}$  NMR (126 MHz,  $\text{CDCl}_3$ )  $\delta$  211.5, 140.9, 128.8, 127.8, 127.0, 52.7, 34.2, 17.5, 8.0; FTIR (NaCl, thin film): 3027, 2976, 2935, 1716, 1600, 1494, 1453, 1374, 1130, 1070, 1029, 957, 758  $\text{cm}^{-1}$ ; LRMS (ESI) calc'd for  $[\text{M}+\text{H}]^+$  163.1, found 163.1.

The optical rotation of the product generated in the presence of (*R,R*)-**L32** was measured as  $[\alpha]_{\text{D}}^{25} = -225.9^\circ$  ( $c = 0.57$ ,  $\text{CHCl}_3$ ). Lit:  $[\alpha]_{\text{D}}^{25} = -76^\circ$  ( $c = 1.2$ ,  $\text{CHCl}_3$ , *R* enantiomer, 95% ee) and  $[\alpha]_{\text{D}}^{21} = -47.2$  ( $c = 1.00$ ,  $\text{CHCl}_3$ ; 73% ee).<sup>4b</sup> Based on the literature precedent, we assign our product as the *R* enantiomer.

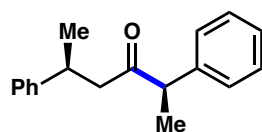
#### (*R*)-5-Methyl-2-phenylhexan-3-one (**116b**)



Prepared from (1-chloroethyl)benzene (**96**, 0.20 mmol) and isovaleroyl chloride (**115b**, 0.24 mmol) according to General Procedure 4. The crude residue was purified by silica gel chromatography (2% ethyl acetate/hexanes) to yield **116b** (27.5 mg, 73% yield) in 88% ee as a clear oil. The enantiomeric excess was determined by chiral SFC analysis (OD-H, 2.5 mL/min, 1% IPA in  $\text{CO}_2$ ,  $\lambda = 210$  nm):  $t_{\text{R}}$  (minor) = 2.2 min,  $t_{\text{R}}$  (major) = 2.7 min.  $[\alpha]_{\text{D}}^{25} = -205.8^\circ$  ( $c = 0.92$ ,  $\text{CHCl}_3$ );  $^1\text{H}$  NMR (500 MHz,  $\text{CDCl}_3$ )  $\delta$  7.35 – 7.29 (m, 2H), 7.28 – 7.23 (m, 1H), 7.23 – 7.18 (m, 2H), 3.72 (q,  $J = 6.9$  Hz, 1H), 2.29 – 2.16 (m, 2H), 2.10 (hept,  $J = 6.7$  Hz, 1H), 1.38 (d,  $J = 7.0$  Hz, 3H), 0.84 (d,  $J = 6.6$  Hz, 3H), 0.75 (d,  $J = 6.6$  Hz, 3H);  $^{13}\text{C}$  NMR (126 MHz,  $\text{CDCl}_3$ )  $\delta$  210.5, 140.5, 128.8, 127.9, 127.0, 53.3, 50.0, 24.3, 22.6, 22.2,

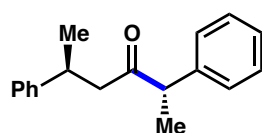
17.4; FTIR (NaCl, thin film): 3027, 2957, 2871, 1712, 1600, 1493, 1453, 1366, 1143, 1071, 1024, 761  $\text{cm}^{-1}$ ; LRMS (ESI) calc'd for  $[\text{M}+\text{H}]^+$  191.1, found 191.2.

**(2*R*,5*S*)-2,5-Diphenylhexan-3-one ((*R,S*)-**116c**)**



Prepared from (1-chloroethyl)benzene (**96**, 0.20 mmol) and (*S*)-3-phenylbutyryl chloride ((*S*)-**115c**, 0.24 mmol) according to General Procedure 4. The crude residue was purified by silica gel chromatography (2% ethyl acetate/hexanes) to yield (*R,S*)-**116c** (34.8 mg, 69% yield) as a clear oil and as a 20:1 mixture of diastereomers (determined by NMR analysis of the purified product).  $[\alpha]_{\text{D}}^{25} = -122.2^{\circ}$  ( $c = 1.71$ ,  $\text{CHCl}_3$ );  $^1\text{H}$  NMR (500 MHz,  $\text{CDCl}_3$ )  $\delta$  7.30 – 7.17 (m, 5H), 7.17 – 7.12 (m, 1H), 7.10 – 7.02 (m, 4H), 3.69 (q,  $J = 7.0$  Hz, 1H), 3.30 (h,  $J = 7.0$  Hz, 1H), 2.70 (dd,  $J = 16.8, 6.8$  Hz, 1H), 2.58 (dd,  $J = 16.8, 7.5$  Hz, 1H), 1.34 (d,  $J = 6.9$  Hz, 3H), 1.20 (d,  $J = 7.0$  Hz, 3H);  $^{13}\text{C}$  NMR (126 MHz,  $\text{CDCl}_3$ )  $\delta$  209.3, 146.1, 140.2, 128.8, 128.3, 127.0, 126.74, 126.73, 126.1, 53.5, 49.2, 35.2, 21.9, 17.2; FTIR (NaCl, thin film): 3061, 3027, 2967, 2930, 1714, 1601, 1493, 1452, 1373, 1125, 1069, 1029, 759  $\text{cm}^{-1}$ ; LRMS (ESI) calc'd for  $[\text{M}+\text{H}]^+$  253.2, found 253.2.

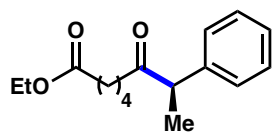
**(2*S*,5*S*)-2,5-Diphenylhexan-3-one ((*S,S*)-**116d**)**



Prepared from (1-chloroethyl)benzene (**26**, 0.20 mmol) and (*S*)-3-phenylbutyryl chloride ((*S*)-**151d**, 0.24 mmol) according to General Procedure 4 except using (*S,S*)-**L36**. The crude residue was purified by silica gel chromatography (2% ethyl acetate/hexanes) to yield (*S,S*)-**152d** (33.7 mg, 67% yield) as a clear oil and as a 12:1 mixture of diastereomers (determined by NMR analysis of the

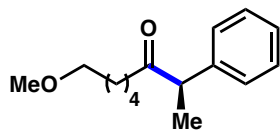
purified product).  $[\alpha]_D^{25} = 121.3^\circ$  ( $c = 1.59$ ,  $\text{CHCl}_3$ );  $^1\text{H NMR}$  (500 MHz,  $\text{CDCl}_3$ )  $\delta$  7.37 – 7.31 (m, 2H), 7.31 – 7.24 (m, 3H), 7.22 – 7.13 (m, 5H), 3.54 (q,  $J = 6.9$  Hz, 1H), 3.29 (h,  $J = 7.3$  Hz, 1H), 2.67 (dd,  $J = 16.3, 6.4$  Hz, 1H), 2.56 (dd,  $J = 16.3, 7.9$  Hz, 1H), 1.32 (d,  $J = 6.9$  Hz, 3H), 1.11 (d,  $J = 7.0$  Hz, 3H);  $^{13}\text{C NMR}$  (126 MHz,  $\text{CDCl}_3$ )  $\delta$  209.5, 146.3, 140.3, 128.9, 128.5, 128.0, 127.1, 126.8, 126.2, 53.4, 49.6, 35.4, 21.5, 17.2; FTIR (NaCl, thin film): 3061, 3027, 2968, 2930, 1714, 1601, 1494, 1452, 1374, 1125, 1068, 1029, 1004, 763  $\text{cm}^{-1}$ ; LRMS (ESI) calc'd for  $[\text{M}+\text{H}]^+$  253.2, found 253.1.

**(R)-Ethyl 6-oxo-7-phenyloctanoate (116e)**



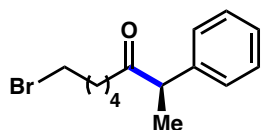
Prepared from (1-chloroethyl)benzene (**96**, 0.20 mmol) and ethyl 6-chloro-6-oxohexanoate (**115e**, 0.24 mmol) according to General Procedure 4 except using 10% v/v DMA/THF. The crude residue was purified by silica gel chromatography (5% ethyl acetate/hexanes) to yield **115f** (33.8 mg, 64% yield) in 92% ee as a clear oil. The enantiomeric excess was determined by chiral SFC analysis (AD-H, 2.5 mL/min, 4% IPA in  $\text{CO}_2$ ,  $\lambda = 210$  nm):  $t_R$  (minor) = 4.9 min,  $t_R$  (major) = 5.3 min.  $[\alpha]_D^{25} = -146.8^\circ$  ( $c = 0.85$ ,  $\text{CHCl}_3$ );  $^1\text{H NMR}$  (500 MHz,  $\text{CDCl}_3$ )  $\delta$  7.35 – 7.29 (m, 2H), 7.28 – 7.23 (m, 1H), 7.22 – 7.18 (m, 2H), 4.09 (q,  $J = 7.1$  Hz, 2H), 3.73 (q,  $J = 7.0$  Hz, 1H), 2.44 – 2.28 (m, 2H), 2.25 – 2.15 (m, 2H), 1.58 – 1.44 (m, 4H), 1.38 (d,  $J = 7.0$  Hz, 3H), 1.22 (t,  $J = 7.1$  Hz, 3H);  $^{13}\text{C NMR}$  (126 MHz,  $\text{CDCl}_3$ )  $\delta$  210.4, 173.4, 140.6, 128.9, 127.8, 127.1, 60.2, 53.0, 40.5, 34.0, 24.3, 23.2, 17.4, 14.2; FTIR (NaCl, thin film): 2977, 2932, 1733, 1714, 1600, 1494, 1453, 1375, 1248, 1181, 1029, 761  $\text{cm}^{-1}$ ; LRMS (ESI) calc'd for  $[\text{M}+\text{H}]^+$  263.2, found 263.2.

**(R)-8-Methoxy-2-phenyloctan-3-one (116f)**



Prepared from (1-chloroethyl)benzene (**96**, 0.20 mmol) and 6-methoxyhexanoyl chloride (**115f**, 0.24 mmol) according to General Procedure 4 except using 20% v/v DMA/THF. The crude residue was purified by silica gel chromatography (5-10% ethyl acetate/hexanes) to yield **116f** (35.0 mg, 75% yield) in 85% ee as a clear oil. The enantiomeric excess was determined by chiral SFC analysis (OD-H, 2.5 mL/min, 3% IPA in CO<sub>2</sub>,  $\lambda$  = 210 nm):  $t_R$  (minor) = 5.4 min,  $t_R$  (major) = 5.8 min.  $[\alpha]_D^{25} = -146.0^\circ$  (c = 1.14, CHCl<sub>3</sub>); <sup>1</sup>H NMR (500 MHz, CDCl<sub>3</sub>)  $\delta$  7.35 – 7.29 (m, 2H), 7.28 – 7.23 (m, 1H), 7.22 – 7.18 (m, 2H), 3.74 (q,  $J$  = 7.0 Hz, 1H), 3.31 – 3.25 (m, 5H), 2.38 – 2.32 (m, 2H), 1.57 – 1.42 (m, 2H), 1.38 (d,  $J$  = 7.0 Hz, 3H), 1.26 – 1.17 (m, 2H); <sup>13</sup>C NMR (126 MHz, CDCl<sub>3</sub>)  $\delta$  210.9, 140.7, 128.9, 127.9, 127.1, 72.5, 58.5, 53.0, 40.9, 29.3, 25.6, 23.6, 17.4; FTIR (NaCl, thin film): 2931, 2866, 2360, 1714, 1600, 1494, 1453, 1373, 1119, 1072, 1029, 761 cm<sup>-1</sup>; LRMS (ESI) calc'd for [M+H]<sup>+</sup> 235.2, found 235.2.

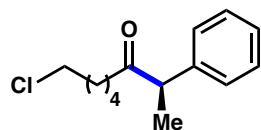
**(R)-8-Bromo-2-phenyloctan-3-one (116g)**



Prepared from (1-chloroethyl)benzene (**96**, 0.20 mmol) and 6-bromohexanoyl chloride (**115g**, 0.24 mmol) according to General Procedure 4 except using 10% v/v DMA/THF. The crude residue was purified by silica gel chromatography (2% ethyl acetate/hexanes) to yield **116g** (40.8 mg, 72% yield) in 86% ee as a clear oil. The enantiomeric excess was determined by chiral SFC analysis (OD-H, 2.5 mL/min, 3% IPA in CO<sub>2</sub>,  $\lambda$  = 210 nm):  $t_R$  (minor) = 7.3 min,  $t_R$  (major) = 8.1 min.  $[\alpha]_D^{25} = -146.8^\circ$  (c = 1.57, CHCl<sub>3</sub>); <sup>1</sup>H NMR (500 MHz,

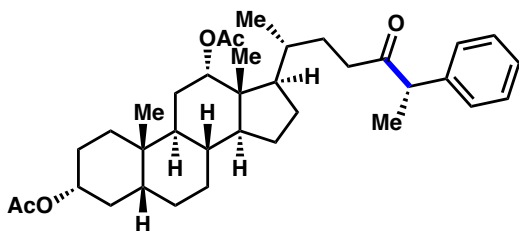
CDCl<sub>3</sub>)  $\delta$  7.37 – 7.30 (m, 2H), 7.29 – 7.24 (m, 1H), 7.23 – 7.18 (m, 2H), 3.74 (q,  $J$  = 7.0 Hz, 1H), 3.32 (t,  $J$  = 6.8 Hz, 2H), 2.46 – 2.28 (m, 2H), 1.80 – 1.70 (m, 2H), 1.56 – 1.44 (m, 2H), 1.39 (d,  $J$  = 7.0 Hz, 3H), 1.37 – 1.24 (m, 2H); <sup>13</sup>C NMR (126 MHz, CDCl<sub>3</sub>)  $\delta$  210.5, 140.6, 128.9, 127.9, 127.2, 53.1, 40.6, 33.6, 32.4, 27.5, 22.9, 17.4; FTIR (NaCl, thin film): 2932, 2867, 1713, 1600, 1494, 1453, 1373, 1252, 1069, 1029, 761 cm<sup>-1</sup>; LRMS (ESI) calc'd for [M+H]<sup>+</sup> 283.1, found 283.1.

**(R)-8-Chloro-2-phenyloctan-3-one (116h)**



Prepared from (1-chloroethyl)benzene (**96**, 0.20 mmol) and 6-chlorohexanoyl chloride (**115h**, 0.24 mmol) according to General Procedure 4 except using 20% v/v DMA/THF. The crude residue was purified by silica gel chromatography (2% ethyl acetate/hexanes) to yield **116h** (36.3 mg, 76% yield) in 92% ee as a clear oil. The enantiomeric excess was determined by chiral SFC analysis (OD-H, 2.5 mL/min, 3% IPA in CO<sub>2</sub>,  $\lambda$  = 210 nm):  $t_R$  (minor) = 5.8 min,  $t_R$  (major) = 6.5 min.  $[\alpha]_D^{25}$  = -163.3° (c = 0.78, CHCl<sub>3</sub>); <sup>1</sup>H NMR (500 MHz, CDCl<sub>3</sub>)  $\delta$  7.36 – 7.30 (m, 2H), 7.29 – 7.23 (m, 1H), 7.23 – 7.18 (m, 2H), 3.74 (q,  $J$  = 7.0 Hz, 1H), 3.45 (t,  $J$  = 6.7 Hz, 2H), 2.46 – 2.28 (m, 2H), 1.73 – 1.61 (m, 2H), 1.57 – 1.44 (m, 2H), 1.39 (d,  $J$  = 7.0 Hz, 3H), 1.34 – 1.24 (m, 2H); <sup>13</sup>C NMR (126 MHz, CDCl<sub>3</sub>)  $\delta$  210.6, 140.6, 128.9, 127.8, 127.2, 53.1, 44.8, 40.6, 32.3, 26.2, 23.0, 17.4; FTIR (NaCl, thin film): 2932, 2867, 2360, 1711, 1599, 1493, 1452, 1374, 1122, 1069, 1029, 760 cm<sup>-1</sup>; LRMS (ESI) calc'd for [M+H]<sup>+</sup> 239.1, found 239.1.

**(3*R*,5*R*,8*R*,9*S*,10*S*,12*S*,13*R*,14*S*,17*R*)-10,13-Dimethyl-17-((2*R*,6*S*)-5-oxo-6-phenylheptan-2-yl)hexadecahydro-1*H*-cyclopenta[*a*]phenanthrene-3,12-diyl diacetate (**116i**)**

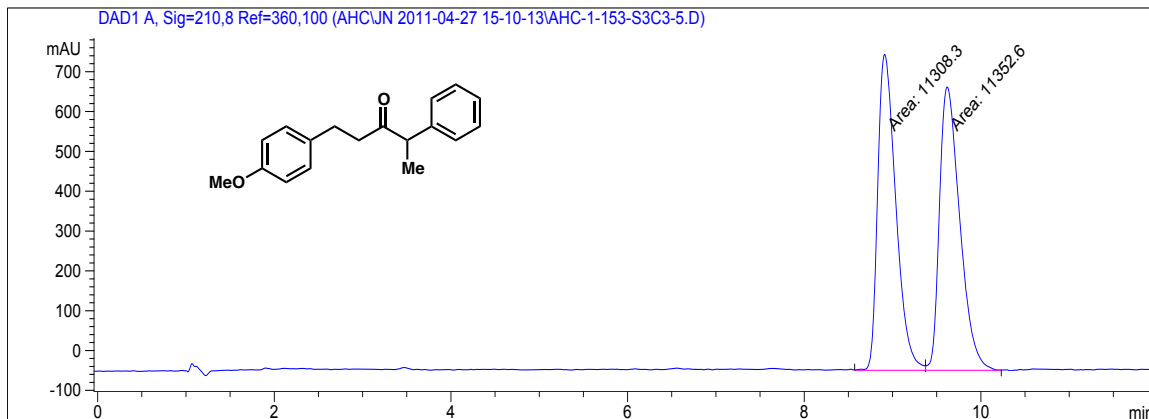


Prepared from (1-chloroethyl)benzene (**96**, 0.20 mmol) and acid chloride **115i** (0.24 mmol) according to General Procedure 4 except using 10% v/v DMA/THF and (*S,S*)-

**L32**. Following extraction, the combined organic layers were washed with sat. aq. NaHCO<sub>3</sub> (1 X 10 mL) and brine (1 X 15 mL). The crude residue was purified by silica gel chromatography (15% ethyl acetate/hexanes) to yield **116i** (72.5 mg, 64% yield) as a fluffy white solid and as a 14:1 mixture of diastereomers (determined by NMR analysis of the purified product).  $[\alpha]_D^{25} = 146.0^\circ$  ( $c = 2.05$ , CHCl<sub>3</sub>); <sup>1</sup>H NMR (500 MHz, Acetone-*d*<sub>6</sub>)  $\delta$  7.39 – 7.31 (m, 2H), 7.30 – 7.22 (m, 3H), 4.99 (t,  $J = 3.0$  Hz, 1H), 4.63 (tt,  $J = 11.4$ , 4.6 Hz, 1H), 3.90 (q,  $J = 6.9$  Hz, 1H), 2.45 – 2.29 (m, 2H), 2.01 (s, 3H), 1.98 – 1.40 (m, 17H), 1.37 – 0.99 (m, 13H), 0.95 (s, 3H), 0.72 (s, 3H), 0.69 (d,  $J = 6.9$  Hz, 3H); <sup>13</sup>C NMR (126 MHz, CDCl<sub>3</sub>)  $\delta$  209.8, 169.5, 169.3, 141.3, 128.7, 127.8, 126.9, 75.2, 73.5, 52.4, 49.4, 47.4, 44.9, 41.7, 37.3, 35.6, 34.6, 34.5, 34.3, 33.9, 32.1, 29.6, 27.0, 26.7, 26.4, 25.8, 25.3, 23.2, 22.5, 20.4, 20.3, 17.1, 16.9, 11.8; FTIR (NaCl, thin film): 2937, 2869, 1735, 1493, 1452, 1377, 1363, 1245, 1194, 1029, 971 cm<sup>-1</sup>; LRMS (ESI) calc'd for [M+H<sub>2</sub>O]<sup>+</sup> 582.4, found 582.4.

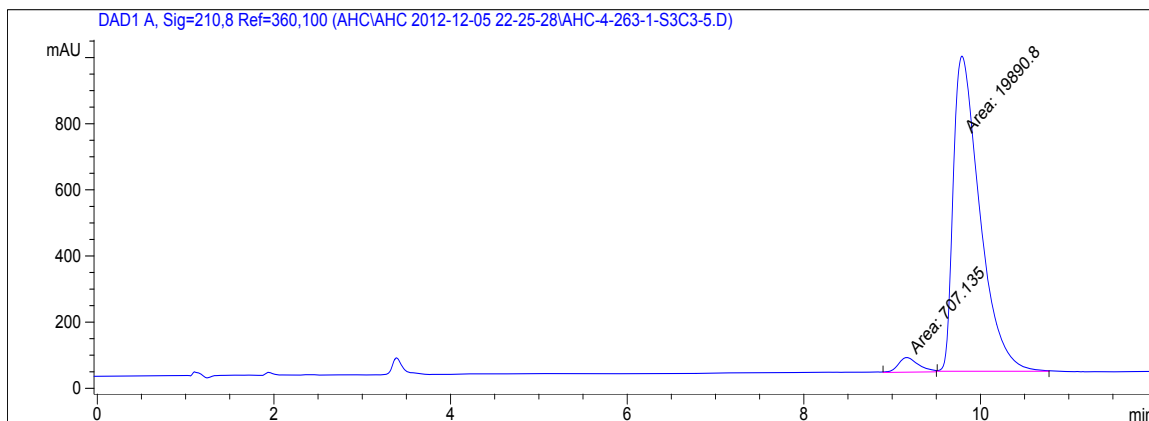
### 2.5.4 SFC Traces of Racemic and Enantioenriched Ketone Products

#### 112a racemic



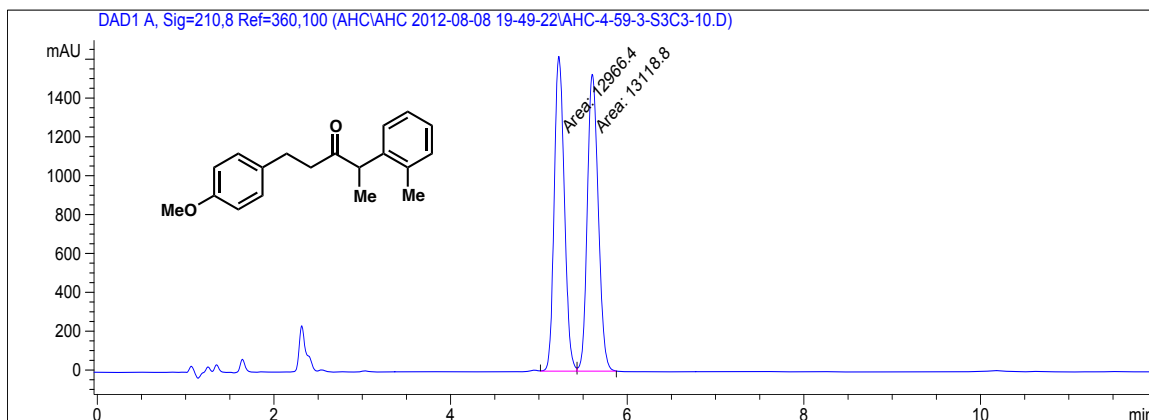
Peak #	RetTime [min]	Type	Width [min]	Area [mAU*s]	Height [mAU]	Area %
1	8.911	MM	0.2376	1.13083e4	793.28162	49.9021
2	9.619	MM	0.2660	1.13526e4	711.29791	50.0979

#### 112a enantioenriched, 93% ee



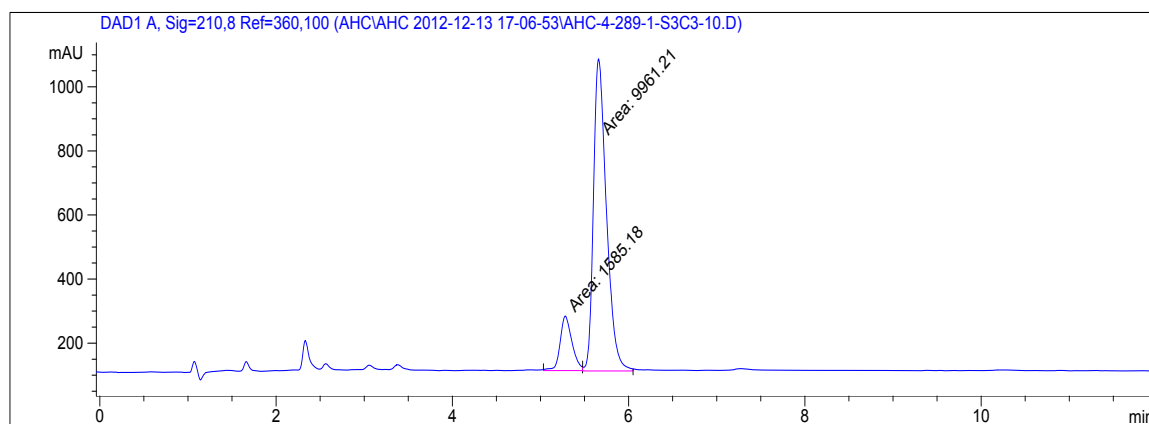
Peak #	RetTime [min]	Type	Width [min]	Area [mAU*s]	Height [mAU]	Area %
1	9.164	MM	0.2646	707.13519	44.53406	3.4330
2	9.790	MM	0.3479	1.98908e4	952.85913	96.5670

**112b** racemic



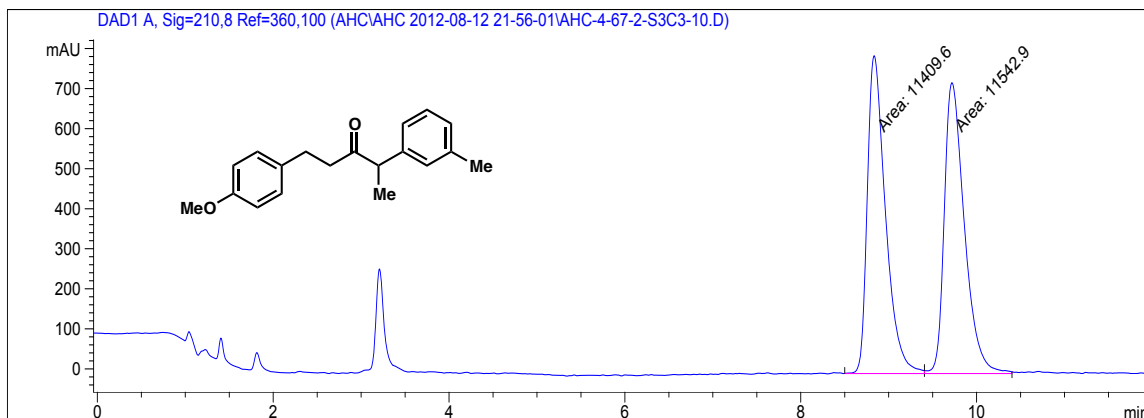
Peak #	RetTime [min]	Type	Width [min]	Area [mAU*s]	Height [mAU]	Area %
1	5.225	MM	0.1332	1.29664e4	1622.72693	49.7079
2	5.604	MM	0.1430	1.31188e4	1529.25037	50.2921

**112b** enantioenriched, 72% ee



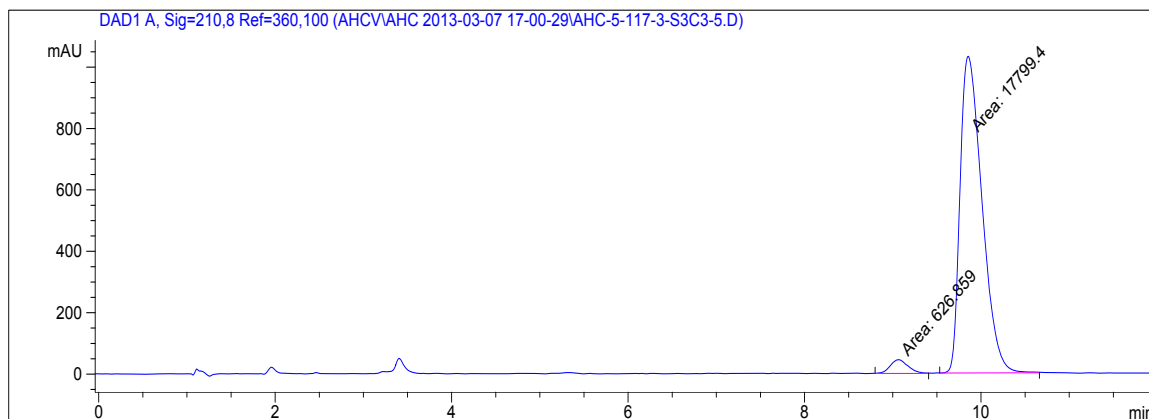
Peak #	RetTime [min]	Type	Width [min]	Area [mAU*s]	Height [mAU]	Area %
1	5.282	MM	0.1551	1585.18311	170.37230	13.7288
2	5.659	MM	0.1703	9961.21484	974.66937	86.2712

**112c racemic**



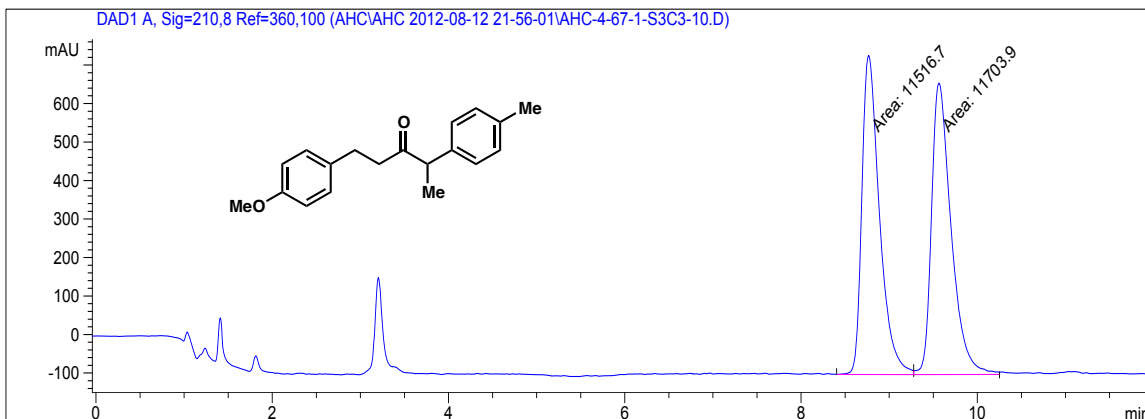
Peak #	RetTime [min]	Type	Width [min]	Area [mAU*s]	Height [mAU]	Area %
1	8.835	MM	0.2395	1.14096e4	794.09918	49.7095
2	9.720	MM	0.2647	1.15429e4	726.79602	50.2905

**112c enantioenriched, 93% ee**



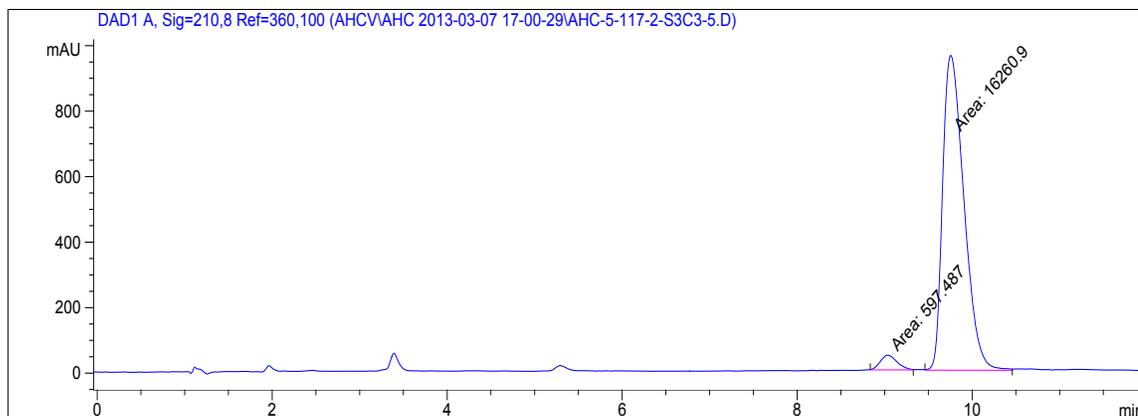
Peak #	RetTime [min]	Type	Width [min]	Area [mAU*s]	Height [mAU]	Area %
1	9.064	MM	0.2335	626.85852	44.73974	3.4020
2	9.854	MM	0.2876	1.77994e4	1031.51978	96.5980

**112d** racemic



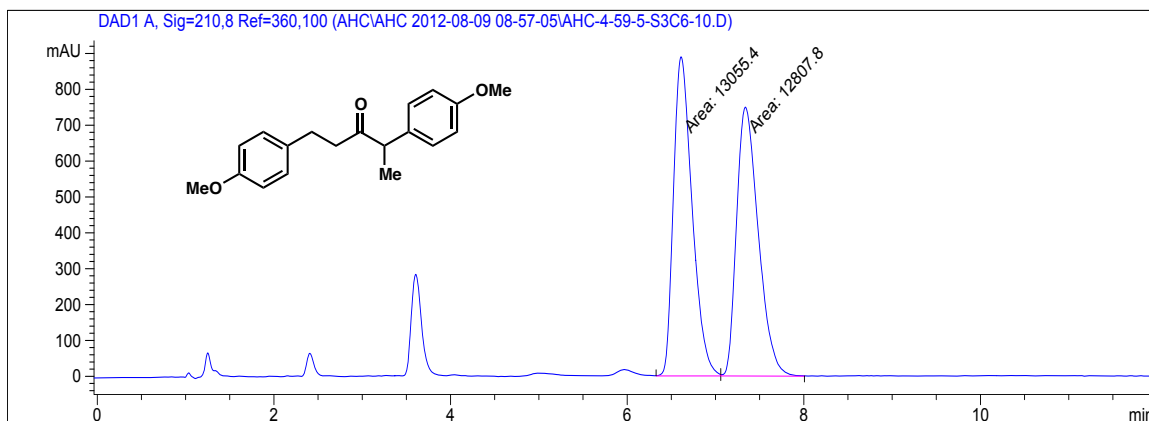
Peak #	RetTime [min]	Type	Width [min]	Area [mAU*s]	Height [mAU]	Area %
1	8.766	MM	0.2315	1.15167e4	829.08398	49.5970
2	9.564	MM	0.2576	1.17039e4	757.13312	50.4030

**112d** enantioenriched, 93% ee



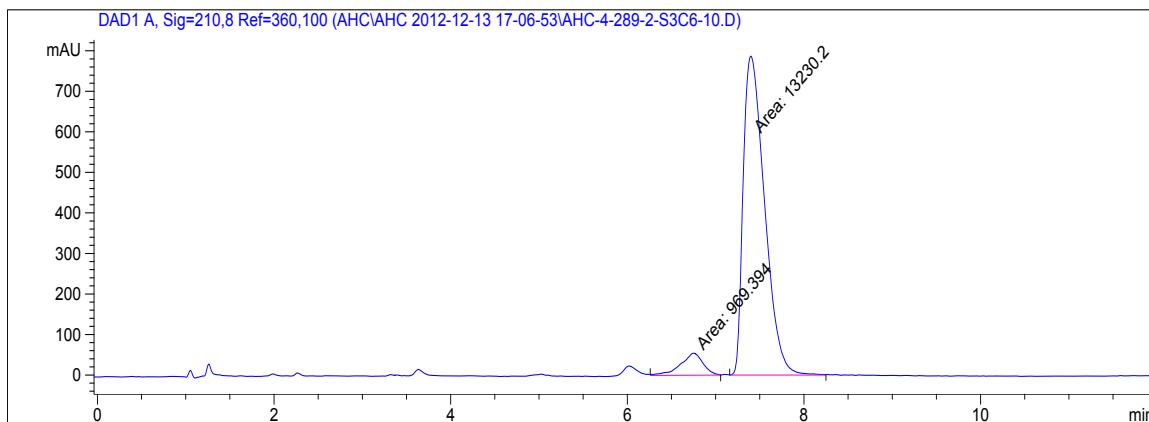
Peak #	RetTime [min]	Type	Width [min]	Area [mAU*s]	Height [mAU]	Area %
1	9.036	MM	0.2206	597.48749	45.14814	3.5442
2	9.756	MM	0.2819	1.62609e4	961.42609	96.4558

**112e racemic**



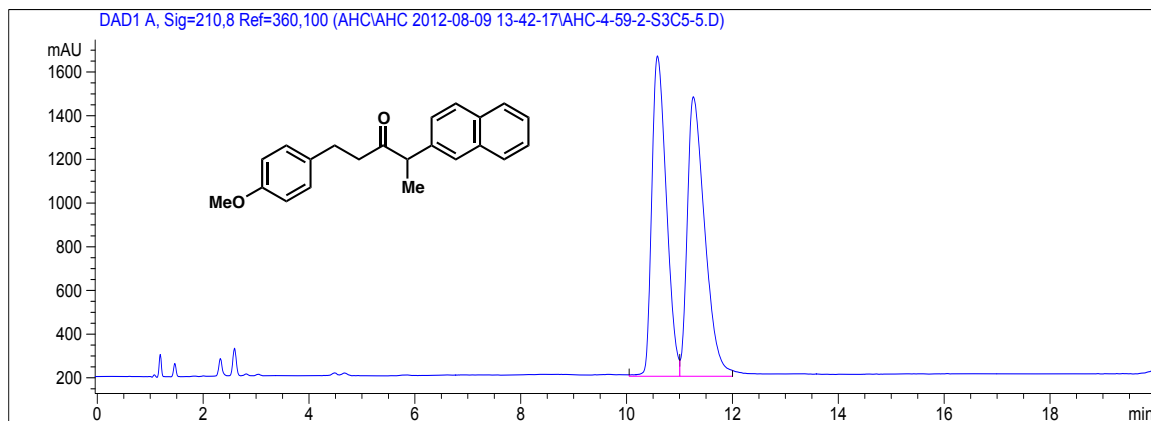
Peak #	RetTime [min]	Type	Width [min]	Area [mAU*s]	Height [mAU]	Area %
1	6.610	MM	0.2445	1.30554e4	889.75983	50.4785
2	7.339	MM	0.2848	1.28078e4	749.64392	49.5215

**112e enantioenriched, 86% ee**



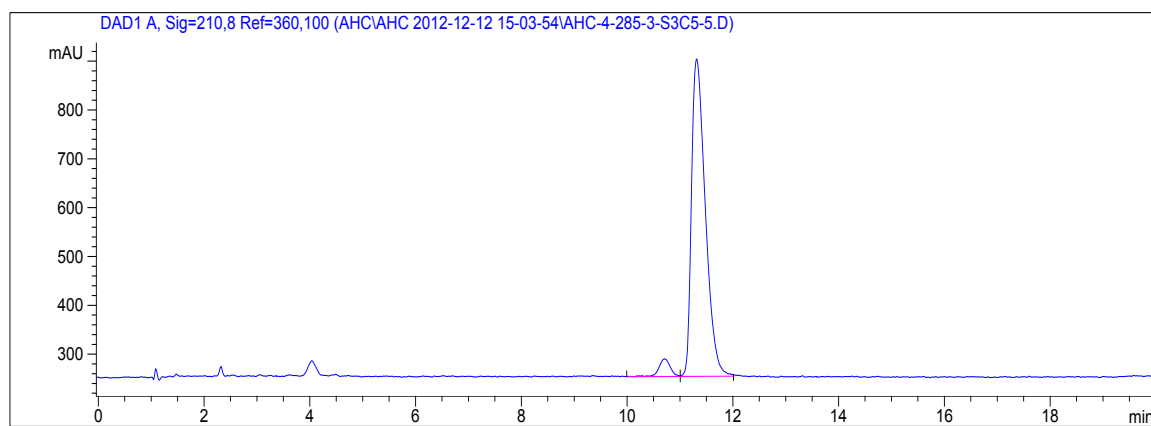
Peak #	RetTime [min]	Type	Width [min]	Area [mAU*s]	Height [mAU]	Area %
1	6.750	MM	0.2970	969.39368	54.40509	6.8269
2	7.399	MM	0.2801	1.32302e4	787.11755	93.1731

**112f** racemic



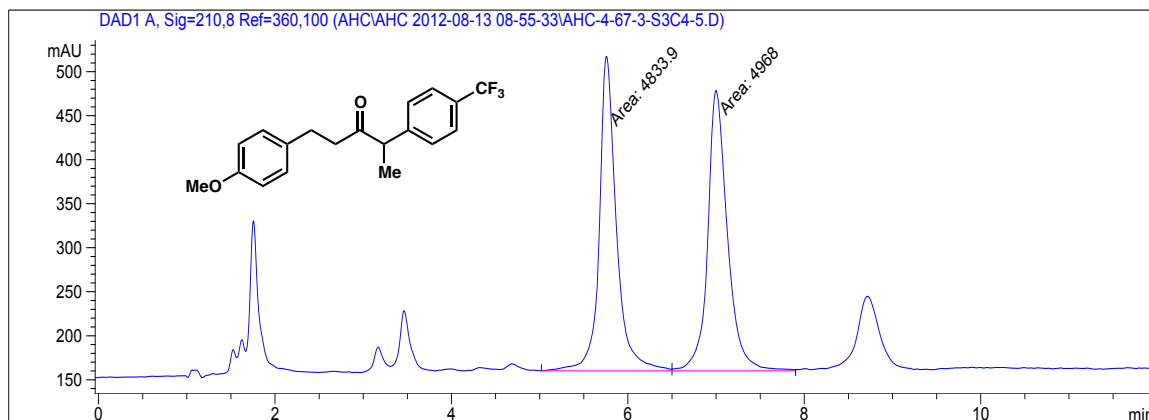
Peak #	RetTime [min]	Type	Width [min]	Area [mAU*s]	Height [mAU]	Area %
1	10.584	VV	0.3032	2.80499e4	1465.87903	48.9009
2	11.263	VBA	0.3473	2.93108e4	1279.38000	51.0991

**112f** enantioenriched, 91% ee



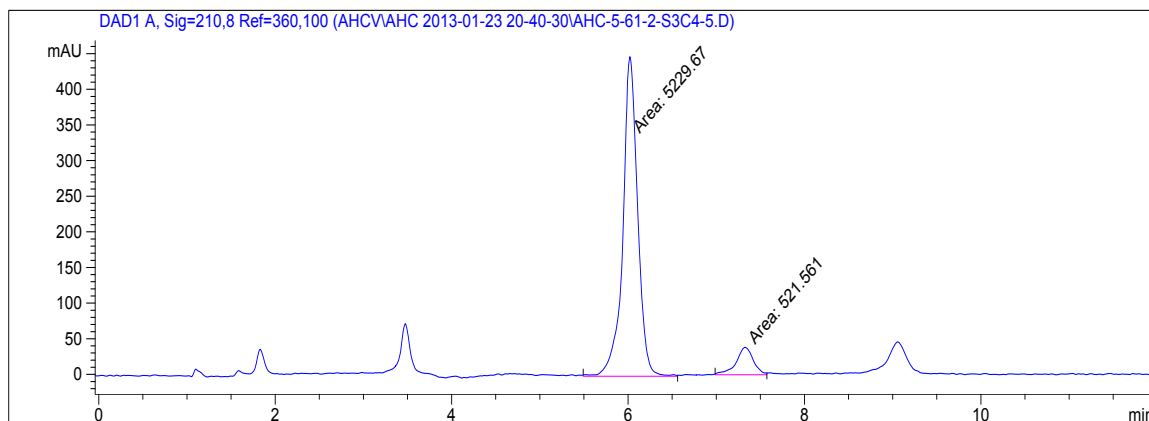
Peak #	RetTime [min]	Type	Width [min]	Area [mAU*s]	Height [mAU]	Area %
1	10.708	VV	0.2364	545.21796	36.05198	4.4227
2	11.316	VBA	0.2797	1.17825e4	649.47711	95.5773

**112h** racemic



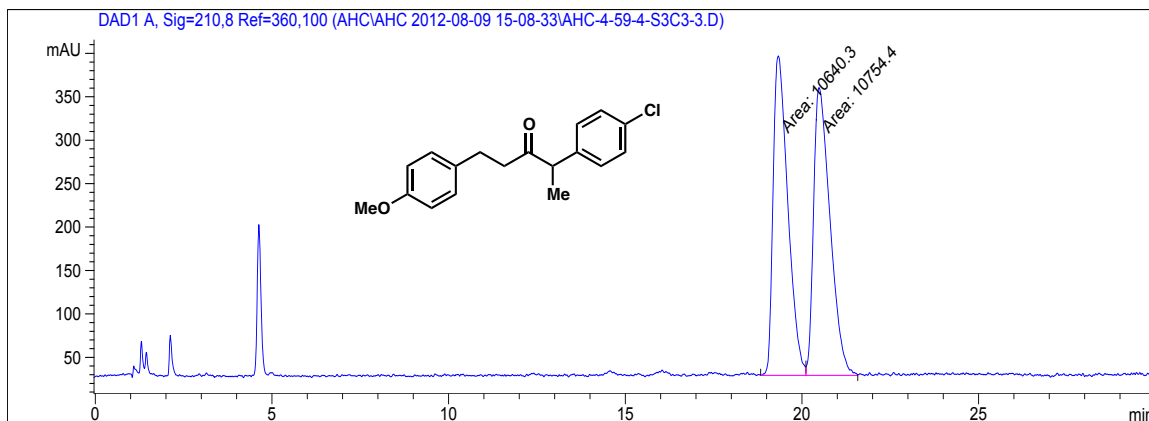
Peak #	RetTime [min]	Type	Width [min]	Area [mAU*s]	Height [mAU]	Area %
1	5.757	MM	0.2253	4833.89893	357.65167	49.3159
2	6.999	MM	0.2598	4967.99951	318.66217	50.6841

**112h** enantioenriched, 82% ee



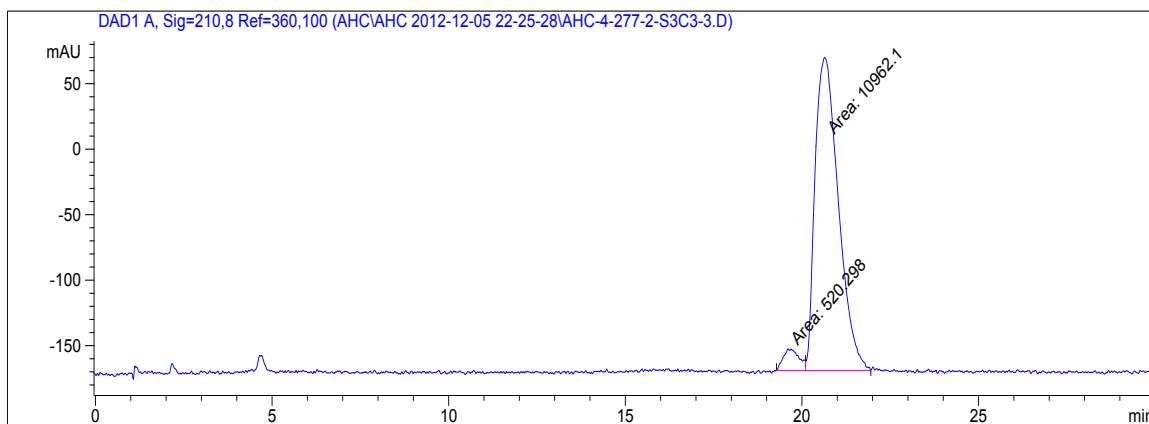
Peak #	RetTime [min]	Type	Width [min]	Area [mAU*s]	Height [mAU]	Area %
1	6.020	MM	0.1943	5229.66602	448.69507	90.9313
2	7.327	MM	0.2264	521.56061	38.39449	9.0687

**112i** racemic

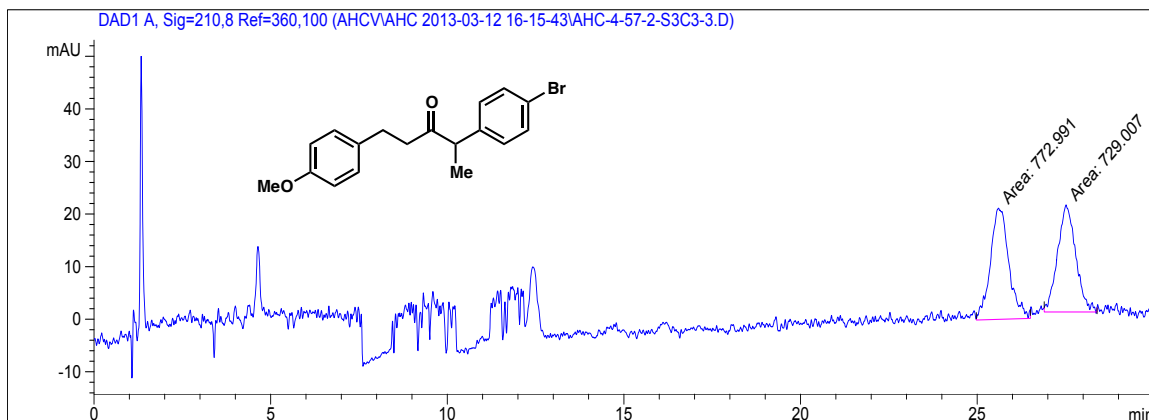


Peak #	RetTime [min]	Type	Width [min]	Area [mAU*s]	Height [mAU]	Area %
1	19.330	MM	0.4822	1.06403e4	367.73328	49.7335
2	20.480	MM	0.5409	1.07544e4	331.38272	50.2665

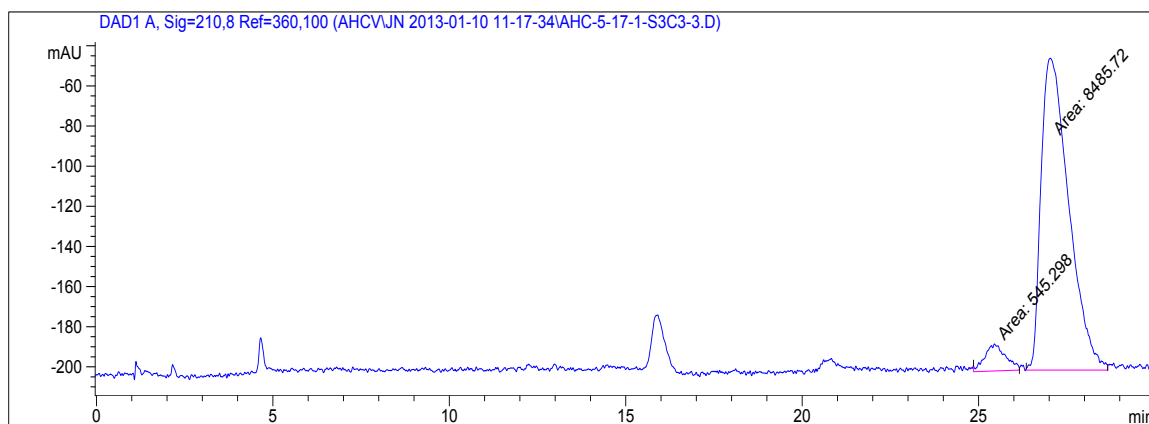
**112i** enantioenriched, 91% ee



Peak #	RetTime [min]	Type	Width [min]	Area [mAU*s]	Height [mAU]	Area %
1	19.605	MM	0.5260	520.29840	16.48751	4.5313
2	20.639	MM	0.7645	1.09621e4	238.97188	95.4687

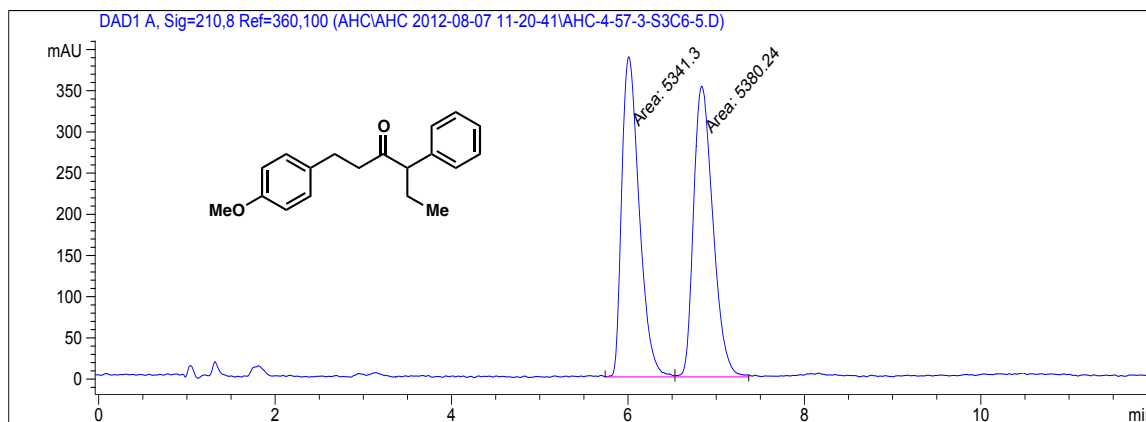
**112j** racemic

Peak #	RetTime [min]	Type	Width [min]	Area [mAU*s]	Height [mAU]	Area %
1	25.604	MM	0.6090	772.99146	21.15472	51.4642
2	27.518	MM	0.5962	729.00677	20.37799	48.5358

**112j** enantioenriched, 86% ee

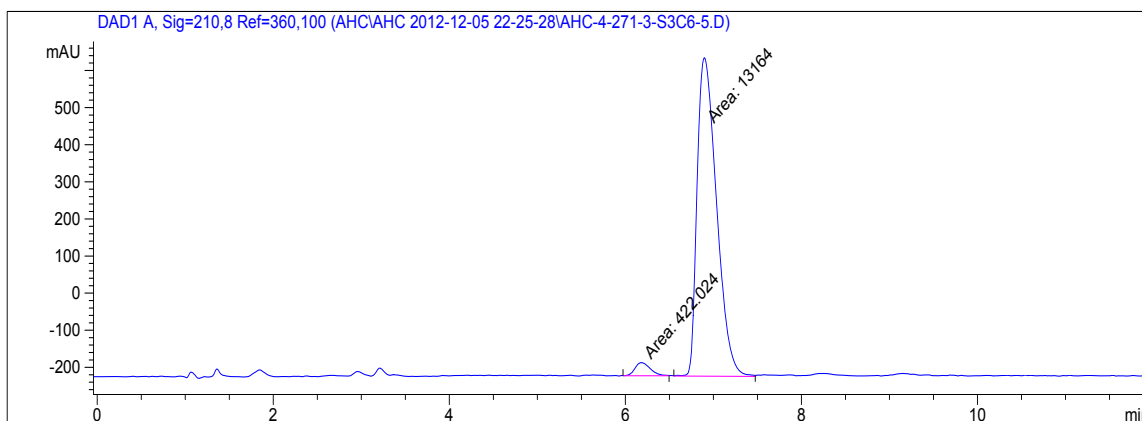
Peak #	RetTime [min]	Type	Width [min]	Area [mAU*s]	Height [mAU]	Area %
1	25.449	MM	0.6766	545.29791	13.43136	6.0381
2	27.030	MM	0.9105	8485.72363	155.33823	93.9619

**114a** racemic



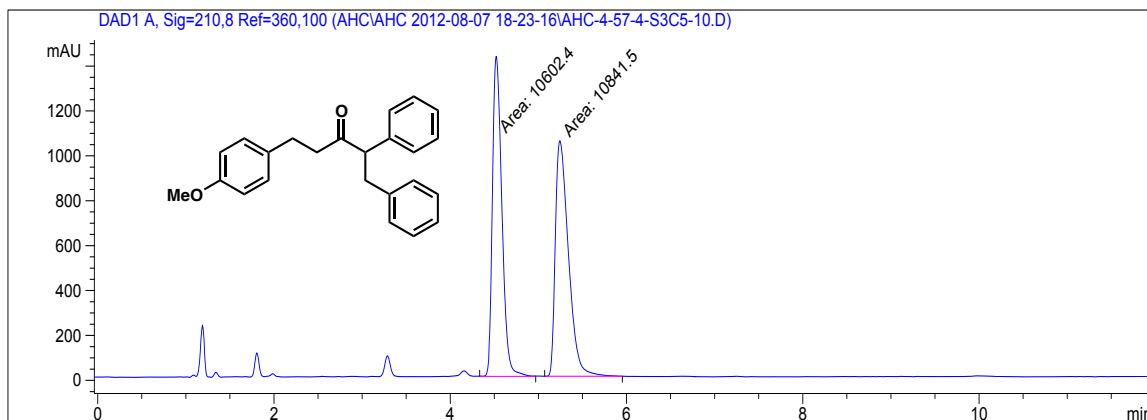
Peak #	RetTime [min]	Type	Width [min]	Area [mAU*s]	Height [mAU]	Area %
1	6.009	MM	0.2291	5341.29736	388.53415	49.8184
2	6.837	MM	0.2540	5380.24316	353.03430	50.1816

**114a** enantioenriched, 94% ee



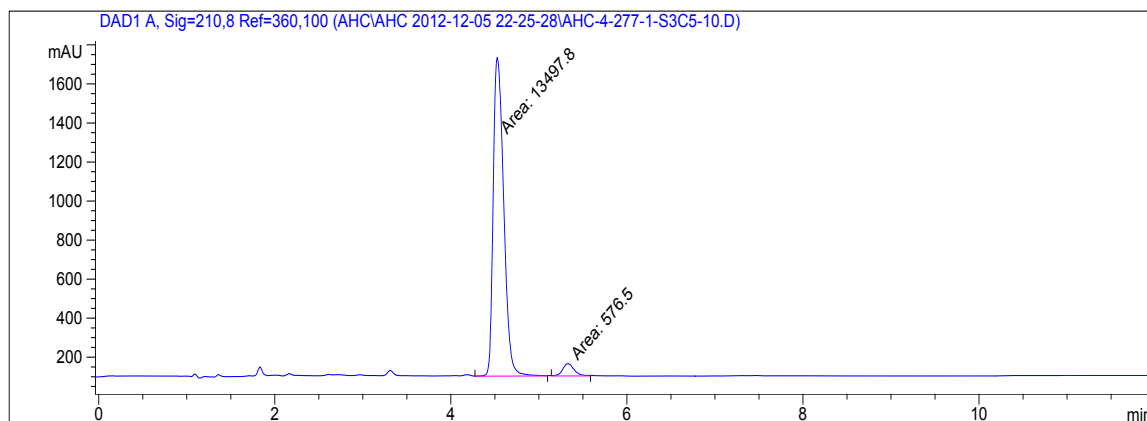
Peak #	RetTime [min]	Type	Width [min]	Area [mAU*s]	Height [mAU]	Area %
1	6.179	MM	0.1983	422.02435	35.47295	3.1063
2	6.898	MM	0.2556	1.31640e4	858.35632	96.8937

**114b** racemic

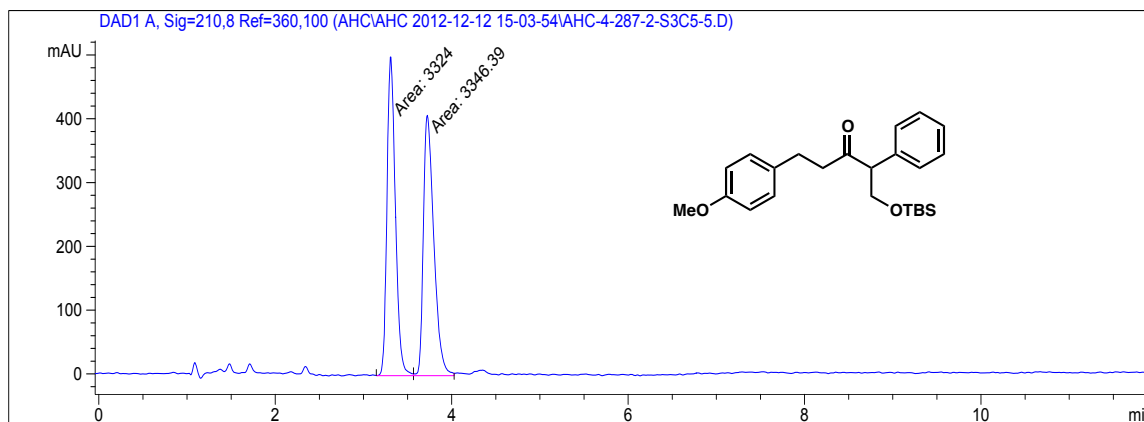


Peak #	RetTime [min]	Type	Width [min]	Area [mAU*s]	Height [mAU]	Area %
1	4.522	MM	0.1239	1.06024e4	1426.70251	49.4425
2	5.244	MM	0.1721	1.08415e4	1050.01685	50.5575

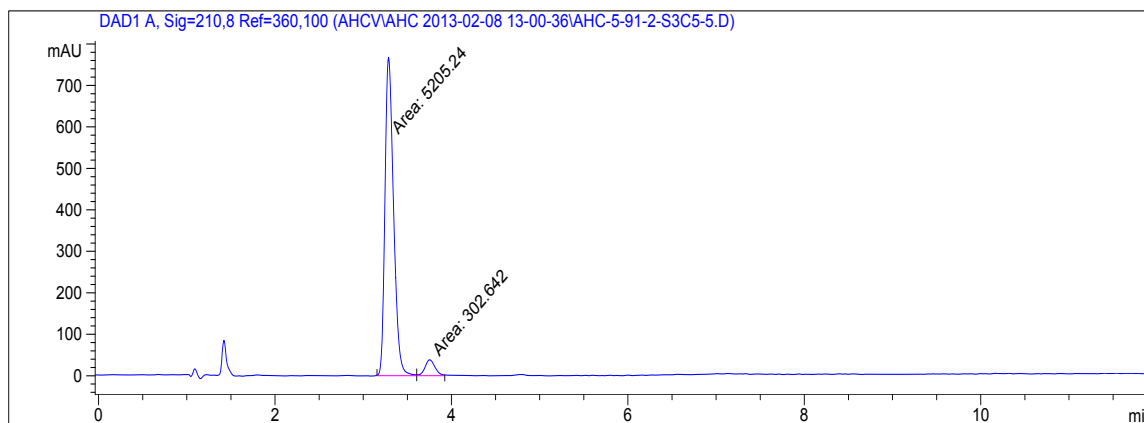
**114b** enantioenriched, 92% ee



Peak #	RetTime [min]	Type	Width [min]	Area [mAU*s]	Height [mAU]	Area %
1	4.528	MM	0.1377	1.34978e4	1634.09204	95.9039
2	5.330	MM	0.1513	576.49988	63.49461	4.0961

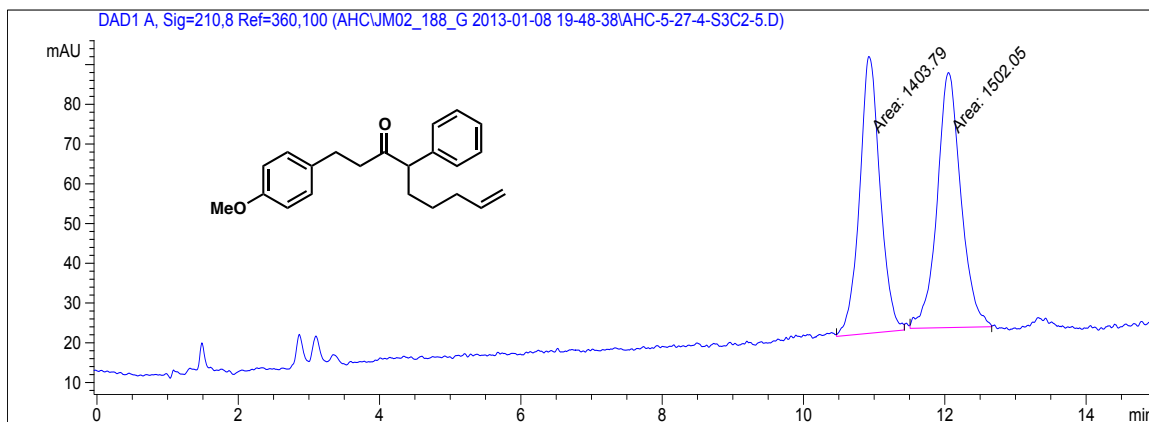
**114c** racemic

Peak #	RetTime [min]	Type	Width [min]	Area [mAU*s]	Height [mAU]	Area %
1	3.308	MM	0.1105	3324.00073	501.56870	49.8322
2	3.723	MM	0.1365	3346.39185	408.55920	50.1678

**114c** enantioenriched, 89% ee

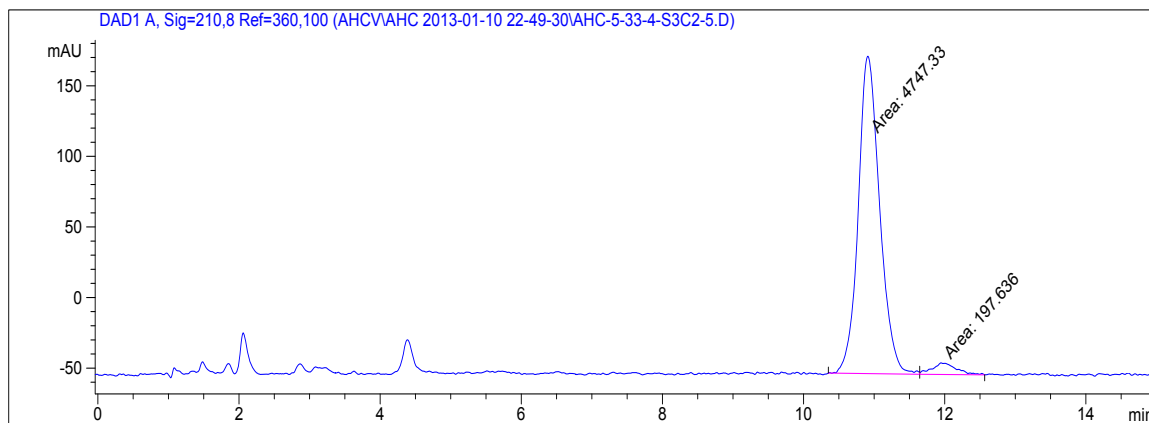
Peak #	RetTime [min]	Type	Width [min]	Area [mAU*s]	Height [mAU]	Area %
1	3.287	MM	0.1129	5205.23877	768.54687	94.5053
2	3.754	MM	0.1313	302.64224	38.40394	5.4947

**114e racemic**

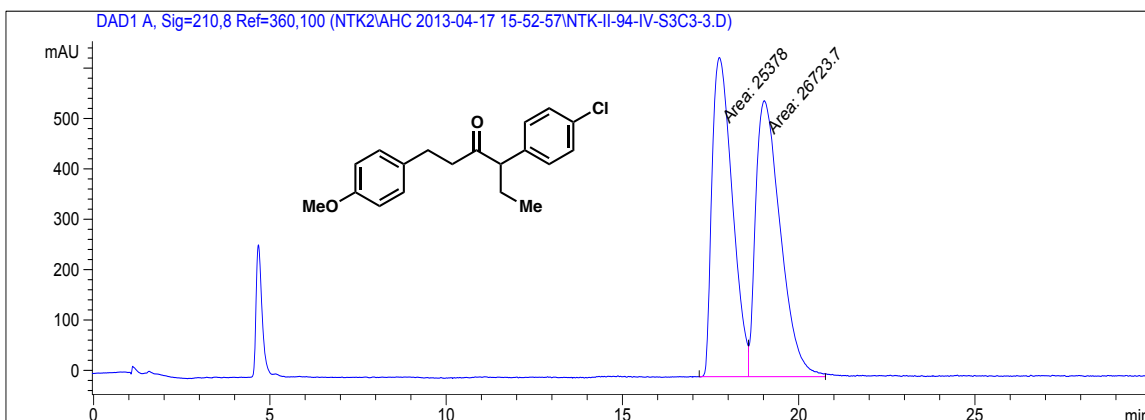


Peak #	RetTime [min]	Type	Width [min]	Area [mAU*s]	Height [mAU]	Area %
1	10.925	MM	0.3357	1403.79077	69.69751	48.3093
2	12.051	MM	0.3898	1502.04858	64.21613	51.6907

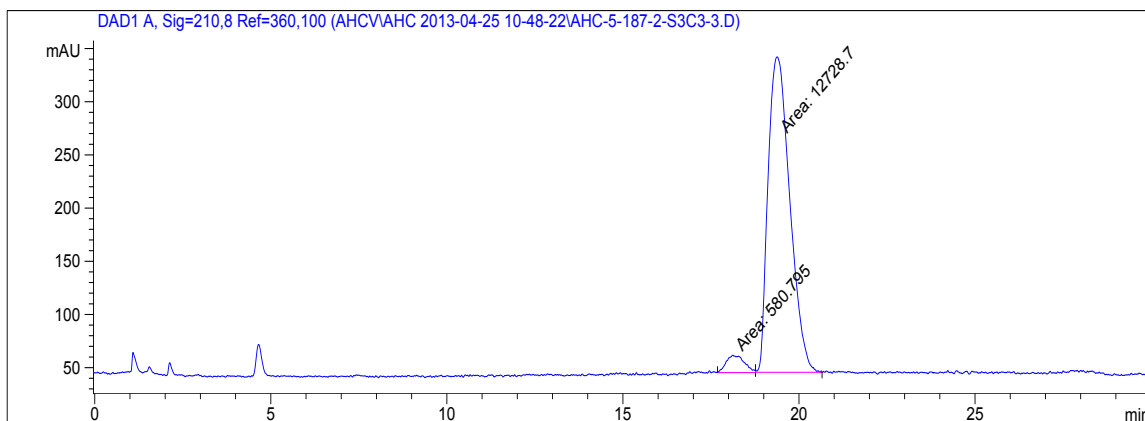
**114e enantioenriched, 92% ee**



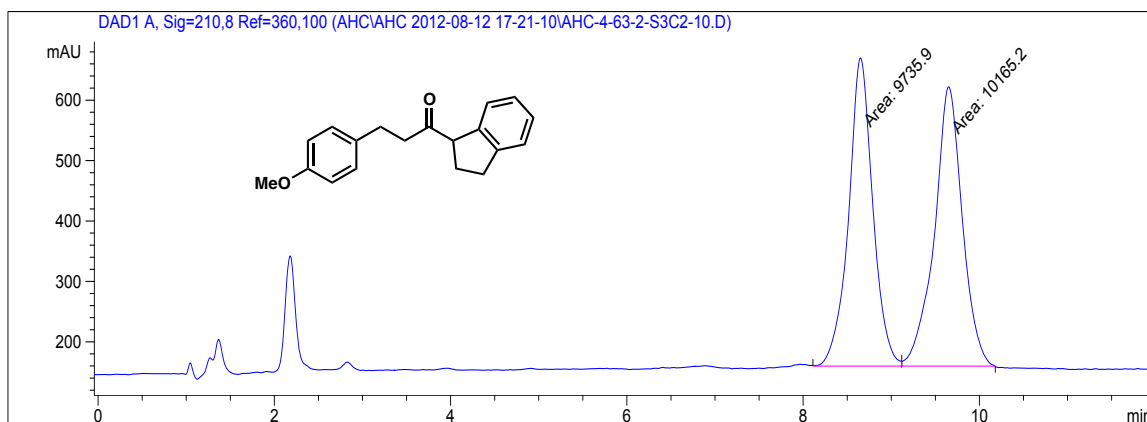
Peak #	RetTime [min]	Type	Width [min]	Area [mAU*s]	Height [mAU]	Area %
1	10.911	MM	0.3519	4747.33496	224.86562	96.0033
2	11.946	MM	0.4028	197.63620	8.17804	3.9967

**114g** racemic

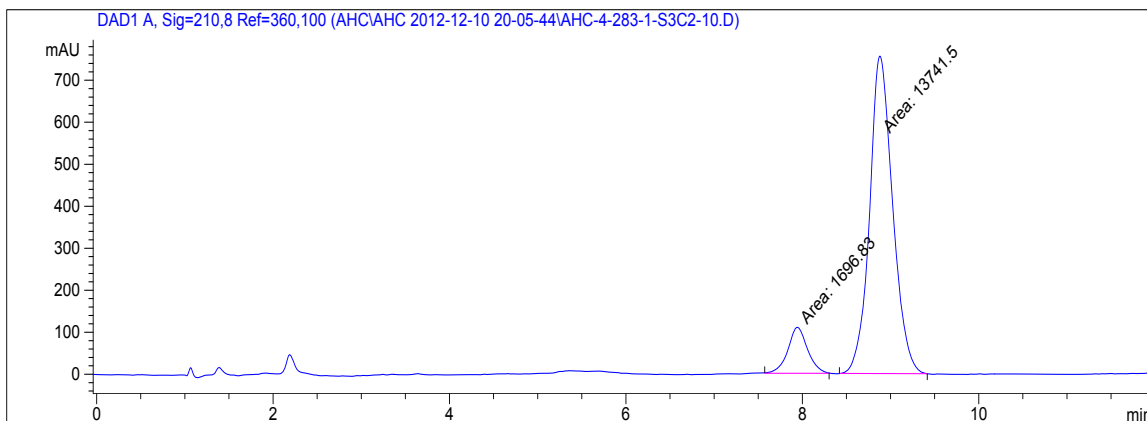
Peak #	RetTime [min]	Type	Width [min]	Area [mAU*s]	Height [mAU]	Area %
1	17.749	MM	0.6673	2.53780e4	633.81763	48.7086
2	19.022	MM	0.8126	2.67237e4	548.09839	51.2914

**114g** enantioenriched, 91% ee

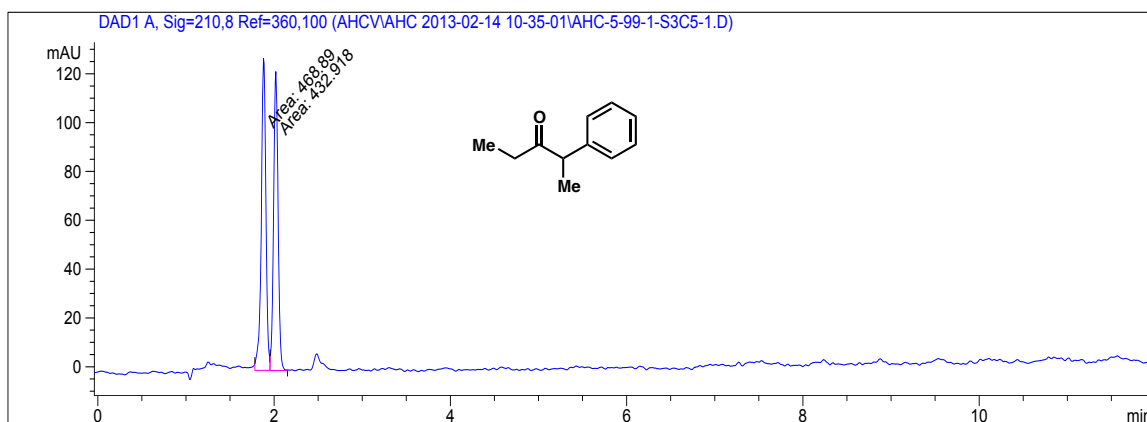
Peak #	RetTime [min]	Type	Width [min]	Area [mAU*s]	Height [mAU]	Area %
1	18.118	MM	0.5944	580.79498	16.28630	4.3637
2	19.381	MM	0.7154	1.27287e4	296.55020	95.6363

**114h** racemic

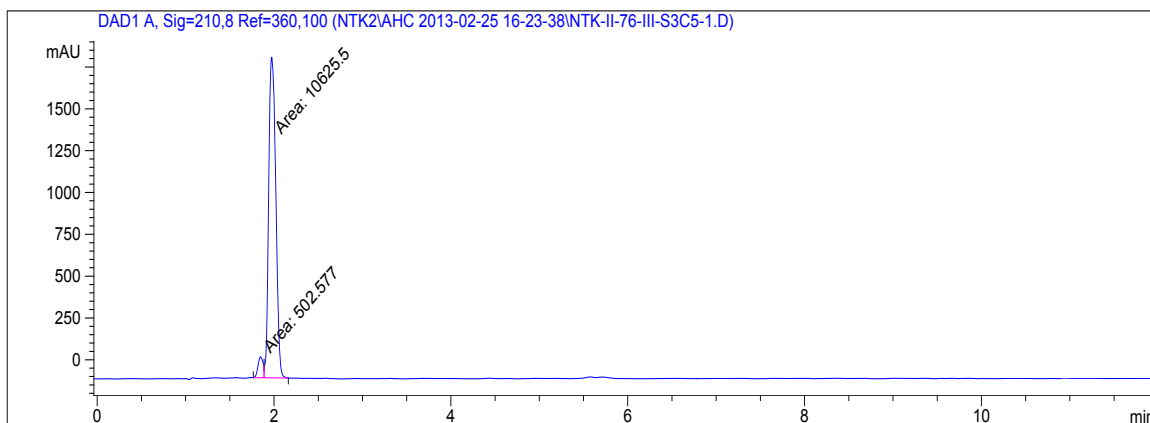
Peak #	RetTime [min]	Type	Width [min]	Area [mAU*s]	Height [mAU]	Area %
1	8.651	MM	0.3179	9735.89941	510.35568	48.9213
2	9.651	MM	0.3663	1.01652e4	462.52780	51.0787

**114h** enantioenriched, 78% ee

Peak #	RetTime [min]	Type	Width [min]	Area [mAU*s]	Height [mAU]	Area %
1	7.943	MM	0.2586	1696.82703	109.37256	10.9910
2	8.880	MM	0.3030	1.37415e4	755.81702	89.0090

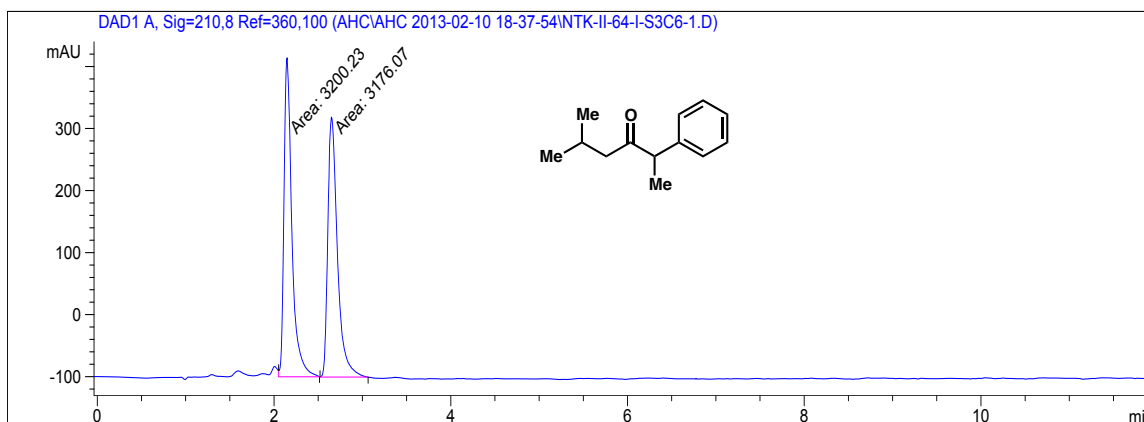
**116a** racemic

Peak #	RetTime [min]	Type	Width [min]	Area [mAU*s]	Height [mAU]	Area %
1	1.882	MM	0.0607	468.89008	128.69202	51.9944
2	2.020	MM	0.0587	432.91794	122.82136	48.0056

**116a** enantioenriched, 89% ee

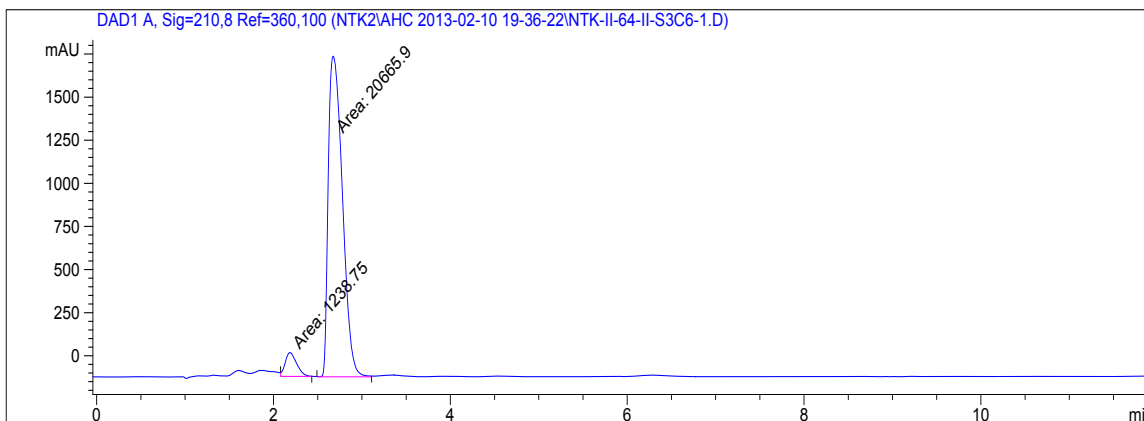
Peak #	RetTime [min]	Type	Width [min]	Area [mAU*s]	Height [mAU]	Area %
1	1.848	MM	0.0672	502.57666	124.59120	4.5163
2	1.973	MM	0.0923	1.06255e4	1918.92407	95.4837

**116b** racemic



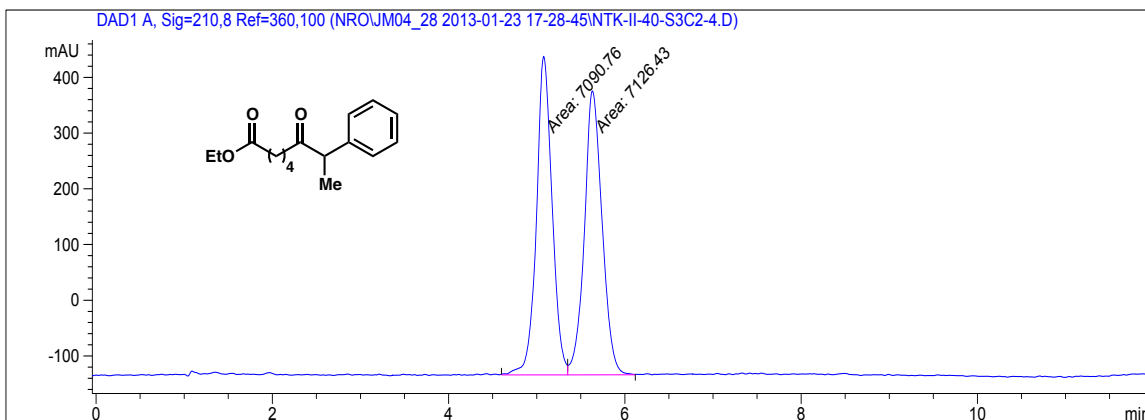
Peak #	RetTime [min]	Type	Width [min]	Area [mAU*s]	Height [mAU]	Area %
1	2.147	MM	0.1035	3200.22705	515.47467	50.1894
2	2.651	MM	0.1261	3176.07007	419.70117	49.8106

**116b** enantioenriched, 88% ee



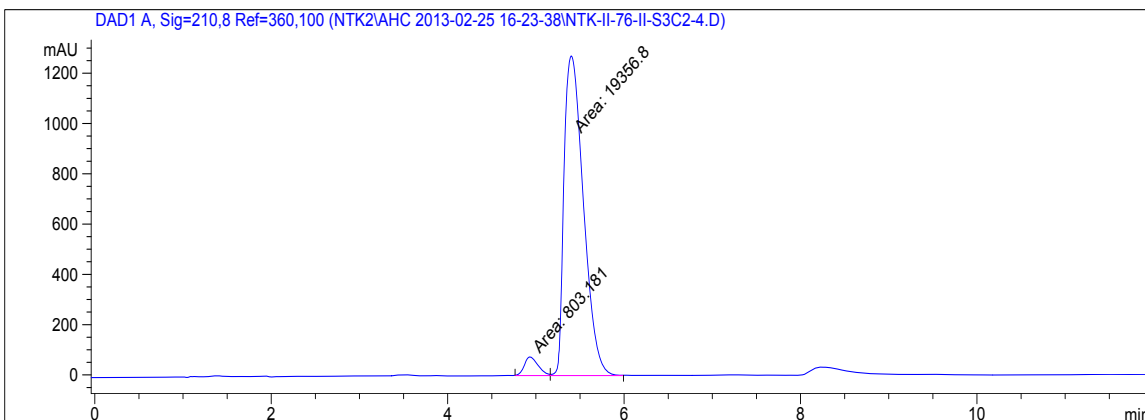
Peak #	RetTime [min]	Type	Width [min]	Area [mAU*s]	Height [mAU]	Area %
1	2.186	MM	0.1493	1238.74841	138.30533	5.6552
2	2.675	MM	0.1852	2.06659e4	1859.45630	94.3448

**116e** racemic

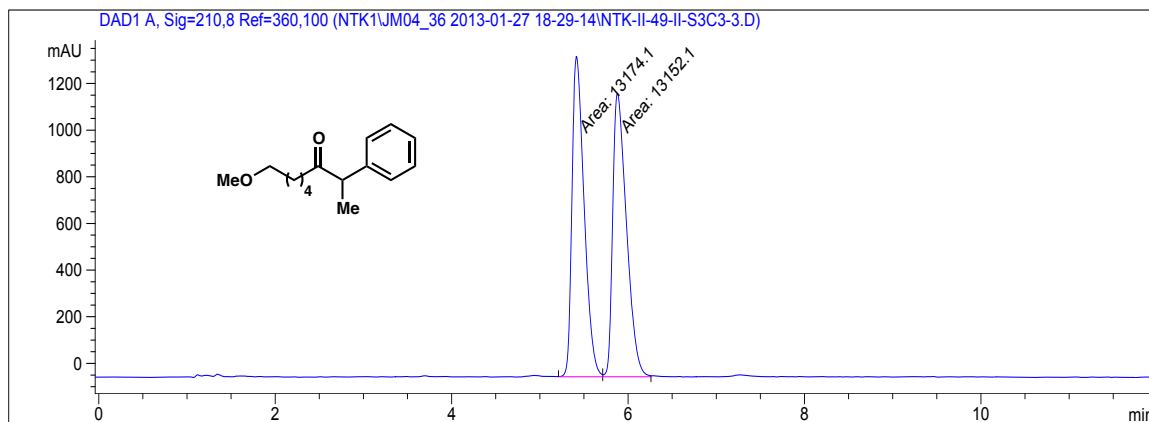
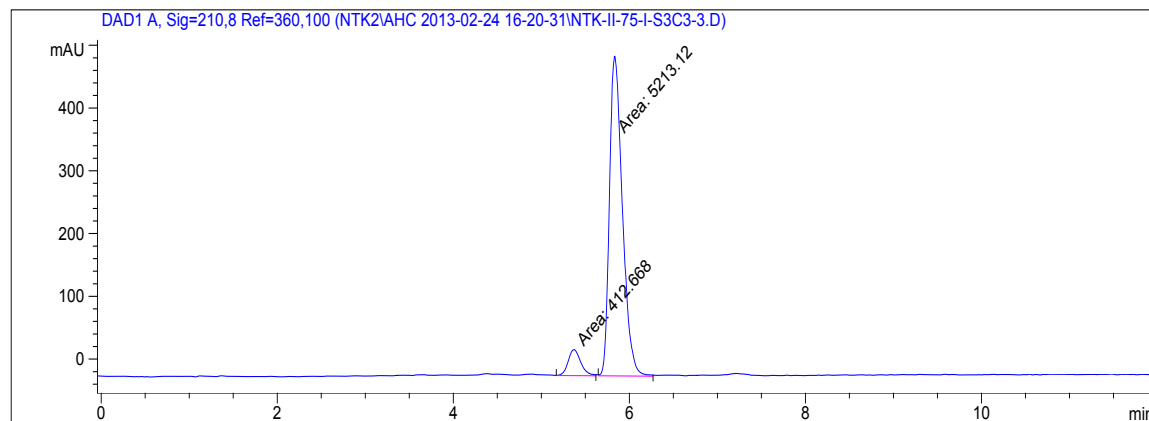


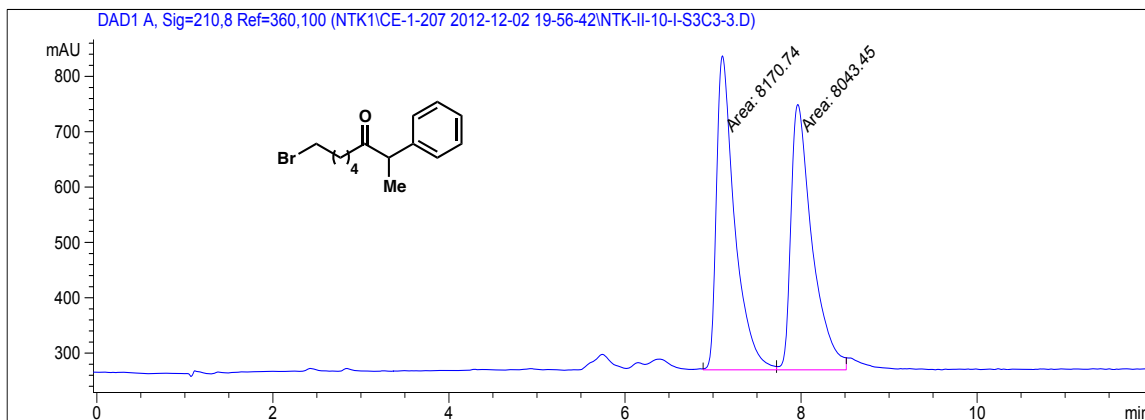
Peak #	RetTime [min]	Type	Width [min]	Area [mAU*s]	Height [mAU]	Area %
1	5.079	MM	0.2066	7090.76221	572.01874	49.8746
2	5.631	MM	0.2330	7126.43066	509.79788	50.1254

**116e** enantioenriched, 92% ee

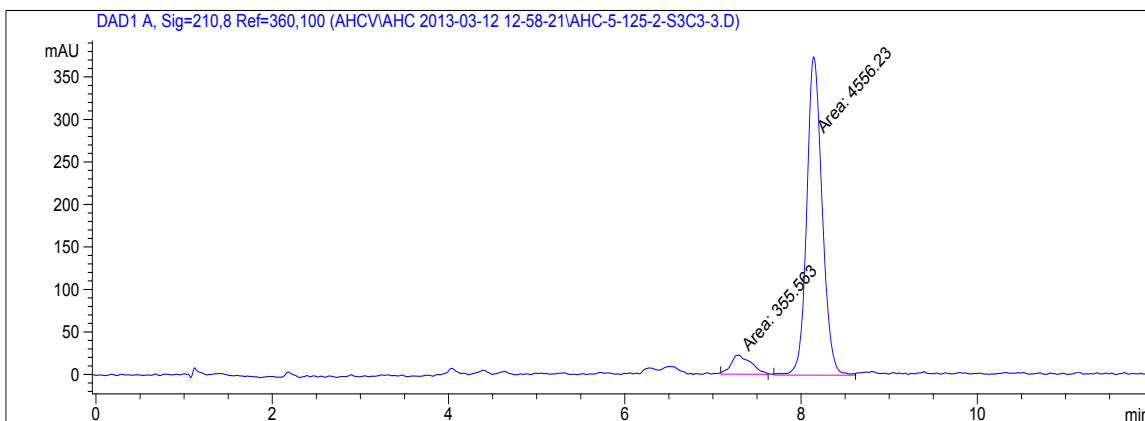


Peak #	RetTime [min]	Type	Width [min]	Area [mAU*s]	Height [mAU]	Area %
1	4.932	MM	0.1805	803.18146	74.16300	3.9840
2	5.401	MM	0.2538	1.93568e4	1271.19958	96.0160

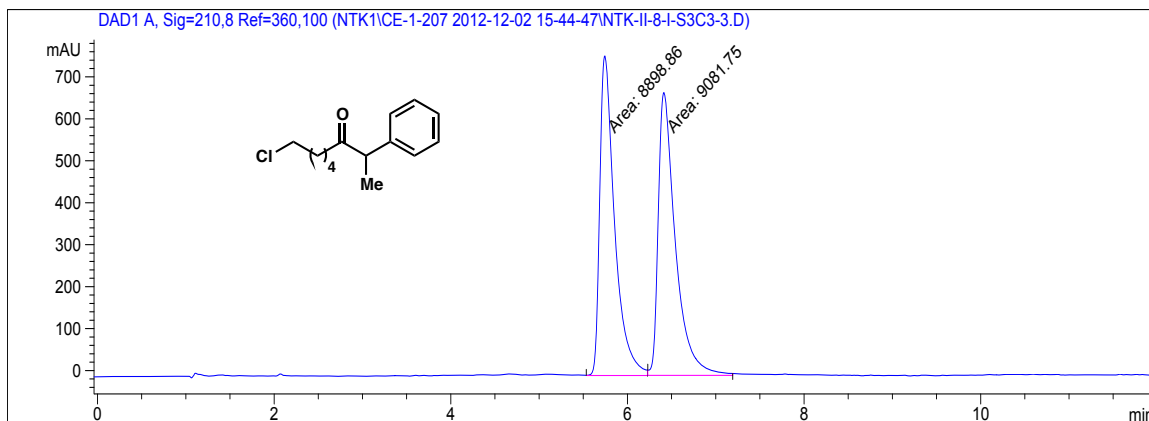
**116f** racemic**116f** enantioenriched, 85% ee

**116g** racemic

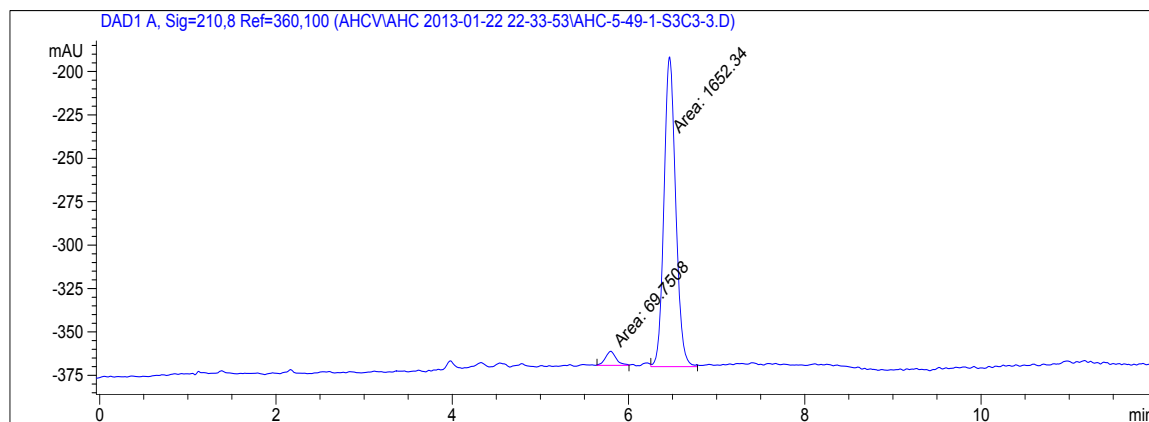
Peak #	RetTime [min]	Type	Width [min]	Area [mAU*s]	Height [mAU]	Area %
1	7.107	MM	0.2399	8170.74316	567.72528	50.3925
2	7.963	MM	0.2795	8043.45215	479.56842	49.6075

**116g** enantioenriched, 86% ee

Peak #	RetTime [min]	Type	Width [min]	Area [mAU*s]	Height [mAU]	Area %
1	7.295	MM	0.2652	355.56323	22.34372	7.2390
2	8.144	MM	0.2027	4556.22852	374.71005	92.7610

**116h** racemic

Peak #	RetTime [min]	Type	Width [min]	Area [mAU*s]	Height [mAU]	Area %
1	5.744	MM	0.1945	8898.86133	762.63263	49.4914
2	6.413	MM	0.2244	9081.74902	674.62744	50.5086

**116h** enantioenriched, 92% ee

Peak #	RetTime [min]	Type	Width [min]	Area [mAU*s]	Height [mAU]	Area %
1	5.798	MM	0.1418	69.75076	8.19656	4.0504
2	6.465	MM	0.1542	1652.33777	178.58195	95.9496

## 2.6 NOTES AND REFERENCES

- (1) (a) Meyers, A. I.; Knaus, G.; Kamata, K. *J. Am. Chem. Soc.* **1974**, *96*, 268; (b) Evans, D. A.; Ennis, M. D.; Mathre, D. J. *J. Am. Chem. Soc.* **1982**, *104*, 1737; (c) Sonnet, P. E.; Heath, R. R. *J. Org. Chem.* **1980**, *45*, 3137; (d) Oppolzer, W.; Moretti, R.; Thomi, S. *Tetrahedron Lett.* **1989**, *30*, 5603; (e) Myers, A. G.; Yang, B. H.; Chen, H.; McKinstry, L.; Kopecky, D. J.; Gleason, J. L. *J. Am. Chem. Soc.* **1997**, *119*, 6496; (f) Stivala, C. E.; Zakarian, A. *J. Am. Chem. Soc.* **2011**, *133*, 11936.
- (2) (a) Beeson, T. D.; Mastracchio, A.; Hong, J. B.; Ashton, K.; MacMillan, D. W. C. *Science* **2007**, *316*, 582; (b) Nicewicz, D. A.; MacMillan, D. W. C. *Science* **2008**, *322*, 77; (c) Shih, H. W.; Vander Wal, M. N.; Grange, R. L.; MacMillan, D. W. C. *J. Am. Chem. Soc.* **2010**, *132*, 13600; (d) Chen, J. P.; Ding, C. H.; Liu, W.; Hou, X. L.; Dai, L. X. *J. Am. Chem. Soc.* **2010**, *132*, 15493; (e) Kim, H.; MacMillan, D. W. C. *J. Am. Chem. Soc.* **2008**, *130*, 398; (f) Dai, X.; Strotman, N. A.; Fu, G. C. *J. Am. Chem. Soc.* **2008**, *130*, 3302; (g) Skucas, E.; MacMillan, D. W. C. *J. Am. Chem. Soc.* **2012**, *134*, 9090; (h) Aleman, J.; Cabrera, S.; Maerten, E.; Overgaard, J.; Jorgensen, K. A. *Angew. Chem. Int. Ed.* **2007**, *46*, 5520; (i) Allen, A. E.; MacMillan, D. W. C. *J. Am. Chem. Soc.* **2011**, *133*, 4260; (j) Bigot, A.; Williamson, A. E.; Gaunt, M. J. *J. Am. Chem. Soc.* **2011**, *133*, 13778; (k) Harvey, J. S.; Simonovich, S. P.; Jamison, C. R.; MacMillan, D. W. C. *J. Am. Chem. Soc.* **2011**, *133*, 13782.
- (3) (a) Trost, B. M.; Xu, J. Y. *J. Am. Chem. Soc.* **2005**, *127*, 17180; (b) Yan, X. X.; Liang, C. G.; Zhang, Y.; Hong, W.; Cao, B. X.; Dai, L. X.; Hou, X. L. *Angew. Chem. Int. Ed.* **2005**, *44*, 6544; (c) Zheng, W. H.; Zheng, B. H.; Zhang, Y.; Hou, X. L. *J. Am. Chem. Soc.* **2007**, *129*, 7718.
- (4) (a) Lou, S.; Fu, G. C. *J. Am. Chem. Soc.* **2010**, *132*, 5010; (b) Lou, S.; Fu, G. C. *J. Am. Chem. Soc.* **2010**, *132*, 1264; (c) Lundin, P. M.; Esquivias, J.; Fu, G. C. *Angew. Chem. Int. Ed.* **2009**, *48*, 154.
- (5) Dieter, R. K. *Tetrahedron* **1999**, *55*, 4177.
- (6) (a) Wang, D. H.; Zhang, Z. G. *Org. Lett.* **2003**, *5*, 4645; (b) Mori, Y.; Seki, M. *Tetrahedron Lett.* **2004**, *45*, 7343; (c) Zhang, Y. D.; Rovis, T. *J. Am. Chem. Soc.* **2004**, *126*, 15964.
- (7) Fausett, B. W.; Liebeskind, L. S. *J. Org. Chem.* **2005**, *70*, 4851.
- (8) Cherney, A. H.; Reisman, S. E. *Tetrahedron* **2014**, *70*, 3259.
- (9) Oost, R.; Misale, A.; Maulide, N. *Angew. Chem. Int. Ed. Engl.* **2016**, *55*, 4587.

- (10) (a) Weix, D. J. *Acc. Chem. Res.* **2015**, *48*, 1767; (b) Moragas, T.; Correa, A.; Martin, R. *Chem. Eur. J.* **2014**, *20*, 8242; (c) Knappke, C. E.; Grupe, S.; Gartner, D.; Corpet, M.; Gosmini, C.; Jacobi von Wangelin, A. *Chem. Eur. J.* **2014**, *20*, 6828.
- (11) (a) Wotal, A. C.; Weix, D. J. *Org. Lett.* **2012**, *14*, 1476; (b) Wotal, A. C.; Ribson, R. D.; Weix, D. J. *Organometallics* **2014**, *33*, 5874; (c) Wotal, A. *Organic Syntheses* **2016**, *93*, 50; (d) Huihui, K. M. M.; Caputo, J. A.; Melchor, Z.; Olivares, A. M.; Spiewak, A. M.; Johnson, K. A.; DiBenedetto, T.; Kim, S.; Ackerman, L. K. G.; Weix, D. J. *J. Am. Chem. Soc.* **2016**; (e) Wu, F.; Lu, W. B.; Qian, Q.; Ren, Q. H.; Gong, H. G. *Org. Lett.* **2012**, *14*, 3044; (f) Gong, H.; Qian, Q.; Lu, W.; Liang, Z.; Zhang, Y.; Wu, F. *Synthesis* **2013**, *45*, 2234; (g) Liang, Z.; Xue, W.; Lin, K.; Gong, H. *Org. Lett.* **2014**, *16*, 5620.
- (12) (a) Gu, J.; Wang, X.; Xue, W.; Gong, H. *Org. Chem. Front.* **2015**, *2*, 1411; (b) Everson, D. A.; Jones, B. A.; Weix, D. J. *J. Am. Chem. Soc.* **2012**, *134*, 6146; (c) Ren, Q.; Jiang, F.; Gong, H. *J. Organomet. Chem.* **2014**, *770*, 130.
- (13) (a) Schley, N. D.; Fu, G. C. *J. Am. Chem. Soc.* **2014**, *136*, 16588; (b) Gutierrez, O.; Tellis, J. C.; Primer, D. N.; Molander, G. A.; Kozlowski, M. C. *J. Am. Chem. Soc.* **2015**, *137*, 4896; (c) Everson, D. A.; Weix, D. J. *J. Org. Chem.* **2014**, *79*, 4793.
- (14) Cherney, A. H.; Kadunce, N. T.; Reisman, S. E. *Chem. Rev.* **2015**, *115*, 9587.
- (15) (a) Yin, H. Y.; Zhao, C. L.; You, H. Z.; Lin, K. H.; Gong, H. G. *Chem. Commun.* **2012**, *48*, 7034; (b) Goossen, L. J.; Ghosh, K. *Angew. Chem. Int. Ed.* **2001**, *40*, 3458.
- (16) Cherney, A. H.; Kadunce, N. T.; Reisman, S. E. *J. Am. Chem. Soc.* **2013**, *135*, 7442.
- (17) Everson, D. A.; Shrestha, R.; Weix, D. J. *J. Am. Chem. Soc.* **2010**, *132*, 3636.
- (18) Giovannini, R.; Stüdemann, T.; Dussin, G.; Knochel, P. *Angew. Chem. Int. Ed.* **1998**, *37*, 2387.
- (19) (a) Cherney, A. H.; Reisman, S. E. *J. Am. Chem. Soc.* **2014**, *136*, 14365; (b) Prinsell, M. R.; Everson, D. A.; Weix, D. J. *Chem. Commun.* **2010**, *46*, 5743.
- (20) Durandetti, M.; Gosmini, C.; Périchon, J. *Tetrahedron* **2007**, *63*, 1146.
- (21) Johnson, K. A.; Biswas, S.; Weix, D. J. *Chem. Eur. J.* **2016**.
- (22) Kadunce, N. T.; Reisman, S. E. *J. Am. Chem. Soc.* **2015**, *137*, 10480.

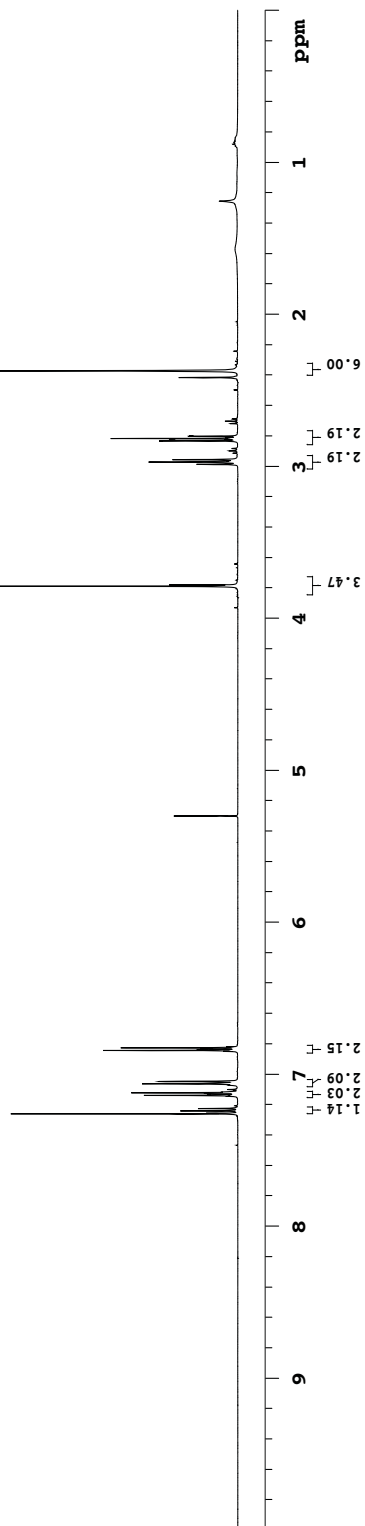
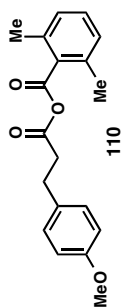
## **APPENDIX 1**

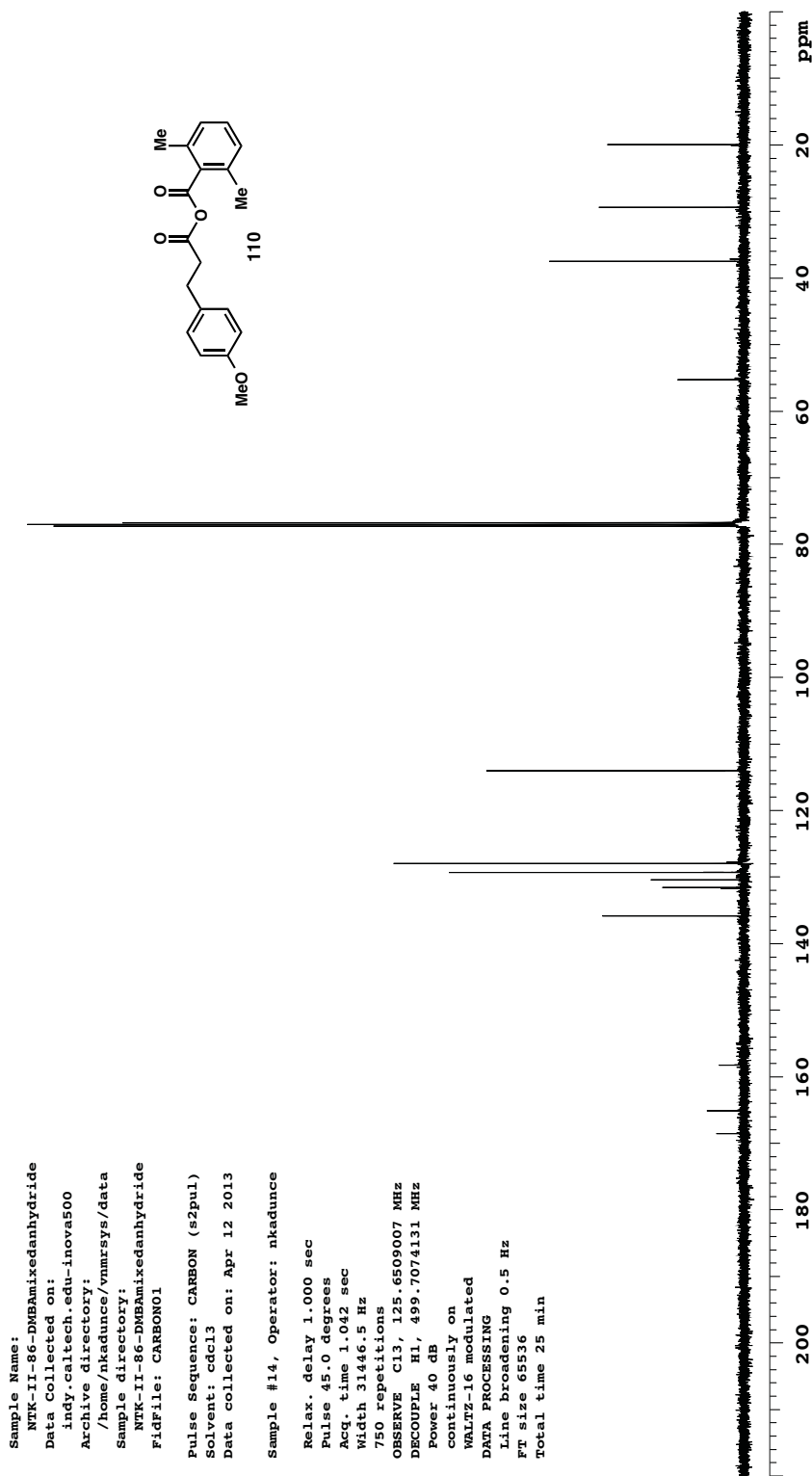
*Spectra Relevant to Chapter 2:*

*Catalytic Asymmetric Reductive Acyl Cross-Coupling: Synthesis of*

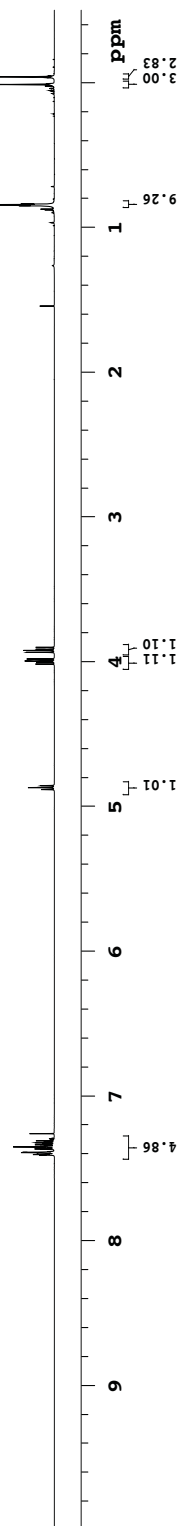
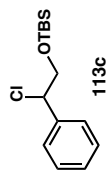
*Enantioenriched Acyclic  $\alpha,\alpha$ -Disubstituted Ketones*

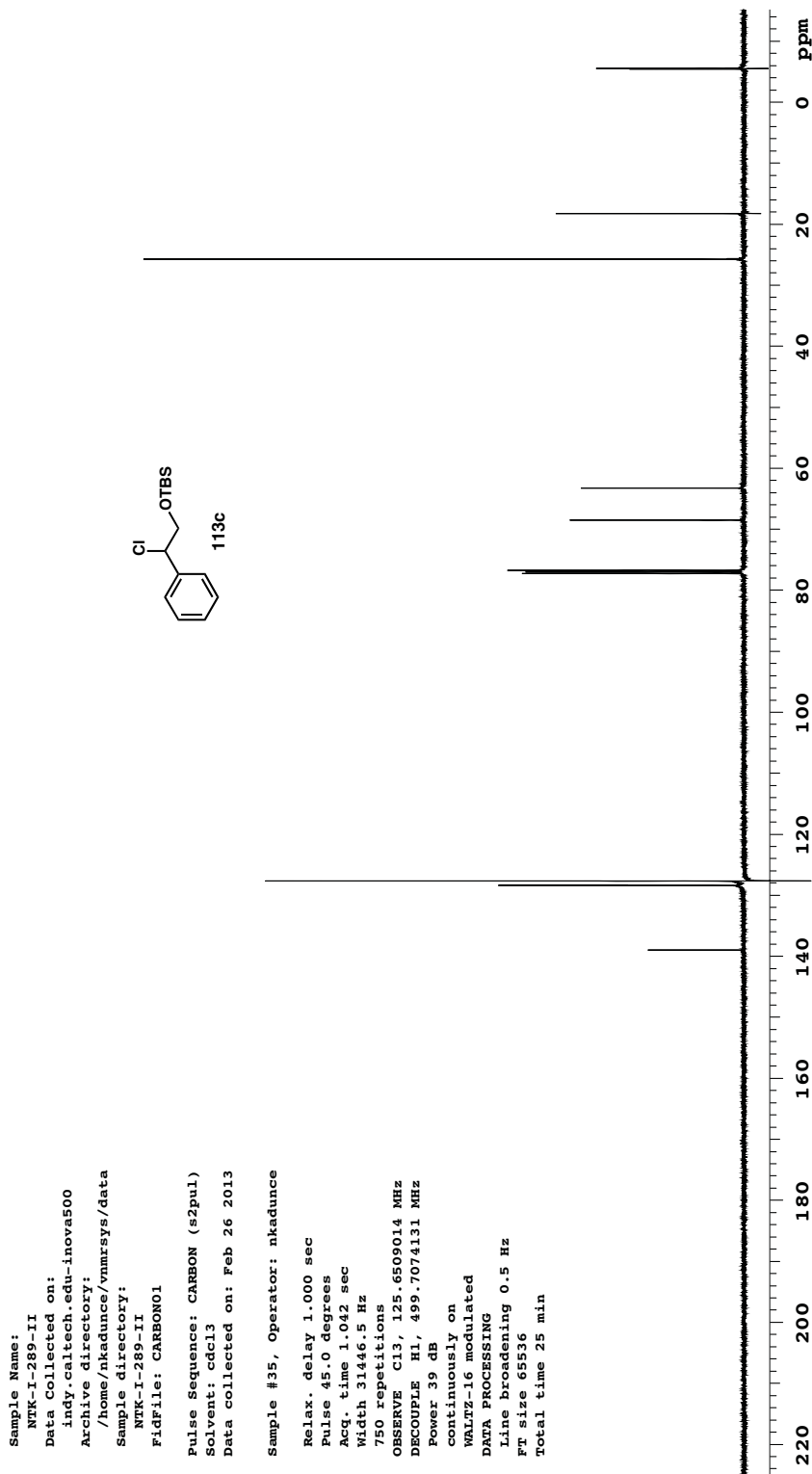
Sample Name:  
 NTK-II-86-DMBAmixedanhydride  
 Data Collected on:  
 indy.caltech.edu-inova500  
 Archive directory:  
 /home/nkadunce/vnmrSYS/data  
 Sample directory:  
 NTK-II-86-DMBAmixedanhydride  
 FidFile: PROTON01  
 Pulse Sequence: PROTON (s2pul)  
 Solvent: cdcl3  
 Data collected on: Apr 12 2013  
 Sample #14, Operator: nkadunce  
 Relax. delay 1.000 sec  
 Pulse 45.0 degrees  
 Acq. time 3.000 sec  
 Width 8000.0 Hz  
 32 repetitions  
 OBSERVE H1, 499.7049145 MHz  
 DATA PROCESSING  
 Line broadening 0.2 Hz  
 FT size 65536  
 Total time 2 min 8 sec



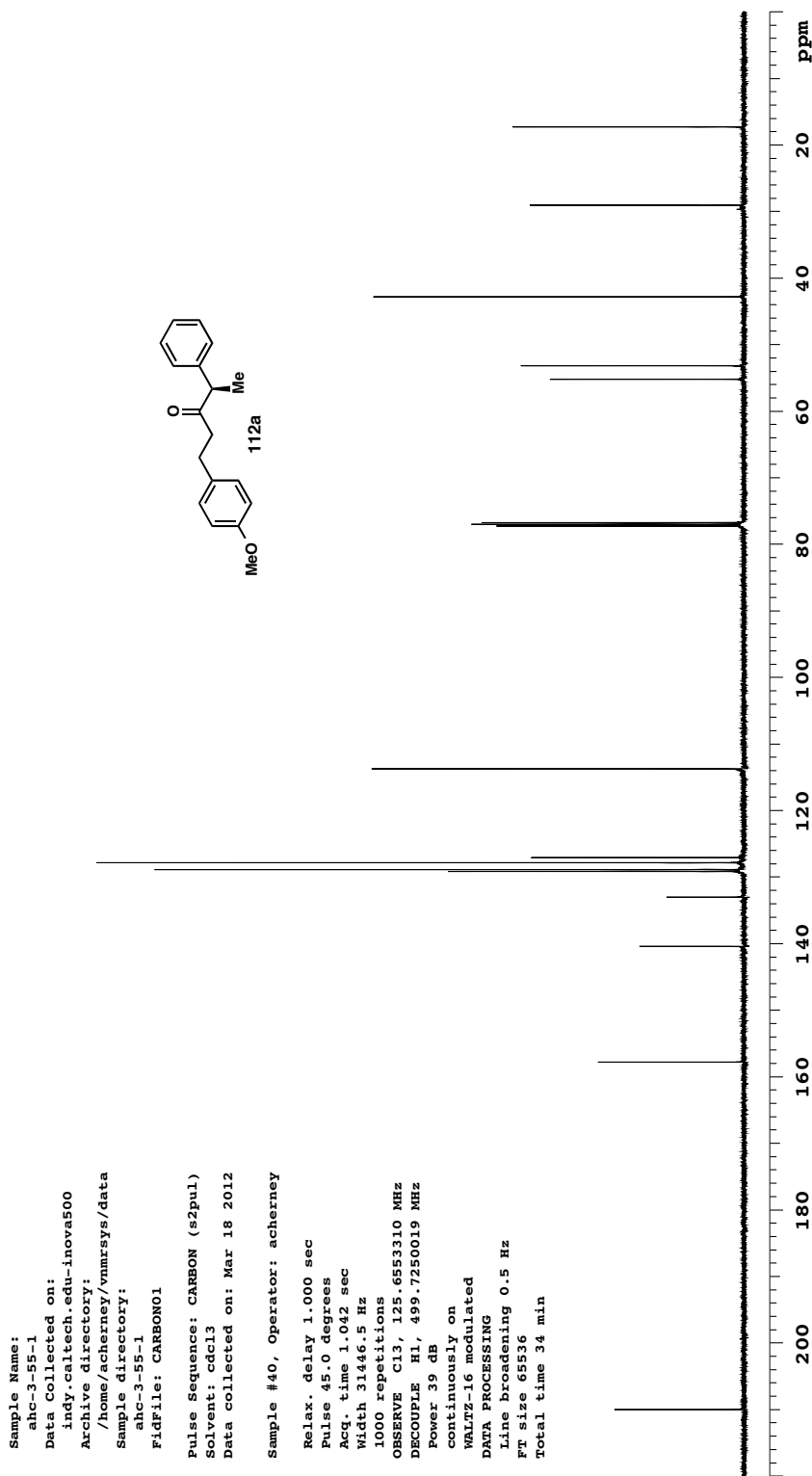


Sample Name:  
 NTK-I-289-II  
 Data Collected on:  
 indy.caltech.edu-inova500  
 Archive directory:  
 /home/nkadunce/vnmrsys/data  
 Sample directory:  
 NTK-I-289-II  
 FidFile: PROTON01  
 Pulse Sequence: PROTON (s2pul)  
 Solvent: cdcl3  
 Data collected on: Feb 26 2013  
 Sample #35, Operator: nkadunce  
 Relax. delay 1.000 sec  
 Pulse 45.0 degrees  
 Acq. time 3.000 sec  
 Width 8000.0 Hz  
 32 repetitions  
 OBSERVE H1, 499.7049145 MHz  
 DATA PROCESSING  
 Line broadening 0.2 Hz  
 FT size 65536  
 Total time 2 min 8 sec

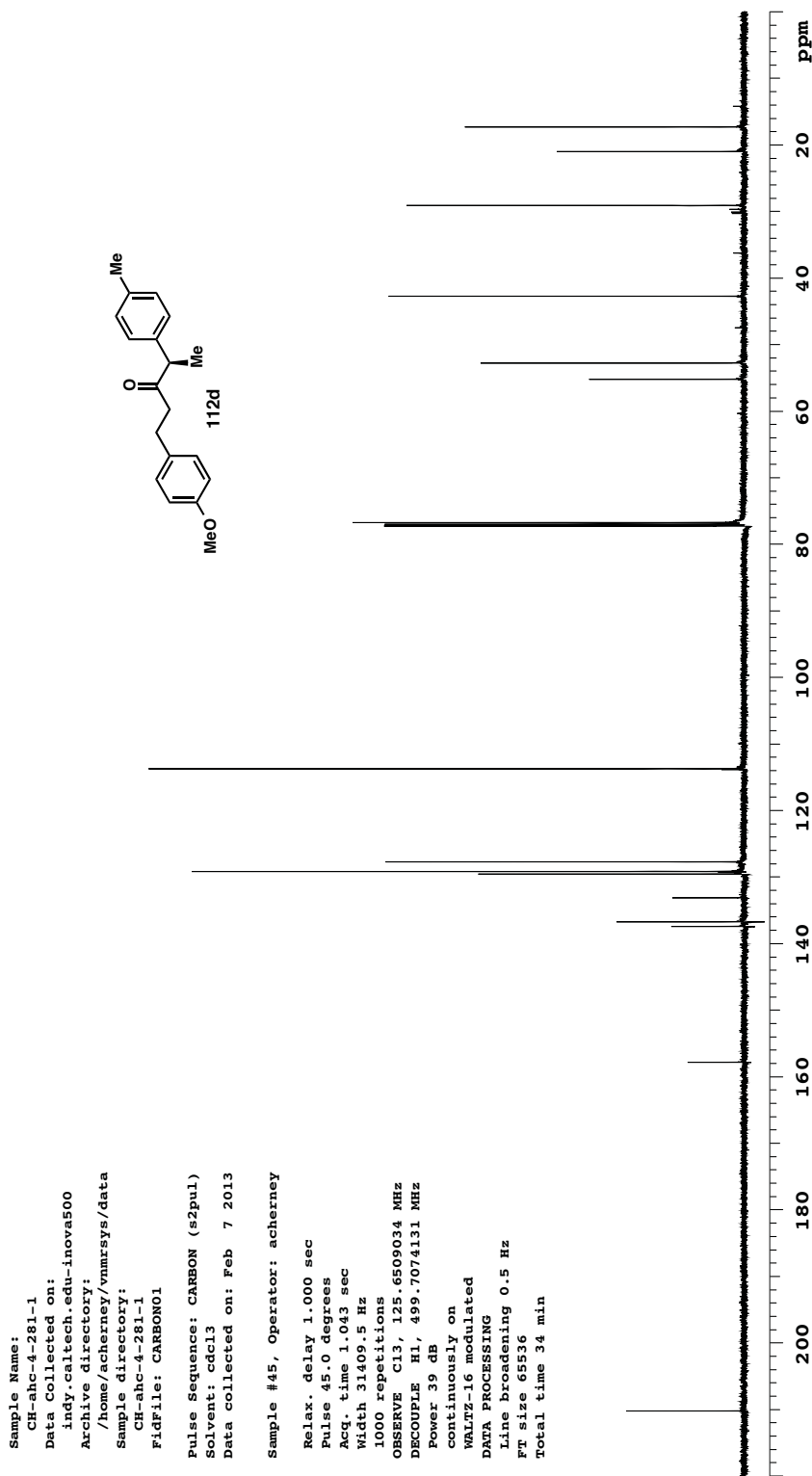




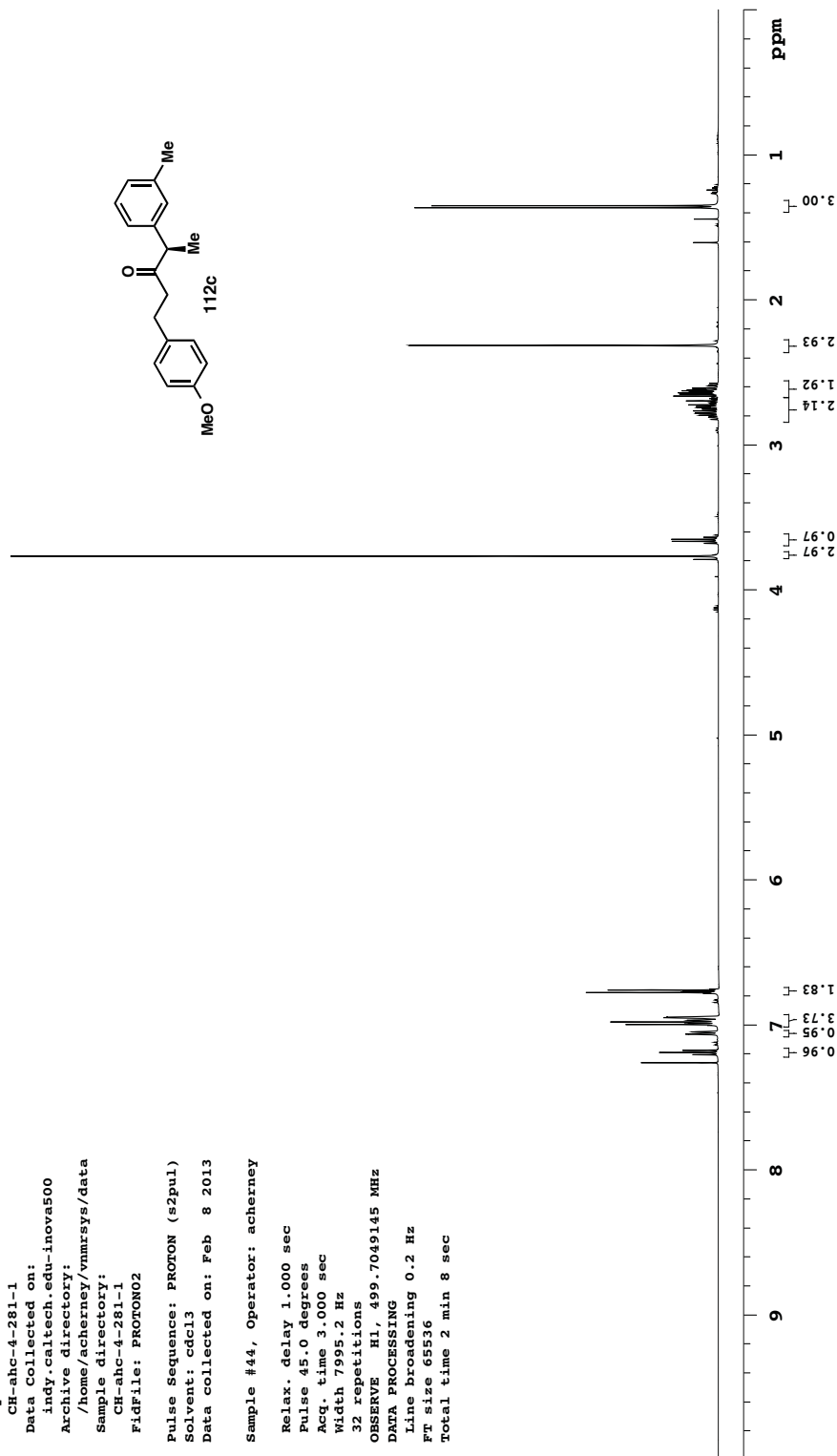
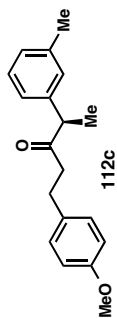


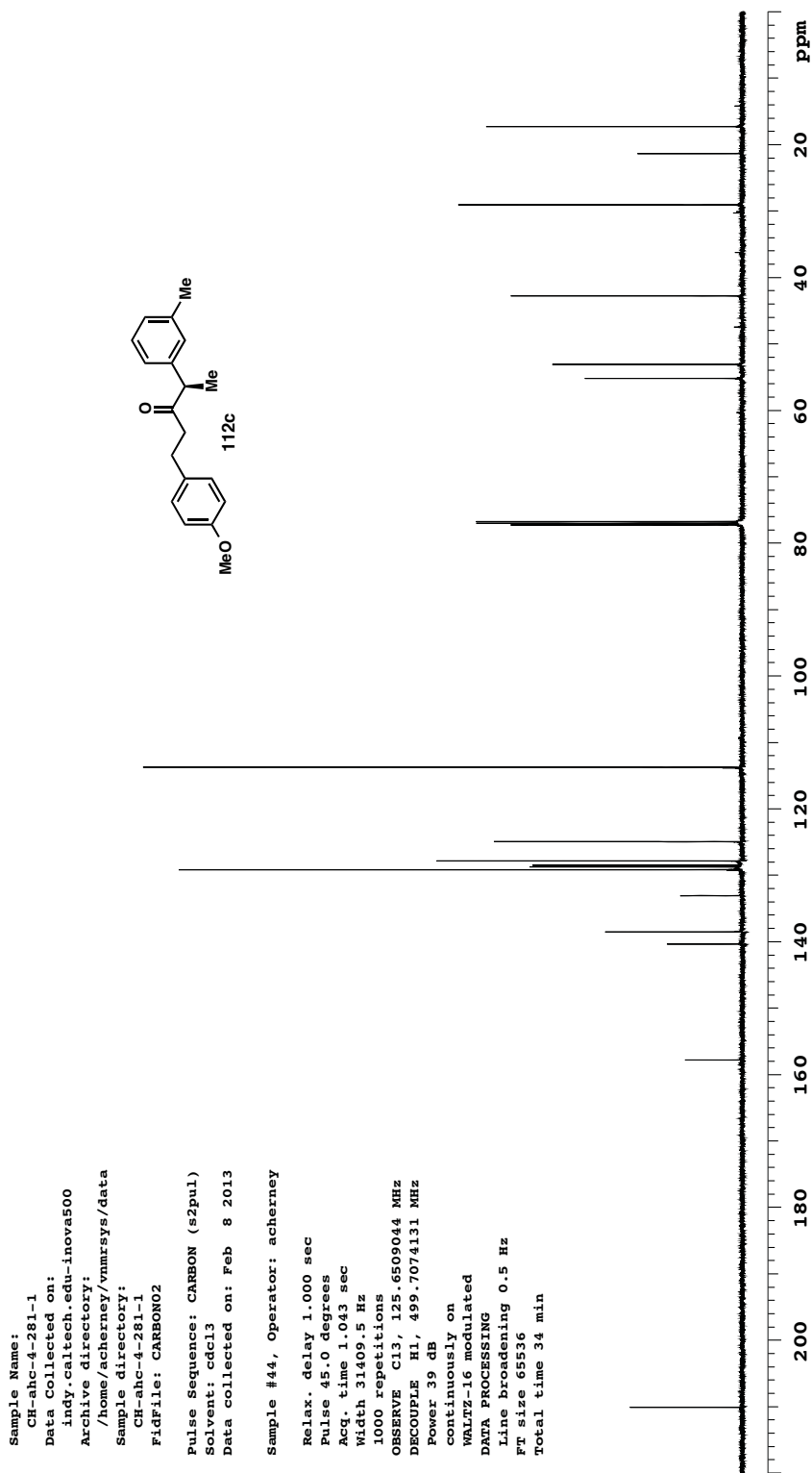


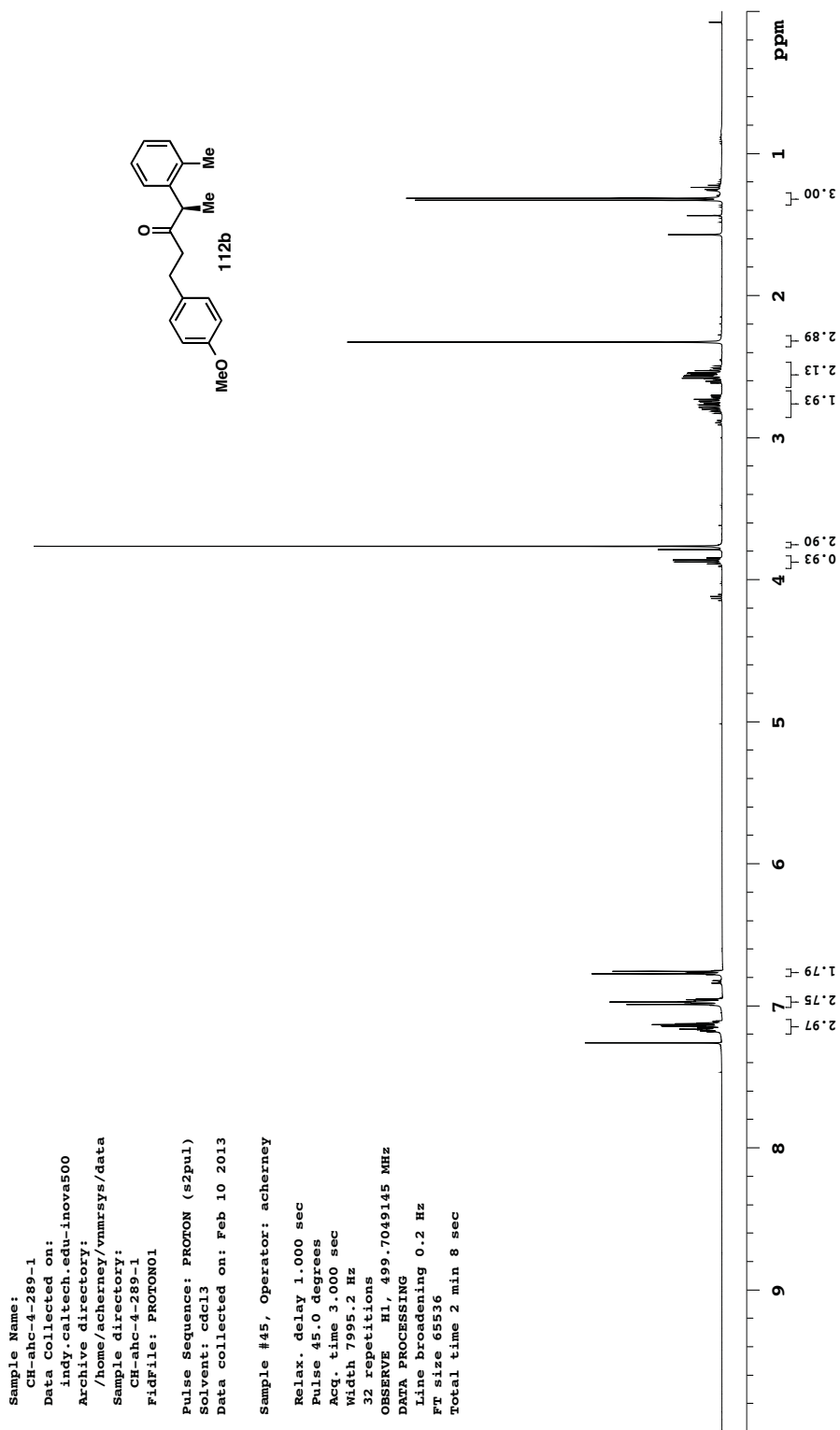


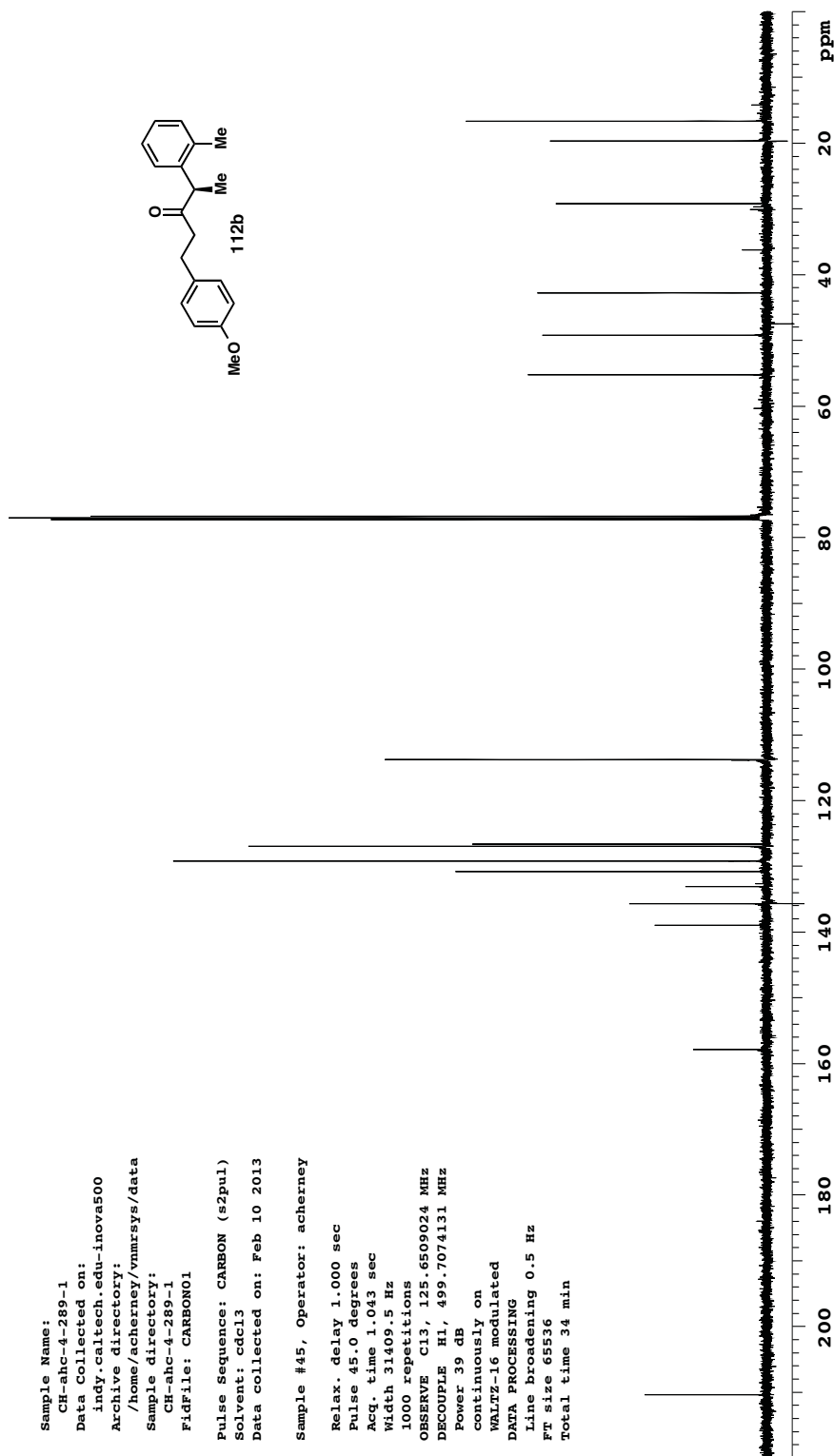


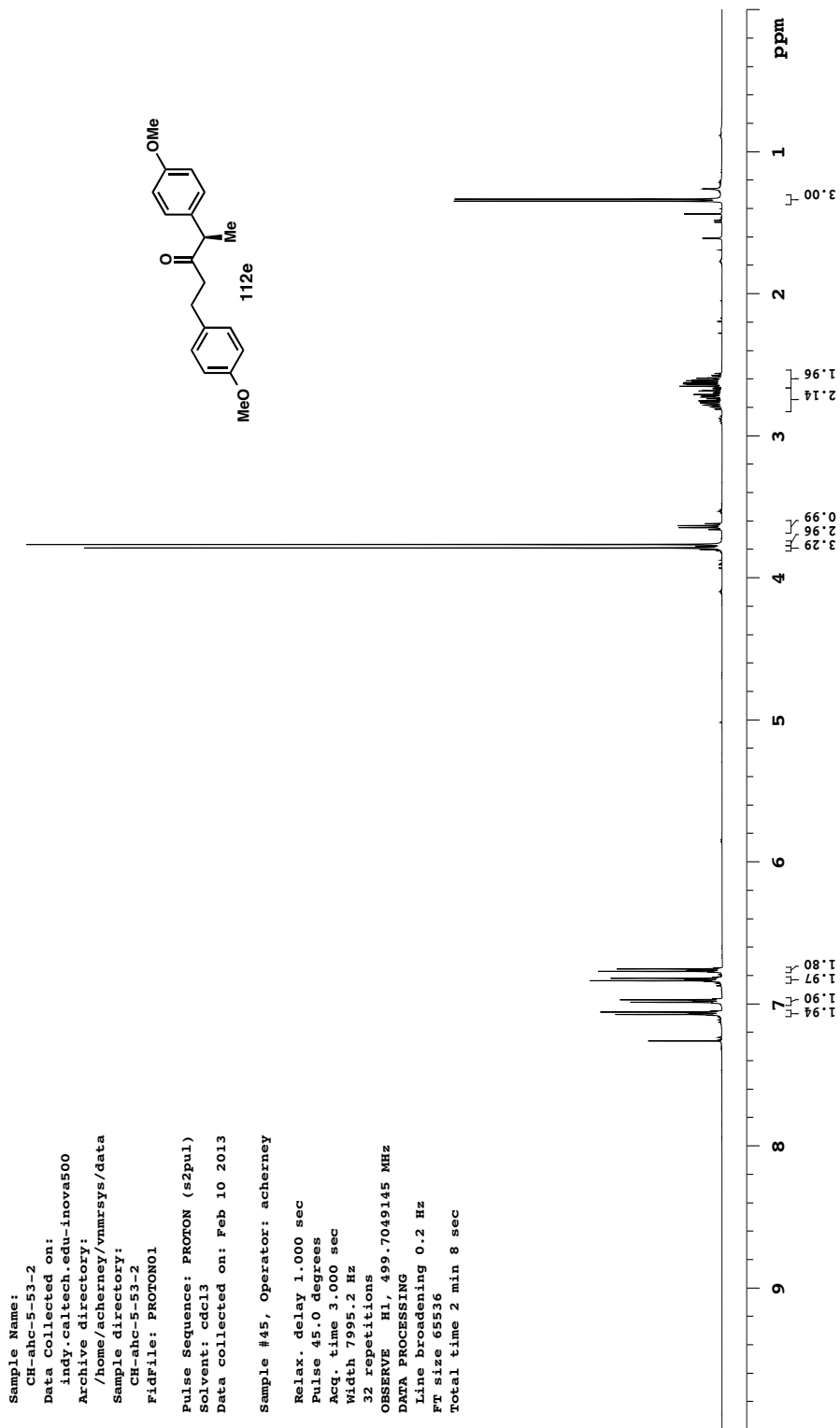
Sample Name:  
 CH-ahc-4-281-1  
 Data Collected on:  
 indy.caltech.edu-inova500  
 Archive directory:  
 /home/acherney/vnmrsys/data  
 Sample directory:  
 CH-ahc-4-281-1  
 FidFile: PROTON02  
 Pulse Sequence: PROTON (s2pul)  
 Solvent: cdcl3  
 Data collected on: Feb 8 2013  
 Sample #44, Operator: acherney  
 Relax. delay 1.000 sec  
 Pulse 45.0 degrees  
 Acq. time 3.000 sec  
 Width 7995.2 Hz  
 32 repetitions  
 OBSERVE H1, 499.7049145 MHz  
 DATA PROCESSING  
 Line broadening 0.2 Hz  
 FT size 65536  
 Total time 2 min 8 sec

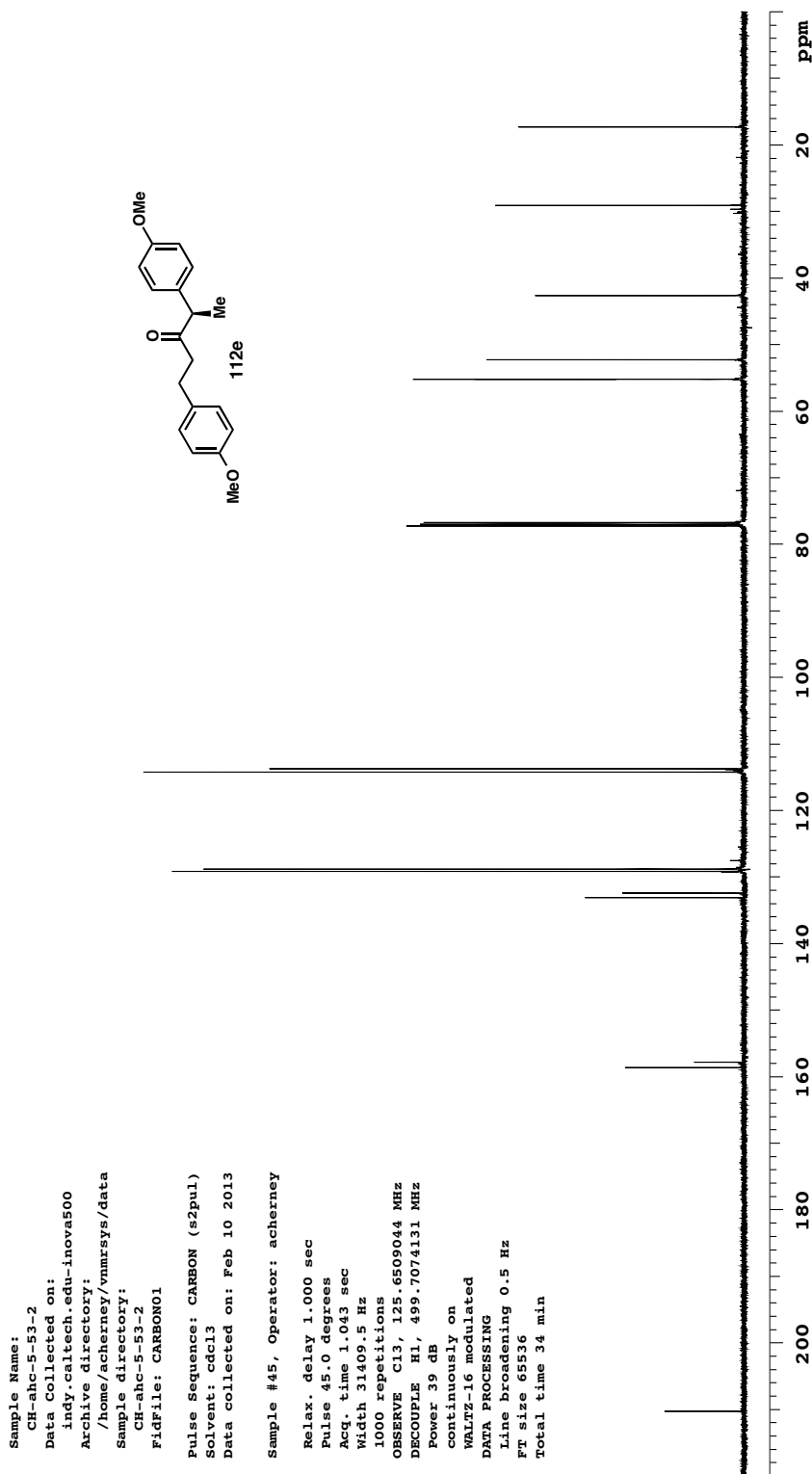


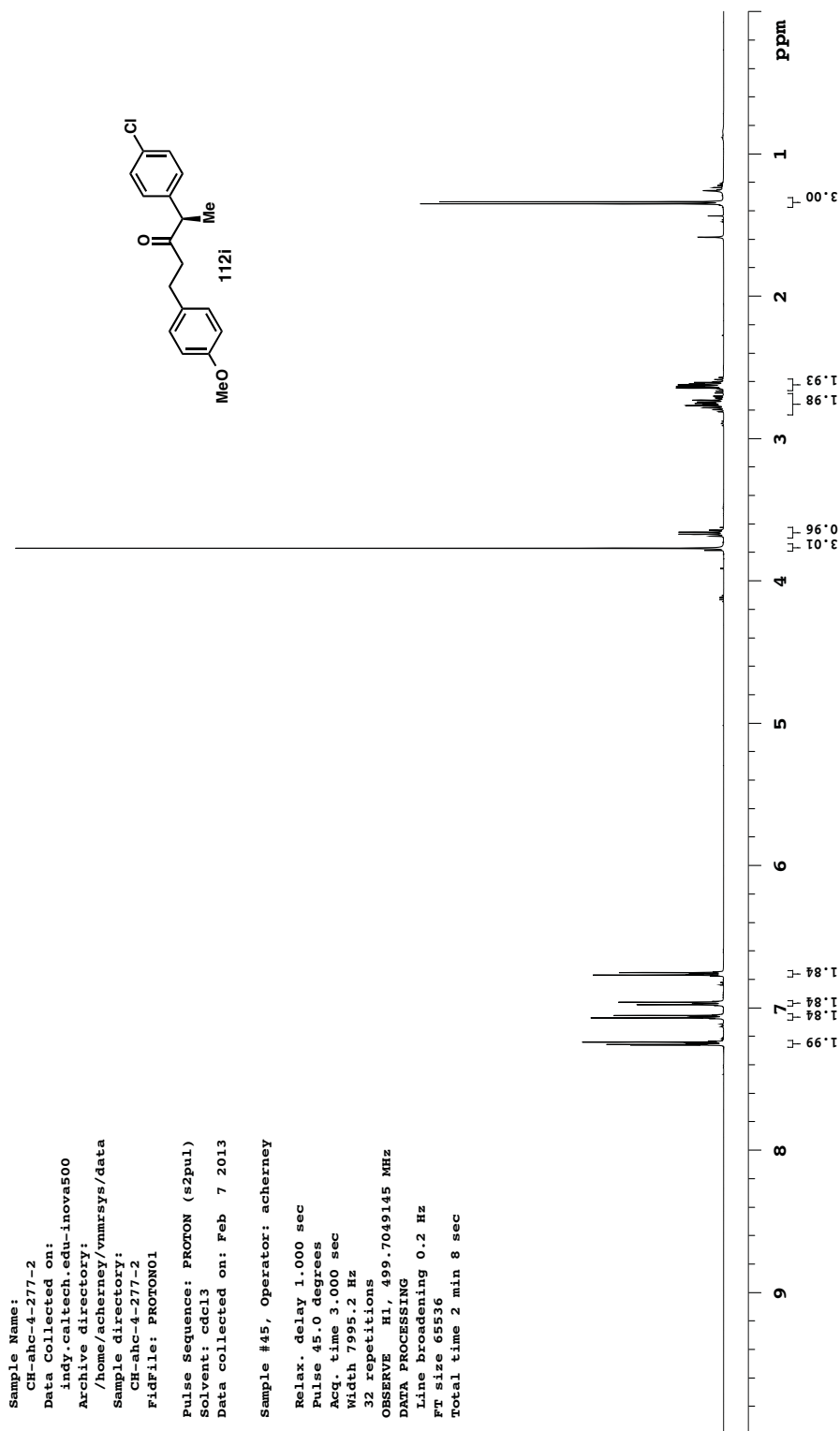


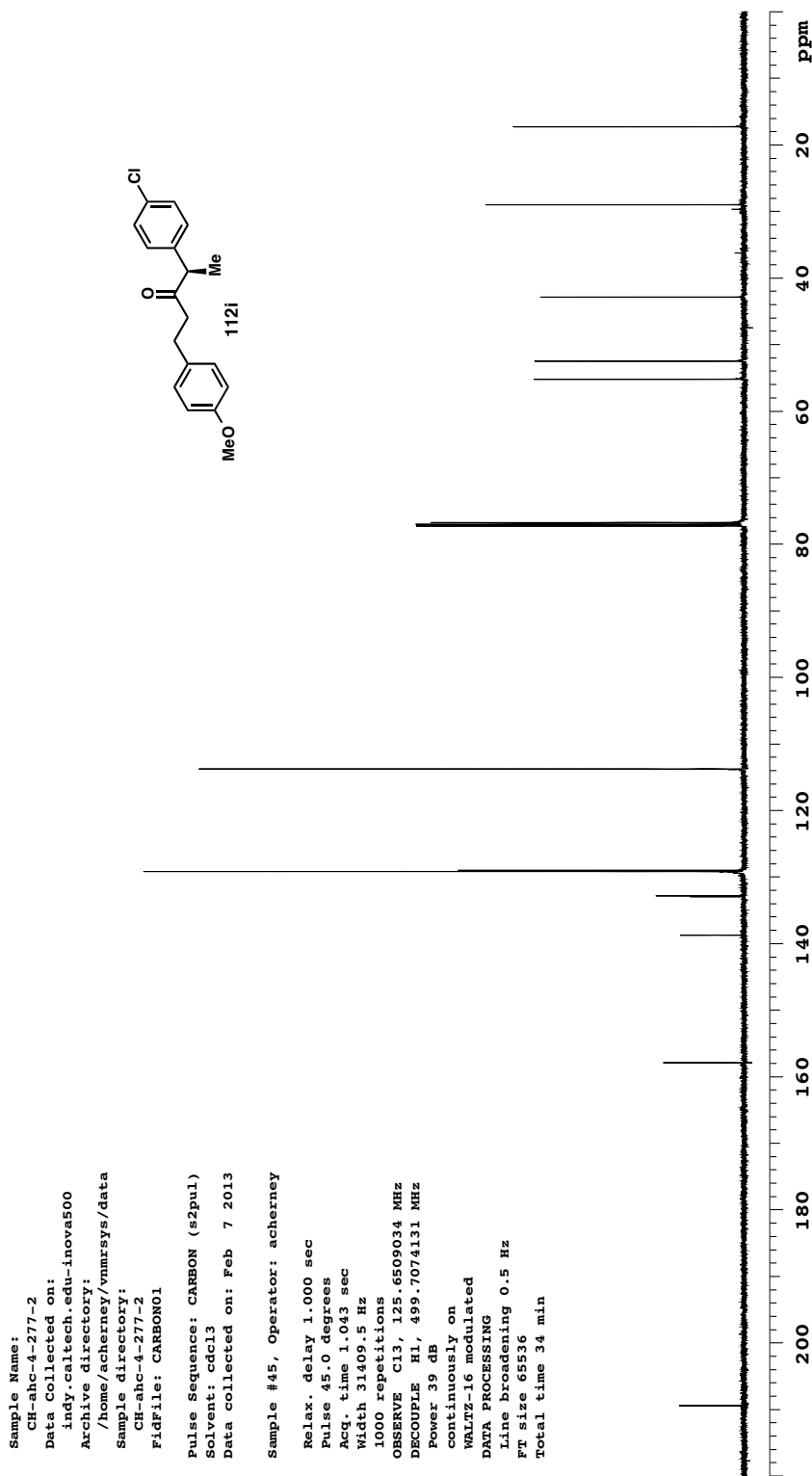


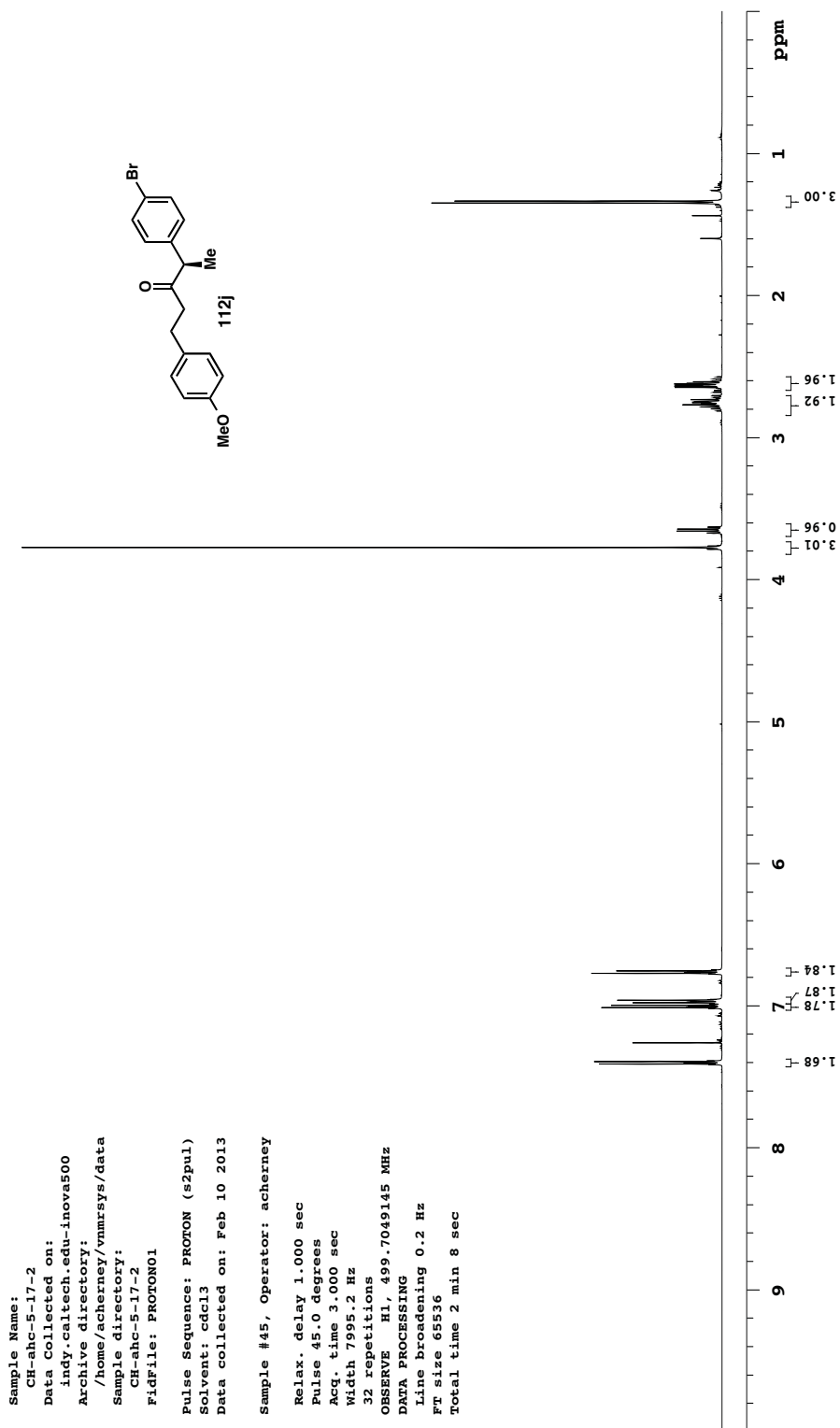


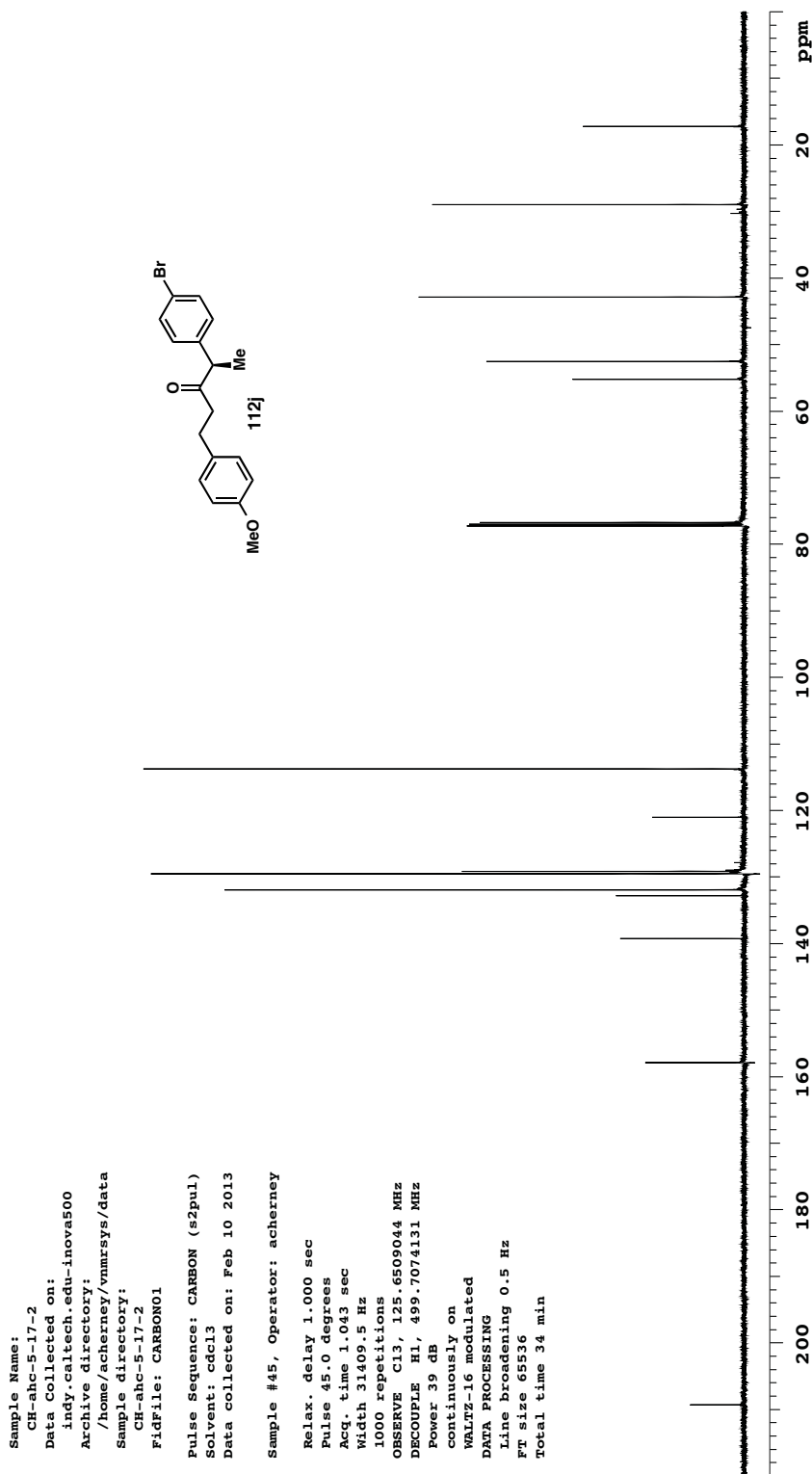




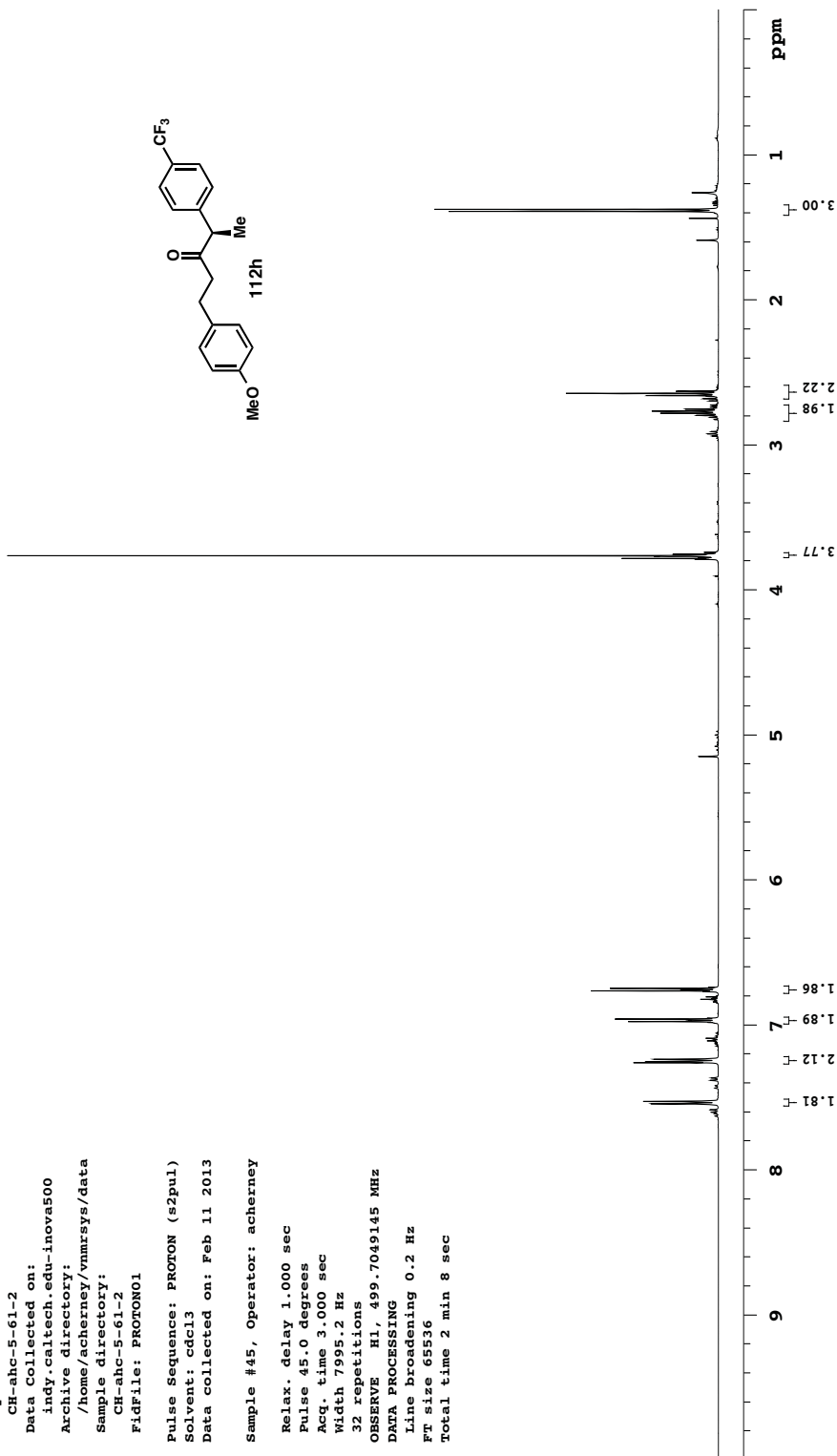


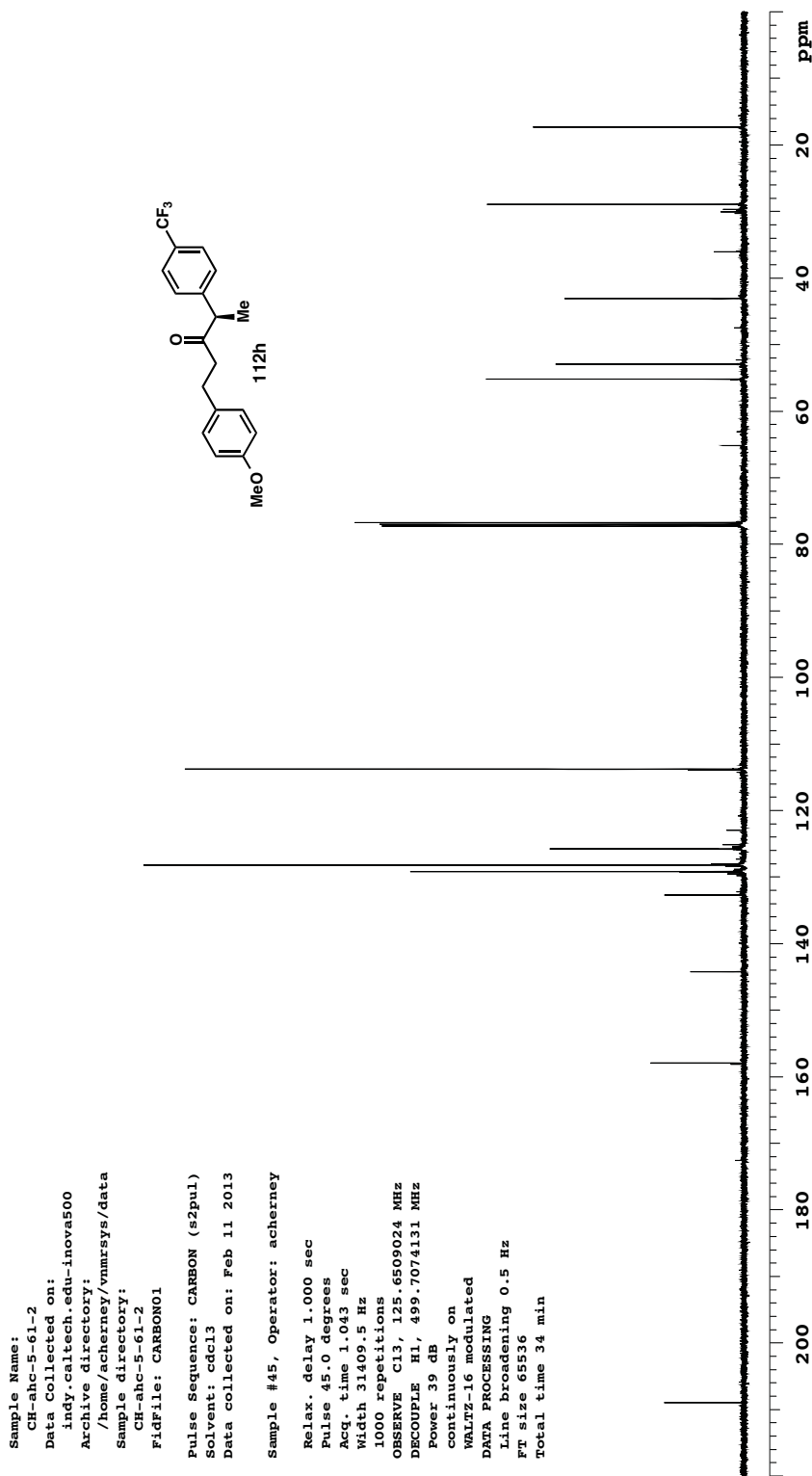


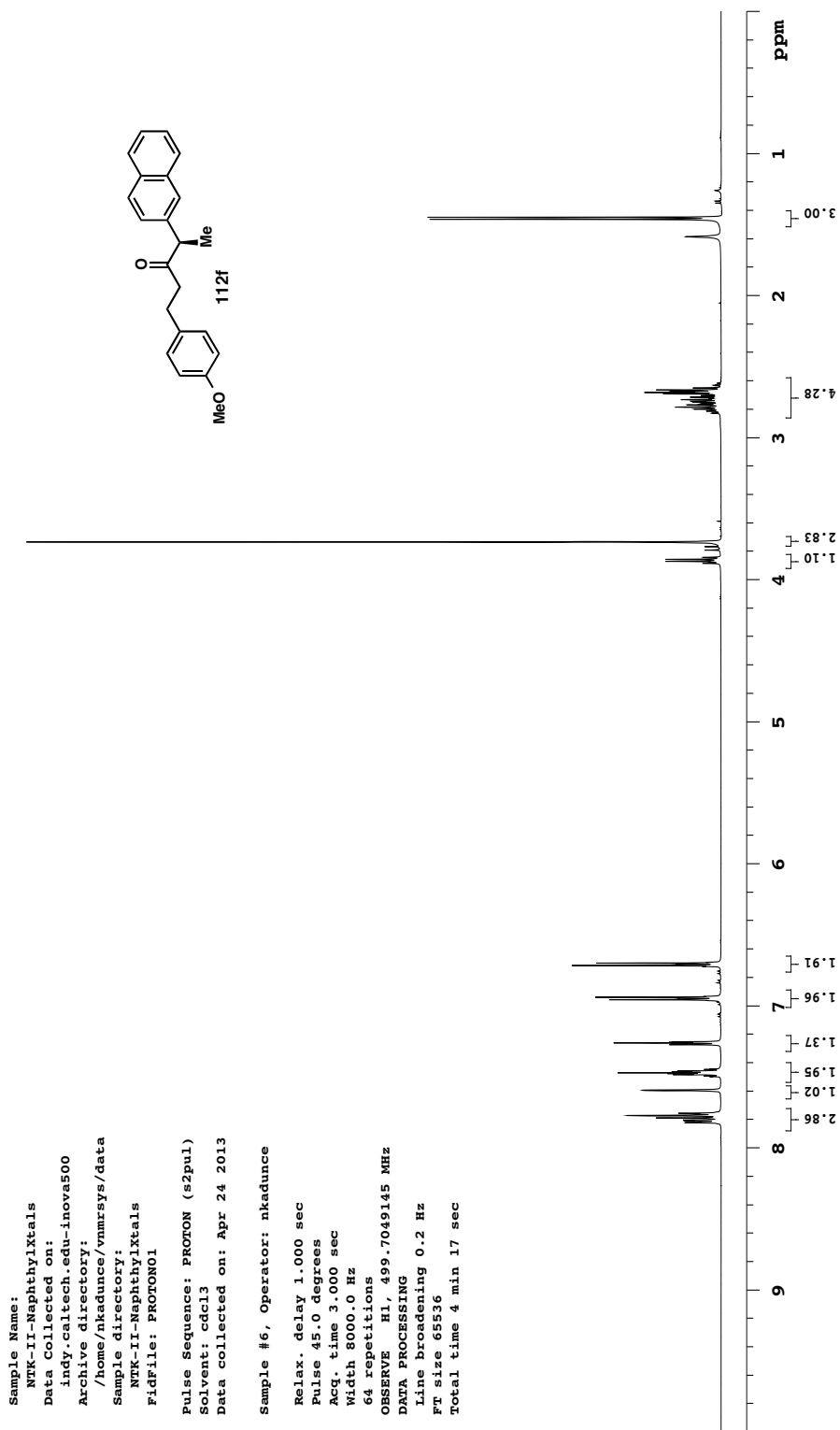


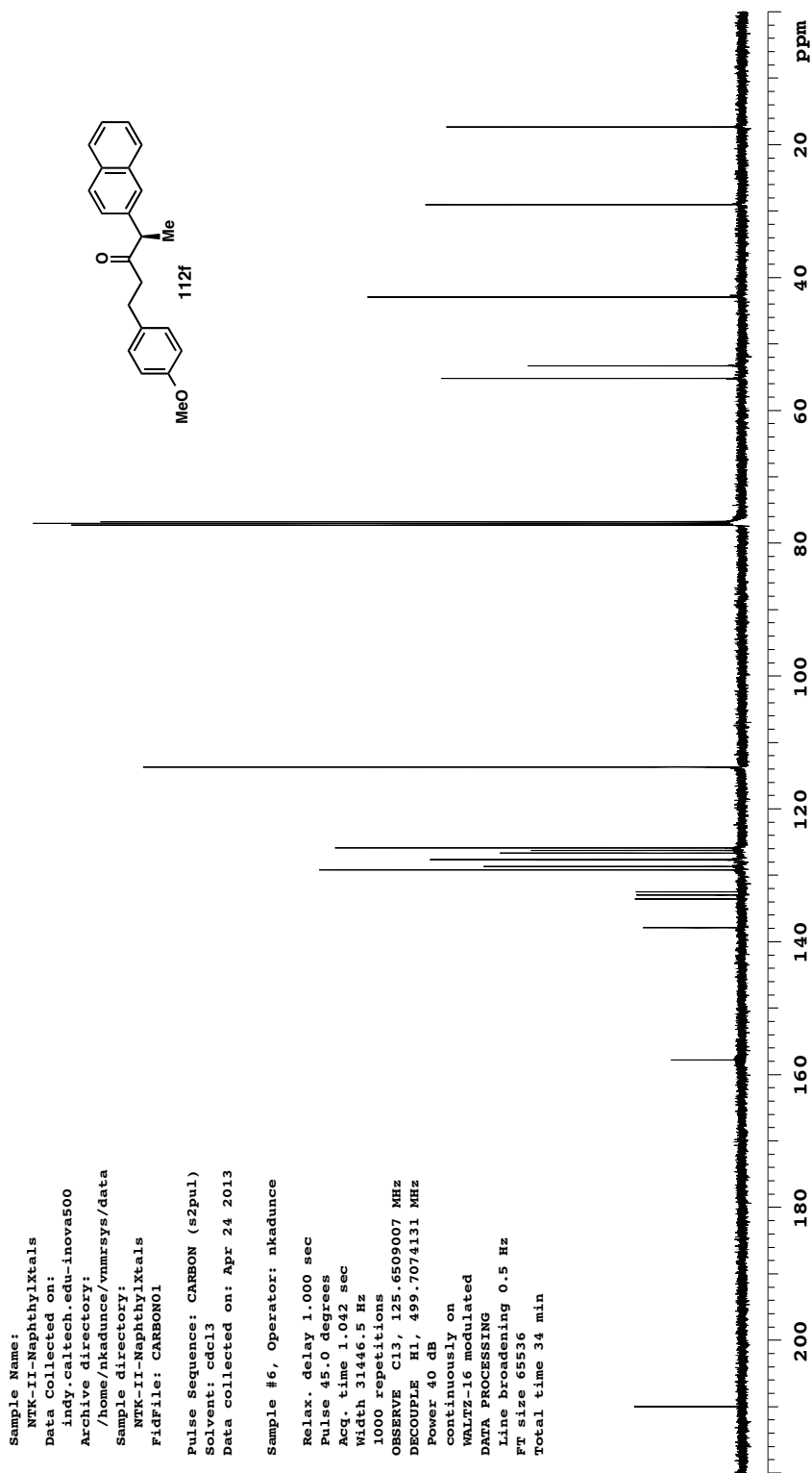


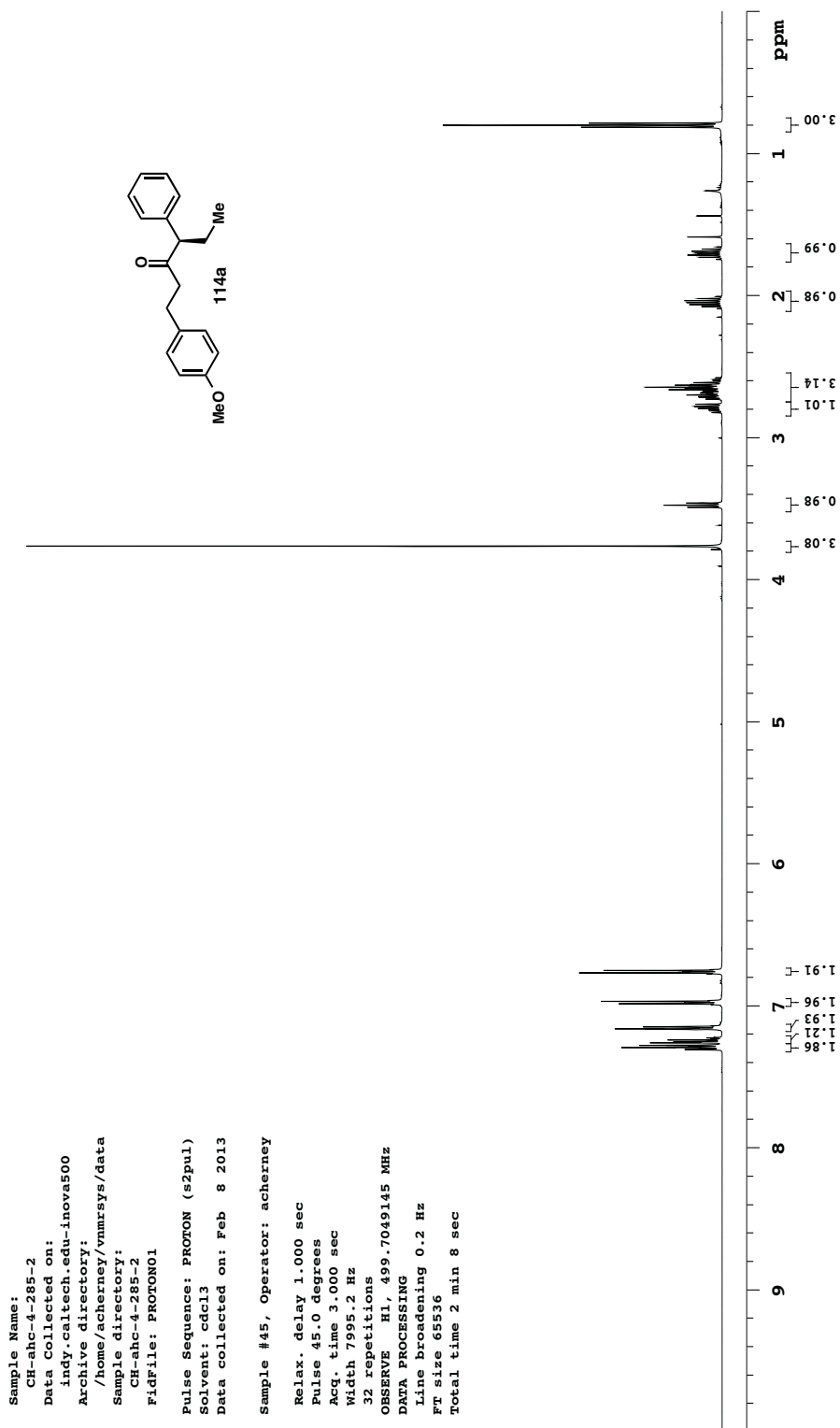
Sample Name:  
 CH-ahc-5-61-2  
 Data Collected on:  
 indy.caltech.edu-inova500  
 Archive directory:  
 /home/acherney/vnmrSYS/data  
 Sample directory:  
 CH-ahc-5-61-2  
 FidFile: PROTON01  
 Pulse Sequence: PROTON (s2pul)  
 Solvent: cdcl3  
 Data collected on: Feb 11 2013  
 Sample #45, Operator: acherney  
 Relax. delay 1.000 sec  
 Pulse 45.0 degrees  
 Acq. time 3.000 sec  
 Width 7995.2 Hz  
 32 repetitions  
 OBSERVE H1, 499.7049145 MHz  
 DATA PROCESSING  
 Line broadening 0.2 Hz  
 FT size 65536  
 Total time 2 min 8 sec

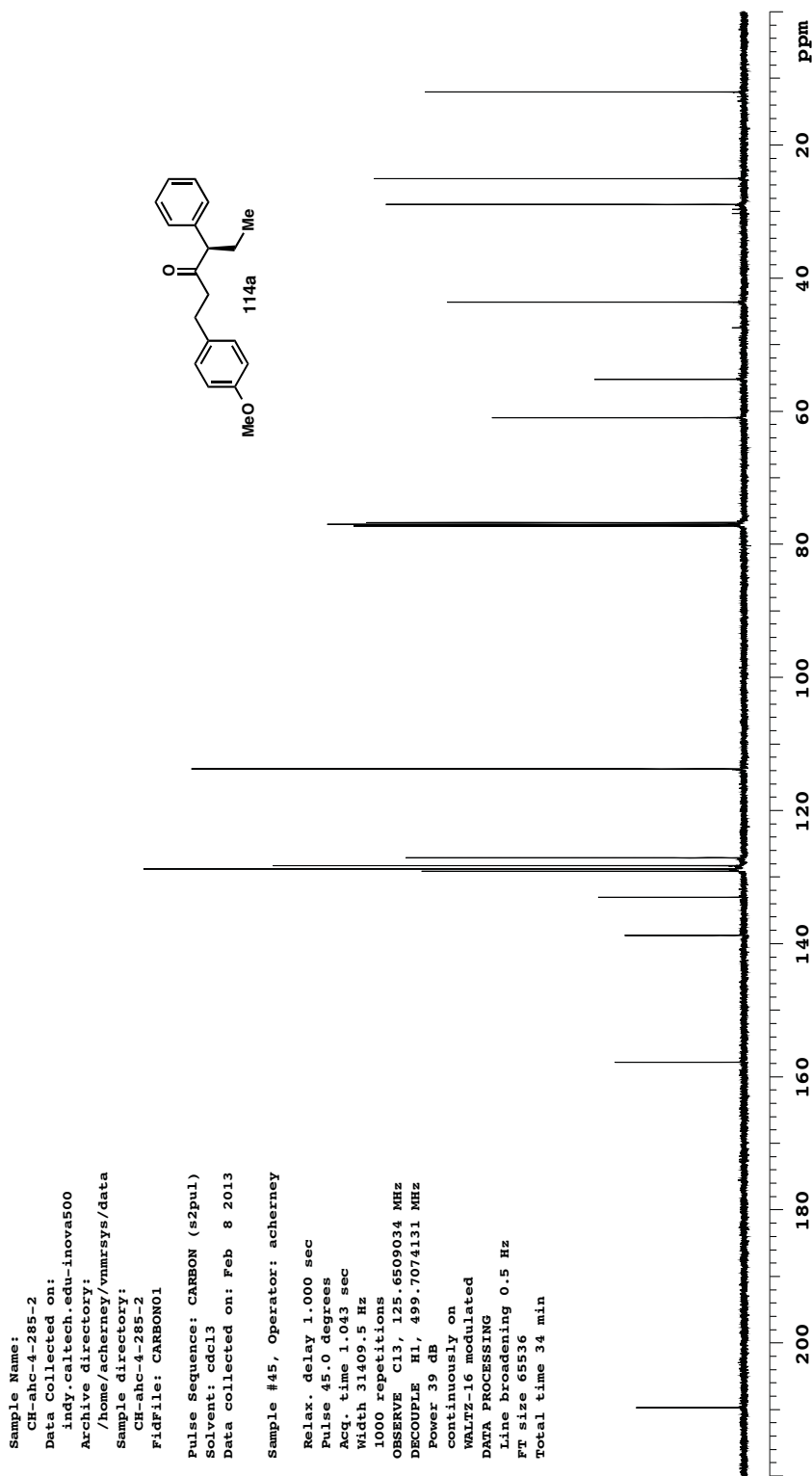


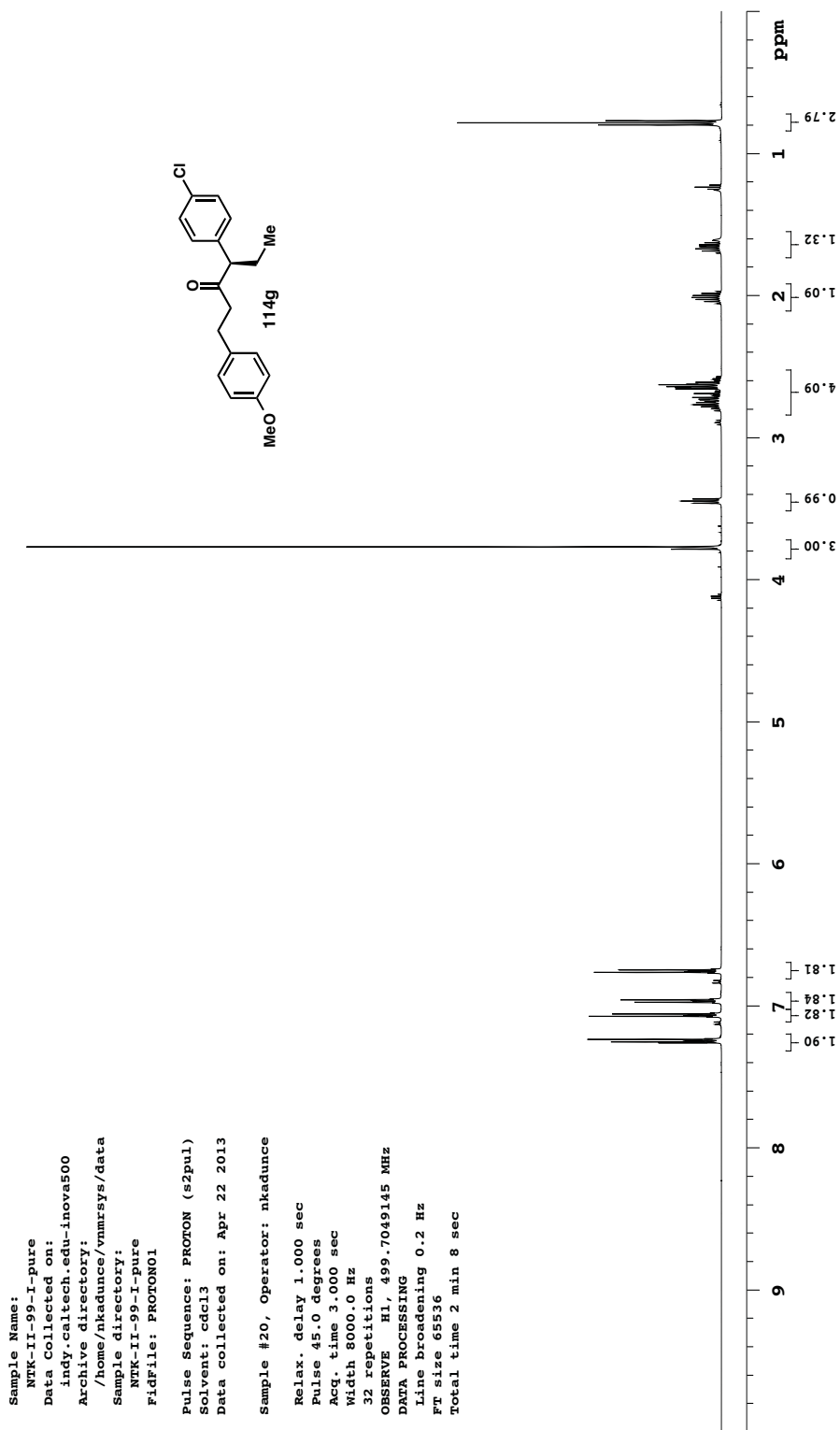


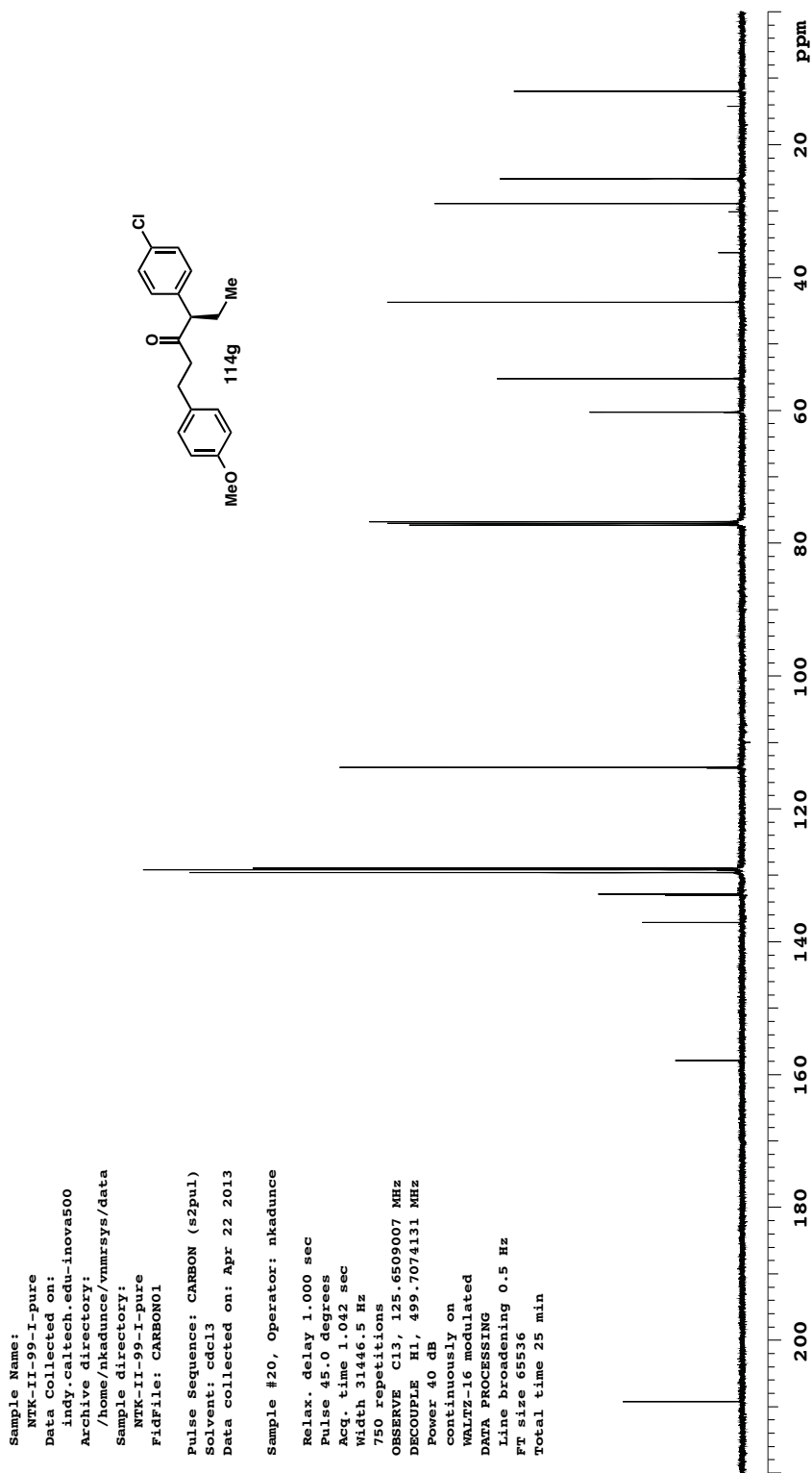








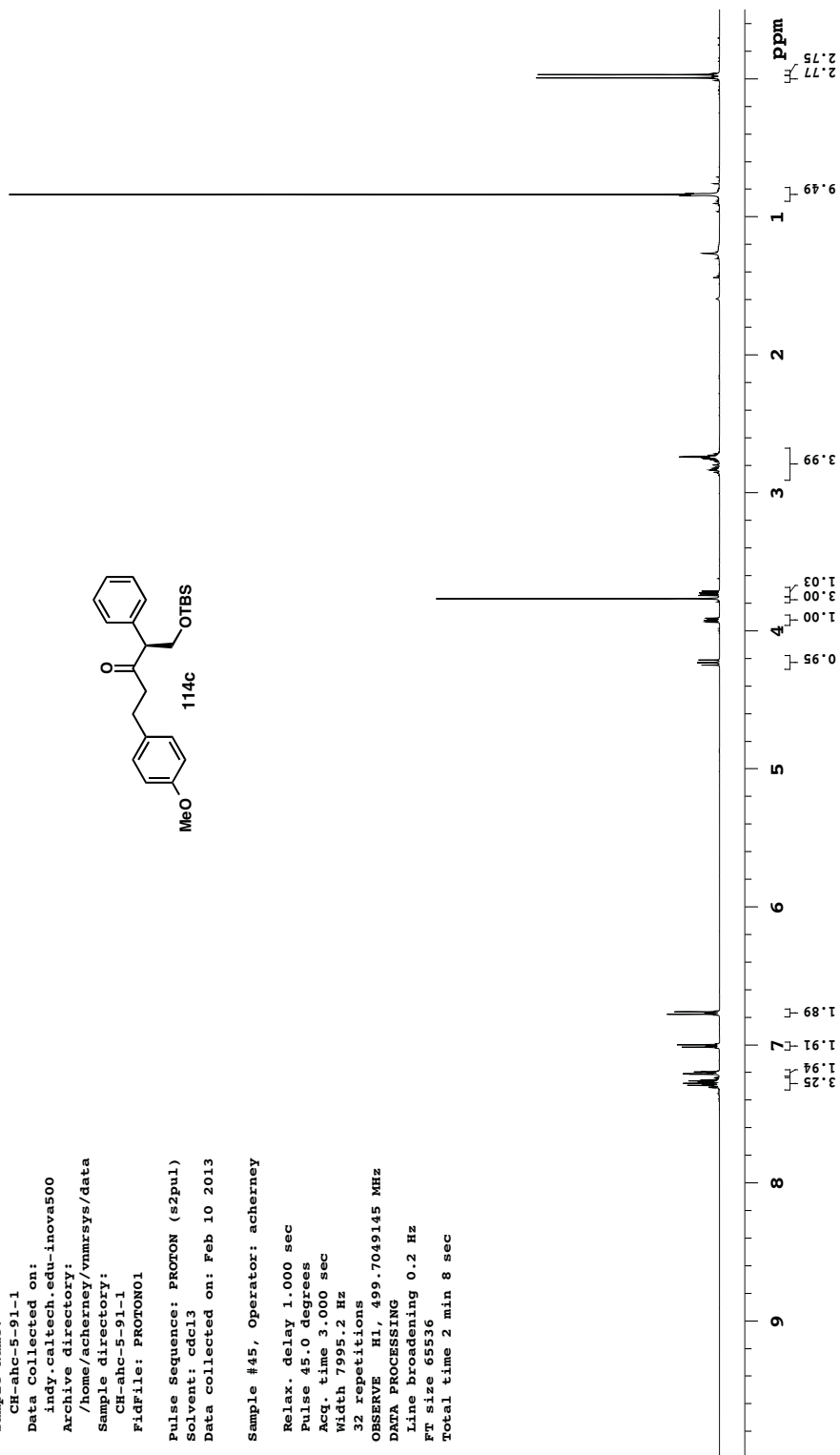
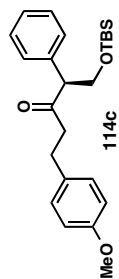




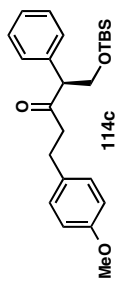




Sample Name:  
 CH-ahc-5-91-1  
 Data Collected on:  
 indy.caltech.edu-inova500  
 Archive directory:  
 /home/acherney/vnmrSYS/data  
 Sample directory:  
 CH-ahc-5-91-1  
 FidFile: PROTON01  
 Pulse Sequence: PROTON (s2pul)  
 Solvent: cdcl3  
 Data collected on: Feb 10 2013  
 Sample #45, Operator: acherney  
 Relax. delay 1.000 sec  
 Pulse 45.0 degrees  
 Acq. time 3.000 sec  
 Width 7995.2 Hz  
 32 repetitions  
 OBSERVE H1, 499.7049145 MHz  
 DATA PROCESSING  
 Line broadening 0.2 Hz  
 FT size 65536  
 Total time 2 min 8 sec



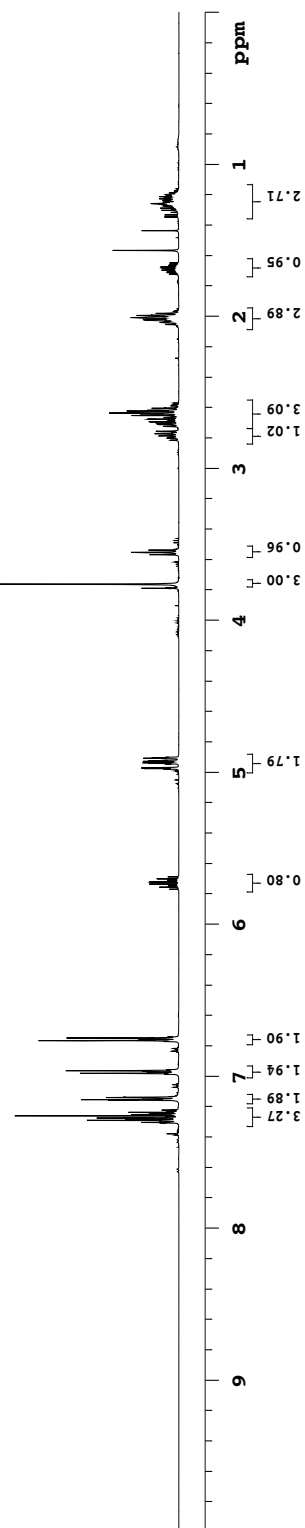
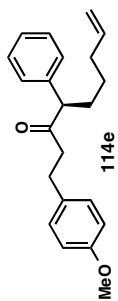
Sample Name:  
 CH-ahc-5-91-1  
 Data Collected on:  
 indy.caltech.edu-inova500  
 Archive directory:  
 /home/acherney/vnmrsys/data  
 Sample directory:  
 CH-ahc-5-91-1  
 FidFile: CARBONO1  
 Pulse Sequence: CARBON (s2pul)  
 Solvent: cdcl3  
 Data collected on: Feb 10 2013  
 Sample #45, Operator: acherney  
 Relax. delay 1.000 sec  
 Pulse 45.0 degrees  
 Acq. time 1.043 sec  
 Width 31409.5 Hz  
 1000 repetitions  
 OBSERVE C13, 125.6509034 MHz  
 DECOUPLE H1, 499.7074131 MHz  
 Power 39 dB  
 continuously on  
 WALTZ-16 modulated  
 DATA PROCESSING  
 Line broadening 0.5 Hz  
 F1 size 65536  
 Total time 34 min

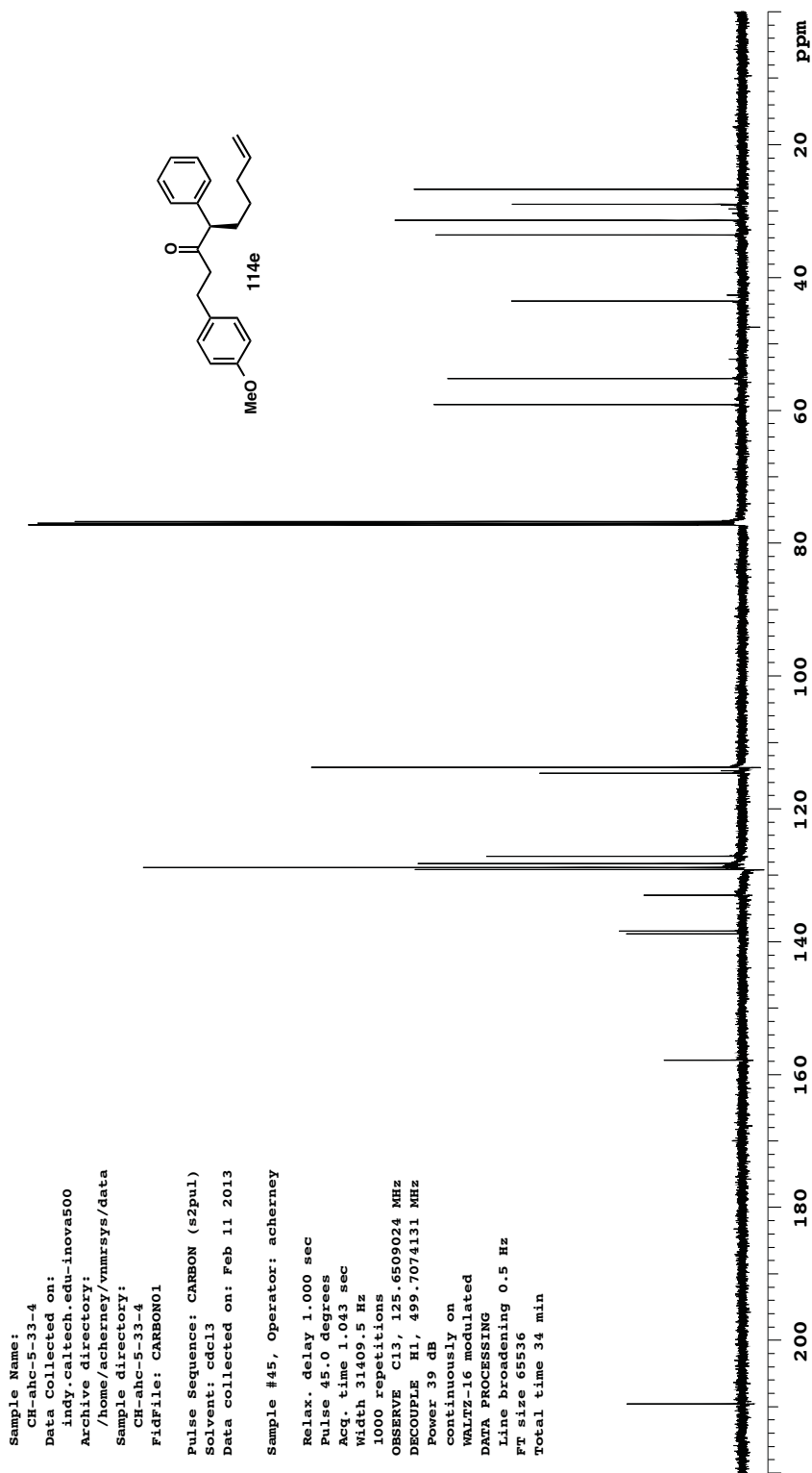


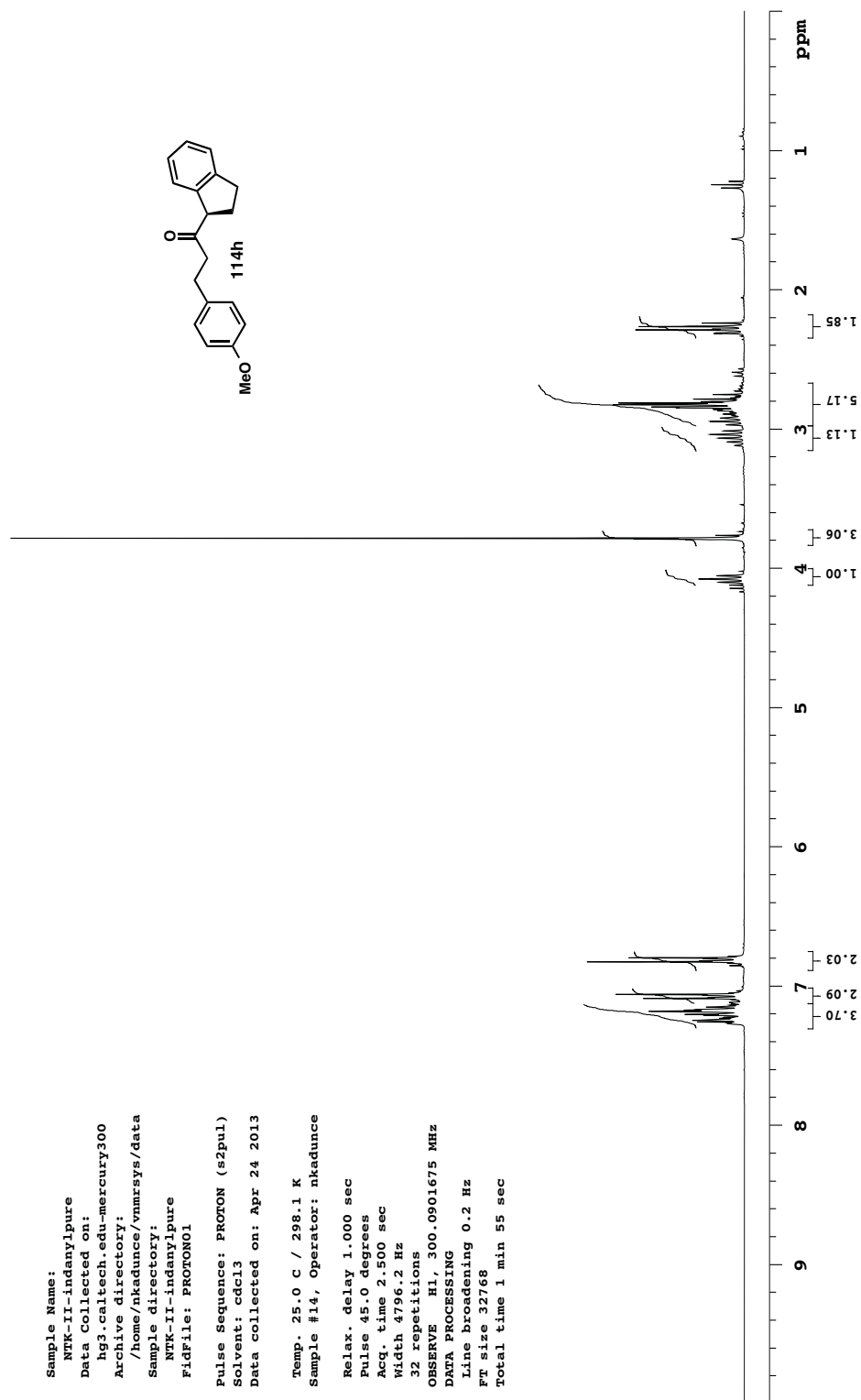
200 180 160 140 120 100 80 60 40 20 0 ppm

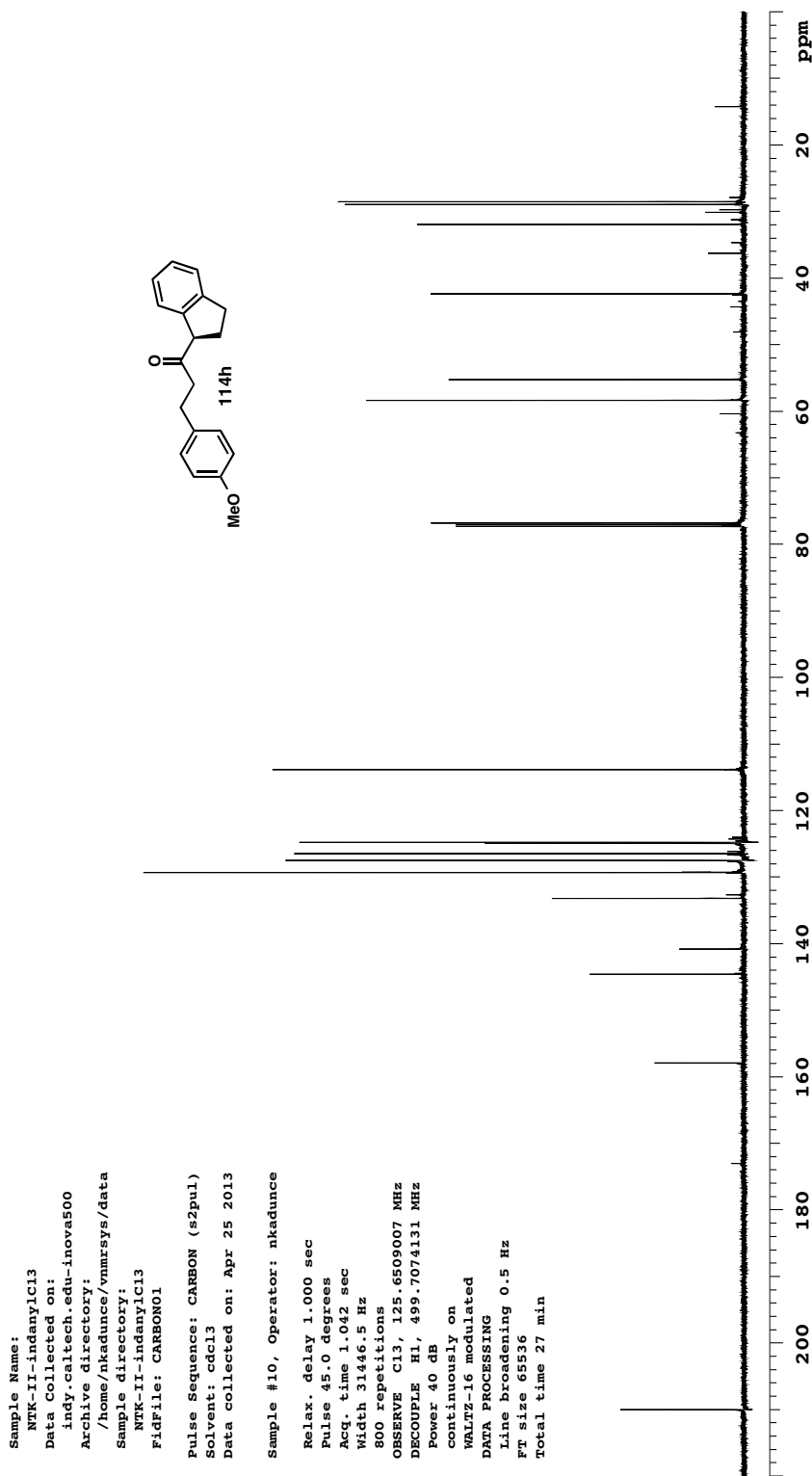


Sample Name:  
 CH-ahc-5-33-4  
 Data Collected on:  
 indy.caltech.edu-inova500  
 Archive directory:  
 /home/acherney/vnmrSYS/data  
 Sample directory:  
 CH-ahc-5-33-4  
 FidFile: PROTON01  
 Pulse Sequence: PROTON (s2pul)  
 Solvent: cdcl3  
 Data collected on: Feb 11 2013  
 Sample #45, Operator: acherney  
 Relax. delay 1.000 sec  
 Pulse 45.0 degrees  
 Acq. time 3.000 sec  
 Width 7995.2 Hz  
 32 repetitions  
 OBSERVE H1, 499.7049145 MHz  
 DATA PROCESSING  
 Line broadening 0.2 Hz  
 FT size 65536  
 Total time 2 min 8 sec

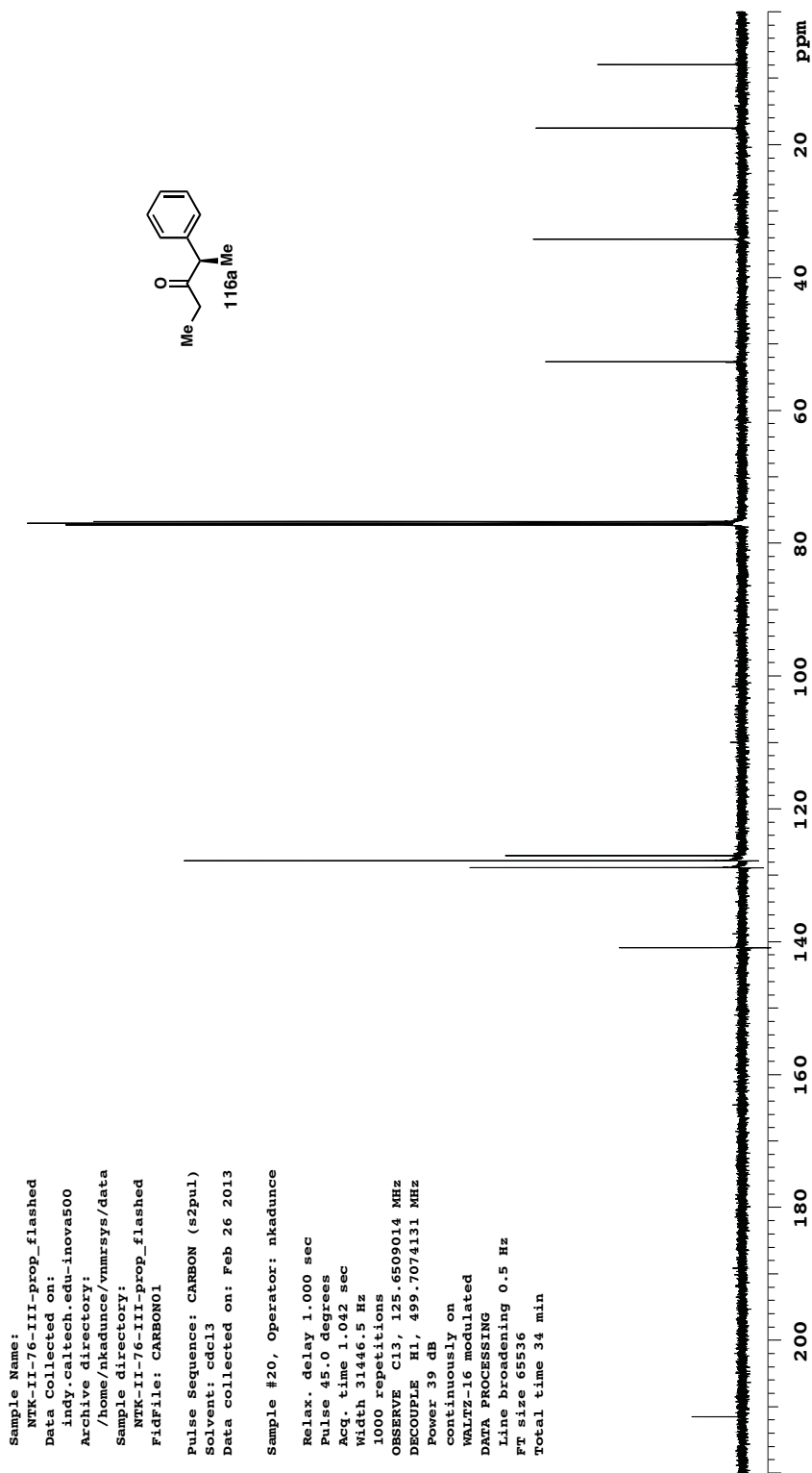




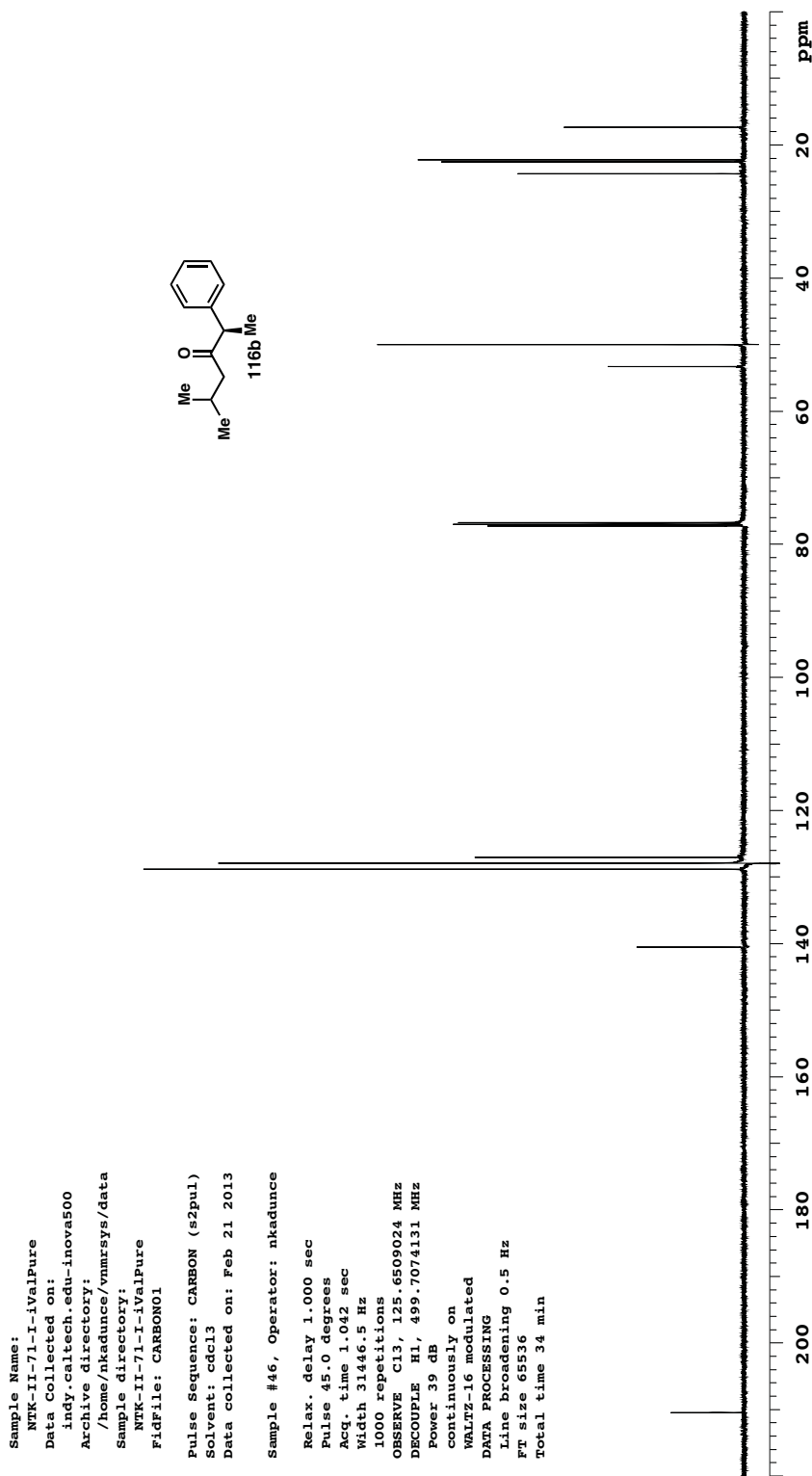




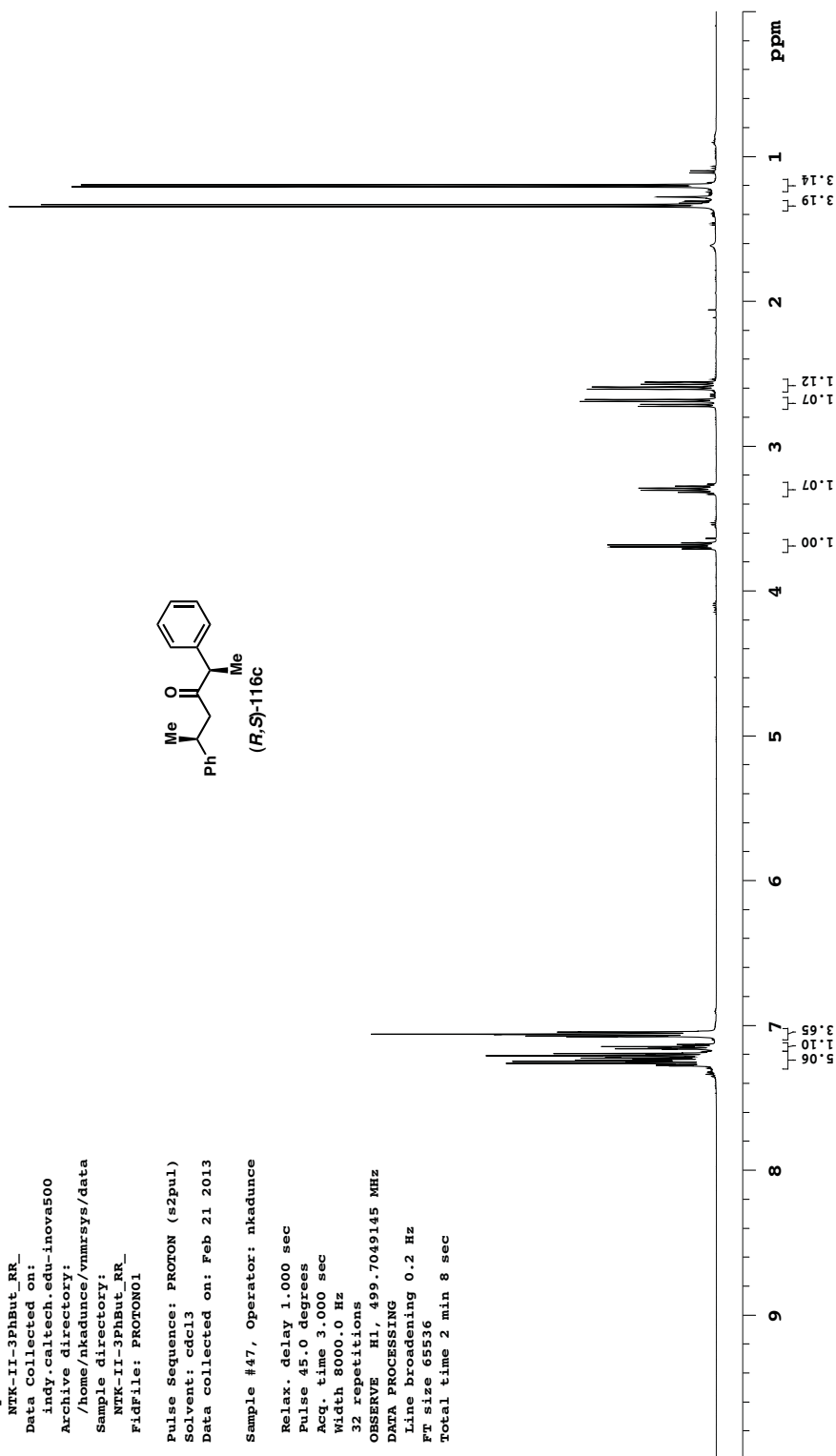
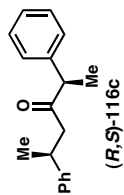


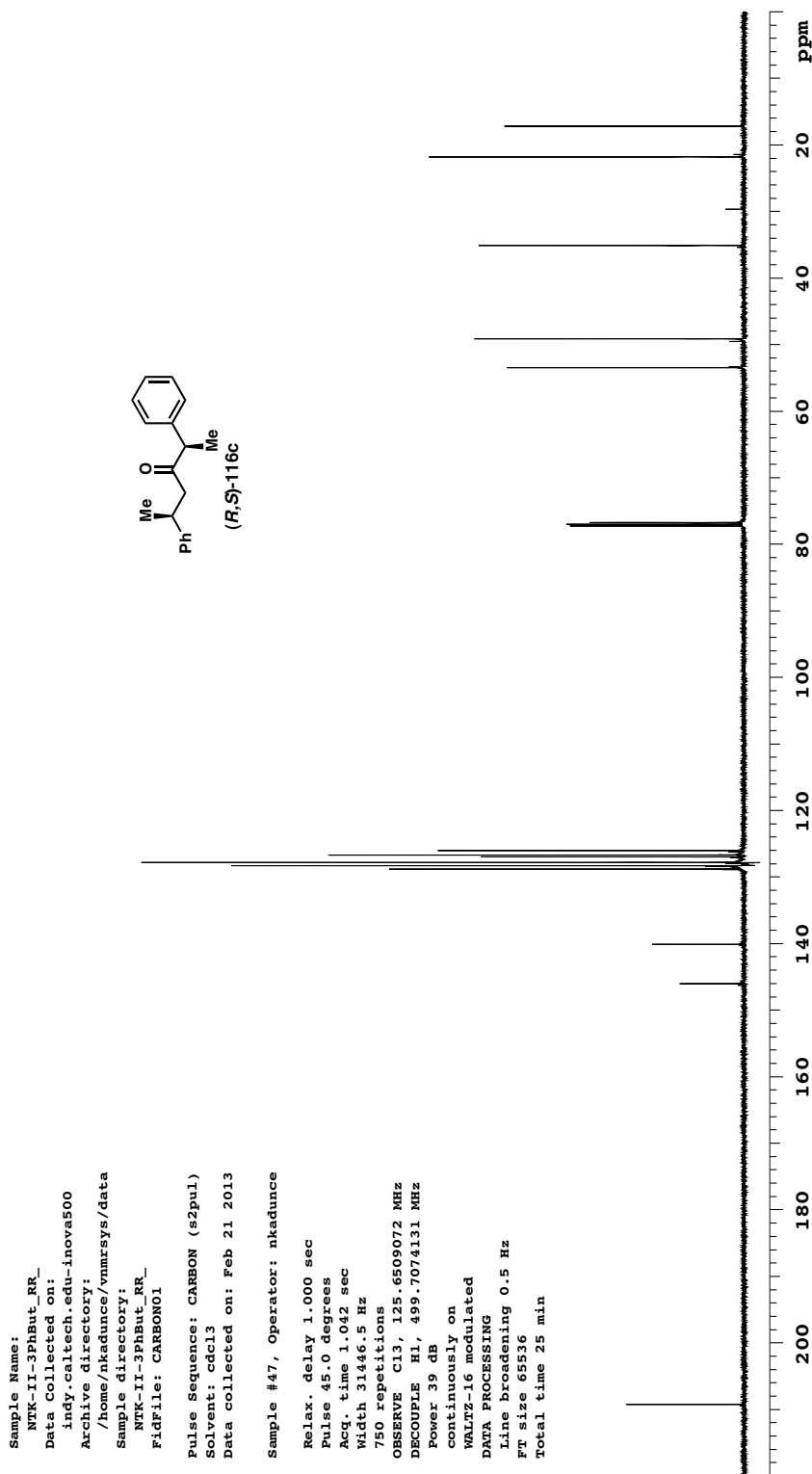




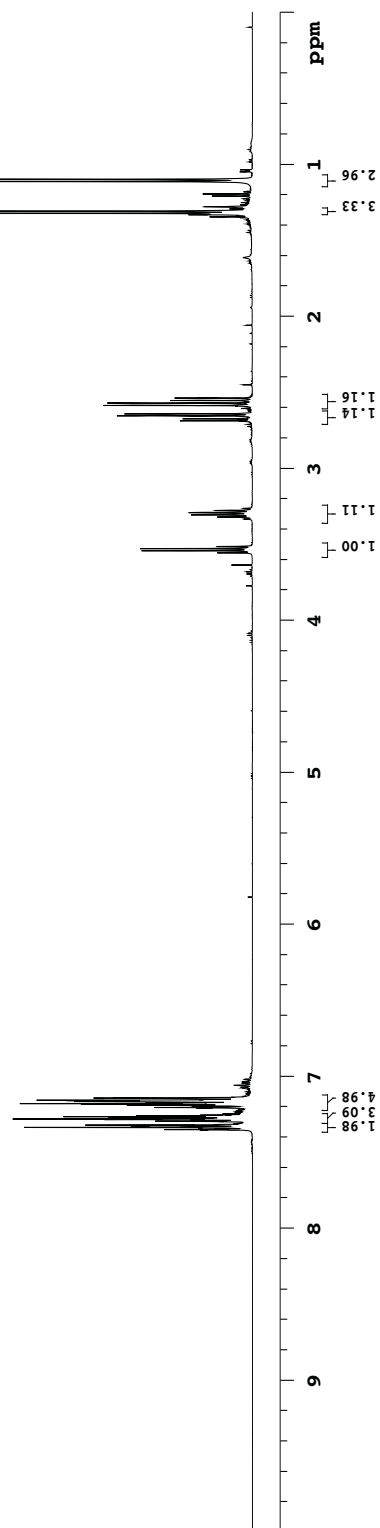
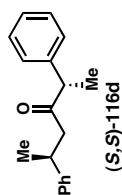


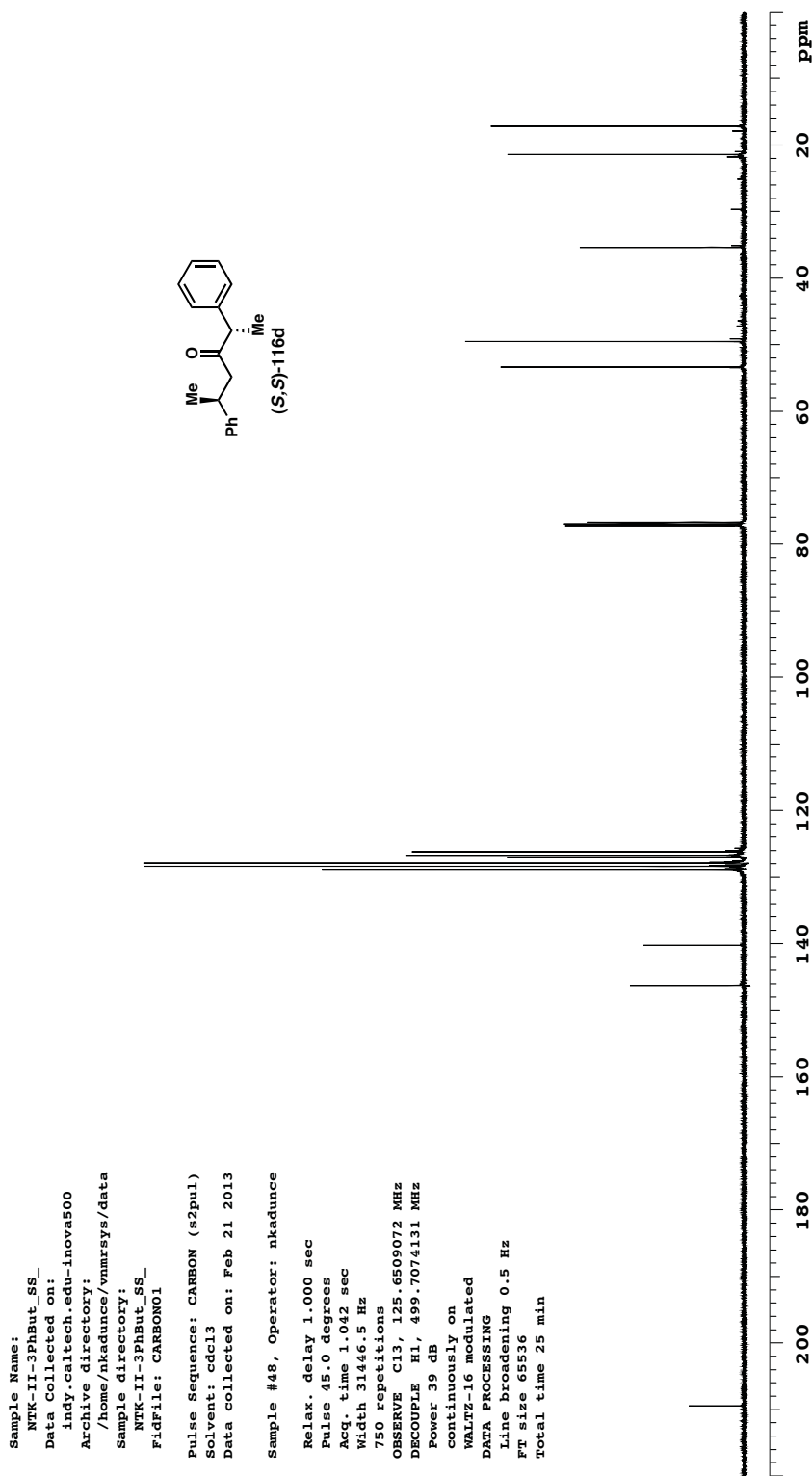
Sample Name: NTK-II-3PhBut\_RR\_  
 Data Collected on: indy.caltech.edu-inova500  
 Archive directory: /home/nkadance/vnmrSYS/data  
 Sample directory: NTK-II-3PhBut\_RR\_  
 FidFile: PROTON01  
 Pulse Sequence: PROTON (s2pul)  
 Solvent: cdcl3  
 Data collected on: Feb 21 2013  
 Sample #47, Operator: nkadance  
 Relax. delay 1.000 sec  
 Pulse 45.0 degrees  
 Acq. time 3.000 sec  
 Width 8000.0 Hz  
 32 repetitions  
 OBSERVE RL, 499.7049145 MHz  
 DATA PROCESSING  
 Line broadening 0.2 Hz  
 FT size 65536  
 Total time 2 min 8 sec

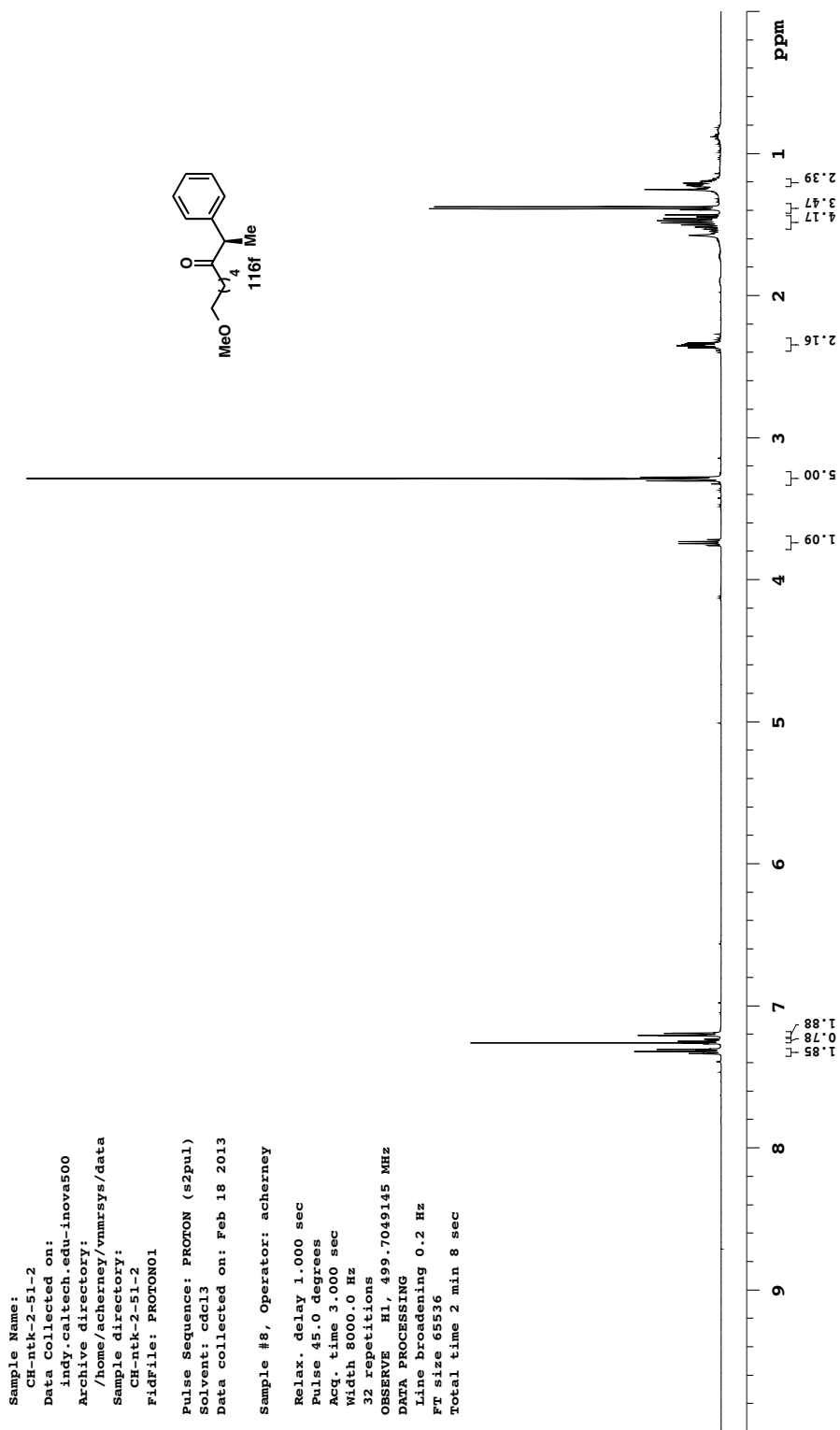


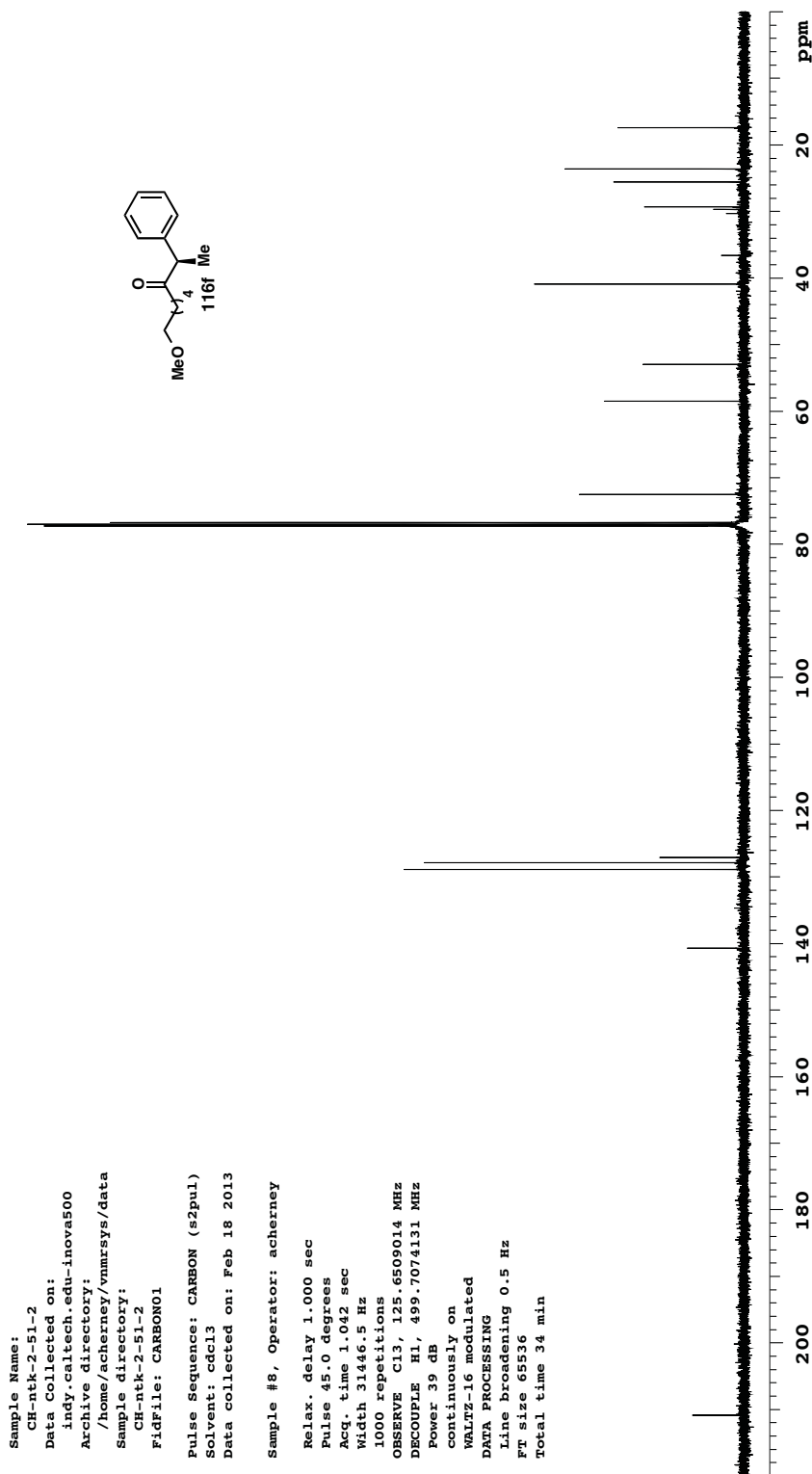


Sample Name: NTK-II-3PhBut\_SS\_  
 Data Collected on: indy.caltech.edu-inova500  
 Archive directory: /home/nkadance/vnmrsys/data  
 Sample directory: NTK-II-3PhBut\_SS\_  
 FidFile: PROTON01  
 Pulse Sequence: PROTON (s2pul)  
 Solvent: cdcl3  
 Data collected on: Feb 21 2013  
 Sample #48, Operator: nkadance  
 Relax. delay 1.000 sec  
 Pulse 45.0 degrees  
 Acq. time 3.000 sec  
 Width 8000.0 Hz  
 32 repetitions  
 OBSERVE H1, 499.7049145 MHz  
 DATA PROCESSING  
 Line broadening 0.2 Hz  
 FT size 65536  
 Total time 2 min 8 sec

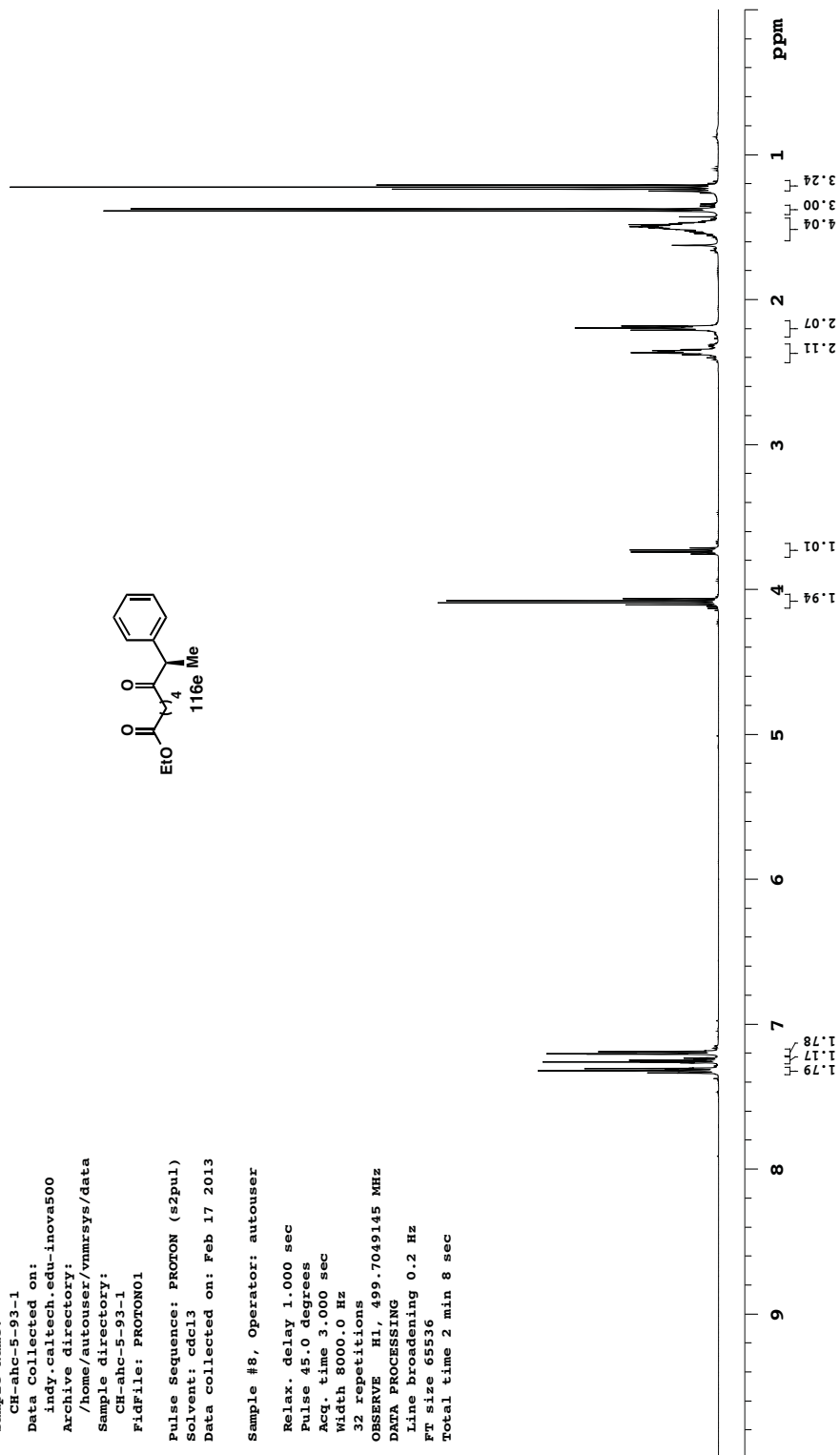
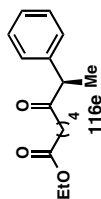


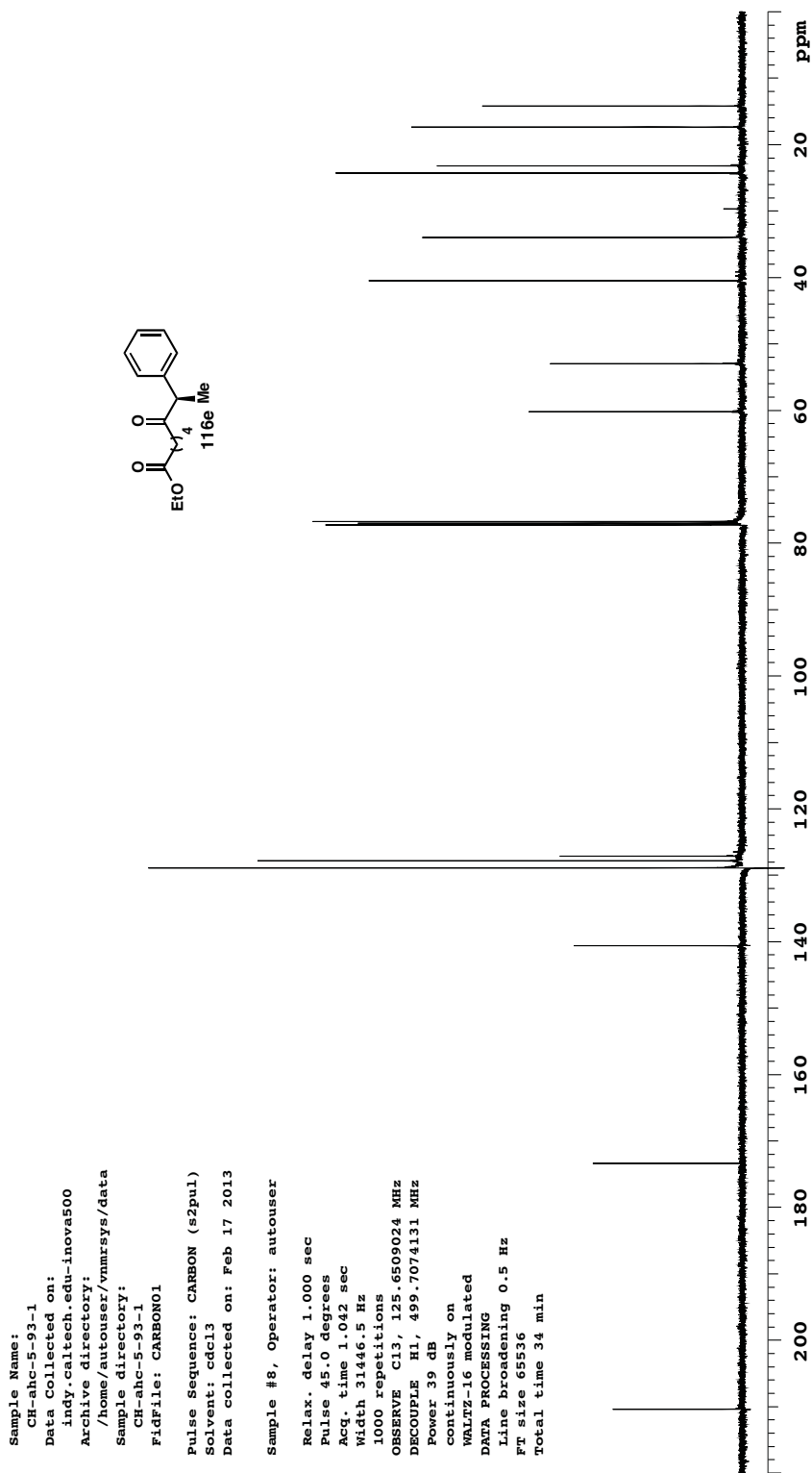




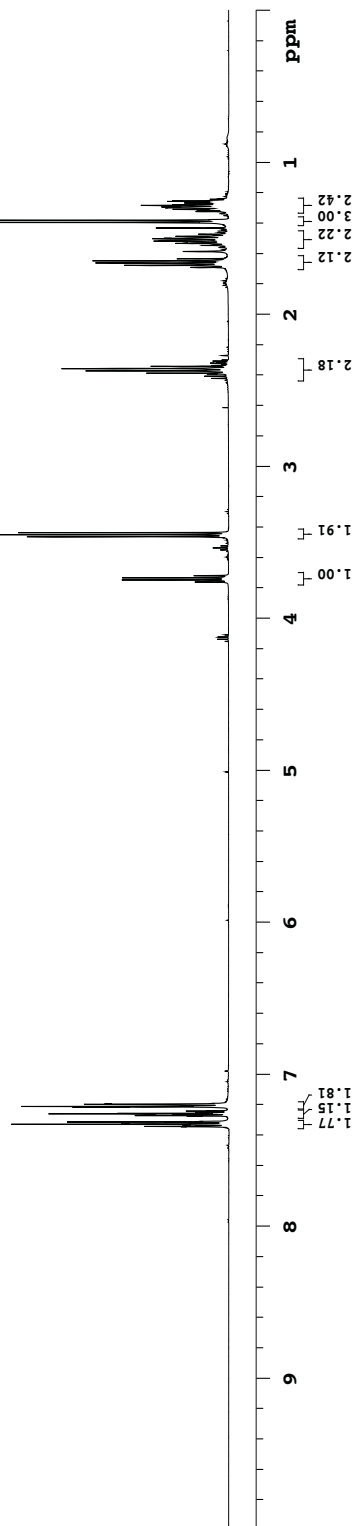
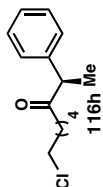


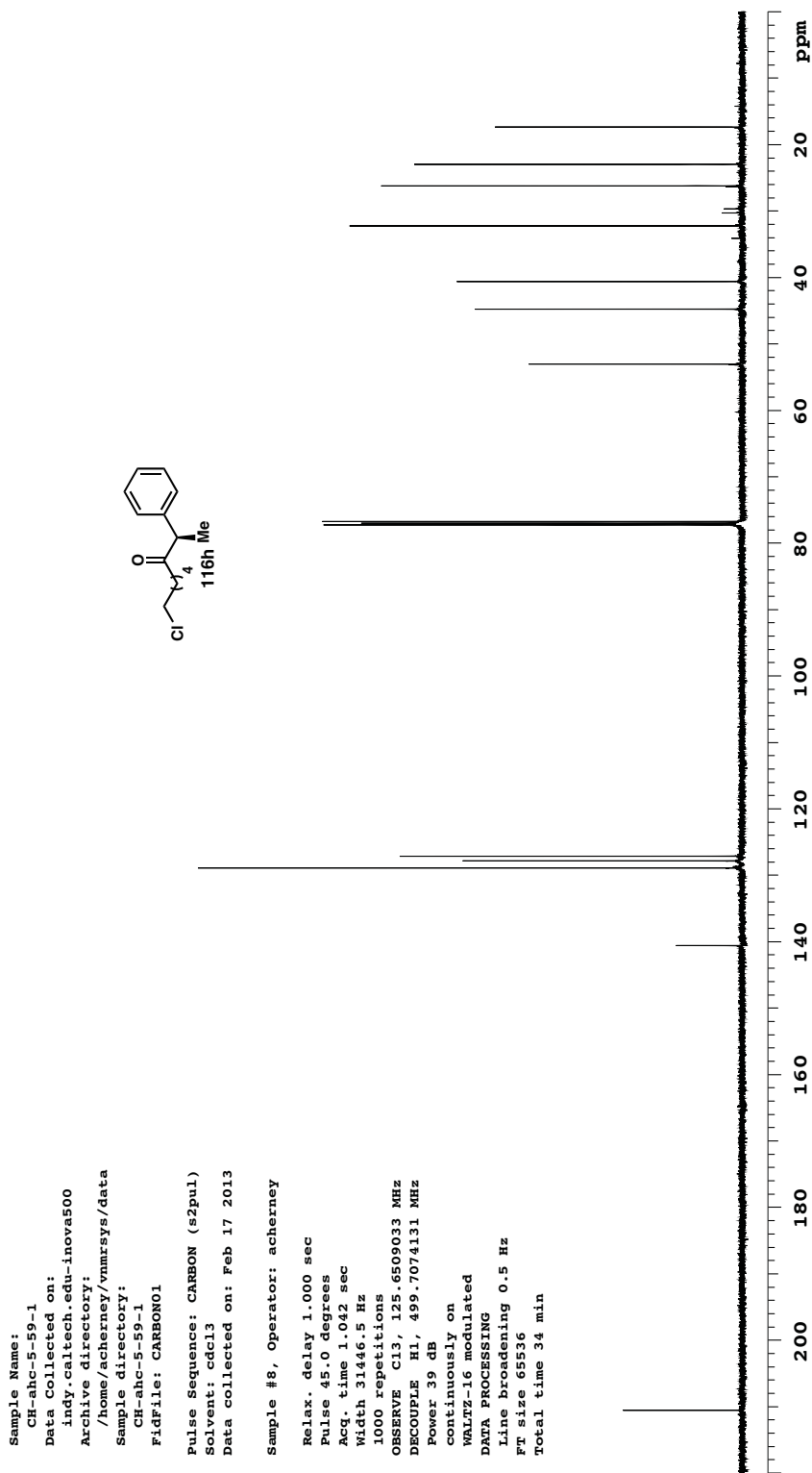
Sample Name:  
 CH-ahc-5-93-1  
 Data Collected on:  
 indy.caltech.edu-inova500  
 Archive directory:  
 /home/autouser/vnmrsys/data  
 Sample directory:  
 CH-ahc-5-93-1  
 FidFile: PROTON01  
 Pulse Sequence: PROTON (s2pul)  
 Solvent: cdcl3  
 Data collected on: Feb 17 2013  
 Sample #8, Operator: autouser  
 Relax. delay 1.000 sec  
 Pulse 45.0 degrees  
 Acq. time 3.000 sec  
 Width 8000.0 Hz  
 32 repetitions  
 OBSERVE H1, 499.7049145 MHz  
 DATA PROCESSING  
 Line broadening 0.2 Hz  
 FT size 65536  
 Total time 2 min 8 sec



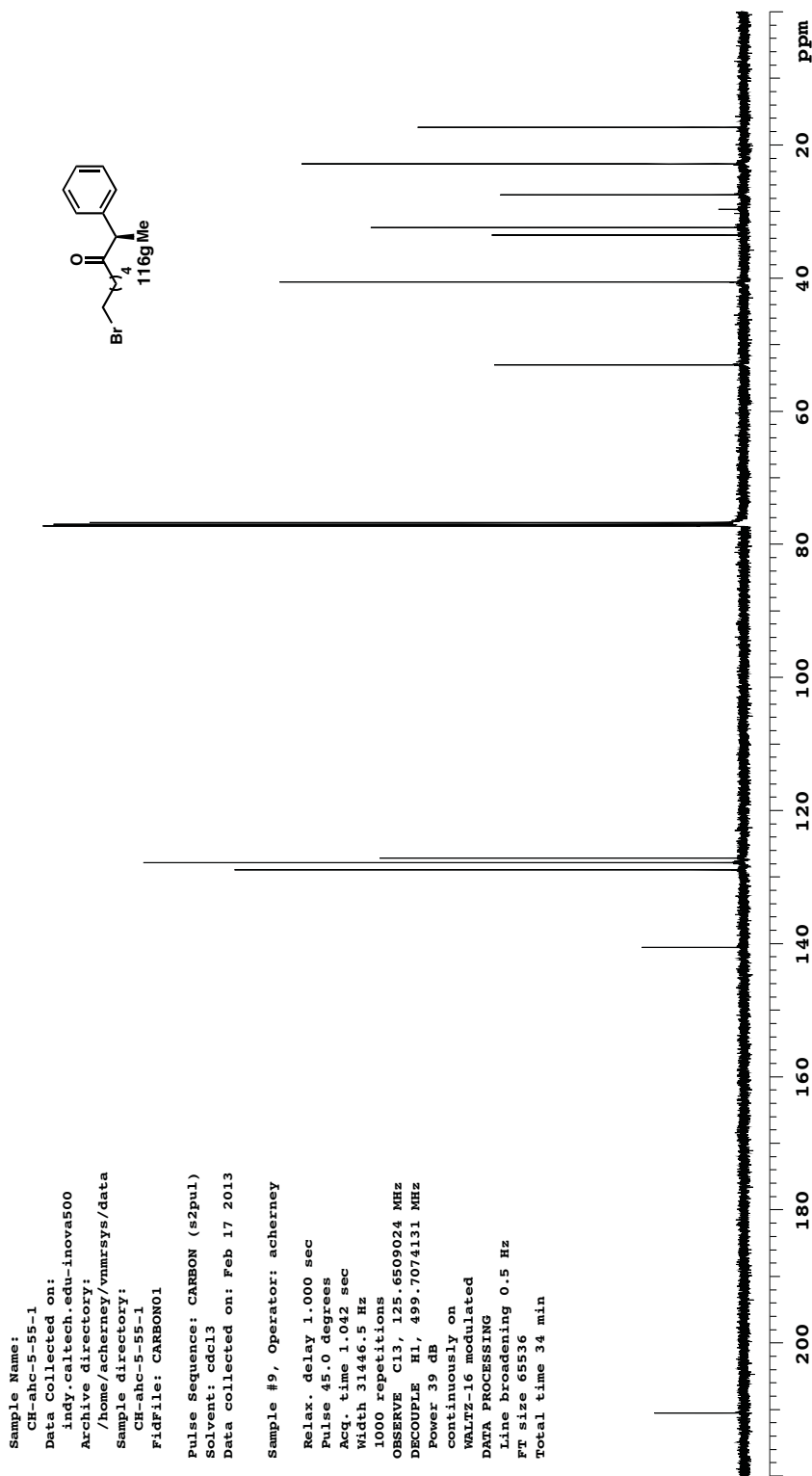


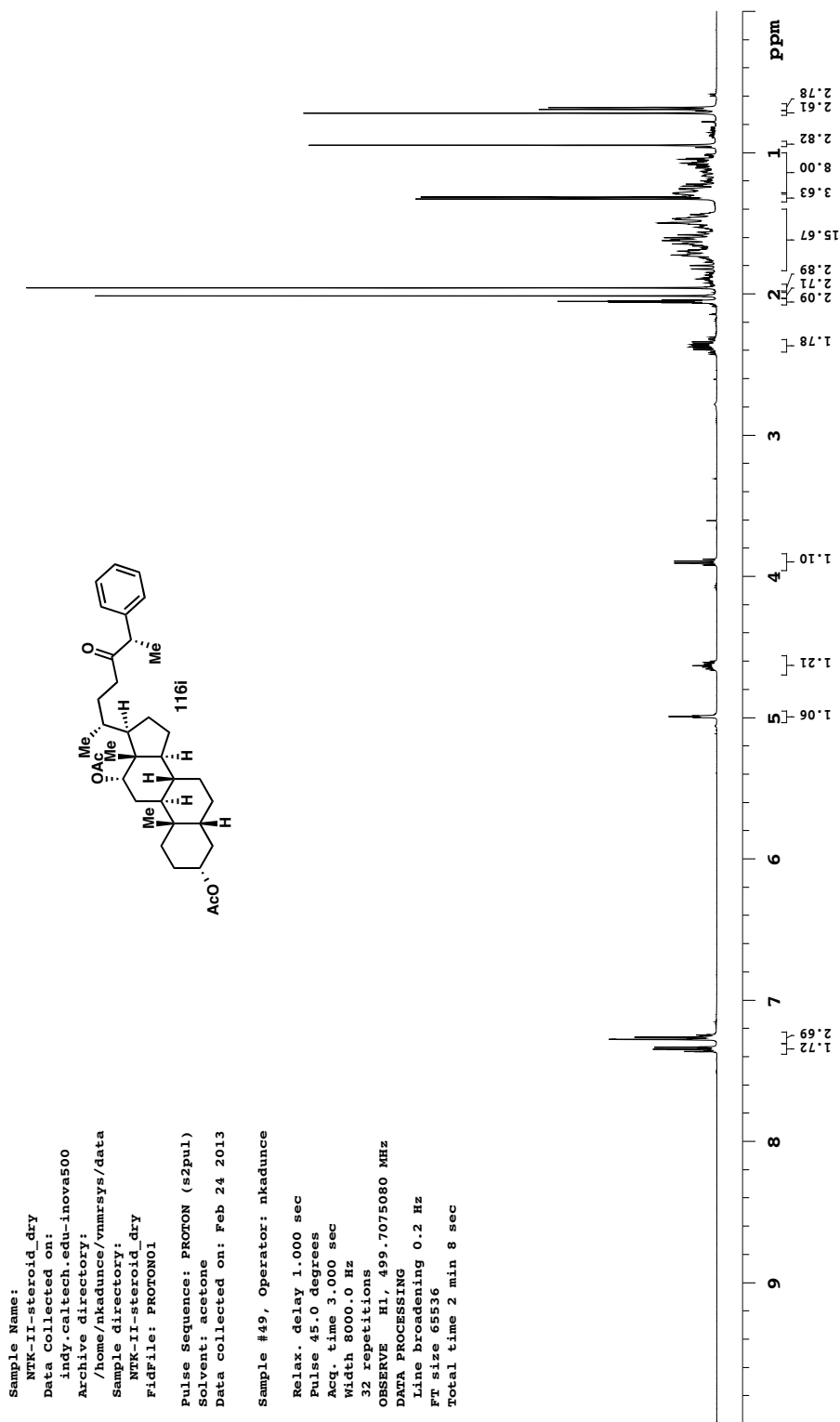
Sample Name:  
 CH-ahc-5-59-1  
 Data Collected on:  
 indy.caltech.edu-inova500  
 Archive directory:  
 /home/acherney/vnmrSYS/data  
 Sample directory:  
 CH-ahc-5-59-1  
 FidFile: PROTON01  
 Pulse Sequence: PROTON (s2pul)  
 Solvent: cdcl3  
 Data collected on: Feb 17 2013  
 Sample #8, Operator: acherney  
 Relax. delay 1.000 sec  
 Pulse 45.0 degrees  
 Acq. time 3.000 sec  
 Width 8000.0 Hz  
 32 repetitions  
 OBSERVE H1, 499.7049145 MHz  
 DATA PROCESSING  
 Line broadening 0.2 Hz  
 FT size 65536  
 Total time 2 min 8 sec

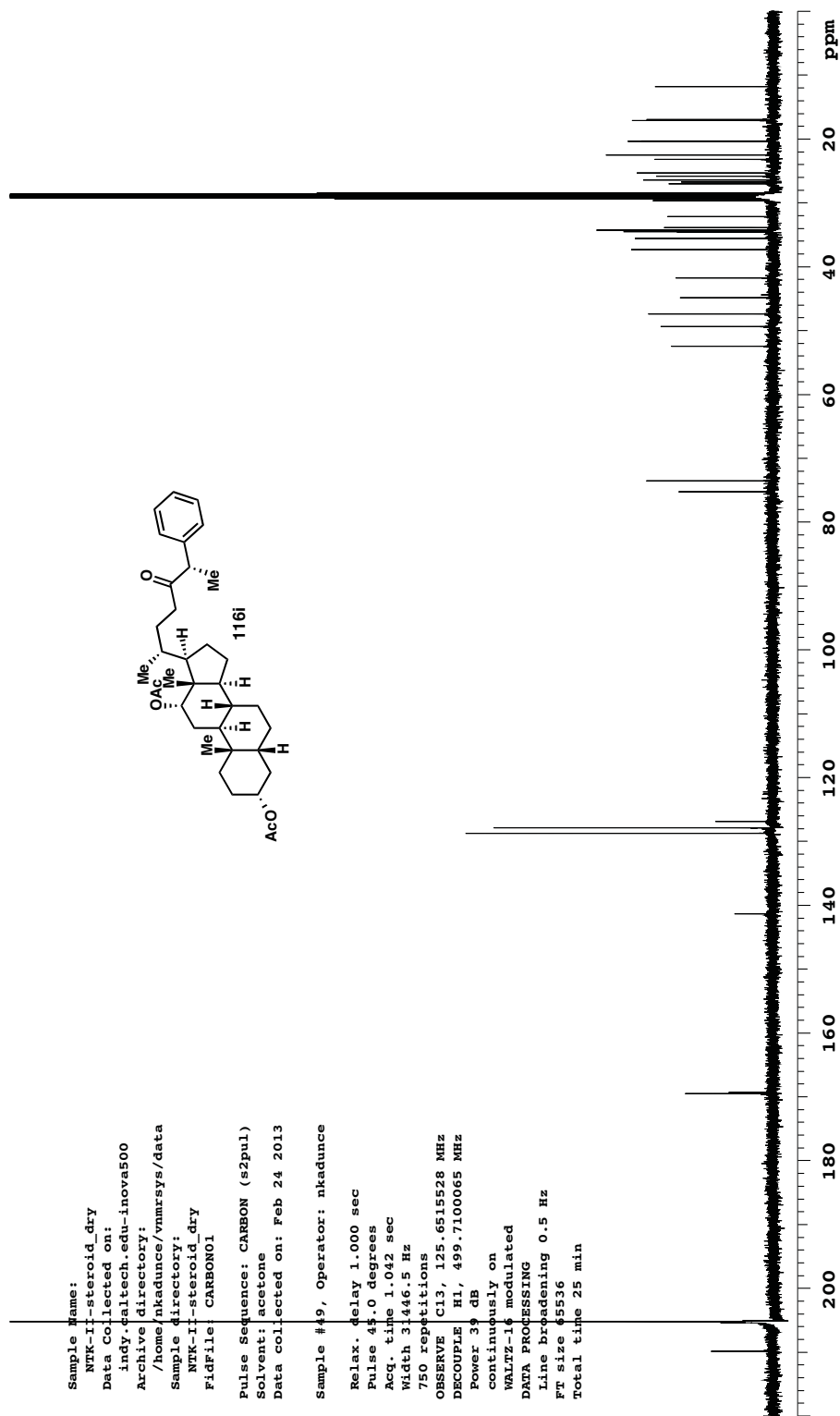












## Chapter 3

### *Nickel-Catalyzed Asymmetric Reductive Cross-Coupling Between Heteroaryl Iodides and $\alpha$ -Chloronitriles<sup>◊</sup>*

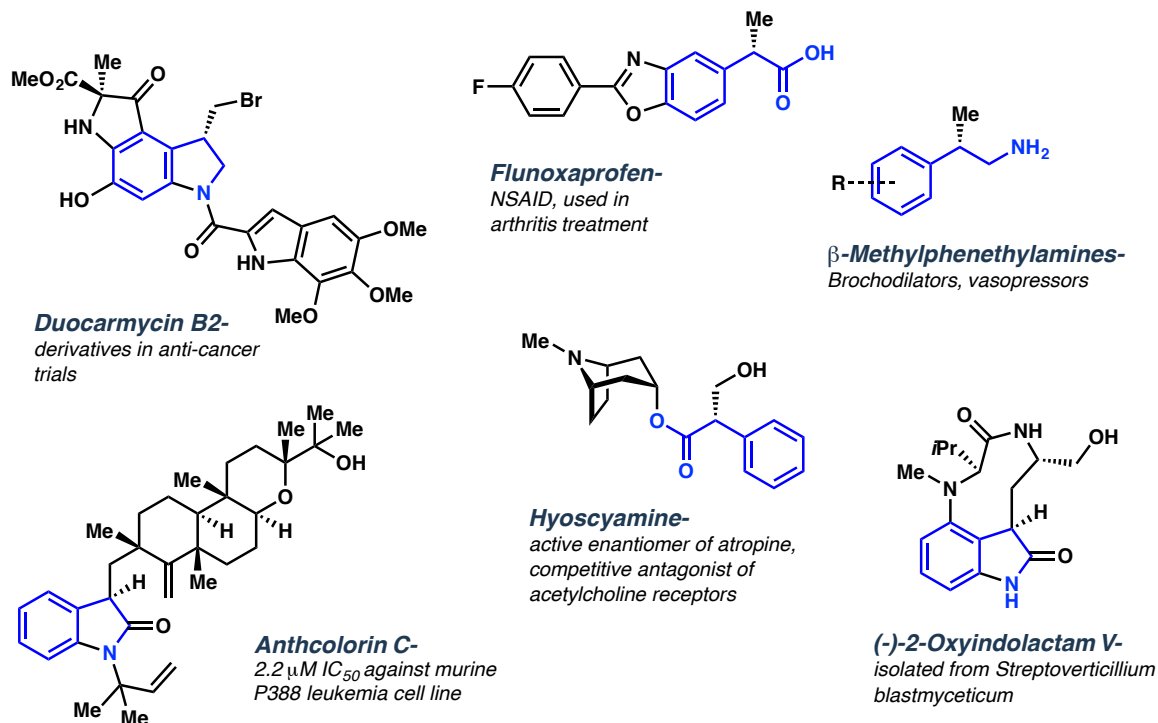
#### 3.1 INTRODUCTION

Benzylic nitriles are a chemically rich and important functionality in organic synthesis. These structural motifs and their derivatives are represented in natural products and bioactive compounds, including pharmaceuticals. They can also serve as valuable synthetic intermediates, being diversifiable to a wide range of more sensitive functionality, such as aldehydes and primary amines. As such, chiral benzylic nitriles present an entry point to enantioenriched products bearing many useful functional groups, as well as being present in desirable targets (**Figure 3.1**). Their hydrolysis to chiral carboxylic acids has been employed in the synthesis of nonsteroidal anti-inflammatories such as naproxen, and their reduction has enabled numerous total syntheses.

---

<sup>◊</sup> Portions of this chapter have been reproduced from published studies (see reference **34**) and the supporting information found therein.

**Figure 3.1.** Bioactive compounds accessible from chiral benzylic nitriles.

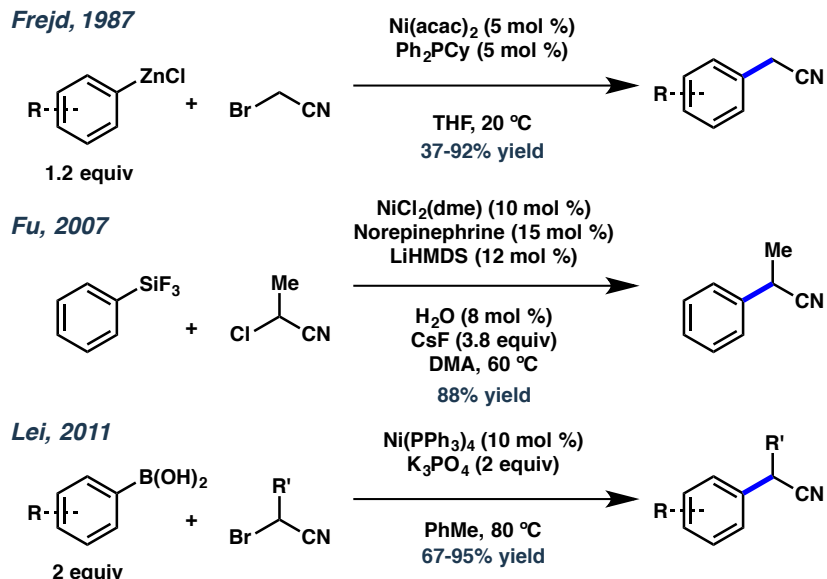


Routes to access these valuable chiral intermediates via asymmetric catalysis have been the focus of numerous research efforts.<sup>1</sup> These approaches have taken two major forms: a) hydrocyanation, including formal conjugate additions, and b) cross-coupling of cyanoelectrophiles. Asymmetric hydrocyanation has been the most widely explored catalytic approach to enantioenriched nitriles, employing HCN (or some surrogate, such as acetone cyanohydrin) and suitable olefin substrates. These reactions can proceed in excellent yield and selectivity, however the substrate scopes of these methods are limited when employing styrenyl olefins. Hydrocyanation of simple styrenes is not amenable to olefin substitution, giving only the  $\alpha$ -methyl nitriles in high enantioselectivity. Conjugate cyanation, on the other hand, has been sparingly developed with  $\beta$ -aryl groups, giving sparse access to the benzylic nitrile class of products. In addition, these methods all

employ some stoichiometric HCN source, making these especially hazardous reactions to conduct.

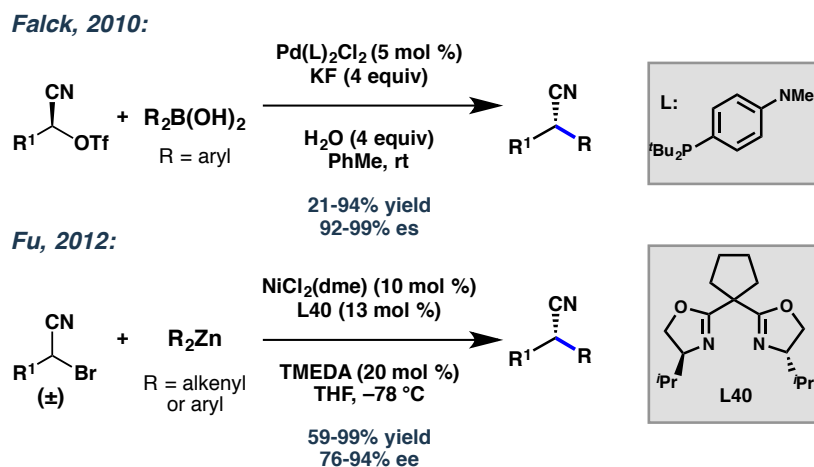
The cross-coupling of  $\alpha$ -halonitriles represents a complementary approach to alkene hydrocyanation. Appealingly, this disconnection introduces the cyano moiety covalently bonded to a substrate, thereby precluding use of an exogenous, potentially hazardous source of cyanide. While asymmetric entries have been reported only recently, the utility of  $\alpha$ -halonitrile electrophiles in cross-coupling was first established in 1987 by Frejd and coworkers (**Scheme 3.1**).<sup>2</sup> The Ni-catalyzed Negishi coupling of bromoacetonitrile with arylzinc reagents proceeds with good to excellent yields to afford the benzylic nitrile products, setting a precedent that went unexplored for another two decades. The next report of these electrophilic partners was by Fu and coworkers in 2007.<sup>3</sup> Importantly, this Hiyama coupling employed a secondary  $\alpha$ -chloronitrile to afford a stereogenic product, albeit in a racemic sense. A similar Suzuki coupling has also been reported by Lei and coworkers with wider substrate scopes for both coupling partners.<sup>4</sup>

**Scheme 3.1.** Racemic cross-coupling of  $\alpha$ -halonitrile electrophiles.



Examples of  $\alpha$ -halonitriles participating in asymmetric cross-coupling reactions have emerged still more recently. Interestingly, both stereospecific and stereoselective examples have been disclosed (**Scheme 3.2**). Falck and coworkers reported the stereospecific Pd-catalyzed Suzuki coupling of enantioenriched cyanohydrin triflates (themselves accessible by asymmetric cyanosilylation of aldehyde precursors).<sup>5</sup> While only a handful of the substrates were prepared asymmetrically, the products of these couplings were furnished with excellent enantiospecificity. In 2012, Fu and coworkers developed a related stereoconvergent transformation: a Negishi coupling employing racemic  $\alpha$ -bromonitriles.<sup>6</sup> Importantly, this report demonstrated the feasibility of a stereoconvergent coupling of halonitrile electrophiles, affording access to the benzylic nitrile products via a chiral Ni catalyst.

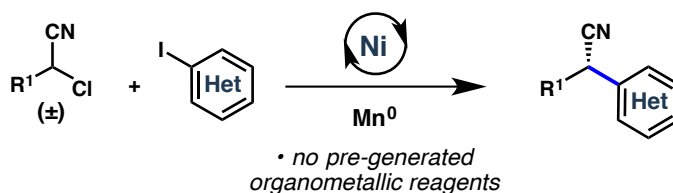
**Scheme 3.2.** Asymmetric cross-coupling of  $\alpha$ -halonitrile electrophiles



With these precedents in mind, we identified  $\alpha$ -halonitriles as desirable electrophiles for Ni-catalyzed asymmetric reductive cross-coupling. To date, the only  $C(sp^3)$  partners employed in enantioselective reductive couplings had been benzylic, providing products with limited prospects for further derivatization. In considering the

mechanistic hypotheses developed for these reactions, the aryl moiety is believed to serve as a radical stabilizing group: the benzylic halides are more susceptible to halide abstraction, generating a prochiral radical intermediate and enabling differentiation of the electrophilic partners (see **Chapter 1**). We hypothesized that a nitrile, while possessing a lower radical stabilization energy than an aryl group, could still facilitate cross-selective coupling with a  $C(sp^2)$  electrophile to afford enantioenriched cyano products (**Scheme 3.3**).<sup>7</sup>

**Scheme 3.3.** Target asymmetric reductive cross-coupling  $\alpha$ -halonitriles.



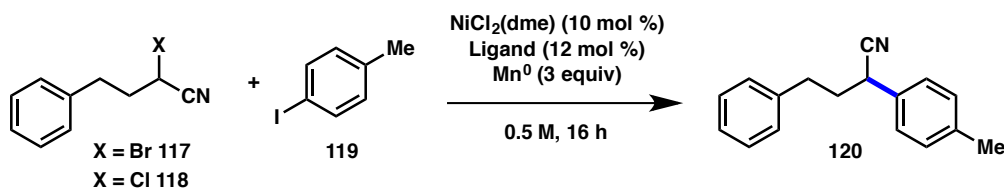
We were also cognizant of potential difficulties employing nitrile-bearing substrates, given that Lewis basic functionality had been poorly tolerated in our previous reaction development. Indeed, nitriles have been shown to form strongly bound  $\sigma$ - and  $\pi$ -adducts with  $Ni^0$  complexes, providing a compelling mechanistic basis for catalyst poisoning.<sup>8</sup> However, we anticipated that if such challenges could be overcome, then other Lewis basic moieties such as heterocycles may be competent coupling partners as well, giving access to desirable products difficult to access via cross-coupling.<sup>9</sup> With this as our goal we set out to evaluate the feasibility of such an asymmetric reductive coupling.

## 3.2 REACTION DEVELOPMENT

Prior to our investigations, there had been no published reports of the catalytic reductive cross-coupling of halonitrile electrophiles. Therefore we chose to begin our

exploration employing achiral ligands to identify conditions capable of affording the desired products. We selected a hydrocinnamaldehyde-derived halonitrile (**117** or **118**) as the C(sp<sup>3</sup>) partner and *p*-iodotoluene (**119**) as the aryl electrophilic component. Based on the conditions employed for the asymmetric reductive cross-coupling of benzylic chlorides with acyl chlorides (see **Chapter 2**), early optimization efforts were conducted employing NiCl<sub>2</sub>(dme) as the precatalyst, Mn<sup>0</sup> as the reductant, polar amide/urea solvents, and various achiral ligands.

**Table 3.1.** Initial exploration with achiral ligands.



Entry	X	Additive	Ligand	Solvent	Temp.	Yield 120
1	Br	--	dtbpy (L64)	DMA	50 °C	--
2	Br	--	dtbpy	NMP	50 °C	--
3	Br	--	dtbpy	DME	50 °C	--
4	Br	--	dtbpy	DMPU	50 °C	5%
5	Br	--	bathophen (L65)	DMPU	50 °C	9%
6	Br	--	bathophen	DMPU	rt	--
7	Br	--	bathophen	DMPU	80 °C	5%
8	Br	TFA	bathophen	DMPU	rt	10%
9	Cl	TFA	dtbpy	DMPU	rt	--
10	Cl	TFA	dtbpy	DMPU	50 °C	10%
11	Cl	TMSCl	dtbpy	DMPU	50 °C	22%
12	Cl	TMSCl	dtbpy	DMPU	rt	8%

Illustrative results from this effort are collected in **Table 3.1**. Attempts to engage bromonitrile **117** (as in the stereoconvergent Fu example, see **Scheme 3.2**) in cross-coupling were met with poor yields not exceeding 10%. However some trends were still identifiable. DMPU was the only solvent in which product was observed, albeit only upon heating (entry 4). Employing acidic surface activating reagents, as reported by

Durandetti and coworkers, enabled some product formation at room temperature (entries 8-12).<sup>10</sup> Taking these results and switching to the analogous chloronitrile **118** proved to be more promising. In the presence of TFA or TMSCl, product could be observed at room temperature, and in excess of 20% yield at 50 °C. In every case, complete consumption of the halonitrile was observed, with protodehalogenated starting material accounting for the remainder of the mass balance. This suggested a poor matching of the substrate reactivities, with the C(sp<sup>3</sup>) partner being consumed and quenched much faster than the aryl component could engage the catalyst.

**Table 3.2.** Preliminary evaluation of chiral ligands and solvents.

Entry	Ligand	Additive	Temp	ee 120
1	<sup>t</sup> BuBiOX (L66)	TFA	50 °C	--
2	<sup>i</sup> PrBiOX (L67)	TFA	50 °C	30%
3	PhBiOX (L68)	TFA	50 °C	20%
4	BnBiOX (L31)	TFA	50 °C	11%
5	<sup>t</sup> BuBOX (L61)	TFA	50 °C	3%
6	<sup>i</sup> PrBOX (L62)	TFA	50 °C	6%
7	PhBOX (L32)	TFA	50 °C	16%
8	BnBOX (L63)	TFA	50 °C	5%
9	<sup>i</sup> PrBiOX (L67)	TMSCl	rt	31%

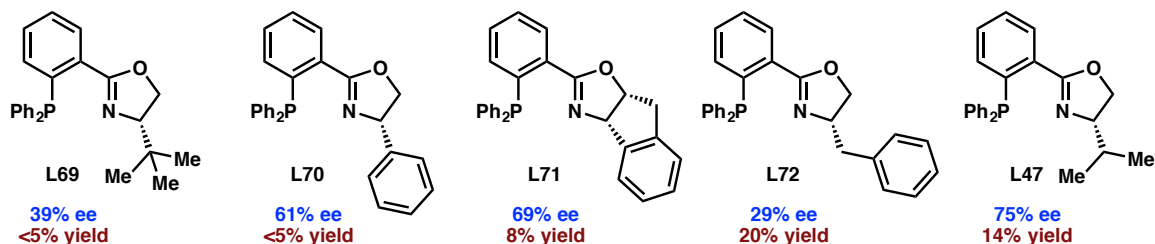
employing <sup>i</sup> PrBiOX (L67):				
Entry	Solvent	Additive	Temp	ee 120
1	DMA	TMSCl	rt	8%
2	DMF	TMSCl	rt	4%
3	DME	TMSCl	rt	44%
4	DMSO	TMSCl	rt	--
5	Dioxane	TMSCl	rt	63%
6	NMP	TMSCl	rt	36%
7	EtOAc	TMSCl	rt	62%
8	THF/DMPU	TMSCl	rt	46%

At this stage, we turned our attention to an initial survey of solvents and chiral ligands. While yields did not improve with any of the surveyed BOX or BiOX ligand scaffolds, we were pleased to observe promising levels of enantioselectivity under the

conditions developed in **Table 3.1** when using  $^i$ PrBiOX **L67** and TMSCl (0.4 equiv) as the activator (**Table 3. 2a, Entry 9**). Running the reaction in 1,4-dioxane as solvent gave a dramatic boost in ee to 63% (**Table 3.2, Entry 5**).

While this result provided us with improved enantioselectivity, the yield (as determined by  $^1$ H NMR spectroscopy of the crude reaction mixture) remained at approximately 10%, and a significant amount of protodehalogenated **118** was still observed. We hypothesized that slow oxidative addition of the aryl iodide relative to the rate of  $\alpha$ -chloronitrile decomposition could be the source of the problem. Therefore we screened a panel of phosphino-oxazoline (PHOX) ligands, anticipating that the more strongly  $\sigma$ -donating phosphine would accelerate oxidative addition of the aryl iodide partner.<sup>11</sup> Gratifyingly, not only were the yields improved twofold (BnPHOX, **L72**), but several ee's were higher than our previous best results (**Figure 3.2**).

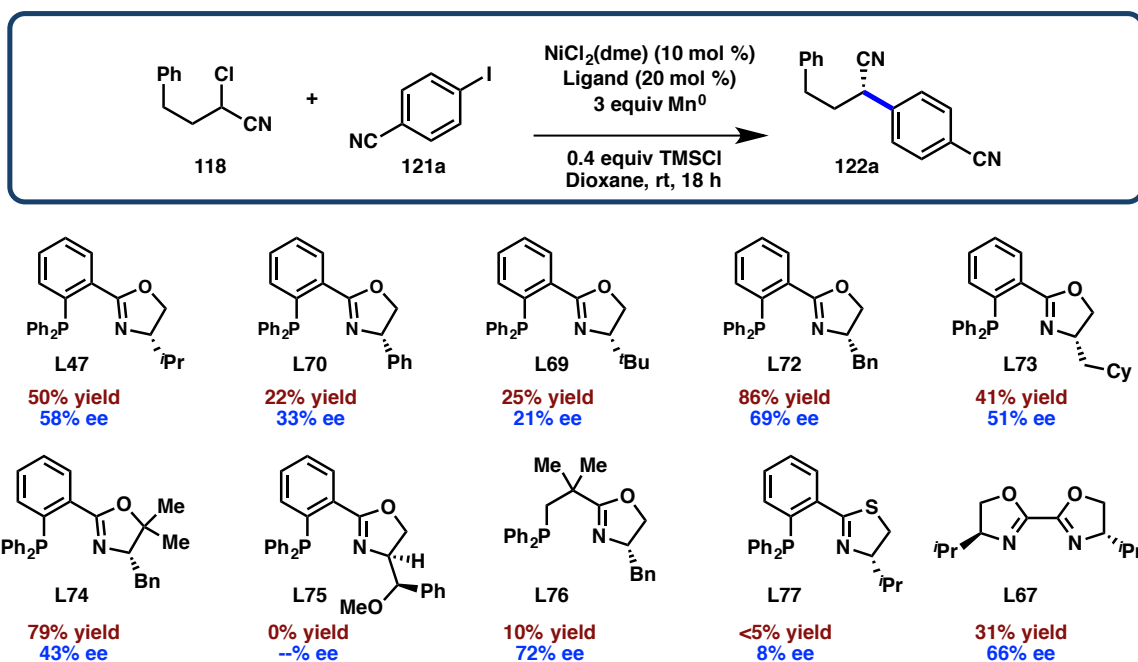
**Figure 3.2.** Initial screen of PHOX ligands.



Based on the improved reactivity using PHOX ligands, we hypothesized that yields might be further improved when coupling electron-deficient aryl halides, which should undergo faster oxidative addition to a Ni<sup>0</sup> complex. This decision also enabled us to leverage our optimization effort toward another of our goals: the tolerance of Lewis basic functionality. We hypothesized that employing 4-iodobenzonitrile **121a** would not only accelerate oxidative addition by virtue of the electron-withdrawing cyano group, but

also incorporate another potentially coordinating functionality. It was our hope that reaction optimization with this substrate would select for conditions tolerant of coordinating groups. Therefore we were pleased to find that aryl iodide **121a** was an improved substrate for the cross-coupling, as shown in **Scheme 3.4**.

**Scheme 3.4.** PHOX ligand evaluation employing 4-iodobenzonitrile (**121a**).

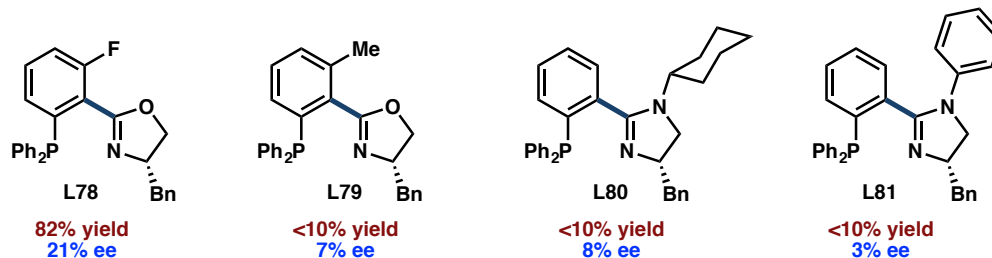


Several entries are included to illustrate the range of ligands explored at this stage. Incorporating branching at the chiral substituent was no longer optimal ( $i\text{PrPHOX}$ , **L47**). Rather,  $\text{BnPHOX}$  (**L72**) was the best-performing ligand, affording **122a** in 86% yield and 69% ee. Scaffolds with steric bulk closer to the binding pocket gave lower yields ( $\text{PhPHOX}$  **L70** and  $i\text{BuPHOX}$  **L69**), although these did perform much better with this substrate than with the previously investigated 4-iodotoluene. A saturated analogue of **L72**,  $\text{CH}_2\text{CyPHOX}$  **L73** did not perform better. Introducing *gem*-dimethyl substitution on the oxazoline ring was expected to orient the  $\text{Bn}$  substituent toward the binding pocket, increasing its effective steric bulk.<sup>12</sup> This substitution afforded lower enantioselectivity

than the corresponding *des*-gem-dimethyl derivative **L72**. Introduction of a methoxy group in **L75** shut down reactivity entirely, suggesting that **L75** may bind Ni in a tridentate fashion, disrupting catalysis.<sup>13</sup> Changing the aryl core of BnPHOX to a neopentyl alkyl linker (**L76**) gave appreciably greater decomposition of the starting materials, indicating that such electron rich phosphine ligands are not well-tolerated.<sup>14</sup> Likewise, changing the oxazoline ring to a thiazoline (**L77**) gave poor reactivity and selectivity.<sup>15</sup> Finally, reinvestigating <sup>i</sup>PrBiOX (**L67**) with this substrate did show an improvement over its performance with 4-iodotoluene, but the ligand was not superior to the PHOX series.

At this stage, BnPHOX (**L72**) stood as the most optimal ligand we had explored, affording **122a** in synthetically useful yields but insufficient ee. To address this, we undertook a systematic exploration of the BnPHOX scaffold, with optimization efforts targeting: a) the bite angle, b) the oxazoline benzyl substituent, and c) the biarylphosphine arm.

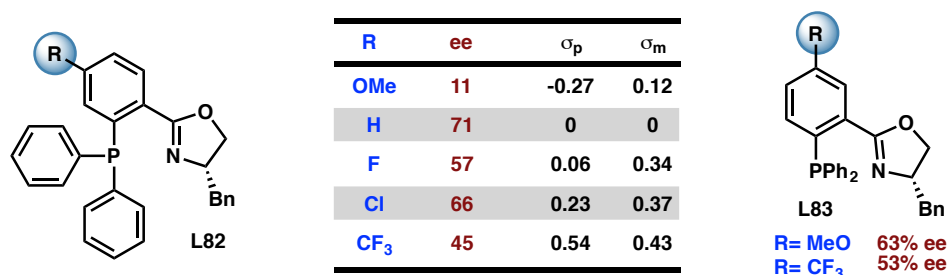
**Figure 3.3.** Perturbation of PHOX ligand bite angles.



Initial studies focused on perturbation of the ligand bite angle (**Figure 3.3**). Substitution of the aryl core *ortho* to the oxazoline was expected to introduce repulsive interactions between the two rings. First, *ortho*-fluoro derivative **L78** was explored, anticipating that an electronic repulsion between the fluoro substituent and the electron

lone pairs of the oxazoline oxygen would lead to a narrowing of the bite angle.<sup>16</sup> While a significant effect was observed, unfortunately it was to the detriment of ee (although the yield was maintained). We then sought to perturb the torsion angle about the aryl-oxazoline bond (highlighted in blue). We anticipated that introduction of bulky substituents on either ring about this bond would lead to steric clashing, disrupting the coplanarity of the rings and therefore altering the ligand bite angle.<sup>17</sup> Therefore, we prepared *ortho*-methyl substituted **L79**, as well as two imidazoline derivatives bearing large groups on the nitrogen atom (**L80** and **L81**). Indeed, all of these ligands displayed a similar reaction profile, affording low yields of nearly racemic product.

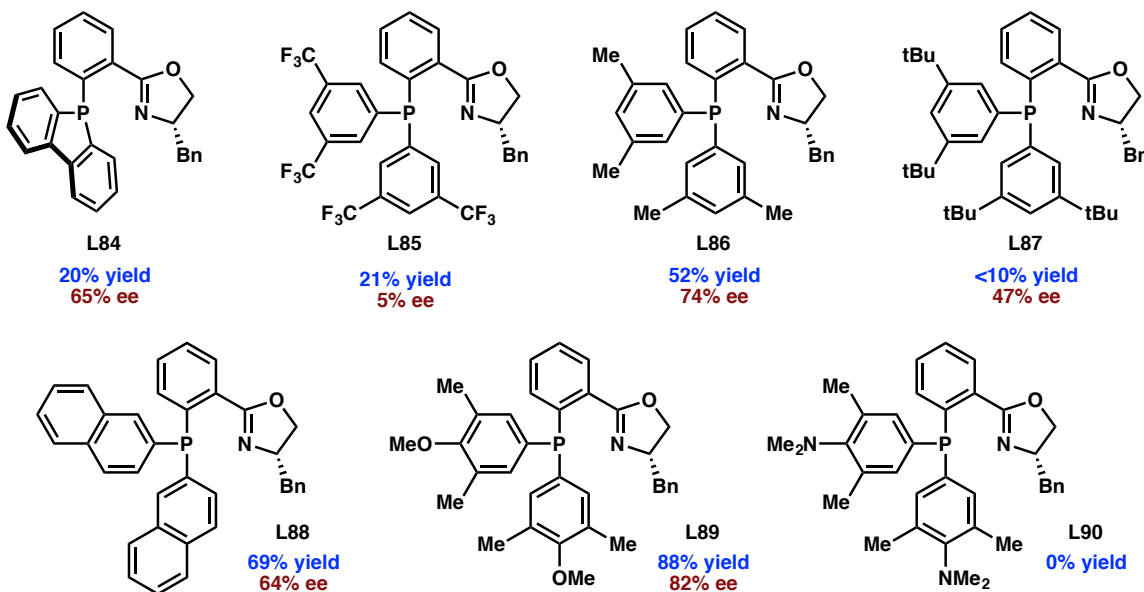
**Figure 3.4.** Electronic tuning of the BnPHOX core and Hammett parameters.



Next, we turned our attention to the electronic profile of the BnPHOX ligand scaffold. Bunt and coworkers have performed extensive studies on the performance of electronically differentiated PHOX ligands in Pd-catalyzed allylic substitution reactions.<sup>18</sup> In these investigations, a substituent at the 4-position (R in **L82**) has been shown to exert a significant effect on both the yield and selectivity of the reaction, an effect attributed to manipulation of the *trans* effect by the substituent. To conduct this study, we prepared the series of 4-substituted BnPHOX derivatives shown in **Figure 3.4**. Unfortunately, no correlation was observed between the product ee and the Hammett parameter  $\sigma_p$  or  $\sigma_m$ , and no substituent outperformed the unsubstituted BnPHOX **L72**. We hypothesize that

this is due to the second-order nature of the perturbation, in which both the oxazoline and phosphine arms are affected by the substituent. We also investigated substitution at the 5-position (**L83**), however neither electron-rich nor electron-withdrawing groups led to an improvement in enantioselectivity.

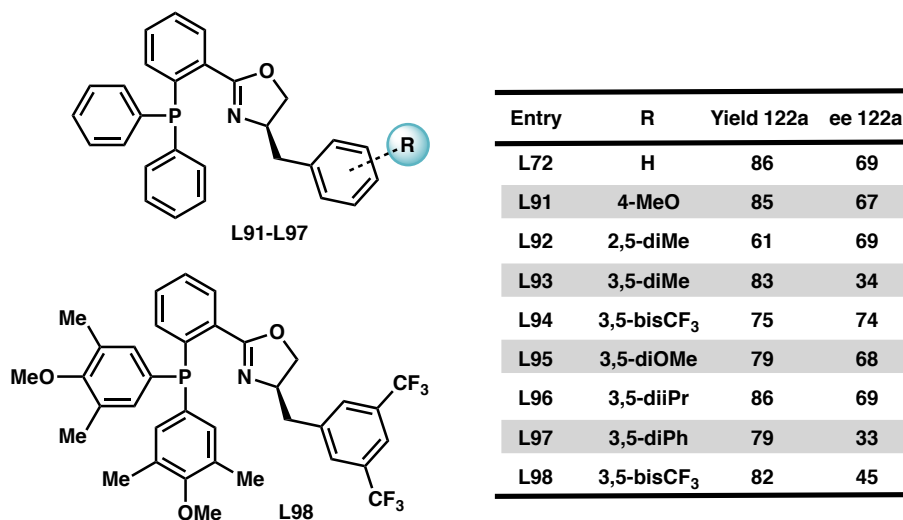
**Figure 3.5.** Optimization of the BnPHOX diarylphosphine arm.



Next, we shifted our focus to the biaryl phosphine arm of BnPHOX. While alkyl phosphines had earlier proven to be too reactive, we hoped that altering the steric and electronic profile of the triarylphosphine moiety might enable more subtle tuning of the reaction.<sup>19</sup> To this end, we first prepared dibenzophosphole-BnPHOX **L84**, in which the phenyl rings of the phosphine are tethered into a planar tricycle.<sup>20</sup> Unfortunately this led to a decrease in the yield of **122a**. Moving instead to substitution about the aryl rings, we focused on 3,5-disubstituted analogues. Preparing electron-deficient and electron-rich derivatives (**L85** and **L86**), we were delighted to see a clear divergence with the trifluoromethylated ligand **L85** giving nearly racemic product while the xylyl **L86** afforded a 5% boost in enantioselectivity over **L72**. While increasing the steric bulk of

the alkyl substituents to 3,5-di(*t*Bu) **L87** nearly shut down reactivity, increasing the electron density of the aryl substituent had the opposite effect: 3,5-dimethyl-4-methoxyphenyl-BnPHOX (**L89**, DMMBnPHOX) afforded **122a** in 88% yield and 82% ee, the best results observed thus far.<sup>11b</sup> Attempts to further increase the electron density of the phenyl rings by introduction of dimethylamino substituents (**L90**) gave no product in the cross-coupling, perhaps due to catalyst destabilization by the aniline moieties.

**Figure 3.6.** Unnatural phenylalanine-derived PHOX ligands.



Pleased to have identified an optimal diarylphosphine arm, we set out to study the benzyl substituent of BnPHOX. We hypothesized that increasing the steric bulk about the aryl ring of the chiral substituent may increase ee by better blocking the occupied quadrant of the coordination sphere, while electronic perturbations may alter subtle secondary interactions during catalysis. The targeted ligand series is shown in **Figure 3.6**. While the chiral oxazoline of all BnPHOX derivatives prepared previously had been derived from natural phenylalanine, the ligands for this study (**L91–L98**) required unnatural phenylalanine derivatives bearing aryl substitution. These were readily accessible via the procedure reported by Jackson and coworkers, a Negishi cross-

coupling between the desired aryl halide partner and the organozinc reagent formed from iodoserine.<sup>21</sup> Unfortunately, most substitutions about the benzyl ring led to catalysts performing no better than BnPHOX (**L72**), with some being markedly worse. However one ligand, 3,5-bis(trifluoromethyl)phenyl **L94** afforded **122a** in 74% ee, a 5% increase over the control.

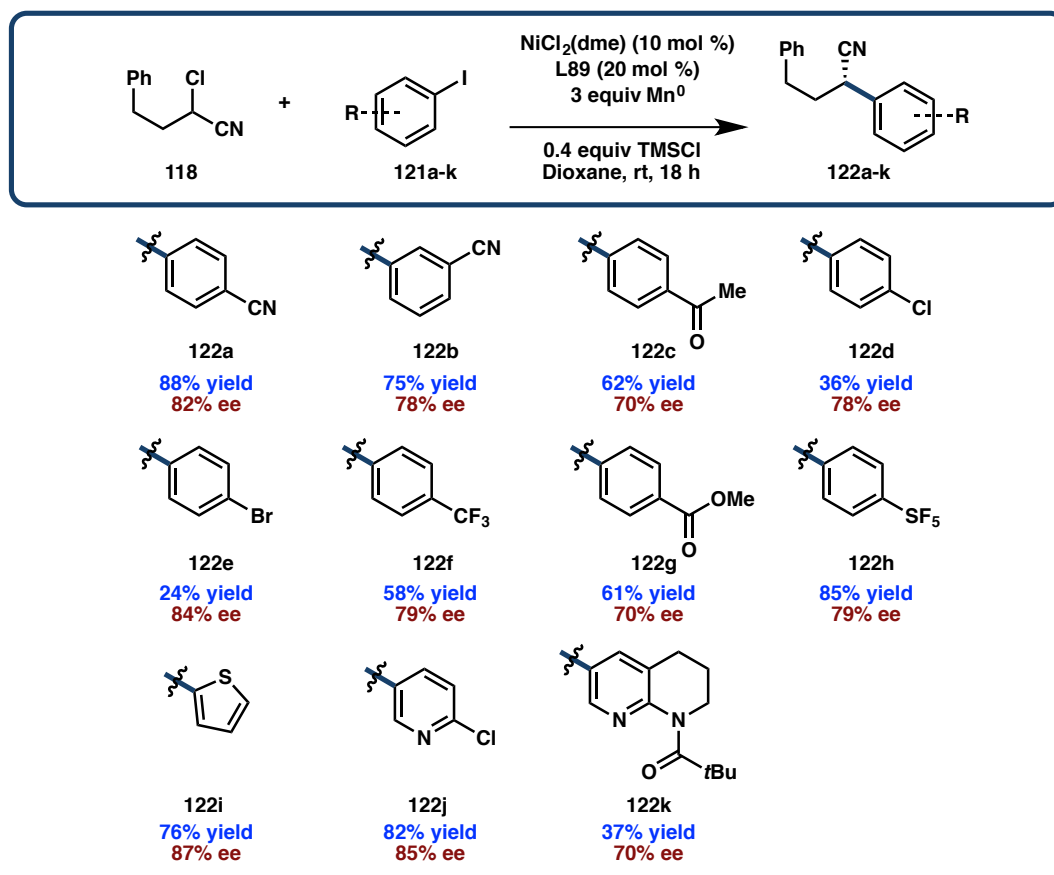
Having identified both a phosphine arm and a benzyl substituent that gave selectivities superior to BnPHOX (**L72**), we prepared the ligand bearing both components (**L98**). We were disappointed that while the yield remained high, the ee of **122a** furnished by this catalyst was only 45%. This result suggests that the two binding arms of the PHOX scaffold are not amenable to independent iterative optimization. Rather, it appears that the phosphine and oxazoline groups must be developed in concert, and that the interplay between the two halves of the ligand during catalysis is nontrivial.

### 3.3 SUBSTRATE SCOPE

With DMMBnPHOX (**L89**) identified as the optimal ligand for the model reductive coupling to afford **122a**, we set out to evaluate the substrate scope of this transformation. We began these studies with a survey of aryl iodide partners bearing various functional groups and a range of electronics (**Scheme 3.5**). It became immediately clear that electron-rich substrates such as 4-iodoanisole did not afford any cross-coupled product (not shown). We attribute this to sluggish oxidative addition of these substrates, even with the optimal PHOX ligand. Substrates bearing mildly electron-withdrawing substitution such as haloarenes **122d** and **122e** gave poor yields but notable chemoselectivity. More strongly electron-withdrawing functionality (**122f–h**) afforded much higher yields, but with ee's generally lower than the model substrate and too low to

be considered synthetically useful. However one class of entries underwent cross-coupling in good yields with enantioselectivities higher than the control: heteroaryl iodides **122i** and **122j**. Both the thiophene and chloropyridine entries reacted cleanly and with high ee.

**Scheme 3.5.** Preliminary screen of aryl iodide substrates.<sup>a</sup>

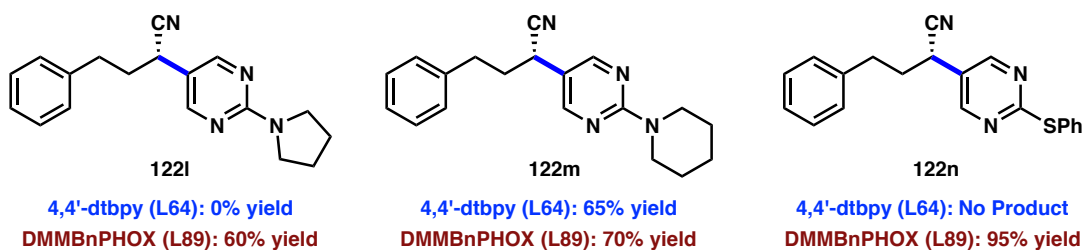


<sup>a</sup> Yields determined by <sup>1</sup>H NMR with an internal standard, reactions conducted on 0.2 or 0.05 mmol scale under an N<sub>2</sub> atmosphere in a glovebox. % ee determined by SFC using a chiral stationary phase.

One of our goals in developing the operative catalyst for this reaction was to select for tolerance of Lewis-basic functionality by utilizing two nitrile-bearing coupling partners. With the preliminary results from substrates **122i** and **122j**, we were hopeful that this had indeed been the outcome of the ligand optimization effort described in **Section 3.2**. Following up on this result, we set out to explore the range of heteroaryl

iodides that may be tolerated by these reaction conditions. We anticipated that these substrates would be of particular interest to the synthetic community, especially with respect to medicinal chemistry.<sup>22</sup> Successful incorporation of a wide range of heteroaryl moieties would also represent an advance in the field of reductive cross-coupling: Previously reported asymmetric examples only include simple arenes, while racemic couplings of heteroarenes require a wide range of varying reaction conditions to achieve only moderate yields in many cases.<sup>23</sup>

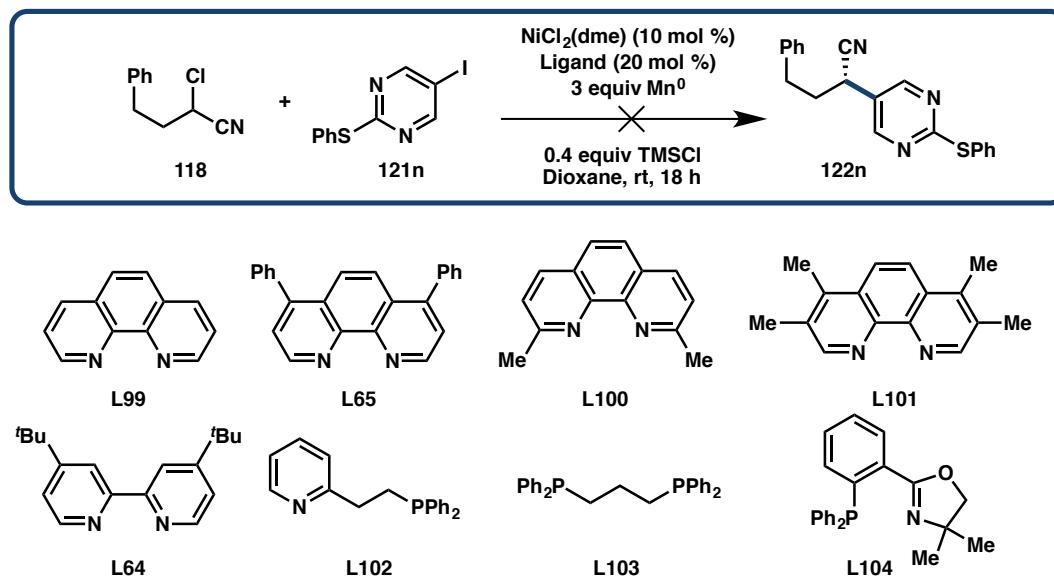
**Figure 3.7.** Heteroaryl cross-coupling behavior with two ligands.



Highlighting the difficulty of utilizing heteroarenes in reductive cross-coupling is **Figure 3.7**, showing the results of employing various substituted iodopyrimidines with **L89** and achiral 4,4'-dtbpy (**L64**). For all coupling products discussed previously, **L64** was the achiral ligand used to obtain racemic material for the development of chiral separation conditions. While **L64** frequently afforded lower yields than the optimal chiral ligands, product was always obtained with both ligands for competent substrates. However, when employing heteroaryl iodides **122l** and **122n** bearing Lewis basic functionality, only DMMBnPHOX **L89** afforded the desired product. An interesting divergence was also observed between pyrrolidinylpyrimidine **122l** and piperidinylpyrimidine **122m** when using achiral **L64**: Product was only observed with the piperidyl substituent, perhaps because the wider C-N-C bond angle of the piperidine

enables blocking of the pyrimidine lone pairs by the methylene protons, preventing catalyst poisoning in this case.

**Scheme 3.6.** Unsuccessful achiral ligands for the coupling of **121n**.

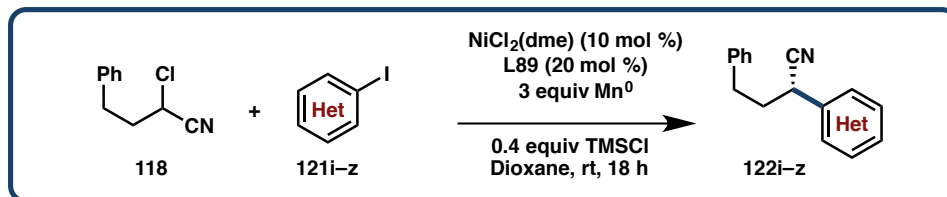


As a result of the difficulties encountered employing achiral ligand **L64** with some heteroaryl substrates, we required a more reliable achiral ligand for the preparation of racemic products (for assay development). Toward this end, we conducted a screen of various achiral ligands in the coupling of phenylthiopyrimidine **121n**. To our surprise, none of the ligands shown in **Scheme 3.6** afforded any cross-coupled product. While this served as a testament to the value of **DMMBnPHOX (L89)** for the cross-coupling of heteroarenes, it did not address the question of accessing racemic products. Ultimately, racemic **BnPHOX L72** prepared from racemic phenylalanine was employed for this purpose.

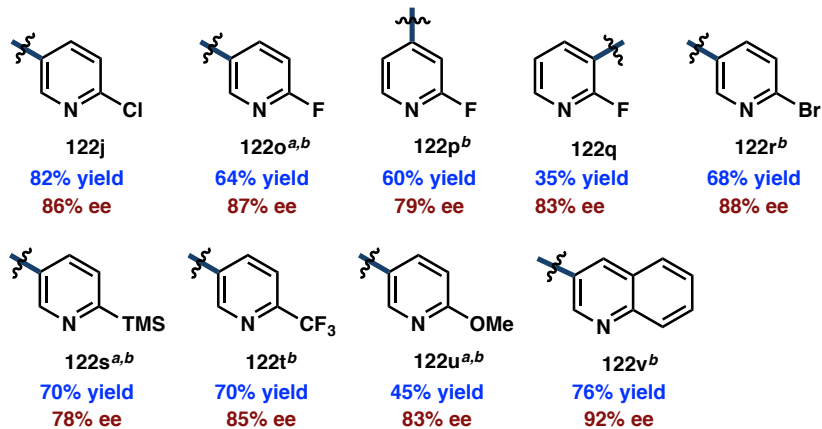
In the course of substrate evaluation and optimization, a wide range of reaction parameters and additives were evaluated. While most of these served only to establish the robustness of the transformation to various perturbations, two advancements were made.

First, the addition of  $\text{NaBF}_4$  to some substrates favorably altered the reaction profile, affording higher yields of the desired products sometimes by increasing conversion and sometimes by decreasing protodehalogenation. Changes in enantioselectivity were also noted, however these tended to be subtler. This is similar to results reported by Molander and coworkers in their reductive cross-couplings of heteroaromatic substrates, which were the impetus for investigating  $\text{NaBF}_4$ . Studies of other salt additives were unfruitful, with only slight or detrimental impacts being observed. It is unclear if the role of  $\text{NaBF}_4$  is as a halide-scavenging agent, a mild Lewis acid, or simply as an ionic electrolyte. Second, several heteroaryl substrates benefited from the use of two equivalents of aryl iodide. The excess substrate was easily recovered during column chromatography, making this a modest sacrifice in the service of improved yields.

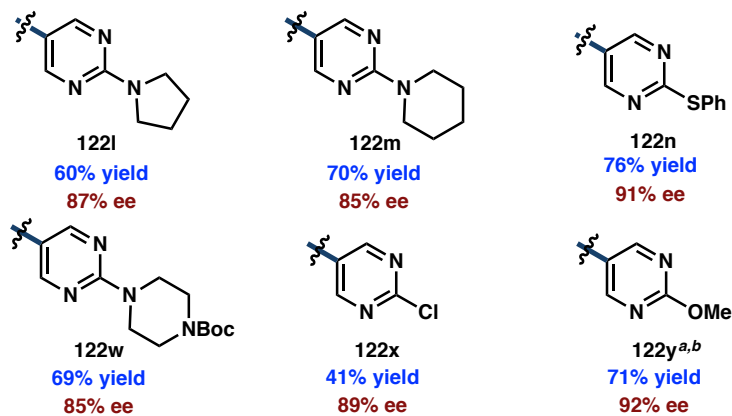
**Scheme 3.7.** Heteroaryl iodide scope.



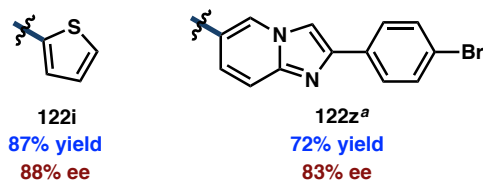
**Pyridines and Quinolines:**



**Pyrimidines:**



**Other heteroarenes:**



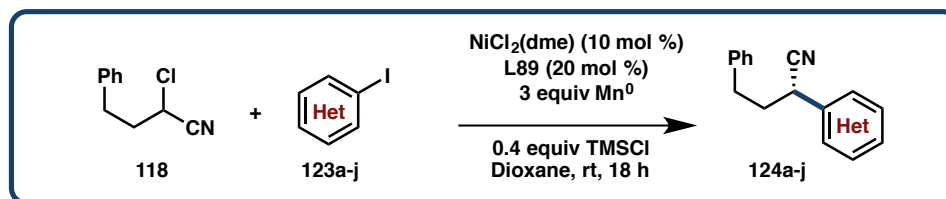
<sup>a</sup> 2 equiv aryl iodide employed. <sup>b</sup> 1 equiv  $\text{NaBF}_4$  added. All yields are isolated on a 0.2 mmol scale. % ee determined by SFC using a chiral stationary phase.

The scope of successful heteroaryl iodide cross-coupling partners is shown in **Scheme 3.7**. We began our screening of these substrates with a series of pyridyl substrates, based on the preliminary success of chloropyridine **121j**. We were pleased to see that a wide range of 2-halopyridines coupled with perfect chemoselectivity for the iodo position, including 2-bromopyridine **121r**. An iodide walk about 2-fluoropyridine demonstrated that while *para* and *meta* substitution were tolerated, 2-fluoro-3-iodopyridine afforded only modest yield of **122q**, albeit with good enantioselectivity. Electron-donating as well as withdrawing groups behaved well, as in **122t** and **122u**. 3-iodoquinoline was an especially good substrate, providing **122v** in excellent ee and high yield. Importantly, 5-iodo-2-trimethylsilylpyridine underwent cross-coupling smoothly (**122s**), providing a nucleophilic handle for further derivatization or a route to access the unsubstituted pyridyl product via protodesilylation.<sup>24</sup>

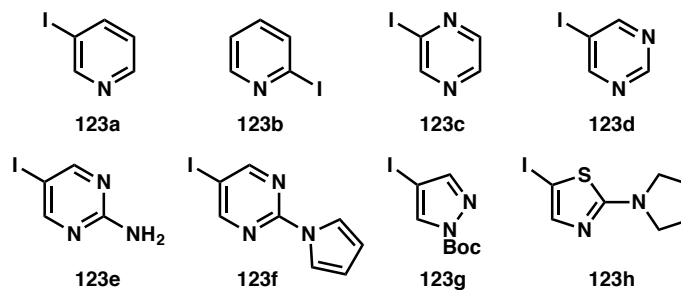
Inspired by the success of the pyridyl series, we went on to prepare and evaluate a range of iodopyrimidine substrates. A series of 2-aminopyrimidines bearing saturated nitrogen heterocycles was of particular interest (**122l**, **122m**, and **122w**), as these compounds find application in medicinal chemistry for a wide range of indications (oncological, cardiovascular, and anti-infective).<sup>22</sup> We were also pleased to find that 2-chloro-5-iodopyrimidine (**121x**) underwent reductive coupling chemoselectively and with excellent ee, providing a functional handle for later  $S_NAr$  or cross-coupling derivatization. Thioether-bearing **122n** was also accessible in high yield and ee, providing an entry to the unsubstituted pyrimidine product via hydrogenation.<sup>25</sup> Finally, we were gratified to find that other heterocyclic scaffolds behaved well in the reaction, including thiophene

**122i** and imidazopyridine **122z** bearing a pendant aryl bromide and containing a fused imidazole moiety.<sup>26</sup>

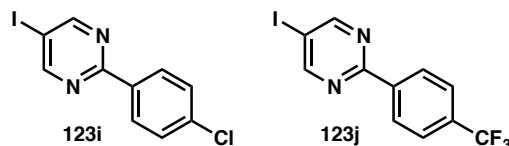
**Scheme 3.8.** Unsuccessful heteroaryl iodides.



*No conversion observed:*



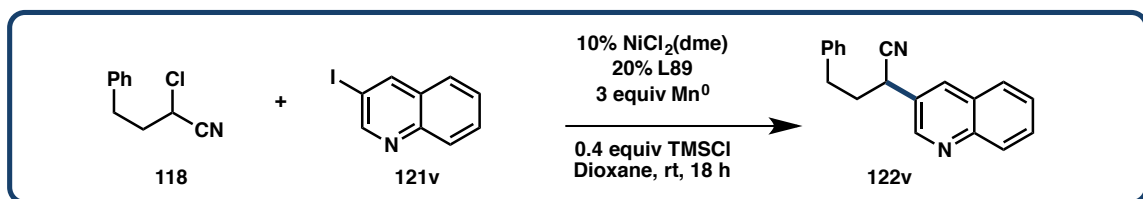
*Racemic product obtained:*



It is important to note current limitations of this methodology. Generally, heteroaromatics with no blocking group adjacent to the heteroatom (**123a** and **123d**) failed to afford product. In addition, placement of the electrophilic iodide at this position also failed to give any reactivity (**123b** and **123c**). Basic amines were generally not tolerated, even when incorporated into electron-withdrawing scaffolds such as **123e**. All of these observations may be attributable to catalyst poisoning by the Lewis basic heteroatoms in these substrates. While we succeeded in introducing a remarkable degree of tolerance for some Lewis basic sites (see **Figure 3.7**), clearly this issue remains a challenge for future development. Much less explicable was the result obtained by

employing 2-arylpyrimidines (**123i** and **123j**). While these substrates afforded the cross-coupled products in excellent yields, the material obtained was racemic. At this time it is unclear whether some mechanistic difference is at play with these substrates, or whether the products obtained are configurationally labile.

**Table 3.3.** Control experiments.

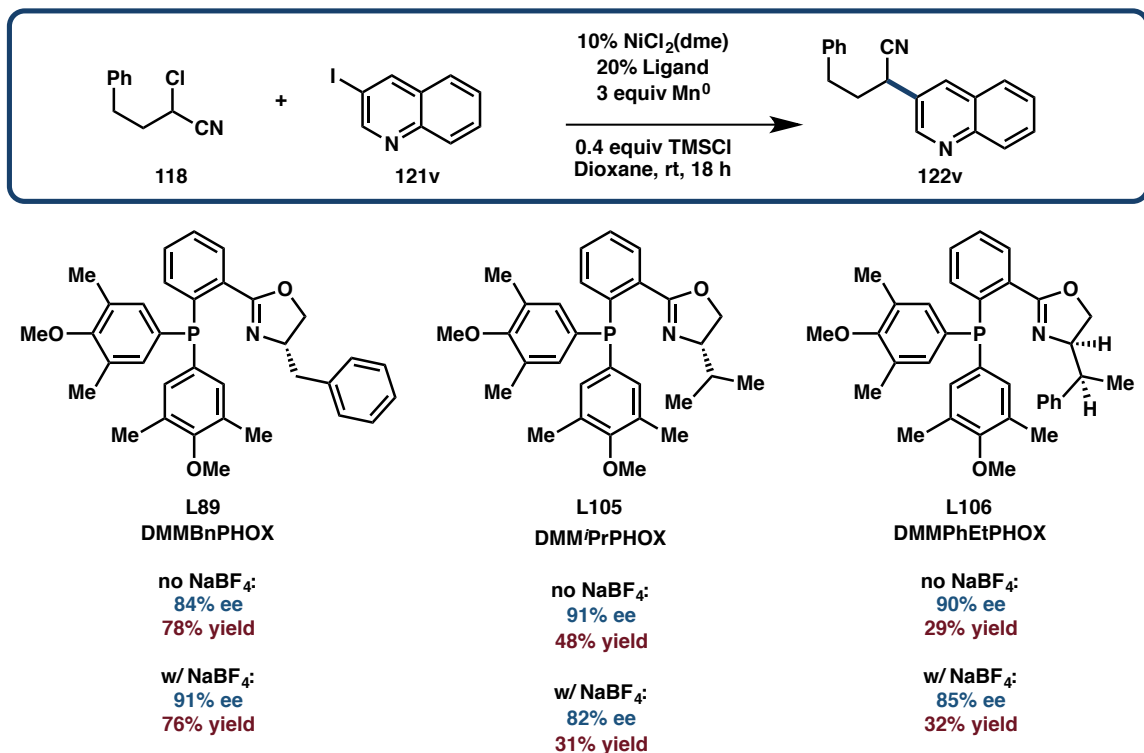


Entry	Deviation	Yield 122v	ee 122v	Yield -Cl
1	None	78	84	20
2	DMA, no dioxane	0	--	62
3	No Ni	0	--	0
4	No Mn <sup>0</sup>	0	--	0
5	No L89	4	0	23
6	No TMSCl	<5	82	<5
7	Zn <sup>0</sup> , no Mn <sup>0</sup>	25	10	32
8	TFA, no TMSCl	48	78	37
9	+ 1 equiv NaBF <sub>4</sub>	76	90	24
10	+ 0.25 equiv NaI	71	84	29
11	RCH(CN)Br, no 118	9	84	36

At this stage, we sought to verify that our reaction conditions were indeed optimal and to establish the necessity of all the reagents employed. **Table 3.3** shows the results of these control experiments conducted with 3-iodoquinoline **121v**. As expected, the reaction does not proceed in the absence of the Ni precatalyst or the Mn<sup>0</sup> reductant, with Mn<sup>0</sup> being superior to Zn<sup>0</sup> in this role. The coupling is also highly ligand-dependent, with only trace product being observed in the absence of ligand. TMSCl was critical for reactivity, with TFA being able to recapitulate only a portion of its effect. For 3-iodoquinoline (**121v**), NaBF<sub>4</sub> proved to be a beneficial additive, while NaI did not

improve reactivity. Finally, employing bromonitrile **117** in place of **118** led to higher levels of protodehalogenation, as well as elimination to form the acrylonitrile.

**Scheme 3.9.** DMM-PHOX derivative series.

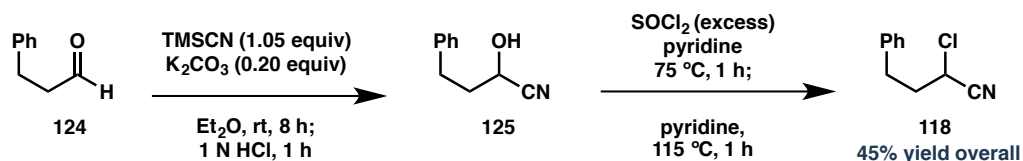


In a final effort toward optimization, we returned to the PHOX ligand scaffold. Having seen the impact on yield, enantioselectivity, and functional group tolerance exerted by **L89** as a result of the DMM-phosphine arm, we prepared a small series of ligands bearing this phosphine component (**Scheme 3.9**). Because <sup>t</sup>PrPHOX (**L34**) had been an early high-performing ligand, we prepared its DMM-phosphine analogue **L105**. Interestingly, **L105** did not benefit from the presence of  $\text{NaBF}_4$ , but excellent ee's were still obtainable, albeit in lower yields. This prompted us to prepare one final DMMBnPHOX analogue, incorporating diastereotopic branching on the benzyl substituent. DMMPPhEtPHOX (**L106**) was accessible from the known unnatural amino

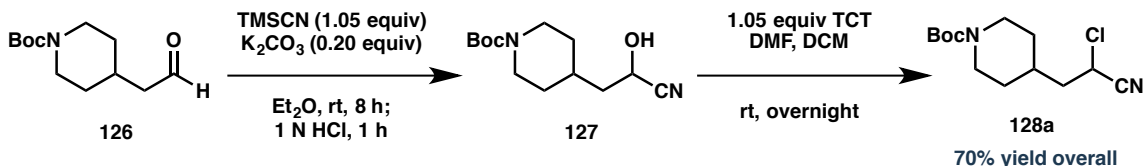
acid  $\beta$ -methylphenylalanine, prepared via asymmetric hydrogenation.<sup>27</sup> Unfortunately, only one diastereomer is easily prepared, with the other requiring commercially unavailable ligands for the analogous hydrogenation step. However **L106** did not provide improved results, affording only the reduced yields of DMM<sup>i</sup>PrPHOX in similar ee. At this point we determined that **L89** was the optimal ligand for this transformation and elected to move forward with substrate scope evaluation.

**Scheme 3.10.** Preparation of  $\alpha$ -chloronitriles.

a) Zelinka, 1974



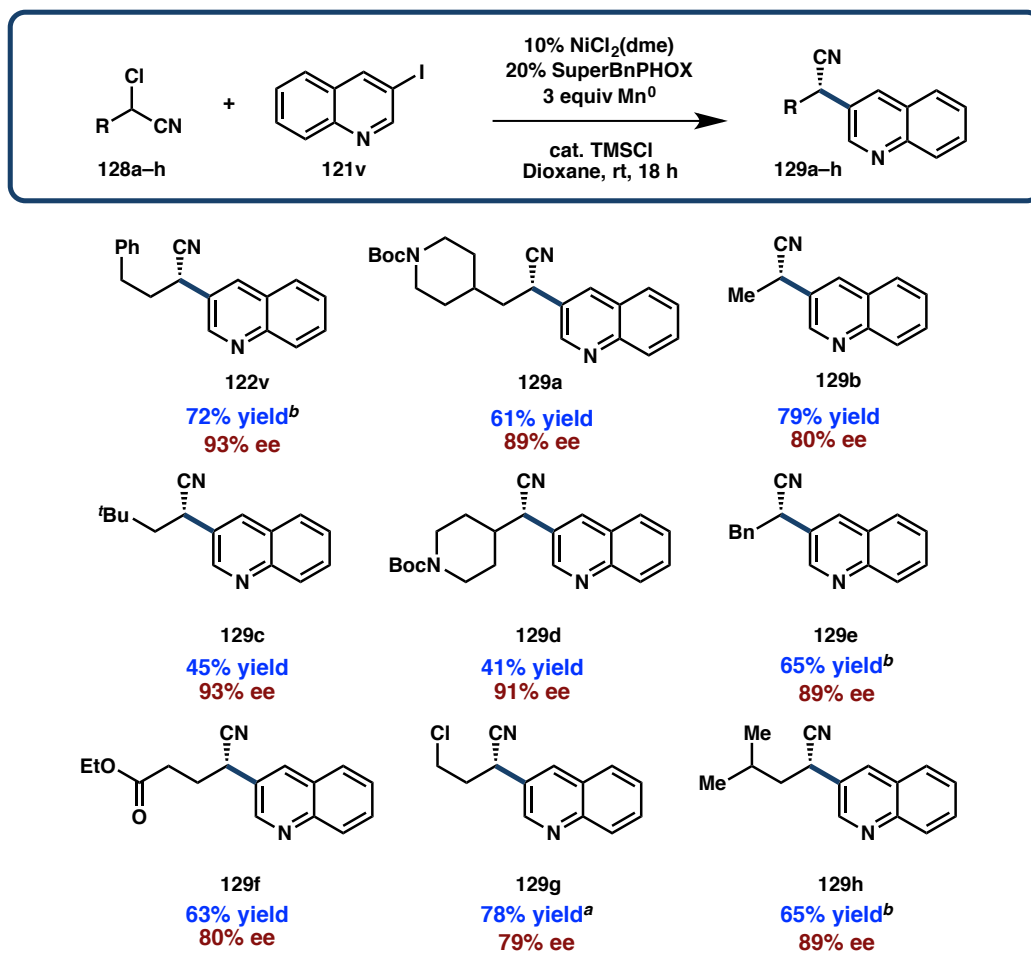
b) Route developed for this work



Having explored a significant range of heteroaryl iodides and established our optimal reaction conditions, we turned our attention to the scope of  $\alpha$ -chloronitrile partners for this reaction. However, before addressing the cross-coupling of these substrates, a method for their general synthesis was required. Indeed, at the time of our investigations, routes for the preparation of  $\alpha$ -chloronitriles were sparsely reported and relied on very harsh reaction conditions. The literature method for the preparation of model chloronitrile **118** is shown in **Scheme 3.10a**.<sup>28</sup> While this procedure did afford sufficient **118** for our initial investigations, it seemed unlikely that these conditions would enable the synthesis of chloronitriles bearing more sensitive functionality. Fortunately,

mild conditions for the chlorination of functionalized alcohols reported by Giacomelli and coworkers furnished chloronitriles from the corresponding cyanohydrins in excellent yields, employing trichlorotriazine (TCT) and DMF (**Scheme 3.10b**).<sup>29</sup> Importantly, these conditions tolerated functional groups such as esters and Boc-protected amines (e.g. **128a**) that would likely have been incompatible with the harsh conditions employed initially. We were pleased that these substrates proved to be not only accessible, but also remarkably stable, undergoing no decomposition over months when stored at  $-20\text{ }^{\circ}\text{C}$ .

**Scheme 3.11.**  $\alpha$ -Chloronitrile substrate scope.

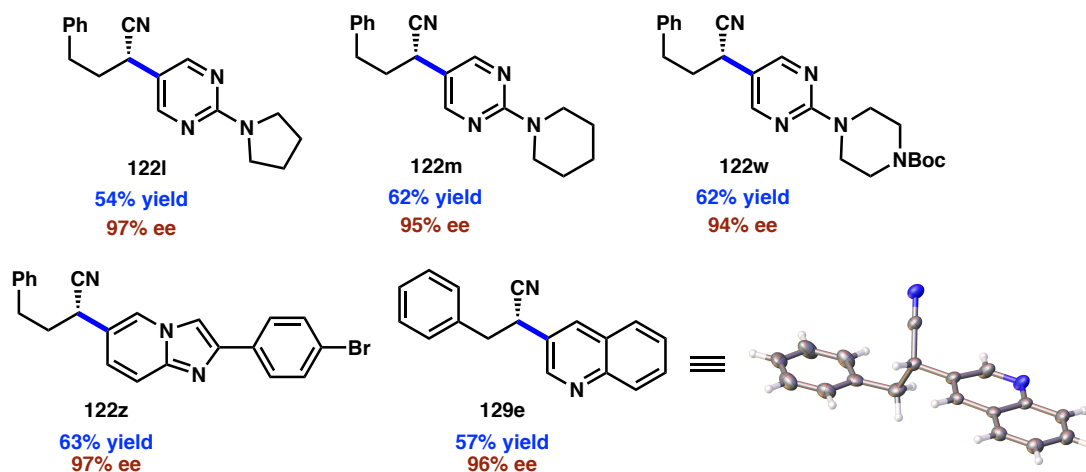


<sup>a</sup> 2 equiv aryl iodide employed. <sup>b</sup> 1 equiv  $\text{NaBF}_4$  added. All yields are isolated on a 0.2 mmol scale. % ee determined by SFC using a chiral stationary phase.

Employing this route, we were able to access a series of diverse  $\alpha$ -chloronitrile substrates from commercially available aldehydes. With the substrates in hand, we evaluated their performance in the reductive cross-coupling reaction utilizing 3-iodoquinoline **121v** as the model aryl iodide. This substrate was chosen because of its simple functionality and high performance in the aryl iodide screen discussed above. What emerged was the trend illustrated in **Scheme 3.11**: Sterically encumbered substrates such as neopentyl **128c** and branched piperidine **128d** afforded the cross-coupled products in excellent ee but with moderate yields, while less hindered substrates such as 2-chloropropionitrile proceeded in excellent yields but with slightly diminished enantioselectivity. Functional group tolerance in this series was excellent, with electrophilic functionality such as pendent ester **128f** and primary alkyl chloride **128g** reacting cleanly and in high yield. Boc protected piperidines **128a** and **128d** were also well-tolerated, demonstrating the feasibility of heteroatom incorporation in the arene, the nitrile moiety, and the alkyl chain of the products.

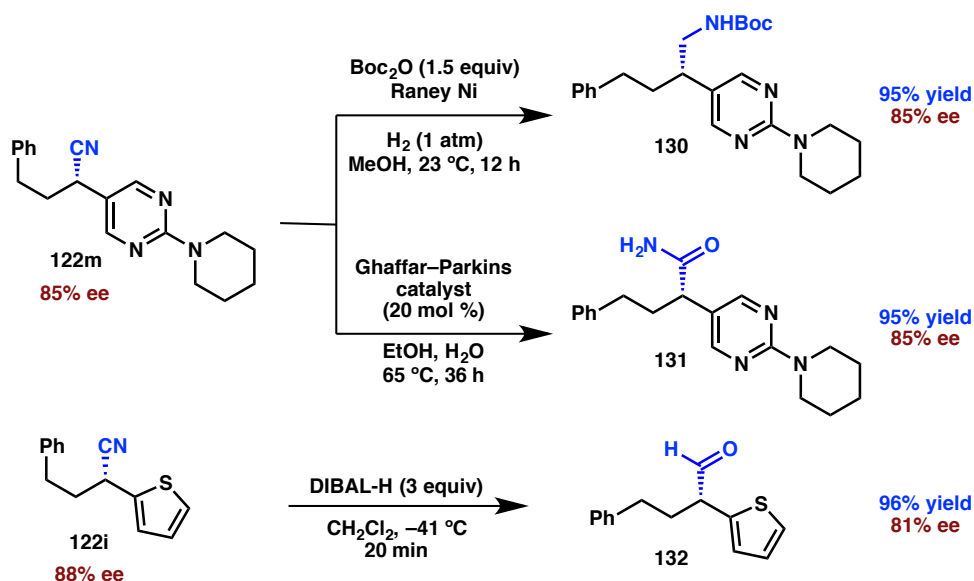
**Figure 3.8.** Recrystallization of selected substrates.

*Yields and ee's following a single recrystallization:*



We noted that many of the products of our substrate scope investigations were isolable as crystalline solids, suggesting that they may be amenable to enantioenrichment via recrystallization. Taking the most promising of these, we subjected the purified products to vapor diffusion recrystallization, affording highly enantioenriched products as shown in **Figure 3.8**. This also enabled the conclusive determination of the absolute stereochemistry of these products as the (*S*)-series, via X-ray diffraction of **129e**.

**Scheme 3.12.** Derivatization of enantioenriched benzylic nitriles.



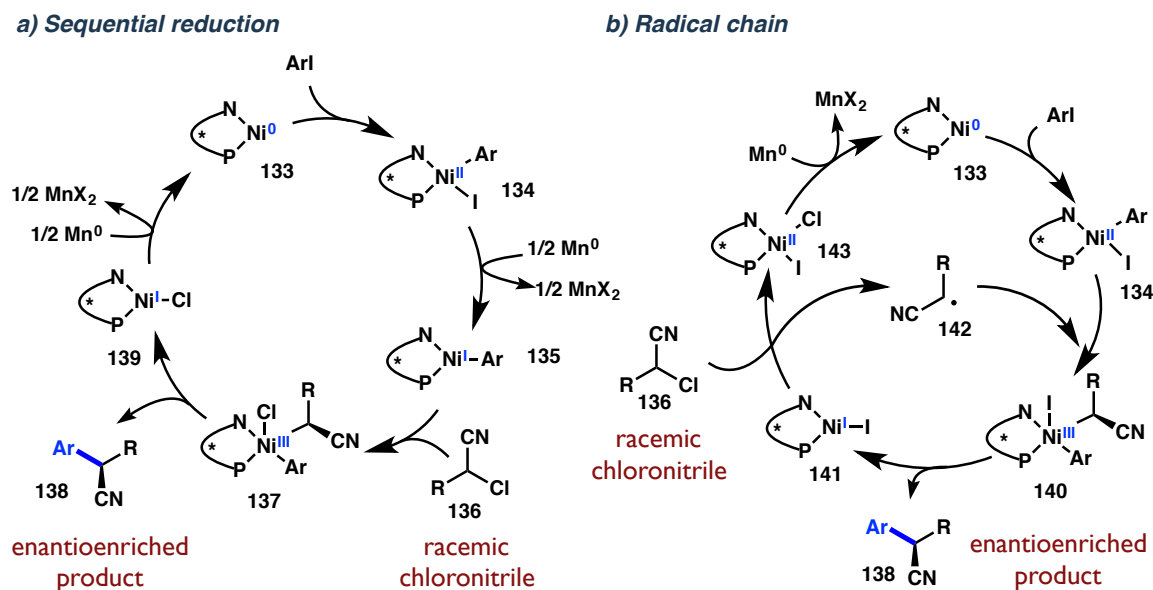
As our final investigation with respect to the substrate scope of this transformation, we set out to demonstrate that the enantioenriched benzylic nitriles obtained via the reductive cross-coupling could be further derivatized to diverse functionality (**Scheme 3.12**). To this end, we subjected piperidylpyrimidine **122m** first to standard Raney Ni hydrogenation in the presence of Boc anhydride, affording the Boc-protected arylethylamine **130** in nearly quantitative yield and with complete preservation of stereochemistry. We anticipate this sequence of reductive cross-coupling followed by hydrogenation to be a valuable route for the preparation of enantioenriched

arylethylamines, a potentially bioactive class of molecules.<sup>30</sup> We also subjected **122m** to Pt-catalyzed hydrolysis, employing the mild conditions developed by Ghaffar and Parkins, to generate the carboxamide product **131** with no loss of ee.<sup>31</sup> Finally, beginning with enantioenriched thiophene **122i**, we conducted a DIBAL-mediated reduction of the stereogenic nitrile to the corresponding aldehyde **132** in excellent yield with only slight degradation of ee under these basic conditions.<sup>32</sup>

### 3.4 MECHANISTIC STUDIES

As described in **Chapter 1**, we hypothesize that asymmetric reductive cross-couplings of radical-stabilized  $C(sp)^3$  electrophiles may proceed through the intermediacy of prochiral radicals derived from halide abstraction. While this hypothesis inspired our substrate selection and helped guide reaction development, we set out to verify the presence of radical intermediates and to elucidate their nature. Two possible mechanisms for this transformation are shown in **Figure 3.9**: a sequential reduction mechanism (**a**) and a radical chain mechanism (**b**).

**Figure 3.9.** Possible mechanisms for the asymmetric reductive cross-coupling.

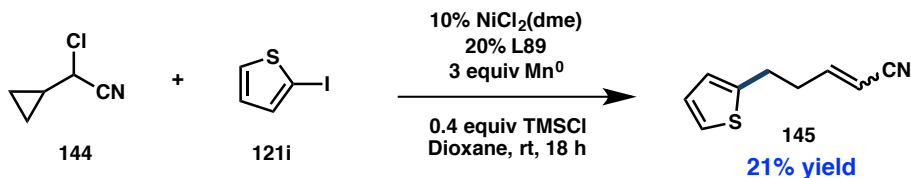


In both mechanisms, cross-selectivity is achieved by matching of substrate hybridization with catalyst oxidation state, affording sequenced oxidative addition steps. That is, the  $C(sp^2)$  aryl iodide coupling partner undergoes facile concerted oxidative addition to  $Ni^0$  species **133**, while the  $C(sp^3)$   $\alpha$ -chloronitrile is expected to favor single-electron oxidative addition via reaction with an odd-electron  $Ni^I$  intermediate (**135** or

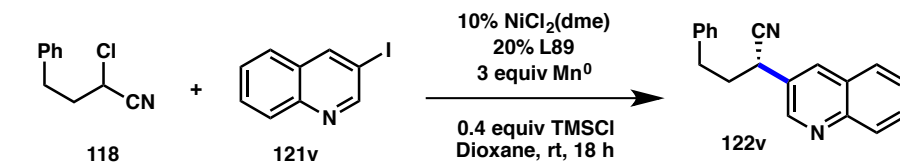
**141**). We postulate that stereoselective recombination of prochiral  $\alpha$ -cyano radical **142** with a chiral Ni<sup>II</sup> complex (**137** or **140**) may be the enantiodetermining step. However if this combination is reversible, then reductive elimination from Ni<sup>III</sup> **137** or **140** may be enantiodetermining via a Curtin-Hammett-type mechanism. The difference between mechanisms **a** and **b** lies in the lifetime of radical **142**. If **142** recombines rapidly with the Ni<sup>II</sup> center that abstracted the halide (a radical rebound process), then sequential reduction is favored. If **142** is sufficiently long-lived to escape the solvent cage and combine with a different Ni<sup>II</sup> center (**134**), then the radical chain process is favored.

**Scheme 3.13.** Mechanistic experiments.

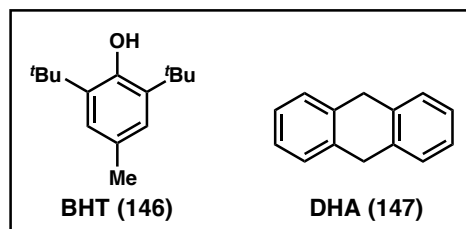
**a) Cyclopropylcarbinyl radical clock**



**b) Radical inhibitor studies**



Control: **72% Yield 84% ee**  
+ 50 mol% BHT: **74% Yield 83% ee**  
+50 mol% DHA: **66% Yield 83% ee**



To ascertain the presence of radicals derived from the C(sp<sup>3</sup>) electrophile, we prepared cyclopropane-bearing chloronitrile **144** (Scheme 3.13a).<sup>33</sup> Subjecting **144** to the reductive cross-coupling conditions with 2-iodothiophene (**121i**), we observed rearranged product **145** as the only cross-coupled product (as a mixture of the *cis* and *trans* isomers).

The remainder of the aryl iodide was unreacted, while the remainder of the  $\alpha$ -chloronitrile afforded volatile decomposition products. This is consistent with the generation of an  $\alpha$ -cyanocyclopropylcarbinyl radical intermediate.

Given the results with radical clock **114**, it was somewhat surprising that the reaction was not impacted by up to 50 mol % of the radical inhibitors BHT or DHA (**Scheme 3.13b**). We would anticipate that cage-escaped radicals generated in the reaction would be quenched by these inhibitors, leading to lower yields or complete inhibition. However, it may be possible that short-lived radicals not escaping the solvent cage may be unaffected by inhibitors. The success of the cross-coupling in the presence of these inhibitors is not consistent with our expectations for a radical chain mechanism, although further studies are required to elucidate if the sequential reduction mechanism is operative or if more complex pathways are at work.

### 3.5 CONCLUSION

In conclusion, a Ni-catalyzed asymmetric reductive cross-coupling between  $\alpha$ -chloronitriles and heteroaryl iodides has been developed.<sup>34</sup> A new chiral PHOX ligand was identified that provides  $\alpha,\alpha$ -disubstituted nitriles in good yields and with high enantioinduction. This is the first example of a Ni-catalyzed asymmetric reductive cross-coupling reaction that tolerates N- and S-heterocyclic coupling partners and demonstrates the feasibility of developing related transformations of electrophiles containing Lewis basic functional groups. The development of such novel asymmetric reductive cross-coupling reactions as well as mechanistic investigations are the subject of ongoing research in our laboratory.

## 3.6 EXPERIMENTAL SECTION

### 3.6.1 Materials and Methods

Unless otherwise stated, reactions were performed under a nitrogen atmosphere using freshly dried solvents. Methylene chloride, diethyl ether, tetrahydrofuran, and toluene were dried by passing through activated alumina. All other commercially obtained reagents were used as received unless specifically indicated. Aryl iodides were purchased from Sigma Aldrich, Combi-Blocks, or Astatech. Manganese powder (>99.9%) was purchased from Sigma Aldrich. NiCl<sub>2</sub>(dme) was purchased from Strem. Ghaffar-Parkins catalyst was purchased from Strem. All reactions were monitored by thin-layer chromatography using EMD/Merck silica gel 60 F254 pre-coated plates (0.25 mm). Silica gel column chromatography was performed as described by Still et al. (W. C. Still, M. Kahn, A. Mitra, *J. Org. Chem.* **1978**, *43*, 2923.) using silica gel (particle size 0.032-0.063) purchased from Silicycle. <sup>1</sup>H and <sup>13</sup>C NMR were recorded on a Varian Inova 500 (at 500 MHz and 125 MHz respectively) or a Varian Inova 600 (at 600 MHz and 150 MHz respectively) and are reported relative to internal chloroform (<sup>1</sup>H,  $\delta$  = 7.26, <sup>13</sup>C,  $\delta$  = 77.0). Data for <sup>1</sup>H NMR spectra are reported as follows: chemical shift ( $\delta$  ppm) (multiplicity, coupling constant (Hz), integration). Multiplicity and qualifier abbreviations are as follows: s = singlet, d = doublet, t = triplet, q = quartet, m = multiplet, br = broad. IR spectra were recorded on a Perkin Elmer Paragon 1000 spectrometer and are reported in frequency of absorption (cm<sup>-1</sup>). Analytical SFC was performed with a Mettler SFC supercritical CO<sub>2</sub> analytical chromatography system with Chiralcel AD-H, OD-H, AS-H, OB-H, and IA columns (4.6 mm x 25 cm). HRMS were acquired using either an Agilent 6200 Series TOF with an Agilent G1978A Multimode

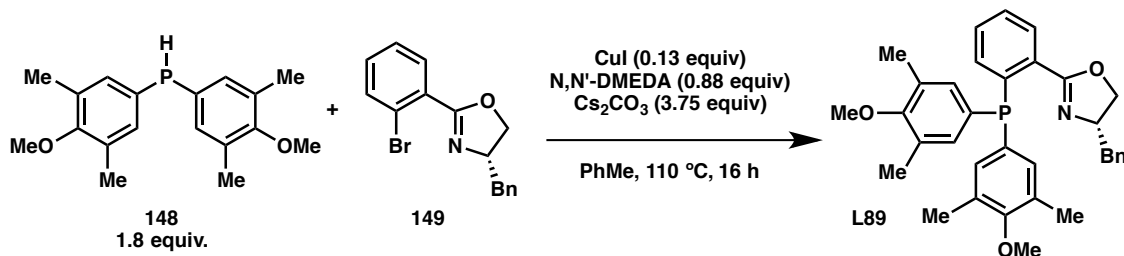
source in electrospray ionization (ESI), atmospheric pressure chemical ionization (APCI), or mixed (MM) ionization mode. Low-temperature X-ray diffraction data ( $\phi$ - and  $\omega$ -scans) were collected on a Bruker AXS D8 VENTURE KAPPA diffractometer coupled to a PHOTON 100 CMOS detector with Cu- $K\alpha$  radiation ( $\lambda = 1.54178 \text{ \AA}$ ) from an I $\mu$ S micro-source.

### 3.6.2 Ligand and Substrate Preparation

#### a. General Procedure 1 for the preparation of BnPHOX derivatives

To a flame-dried flask was added CuI (0.13 equiv), followed by anhydrous toluene (0.5 mL/1 mmol bromoarene). To this solution was added N,N'-DMEDA (0.88 equiv) and diarylphosphine (1.8 equiv). These were stirred for 15 minutes at room temperature. To the reaction was then added Cs<sub>2</sub>CO<sub>3</sub> (3.75 equiv), followed by bromoarene (1 equiv) as a solution in toluene (0.5 mL/1 mmol bromoarene). The reaction was heated to 110 °C for 16 h. After cooling to room temperature, the reaction was filtered through a plug of Celite and washed with degassed anhydrous DCM. The solution was concentrated and quickly purified via column chromatography using a positive pressure of argon and degassed solvent to afford the BnPHOX ligand.

**(S)-4-benzyl-2-(2-(bis(4-methoxy-3,5-dimethylphenyl)phosphanyl)phenyl)-4,5-dihydrooxazole (L89, DMMBnPHOX)**

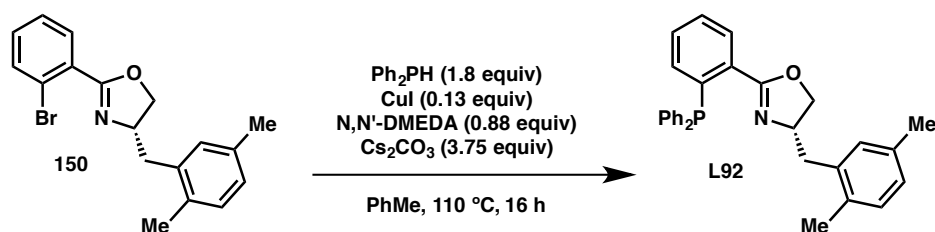


Prepared according to General Procedure 1: To a flame-dried flask was added CuI (0.13 equiv, 241 mg, 1.3 mmol), followed by anhydrous toluene (40 mL). To this solution was added N,N'-DMEDA (0.88 equiv, 0.93 mL, 8.6 mmol) and diarylphosphine **148** (1.8 equiv, 5.3 g, 17.5 mmol). These were stirred for 15 minutes at room temperature. To the reaction was then added Cs<sub>2</sub>CO<sub>3</sub> (3.75 equiv, 12.4 g, 36.7 mmol), followed by bromoarene **149** (1 equiv, 3.1 g, 9.8 mmol) as a solution in toluene (40 mL). The reaction was heated to 110 °C for 16 h. After cooling to room temperature, the reaction was filtered through a plug of Celite and washed with degassed anhydrous DCM. The solution was concentrated and quickly purified via column chromatography using a positive pressure of argon and degassed solvent (10-40% Et<sub>2</sub>O/Hexanes) to afford **L89** as a white foamy solid (1.62 g, 3.01 mmol, 31% yield). <sup>1</sup>H NMR (500 MHz, Chloroform-*d*)  $\delta$  7.90 – 7.82 (m, 1H), 7.40 – 7.32 (m, 2H), 7.32 – 7.27 (m, 2H), 7.26 – 7.20 (m, 1H), 7.15 – 7.10 (m, 2H), 7.05 (dd, *J* = 12.7, 7.9 Hz, 4H), 6.93 (ddd, *J* = 7.7, 4.5, 1.5 Hz, 1H), 4.44 – 4.29 (m, 1H), 4.06 (dd, *J* = 9.3, 8.3 Hz, 1H), 3.78 (dd, *J* = 8.4, 7.4 Hz, 1H), 3.75 (d, *J* = 4.0 Hz, 6H), 2.99 (dd, *J* = 13.7, 5.0 Hz, 1H), 2.28 (d, *J* = 13.0 Hz, 12H), 2.17 – 2.06 (m, 1H); <sup>13</sup>C NMR (126 MHz, cdCl<sub>3</sub>)  $\delta$  164.32, 164.30, 157.71, 157.63, 139.88, 139.68, 138.19, 135.02, 134.84, 134.72, 134.54, 133.40, 133.38, 132.43, 132.41,

132.36, 132.33, 131.49, 131.35, 131.01, 130.95, 130.90, 130.83, 130.36, 129.91, 129.89, 129.08, 128.48, 127.65, 126.34, 71.55, 67.90, 59.68, 59.62, 41.25, 16.22, 16.17;  $^{31}\text{P}$  NMR (121 MHz,  $\text{cdCl}_3$ )  $\delta$  -6.15; IR (NaCl/thin film): 3564.92, 2935.84, 1651.78, 1474.78, 1274.72, 1217.33, 1113.02, 1014.45, 909.83, 732.11, 700.48, 607.77  $\text{cm}^{-1}$ ;  $[\alpha]_{\text{D}}^{25} = +37.355$  ( $c = 1.285$ ,  $\text{CHCl}_3$ ). HRMS (MM) calc'd for  $[\text{M}+\text{H}_2\text{O}]^+$  555.2533, found 555.2544.

**(S)-4-(2,5-dimethylbenzyl)-2-(2-(diphenylphosphanyl)phenyl)-4,5-dihydrooxazole**

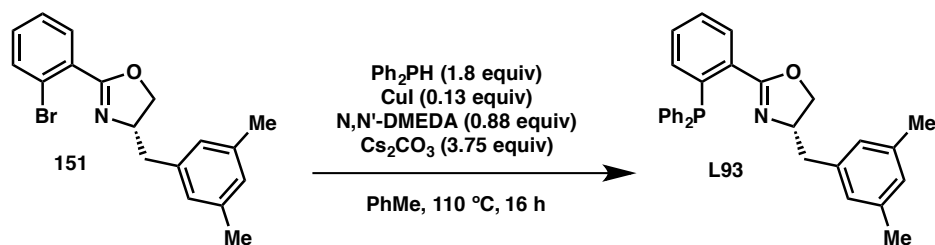
**(L92)**



Prepared from bromoarene **150** (4.24 mmol, 1.46 g) according to General Procedure 1 and purified by flash column chromatography in 10-20% EtOAc/hexanes to afford 1.1 g (58% yield) of **L92** a clear tacky resin.  $^1\text{H}$  NMR (500 MHz, Chloroform- $d$ )  $\delta$  7.97 (ddd,  $J = 7.6, 3.5, 1.5$  Hz, 1H), 7.46 – 7.29 (m, 12H), 7.07 (d,  $J = 7.7$  Hz, 1H), 7.00 – 6.85 (m, 3H), 4.41 (tdd,  $J = 9.6, 7.2, 4.8$  Hz, 1H), 4.09 (t,  $J = 8.8$  Hz, 1H), 3.87 (dd,  $J = 8.4, 7.2$  Hz, 1H), 2.96 (dd,  $J = 14.3, 4.9$  Hz, 1H), 2.34 (s, 3H), 2.27 (s, 3H), 2.12 (dd,  $J = 14.3, 9.9$  Hz, 1H).

**(S)-4-(3,5-dimethylbenzyl)-2-(2-(diphenylphosphanyl)phenyl)-4,5-dihydrooxazole**

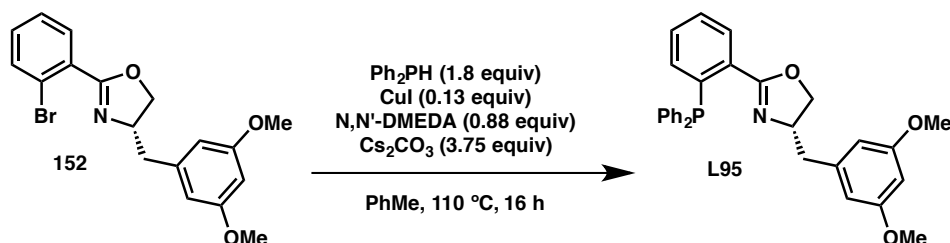
**(L93)**



Prepared from bromoarene **151** (4.24 mmol, 1.46 g) according to General Procedure 1 and purified by flash column chromatography in 10-20% EtOAc/hexanes to afford 210 mg (11% yield) of **L93** a clear tacky resin.  $^1\text{H}$  NMR (500 MHz, Chloroform- $d$ )  $\delta$  7.90 (s, 1H), 7.45 – 7.18 (m, 12H), 6.95 – 6.79 (m, 2H), 6.71 (s, 2H), 4.49 – 4.21 (m, 1H), 4.02 (t,  $J = 8.9$  Hz, 1H), 3.81 (d,  $J = 8.1$  Hz, 1H), 2.89 (d,  $J = 13.8$  Hz, 1H), 2.28 (d,  $J = 0.7$  Hz, 6H), 2.02 (q,  $J = 12.0, 10.4$  Hz, 1H).

**(S)-4-(3,5-dimethoxybenzyl)-2-(2-(diphenylphosphanyl)phenyl)-4,5-dihydrooxazole**

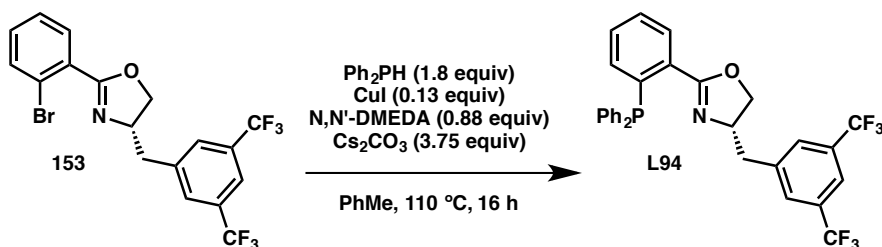
**(L95)**



Prepared from bromoarene **152** (5.60 mmol, 2.11 g) according to General Procedure 1 and purified by flash column chromatography in 10-50% EtOAc/hexanes to afford 414 mg (15% yield) of **L95** a white solid.  $^1\text{H}$  NMR (300 MHz, Acetonitrile- $d_3$ )  $\delta$  7.86 – 7.74 (m, 1H), 7.52 – 7.22 (m, 12H), 6.98 – 6.88 (m, 1H), 6.39 (d,  $J = 2.3$  Hz, 2H), 6.35 (t,  $J = 2.3$  Hz, 1H), 4.45 – 4.23 (m, 1H), 4.13 (dd,  $J = 9.4, 8.3$  Hz, 1H), 3.76 (m, 7H),

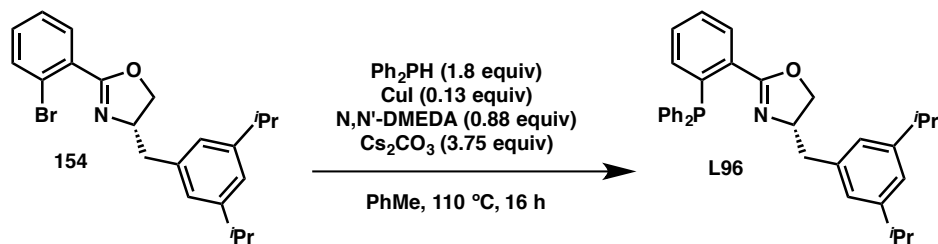
2.68 (dd,  $J = 13.7, 6.4$  Hz, 1H), 2.32 (dd,  $J = 13.7, 7.4$  Hz, 1H);  $^{31}\text{P}$  NMR (121 MHz,  $\text{cd}_3\text{cn}$ )  $\delta$  -6.56.

**(S)-4-(3,5-bis(trifluoromethyl)benzyl)-2-(2-(diphenylphosphanyl)phenyl)-4,5-dihydrooxazole (L94)**



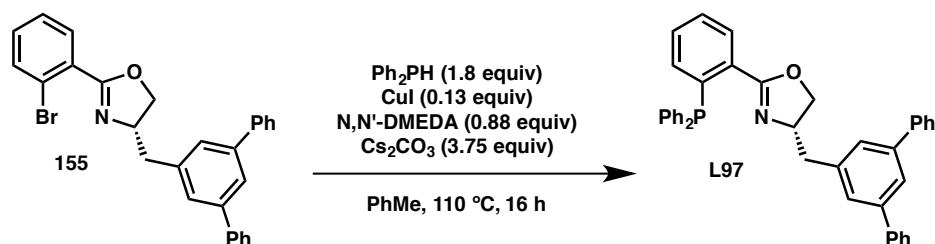
Prepared from bromoarene **153** (1.05 mmol, 475 mg) according to General Procedure 1 and purified by flash column chromatography in 10-20% EtOAc/hexanes to afford 240 mg (41% yield) of **L94** a colorless viscous oil.  $^1\text{H}$  NMR (300 MHz, Acetonitrile- $d_3$ )  $\delta$  7.88 (s, 3H), 7.82 – 7.72 (m, 1H), 7.52 – 7.10 (m, 12H), 6.98 – 6.85 (m, 1H), 4.49 – 4.29 (m, 1H), 4.25 (dd,  $J = 9.5, 8.3$  Hz, 1H), 3.84 (dd,  $J = 8.3, 7.3$  Hz, 1H), 2.84 (dd,  $J = 14.0, 5.0$  Hz, 1H), 2.69 (dd,  $J = 14.0, 8.2$  Hz, 1H);  $^{31}\text{P}$  NMR (121 MHz,  $\text{cd}_3\text{cn}$ )  $\delta$  -6.50.

**(S)-4-(3,5-diisopropylbenzyl)-2-(2-(diphenylphosphanyl)phenyl)-4,5-dihydrooxazole (L96)**



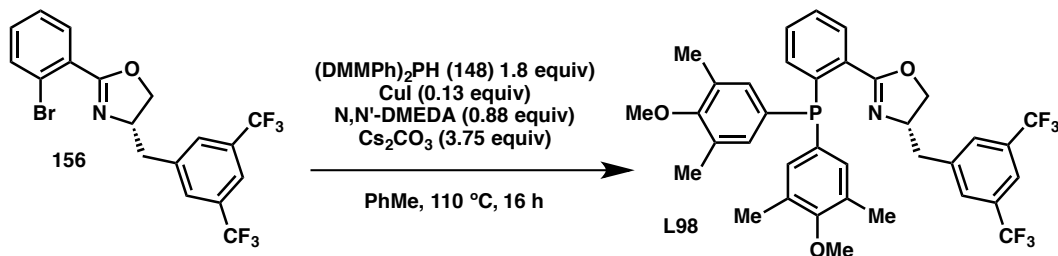
Prepared from bromoareene **154** (5.30 mmol, 2.12 g) according to General Procedure 1 and purified by flash column chromatography in 5-20% EtOAc/hexanes to afford 930 mg (35% yield) of **L96** a white solid.  $^1\text{H}$  NMR (300 MHz, Acetonitrile- $d_3$ )  $\delta$  7.85 – 7.74 (m, 1H), 7.50 – 7.21 (m, 10H), 6.99 (t,  $J = 1.7$  Hz, 1H), 6.97 – 6.86 (m, 3H), 4.31 (dtd,  $J = 9.4, 7.4, 6.2$  Hz, 1H), 4.10 (dd,  $J = 9.4, 8.3$  Hz, 1H), 3.77 (dd,  $J = 8.3, 7.5$  Hz, 1H), 2.86 (p,  $J = 6.9$  Hz, 2H), 2.69 (dd,  $J = 13.7, 6.3$  Hz, 1H), 2.37 (dd,  $J = 13.7, 7.3$  Hz, 1H), 1.22 (d,  $J = 6.9$  Hz, 12H);  $^{31}\text{P}$  NMR (121 MHz,  $\text{cd}_3\text{cn}$ )  $\delta$  -6.43.

**(S)-4-([1,1':3',1''-terphenyl]-5'-ylmethyl)-2-(2-(diphenylphosphanyl)phenyl)-4,5-dihydrooxazole (L97)**



Prepared from bromoarene **155** (5.97 mmol, 2.80 g) according to General Procedure 1 and purified by flash column chromatography in 10-30% EtOAc/hexanes to afford 830 mg (24% yield) of **L97** a white solid.  $^1\text{H}$  NMR (300 MHz, Acetonitrile- $d_3$ )  $\delta$  7.93 – 7.77 (m, 1H), 7.77 – 7.69 (m, 5H), 7.53 (d,  $J = 1.7$  Hz, 2H), 7.51 – 7.07 (m, 13H), 6.94 (ddd,  $J = 6.3, 3.8, 1.9$  Hz, 1H), 4.54 – 4.34 (m, 1H), 4.33 – 4.16 (m, 1H), 4.00 – 3.82 (m, 1H), 2.89 – 2.60 (m, 2H);  $^{31}\text{P}$  NMR (121 MHz,  $\text{cd}_3\text{cn}$ )  $\delta$  -7.08.

**(S)-2-(2-(bis(4-methoxy-3,5-dimethylphenyl)phosphanyl)phenyl)-4-(3,5-bis(trifluoromethyl)benzyl)-4,5-dihydrooxazole (L98)**

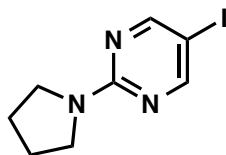


Prepared from bromoarene **156** (3.0 mmol, 1.36 g) according to General Procedure 1 and purified by flash column chromatography in 10-20% Et<sub>2</sub>O/hexanes to afford 300 mg (15% yield) of **L98** a clear yellow oil. <sup>1</sup>H NMR (300 MHz, Acetonitrile-*d*<sub>3</sub>)  $\delta$  8.07 – 7.63 (m, 3H), 7.57 – 7.15 (m, 3H), 6.95 (dd, *J* = 7.9, 4.0 Hz, 5H), 4.42 – 4.05 (m, 1H), 3.86 – 3.44 (m, 8H), 2.88 – 2.45 (m, 2H), 2.16 (s, 6H), 1.96 (s, 6H).; <sup>19</sup>F NMR (282 MHz, cd<sub>3</sub>cn)  $\delta$  -63.09.; <sup>31</sup>P NMR (121 MHz, cd<sub>3</sub>cn)  $\delta$  -6.78.

**b. General Procedure 2 for preparation of heteroaryl iodides.**

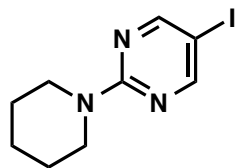
To a flame-dried flask was added copper(I) iodide (0.05 equiv), followed by 1,4-dioxane and N,N'-DMEDA (0.10 equiv), then aryl bromide (1.0 equiv) and sodium iodide (2.0 equiv). The reaction was heated to 110 °C for 24 h. Upon cooling to room temperature, the reaction was filtered over Celite and washed with DCM. The solution was concentrated to afford the aryl iodide as a light solid. Purification by recrystallization was possible for all substrates but was generally unnecessary. Aryl iodides were employed in the coupling reactions as is.

### 5-iodo-2-(pyrrolidin-1-yl)pyrimidine (**121l**)



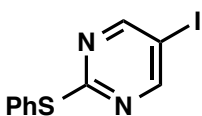
Prepared from 5-bromo-2-(pyrrolidin-1-yl)pyrimidine (10.3 mmol, 2.35 g) following General Procedure 2 to yield 2.75 g (97% yield) of **121l** as a very light pink solid.  $^1\text{H}$  NMR (500 MHz, Chloroform-*d*)  $\delta$  8.37 (s, 2H), 3.57 – 3.47 (m, 4H), 2.18 – 1.77 (m, 4H);  $^{13}\text{C}$  NMR (126 MHz,  $\text{cdCl}_3$ )  $\delta$  162.34, 158.19, 74.37, 46.74, 25.52; IR (NaCl/thin film): 2944.10, 2864.32, 1565.22, 1518.02, 1511.96, 1333.11, 1286.14, 1153.17, 940.39, 782.61, 639.66  $\text{cm}^{-1}$ ; HRMS (MM) calc'd for  $[\text{M}]^+$  274.9914, found 274.9874.

### 5-iodo-2-(piperidin-1-yl)pyrimidine (**121m**)



Prepared from 5-bromo-2-(piperidin-1-yl)pyrimidine (10.3 mmol, 2.49 g) following General Procedure 2 to yield 2.86 g (96% yield) of **121m** as a light yellow solid.  $^1\text{H}$  NMR (500 MHz, Chloroform-*d*)  $\delta$  8.34 (s, 2H), 3.78 – 3.69 (m, 4H), 1.71 – 1.63 (m, 2H), 1.59 (tt,  $J = 7.8, 4.5$  Hz, 4H);  $^{13}\text{C}$  NMR (126 MHz,  $\text{cdCl}_3$ )  $\delta$  162.34, 159.63, 74.30, 44.87, 25.64, 24.71; IR (NaCl/thin film): 2929.42, 2849.82, 1558.04, 1505.31, 1360.11, 1266.59, 1253.66, 1023.84, 945.12, 851.36, 784.80, 642.34  $\text{cm}^{-1}$ ; HRMS (MM) calc'd for  $[\text{M}]^+$  289.0070, found 289.0033.

### 5-iodo-2-phenylthiopyrimidine (**121n**)



Prepared from 5-bromo-2-phenylthiopyrimidine (10.3 mmol, 2.75 g) following General Procedure 2 to yield 3.14 g (97% yield) of **121n** as a light tan solid.  $^1\text{H}$  NMR (500 MHz, Chloroform-*d*)  $\delta$  8.62 (s, 2H), 7.65 – 7.56 (m, 2H), 7.48 – 7.40 (m, 3H);  $^{13}\text{C}$  NMR (126 MHz,  $\text{cdCl}_3$ )  $\delta$  171.40, 162.64, 135.25, 129.61,

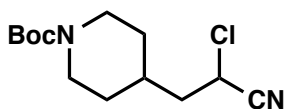
129.34, 128.88, 87.17; IR (NaCl/thin film): 3057.57, 1537.84, 1514.30, 1440.03, 1382.13, 1184.77, 994.96, 745.51, 687.91, 630.05  $\text{cm}^{-1}$ ; HRMS (MM) calc'd for  $[\text{M}]^+$  313.9369, found 313.9579.

**c. General Procedure 3 for preparation of  $\alpha$ -chloronitriles.**

To a flame-dried flask was added aldehyde starting material (1 equiv) followed by anhydrous  $\text{Et}_2\text{O}$  and  $\text{K}_2\text{CO}_3$  (0.2 equiv). To this suspension was added  $\text{TMSCN}$  (1.02 equiv) (Warning: acutely toxic, handle with care). Reaction was stirred at room temperature overnight. Reaction was then quenched with saturated aqueous  $\text{NaHCO}_3$  (1 mL/mmol). Layers were separated and the aqueous phase was extracted twice with  $\text{Et}_2\text{O}$ . Organic layers were combined and concentrated. The resulting oil was suspended in 1 N  $\text{HCl}$  and stirred at rt for 2 hours. The reaction was then washed twice with  $\text{Et}_2\text{O}$  and the organics were dried over  $\text{Na}_2\text{SO}_4$  and concentrated to afford the crude cyanohydrin. A new flame-dried flask was charged with a large stirbar and cyanuric chloride (1.05 equiv). To this was added  $\text{DMF}$  (1.1 mL/gram cyanuric chloride) and the suspension was stirred vigorously until a white solid was obtained. The solid was then suspended by addition of  $\text{DCM}$  (0.5 M). The crude cyanohydrin was added to the reaction as a solution in  $\text{DCM}$  and stirred at room temperature for 24 hours. The reaction was quenched by addition of water and stirred for 10 minutes. Layers were separated and the aqueous layer was washed with  $\text{DCM}$ . Organic phases were combined and washed with saturated  $\text{Na}_2\text{CO}_3$ , then 1 N  $\text{HCl}$ , then brine. Organics were then dried over  $\text{Na}_2\text{SO}_4$  and concentrated to afford the crude chloronitrile. Crude oils were purified by column

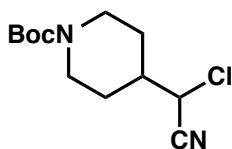
chromatography to afford clear oils or white solids. Substrate preparations were unoptimized and the reported reactions were performed once.

***tert*-Butyl-4-(2-chloro-2-cyanoethyl)piperidine-1-carboxylate (128a)**



Prepared from 2-(1-Boc-4-piperidyl)acetaldehyde (1.0 g, 4.4 mmol) following General Procedure 3. The crude residue was purified by silica gel chromatography (5:95 to 20:80 EtOAc:hexanes) to yield 837 mg (70% yield) of **128a** as a white solid.  $^1\text{H}$  NMR (500 MHz, Chloroform-*d*)  $\delta$  4.49 (t,  $J$  = 7.6 Hz, 1H), 4.12 (bs, 2H), 2.71 (bs, 2H), 2.10 – 1.94 (m, 2H), 1.80 (ddd,  $J$  = 11.3, 7.6, 4.2 Hz, 1H), 1.72 – 1.67 (m, 2H), 1.45 (s, 9H), 1.28 – 1.06 (m, 2H);  $^{13}\text{C}$  NMR (126 MHz,  $\text{cdCl}_3$ )  $\delta$  154.64, 117.08, 79.61, 43.72, 43.20, 42.63, 40.18, 33.02, 31.44, 31.08, 28.42; IR (NaCl/thin film): 2929.41, 1673.87, 1417.84, 1246.54, 1161.38, 1127.43, 966.65, 865.88, 769.18, 741.68, 677.80  $\text{cm}^{-1}$ ; HRMS (MM) calc'd for  $[\text{M}+\text{H}]^+$  273.1364, found 273.1352.

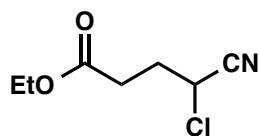
***tert*-Butyl-4-(chloro(cyano)methyl)piperidine-1-carboxylate (128d)**



Prepared from 1-Boc-piperidine-4-carboxaldehyde (2.0 g, 9.39 mmol) following General Procedure 3. The crude residue was purified by silica gel chromatography (5:95 to 20:80 EtOAc:hexanes) to yield 570 mg (24% yield) of **128d** as a white solid.  $^1\text{H}$  NMR (500 MHz, Chloroform-*d*)  $\delta$  4.34 (d,  $J$  = 6.1 Hz, 1H), 4.24 (bs, 2H), 2.70 (bs, 2H), 2.10 – 1.98 (m, 1H), 1.98 – 1.84 (m, 2H), 1.46 (s, m, 11H);  $^{13}\text{C}$  NMR (126 MHz,  $\text{cdCl}_3$ )  $\delta$  154.47, 115.76, 79.95, 47.27, 43.17, 42.70, 41.59, 28.39, 28.35, 27.96; IR (NaCl/thin film): 1976.08, 1945.79, 2859.74, 1682.85, 1422.81, 1366.50, 1280.82, 1239.82, 1166.99,

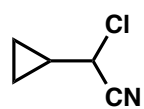
1128.02, 973.46, 866.39, 760.71  $\text{cm}^{-1}$ ; HRMS (MM) calc'd for  $[\text{M}+\text{H}]^+$  259.1208, found 259.1256.

#### Ethyl 4-chloro-4-cyanobutyrate (**128f**)



Prepared from ethyl hemisuccinaldehyde (1.82 g, 14 mmol) following General Procedure 3. The crude residue was purified by silica gel chromatography (5:95 to 20:80 EtOAc:hexanes) to yield 1.77 g (72% yield) of **128f** as a clear oil.  $^1\text{H}$  NMR (500 MHz, Chloroform-*d*)  $\delta$  4.70 (dd,  $J = 7.5, 6.2$  Hz, 1H), 4.17 (q,  $J = 7.1$  Hz, 2H), 2.73 – 2.53 (m, 2H), 2.49 – 2.28 (m, 2H), 1.28 (t,  $J = 7.1$  Hz, 3H), ;  $^{13}\text{C}$  NMR (126 MHz,  $\text{cdCl}_3$ )  $\delta$  171.34, 116.62, 61.14, 41.50, 31.39, 29.66, 14.15; IR (NaCl/thin film): 2983.27, 2249.74, 1734.19, 1608.59, 1564.56, 1419.07, 1378.34, 1193.90, 1096.48, 1024.20, 852.08, 795.42, 665.51  $\text{cm}^{-1}$ ; HRMS (MM) calc'd for  $[\text{M}]^+$  175.0395, found 175.0380.

#### 2-chloro-2-cyclopropylacetonitrile (**144**)



Prepared from cyclopropane carboxaldehyde (1 mL, 13.4 mmol) following General Procedure 3. The crude residue was purified by kugelrohr distillation followed by silica gel chromatography (100% pentanes) to yield 205 mg (13% yield) of **144** as a clear mobile liquid. The product was isolated with some residual pentane due to its volatility.  $^1\text{H}$  NMR (500 MHz, Chloroform-*d*)  $\delta$  4.22 (d,  $J = 7.7$  Hz, 1H), 1.53 (qt,  $J = 7.9, 4.8$  Hz, 1H), 0.94 – 0.84 (m, 2H), 0.74 – 0.62 (m, 2H);  $^{13}\text{C}$  NMR (126 MHz,  $\text{cdCl}_3$ )  $\delta$  115.79, 46.91, 16.59, 6.09, 5.40; IR (NaCl/thin film): 3091.35,

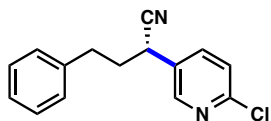
3013.92, 2958.47, 2247.22, 1732.61, 1430.84, 1220.80, 1029.90, 991.98, 926.86, 832.41, 728.05  $\text{cm}^{-1}$ ; HRMS (MM) calc'd for  $[\text{M}+\text{H}]^+$  116.0262, found 116.0258.

### 3.6.3 Enantioselective Reductive Cross-Coupling

#### General Procedure 4 for reductive cross-couplings.

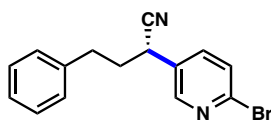
A 20 mL scintillation vial was charged with a cross stirbar,  $\text{Mn}^0$  powder (3 equiv, 33 mg, 0.6 mmol), aryl iodide (*if solid*, 1 or 2 equiv, 0.2 or 0.4 mmol),  $\text{NiCl}_2(\text{dme})$  (0.1 equiv, 4.4 mg, 0.02 mmol), **L89** (0.2 equiv, 21.6 mg, 0.04 mmol) and  $\text{NaBF}_4$  if applicable (1 equiv, 22 mg, 0.2 mmol). To this was added 1,4-dioxane (0.68 mL, 0.3M), aryl iodide (*if liquid*, 1 or 2 equiv, 0.2 or 0.4 mmol) and  $\text{TMSCl}$  (0.4 equiv, 33  $\mu\text{L}$ , 0.08 mmol), followed by chloronitrile (1 equiv, 0.2 mmol). Reaction was sealed with a Teflon-lined cap and stirred on the benchtop at 500 RPM for 16 hours. Over this interval reactions turn from dark purple to cloudy red or yellow with significant white precipitate. Reactions were diluted with 1 mL of hexane, leading to additional salt precipitation. This slurry was loaded directly onto a silica gel or florisil column and eluted in a hexane/EtOAc gradient. Excess aryl iodide could be recovered in the first several fractions, with cross-coupled product being the most polar component. Reaction success is critically dependent on stirring. A stirbar too small for the reaction vessel will fail to suspend the Mn powder and lead to low conversions. The reaction vessel should be sufficiently large (solvent height should be sufficiently low) to allow even distribution of Mn powder with vigorous stirring.

### 2-(6-chloropyridin-3-yl)-4-phenylbutanenitrile (**122j**)



Prepared from 2-chloro-5-iodopyridine (48.0 mg, 0.2 mmol) and 2-chloro-4-phenylbutanenitrile (36 mg, 0.2 mmol) following General Procedure 4. The crude residue was purified by silica gel chromatography (0:100 to 10:90 EtOAc:hexanes) to yield 39.8 mg (78% yield) of **122j** as a clear oil. The enantiomeric excess was determined to be 85% by chiral SFC analysis (AD, 2.5 mL/min, 8% IPA in CO<sub>2</sub>,  $\lambda$  = 210 nm):  $t_R$ (minor) = 9.8 min,  $t_R$ (major) = 13.0 min. <sup>1</sup>H NMR (500 MHz, Chloroform-*d*)  $\delta$  8.31 (d,  $J$  = 2.6 Hz, 1H), 7.66 (dd,  $J$  = 8.3, 2.7 Hz, 1H), 7.40 – 7.28 (m, 3H), 7.28 – 7.22 (m, 1H), 7.22 – 7.17 (m, 2H), 3.77 (dd,  $J$  = 9.2, 6.0 Hz, 1H), 2.87 – 2.81 (m, 2H), 2.34 – 2.27 (m, 1H), 2.16 (dddd,  $J$  = 13.7, 8.5, 7.6, 6.0 Hz, 1H); <sup>13</sup>C NMR (126 MHz, cdCl<sub>3</sub>)  $\delta$  151.54, 148.52, 138.91, 137.56, 130.54, 128.89, 128.40, 126.84, 124.78, 119.22, 37.00, 33.47, 32.86.; IR (NaCl/thin film): 3027.23, 2926.09, 2242.46, 1586.64, 1566.17, 1496.29, 1460.14, 1389.42, 1141.53, 1108.27, 1022.71, 832.61, 741.61, 700.19 cm<sup>-1</sup>;  $[\alpha]_D^{25}$  = -12.081 ( $c$  = 1.410, CHCl<sub>3</sub>). HRMS (MM) calc'd for [M+Na]<sup>+</sup> 279.0659, found 279.0702.

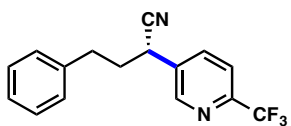
### 2-(6-bromopyridin-3-yl)-4-phenylbutanenitrile (**122r**)



Prepared from 2-bromo-5-iodopyridine (56.8 mg, 0.2 mmol) and 2-chloro-4-phenylbutanenitrile (36 mg, 0.2 mmol) with NaBF<sub>4</sub> (22 mg, 0.2 mmol) following General Procedure 4. The crude residue was purified by silica gel chromatography (0:100 to 10:90 EtOAc:hexanes) to yield 40.9 mg (68% yield) of **122r** as a clear oil. The enantiomeric excess was determined to be 88% by chiral SFC analysis (AD, 2.5 mL/min, 10% IPA in CO<sub>2</sub>,  $\lambda$  = 280 nm):  $t_R$ (minor) = 9.5 min,  $t_R$ (major)

= 12.2 min.  $^1\text{H}$  NMR (500 MHz, Chloroform-*d*)  $\delta$  8.29 (dt,  $J = 2.5, 0.6$  Hz, 1H), 7.54 (qd,  $J = 8.3, 1.7$  Hz, 2H), 7.42 – 7.29 (m, 2H), 7.29 – 7.22 (m, 1H), 7.22 – 7.14 (m, 2H), 3.74 (dd,  $J = 9.2, 6.0$  Hz, 1H), 2.90 – 2.78 (m, 2H), 2.29 (dddd,  $J = 13.9, 9.3, 8.0, 6.0$  Hz, 1H), 2.16 (dddd,  $J = 13.7, 8.5, 7.6, 6.0$  Hz, 1H);  $^{13}\text{C}$  NMR (126 MHz,  $\text{cdCl}_3$ )  $\delta$  148.97, 142.08, 138.88, 137.29, 130.97, 128.89, 128.57, 128.40, 126.85, 119.13, 36.95, 33.53, 32.85; IR (NaCl/thin film): 3026.73, 2925.74, 2859.37, 2242.11, 1734.00, 1581.13, 1561.56, 1496.15, 1455.35, 1385.97, 1090.22, 1019.79, 830.73, 735.64, 699.99  $\text{cm}^{-1}$ ;  $[\alpha]_{\text{D}}^{25} = -4.695$  ( $c = 1.180, \text{CHCl}_3$ ). HRMS (MM) calc'd for  $[\text{M}+\text{H}]^+$  301.0335, found 301.0341.

#### 4-phenyl-2-(6-(trifluoromethyl)pyridin-3-yl)butanenitrile (**122t**)

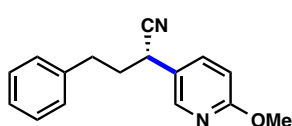


Prepared from 5-iodo-2-trifluoromethylpyridine (54.6 mg, 0.2 mmol) and 2-chloro-4-phenylbutanenitrile (36 mg, 0.2 mmol) with  $\text{NaBF}_4$  (22 mg, 0.2 mmol) following General Procedure 4.

The crude residue was purified by silica gel chromatography (0:100 to 10:90 EtOAc:hexanes) to yield 39.7 mg (68% yield) of **122t** as a clear oil. The enantiomeric excess was determined to be 85% by chiral SFC analysis (AD, 2.5 mL/min, 7% IPA in  $\text{CO}_2$ ,  $\lambda = 254$  nm):  $t_{\text{R}}$ (minor) = 3.0 min,  $t_{\text{R}}$ (major) = 4.7 min.  $^1\text{H}$  NMR (500 MHz, Chloroform-*d*)  $\delta$  8.64 (d,  $J = 2.2$  Hz, 1H), 7.89 (dd,  $J = 8.1, 2.3$  Hz, 1H), 7.73 (dd,  $J = 8.2, 0.8$  Hz, 1H), 7.40 – 7.29 (m, 2H), 7.29 – 7.22 (m, 1H), 7.22 – 7.14 (m, 2H), 3.87 (dd,  $J = 9.3, 5.9$  Hz, 1H), 2.93 – 2.82 (m, 2H), 2.39 – 2.28 (m, 1H), 2.21 (dddd,  $J = 13.7, 8.5, 7.7, 5.9$  Hz, 1H);  $^{13}\text{C}$  NMR (126 MHz,  $\text{cdCl}_3$ )  $\delta$  148.93,  $\delta$  148.18 (q,  $J_{\text{C-F}} = 35.3$  Hz), 138.77, 136.28, 134.83, 128.92, 128.40, 128.38, 126.91, 126.89, 120.81 (q,  $J_{\text{C-F}} = 2.7$  Hz),

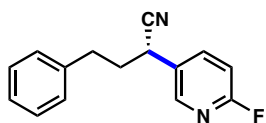
118.87, 37.02, 34.03, 32.90.; IR (NaCl/thin film): 3028.51, 2928.97, 2862.95, 2243.85, 1735.25, 1602.71, 1496.75, 1454.95, 1403.90, 1339.65, 1178.34, 1137.96, 1088.63, 1027.88, 850.30, 751.10, 700.69  $\text{cm}^{-1}$ ;  $[\alpha]_{\text{D}}^{25} = -21.304$  ( $c = 1.475$ ,  $\text{CHCl}_3$ ). HRMS (MM) calc'd for  $[\text{M}+\text{H}]^+$  291.1104, found 291.1181.

### 2-(6-methoxypyridin-3-yl)-4-phenylbutanenitrile (**122u**)



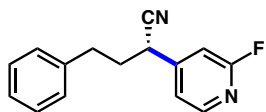
Prepared from 5-iodo-2-methoxypyridine (94.0 mg, 0.4 mmol) and 2-chloro-4-phenylbutanenitrile (36 mg, 0.2 mmol) with  $\text{NaBF}_4$  (22 mg, 0.2 mmol) following General Procedure 4. The crude residue was purified by silica gel chromatography (0:100 to 20:80 EtOAc:hexanes) to yield 22.8 mg (45% yield) of **122u** as a clear oil. The enantiomeric excess was determined to be 83% by chiral SFC analysis (AD, 2.5 mL/min, 8% IPA in  $\text{CO}_2$ ,  $\lambda = 245$  nm):  $t_{\text{R}}$ (minor) = 6.5 min,  $t_{\text{R}}$ (major) = 7.5 min.  $^1\text{H}$  NMR (500 MHz, Chloroform-*d*)  $\delta$  8.07 (dt,  $J = 2.6, 0.6$  Hz, 1H), 7.55 (ddd,  $J = 8.6, 2.6, 0.4$  Hz, 1H), 7.37 – 7.28 (m, 2H), 7.26 – 7.21 (m, 1H), 7.21 – 7.17 (m, 2H), 6.78 (dd,  $J = 8.6, 0.7$  Hz, 1H), 3.94 (s, 3H), 3.69 (dd,  $J = 8.8, 6.3$  Hz, 1H), 2.81 (td,  $J = 8.1, 3.5$  Hz, 2H), 2.35 – 2.21 (m, 1H), 2.14 (dddd,  $J = 13.8, 8.5, 7.5, 6.4$  Hz, 1H);  $^{13}\text{C}$  NMR (126 MHz,  $\text{cdCl}_3$ )  $\delta$  164.04, 145.68, 139.41, 137.39, 128.77, 128.42, 126.64, 124.09, 120.16, 111.56, 53.67, 37.04, 33.28, 32.85.; IR (NaCl/thin film): 2925.19, 1849.43, 2240.05, 1608.56, 1572.83, 1494.73, 1395.28, 1290.62, 1024.55, 831.08, 750.29, 699.95  $\text{cm}^{-1}$ ;  $[\alpha]_{\text{D}}^{25} = -9.806$  ( $c = 0.790$ ,  $\text{CHCl}_3$ ). HRMS (MM) calc'd for  $[\text{M}+\text{Na}]^+$  275.1155, found 275.1175.

**2-(6-fluoropyridin-3-yl)-4-phenylbutanenitrile (122o)**



Prepared from 2-fluoro-5-iodopyridine (89.2 mg, 0.4 mmol) and 2-chloro-4-phenylbutanenitrile (36 mg, 0.2 mmol) following General Procedure 4. The crude residue was purified by silica gel chromatography (0:100 to 10:90 EtOAc:hexanes) to yield 30.7 mg (64% yield) of **122o** as a clear oil. The enantiomeric excess was determined to be 87% by chiral SFC analysis (AD, 2.5 mL/min, 8% IPA in CO<sub>2</sub>,  $\lambda$  = 254 nm):  $t_R$ (minor) = 5.2 min,  $t_R$ (major) = 6.4 min. <sup>1</sup>H NMR (500 MHz, Chloroform-*d*)  $\delta$  8.18 – 8.10 (m, 1H), 7.79 (ddd,  $J$  = 8.5, 7.2, 2.7 Hz, 1H), 7.38 – 7.28 (m, 2H), 7.28 – 7.22 (m, 1H), 7.22 – 7.16 (m, 2H), 6.99 (ddd,  $J$  = 8.5, 3.1, 0.6 Hz, 1H), 3.78 (dd,  $J$  = 9.2, 6.0 Hz, 1H), 2.93 – 2.77 (m, 2H), 2.31 (dddd,  $J$  = 14.0, 9.3, 8.1, 6.0 Hz, 1H), 2.17 (dddd,  $J$  = 13.7, 8.5, 7.6, 6.0 Hz, 1H); <sup>13</sup>C NMR (126 MHz, cdcl<sub>3</sub>)  $\delta$  163.33 (d,  $J_{C-F}$  = 241.3 Hz), 146.57 (d,  $J_{C-F}$  = 15.3 Hz), 140.02 (d,  $J_{C-F}$  = 8.2 Hz), 138.98, 129.33 (d,  $J_{C-F}$  = 4.7 Hz), 128.87, 128.40, 126.82, 119.45, 110.26 (d,  $J_{C-F}$  = 37.6 Hz), 37.11, 33.29 (d,  $J_{C-F}$  = 1.6 Hz), 32.88. ; IR (NaCl/thin film): 3027.76, 2926.65, 2859.25, 2242.02, 1599.81, 1484.95, 1399.59, 1256.76, 1127.35, 1025.00, 831.20, 748.87, 700.31 cm<sup>-1</sup>;  $[\alpha]_D^{25}$  = -27.336 ( $c$  = 1.155, CHCl<sub>3</sub>). HRMS (MM) calc'd for [M+H]<sup>+</sup> 241.1136, found 241.1210.

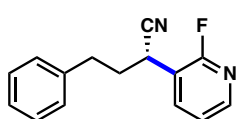
**2-(2-fluoropyridin-4-yl)-4-phenylbutanenitrile (122p)**



Prepared from 2-fluoro-4-iodopyridine (44.6 mg, 0.2 mmol) and 2-chloro-4-phenylbutanenitrile (36 mg, 0.2 mmol) with NaBF<sub>4</sub> (22 mg, 0.2 mmol) following General Procedure 4. The crude residue was purified by silica gel chromatography (0:100 to 10:90 EtOAc:hexanes) to yield 28.8 mg (60% yield) of

**122p** as a clear oil. The enantiomeric excess was determined to be 79% by chiral SFC analysis (AD, 2.5 mL/min, 8% IPA in CO<sub>2</sub>,  $\lambda$  = 210 nm):  $t_R$ (minor) = 4.7 min,  $t_R$ (major) = 5.5 min. <sup>1</sup>H NMR (500 MHz, Chloroform-*d*)  $\delta$  8.25 (d,  $J$  = 5.2 Hz, 1H), 7.36 – 7.31 (m, 2H), 7.29 – 7.23 (m, 1H), 7.22 – 7.18 (m, 2H), 7.17 – 7.14 (m, 1H), 6.92 (td,  $J$  = 1.5, 0.7 Hz, 1H), 3.79 (dd,  $J$  = 9.4, 5.6 Hz, 1H), 2.92 – 2.83 (m, 2H), 2.29 (dddd,  $J$  = 13.7, 9.5, 8.2, 5.5 Hz, 1H), 2.23 – 2.15 (m, 1H); <sup>13</sup>C NMR (126 MHz, cdcl<sub>3</sub>)  $\delta$  164.13 (d,  $J_{C-F}$  = 240.5 Hz), 163.17, 150.09, 148.71 (d,  $J_{C-F}$  = 15.3 Hz), 138.83, 128.91, 128.39, 126.90, 120.00 (d,  $J_{C-F}$  = 4.4 Hz), 118.59, 108.40 (d,  $J_{C-F}$  = 38.8 Hz), 36.61, 35.85 (d,  $J_{C-F}$  = 3.3 Hz), 32.90. ; IR (NaCl/thin film): 2923.87, 2851.17, 2244.02, 1734.43, 1611.28, 1569.24, 1454.61, 1414.02, 1277.86, 839.28, 751.37, 700.44 cm<sup>-1</sup>;  $[\alpha]_D^{25}$  = -22.036 ( $c$  = 0.45, CHCl<sub>3</sub>). HRMS (MM) calc'd for [M+H]<sup>+</sup> 241.1136, found 241.1134.

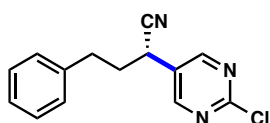
### 2-(2-fluoropyridin-3-yl)-4-phenylbutanenitrile (**122q**)



Prepared from 2-fluoro-3-iodopyridine (44.6 mg, 0.2 mmol) and 2-chloro-4-phenylbutanenitrile (36 mg, 0.2 mmol) following General Procedure 4. The crude residue was purified by silica gel chromatography (0:100 to 10:90 EtOAc:hexanes) to yield 16.7 mg (35% yield) of **122q** as a clear oil. The enantiomeric excess was determined to be 83% by chiral SFC analysis (AD, 2.5 mL/min, 6% IPA in CO<sub>2</sub>,  $\lambda$  = 245 nm):  $t_R$ (minor) = 4.9 min,  $t_R$ (major) = 5.8 min. <sup>1</sup>H NMR (500 MHz, Chloroform-*d*)  $\delta$  8.21 (ddd,  $J$  = 4.9, 1.9, 1.2 Hz, 1H), 7.98 – 7.87 (m, 1H), 7.35 – 7.29 (m, 2H), 7.29 – 7.22 (m, 2H), 7.22 – 7.18 (m, 2H), 4.03 (t,  $J$  = 7.4 Hz, 1H), 2.94 – 2.80 (m, 2H), 2.30 – 2.18 (m, 2H); <sup>13</sup>C NMR (126 MHz, cdcl<sub>3</sub>)  $\delta$  160.30 (d,  $J_{C-F}$  = 239.3 Hz), 147.65 (d,  $J_{C-F}$  = 14.8 Hz), 139.59 (d,  $J_{C-F}$  = 4.3 Hz), 139.02, 128.78, 128.37, 126.74,

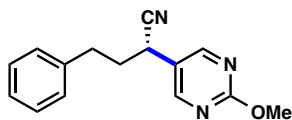
122.09 (d,  $J_{C-F} = 4.3$  Hz), 118.80, 118.23 (d,  $J_{C-F} = 29.6$  Hz), 35.26, 33.06, 30.83 (d,  $J_{C-F} = 2.5$  Hz); IR (NaCl/thin film): 2925.09, 2853.97, 2244.15, 1734.36, 1606.84, 1577.55, 1441.07, 1248.36, 1101.26, 805.44, 750.96, 699.91  $\text{cm}^{-1}$ ;  $[\alpha]_D^{25} = -29.296$  ( $c = 0.635$ ,  $\text{CHCl}_3$ ). HRMS (MM) calc'd for  $[\text{M}+\text{H}]^+$  241.1136, found 241.1133.

### 2-(2-chloropyrimidin-5-yl)-4-phenylbutanenitrile (**122x**)



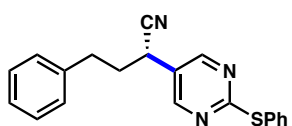
Prepared from 2-chloro-5-iodopyrimidine (48.1 mg, 0.2 mmol) and 2-chloro-4-phenylbutanenitrile (36 mg, 0.2 mmol) following General Procedure 4. The crude residue was purified by flash column chromatography using Florisil<sup>®</sup> stationary phase (0:100 to 15:85 EtOAc:hexanes) to yield 21.2 mg (41% yield) of **122x** as a clear oil. The enantiomeric excess was determined to be 89% by chiral SFC analysis (AD, 2.5 mL/min, 10% IPA in  $\text{CO}_2$ ,  $\lambda = 210$  nm):  $t_R(\text{minor}) = 6.2$  min,  $t_R(\text{major}) = 7.0$  min.  $^1\text{H}$  NMR (500 MHz, Chloroform- $d$ )  $\delta$  8.59 (d,  $J = 0.5$  Hz, 2H), 7.37 – 7.31 (m, 2H), 7.30 – 7.24 (m, 1H), 7.22 – 7.17 (m, 2H), 3.78 (dd,  $J = 9.4, 5.9$  Hz, 1H), 2.95 – 2.84 (m, 2H), 2.34 (dddd,  $J = 13.6, 9.4, 7.7, 5.8$  Hz, 1H), 2.19 (dtd,  $J = 13.8, 8.0, 5.9$  Hz, 1H);  $^{13}\text{C}$  NMR (126 MHz,  $\text{cdCl}_3$ )  $\delta$  161.50, 158.30, 138.35, 129.03, 128.39, 128.36, 127.07, 118.06, 36.65, 32.80, 31.36; IR (NaCl/thin film): 2923.61, 2850.58, 2243.80, 1735.29, 1580.36, 1550.38, 1401.12, 1160.95, 772.57, 748.86, 700.55, 640.20  $\text{cm}^{-1}$ ;  $[\alpha]_D^{25} = -14.892$  ( $c = 0.305$ ,  $\text{CHCl}_3$ ). HRMS (MM) calc'd for  $[\text{M}+\text{H}]^+$  258.0793, found 258.0257.

### 2-(2-methoxypyrimidin-5-yl)-4-phenylbutanenitrile (**122y**)



Prepared from 5-iodo-2-methoxypyrimidine (89.2 mg, 0.4 mmol) and 2-chloro-4-phenylbutanenitrile (36 mg, 0.2 mmol) with  $\text{NaBF}_4$  (22 mg, 0.2 mmol) following General Procedure 4. The crude residue was purified by florisil gel chromatography (0:100 to 40:60 EtOAc:hexanes) to yield 35.8 mg (71% yield) of **122y** as a clear oil. The enantiomeric excess was determined to be 92% by chiral SFC analysis (AS, 2.5 mL/min, 10% IPA in  $\text{CO}_2$ ,  $\lambda = 254$  nm):  $t_{\text{R}}(\text{minor}) = 4.5$  min,  $t_{\text{R}}(\text{major}) = 5.0$  min.  $^1\text{H}$  NMR (500 MHz, Chloroform-*d*)  $\delta$  8.47 (d,  $J = 0.4$  Hz, 2H), 7.38 – 7.29 (m, 2H), 7.28 – 7.23 (m, 1H), 7.22 – 7.17 (m, 2H), 4.04 (s, 3H), 3.71 (dd,  $J = 9.1, 6.1$  Hz, 1H), 2.89 – 2.82 (m, 2H), 2.31 (dddd,  $J = 13.9, 9.2, 7.9, 6.1$  Hz, 1H), 2.16 (dddd,  $J = 13.7, 8.4, 7.6, 6.1$  Hz, 1H);  $^{13}\text{C}$  NMR (126 MHz,  $\text{CDCl}_3$ )  $\delta$  165.54, 158.16, 138.84, 128.91, 128.40, 126.86, 122.72, 119.06, 55.30, 36.79, 32.79, 31.17; IR (NaCl/thin film): 3026.71, 2928.66, 2241.18, 1600.01, 1560.30, 1474.60, 1410.27, 1331.54, 1031.65, 803.93, 700.50  $\text{cm}^{-1}$ ;  $[\alpha]_{\text{D}}^{25} = -17.013$  ( $c = 0.395$ ,  $\text{CHCl}_3$ ). HRMS (MM) calc'd for  $[\text{M}+\text{H}]^+$  254.1288, found 254.1310.

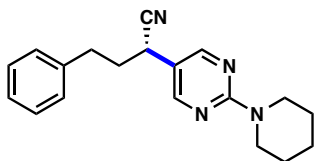
### 4-phenyl-2-(2-phenylthio)pyrimidin-5-yl)butanenitrile (**122n**)



Prepared from 5-iodo-2-phenylthiopyrimidine (62.8 mg, 0.2 mmol) and 2-chloro-4-phenylbutanenitrile (36 mg, 0.2 mmol) following General Procedure 4. The crude residue was purified by silica gel chromatography (0:100 to 30:70 EtOAc:hexanes) to yield 50.3 mg (76% yield) of **122n** as a clear oil. The enantiomeric excess was determined to be 91% by chiral SFC analysis (AD, 2.5 mL/min, 15% IPA in  $\text{CO}_2$ ,  $\lambda = 280$  nm):  $t_{\text{R}}(\text{minor}) = 11.3$  min,  $t_{\text{R}}(\text{major}) = 12.7$

min.  $^1\text{H}$  NMR (500 MHz, Chloroform-*d*)  $\delta$  8.44 (s, 2H), 7.70 – 7.56 (m, 2H), 7.50 – 7.40 (m, 3H), 7.37 – 7.29 (m, 2H), 7.28 – 7.22 (m, 1H), 7.20 – 7.14 (m, 2H), 3.67 (dd,  $J = 9.0$ , 6.0 Hz, 1H), 2.89 – 2.79 (m, 2H), 2.28 (dddd,  $J = 13.9$ , 9.2, 7.9, 6.1 Hz, 1H), 2.13 (dddd,  $J = 13.7$ , 8.4, 7.7, 6.1 Hz, 1H);  $^{13}\text{C}$  NMR (126 MHz,  $\text{cdCl}_3$ )  $\delta$  173.10, 156.34, 138.73, 135.37, 129.65, 129.37, 128.92, 128.80, 128.38, 126.89, 124.93, 118.64, 36.64, 32.74, 31.50; IR (NaCl/thin film): 3025.13, 2926.01, 2242.07, 1734.06, 1580.58, 1539.37, 1399.77, 1170.57, 748.46, 701.21, 689.27  $\text{cm}^{-1}$ ;  $[\alpha]_{\text{D}}^{25} = +10.214$  ( $c = 1.965$ ,  $\text{CHCl}_3$ ). HRMS (MM) calc'd for  $[\text{M}+\text{H}]^+$  332.1216, found 332.1746.

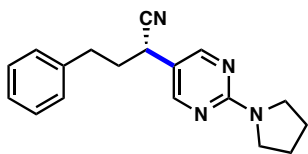
#### 4-phenyl-2-(2-(piperidin-1-yl)pyrimidin-5-yl)butanenitrile (**122m**)



Prepared from 5-iodo-2-(piperidin-1-yl)pyrimidine (57.8 mg, 0.2 mmol) and 2-chloro-4-phenylbutanenitrile (36.0 mg, 0.2 mmol) following General Procedure 4. The crude residue was purified by silica gel chromatography (0:100 to 40:60 EtOAc:hexanes) to yield 43.1 mg (70% yield) of **122m** as a white solid. The enantiomeric excess was determined to be 85% by chiral SFC analysis (AD, 2.5 mL/min, 15% IPA in  $\text{CO}_2$ ,  $\lambda = 254$  nm):  $t_{\text{R}}(\text{minor}) = 7.5$  min,  $t_{\text{R}}(\text{major}) = 8.6$  min. The product could be further enriched via recrystallization by vapor diffusion of pentane to a saturated solution of **122m** in DCM, affording 38.4 mg (89% recovery) of white needles. The enantiomeric excess of recrystallized **7k** was determined to be 95%.  $^1\text{H}$  NMR (500 MHz, Chloroform-*d*)  $\delta$  8.22 (s, 2H), 7.35 – 7.29 (m, 2H), 7.26 – 7.21 (m, 1H), 7.21 – 7.16 (m, 2H), 3.93 – 3.70 (m, 4H), 3.55 (dd,  $J = 8.6$ , 6.5 Hz, 1H), 2.81 (td,  $J = 8.0$ , 7.3, 2.1 Hz, 2H), 2.25 (dddd,  $J = 13.6$ , 8.6, 7.9, 6.5 Hz, 1H), 2.11 (dddd,  $J = 13.7$ , 8.3, 7.4, 6.5 Hz, 1H), 1.76 – 1.65 (m,

2H), 1.65 – 1.54 (m, 4H);  $^{13}\text{C}$  NMR (126 MHz,  $\text{cdCl}_3$ )  $\delta$  161.27, 156.64, 139.33, 128.78, 128.42, 126.64, 119.91, 115.78, 44.89, 36.74, 32.73, 31.18, 25.71, 24.78.; IR (NaCl/thin film): 2932.29, 2853.60, 2239.17, 1605.13, 1514.57, 1448.02, 1364.20, 1271.93, 1024.80, 947.51, 797.14, 700.19  $\text{cm}^{-1}$ ;  $[\alpha]_{\text{D}}^{25} = +13.073$  ( $c = 1.595$ ,  $\text{CHCl}_3$ ). HRMS (MM) calc'd for  $[\text{M}+\text{H}]^+$  307.1917, found 307.1848.

#### 4-phenyl-2-(2-(pyrrolidin-1-yl)pyrimidin-5-yl)butanenitrile (**122I**)

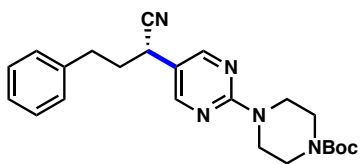


Prepared from 5-iodo-2-(pyrrolidin-1-yl)pyrimidine (55 mg, 0.2 mmol) and 2-chloro-4-phenylbutanenitrile (36.0 mg, 0.2 mmol) following General Procedure 4. The crude residue was purified by silica gel chromatography (0:100 to 40:60 EtOAc:hexanes) to yield 35.0 mg (60% yield) of **122I** as a white solid. The enantiomeric excess was determined to be 85% by chiral SFC analysis (AD, 2.5 mL/min, 12% IPA in  $\text{CO}_2$ ,  $\lambda = 235$  nm):  $t_{\text{R}}$ (minor) = 10.8 min,  $t_{\text{R}}$ (major) = 12.5 min. The product could be further enriched via recrystallization by vapor diffusion of pentane to a saturated solution of **122I** in DCM, affording 31.8 mg (91% recovery) of white needles. The enantiomeric excess of recrystallized **122I** was determined to be 97%.  $^1\text{H}$  NMR (500 MHz, Chloroform-*d*)  $\delta$  8.25 (s, 2H), 7.34 – 7.29 (m, 2H), 7.26 – 7.21 (m, 1H), 7.21 – 7.16 (m, 2H), 3.66 – 3.49 (m, 5H), 2.81 (t,  $J = 7.6$  Hz, 2H), 2.26 (ddt,  $J = 13.7, 8.5, 7.2$  Hz, 1H), 2.11 (dtd,  $J = 13.6, 7.8, 6.6$  Hz, 1H), 2.05 – 1.96 (m, 4H).;  $^{13}\text{C}$  NMR (126 MHz,  $\text{cdCl}_3$ )  $\delta$  156.64, 139.30, 128.79, 128.42, 126.65, 121.43, 119.93, 115.75, 46.78, 36.76, 32.72, 31.22, 25.52; IR (NaCl/thin film): 2927.97, 2866.57, 2238.90, 1603.00, 1524.42, 1483.96, 1460.18, 1335.03, 798.26, 699.99  $\text{cm}^{-1}$ ;

$[\alpha]_D^{25} = +12.942$  ( $c = 1.130$ ,  $\text{CHCl}_3$ ). HRMS (MM) calc'd for  $[\text{M}+\text{H}_3\text{O}]^+$  311.1826, found 311.1825.

***tert*-butyl-4-(5-(1-cyano-3-phenylpropyl)pyrimidin-2-yl)piperazine-1-carboxylate**

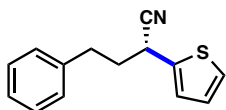
**(122w)**



Prepared from 5-iodo-2-(4-Boc-piperazin-1-yl)pyrimidine (78.0 mg, 0.2 mmol) and 2-chloro-4-phenylbutanenitrile (36.0 mg, 0.2 mmol) following General Procedure 4. The crude residue was purified by silica gel chromatography (0:100 to 40:60 EtOAc:hexanes) to yield 56.5 mg (69% yield) of **122w** as a white solid. The enantiomeric excess was determined to be 85% by chiral SFC analysis (AD, 2.5 mL/min, 15% IPA in  $\text{CO}_2$ ,  $\lambda = 235$  nm):  $t_R(\text{minor}) = 7.5$  min,  $t_R(\text{major}) = 9.0$  min. The product could be further enriched via recrystallization by vapor diffusion of pentane to a saturated solution of **122w** in benzene, affording 51.0 mg (90% recovery) of white needles. The enantiomeric excess of recrystallized **122w** was determined to be 94%.  $^1\text{H}$  NMR (500 MHz,  $\text{CHCl}_3$ )  $\delta$  8.25 (s, 2H), 7.37 – 7.27 (m, 2H), 7.25 – 7.20 (m, 1H), 7.20 – 7.15 (m, 2H), 3.83 – 3.79 (m, 4H), 3.58 (dd,  $J = 8.7, 6.4$  Hz, 1H), 3.50 (t,  $J = 5.3$  Hz, 4H), 2.90 – 2.73 (m, 2H), 2.26 (dddd,  $J = 13.6, 8.7, 7.2, 4.1$  Hz, 1H), 2.11 (dddd,  $J = 13.7, 8.4, 7.5, 6.4$  Hz, 1H), 1.49 (s, 9H);  $^{13}\text{C}$  NMR (126 MHz,  $\text{CDCl}_3$ )  $\delta$  161.27, 156.70, 154.78, 139.21, 128.81, 128.40, 126.69, 119.71, 117.11, 80.07, 43.65, 42.86 (br), 36.74, 32.74, 31.18, 28.43; IR (NaCl/thin film): 2977.91, 2927.86, 2861.14, 2243.21, 1687.28, 1607.00, 1517.48, 1496.25, 1424.34, 1364.59, 1247.24, 1176.22, 1129.18, 999.26, 793.95, 696.53  $\text{cm}^{-1}$ ;

$[\alpha]_D^{25} = +13.500$  ( $c = 1.980$ ,  $\text{CHCl}_3$ ). HRMS (MM) calc'd for  $[\text{M}+\text{Na}]^+$  430.2213, found 430.2294.

#### 4-phenyl-2-(thiophen-2-yl)butanenitrile (**122i**)



Prepared from 2-iodothiophene (111  $\mu\text{L}$ , 1.0 mmol) and 2-chloro-4-phenylbutanenitrile (180 mg, 1.0 mmol) following General Procedure 4. The crude residue was purified by silica gel chromatography (0:100 to 10:90 EtOAc:hexanes) to yield 170 mg (75% yield) of **122i** as a clear oil. The enantiomeric excess was determined to be 88% by chiral SFC analysis (AD, 2.5 mL/min, 8% IPA in  $\text{CO}_2$ ,  $\lambda = 245$  nm):  $t_R(\text{minor}) = 5.8$  min,  $t_R(\text{major}) = 7.1$  min.  $^1\text{H}$  NMR (500 MHz, Chloroform- $d$ )  $\delta$  7.36 – 7.31 (m, 2H), 7.29 (dd,  $J = 5.1, 1.3$  Hz, 1H), 7.27 – 7.23 (m, 1H), 7.22 (dq,  $J = 7.6, 0.7$  Hz, 2H), 7.08 (dt,  $J = 3.5, 1.0$  Hz, 1H), 7.00 (dd,  $J = 5.1, 3.5$  Hz, 1H), 4.03 (ddd,  $J = 8.6, 6.3, 0.8$  Hz, 1H), 2.94 – 2.82 (m, 2H), 2.41 – 2.24 (m, 2H);  $^{13}\text{C}$  NMR (126 MHz,  $\text{cdCl}_3$ )  $\delta$  139.49, 137.62, 128.76, 128.50, 127.13, 126.62, 126.31, 125.61, 119.74, 37.32, 32.85, 31.66; IR (NaCl/thin film): 3085.49, 3062.55, 3026.78, 2927.12, 2860.88, 2241.68, 1602.83, 1496.13, 1454.38, 1238.04, 1080.89, 1029.74, 833.92, 750.39, 699.80  $\text{cm}^{-1}$ ;  $[\alpha]_D^{25} = -27.559$  ( $c = 1.455$ ,  $\text{CHCl}_3$ ). HRMS (MM) calc'd for  $[\text{M}+\text{H}_3\text{O}]^+$  246.0947, found 246.1107.

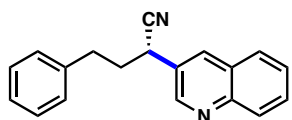
#### 2-(2-(4-bromophenyl)imidazo[1,2-*a*]pyridin-6-yl)-4-phenylbutanenitrile (**122z**)



Prepared from 2-(4-bromophenyl)-6-iodoimidazo[1,2-*a*]pyridine (159.6 mg, 0.4 mmol) and 2-chloro-4-phenylbutanenitrile (36.0 mg, 0.2 mmol) following General Procedure 4. The crude

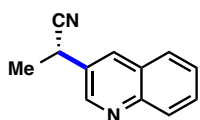
residue was purified by silica gel chromatography (5:95 to 20:80 acetone:hexanes) to yield 60.0 mg (72% yield) of **122z** as a white solid. The enantiomeric excess was determined to be 87% by chiral SFC analysis (IA, 2.5 mL/min, 40% IPA in CO<sub>2</sub>,  $\lambda$  = 245 nm):  $t_R$ (minor) = 10.7 min,  $t_R$ (major) = 14.3 min. The product could be further enriched via recrystallization by vapor diffusion of pentane to a saturated solution of **7o** in DCM, affording 52.2 mg (87% recovery) of white needles. The enantiomeric excess of recrystallized **122z** was determined to be 97%. Following column chromatography, a UV active peak remained in the SFC trace ( $t_R$  = 8.6 min) that was not observed in any other analysis. This peak was significantly diminished following recrystallization. <sup>1</sup>H NMR (500 MHz, Chloroform-*d*)  $\delta$  8.19 – 8.11 (m, 1H), 7.86 (d,  $J$  = 0.7 Hz, 1H), 7.85 – 7.78 (m, 2H), 7.64 (d,  $J$  = 9.4 Hz, 1H), 7.60 – 7.53 (m, 2H), 7.38 – 7.30 (m, 2H), 7.28 – 7.23 (m, 1H), 7.21 (dq,  $J$  = 7.7, 0.7 Hz, 2H), 7.07 (dd,  $J$  = 9.3, 1.9 Hz, 1H), 3.77 (dd,  $J$  = 9.0, 5.7 Hz, 1H), 2.93 – 2.83 (m, 2H), 2.33 (dddd,  $J$  = 13.8, 9.1, 8.2, 5.7 Hz, 1H), 2.25 (dddd,  $J$  = 13.7, 8.5, 7.7, 5.8 Hz, 1H); <sup>13</sup>C NMR (126 MHz, cdcl<sub>3</sub>)  $\delta$  145.73, 144.82, 139.13, 132.34, 131.93, 128.86, 128.41, 127.59, 126.80, 124.07, 123.75, 122.23, 121.06, 119.44, 118.31, 108.76, 36.51, 33.80, 32.88; IR (NaCl/thin film): 2924.20, 2854.07, 2240.70, 1472.83, 1435.81, 1354.99, 1208.78, 1067.55, 1009.04, 833.96, 806.47, 738.54, 700.04 cm<sup>-1</sup>;  $[\alpha]_D^{25}$  = +28.004 ( $c$  = 0.275, CHCl<sub>3</sub>). HRMS (MM) calc'd for [M+H]<sup>+</sup> 416.0757, found 416.0698.

#### 4-phenyl-2-(quinolin-3-yl)butanenitrile (**122v**)



Prepared from 3-iodoquinoline (51.2 mg, 0.2 mmol) and 2-chloro-4-phenylbutanenitrile (36.0 mg, 0.2 mmol) with  $\text{NaBF}_4$  (22.0 mg, 0.2 mmol) following General Procedure 4. The crude residue was purified by silica gel chromatography (0:100 to 40:60 EtOAc:hexanes) to yield 39.4 mg (72% yield) of **3a** as a light yellow oil that solidified on standing. The enantiomeric excess was determined to be 92% by chiral SFC analysis (AD, 2.5 mL/min, 20% IPA in  $\text{CO}_2$ ,  $\lambda = 280$  nm):  $t_R$ (major) = 6.1 min,  $t_R$ (minor) = 6.8 min.  $^1\text{H}$  NMR (500 MHz, Chloroform-*d*)  $\delta$  8.81 (s, 1H), 8.18 (d,  $J = 2.3$  Hz, 1H), 8.12 (d,  $J = 8.4$  Hz, 1H), 7.85 (dd,  $J = 8.2, 1.3$  Hz, 1H), 7.76 (ddd,  $J = 8.4, 6.9, 1.5$  Hz, 1H), 7.61 (ddd,  $J = 8.1, 6.8, 1.1$  Hz, 1H), 7.38 – 7.28 (m, 2H), 7.28 – 7.15 (m, 3H), 3.99 (dd,  $J = 9.0, 5.9$  Hz, 1H), 2.95 – 2.82 (m, 2H), 2.39 (dddd,  $J = 14.0, 9.2, 7.9, 6.2$  Hz, 1H), 2.30 (dddd,  $J = 13.7, 8.5, 7.7, 5.9$  Hz, 1H);  $^{13}\text{C}$  NMR (126 MHz,  $\text{cdCl}_3$ )  $\delta$  149.22, 147.75, 139.21, 134.28, 130.18, 129.42, 128.85, 128.57, 128.45, 127.78, 127.62, 127.56, 126.76, 119.74, 37.18, 34.39, 32.99; IR (NaCl/thin film): 3026.11, 2926.11, 2241.03, 1603.40, 1571.03, 1495.05, 1454.48, 1125.63, 906.13, 787.96, 751.66, 700.17  $\text{cm}^{-1}$ ;  $[\alpha]_D^{25} = -1.617$  ( $c = 0.952$ ,  $\text{CHCl}_3$ ). HRMS (MM) calc'd for  $[\text{M}+\text{H}]^+$  273.1386, found 273.1589.

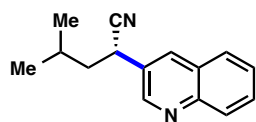
#### 2-(quinolin-3-yl)propanenitrile (**129b**)



Prepared from 3-iodoquinoline (51.2 mg, 0.2 mmol) and 2-chloropropanenitrile (17  $\mu\text{L}$ , 0.2 mmol) following General Procedure 4. The crude residue was purified by silica gel chromatography (0:100 to 20:80 EtOAc:hexanes) to yield 28.7 mg (79% yield) of **129b** as a clear oil. The enantiomeric

excess was determined to be 81% by chiral SFC analysis (AD, 2.5 mL/min, 10% IPA in CO<sub>2</sub>,  $\lambda$  = 254 nm):  $t_R$ (major) = 7.8 min,  $t_R$ (minor) = 8.8 min. <sup>1</sup>H NMR (300 MHz, Chloroform-*d*)  $\delta$  8.87 (d,  $J$  = 2.4 Hz, 1H), 8.23 (d,  $J$  = 2.4 Hz, 1H), 8.14 (d,  $J$  = 8.5 Hz, 1H), 7.92 – 7.84 (m, 1H), 7.77 (ddd,  $J$  = 8.4, 6.9, 1.5 Hz, 1H), 7.62 (ddd,  $J$  = 8.2, 6.9, 1.2 Hz, 1H), 4.16 (q,  $J$  = 7.3 Hz, 1H), 1.78 (dd,  $J$  = 7.3, 0.5 Hz, 3H); <sup>13</sup>C NMR (126 MHz, cdcl<sub>3</sub>)  $\delta$  149.01, 147.67, 133.57, 130.13, 129.83, 129.34, 127.78, 127.58, 127.54, 120.60, 29.26, 21.39; IR (NaCl/thin film): 2924.03, 2850.94, 2241.83, 1570.25, 1496.55, 1457.22, 1378.86, 1126.13, 1082.83, 966.72, 907.45, 787.48, 752.77, 617.35 cm<sup>-1</sup>; [ $\alpha$ ]<sub>D</sub><sup>25</sup> = -20.200 ( $c$  = .355, CHCl<sub>3</sub>). HRMS (MM) calc'd for [M+H<sub>3</sub>O]<sup>+</sup> 201.1022, found 201.1022.

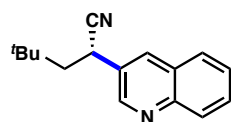
#### 4-methyl-2-(quinolin-3-yl)pentanenitrile (**129h**)



Prepared from 3-iodoquinoline (51.2 mg, 0.2 mmol) and 2-chloro-4-methylpentanenitrile (26.2 mg, 0.2 mmol) following General Procedure 4. The crude residue was purified by silica gel chromatography (0:100 to 30:70 EtOAc:hexanes) to yield 29.1 mg (65% yield) of **129h** as a clear oil. The enantiomeric excess was determined to be 89% by chiral SFC analysis (OB-H, 2.5 mL/min, 5% IPA in CO<sub>2</sub>,  $\lambda$  = 254 nm):  $t_R$ (minor) = 4.2 min,  $t_R$ (major) = 4.6 min. <sup>1</sup>H NMR (500 MHz, Chloroform-*d*)  $\delta$  8.83 (d,  $J$  = 2.4 Hz, 1H), 8.19 (d,  $J$  = 2.4 Hz, 1H), 8.13 (dq,  $J$  = 8.5, 0.9 Hz, 1H), 7.85 (ddd,  $J$  = 8.1, 1.3, 0.7 Hz, 1H), 7.76 (ddd,  $J$  = 8.5, 6.9, 1.4 Hz, 1H), 7.61 (ddd,  $J$  = 8.1, 6.9, 1.2 Hz, 1H), 4.05 (dd,  $J$  = 9.8, 6.2 Hz, 1H), 2.06 – 1.97 (m, 1H), 1.96 – 1.86 (m, 1H), 1.75 (ddd,  $J$  = 13.5, 8.6, 6.2 Hz, 1H), 1.04 (dd,  $J$  = 11.3, 6.6 Hz, 6H); <sup>13</sup>C NMR (126 MHz, cdcl<sub>3</sub>)  $\delta$  149.31, 147.66, 134.09, 130.08, 129.34, 129.21, 127.73,

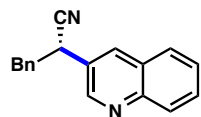
127.63, 127.50, 120.06, 44.85, 33.43, 26.23, 22.59, 21.58; IR (NaCl/thin film): 2957.60, 2928.61, 2238.86, 1653.55, 1570.26, 1494.77, 1467.80, 1369.63, 1280.03, 1116.26, 787.30, 752.79  $\text{cm}^{-1}$ ;  $[\alpha]_{\text{D}}^{25} = -22.811$  ( $c = 0.350$ ,  $\text{CHCl}_3$ ). HRMS (MM) calc'd for  $[\text{M}+\text{H}_3\text{O}]^+$  243.1492, found 243.1194.

#### 4,4-dimethyl-2-(quinolin-3-yl)pentanenitrile (**129c**)



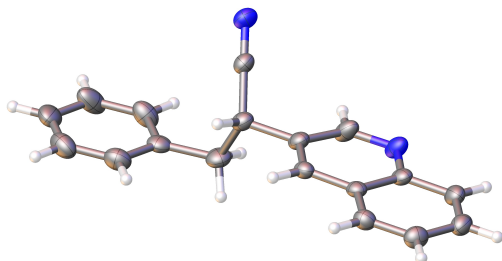
Prepared from 3-iodoquinoline (51.2 mg, 0.2 mmol) and 2-chloro-4,4-dimethylpentanenitrile (29.1 mg, 0.2 mmol) following General Procedure 4. The crude residue was purified by silica gel chromatography (0:100 to 30:70 EtOAc:hexanes) to yield 21.4 mg (45% yield) of **129c** as a clear oil. The enantiomeric excess was determined to be 93% by chiral SFC analysis (AD, 2.5 mL/min, 12% IPA in  $\text{CO}_2$ ,  $\lambda = 280$  nm):  $t_{\text{R}}$ (major) = 5.5 min,  $t_{\text{R}}$ (minor) = 6.8 min.  $^1\text{H}$  NMR (500 MHz, Chloroform- $d$ )  $\delta$  8.81 (d,  $J = 2.4$  Hz, 1H), 8.20 (d,  $J = 2.4$  Hz, 1H), 8.12 (dd,  $J = 8.5, 1.0$  Hz, 1H), 7.84 (ddt,  $J = 8.1, 1.3, 0.6$  Hz, 1H), 7.75 (ddd,  $J = 8.4, 6.9, 1.5$  Hz, 1H), 7.60 (ddd,  $J = 8.1, 6.9, 1.2$  Hz, 1H), 4.00 (dd,  $J = 10.3, 3.4$  Hz, 1H), 2.15 (dd,  $J = 14.2, 10.4$  Hz, 1H), 1.76 (dd,  $J = 14.2, 3.4$  Hz, 1H), 1.12 (s, 9H);  $^{13}\text{C}$  NMR (126 MHz,  $\text{cdCl}_3$ )  $\delta$  149.40, 147.52, 133.87, 130.57, 130.04, 129.32, 127.73, 127.61, 127.50, 121.19, 50.25, 31.37, 31.16, 29.40. IR (NaCl/thin film): 2956.95, 2239.66, 1734.18, 1495.05, 1477.11, 1280.54, 1116.30, 1012.66, 897.41, 788.79, 752.85, 619.63  $\text{cm}^{-1}$ ;  $[\alpha]_{\text{D}}^{25} = -55.546$  ( $c = 0.515$ ,  $\text{CHCl}_3$ ). HRMS (MM) calc'd for  $[\text{M}+\text{H}]^+$  239.1543, found 239.1530.

### 3-phenyl-2-(quinolin-3-yl)propanenitrile (**129e**)

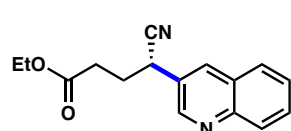


Prepared from 3-iodoquinoline (51.2 mg, 0.2 mmol) and 2-chloro-3-phenylpropanenitrile (33.1 mg, 0.2 mmol) with  $\text{NaBF}_4$  (22 mg, 0.2 mmol) following General Procedure 4. The crude residue was purified by silica gel chromatography (0:100 to 30:70 EtOAc:hexanes) to yield 33.8 mg (65% yield) of **3e** as a light yellow solid. The enantiomeric excess was determined to be 90% by chiral SFC analysis (AD, 2.5 mL/min, 20% IPA in  $\text{CO}_2$ ,  $\lambda = 280$  nm):  $t_{\text{R}}(\text{major}) = 5.9$  min,  $t_{\text{R}}(\text{minor}) = 6.8$  min. The product could be further enriched via recrystallization by vapor diffusion of pentane to a saturated solution of **129e** in DCM, affording 29.7 mg (88% recovery) of clear pyramidal crystals suitable for X-Ray diffraction. The enantiomeric excess of recrystallized **3e** was determined to be 96%. The structure was solved by direct methods using SHELXS and refined against  $F^2$  on all data by full-matrix least squares with SHELXL-2014 using established refinement techniques and with an extinction coefficient of 0.0069(7). All non-hydrogen atoms were refined anisotropically. All hydrogen atoms were included into the model at geometrically calculated positions and refined using a riding model. Compound **129e** crystallizes in the orthorhombic space group  $P2_12_12_1$  and absolute configuration was determined by anomalous dispersion (Flack = -0.15(8)).  $^1\text{H}$  NMR (500 MHz, Chloroform- $d$ )  $\delta$  8.71 (d,  $J = 2.4$  Hz, 1H), 8.16 – 8.10 (m, 1H), 8.07 (d,  $J = 2.3$  Hz, 1H), 7.81 (dd,  $J = 8.2, 1.4$  Hz, 1H), 7.77 (ddd,  $J = 8.4, 6.9, 1.4$  Hz, 1H), 7.61 (ddd,  $J = 8.1, 6.9, 1.2$  Hz, 1H), 7.33 – 7.27 (m, 3H), 7.17 – 7.11 (m, 2H), 4.32 – 4.25 (m, 1H), 3.36 – 3.23 (m, 2H);  $^{13}\text{C}$  NMR (126 MHz,  $\text{cdCl}_3$ )  $\delta$  149.35, 147.68, 135.32, 134.61, 130.18, 129.35, 129.29, 128.84, 127.96, 127.80, 127.76, 127.49, 127.45, 119.51, 41.90, 37.50; IR (NaCl/thin film): 3029.15, 2925.55, 2855.78, 2242.14,

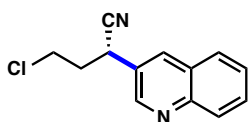
1604.24, 1571.67, 1495.10, 1455.39, 1382.41, 1125.96, 908.49, 787.51, 752.04, 734.70, 699.30  $\text{cm}^{-1}$ ;  $[\alpha]_{\text{D}}^{25} = -1.218$  ( $c = 0.870$ ,  $\text{CHCl}_3$ ). HRMS (MM) calc'd for  $[\text{M}+\text{H}]^+$  259.1230, found 259.1427.



#### Ethyl 4-cyano-4-(quinolin-3-yl)butanoate (**129f**)

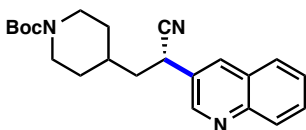
 Prepared from 3-iodoquinoline (51.2 mg, 0.2 mmol) and ethyl 4-chloro-4-cyanobutyrate (35.1 mg, 0.2 mmol) following General Procedure 4. The crude residue was purified by silica gel chromatography (0:100 to 30:70 EtOAc:hexanes) to yield 34.0 mg (63% yield) of **129f** as a clear oil. The enantiomeric excess was determined to be 80% by chiral SFC analysis (AD, 2.5 mL/min, 12% IPA in  $\text{CO}_2$ ,  $\lambda = 254$  nm):  $t_{\text{R}}$ (major) = 7.2 min,  $t_{\text{R}}$ (minor) = 8.3 min.  $^1\text{H}$  NMR (500 MHz, Chloroform- $d$ )  $\delta$  8.91 (s, 1H), 8.20 (s, 2H), 7.86 (dd,  $J = 8.2, 1.1$  Hz, 1H), 7.77 (d,  $J = 6.7$  Hz, 1H), 7.61 (dd,  $J = 8.1, 6.8$  Hz, 1H), 4.28 (dd,  $J = 8.7, 6.0$  Hz, 1H), 4.15 (q,  $J = 7.1$  Hz, 2H), 2.62 (dt,  $J = 16.9, 7.5$  Hz, 1H), 2.53 (dt,  $J = 17.0, 6.5$  Hz, 1H), 2.41 – 2.21 (m, 2H), 1.27 (t,  $J = 7.1$  Hz, 3H);  $^{13}\text{C}$  NMR (126 MHz,  $\text{cdCl}_3$ )  $\delta$  171.81, 149.29, 148.04, 134.40, 130.30, 129.54, 128.12, 127.83, 127.61, 127.59, 119.40, 61.01, 34.27, 30.92, 30.72, 14.17; IR (NaCl/thin film): 2979.77, 2926.59, 2242.45, 1731.81, 1495.27, 1377.67, 1312.77, 1189.37, 1024.39, 909.00, 788.82, 754.73  $\text{cm}^{-1}$ ;  $[\alpha]_{\text{D}}^{25} = -9.319$  ( $c = 0.860$ ,  $\text{CHCl}_3$ ). HRMS (MM) calc'd for  $[\text{M}+\text{H}]^+$  269.1285, found 269.1313.

### 3-chloro-2-(quinolin-3-yl)propanenitrile (**129g**)



Prepared from 3-iodoquinoline (102.4 mg, 0.4 mmol) and 2,4-dichlorobutanenitrile (27.6 mg, 0.2 mmol) following General Procedure 4. The crude residue was purified by silica gel chromatography (0:100 to 30:70 EtOAc:hexanes) to yield 35.8 mg (78% yield) of **129g** as a clear oil that slowly solidified on standing. The enantiomeric excess was determined to be 79% by chiral SFC analysis (AD, 2.5 mL/min, 12% IPA in CO<sub>2</sub>,  $\lambda$  = 254 nm):  $t_R$ (major) = 7.1 min,  $t_R$ (minor) = 9.7 min. <sup>1</sup>H NMR (500 MHz, Chloroform-*d*)  $\delta$  8.88 (d,  $J$  = 2.4 Hz, 1H), 8.22 (d,  $J$  = 2.4 Hz, 1H), 8.14 (dd,  $J$  = 8.5, 1.0 Hz, 1H), 7.90 – 7.83 (m, 1H), 7.78 (ddd,  $J$  = 8.4, 6.9, 1.4 Hz, 1H), 7.63 (ddd,  $J$  = 8.1, 6.9, 1.2 Hz, 1H), 4.41 (dd,  $J$  = 8.6, 6.7 Hz, 1H), 3.79 (ddd,  $J$  = 11.5, 8.2, 4.6 Hz, 1H), 3.60 (ddd,  $J$  = 11.4, 6.4, 4.8 Hz, 1H), 2.54 (dddd,  $J$  = 14.4, 8.7, 6.5, 4.5 Hz, 1H), 2.40 (dddd,  $J$  = 14.4, 8.2, 6.7, 4.8 Hz, 1H); <sup>13</sup>C NMR (126 MHz, cdcl<sub>3</sub>)  $\delta$  149.09, 147.92, 134.63, 130.42, 129.44, 127.77, 127.71, 127.51, 127.27, 119.08, 41.02, 38.07, 32.28; IR (NaCl/thin film): 2960.74, 2922.28, 2242.62, 1571.06, 1495.00, 1443.08, 1382.69, 1125.91, 957.61, 906.20, 787.55, 753.85, 619.73 cm<sup>-1</sup>;  $[\alpha]_D^{25}$  = +9.150 ( $c$  = 0.665, CHCl<sub>3</sub>). HRMS (MM) calc'd for [M+H<sub>3</sub>O]<sup>+</sup> 249.0789, found 249.0270.

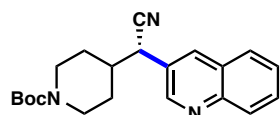
### *tert*-butyl-4-(2-cyano-2-(quinolin-3-yl)ethyl)piperidine-1-carboxylate (**129a**)



Prepared from 3-iodoquinoline (51.2 mg, 0.2 mmol) and *tert*-Butyl-4-(2-chloro-2-cyanoethyl)piperidine-1-carboxylate (54.6 mg, 0.2 mmol) following General Procedure 4. The crude residue was purified by silica gel chromatography (0:100 to 40:60 EtOAc:hexanes) to yield 44.7 mg (61% yield) of **129a** as a clear oil. The enantiomeric excess was

determined to be 89% by chiral SFC analysis (AD, 2.5 mL/min, 25% IPA in CO<sub>2</sub>,  $\lambda$  = 280 nm):  $t_R$ (major) = 4.8 min,  $t_R$ (minor) = 6.0 min. <sup>1</sup>H NMR (500 MHz, Chloroform-*d*)  $\delta$  8.81 (d,  $J$  = 2.3 Hz, 1H), 8.18 (d,  $J$  = 2.3 Hz, 1H), 8.12 (dd,  $J$  = 8.4, 1.0 Hz, 1H), 7.84 (dd,  $J$  = 8.1, 1.4 Hz, 1H), 7.76 (ddd,  $J$  = 8.4, 6.9, 1.4 Hz, 1H), 7.60 (ddd,  $J$  = 8.1, 6.8, 1.1 Hz, 1H), 4.10 (br, dd,  $J$  = 10.1, 5.6 Hz, 3H), 2.72 (br, 2H), 2.13 – 1.99 (m, 1H), 1.94 – 1.63 (m, 4H), 1.46 (s, 9H), 1.33 – 1.12 (m, 2H); <sup>13</sup>C NMR (126 MHz, cdcl<sub>3</sub>)  $\delta$  154.68, 149.12, 147.72, 134.10, 130.21, 129.37, 128.78, 127.73, 127.60, 127.58, 119.77, 79.55, 43.88 (br), 43.20 (br), 42.58, 33.99, 32.58, 32.10, 31.22, 28.44; IR (NaCl/thin film): 2974.27, 2926.66, 2852.75, 2239.98, 1685.09, 1495.27, 1424.19, 1365.34, 1278.99, 1244.13, 1163.05, 1125.17, 970.82, 865.20, 787.79, 755.04, 736.24, 620.45 cm<sup>-1</sup>;  $[\alpha]_D^{25}$  = -4.158 ( $c$  = 1.900, CHCl<sub>3</sub>). HRMS (MM) calc'd for [M+Mg]<sup>+</sup> 389.1948, found 389.2091.

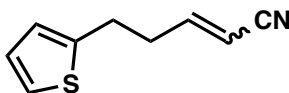
***tert*-butyl-4-(cyano(quinolin-3-yl)methyl)piperidine-1-carboxylate (**129d**)**



Prepared from 3-iodoquinoline (51.2 mg, 0.2 mmol) and *tert*-Butyl-4-(chloro(cyano)methyl)piperidine-1-carboxylate (51.8 mg, 0.2 mmol) following General Procedure 4. The crude residue was purified by silica gel chromatography (0:100 to 40:60 EtOAc:hexanes) to yield 28.6 mg (41% yield) of **129d** as a clear oil. The enantiomeric excess was determined to be 91% by chiral SFC analysis (AD, 2.5 mL/min, 12% IPA in CO<sub>2</sub>,  $\lambda$  = 280 nm):  $t_R$ (minor) = 18.5 min,  $t_R$ (major) = 19.5 min. <sup>1</sup>H NMR (500 MHz, Chloroform-*d*)  $\delta$  8.79 (d,  $J$  = 2.4 Hz, 1H), 8.16 (d,  $J$  = 2.3 Hz, 1H), 8.13 (dq,  $J$  = 8.5, 0.8 Hz, 1H), 7.86 (dd,  $J$  = 8.1, 1.3 Hz, 1H), 7.77 (ddd,  $J$  = 8.4, 6.9, 1.4 Hz, 1H), 7.62 (ddd,  $J$  = 8.1, 6.9, 1.2 Hz, 1H), 4.19 (s, 2H), 3.94 (d,  $J$  = 6.8 Hz, 1H), 2.64 (s, 2H), 2.03 (tdd,  $J$  = 12.0, 6.9, 3.5 Hz, 1H), 1.88 – 1.71 (m, 1H), 1.67 (dt,  $J$  = 12.9,

3.0 Hz, 1H), 1.45 (s, 11H);  $^{13}\text{C}$  NMR (126 MHz,  $\text{cdCl}_3$ )  $\delta$  154.49, 149.48, 147.80, 135.05, 130.33, 129.37, 127.79, 127.66, 127.41, 126.70, 118.57, 79.85, 43.53, 42.89, 41.41, 41.34, 30.11, 28.80, 28.40; IR (NaCl/thin film): 2975.09, 2929.55, 2853.85, 2240.07, 1688.65, 1424.27, 1365.82, 1248.34, 1165.15, 1121.49, 1059.13, 756.02  $\text{cm}^{-1}$ ;  $[\alpha]_{\text{D}}^{25} = -21.275$  ( $c = 0.640$ ,  $\text{CHCl}_3$ ). HRMS (MM) calc'd for  $[\text{M}+\text{Mg}]^+$  377.1948, found 377.2042.

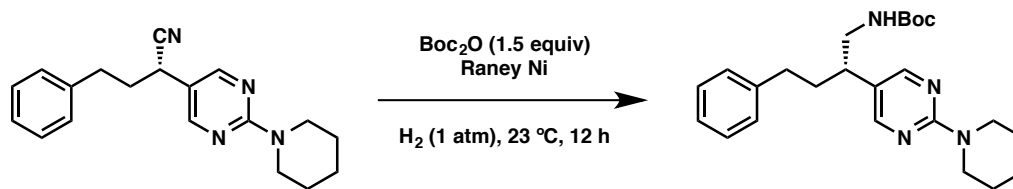
### 5-(thiophen-2-yl)pent-2-enitrile (1:1 *cis/trans*) (**145**)



Prepared from 2-iodothiophene (11  $\mu\text{L}$ , 0.1 mmol) and 2-chloro-2-cyclopropylacetonitrile (11.6 mg, 0.1 mmol) following General Procedure 4. The crude residue was purified by preparative thin layer chromatography (15:85 EtOAc:hexanes) to yield 3.5 mg (21% yield) of **145** as a clear oil as a 1:1 mixture of *cis*<sup>\*</sup> and *trans*<sup>§</sup> isomers. Analysis of the crude NMR indicated no other conversion of the aryl iodide, with no cyclopropane-containing product detected. No unreacted chloronitrile was observed, presumably consumed by non-productive reaction pathways.  $^1\text{H}$  NMR (500 MHz, Chloroform-*d*)  $\delta$  7.16 (ddd,  $J = 5.1, 1.2, 0.7$  Hz, 2H)<sup>\*§</sup>, 6.94 (ddd,  $J = 5.2, 3.4, 1.9$  Hz, 2H)<sup>\*§</sup>, 6.86 – 6.77 (m, 2H)<sup>\*§</sup>, 6.73 (dt,  $J = 16.3, 6.9$  Hz, 1H)<sup>§</sup>, 6.50 (dt,  $J = 10.9, 7.5$  Hz, 1H)<sup>\*</sup>, 5.45 – 5.27 (m, 2H)<sup>\*§</sup>, 3.02 (dtd,  $J = 15.6, 7.4, 0.8$  Hz, 4H)<sup>\*§</sup>, 2.87 – 2.78 (m, 2H)<sup>\*</sup>, 2.62 (ddd,  $J = 7.7, 6.9, 1.7$  Hz, 2H)<sup>§</sup>.  $^{13}\text{C}$  NMR (126 MHz,  $\text{cdCl}_3$ )  $\delta$  153.94, 153.14, 142.38, 142.30, 126.95, 124.91, 123.78, 123.76, 100.98, 100.70, 35.11, 33.46, 28.43, 28.09; IR (NaCl/thin film): 2916.78, 2848.47, 2220.22, 1558.05, 1683.13, 848.26, 689.00, 668.02  $\text{cm}^{-1}$ . HRMS (MM) calc'd for  $[\text{M}]^+$  163.0450, found 163.0765.

### 3.6.4 Derivatization of Enantioenriched Nitrile Products

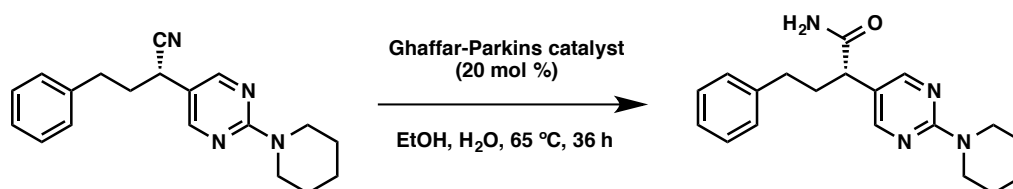
#### a. Hydrogenation of **122m** over Raney Ni to Boc-amine **130**.



Raney Ni (75 mg) was rinsed with dry MeOH 3 times to remove excess water and added to a flame-dried flask. To this was added dry MeOH (5 mL), 4-phenyl-2-(2-(piperidin-1-yl)pyrimidin-5-yl)butanenitrile (**122m**, 30 mg, 0.10 mmol, 85% ee), and Boc anhydride (33 mg, 0.15 mmol). The flask was purged with N<sub>2</sub> for 15 min, then flushed with two balloons of H<sub>2</sub>. The flask was equipped with a balloon of H<sub>2</sub> and stirred for 3.5 hours. The reaction was then filtered over Celite with EtOAc to afford a viscous resinous clear oil. The crude residue was purified by silica gel chromatography (0:100 to 50:50 EtOAc:hexanes) to yield 39 mg (95% yield) of **130** as a clear oil that solidified slowly upon standing. The enantiomeric excess was determined to be 85% by chiral SFC analysis (AD, 2.5 mL/min, 15% IPA in CO<sub>2</sub>,  $\lambda$  = 235 nm):  $t_R$ (major) = 10.5 min,  $t_R$ (minor) = 12.3 min. <sup>1</sup>H NMR (500 MHz, Chloroform-*d*)  $\delta$  8.14 (s, 2H), 7.29 – 7.21 (m, 2H), 7.21 – 7.13 (m, 1H), 7.13 – 7.06 (m, 2H), 4.45 (s, 1H), 3.86 – 3.70 (m, 4H), 3.45 (dt,  $J$  = 13.1, 6.4 Hz, 1H), 3.12 (ddd,  $J$  = 13.9, 8.8, 5.4 Hz, 1H), 2.69 – 2.41 (m, 3H), 1.99 (dddd,  $J$  = 13.6, 9.8, 6.9, 4.8 Hz, 1H), 1.84 (dtd,  $J$  = 13.5, 9.8, 5.3 Hz, 1H), 1.74 – 1.55 (m, 6H), 1.40 (s, 9H); <sup>13</sup>C NMR (126 MHz, cdCl<sub>3</sub>)  $\delta$  161.26, 157.43, 155.82, 141.54, 128.42, 128.33, 125.93, 121.66, 79.40, 46.02, 44.85, 40.52, 34.57, 33.28, 28.34, 25.75, 24.84; IR (NaCl/thin film): 3337.97, 2930.35, 2853.42, 1712.79, 1602.18, 1504.75, 1449.34, 1364.47, 1271.22, 1255.54, 1169.92, 1028.05, 947.36, 798.75, 699.89 cm<sup>-1</sup>;

$[\alpha]_D^{25} = -15.883$  ( $c = 2.365$ ,  $\text{CHCl}_3$ ). HRMS (MM) calc'd for  $[\text{M}]^+$  410.2676, found 410.2101.

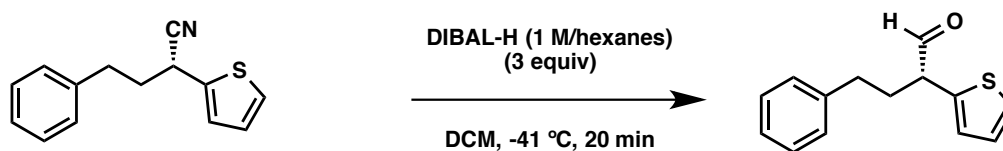
**b. Hydrolysis of 122m with Ghaffar-Parkins catalyst to carboxamide 131.**



In a 1-dram vial, 4-phenyl-2-(2-(piperidin-1-yl)pyrimidin-5-yl)butanenitrile (**122m**, 30 mg, 0.10 mmol, 85% ee) was suspended in EtOH (0.4 mL) and H<sub>2</sub>O (0.1 mL). To this was added hydrido(dimethylphosphinous acid-kP)[hydrogen bis(dimethylphosphinito-kP)]platinum(II) (9 mg, 20  $\mu$ mol). The reaction was sealed with a Teflon-lined cap and heated to 65 °C for 36 h. After cooling to room temperature, the reaction was diluted with DCM and filtered through a short plug of silica gel and Na<sub>2</sub>SO<sub>4</sub>. The plug was washed with additional DCM and the organics were concentrated to afford the carboxamide as a clear oil. The crude residue was purified by silica gel chromatography (30:70 to 60:40 EtOAc:hexanes) to yield 30.8 mg (95% yield) of **131** as a viscous clear oil. The enantiomeric excess was determined to be 85% by <sup>1</sup>H NMR using Europium(III) tris[3-(trifluoromethylhydroxymethylene)-*d*-camphorate] (30 mol %) as a chiral shift reagent. <sup>1</sup>H NMR (500 MHz, Chloroform-*d*)  $\delta$  8.23 (s, 2H), 7.27 (d,  $J = 7.2$  Hz, 2H), 7.22 – 7.16 (m, 1H), 7.16 – 7.11 (m, 2H), 5.66 (s, 1H), 5.45 (s, 1H), 3.92 – 3.61 (m, 4H), 3.12 (dd,  $J = 8.4, 6.8$  Hz, 1H), 2.67 – 2.54 (m, 2H), 2.43 (ddt,  $J = 13.8, 8.7, 6.9$  Hz, 1H), 2.12 – 1.97 (m, 1H), 1.68 (td,  $J = 6.7, 6.3, 4.7$  Hz, 2H), 1.65 – 1.55 (m, 4H); <sup>13</sup>C NMR (126 MHz, cdCl<sub>3</sub>)  $\delta$  175.22, 161.24, 157.30, 140.84, 128.51, 126.13, 119.40,

46.14, 44.86, 34.06, 33.17, 25.72, 24.82; IR (NaCl/thin film): 3333.85, 3190.50, 2932.50, 2853.02, 1667.77, 1602.06, 1504.96, 1446.89, 1364.61, 1271.06, 1256.15, 1178.28, 1024.54, 947.10, 797.03, 733.36, 699.53  $\text{cm}^{-1}$   $[\alpha]_{\text{D}}^{25} = +35.005$  ( $c = 2.455$ ,  $\text{CHCl}_3$ ). HRMS (MM) calc'd for  $[\text{M}]^+$  324.1945, found 324.1904.

**c. DIBAL-H reduction of **122i** to carboxaldehyde **132**.**

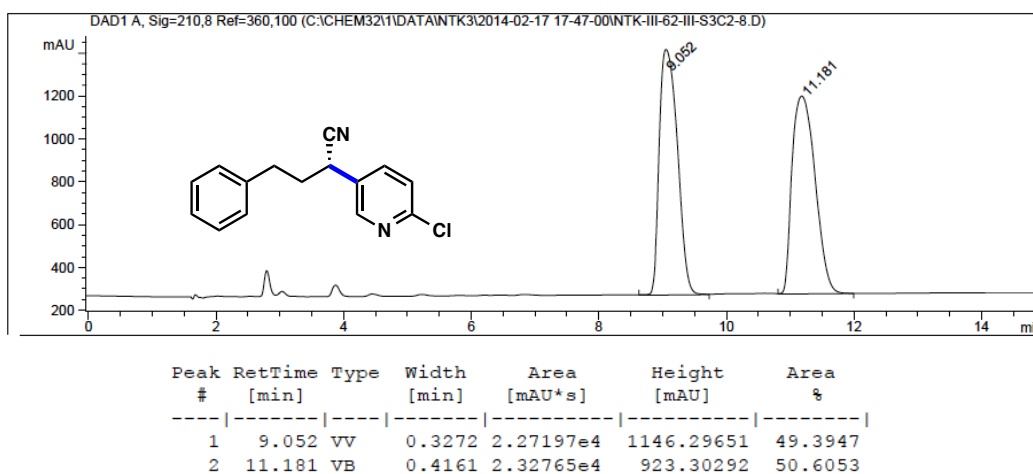


To a flame-dried flask was added 4-phenyl-2-(thiophen-2-yl)butanenitrile (**122i**, 46 mg, 0.2 mmol, 88% ee) and DCM (30 mL). The reaction was cooled to -41 °C and a 1 M solution of DIBAL-H in hexanes (3 equiv, 0.6 mL, 0.6 mmol) was added slowly via syringe. The reaction was complete by TLC after 20 min. A 5% AcOH/ $\text{H}_2\text{O}$  solution (12 mL) was added and the reaction was allowed to warm to room temperature. The reaction was stirred vigorously for 30 min and then the layers were separated. The organics were washed with dilute sodium bicarbonate, dried over sodium sulfate, and concentrated to afford light yellow oil. The crude residue was purified by silica gel chromatography (0:100 to 10:90 EtOAc:hexanes) to yield 44 mg (96% yield) of **132** as a yellow oil that was stored frozen in benzene. The enantiomeric excess was determined to be 81% by chiral SFC analysis (AD, 2.5 mL/min, 8% IPA in  $\text{CO}_2$ ,  $\lambda = 235$  nm):  $t_{\text{R}}$ (minor) = 4.5 min,  $t_{\text{R}}$ (major) = 5.1 min.  $^1\text{H}$  NMR (500 MHz, Chloroform- $d$ )  $\delta$  9.61 (d,  $J = 2.1$  Hz, 1H), 7.34 – 7.28 (m, 3H), 7.25 – 7.20 (m, 1H), 7.18 (dq,  $J = 7.6, 0.7$  Hz, 2H), 7.07 (dd,  $J = 5.1, 3.5$  Hz, 1H), 6.95 (ddd,  $J = 3.5, 1.2, 0.7$  Hz, 1H), 3.79 (ddd,  $J = 8.4, 6.3, 2.1$  Hz, 1H), 2.73

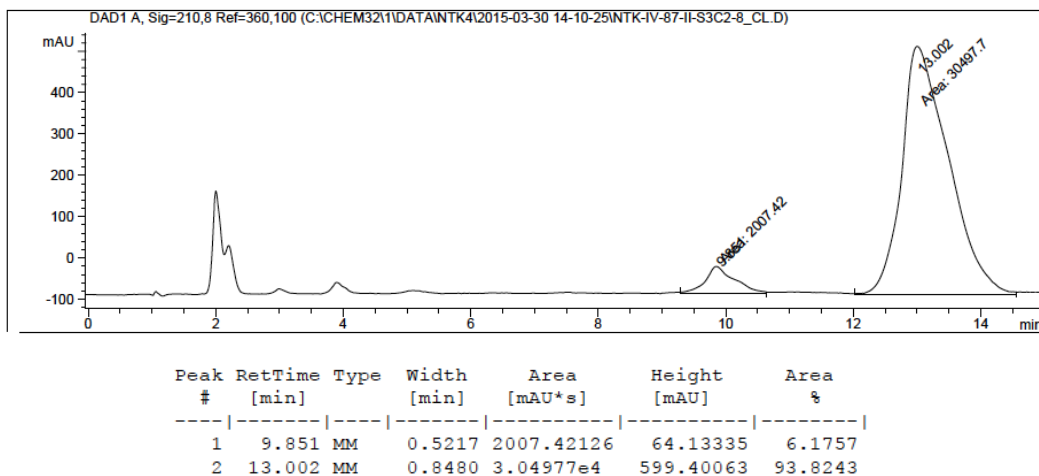
(ddd,  $J = 14.4, 9.0, 5.7$  Hz, 1H), 2.64 (ddd,  $J = 13.8, 8.8, 7.0$  Hz, 1H), 2.43 (dddd,  $J = 13.6, 9.0, 7.1, 6.3$  Hz, 1H), 2.17 – 2.07 (m, 1H);  $^{13}\text{C}$  NMR (126 MHz,  $\text{cdcl}_3$ )  $\delta$  198.65, 140.80, 138.31, 128.54, 128.52, 127.54, 126.43, 126.22, 125.56, 52.86, 32.84, 32.05; IR (NaCl/thin film): 3025.79, 2924.74, 1725.05, 1496.21, 1454.03, 750.13, 699.05  $\text{cm}^{-1}$ ;  $[\alpha]_{\text{D}}^{25} = +4.156$  ( $c = 0.70$ ,  $\text{CHCl}_3$ ). HRMS (MM) calc'd for  $[\text{M}]^+$  410.2676, found 410.2101.

### 3.6.5 SFC Traces of Racemic and Enantioenriched Nitrile Products

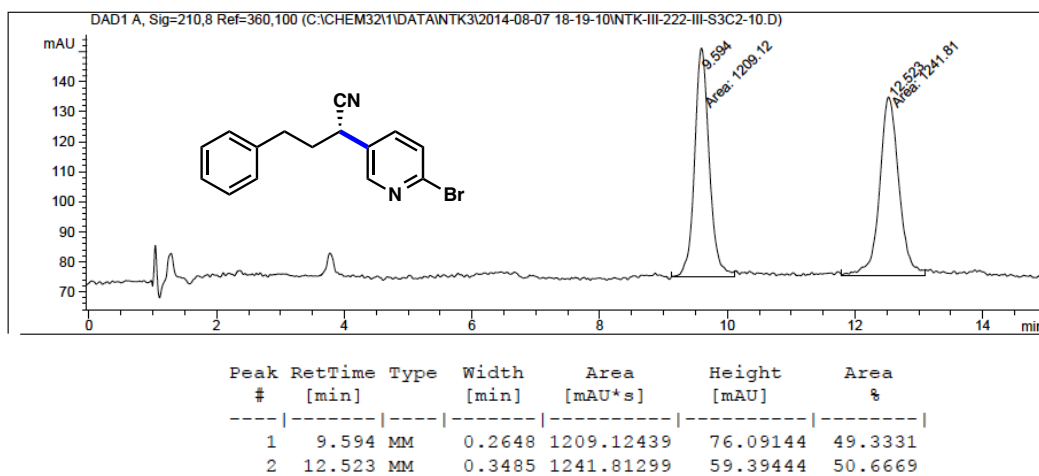
**122j** racemic



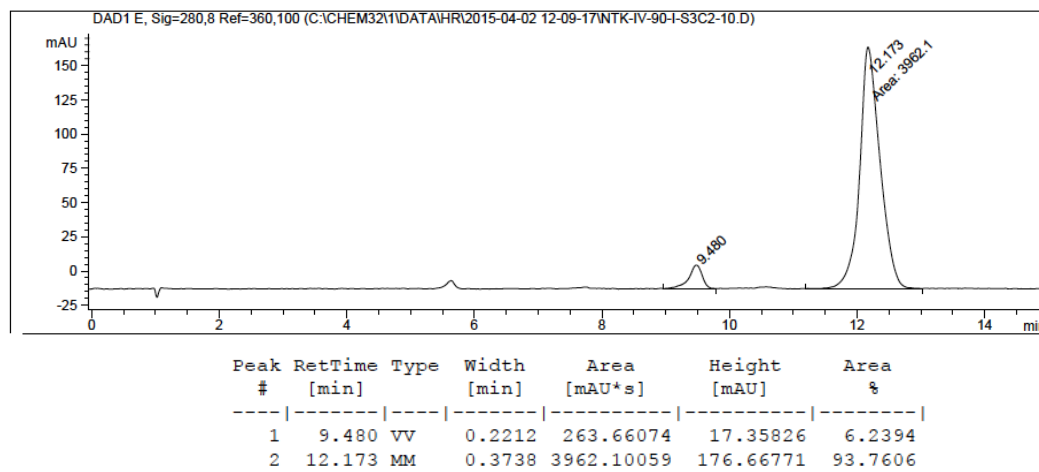
**122j** enantioenriched, 88% ee



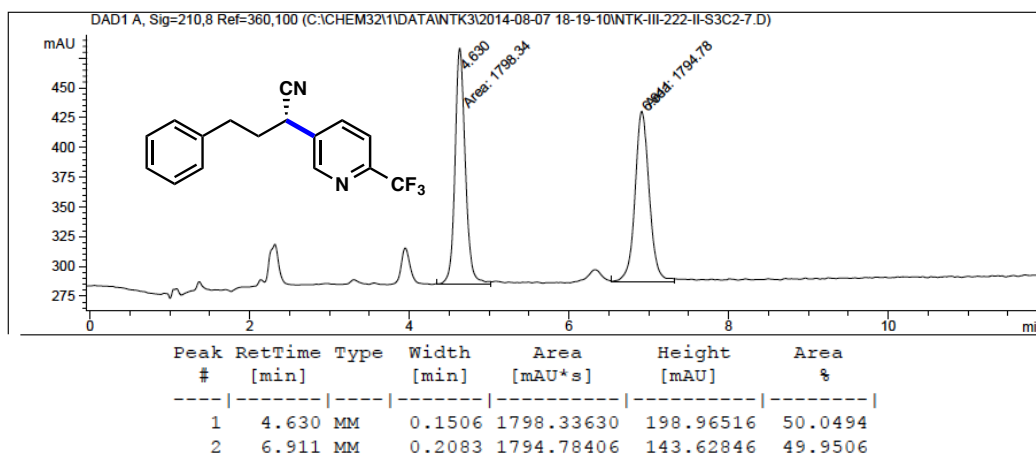
**122r** racemic



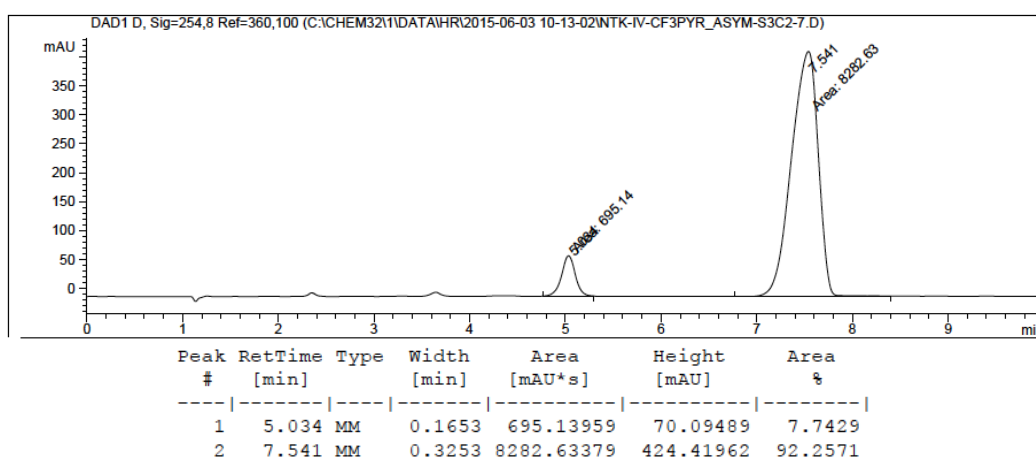
**122r** enantioenriched, 88% ee



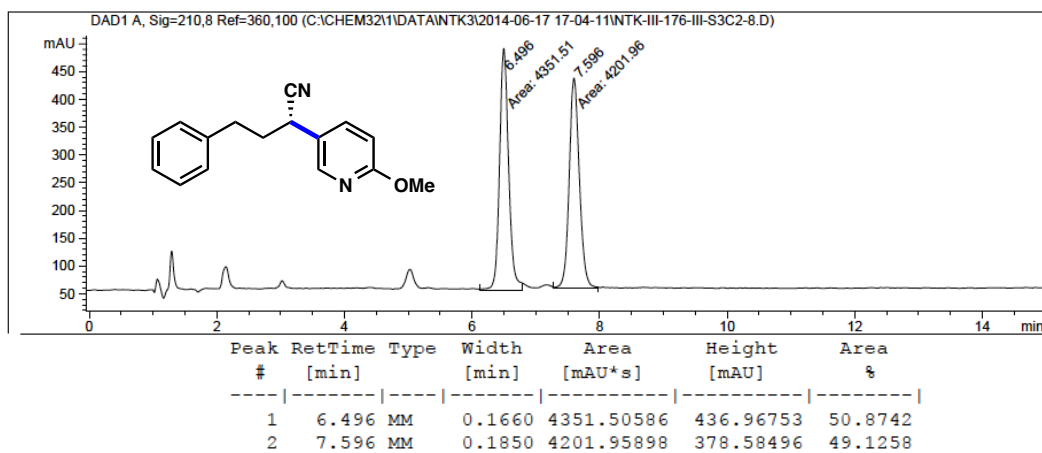
**122t** racemic



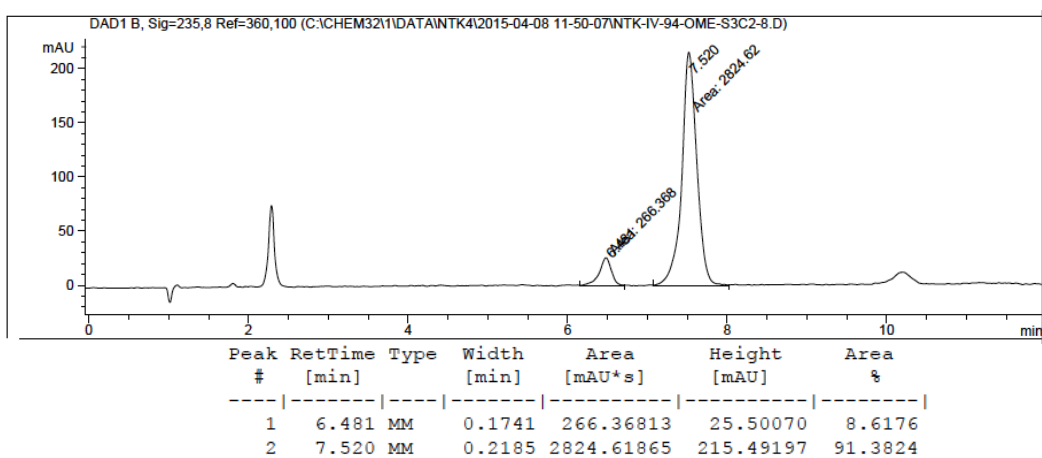
**122t** enantioenriched, 85% ee



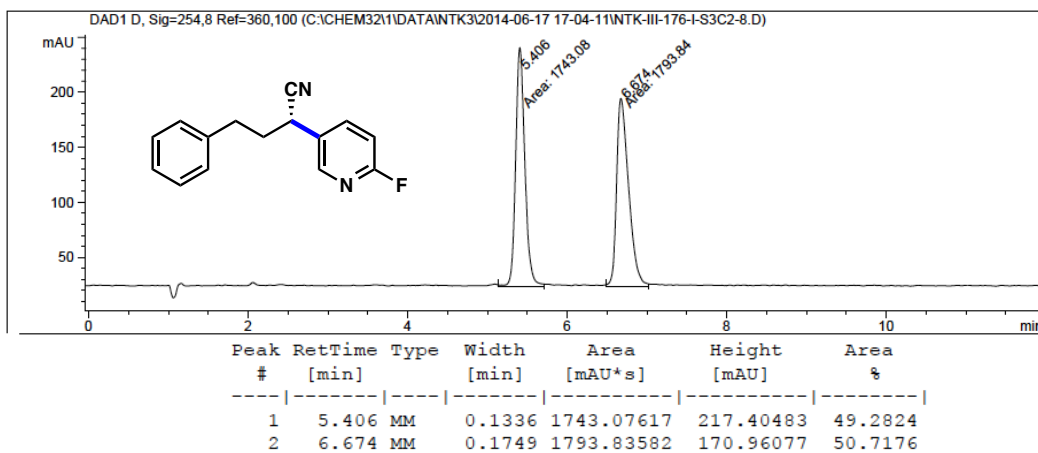
**122u** racemic



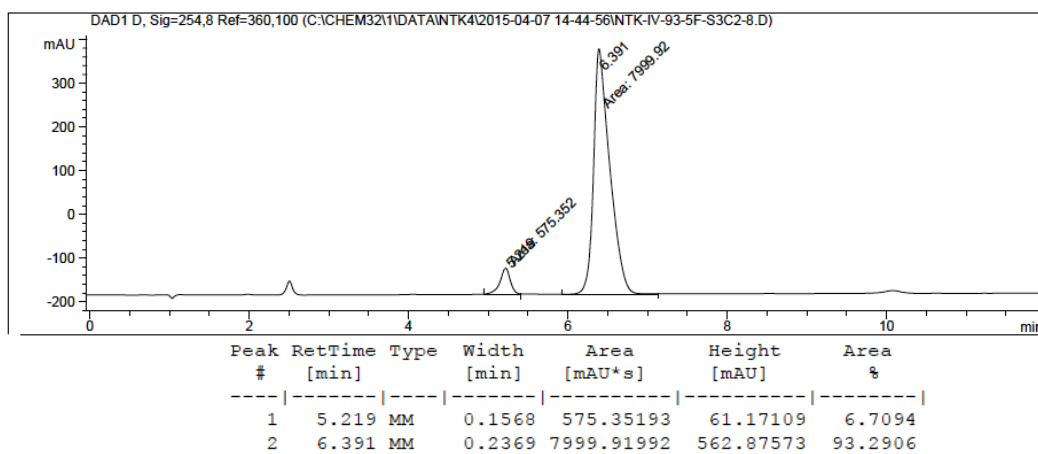
**122u** enantioenriched, 83% ee



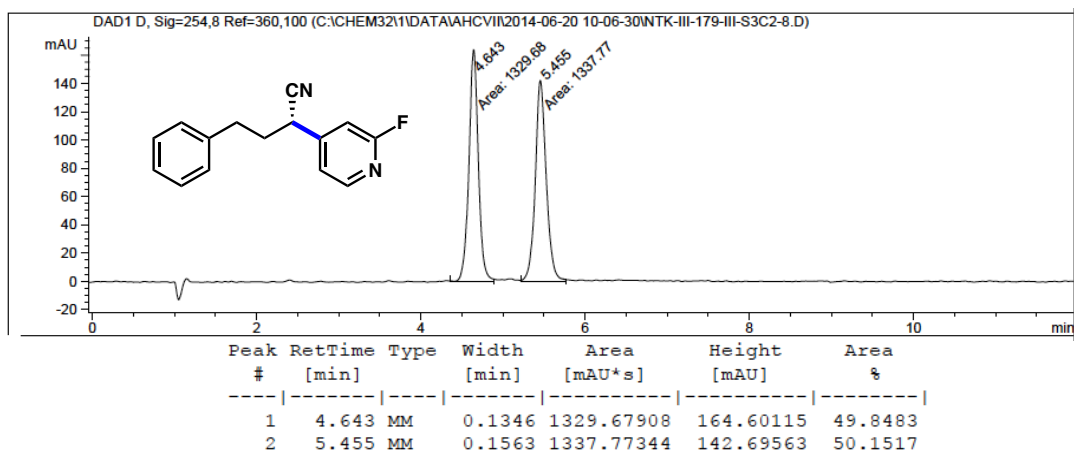
**122o** racemic



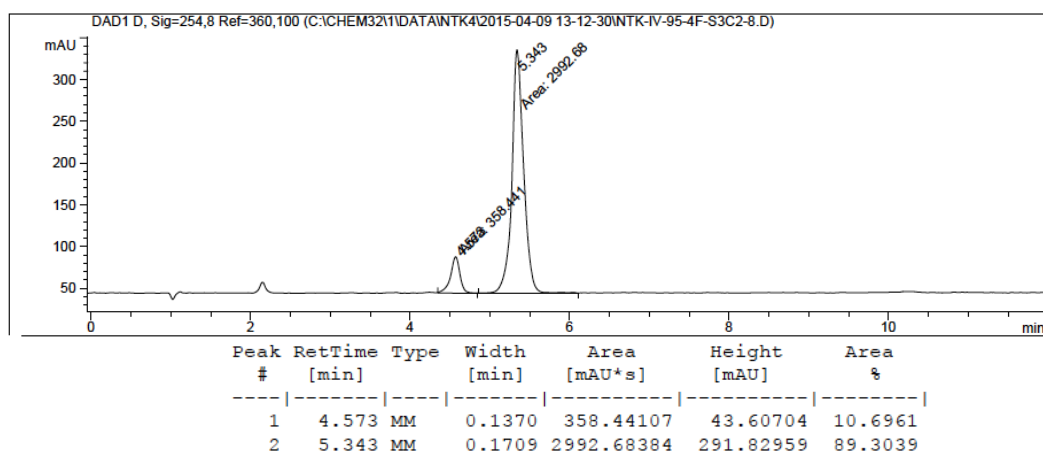
**122o** enantioenriched, 87% ee



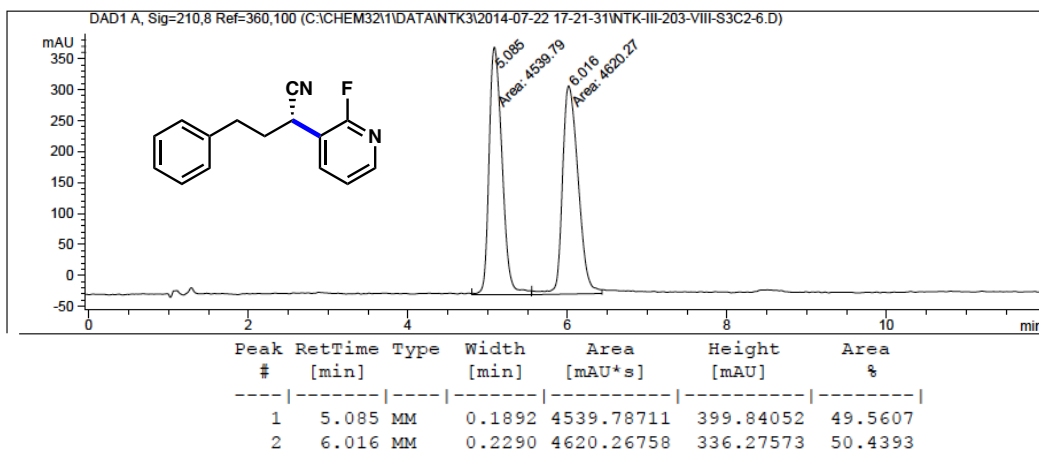
**122p** racemic



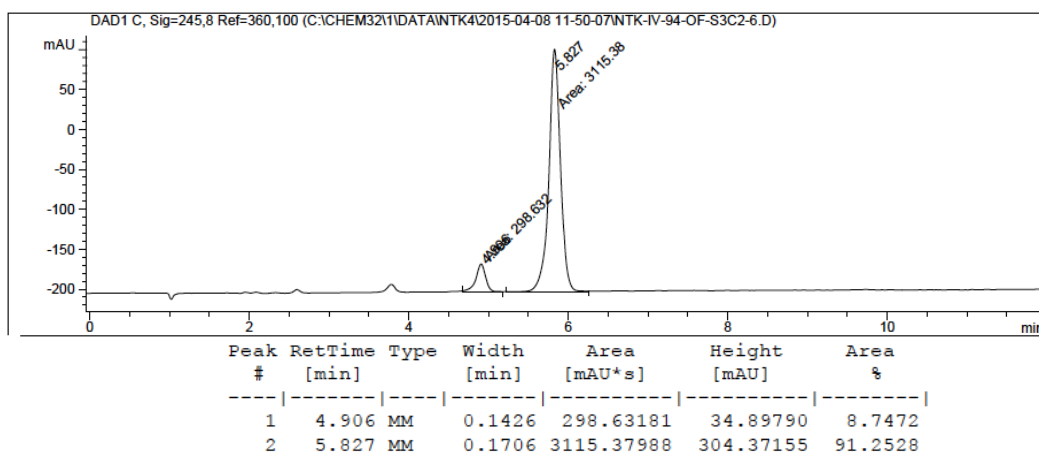
**122p** enantioenriched, 79% ee



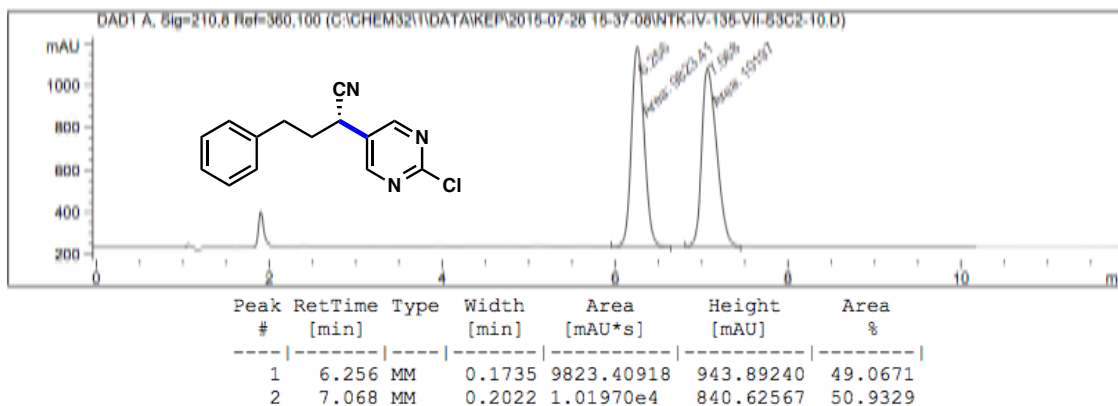
**122q** racemic



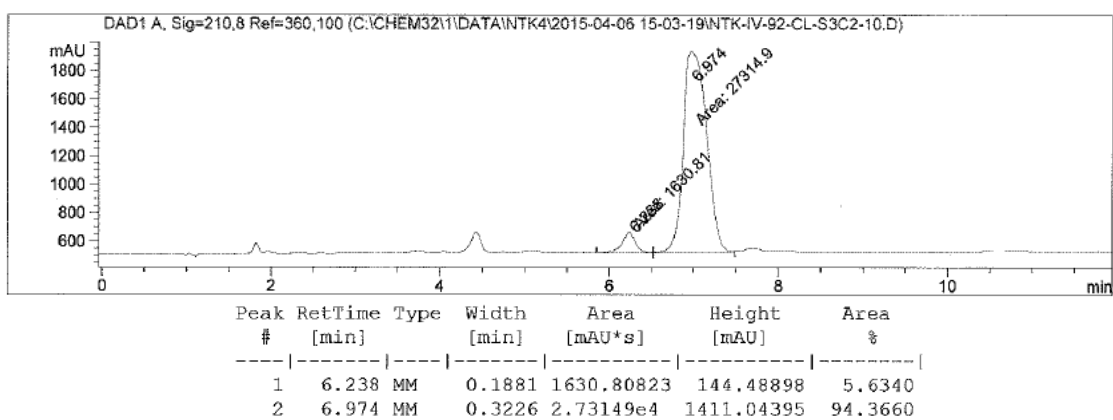
**122q** enantioenriched, 83% ee



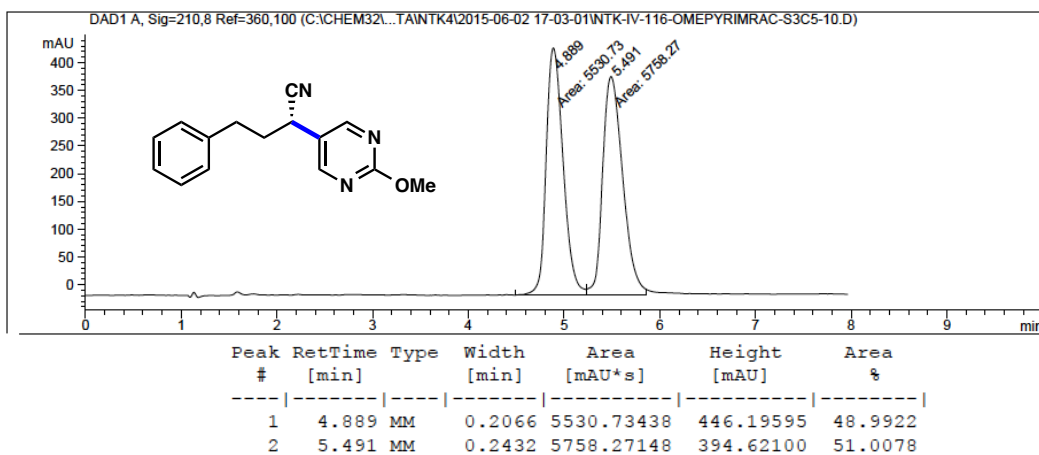
**122x racemic**



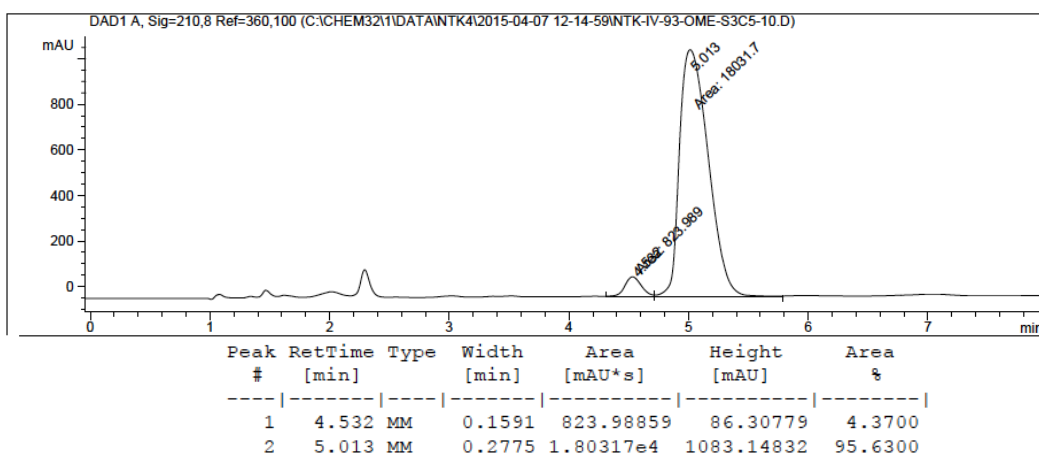
**122x enantioenriched, 89% ee**



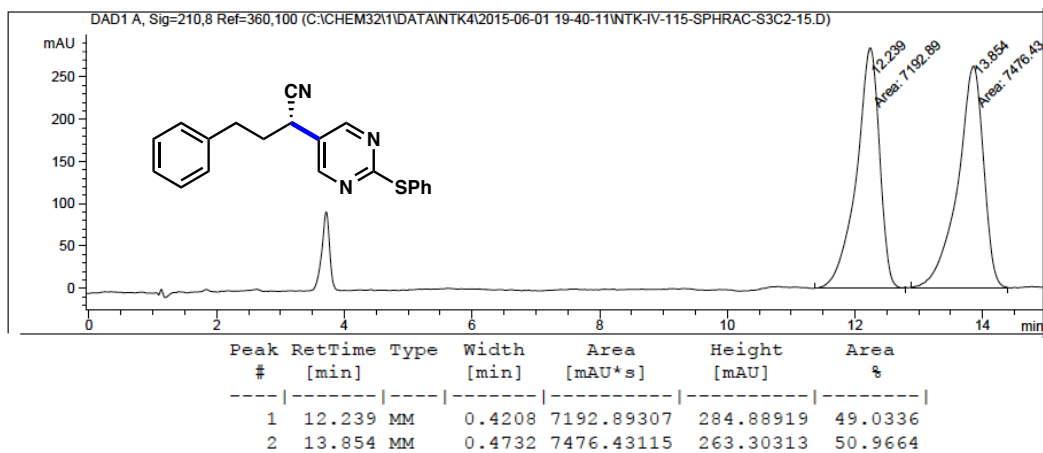
**122y** racemic



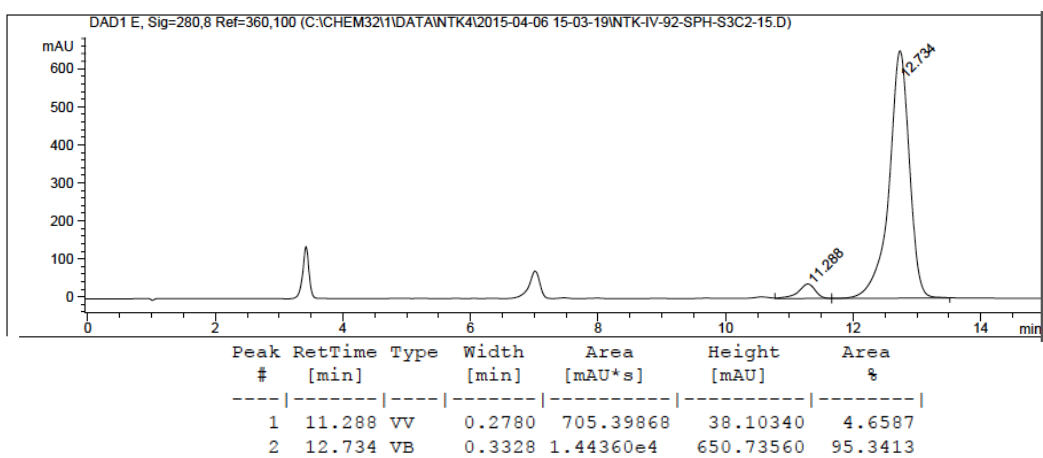
**122y** enantioenriched, 92% ee



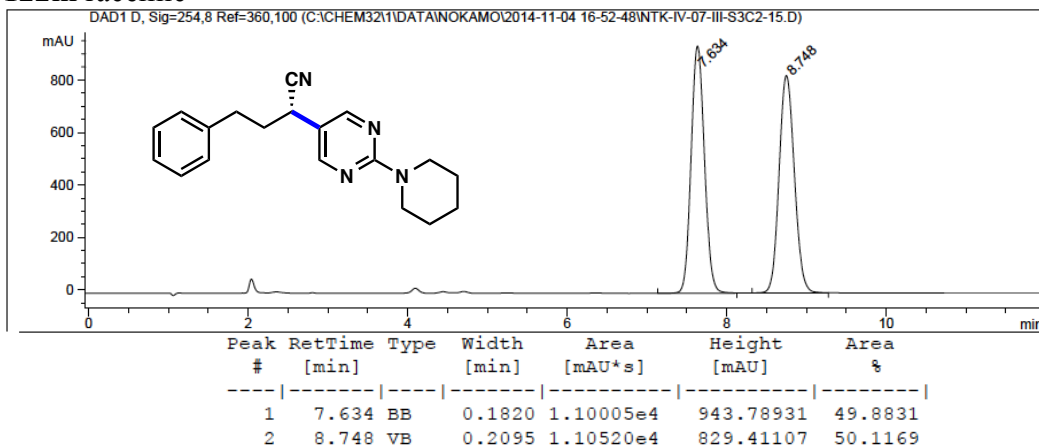
**122n** racemic



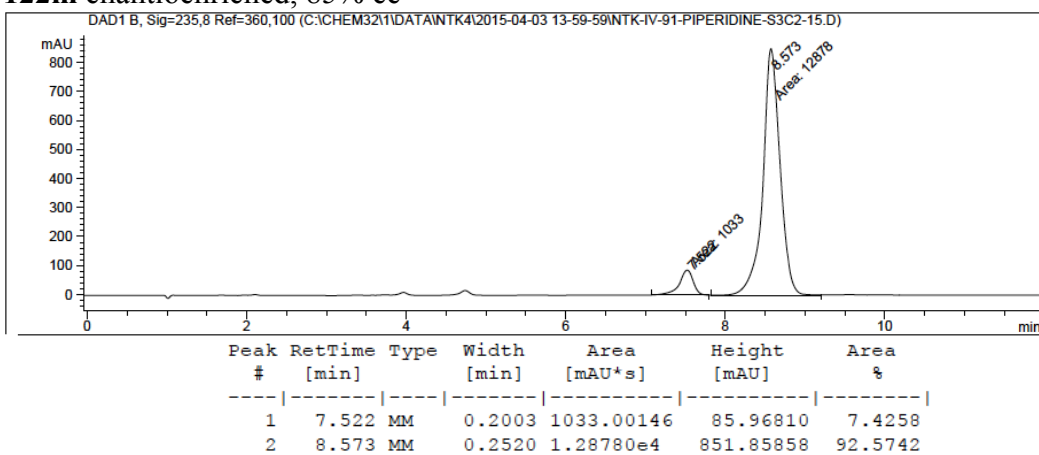
**122n** enantioenriched, 91% ee



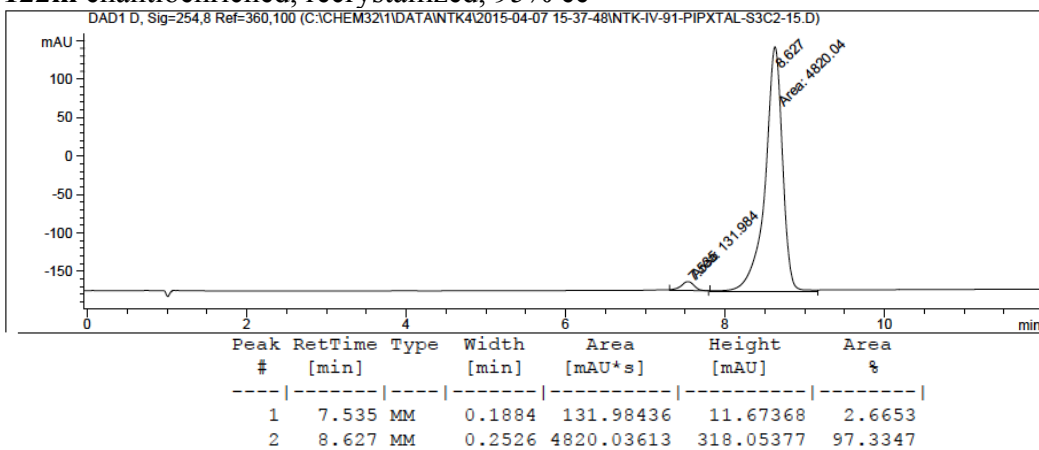
**122m racemic**



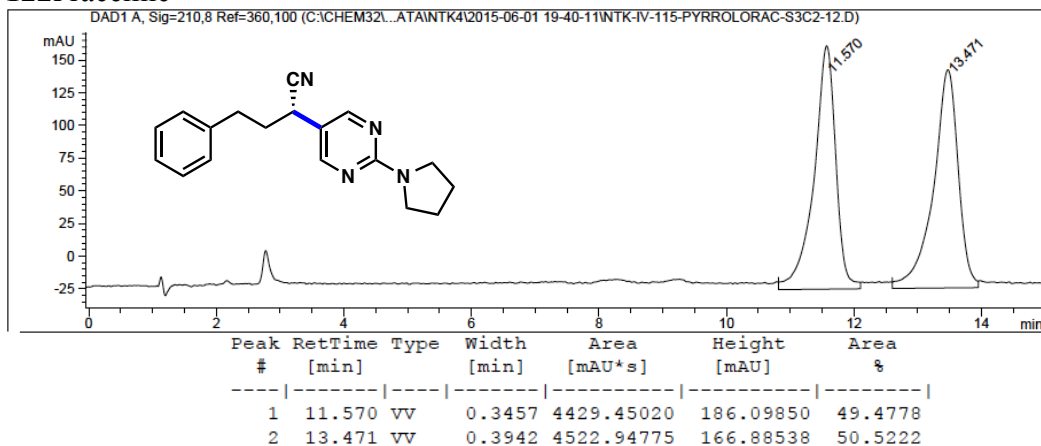
**122m enantioenriched, 85% ee**



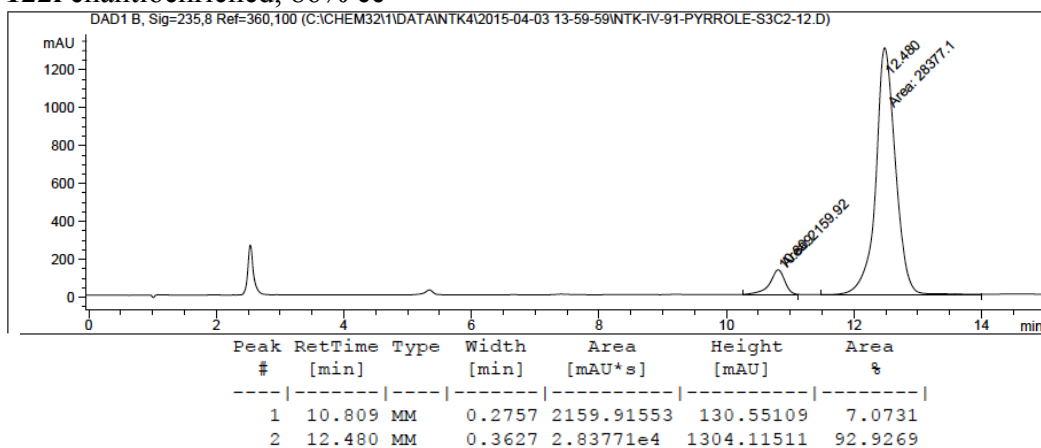
**122m enantioenriched, recrystallized, 95% ee**



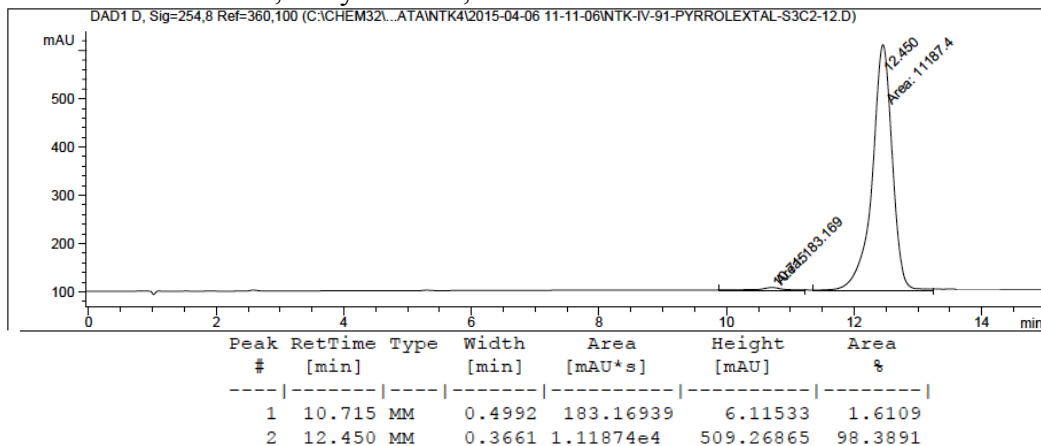
**122l** racemic



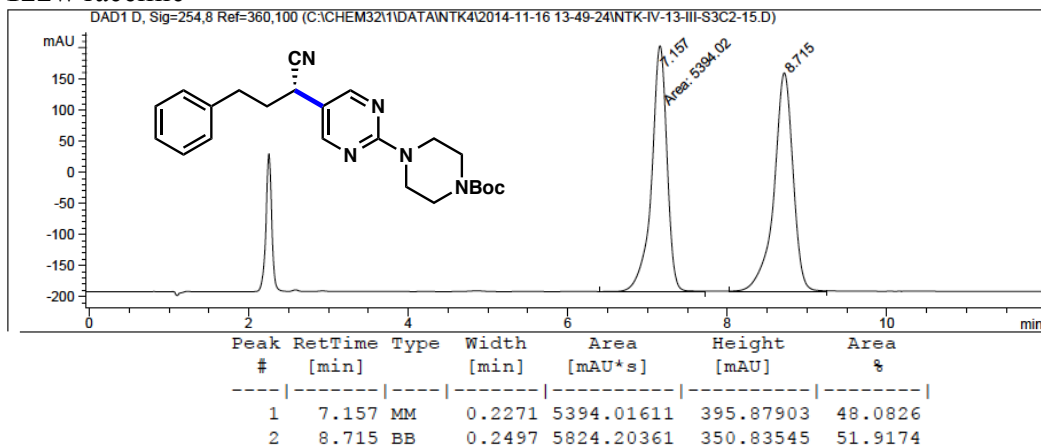
**122l** enantioenriched, 86% ee



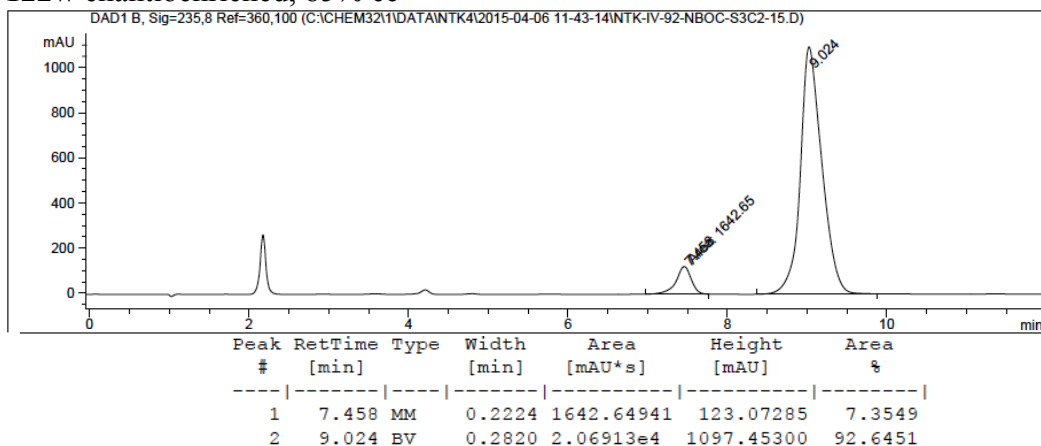
**122l** enantioenriched, recrystallized, 97% ee



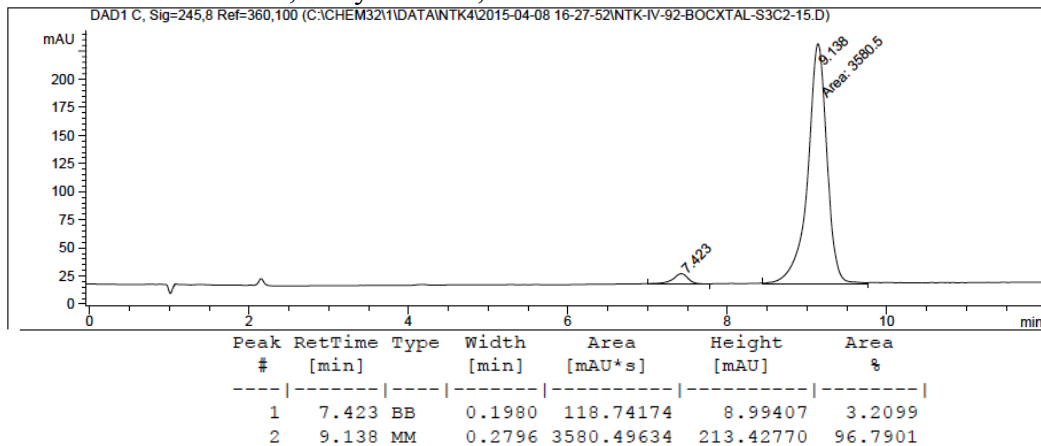
**122w racemic**



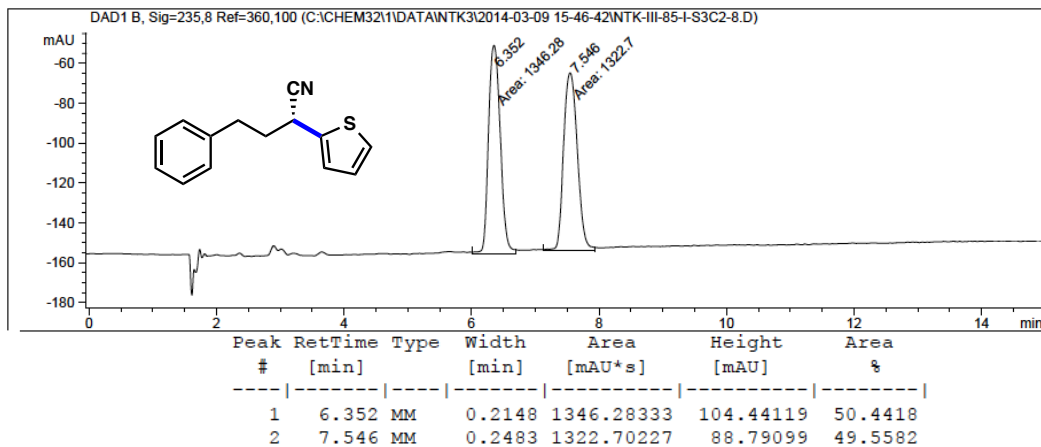
**122w enantioenriched, 85% ee**



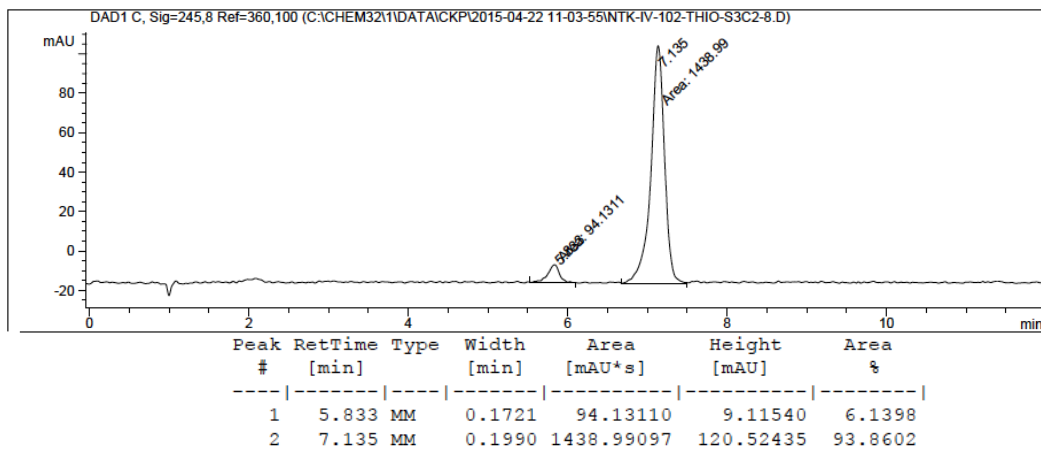
**122w enantioenriched, recrystallized, 94% ee**



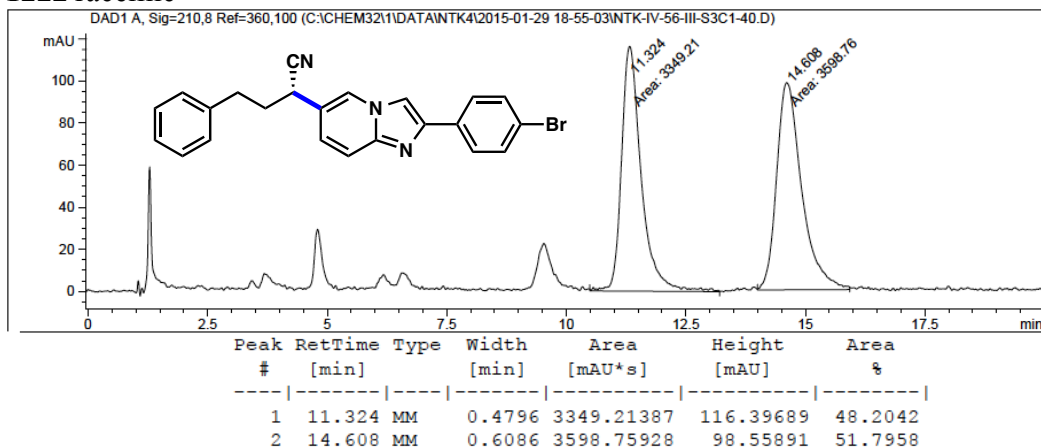
**122i** racemic



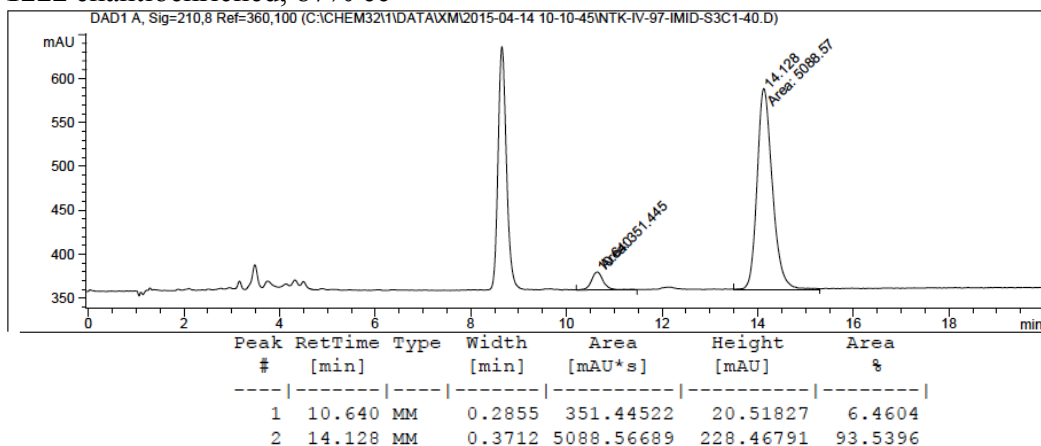
**122i** enantioenriched, 88% ee



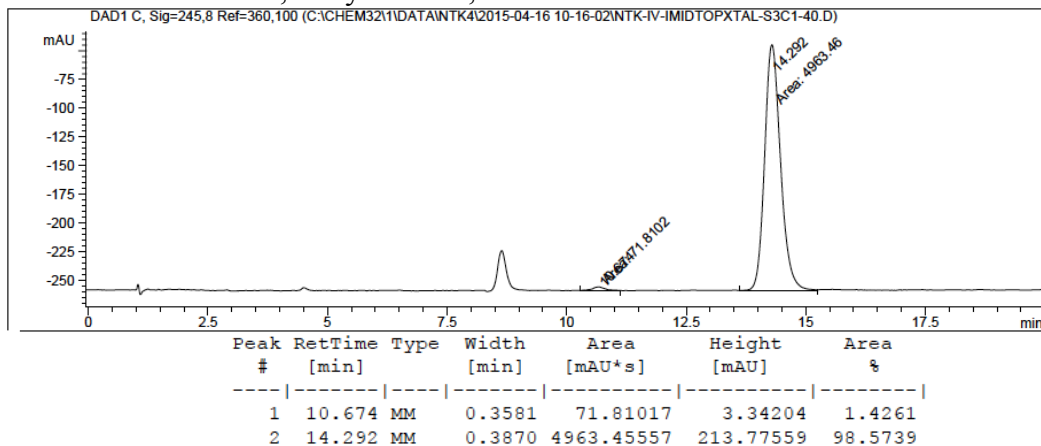
**122z** racemic



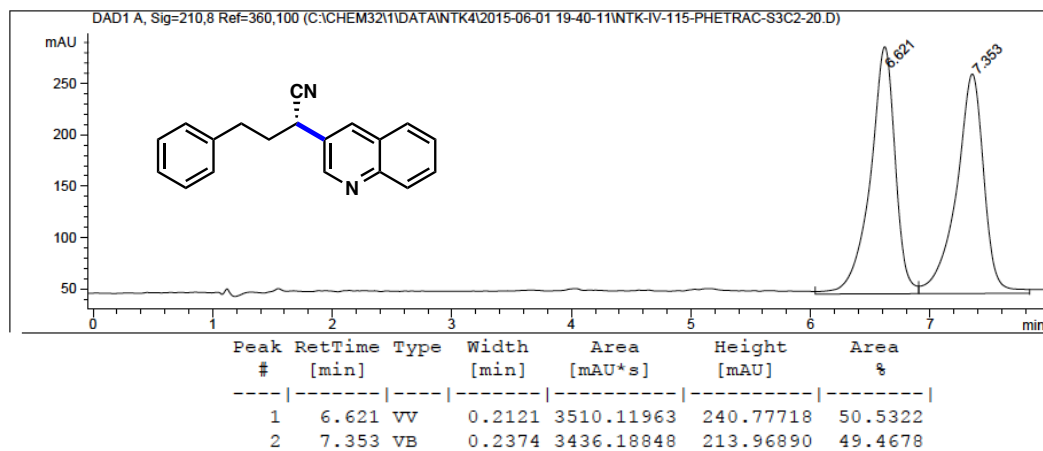
**122z** enantioenriched, 87% ee



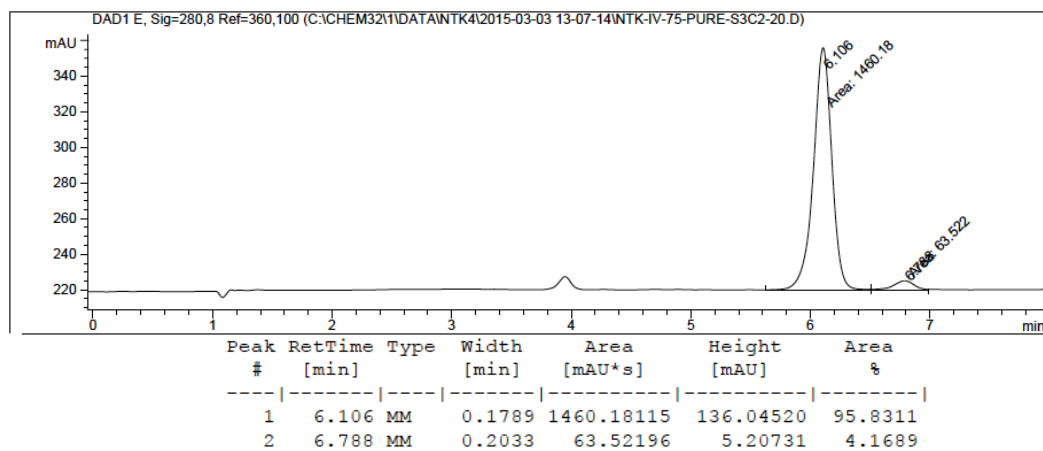
**122z** enantioenriched, recrystallized, 97% ee



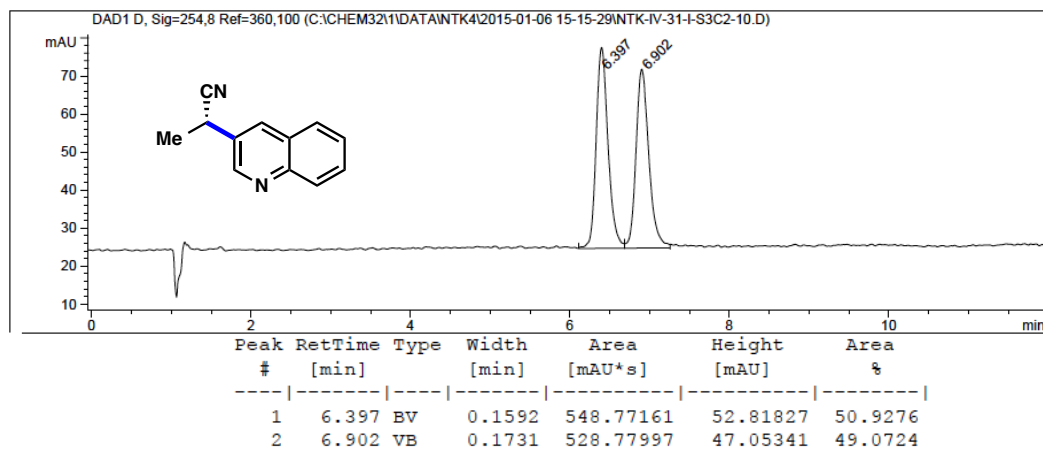
**122v** racemic



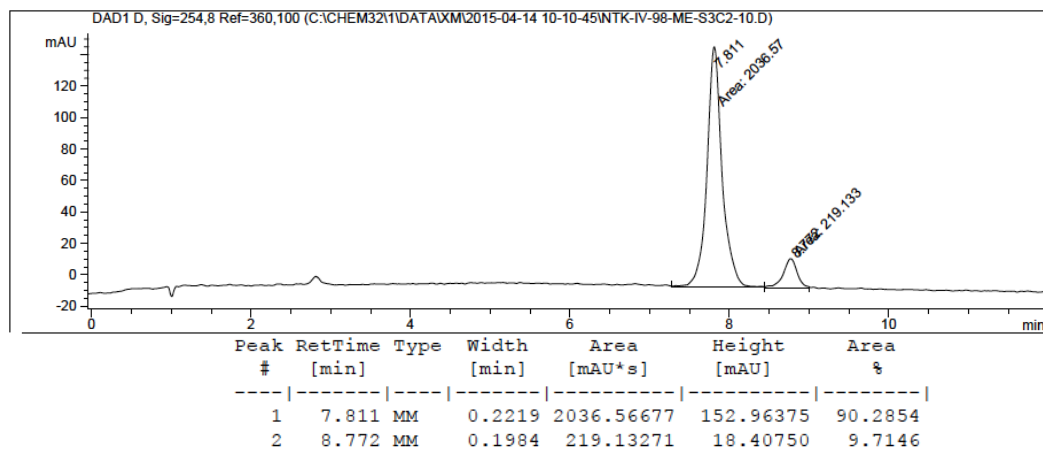
**122v** enantioenriched, 92% ee



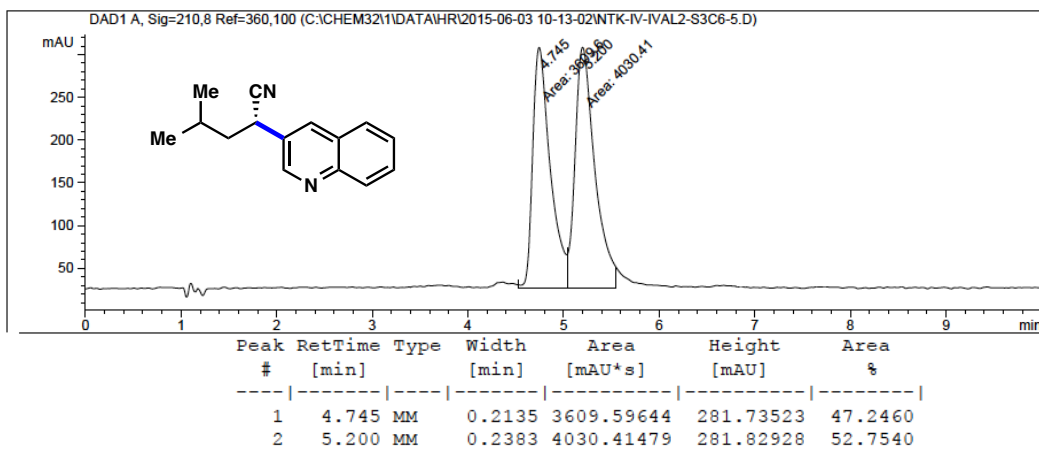
**129b** racemic



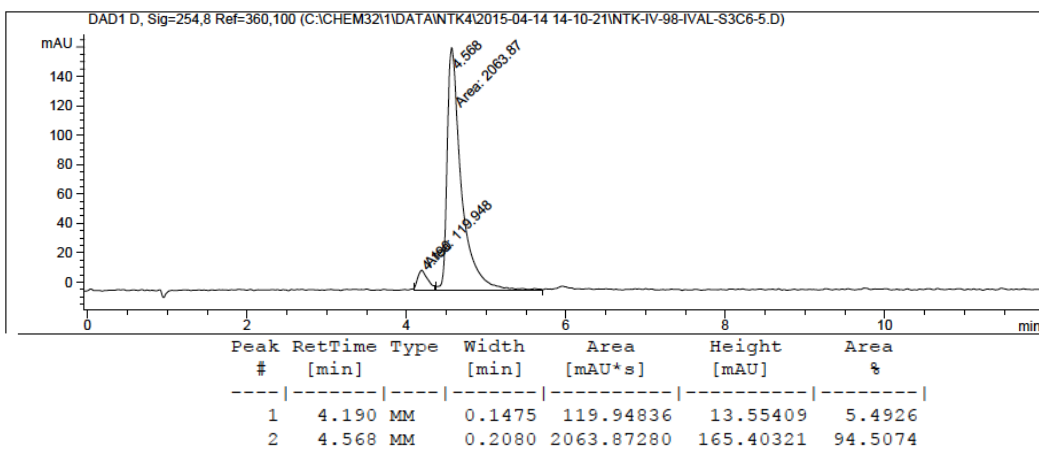
**129b** enantioenriched, 81% ee



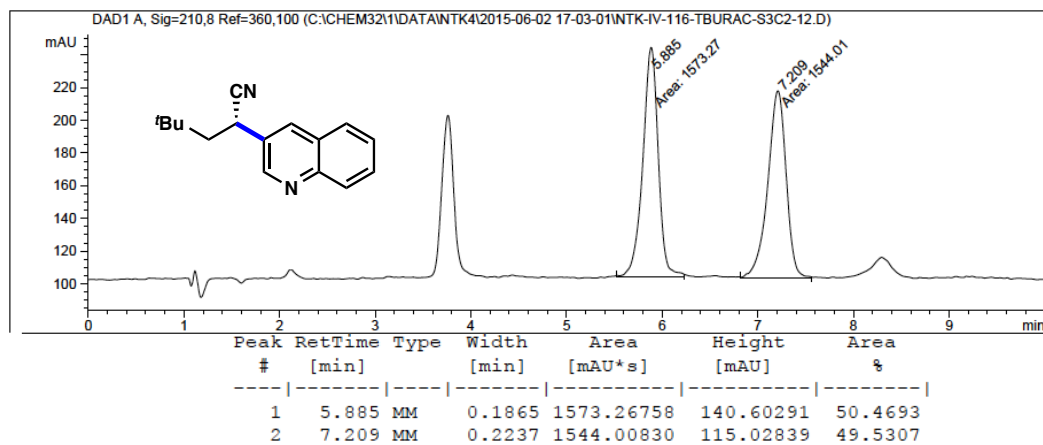
**129h** racemic



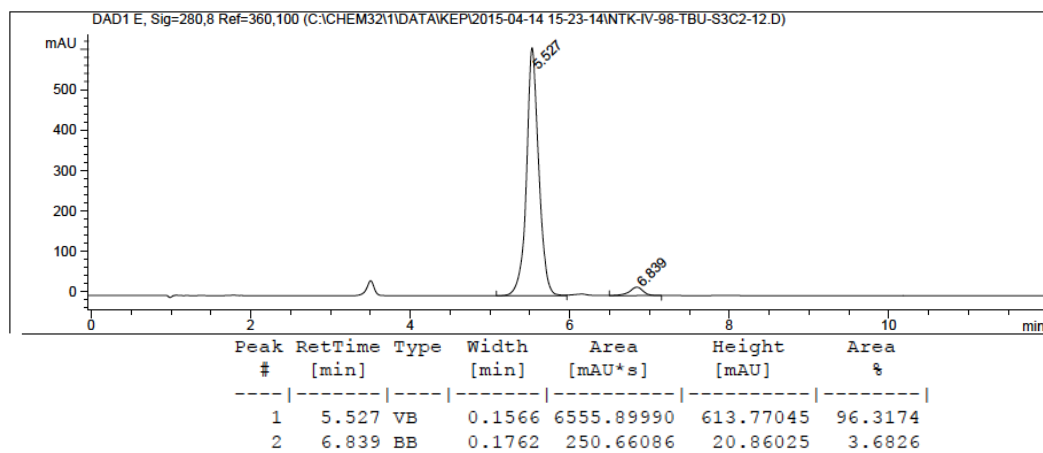
**129h** enantioenriched, 89% ee



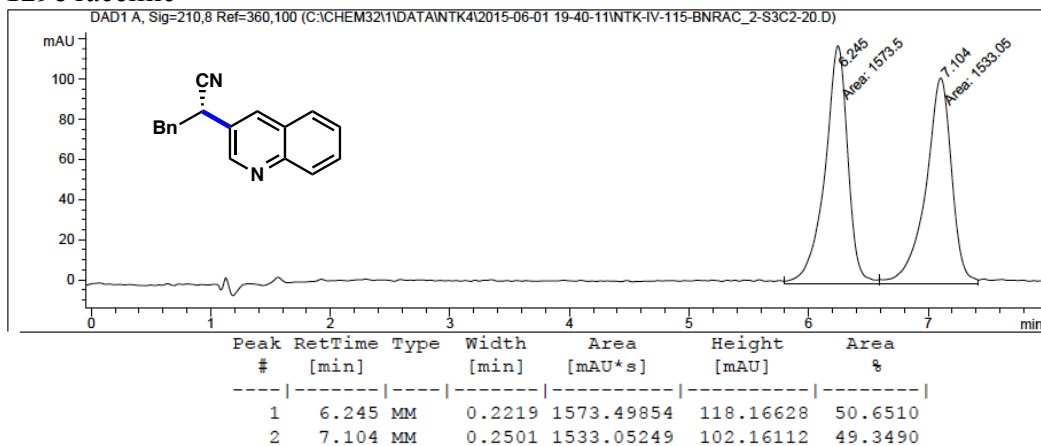
**129c** racemic



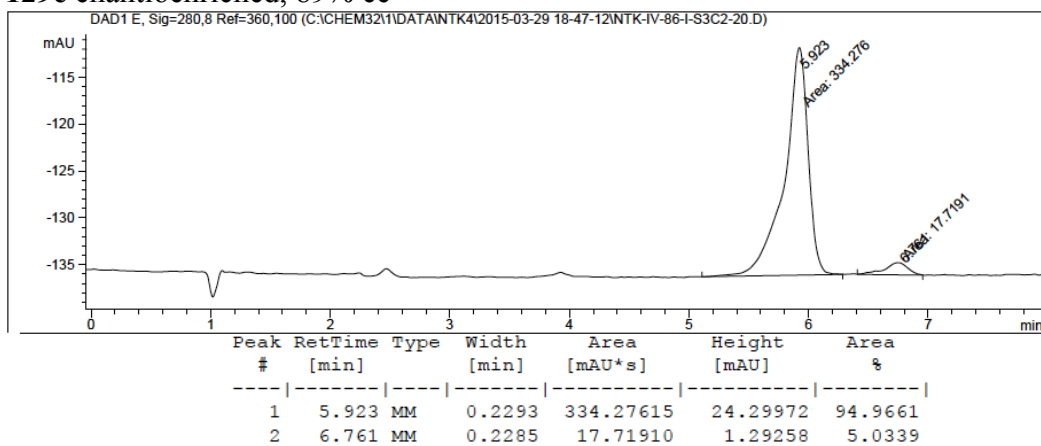
**129c** enantioenriched, 93% ee



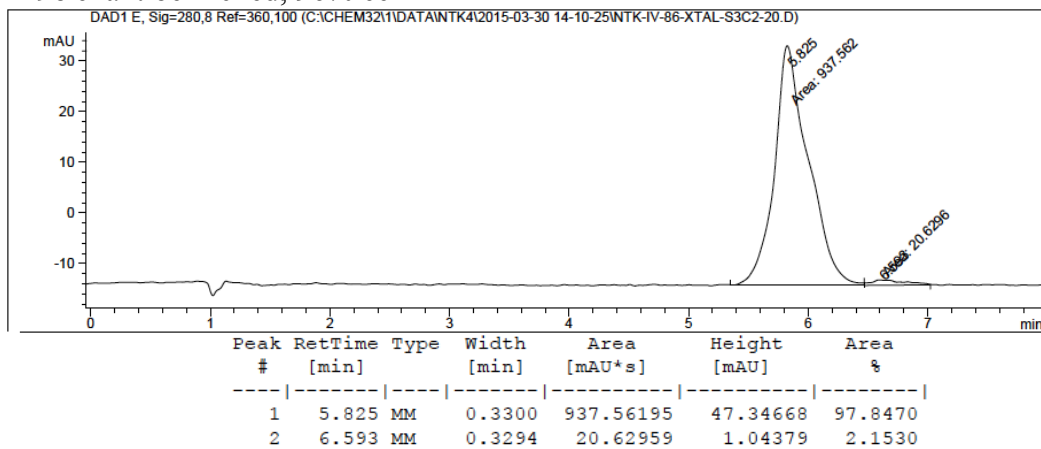
**129e** racemic



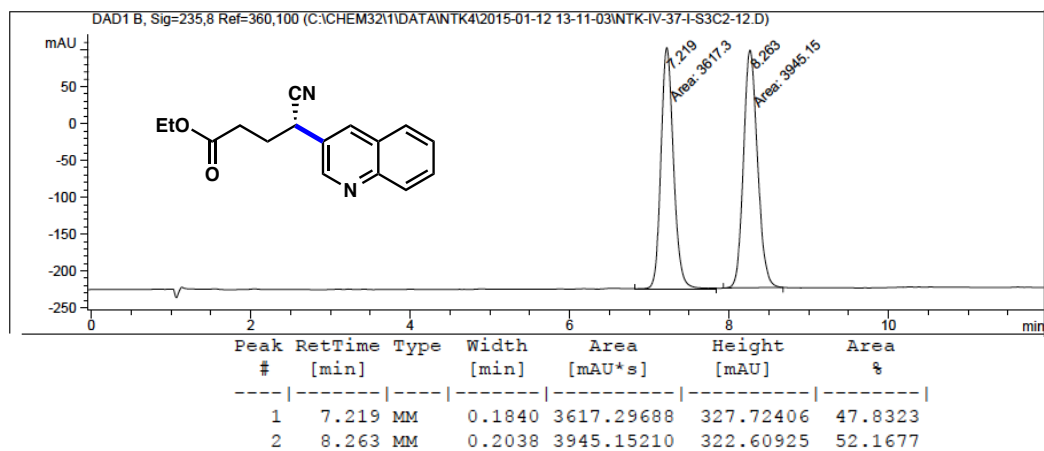
**129e** enantioenriched, 89% ee



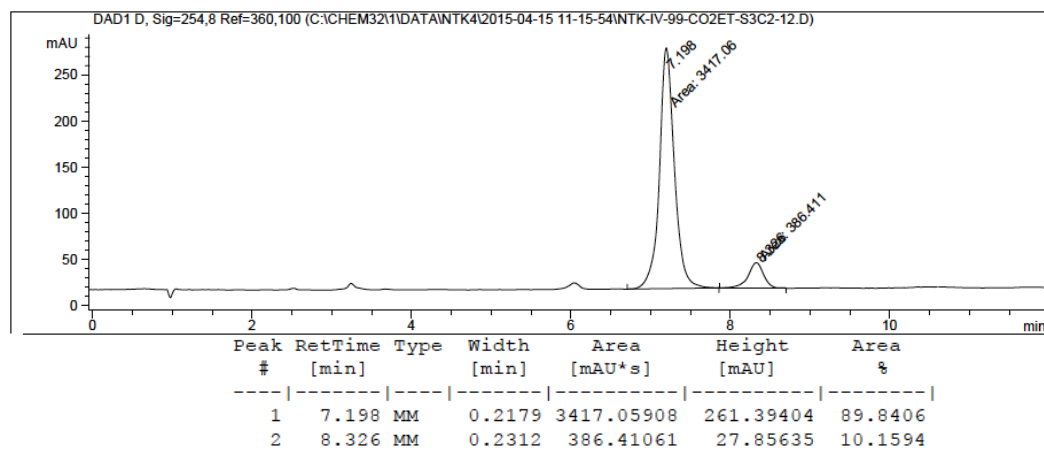
**129e** enantioenriched, 96% ee



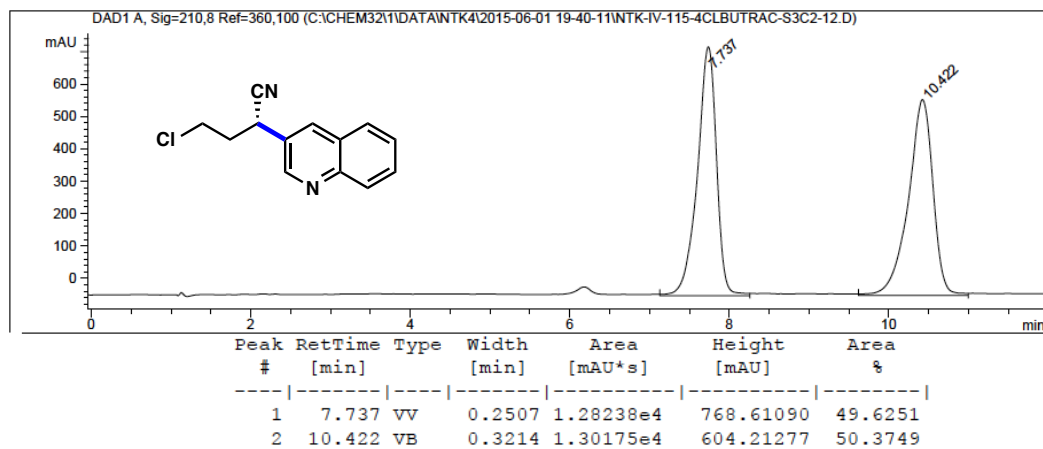
**129f** racemic



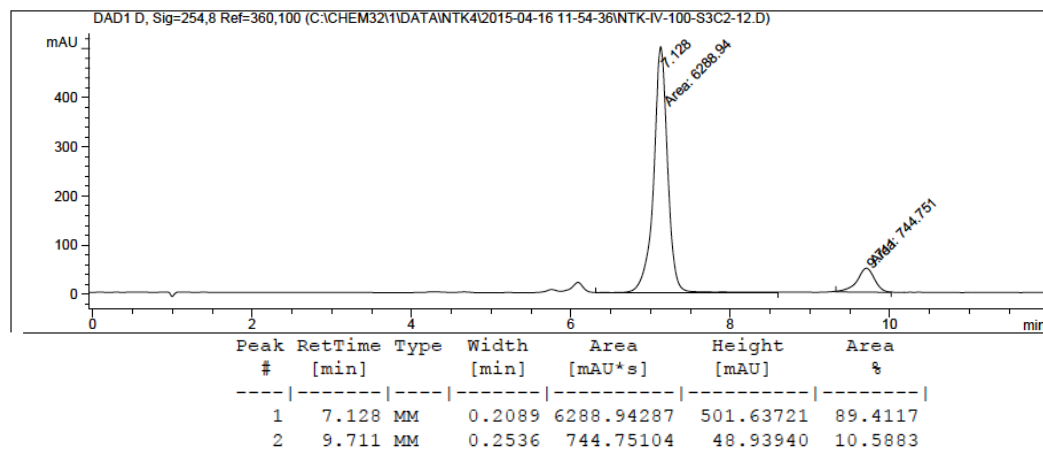
**129f** enantioenriched, 80% ee



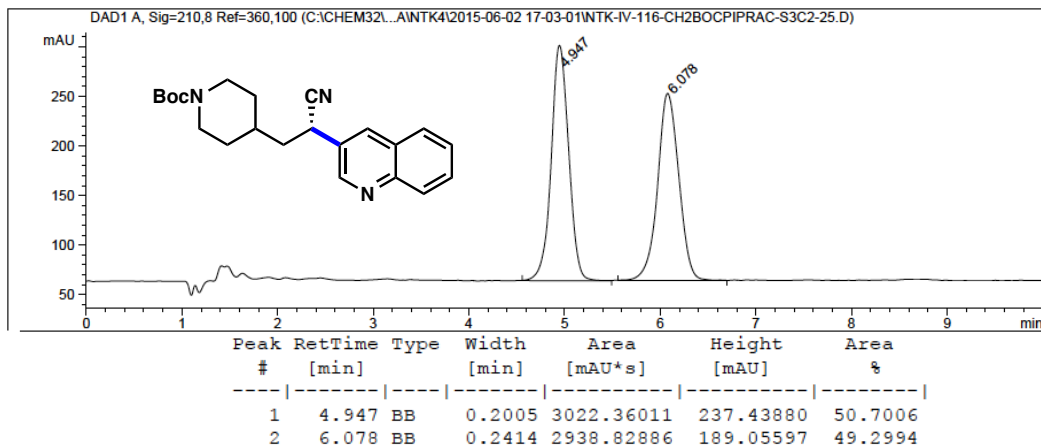
**129g racemic**



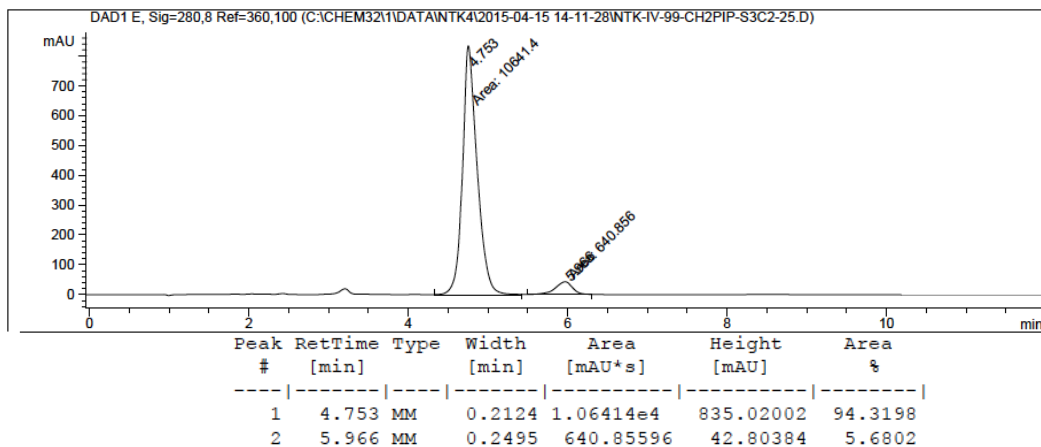
**129g enantioenriched, 79% ee**



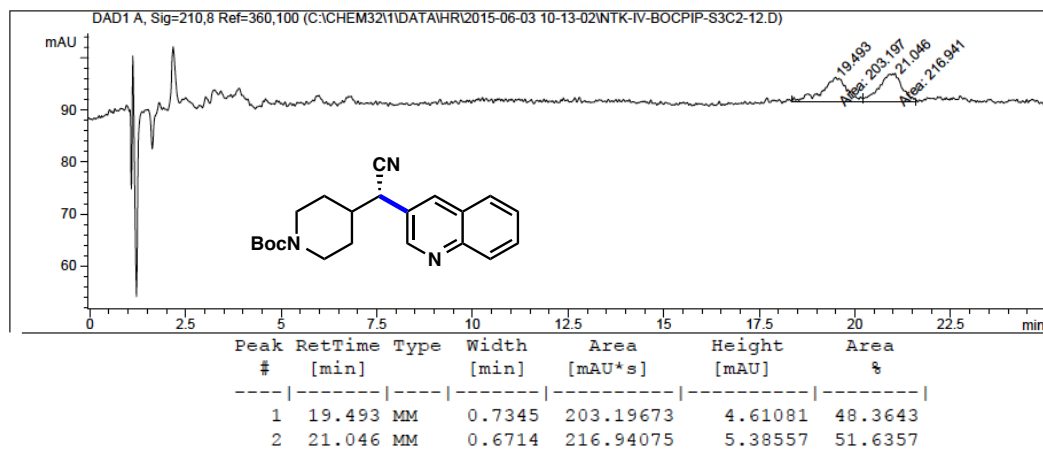
**129a** racemic



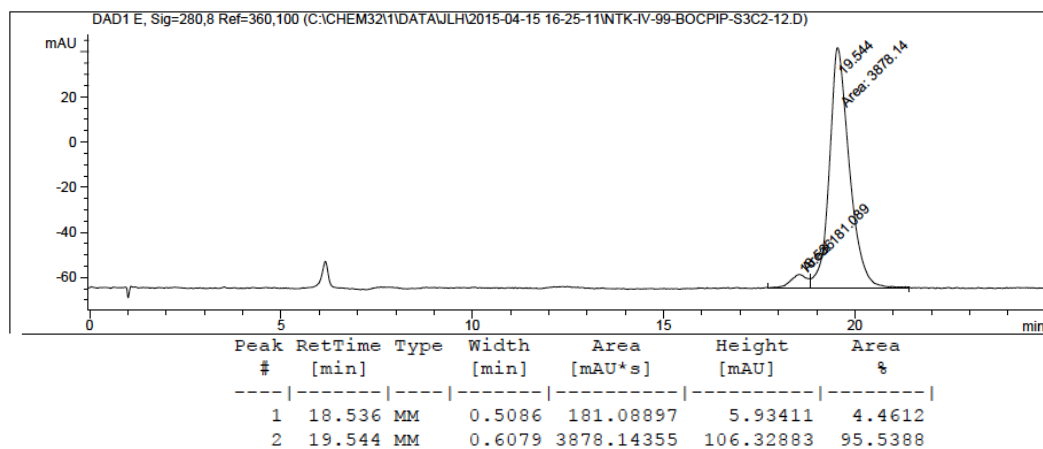
**129a** enantioenriched, 89% ee



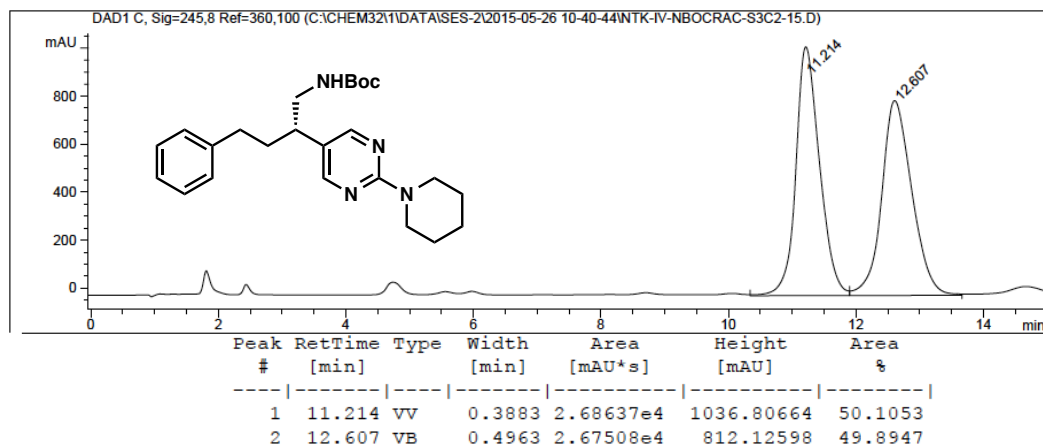
**129d** racemic



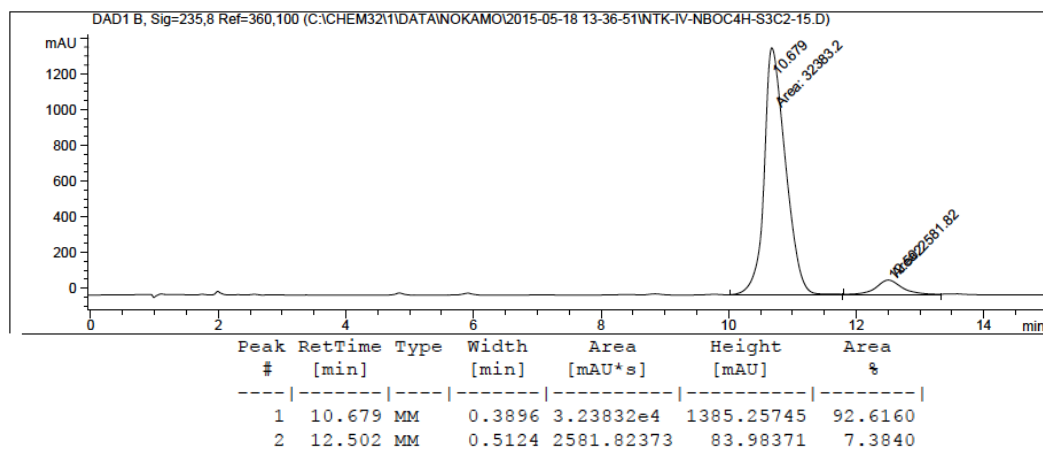
**129d** enantioenriched, 91% ee



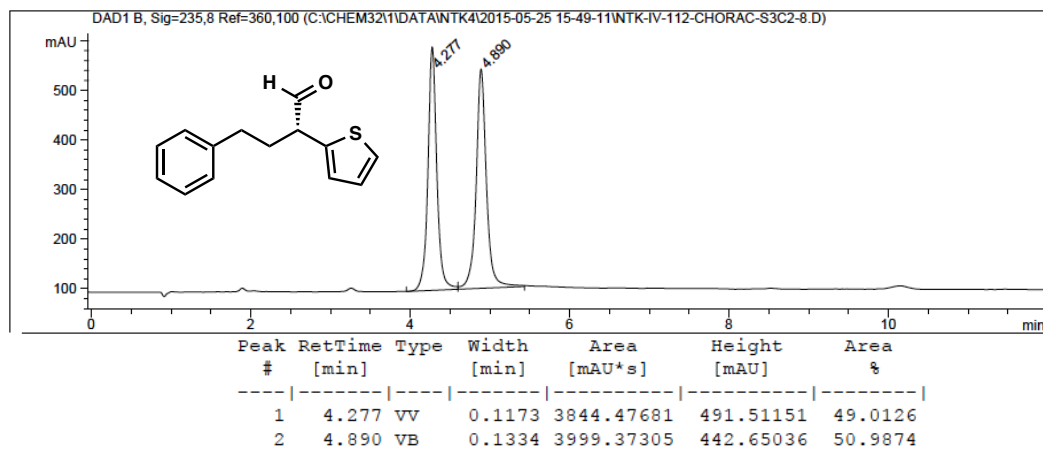
**130** racemic



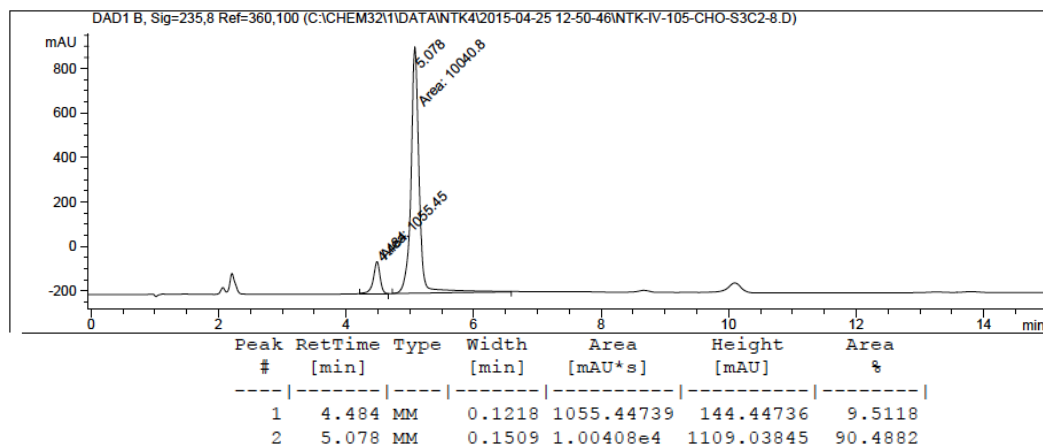
**130** enantioenriched, 85% ee



**132** racemic



**132** enantioenriched, 81% ee



### 3.7 NOTES AND REFERENCES

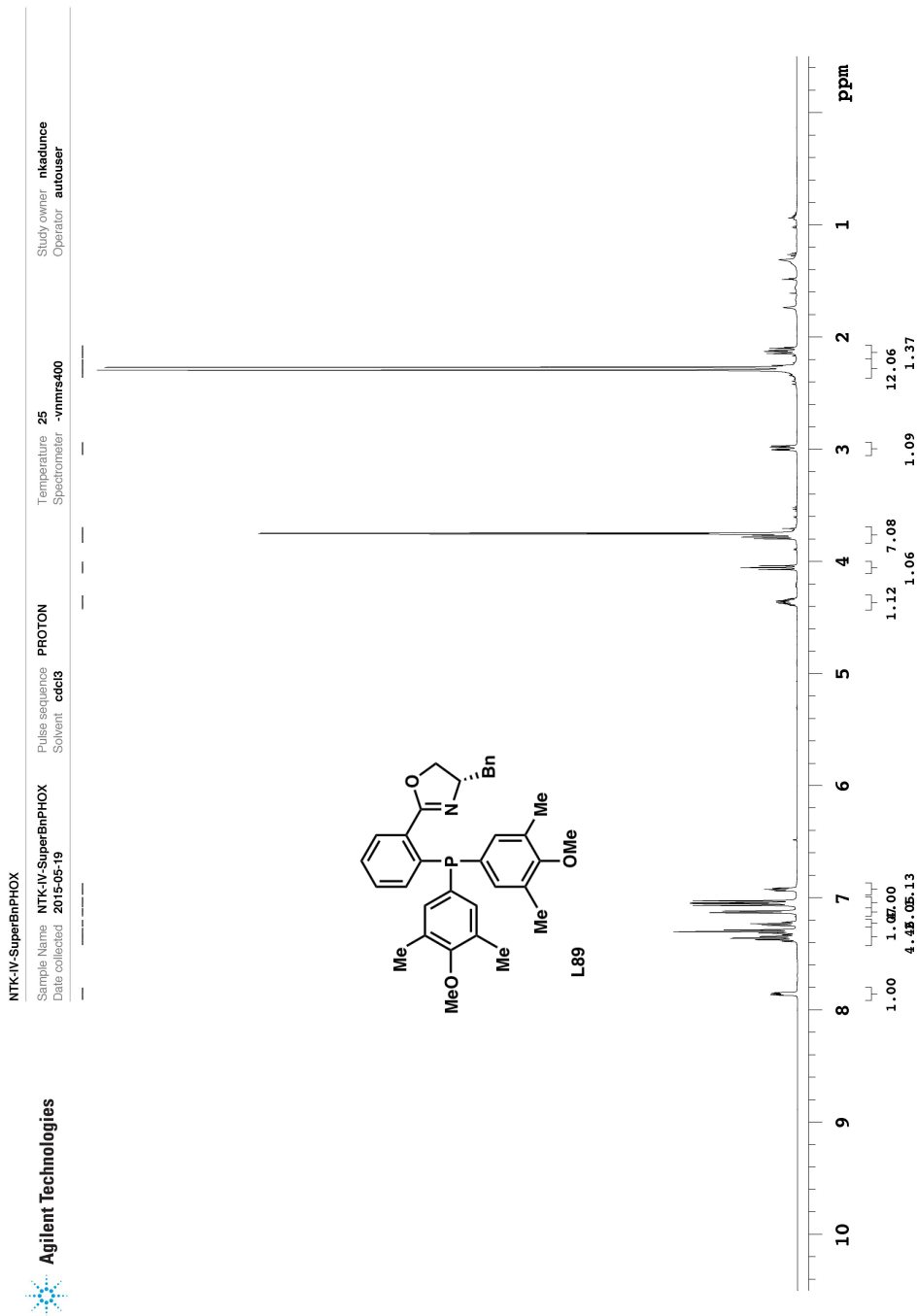
- (1) Kurono, N.; Ohkuma, T. *ACS Catalysis* **2016**, *6*, 989.
- (2) Frejd, T.; Klingstedt, T. *Synthesis* **1987**, *1987*, 40.
- (3) Strotman, N. A.; Sommer, S.; Fu, G. C. *Angew. Chem. Int. Ed. Engl.* **2007**, *46*, 3556.
- (4) Yang, Y.; Tang, S.; Liu, C.; Zhang, H.; Sun, Z.; Lei, A. *Org. Biomol. Chem.* **2011**, *9*, 5343.
- (5) He, A.; Falck, J. R. *J. Am. Chem. Soc.* **2010**, *132*, 2524.
- (6) Choi, J.; Fu, G. C. *J. Am. Chem. Soc.* **2012**, *134*, 9102.
- (7) Henry, D. J.; Parkinson, C. J.; Mayer, P. M.; Radom, L. *J. Phys. Chem. A* **2001**, *105*, 6750.
- (8) (a) Abila, M.; Yamamoto, T. *J. Organomet. Chem.* **1997**, *532*, 267; (b) Favero, G.; Morvillo, A.; Turco, A. *J. Organomet. Chem.* **1983**, *241*, 251; (c) Green, R. A.; Hartwig, J. F. *Angew. Chem. Int. Ed. Engl.* **2015**, *54*, 3768; (d) Ge, S.; Green, R. A.; Hartwig, J. F. *J. Am. Chem. Soc.* **2014**, *136*, 1617; (e) Ge, S.; Hartwig, J. F. *J. Am. Chem. Soc.* **2011**, *133*, 16330.
- (9) Slagt, V. F.; de Vries, A. H. M.; de Vries, J. G.; Kellogg, R. M. *Organic Process Research & Development* **2010**, *14*, 30.
- (10) Lhermet, R.; Durandetti, M.; Maddaluno, J. *Beilstein J. Org. Chem.* **2013**, *9*, 710.
- (11) (a) Helmchen, G.; Pfaltz, A. *Acc. Chem. Res.* **2000**, *33*, 336; (b) Tani, K.; Behenna, D. C.; McFadden, R. M.; Stoltz, B. M. *Org. Lett.* **2007**, *9*, 2529.
- (12) Craig, R. A., 2nd; Stoltz, B. M. *Tetrahedron Lett.* **2015**, *56*, 4670.
- (13) Frolander, A.; Lutsenko, S.; Privalov, T.; Moberg, C. *J. Org. Chem.* **2005**, *70*, 9882.
- (14) Schrems, M. G.; Pfaltz, A. *Chem. Commun.* **2009**, 6210.
- (15) Abrunhosa, I.; Delain-Bioton, L.; Gaumont, A.-C.; Gulea, M.; Masson, S. *Tetrahedron* **2004**, *60*, 9263.
- (16) Zhang, C.; Santiago, C. B.; Crawford, J. M.; Sigman, M. S. *J. Am. Chem. Soc.* **2015**, *137*, 15668.

- (17) Menges, F.; Neuburger, M.; Pfaltz, A. *Org. Lett.* **2002**, *4*, 4713.
- (18) Armstrong, P. B.; Dembicer, E. A.; DesBois, A. J.; Fitzgerald, J. T.; Gehrman, J. K.; Nelson, N. C.; Noble, A. L.; Bunt, R. C. *Organometallics* **2012**, *31*, 6933.
- (19) Tolman, C. A. *Chem. Rev.* **1977**, *77*, 313.
- (20) Aeby, A.; Bangerter, F.; Consiglio, G. *Helv. Chim. Acta* **1998**, *81*, 764.
- (21) Ross, A. J.; Lang, H. L.; Jackson, R. F. *J. Org. Chem.* **2010**, *75*, 245.
- (22) Vitaku, E.; Smith, D. T.; Njardarson, J. T. *J. Med. Chem.* **2014**, *57*, 10257.
- (23) (a) Molander, G. A.; Traister, K. M.; O'Neill, B. T. *J. Org. Chem.* **2014**, *79*, 5771; (b) Cherney, A. H.; Reisman, S. E. *J. Am. Chem. Soc.* **2014**, *136*, 14365.
- (24) (a) Blakemore, D. C.; Marples, L. A. *Tetrahedron Lett.* **2011**, *52*, 4192; (b) Ikawa, T.; Urata, H.; Fukumoto, Y.; Sumii, Y.; Nishiyama, T.; Akai, S. *Chem. Eur. J.* **2014**, *20*, 16228.
- (25) Graham, T. H.; Liu, W.; Shen, D. M. *Org. Lett.* **2011**, *13*, 6232.
- (26) Dyminska, L. *Bioorg. Med. Chem.* **2015**, *23*, 6087.
- (27) Burk, M. J.; Gross, M. F.; Martinez, J. P. *J. Am. Chem. Soc.* **1995**, *117*, 9375.
- (28) Procházka, M.; Uchytíl, B.; Zelinka, J. *Collect. Czech. Chem. Commun.* **1974**, *39*, 1342.
- (29) De Luca, L.; Giacomelli, G.; Porcheddu, A. *Org. Lett.* **2002**, *4*, 553.
- (30) Freeman, S.; Alder, J. F. *Eur. J. Med. Chem.* **2002**, *37*, 527.
- (31) (a) Ghaffar, T.; Parkins, A. W. *J. Mol. Catal. A: Chem.* **2000**, *160*, 249; (b) Ghaffar, T.; Parkins, A. W. *Tetrahedron Lett.* **1995**, *36*, 8657.
- (32) Levin, S.; Nani, R. R.; Reisman, S. E. *J. Am. Chem. Soc.* **2011**, *133*, 774.
- (33) Nonhebel, D. C. *Chem. Soc. Rev.* **1993**, *22*, 347.
- (34) Kadunce, N. T.; Reisman, S. E. *J. Am. Chem. Soc.* **2015**, *137*, 10480.

## **APPENDIX 2**

*Spectra Relevant to Chapter 3:*

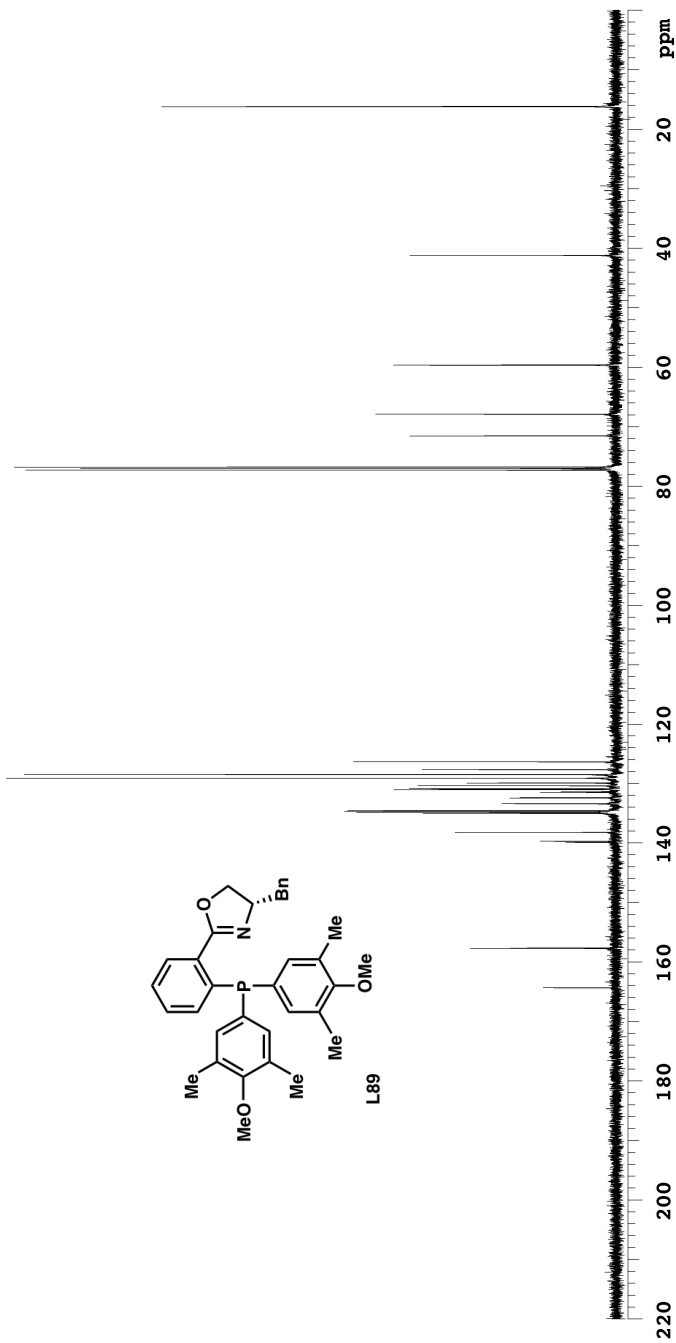
*Nickel-Catalyzed Asymmetric Reductive Cross-Coupling Between  
Heteroaryl Iodides and  $\alpha$ -Chloronitriles*



Data file: /ndy/nkadunce/vnmisys/data/NTK-IV-SuperBnPHOX/PROTON01.fid

Pict date: 2015-05-29

NTK-IV-SuperBnPHOX  
 Sample Name: NTK-IV-SuperBnPHOX  
 Date collected: 2015-05-19  
 Pulse sequence: CARBON  
 Solvent: cdf38  
 Temperature Spectrometer: 25 -vnmrs400  
 Study owner: nkadunce  
 Operator: autouser



Plot date 2015-05-29

Data file /ndy/ncadunce/vnmrsys/data/NTK-IV-SuperBnPHOX/CARBON01.fid



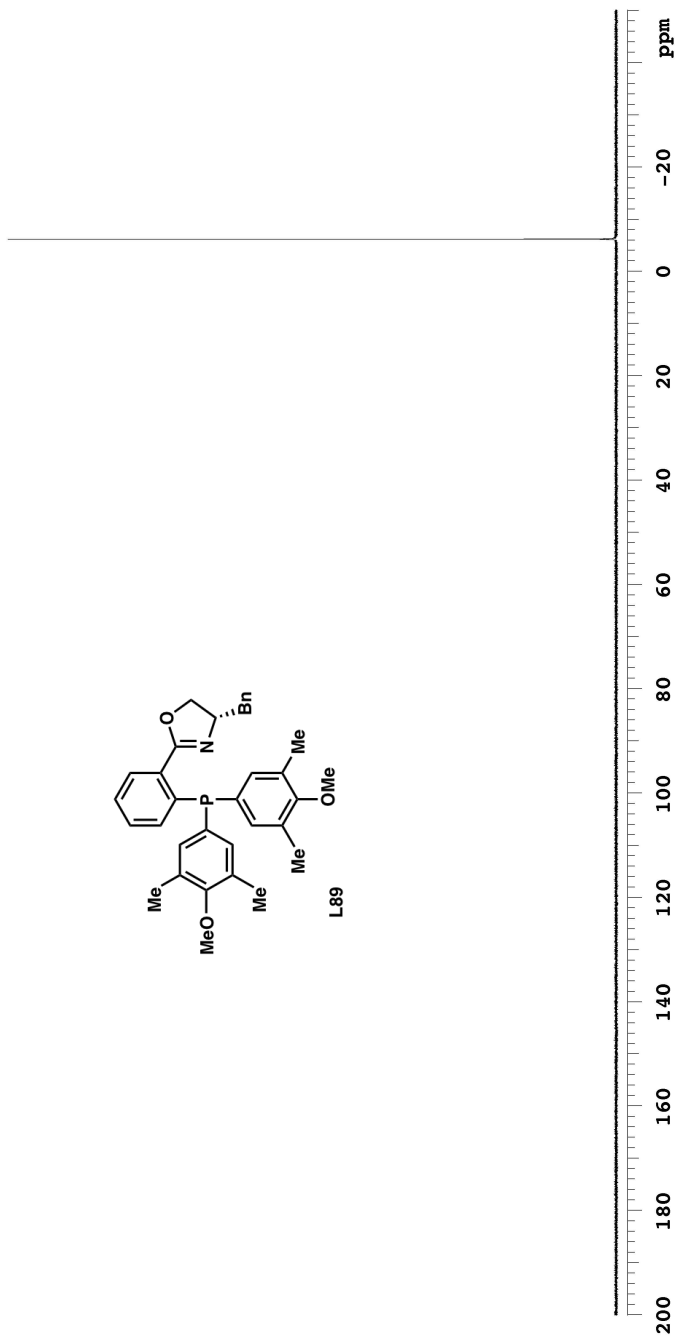
NTK-IV-SuperEnPHOX31P

Sample Name: NTK-IV-SuperEnPHOX31P  
Date collected: 2015-05-19

Pulse sequence: PHOSPHORUS  
Solvent: cdc13

Temperature: 25  
Spectrometer: vnmrns400

Study owner: ntheaduince  
Operator: autouser



Data file: /hg3/nk/aduince/vnmrnsys/data/NTK-IV-SuperEnPHOX31P/PHOSPHORUS01.fid

Plot date: 2015-05-29

NFK-III-252-2\_5-F1

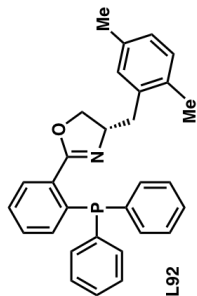
Sample Name:  
 NFK-III-252-2\_5-F1  
 Data Collected on:  
 indy.caltech.edu-inova500  
 Archive directory:  
 /home/nkadance/vmrsys/data  
 Sample directory:  
 NFK-III-252-2\_5-F1  
 FIDfile: PROTON01

Pulse sequence: PROTON (s2pul)  
 Solvent: cdcl3  
 Data collected on: Sep 5 2014

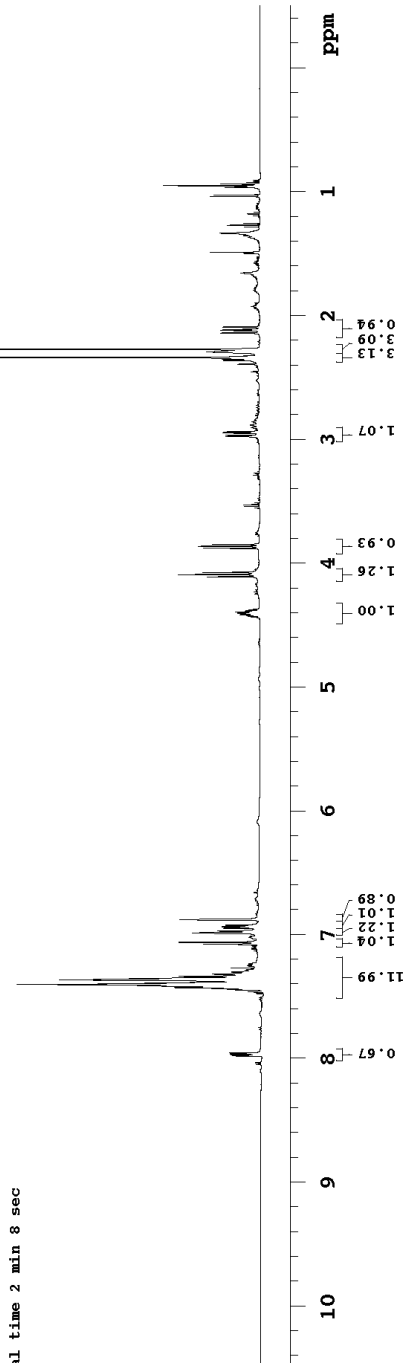
Temp. 25.0 C / 298.1 K  
 Sample #24, Operator: nkadance

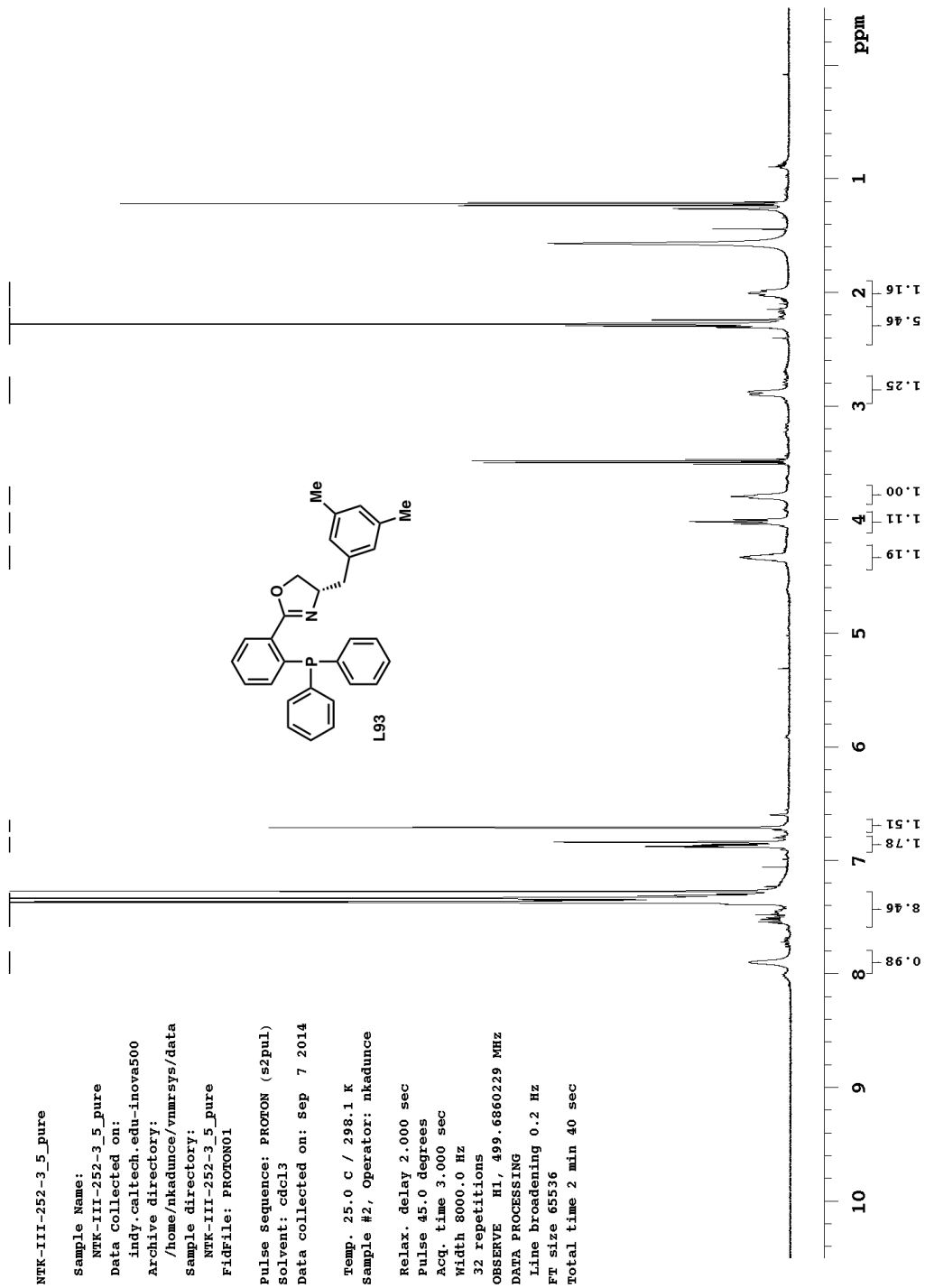
Relax. delay 1.000 sec  
 Pulse 45.0 degrees  
 Acq. time 3.000 sec  
 Width 8000.0 Hz

32 repetitions  
 OBSERVE H1, 499.6860229 MHz  
 DATA PROCESSING  
 Line broadening 0.2 Hz  
 FT size 65536  
 Total time 2 min 8 sec



L92





NTK-III-279-OMe

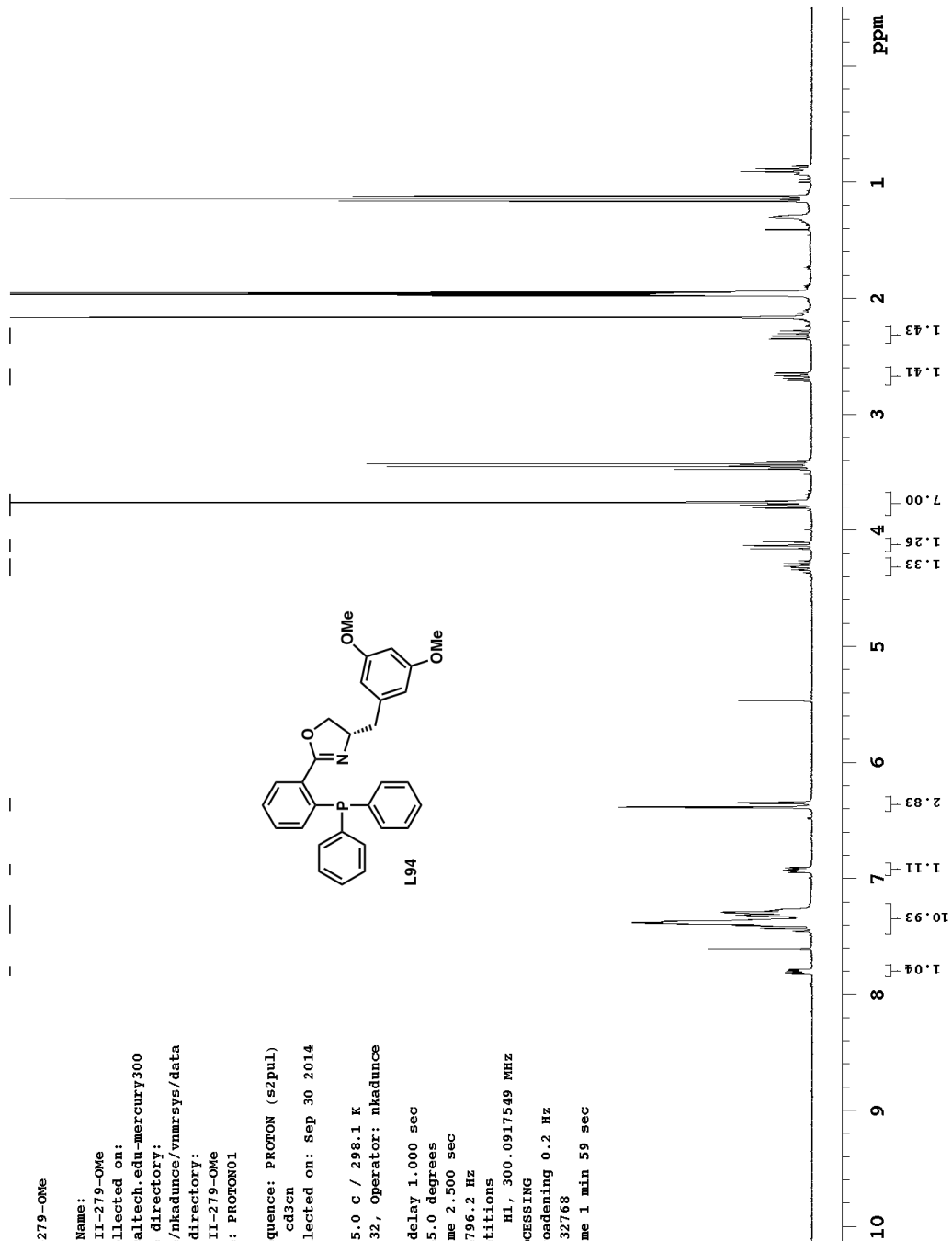
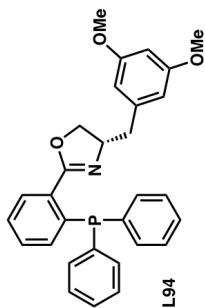
Sample Name:  
NTK-III-279-OMe  
Data Collected on:  
hg3.caltech.edu-mercury300  
Archive directory:  
/home/nkadance/vnmrSYS/data  
Sample directory:  
NTK-III-279-OMe  
Fidfile: PROTON01

Pulse Sequence: PROTON (s2pul)  
Solvent: cd3cn  
Data collected on: sep 30 2014

Temp. 25.0 C / 298.1 K  
Sample #32, Operator: nkadance

Relax. delay 1.000 sec  
Pulse 45.0 degrees  
Acq. time 2.500 sec  
Width 4796.2 Hz  
32 repetitions

OBSERVE H1, 300.0917549 MHz  
DATA PROCESSING  
Line broadening 0.2 Hz  
FT size 32768  
Total time 1 min 59 sec

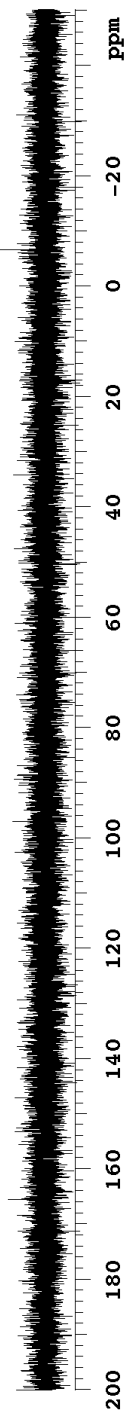
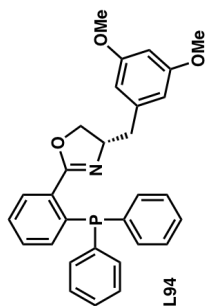


NTK-III-279-OMe

Sample Name:  
NTK-III-279-OMe  
Data Collected on:  
hg3.caltech.edu-mercury300  
Archive directory:  
/home/nkadance/vmrsys/data  
Sample directory:  
NTK-III-279-OMe  
Fidfile: PHOSPHORUS01

Pulse Sequence: PHOSPHORUS (s2pul)  
Solvent: cd3cn  
Data collected on: Sep 30 2014

Temp. 25.0 C / 298.1 K  
Sample #32, Operator: nkadance  
Relax. delay 1.000 sec  
Pulse 45.0 degrees  
Acq. time 1.078 sec  
Width 30395.1 Hz  
64 repetitions  
OBSERVE F31, 121.4793691 MHz  
DECOUPLE H1, 300.0933075 MHz  
Power 34 dB  
on during acquisition  
off during delay  
WALTZ-16 modulated  
DATA PROCESSING  
Line broadening 0.5 Hz  
FT size 65536  
Total time 2 min 24 sec



NTK-III-278-CF3

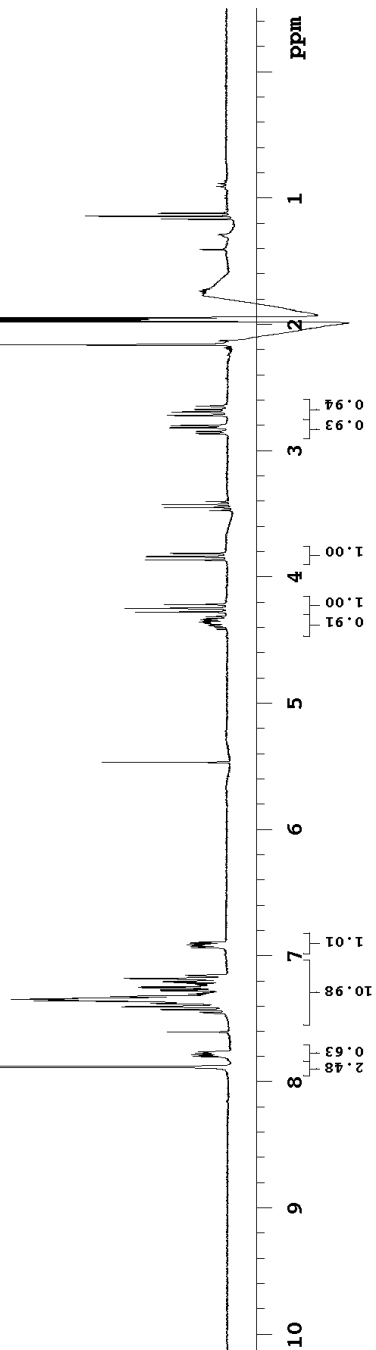
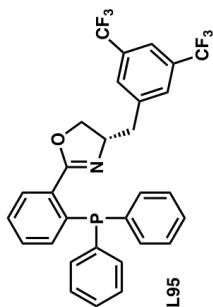
Sample Name:  
NTK-III-278-CF3  
Data Collected on:  
hg3.caltech.edu-mercury300  
Archive directory:  
/home/nkadance/vnmrSYS/data  
Sample directory:  
NTK-III-278-CF3  
Fidfile: PROTON01

Pulse Sequence: PROTON (s2pul)  
Solvent: cd3cn  
Data collected on: sep 29 2014

Temp. 25.0 C / 298.1 K  
Sample #40, Operator: nkadance

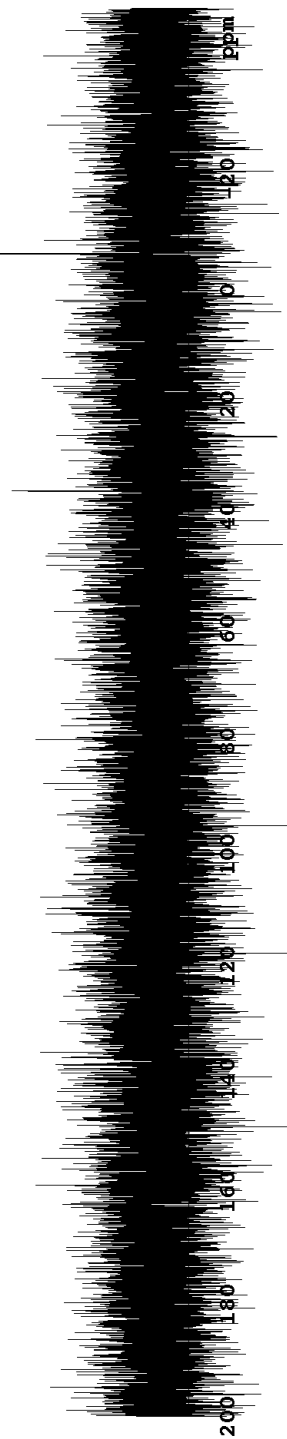
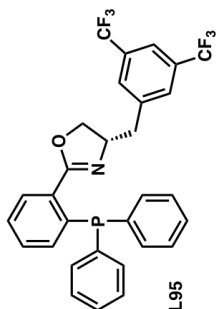
Relax. delay 1.000 sec  
Pulse 45.0 degrees  
Acq. time 2.500 sec  
Width 4796.2 Hz  
32 repetitions

OBSERVE H1, 300.0917549 MHz  
DATA PROCESSING  
Line broadening 0.2 Hz  
FT size 32768  
Total time 1 min 59 sec



## STANDARD PHOSPHORUS PARAMETERS

Sample Name:  
 NTK-III-278-CF3  
 Data Collected on:  
 hg3.caltech.edu-mercury300  
 Archive directory:  
 /home/nkadance/vnmrSYS/data  
 Sample directory:  
 NTK-III-278-CF3  
 Fidfile: PHOSPHORUS01  
 Pulse Sequence: PHOSPHORUS (s2pul)  
 Solvent: cd3cn  
 Data collected on: Sep 29 2014  
 Temp. 25.0 C / 298.1 K  
 Sample #40, Operator: nkadance  
 Relax. delay 1.000 sec  
 Pulse 45.0 degrees  
 Acq. time 1.078 sec  
 Width 30395.1 Hz  
 64 repetitions  
 OBSERVE P31, 121.4793691 MHZ  
 DECOUPLE H1, 300.0933075 MHZ  
 Power 34 dB  
 on during acquisition  
 off during delay  
 WALTZ-16 modulated  
 DATA PROCESSING  
 Line broadening 0.5 Hz  
 FT size 6536  
 Total time 2 min 24 sec





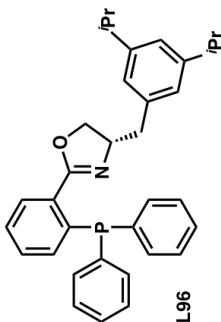
NTK-III-279-IPr\_2

Sample Name:  
 NTK-III-279-IPr\_2  
 Data Collected on:  
 hg3.caltech.edu-mercury300  
 Archive directory:  
 /home/nkadance/vnmrSYS/data  
 Sample directory:  
 NTK-III-279-IPr\_2  
 Fidfile: PHOSPHORUS01

Pulse Sequence: PHOSPHORUS (s2pul)  
 Solvent: cdcl3  
 Data collected on: Sep 30 2014

Temp. 25.0 C / 298.1 K  
 sample #36, Operator: nkadance

Relax. delay 1.000 sec  
 Pulse 45.0 degrees  
 Acq. time 1.078 sec  
 Width 30395.1 Hz  
 64 repetitions  
 OBSERVE P31, 121.4787265 MHZ  
 DECOUPLE H1, 300.0917200 MHZ  
 Power 34 dB  
 on during acquisition  
 off during delay  
 WALTZ-16 modulated  
 DATA PROCESSING  
 Line broadening 0.5 Hz  
 FT size 65536  
 Total time 2 min 24 sec



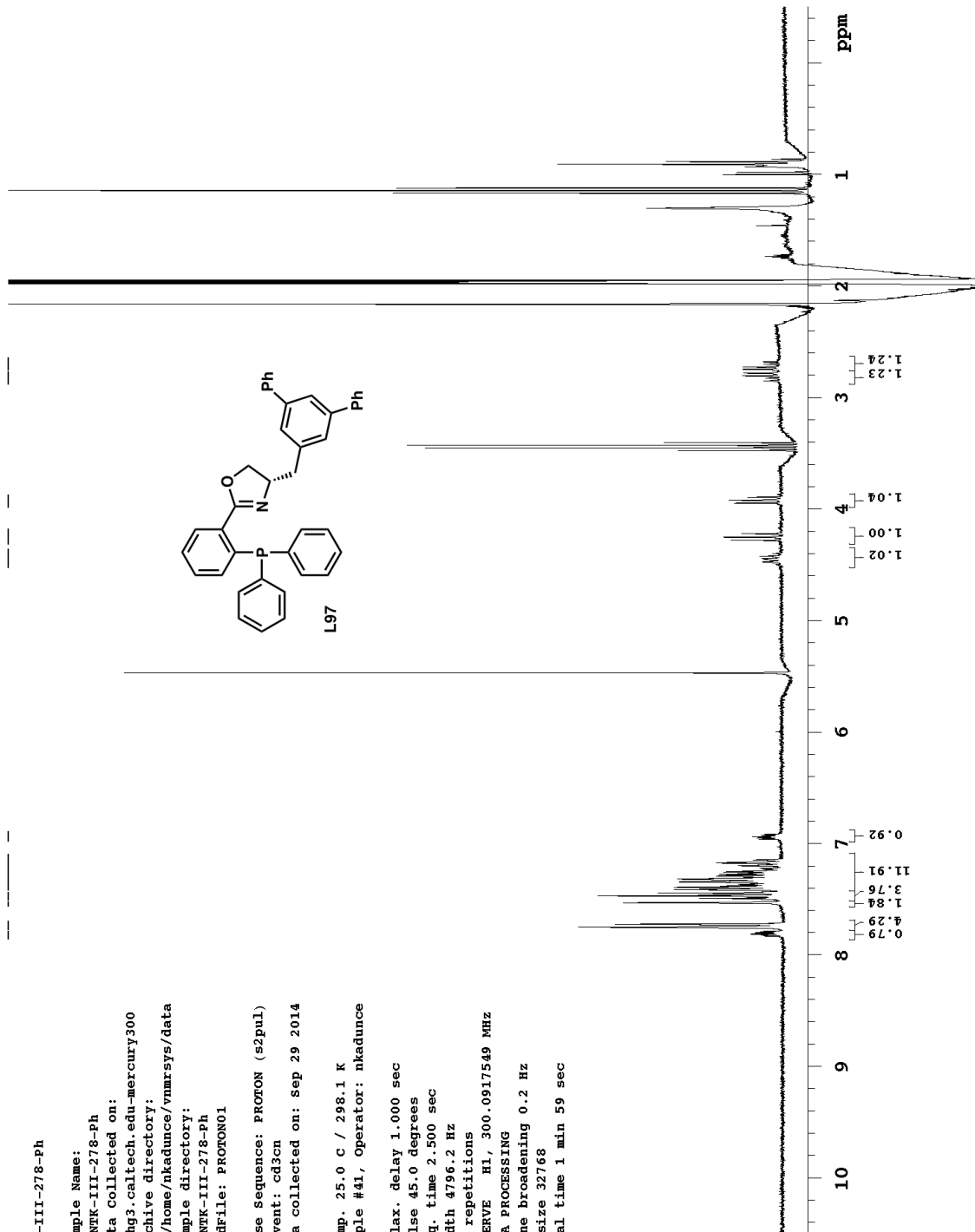
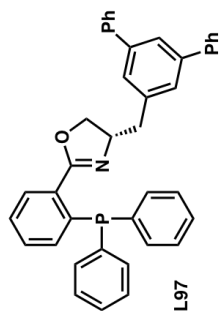
NTK-III-278-Ph

Sample Name:  
 NTK-III-278-Ph  
 Data Collected on:  
 hg3.caltech.edu-mercury300  
 Archive directory:  
 /home/nkadance/vnmrsys/data  
 Sample directory:  
 NTK-III-278-Ph  
 FIDfile: PROTON01

Pulse Sequence: PROTON (s2pul)  
 Solvent: cd3cn  
 Data collected on: Sep 29 2014

Temp. 25.0 C / 298.1 K  
 sample #41, Operator: nkadance

Relax. delay 1.000 sec  
 Pulse 45.0 degrees  
 Acq. time 2.500 sec  
 Width 4796.2 Hz  
 32 repetitions  
 OBSERVE H1, 300.0917549 MHZ  
 DATA PROCESSING  
 Line broadening 0.2 Hz  
 FT size 32768  
 Total time 1 min 59 sec

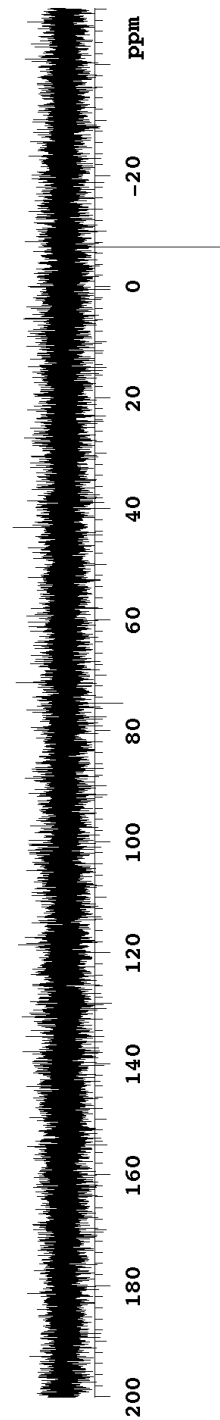
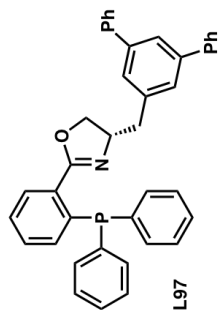


NTK-III-278-Ph

Sample Name:  
NTK-III-278-Ph  
Data Collected on:  
hg3.caltech.edu-mercury300  
Archive directory:  
/home/nkadance/vnmrSYS/data  
Sample directory:  
NTK-III-278-Ph  
Fidfile: PHOSPHORUS01

Pulse Sequence: PHOSPHORUS (s2pul)  
Solvent: cd3cn  
Data collected on: sep 29 2014

Temp. 25.0 C / 298.1 K  
Sample #41, Operator: nkadance  
Relax. delay 1.000 sec  
Pulse 45.0 degrees  
Acq. time 1.078 sec  
Width 30395.1 Hz  
64 repetitions  
OBSERVE F31, 121.4793691 MHz  
DECOUPLE H1, 300.0933075 MHz  
Power 34 dB  
on during acquisition  
off during delay  
NALZ-16 modulated  
DATA PROCESSING  
Line broadening 0.5 Hz  
FT size 65536  
Total time 2 min 24 sec



NTK-III-287-UltrabnPHOX\_2

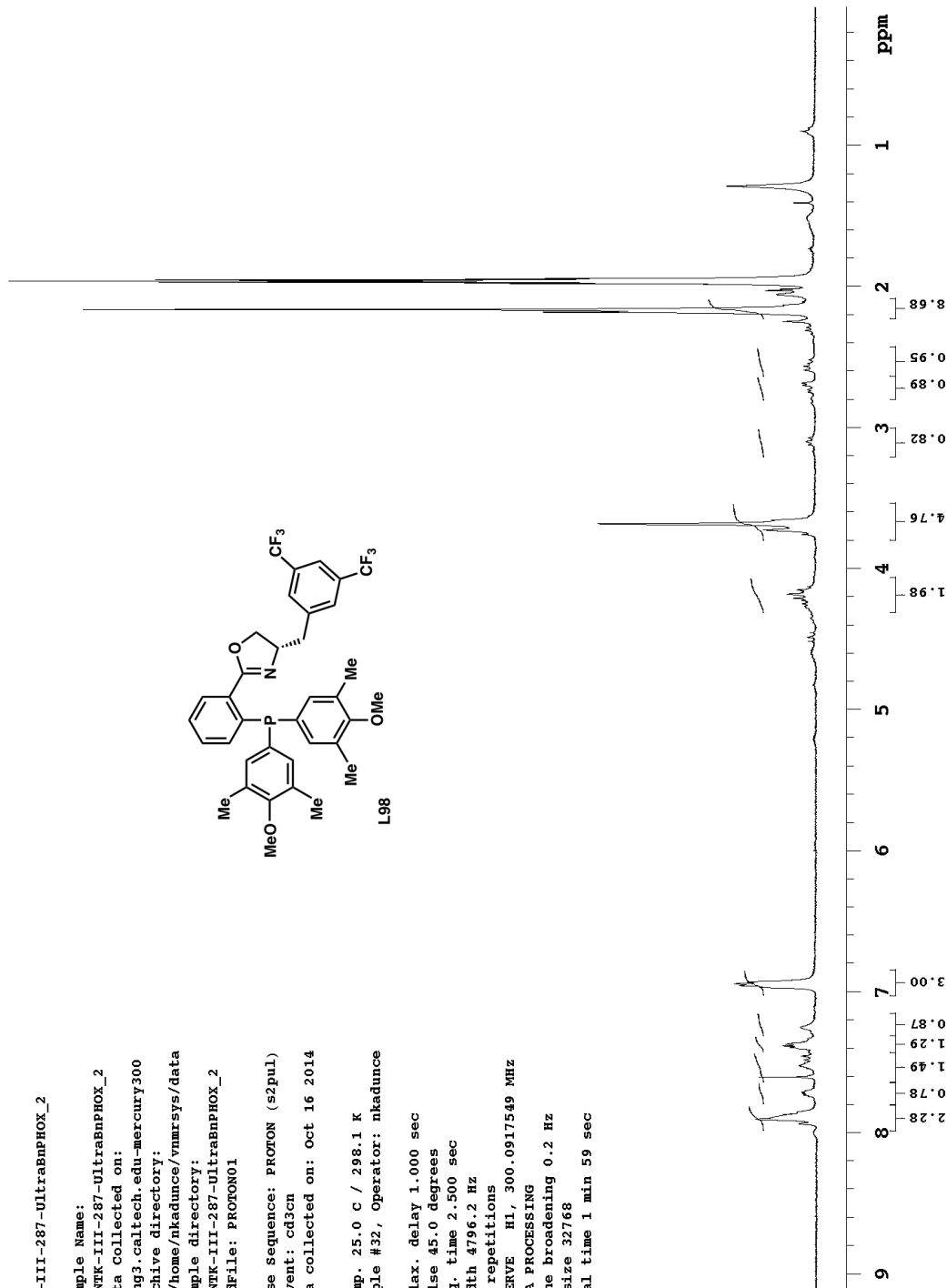
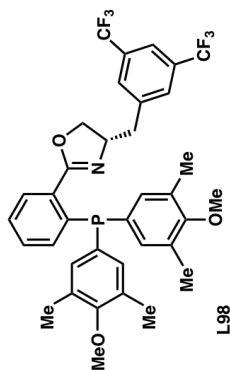
Sample Name:  
 NTK-III-287-UltrabnPHOX\_2  
 Data Collected on:  
 hg3.caltech.edu-mercury300  
 Archive directory:  
 /home/nkadance/vnmrsys/data  
 Sample directory:  
 NTK-III-287-UltrabnPHOX\_2  
 FIDfile: PROTON01

Pulse Sequence: PROTON (s2pul)  
 Solvent: cd3cn  
 Data collected on: Oct 16 2014

Temp. 25.0 C / 298.1 K  
 sample #32, Operator: nkadance

Relax. delay 1.000 sec  
 Pulse 45.0 degrees  
 Acq. time 2.500 sec  
 Width 4796.2 Hz  
 32 repetitions

OBSERVE H1, 300.0917549 MHZ  
 DATA PROCESSING  
 Line broadening 0.2 Hz  
 FT size 32768  
 Total time 1 min 59 sec



NTK-III-287-UltrabnPHOX\_2

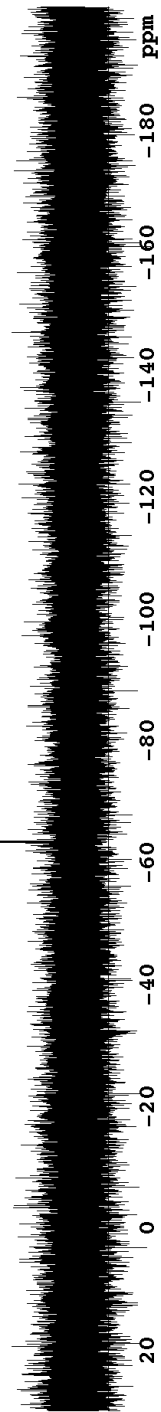
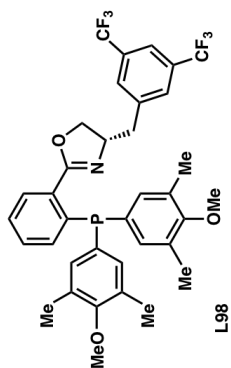
Sample Name:  
 NTK-III-287-UltrabnPHOX\_2  
 Data Collected on:  
 hg3.caltech.edu-mercury300  
 Archive directory:  
 /home/nkadance/vnmrsys/data  
 Sample directory:  
 NTK-III-287-UltrabnPHOX\_2  
 Fidfile: FLUORINE01

Pulse Sequence: FLUORINE (s2pul)  
 Solvent: cd3cn  
 Data collected on: Oct 16 2014

Temp. 25.0 C / 298.1 K  
 Sample #32, Operator: nkadance

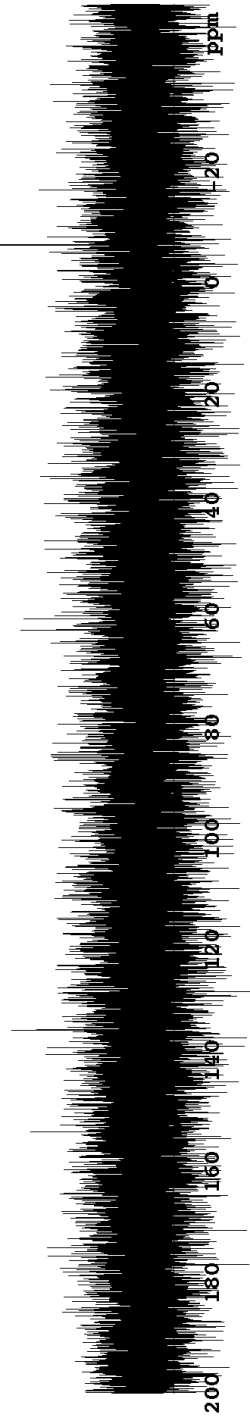
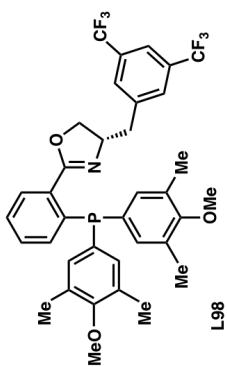
Relax. delay 1.000 sec  
 Pulse 30.0 degrees  
 Acq. time 0.986 sec  
 Width 64935.1 Hz  
 16 repetitions

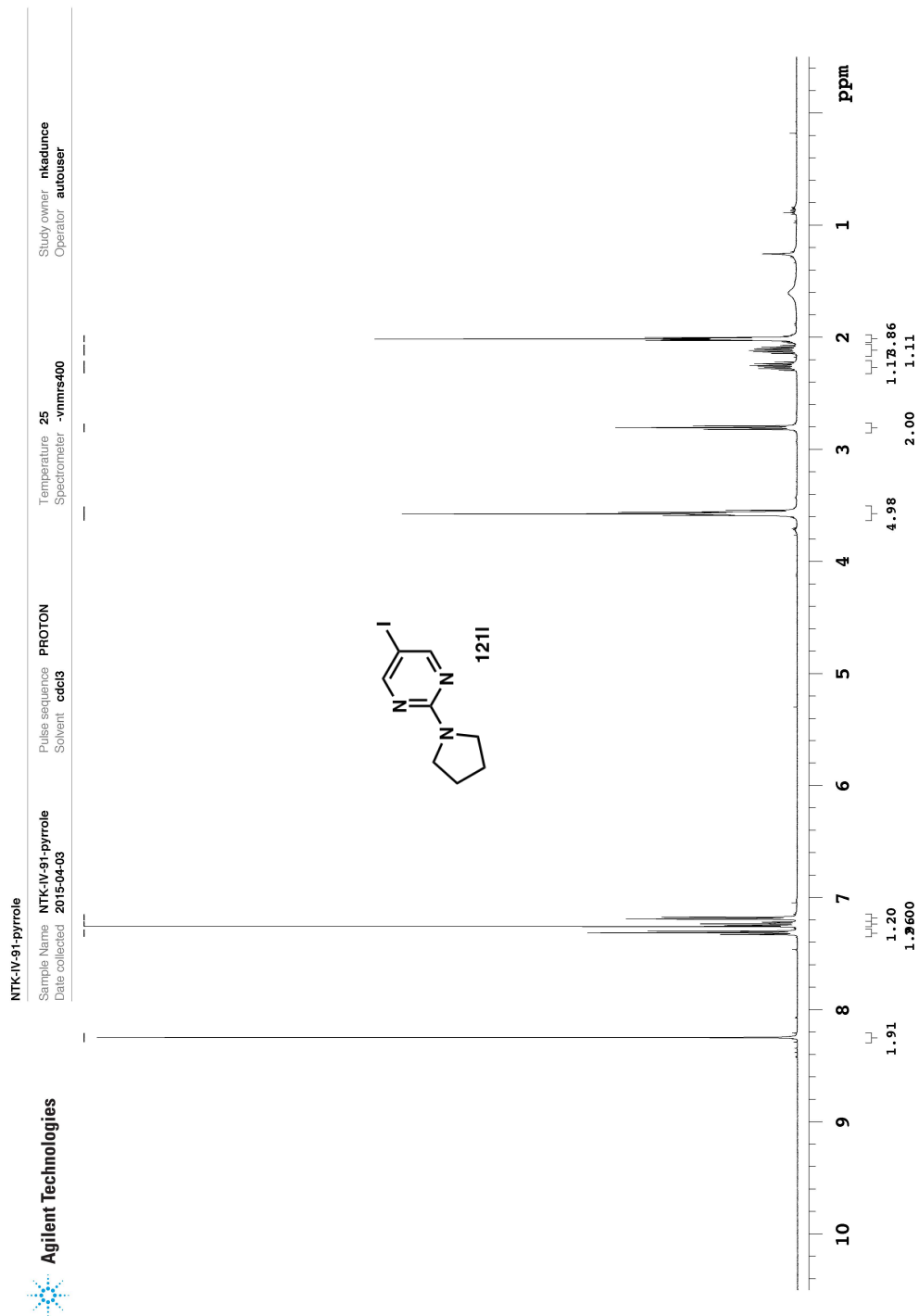
OBSERVE F19, 282.3683689 MHz  
 DATA PROCESSING  
 FT size 131072  
 Total time 0 min 45 sec



## STANDARD PHOSPHORUS PARAMETERS

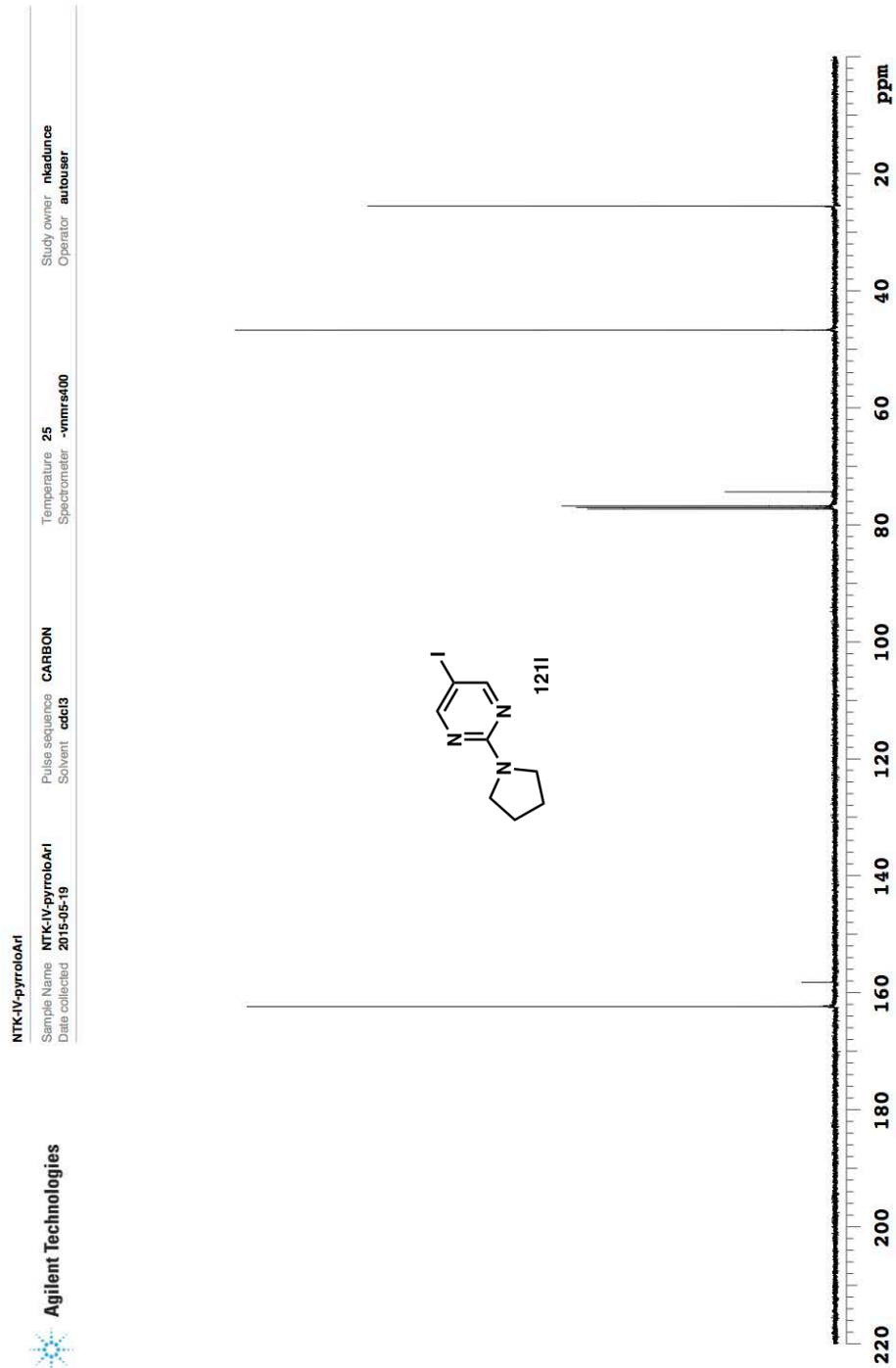
Sample Name:  
 NTK-III-287-UltraBnPHOX\_2  
 Data Collected on:  
 hg3.caltech.edu-mercury300  
 Archive directory:  
 /home/nkadance/vnmrSYS/data  
 Sample directory:  
 NTK-III-287-UltraBnPHOX\_2  
 FIDfile: PHOSPHORUS01  
 Pulse Sequence: PHOSPHORUS (s2pul)  
 Solvent: cd3cn  
 Data collected on: Oct 16 2014  
 Temp. 25.0 C / 298.1 K  
 Sample #32, Operator: nkadance  
 Relax. delay 1.000 sec  
 Pulse 45.0 degrees  
 Acq. time 1.078 sec  
 Width 30395.1 Hz  
 128 repetitions  
 OBSERVE F31, 121.4793691 MHz  
 DECOUPLE H1, 300.0933075 MHz  
 Power 34 dB  
 on during acquisition  
 off during delay  
 NALZ-16 modulated  
 DATA PROCESSING  
 Line broadening 0.5 Hz  
 FT size 65536  
 Total time 4 min 43 sec

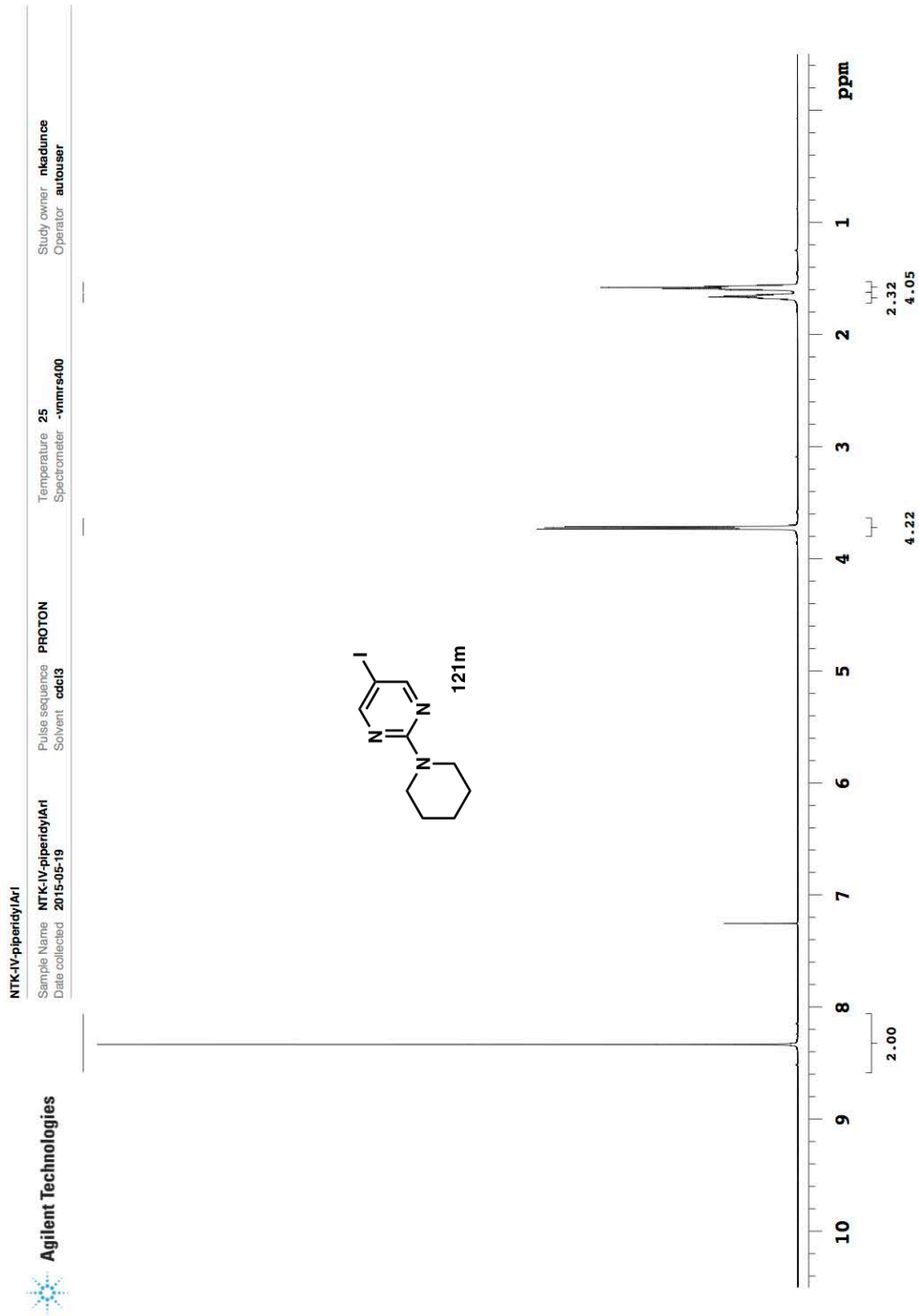




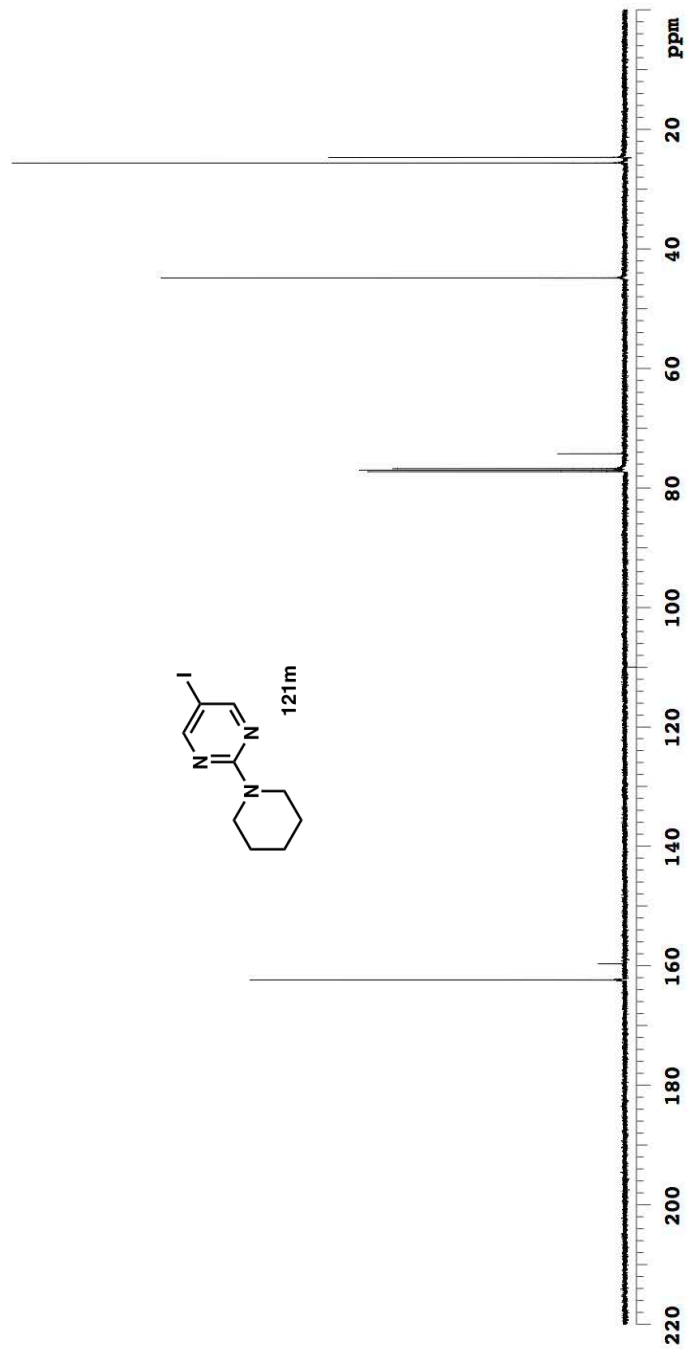
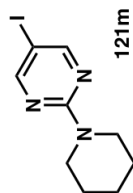
Plot date 2015-05-29

Data file: /ind/nkadunce/vnmrsys/data/NTK-IV-91-pyrrole/PROTON01.fid

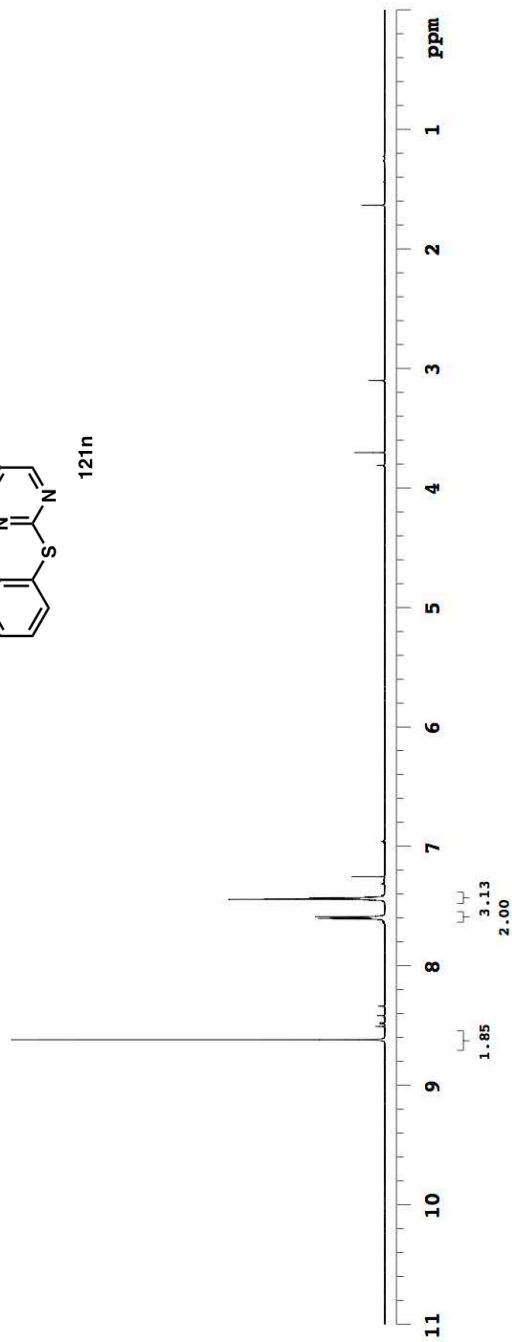
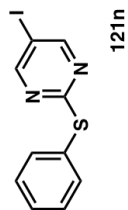




NTK-IV-piperdyIArI  
 Sample Name NTK-IV-piperdyIArI  
 Date collected 2015-05-19  
 Pulse sequence CARBON  
 Solvent cdcl3  
 Temperature 25  
 Spectrometer -vnmr400  
 Study owner nksadunice  
 Operator autobuser



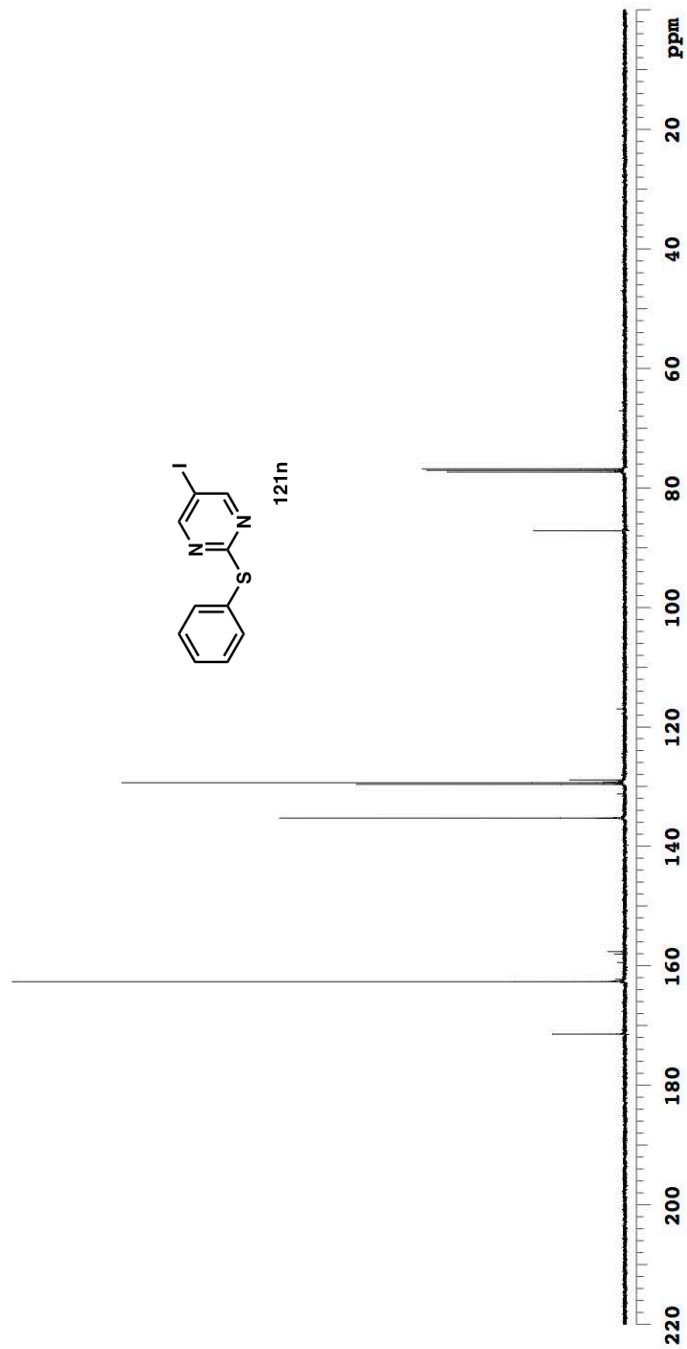
**NTK-IV-SPhArI**  
 Sample Name **NTK-IV-SPhArI**      Pulse sequence **PROTON**      Temperature **25**      Study owner **nkadunce**  
 Date collected **2015-05-19**      Solvent **cdcl3**      Spectrometer **-vnmrsl400**      Operator **autouser**

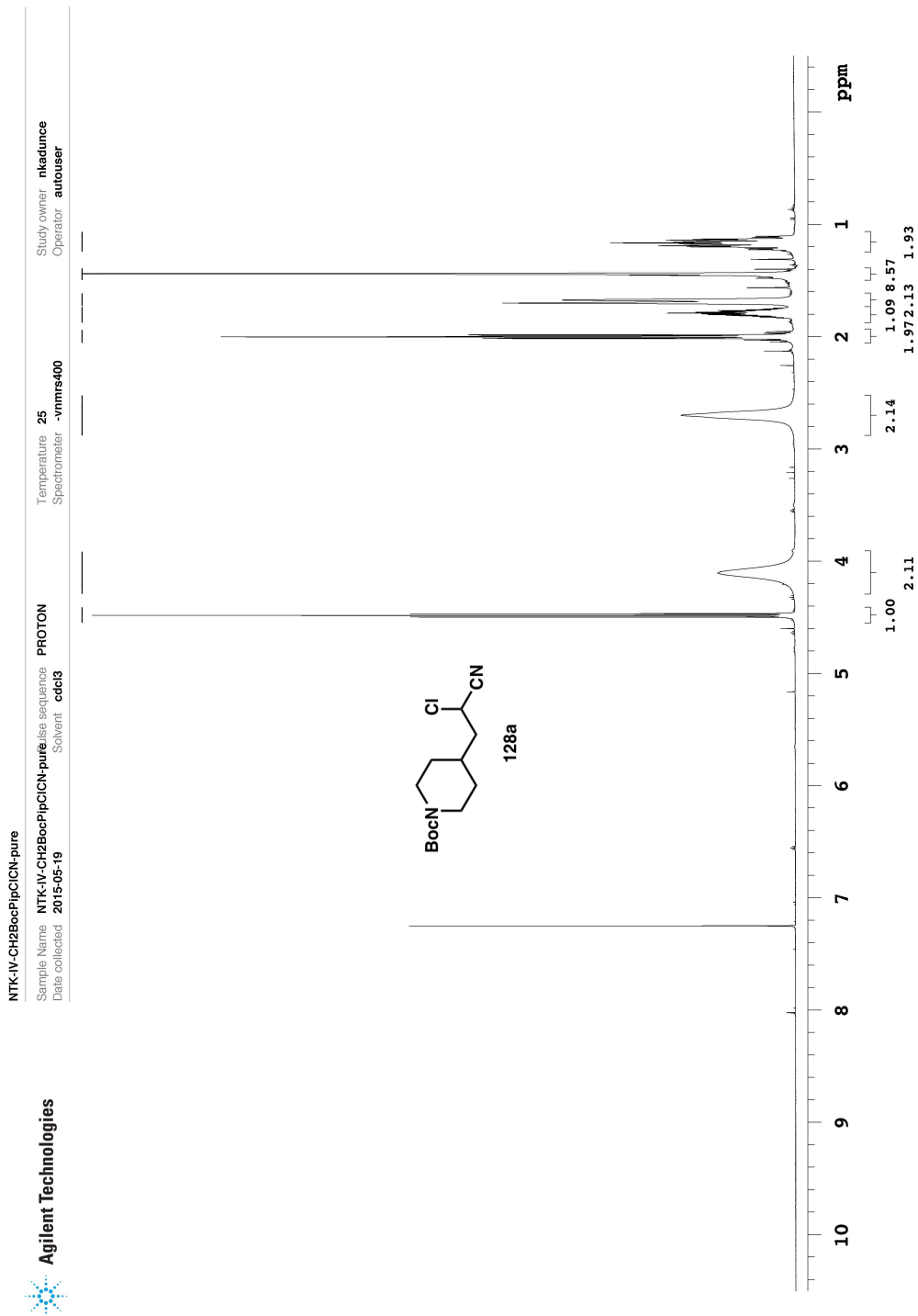


**NTK-IV-SPhArI**  
 Sample Name **NTK-IV-SPhArI** Temperature **25** Study owner **nkadunice**  
 Date collected **2015-05-19** Spectrometer **-vnmrsl400** Operator **autouser**

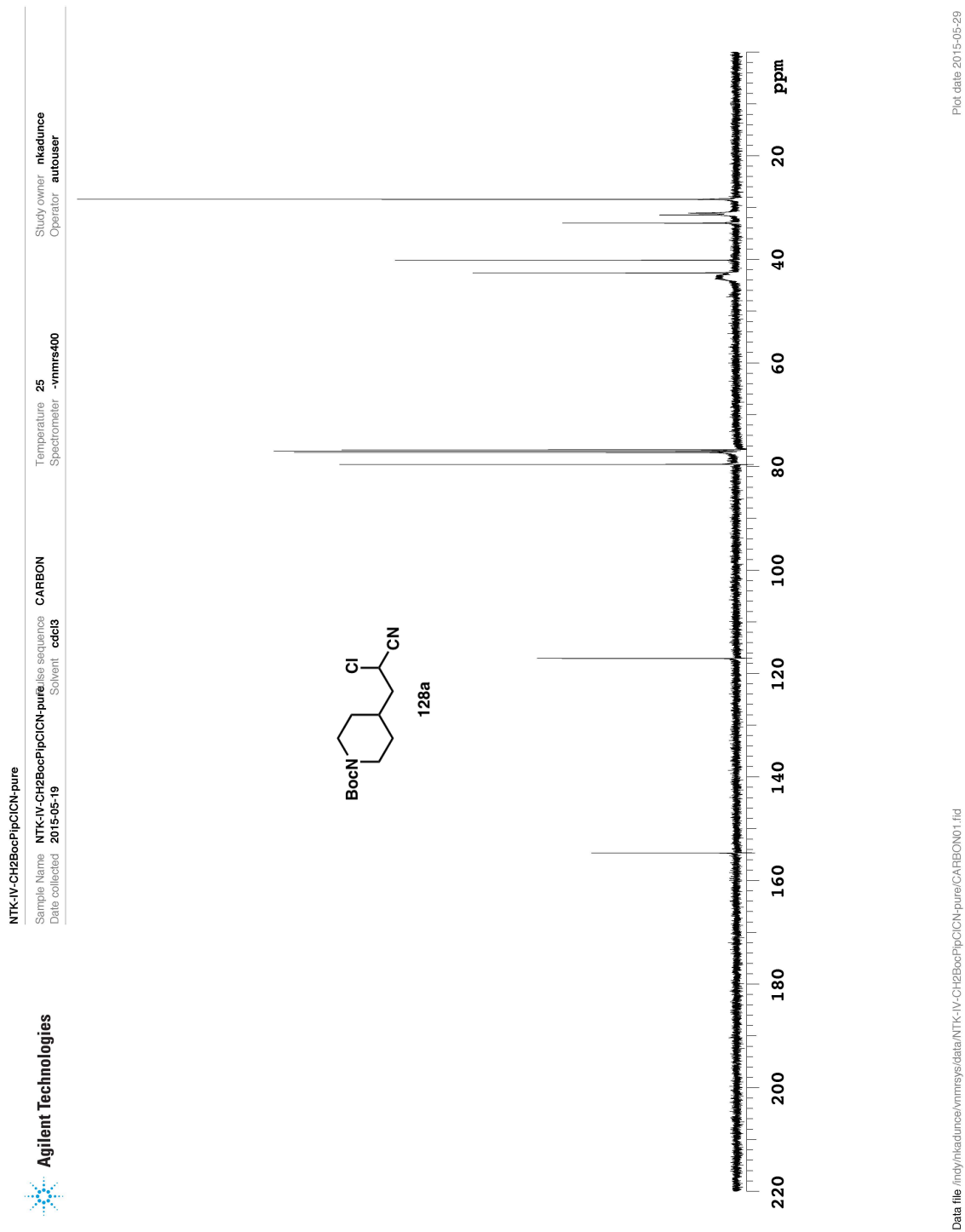


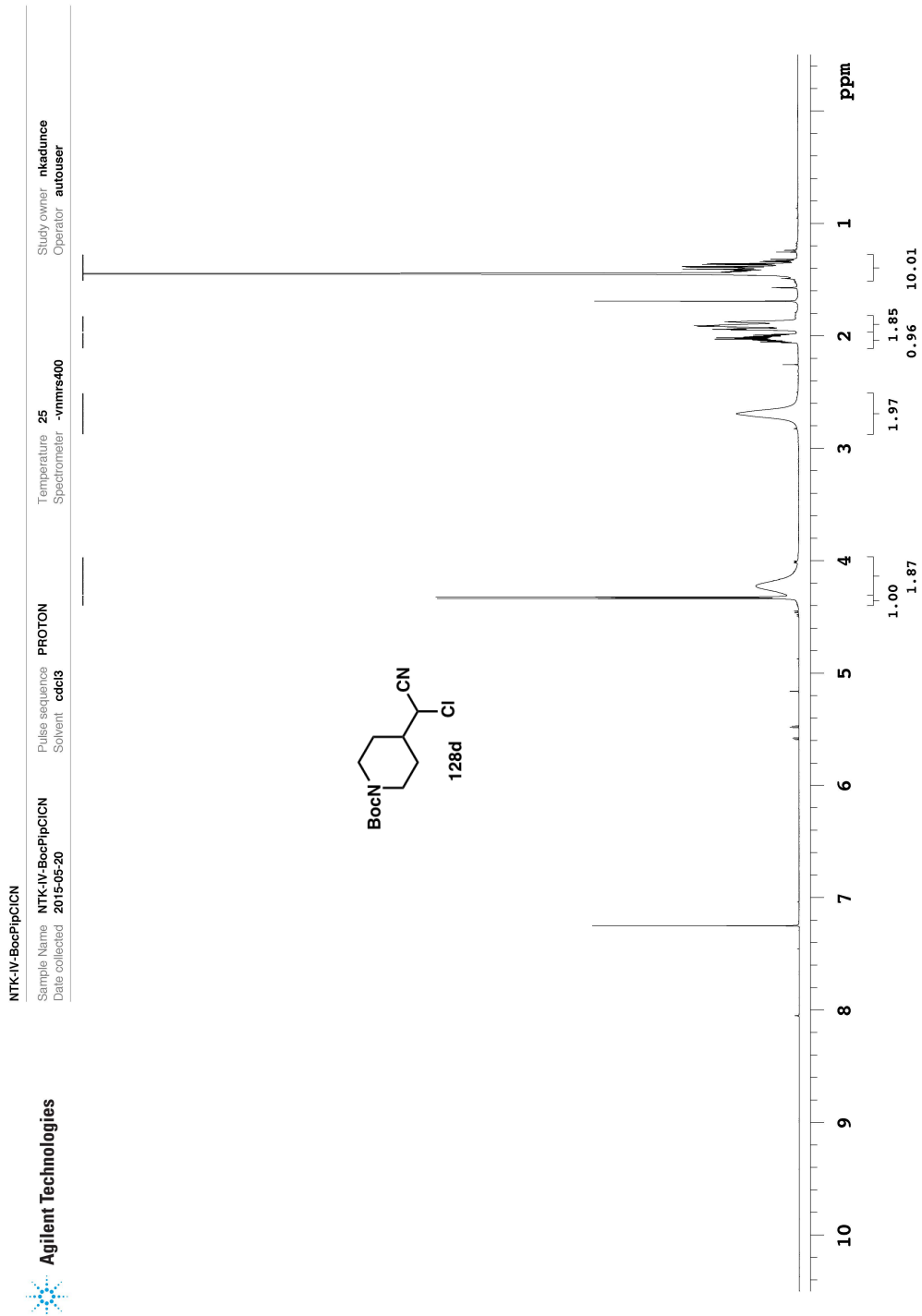
Pulse sequence **CARBON**  
 Solvent **cdcl3**





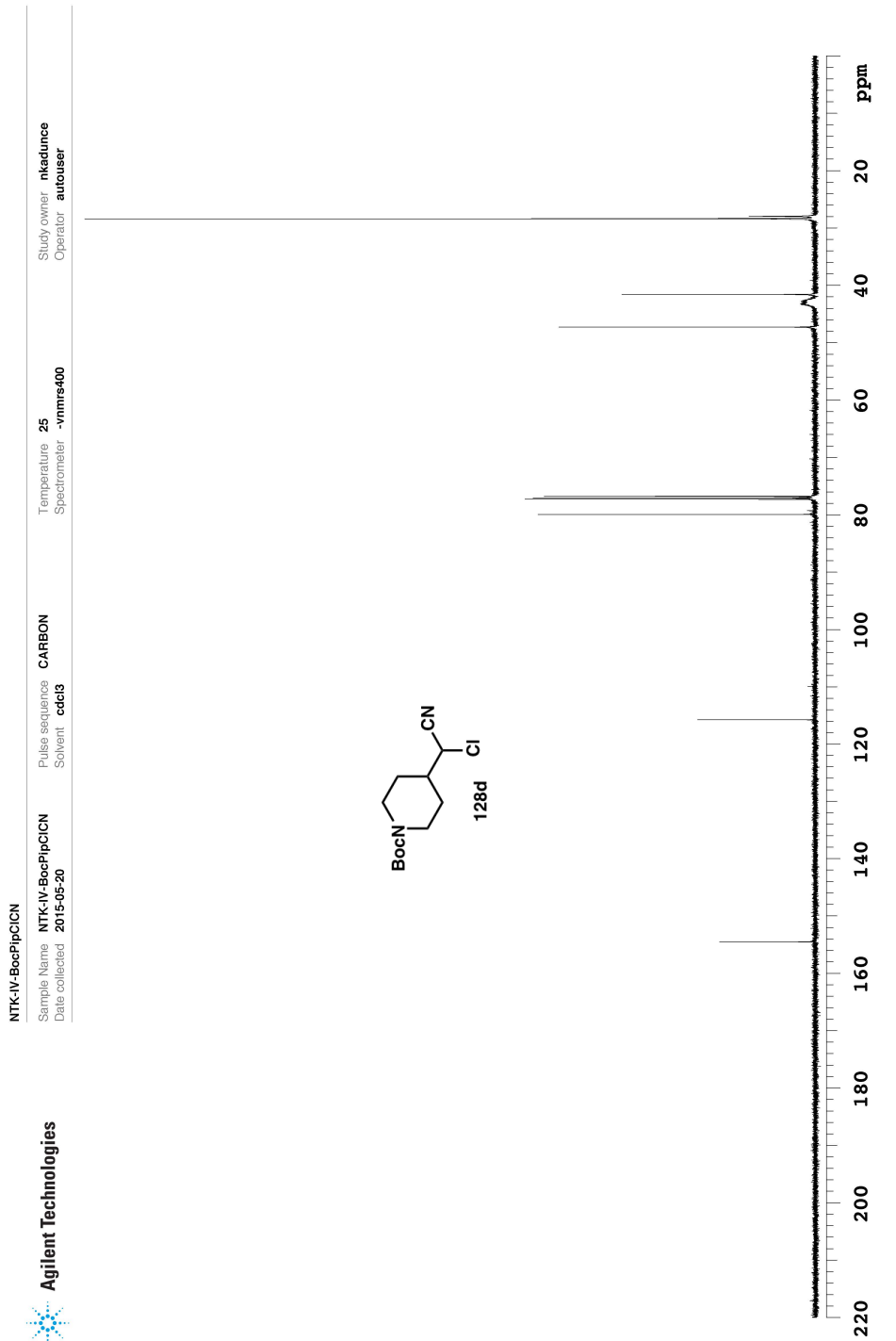
Data file: /ndy/nkadunce/vnmrsys/data/NTK-IV-CH2BocPipClCN-pure/PROTON01.fid  
 Plot date: 2015-05-29





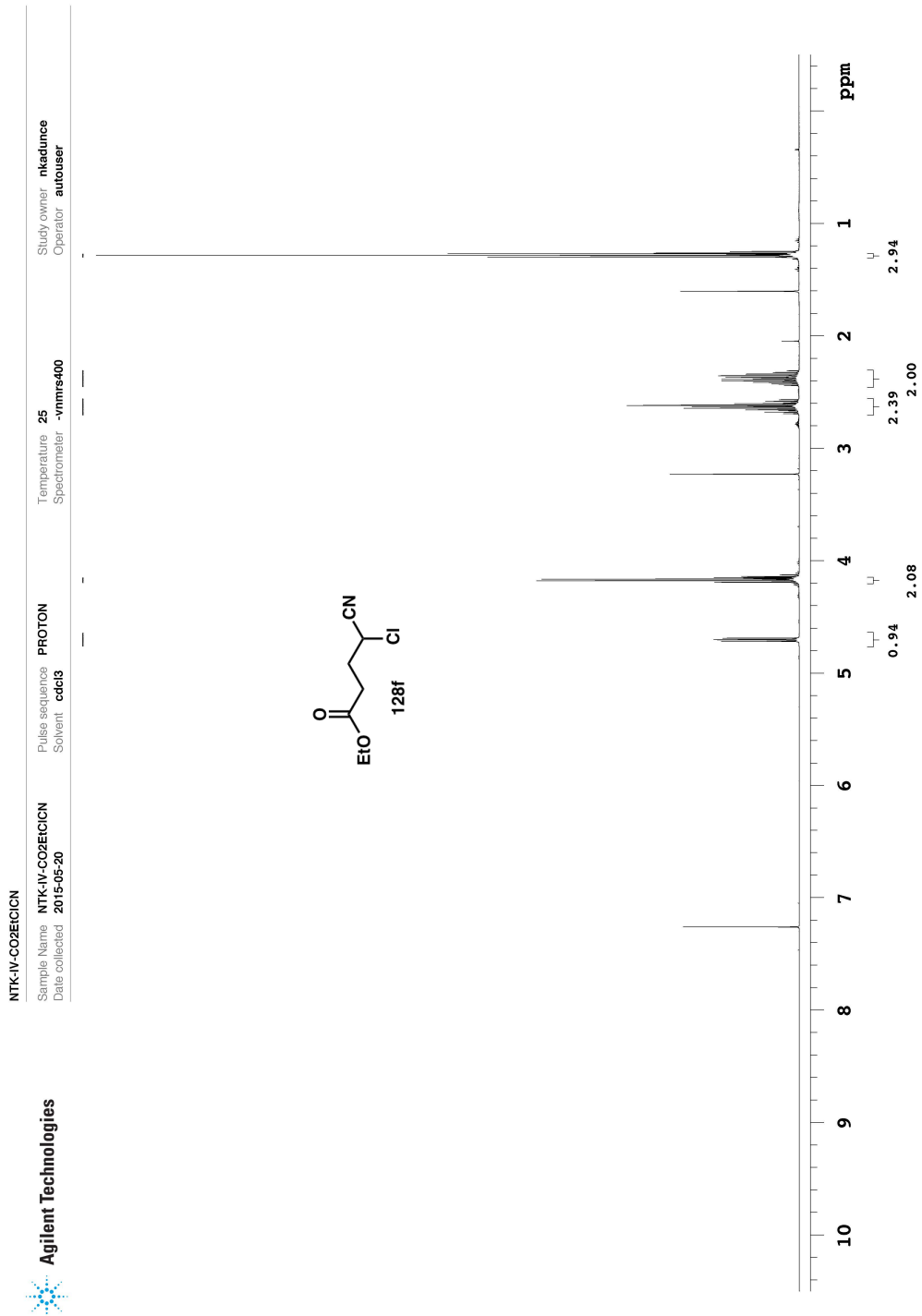
Plot date 2015-05-29

Data file: /ind/nkaadunce/vnmrsys/data/NTK-IV-BocPipClCN/PROTON01.fid



Plot date 2015-05-29

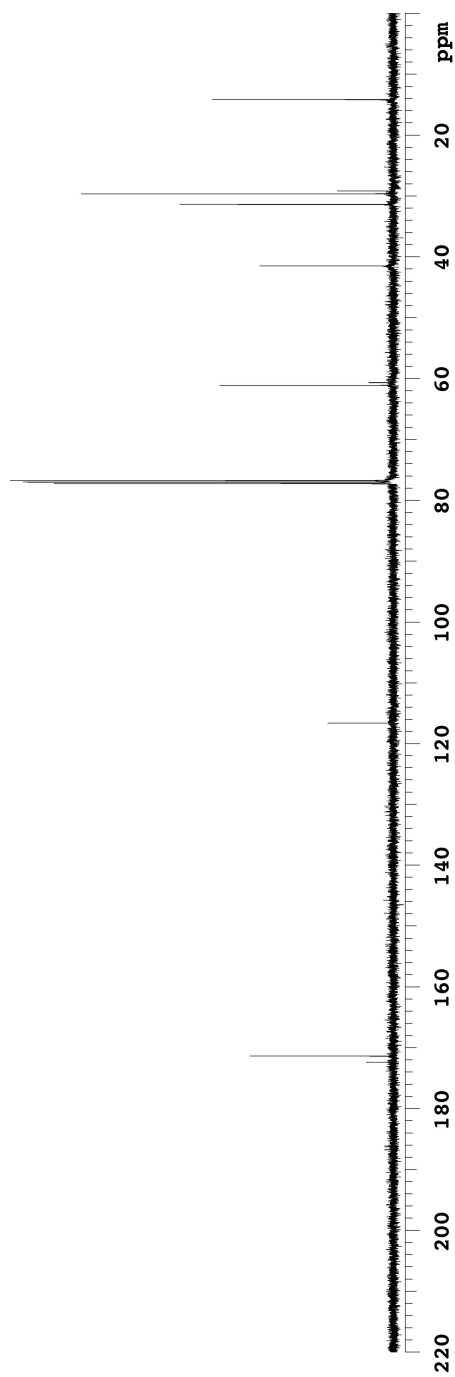
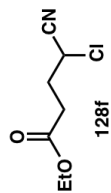
Data file: /ind/nkaclunice/vnmrsys/data/NTK-IV-BocPipClCN/CARBON01.fid



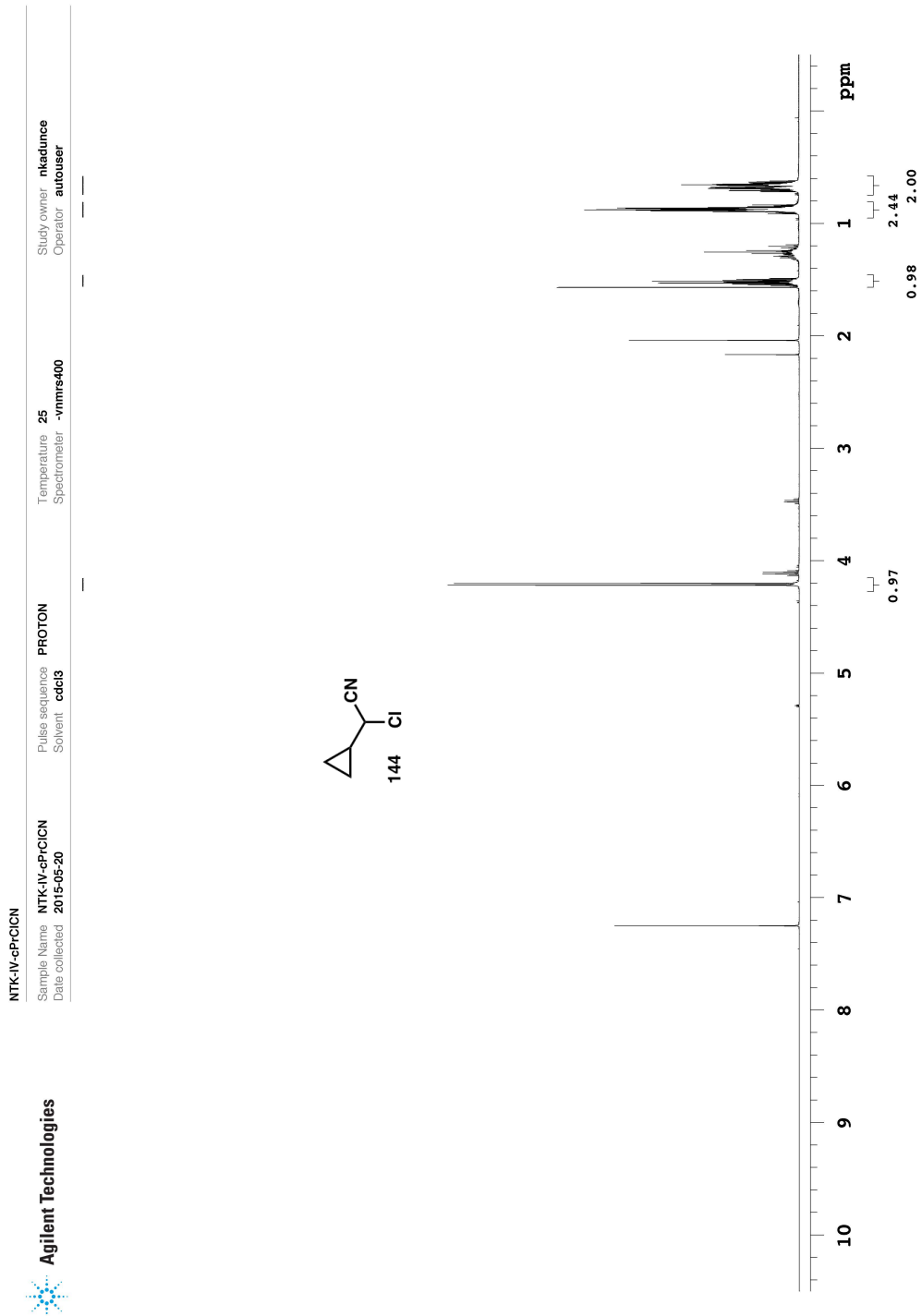
Plot date 2015-05-29

Data file f:\ndy\nkaelunce\vnmrs\data\NTK-IV-CO2E1C1CN\PROTON01.fid

NTK-IV-CO2EIC1CN  
 Sample Name NTK-IV-CO2EIC1CN CARBON  
 Date collected 2015-05-20 Pulse sequence  
 Solvent cdc13 Temperature 25  
 Spectrometer -vnmrs400  
 Study owner nkaclunice  
 Operator autouser



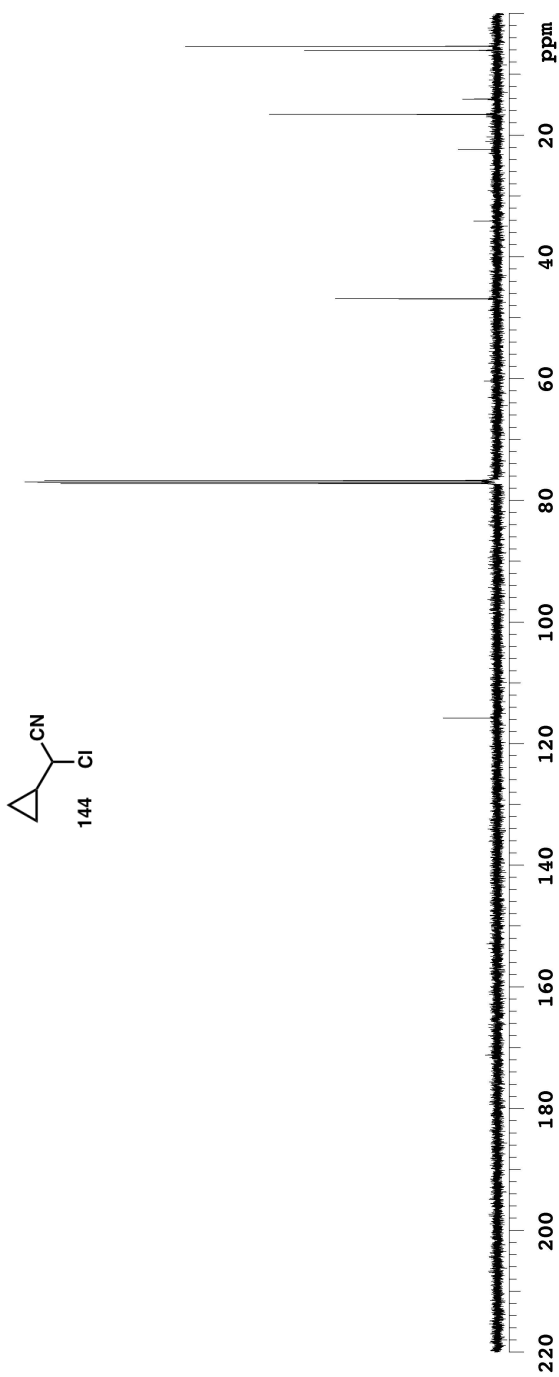
Data file f:\ndy\nkaclunice\vmmsys\data\NTK-IV-CO2EIC1CN\CARBON01.fid  
 Plot date 2015-05-29



Plot date: 2015-05-29

Data file: /ind/nkaelunce/vnmr400/data/NTK-IV-cPrClCN/PROTON01.fid

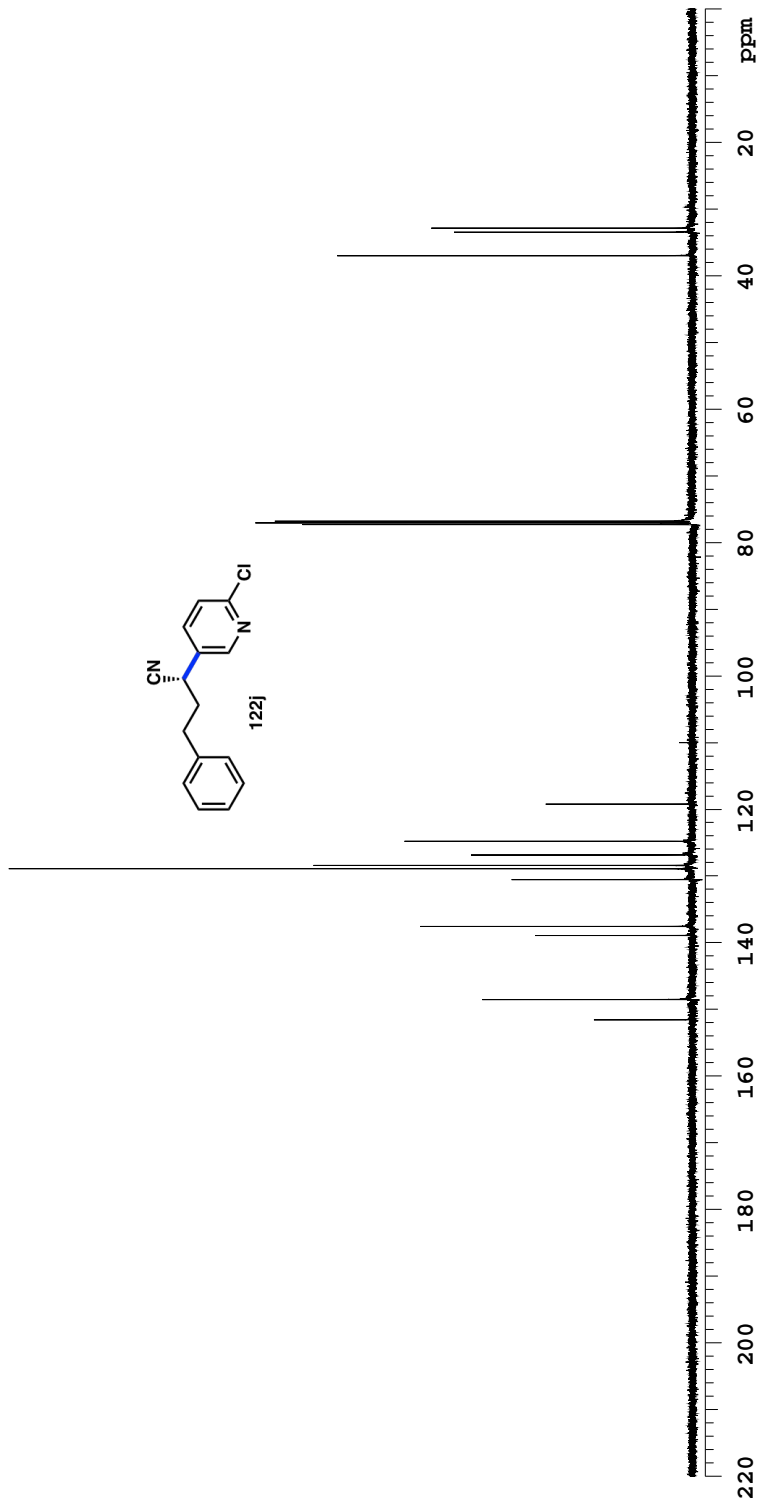
NTK-IV-cPrClCN  
 Sample Name NTK-IV-cPrClCN  
 Date collected 2015-05-20  
 Pulse sequence CARBON  
 Solvent cdc13  
 Temperature 25  
 Spectrometer vnmr400  
 Study owner nkaalunce  
 Operator autouser



Data file /ind/nkaalunce/vnmrsys/data/NTK-IV-cPrClCN/CARBON01.fid  
 Plot date 2015-05-29

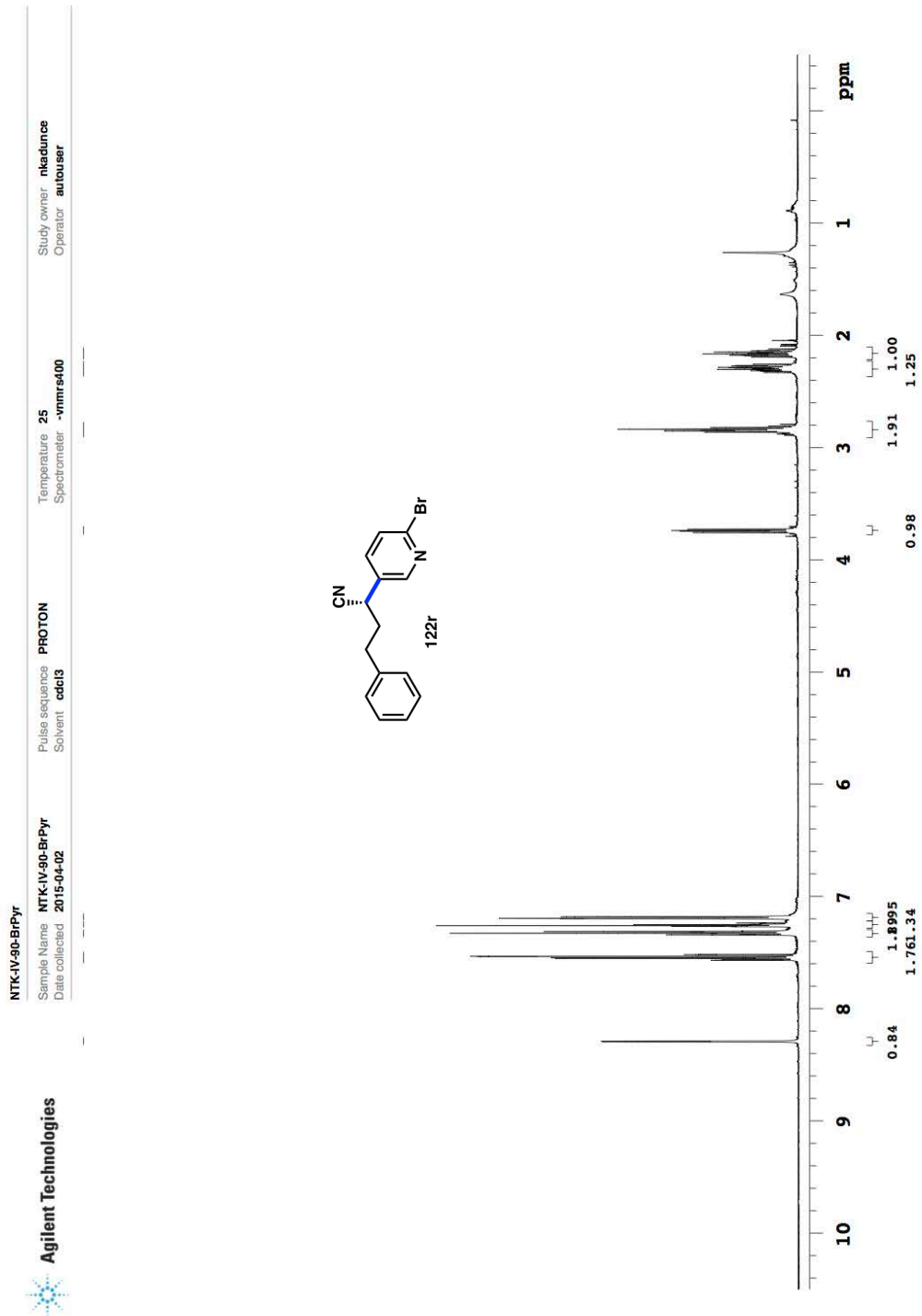


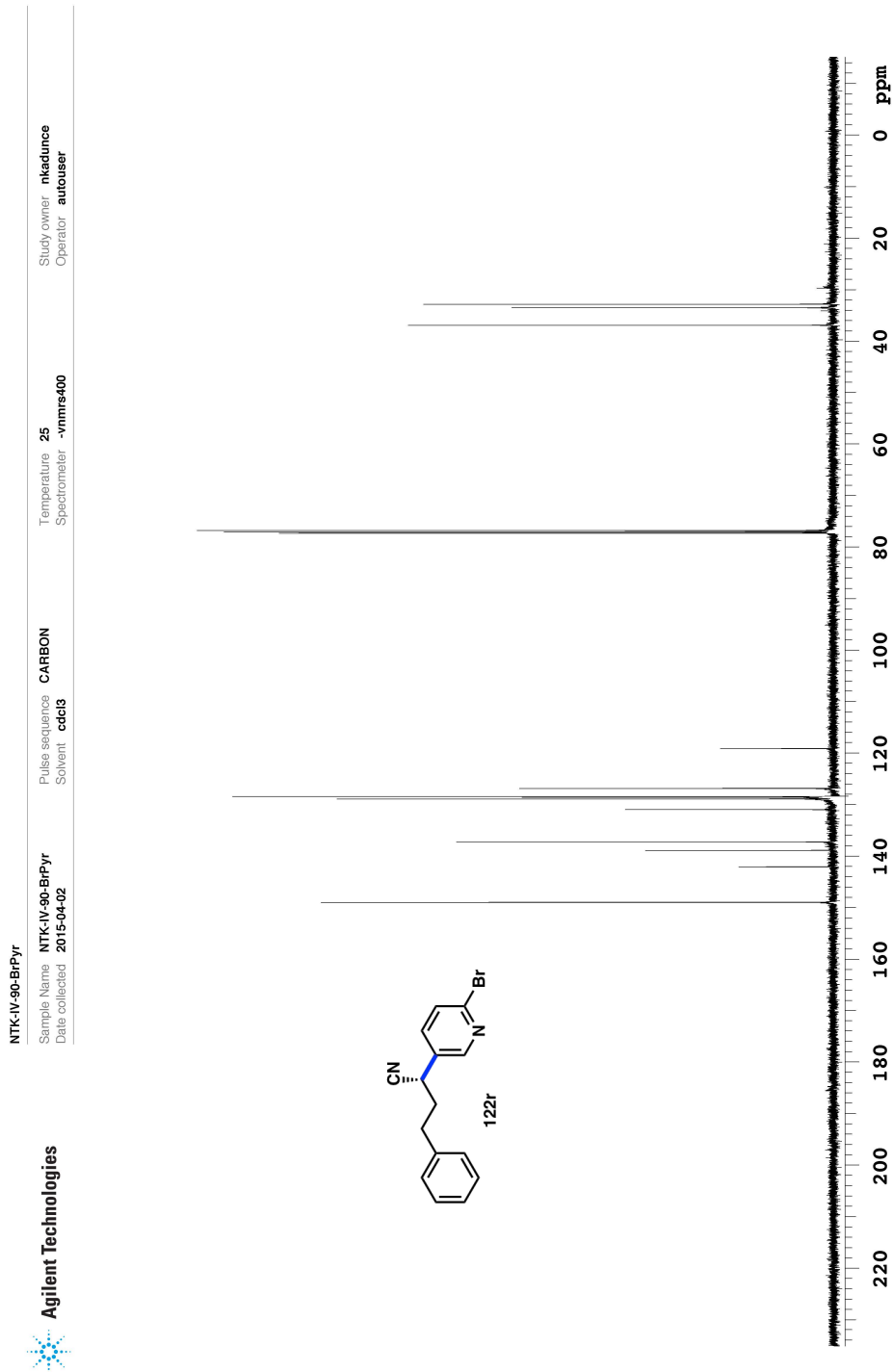
NTK-IV\_2ClPyr\_clean  
Sample Name NTK-IV\_2ClPyr\_clean  
Date collected 2015-05-17  
Pulse sequence CARBON  
Solvent cdcl3  
Temperature 25  
Spectrometer -vnmrs400  
Study owner nkadunce  
Operator autouser



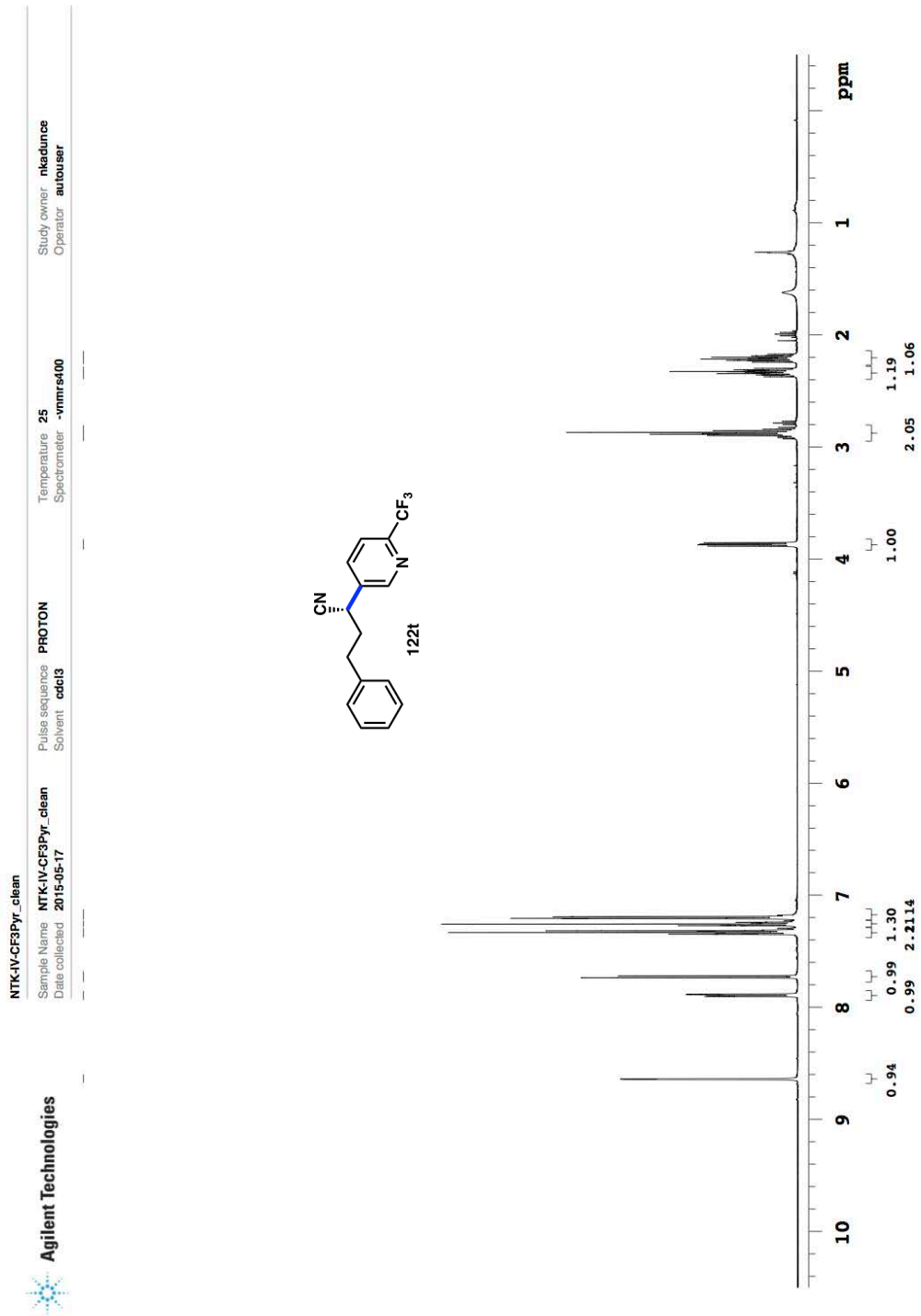
Plot date 2015-05-29

Data file j:\ndy\inkadunce\vnmsys\data\NTK-IV\_2ClPyr\_clean\CARBOND1.fid



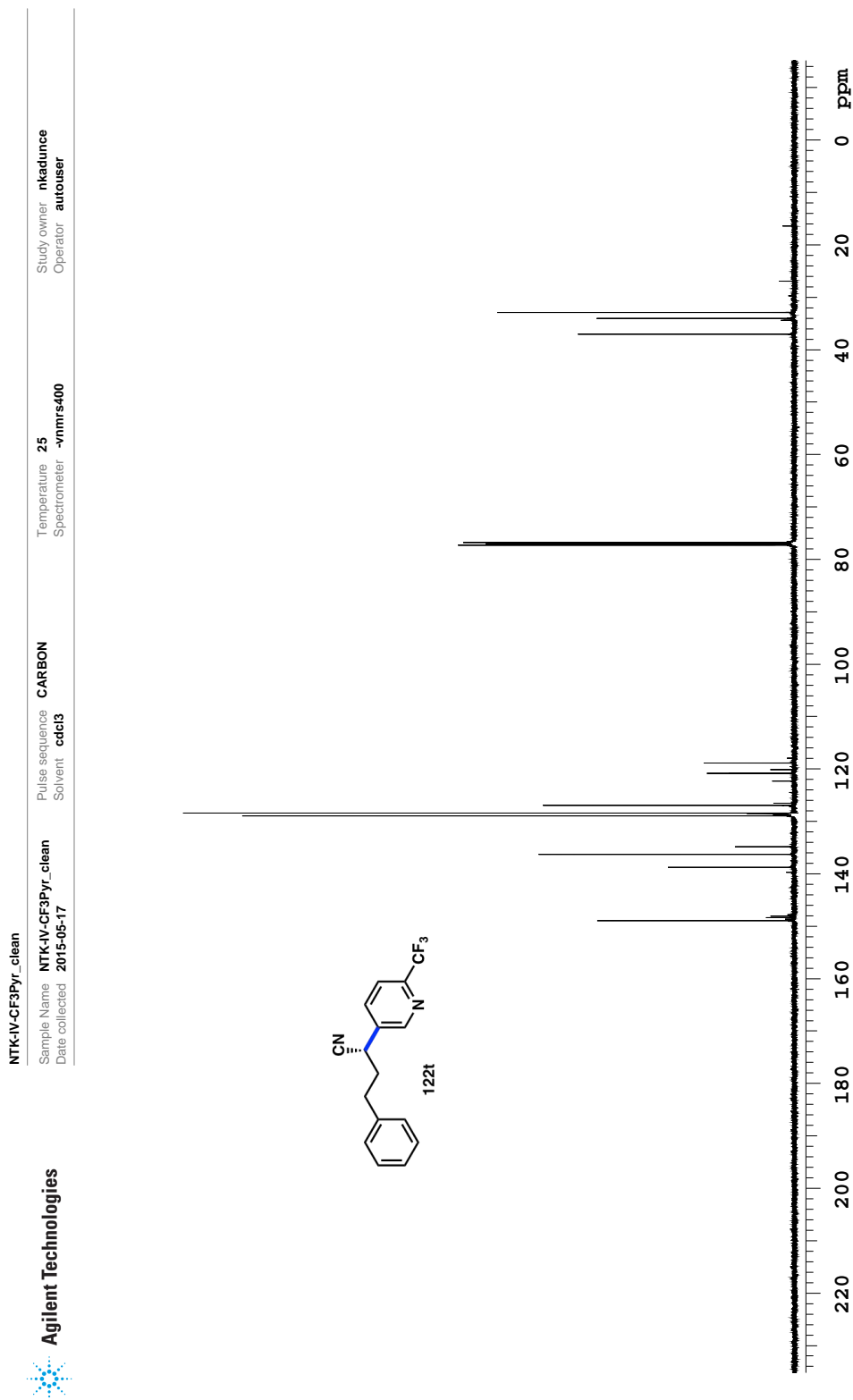


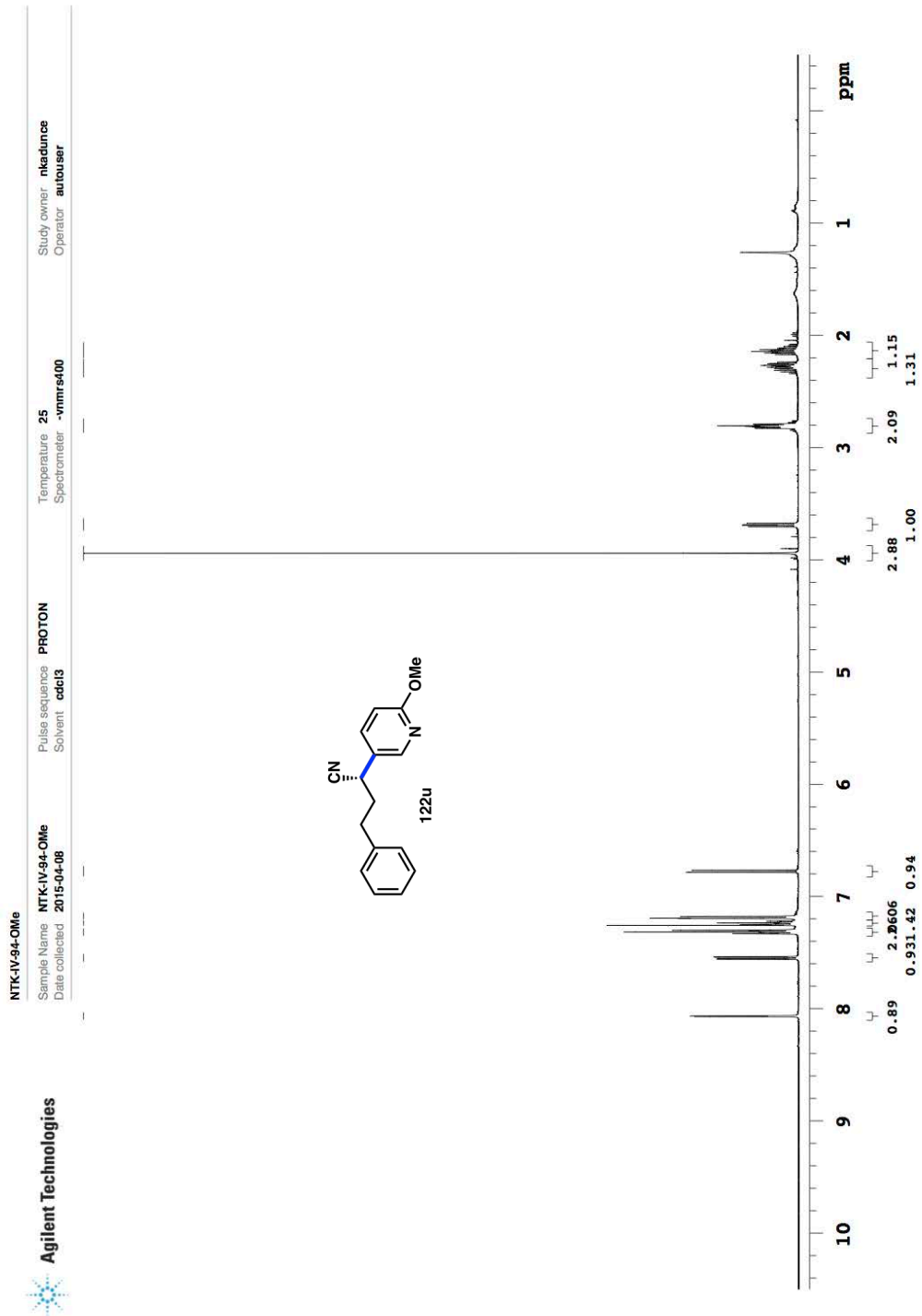
Data file: /ind/nkaadunce/vnmrsys/data/NTK-IV-90-BfPyr/CARBON01.fid  
Plot date: 2015-05-29



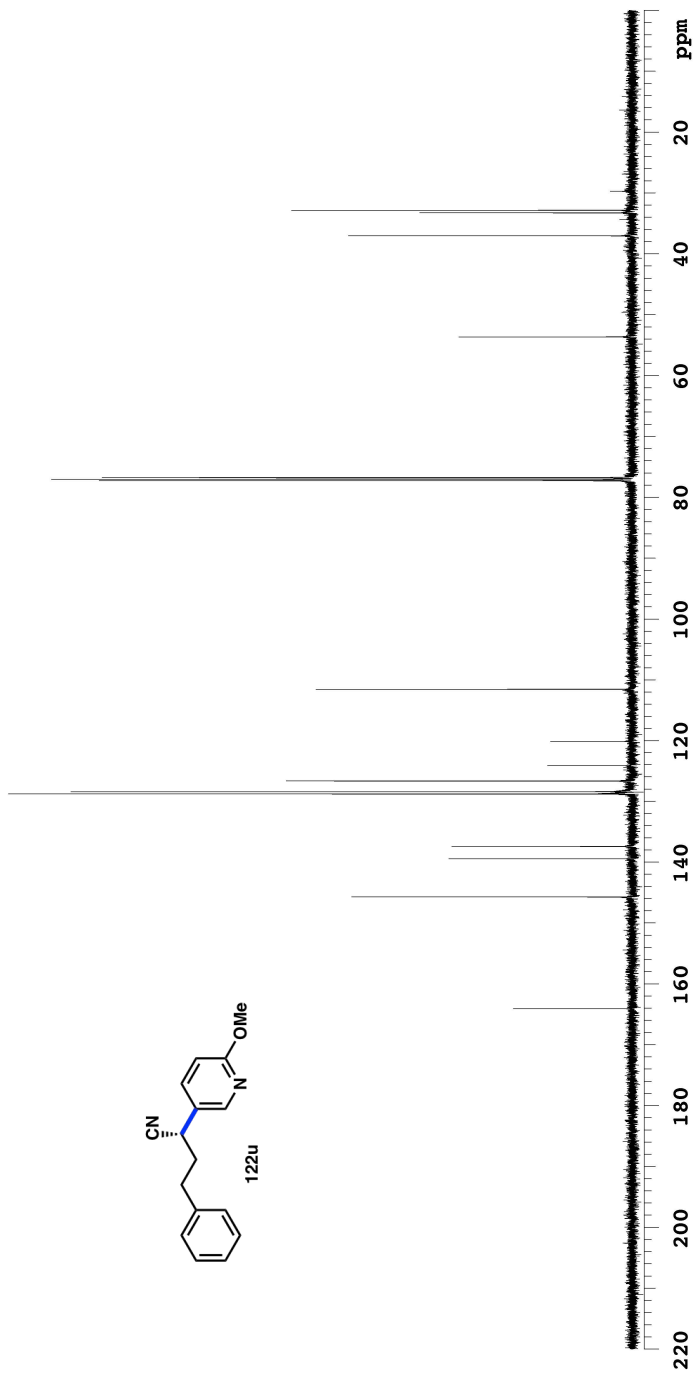
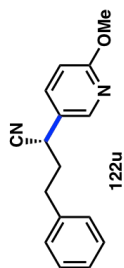
Plot date 2015-06-18

Data file /data/ndy/hkadunce/vnmrsys/data/NTK-IV-CF3Pyr\_clean/PROTON01.fid





NTK-IV-94-OMe  
 Sample Name NTK-IV-94-OMe  
 Date collected 2015-04-08  
 Pulse sequence CARBON  
 Solvent cdc13  
 Temperature 25  
 Spectrometer -vnmrs400  
 Study owner nkaclunice  
 Operator autouser



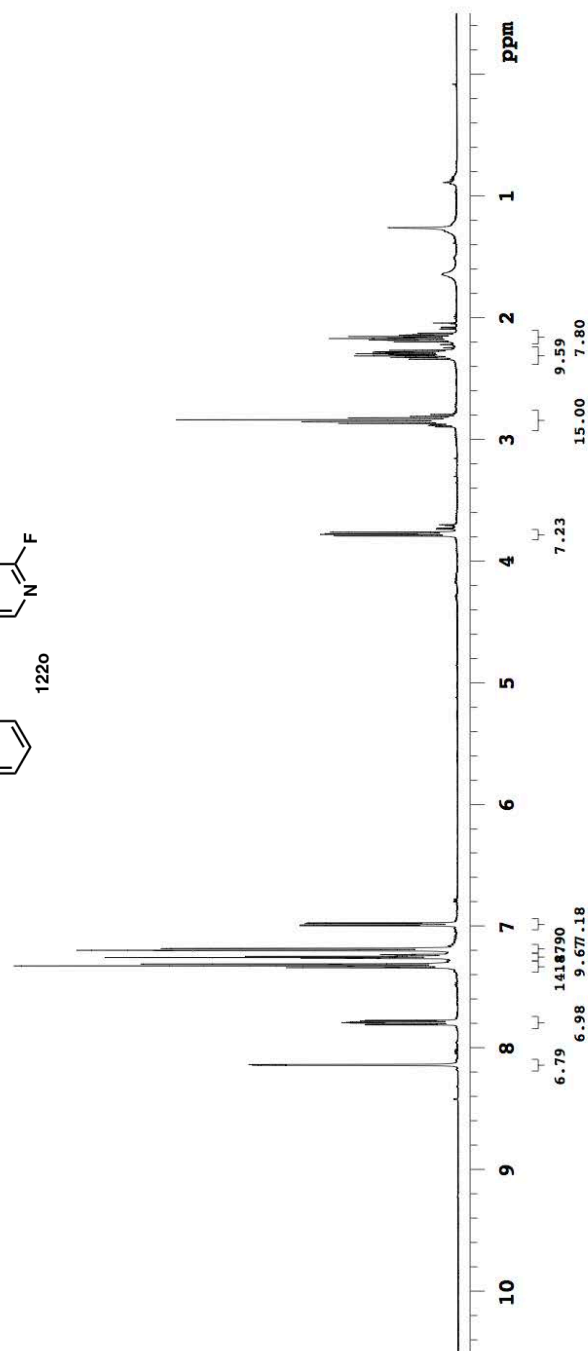
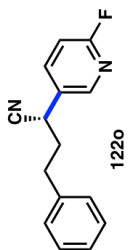
Data file f:\ndy\nkaclunice\vnmrs\data\NTK-IV-94-OMe\CARBON01.tid  
 Plot date 2015-05-29

**Agilent Technologies**

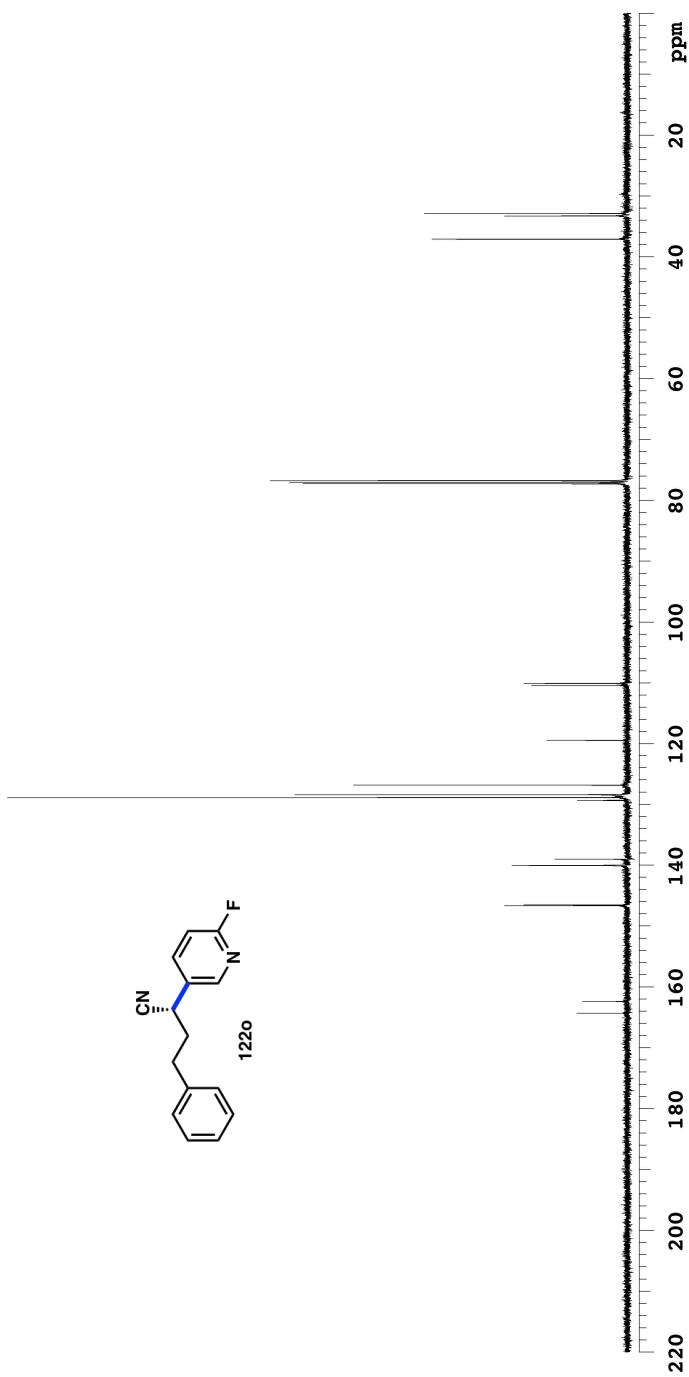
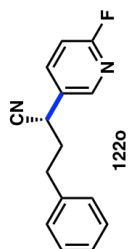
---

**NTK-IV-93-5Fpyridine**

Sample Name	NTK-IV-93-5Fpyridine	Pulse sequence	PROTON
Date collected	2015-04-07	Solvent	cdcl3
		Temperature	25
		Spectrometer	-vnmrs400
		Study owner	rhadunce
		Operator	autouser

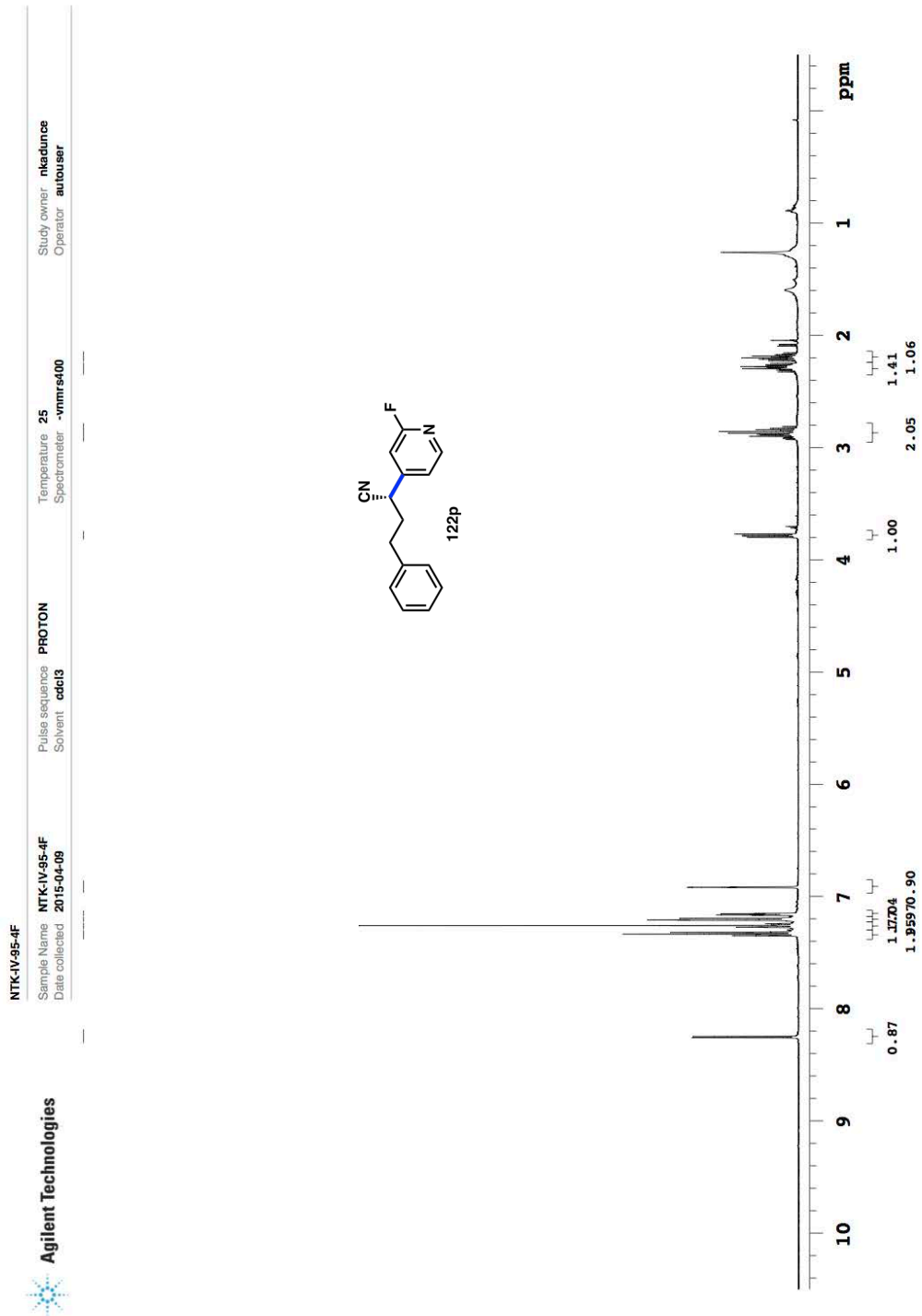


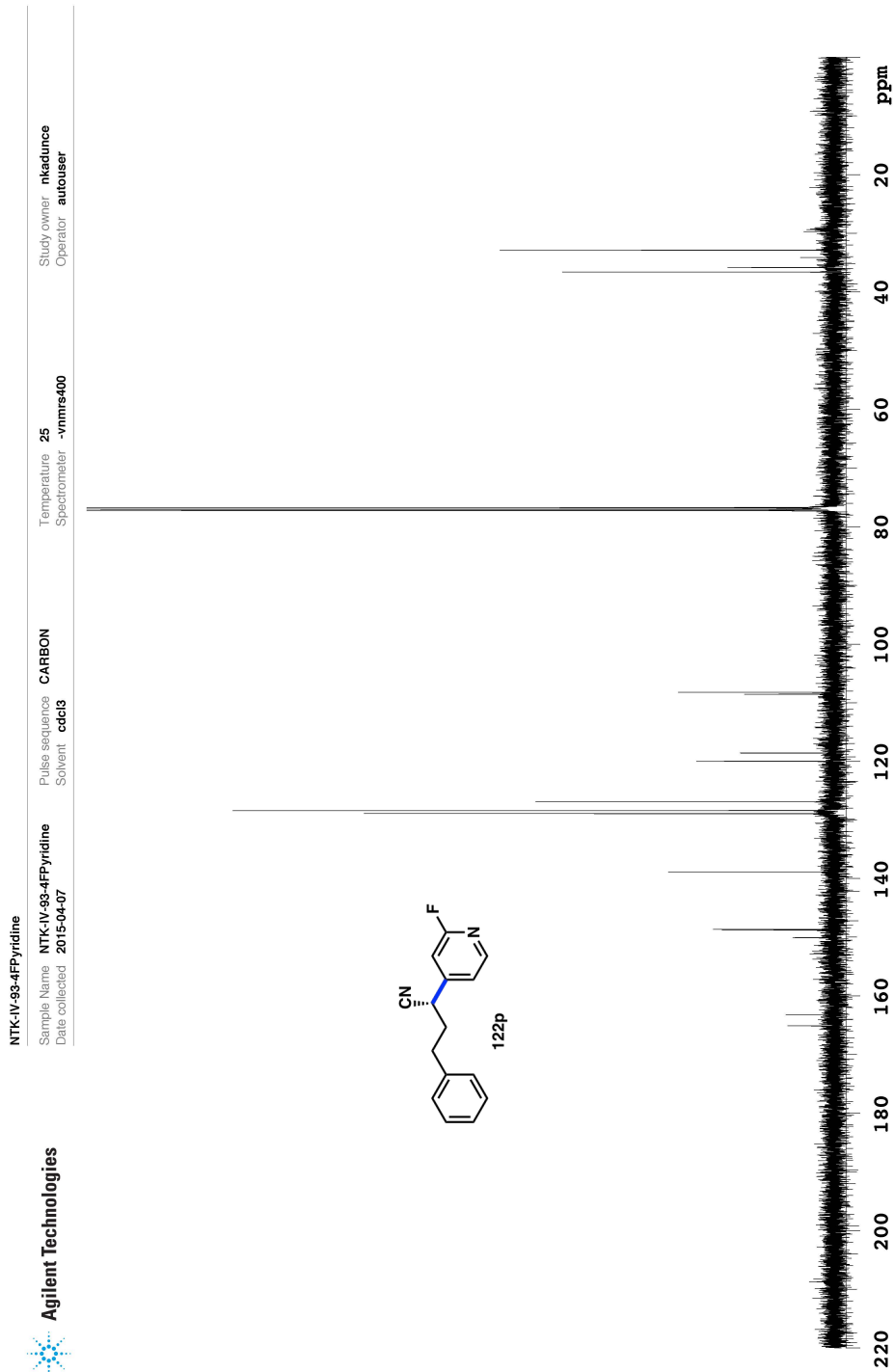
NTK-IV-93-5Pyridine  
 Sample Name NTK-IV-93-5Pyridine  
 Date collected 2015-04-07  
 Pulse sequence CARBON  
 Solvent cdc13  
 Temperature 25  
 Spectrometer -vms400  
 Study owner nkaclunce  
 Operator autouser



Plot date 2015-05-29

Data file /ind/nkaclunce/vmmsys\data/NTK-IV-93-5Pyridine/CARBON01.tid





Plot date 2015-05-29

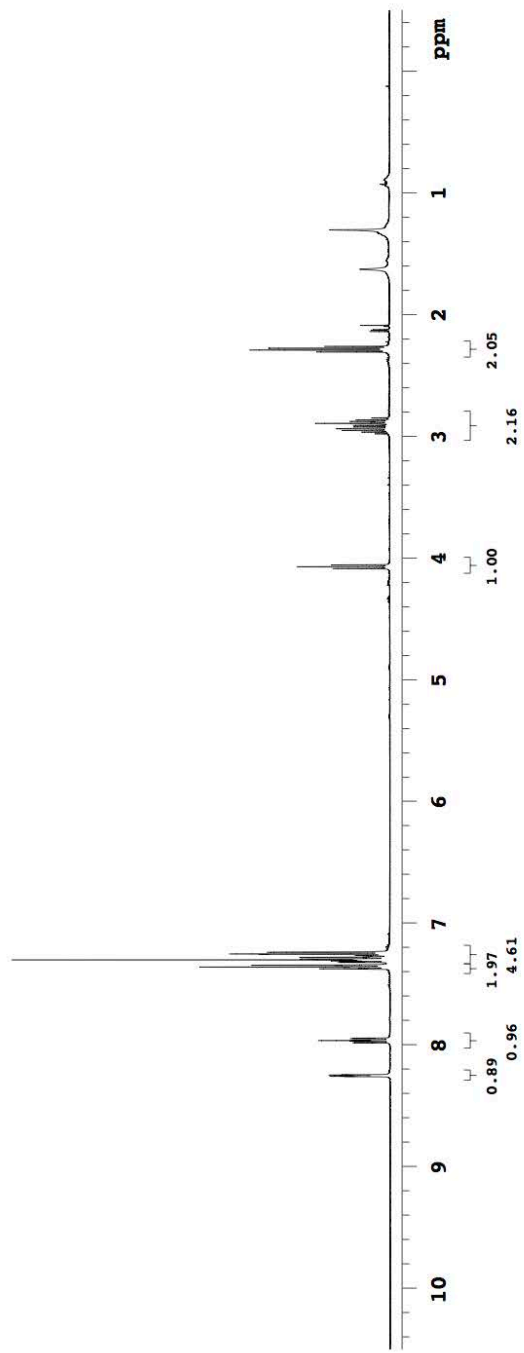
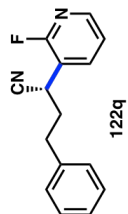
Data file: /ind/nkaadunce/vmsms/data/NTK-IV-93-4FPyridine/CARBON01.fid

**Agilent Technologies**

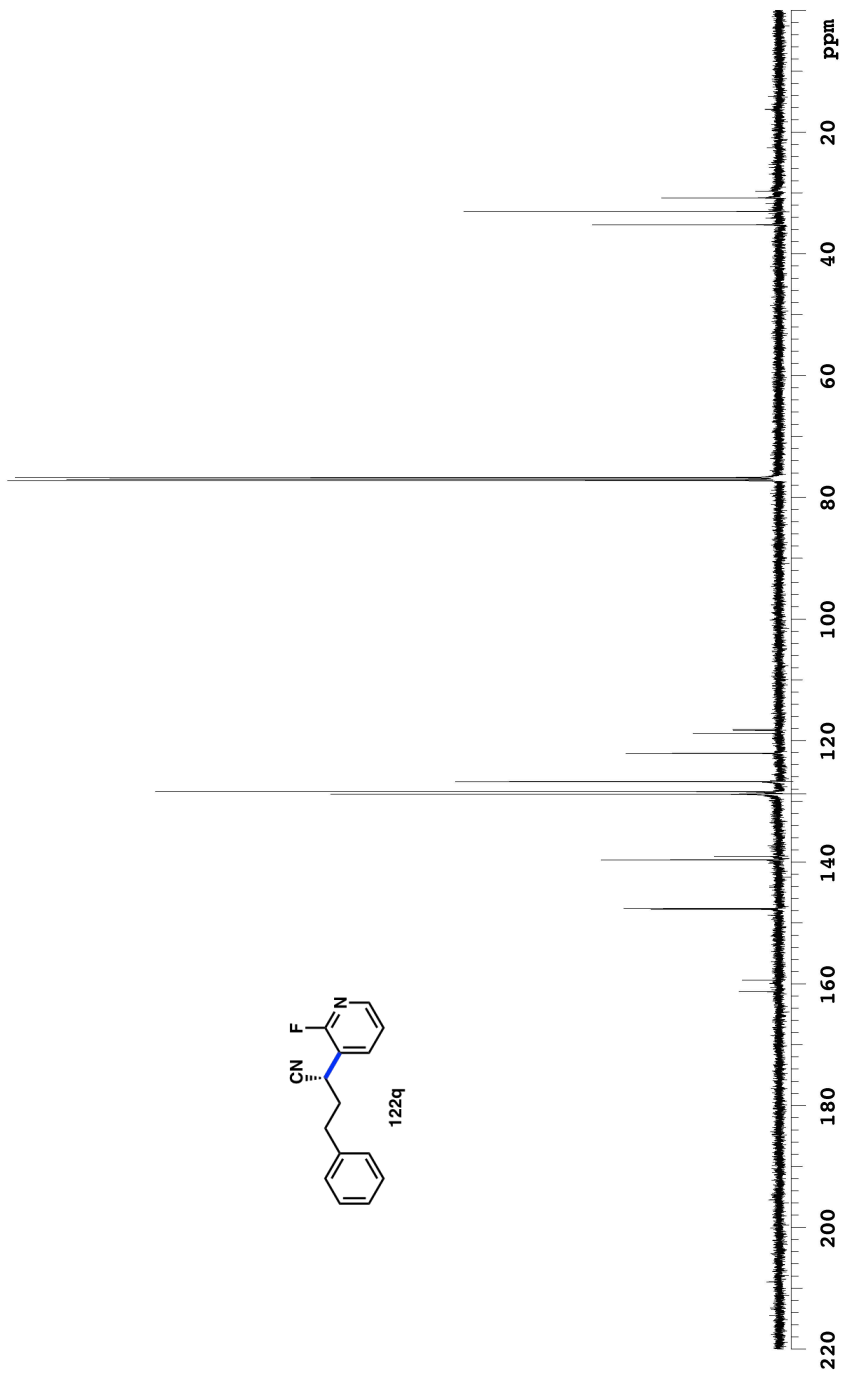
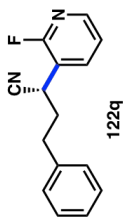
---

**NTK-IV-94-orthoF**

Sample Name	NTK-IV-94-orthoF	Pulse sequence	PROTON	Study owner	rheadunce
Date collected	2015-04-12	Solvent	cdcl3	Operator	autouser
		Temperature	25		
		Spectrometer	-vnmr500		

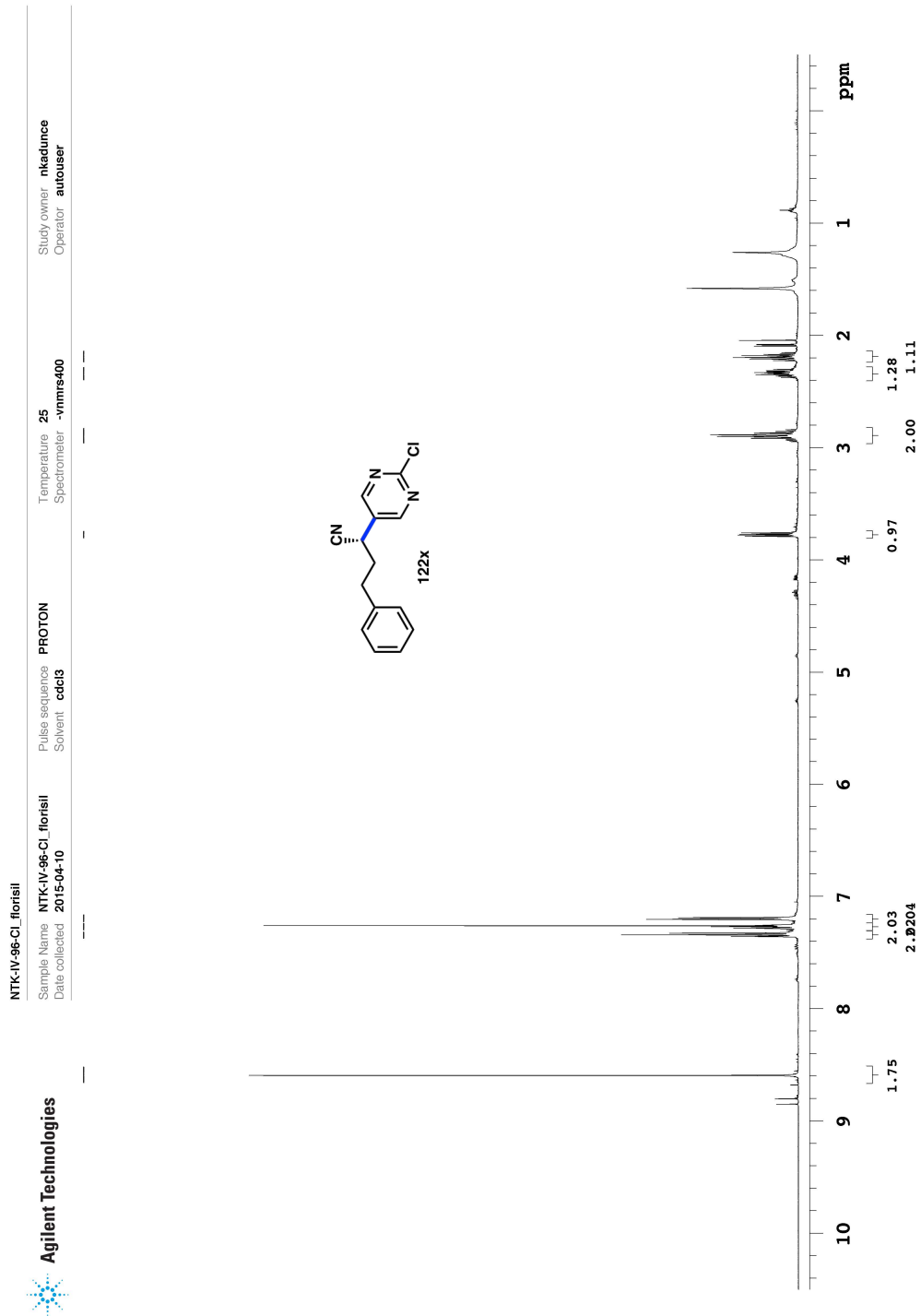


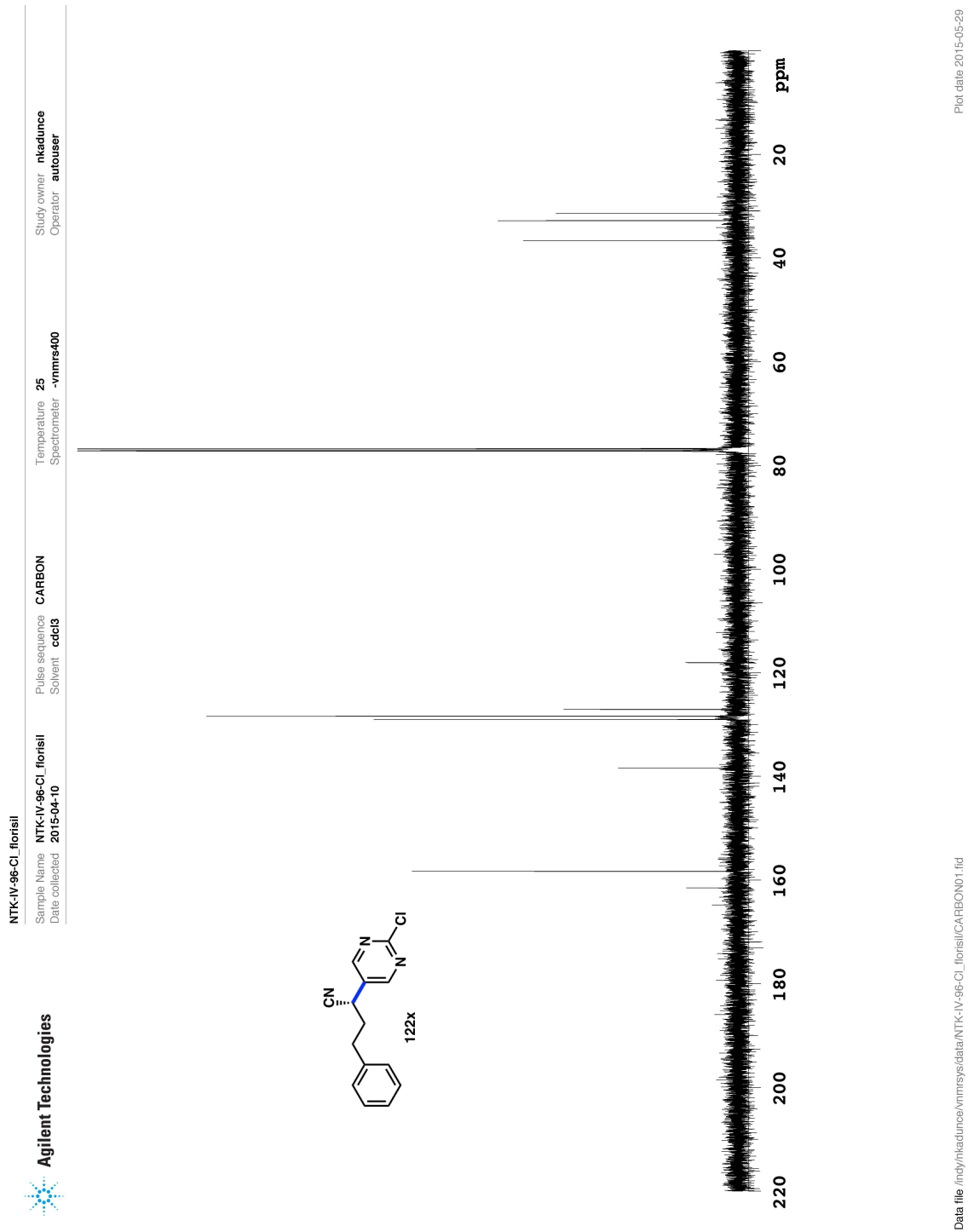
NTK-IV-94-orthoF  
 Sample Name NTK-IV-94-orthoF  
 Date collected 2015-04-08  
 Pulse sequence CARBON  
 Solvent cdc13  
 Temperature 25  
 Spectrometer -vnmrs400  
 Study owner nkaclunce  
 Operator autouser

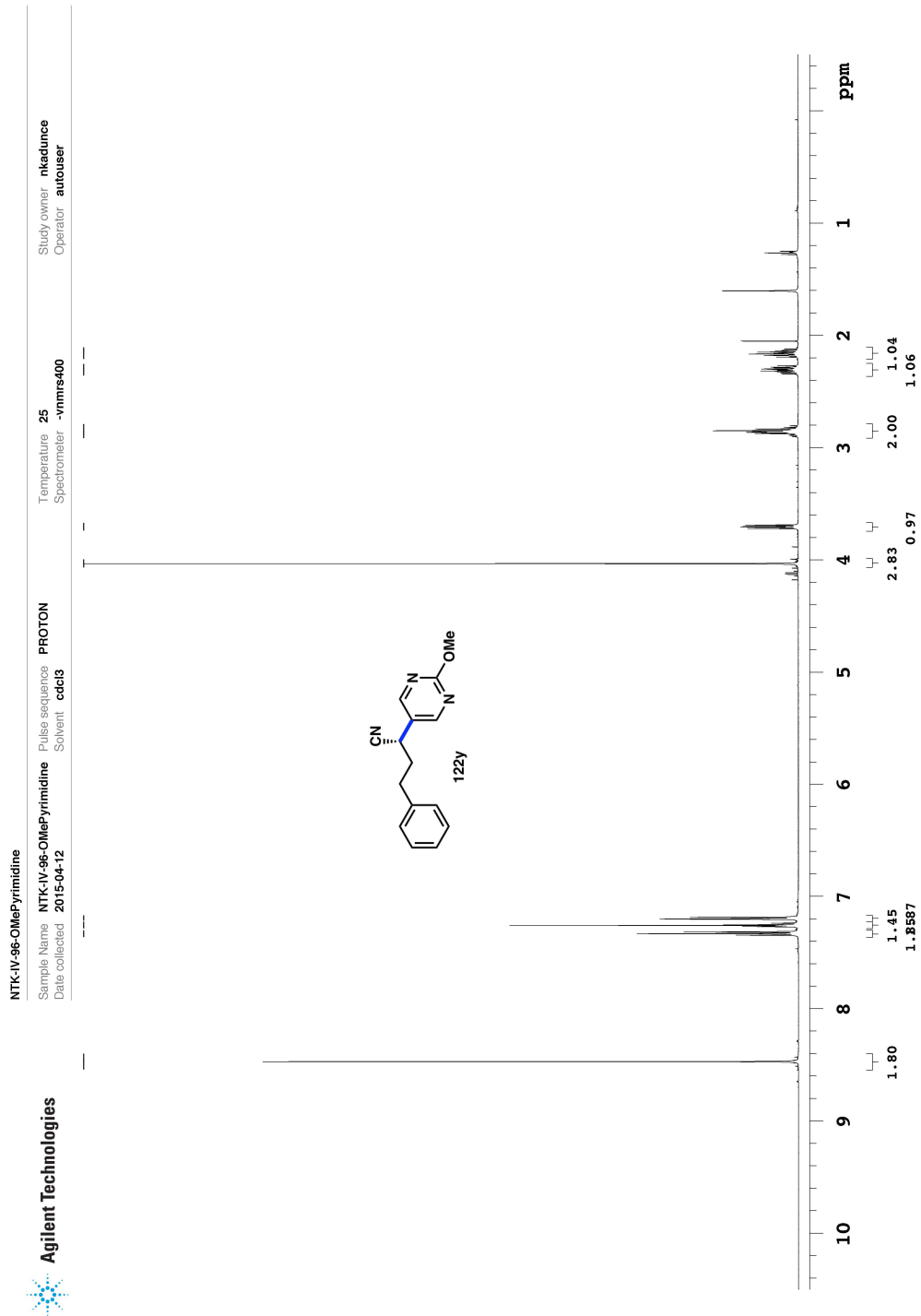


Plot date 2015-05-29

Data file /ind/nkaclunce/vnmrsys/data/NTK-IV-94-orthoF/CARBON01.fid

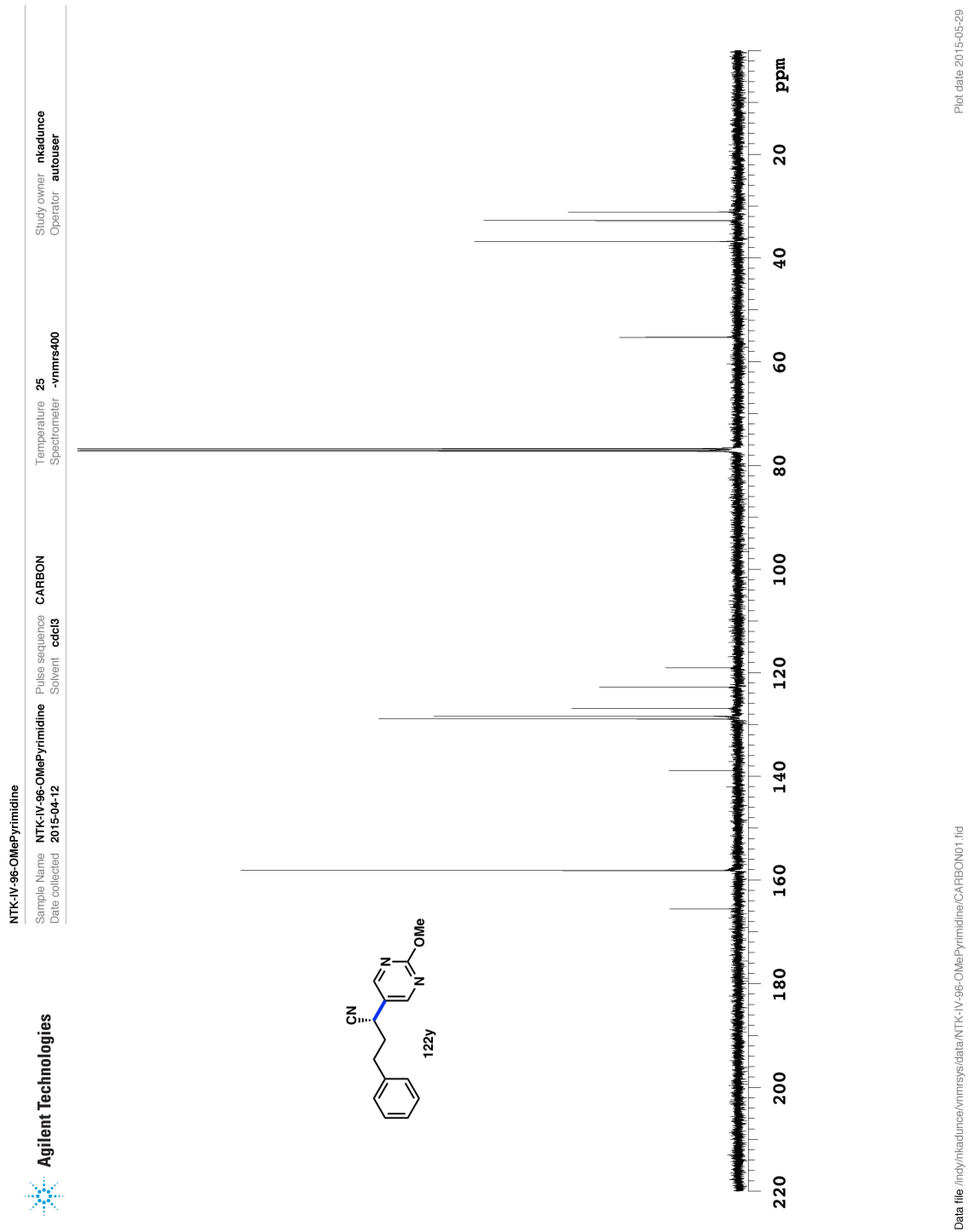


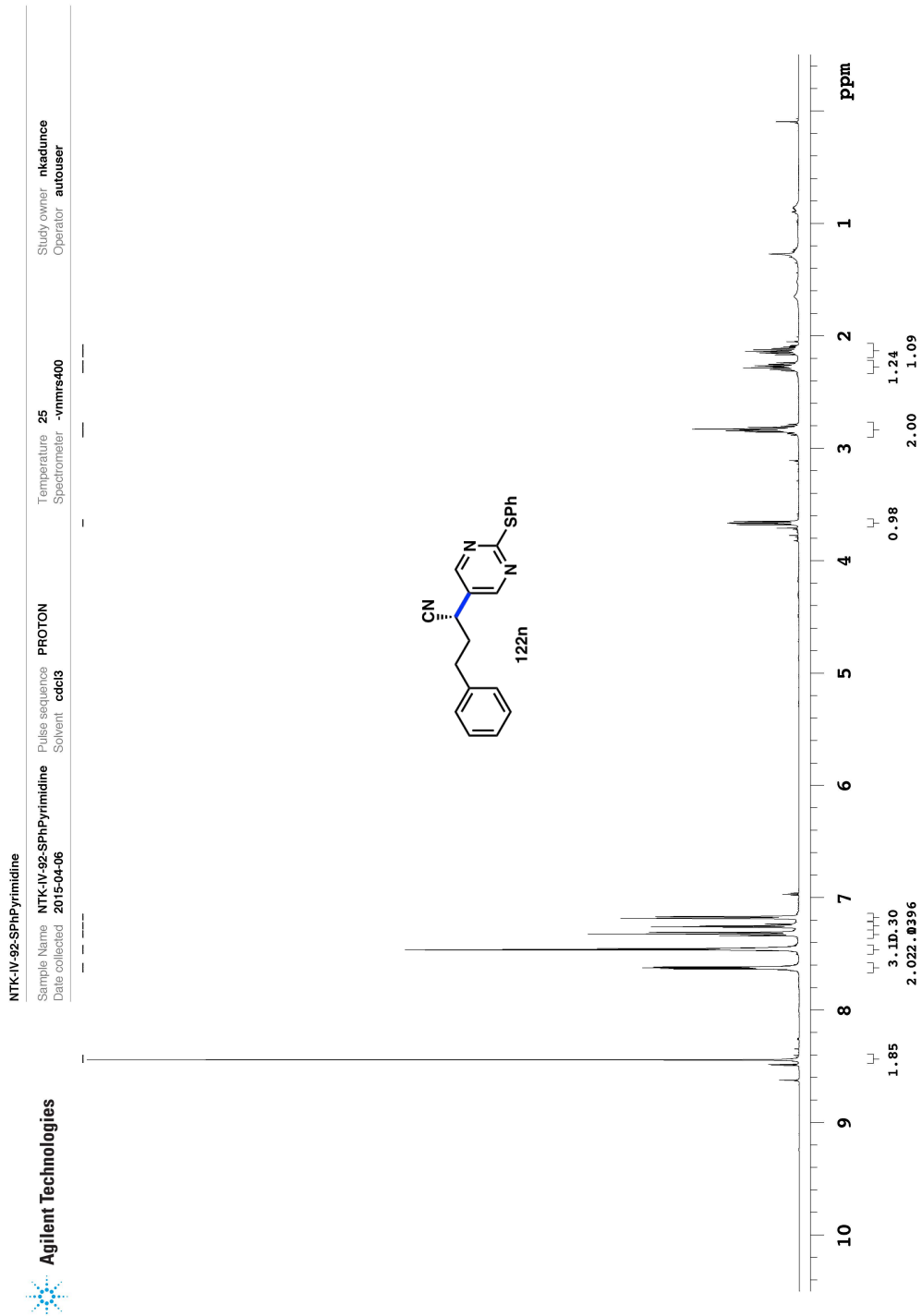




Plot date: 2015-05-29

Data file: /ndy/nkadunce/vnmrsys/data/NTK-IV-96-OMePyrimidine/PROTON01.fid

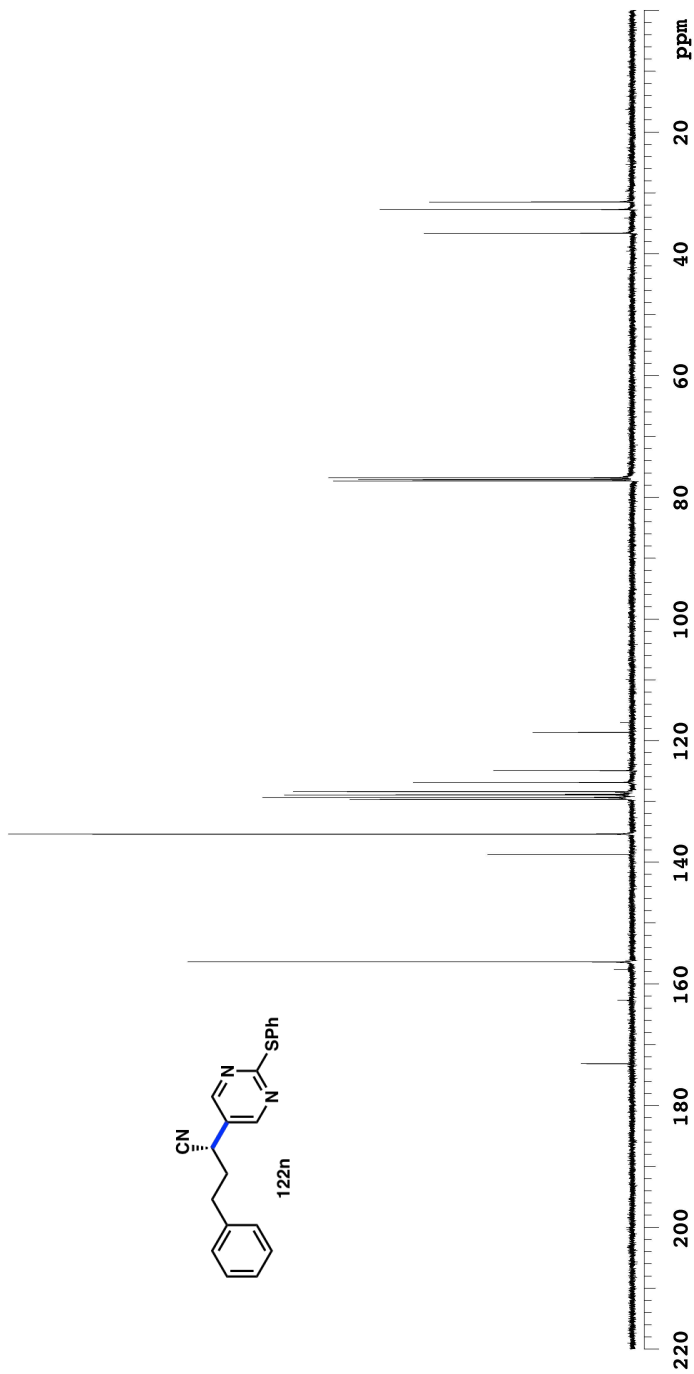
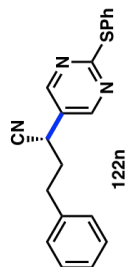




Plot date 2015-05-29

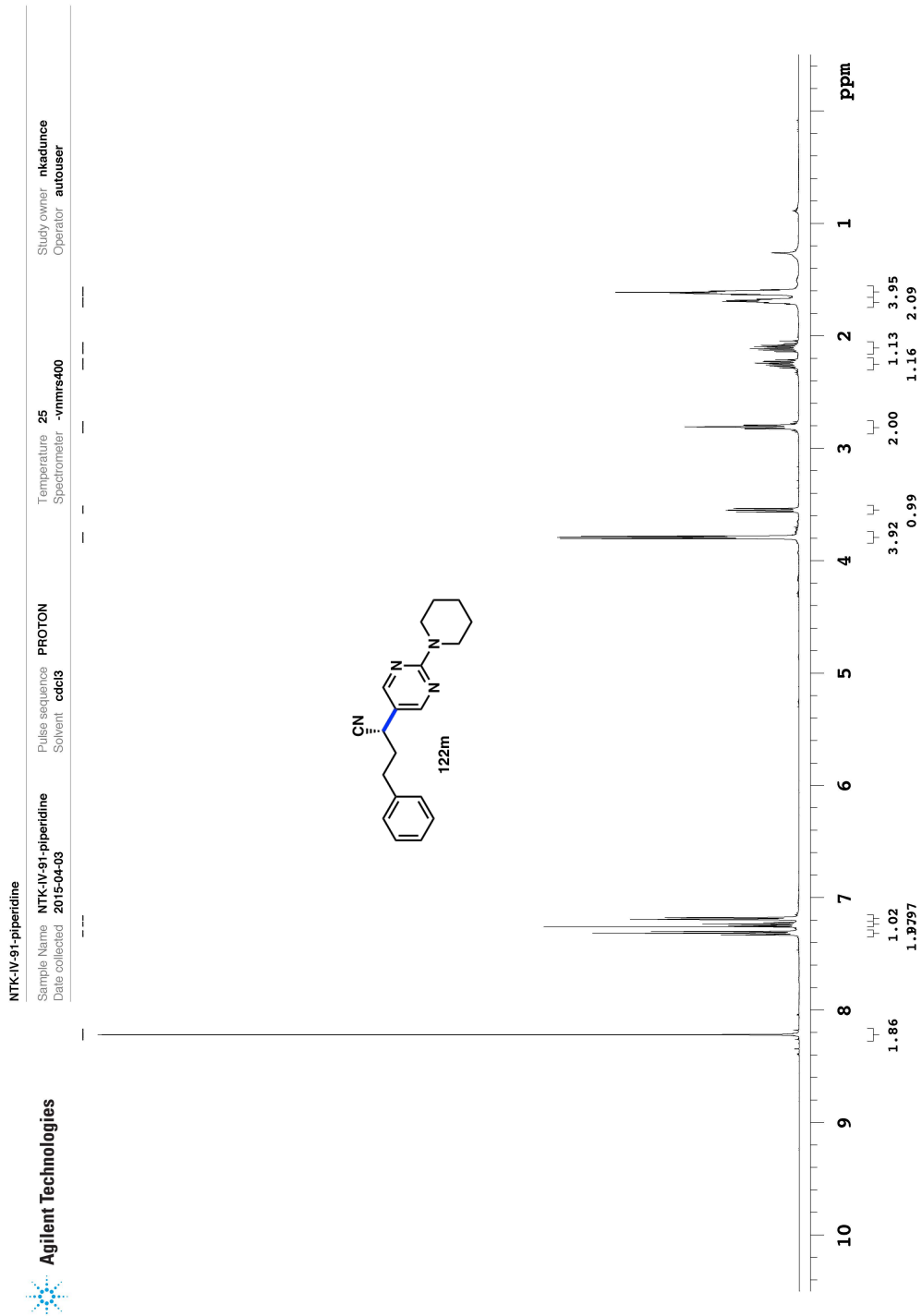
Data file: /ind/nkauduce/vmmsys/data/NTK-IV-92-SPhPyrimidine/PROTON01.fid

NTK-IV-92-SPhPyrimidine  
 Sample Name NTK-IV-92-SPhPyrimidine  
 Date collected 2015-04-06  
 Pulse sequence CARBON  
 Solvent cdcl3  
 Temperature 25  
 Spectrometer -vnmrs400  
 Study owner nkaclunice  
 Operator autouser



Plot date 2015-05-29

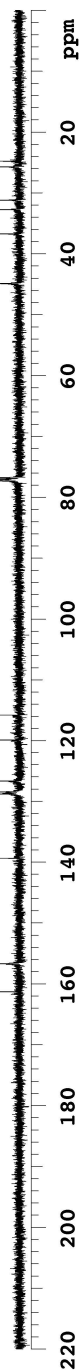
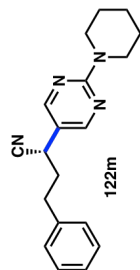
Data file f:\ndy\nkaclunice\vnmsys\data\NTK-IV-92-SPhPyrimidine\CARBON01.fid



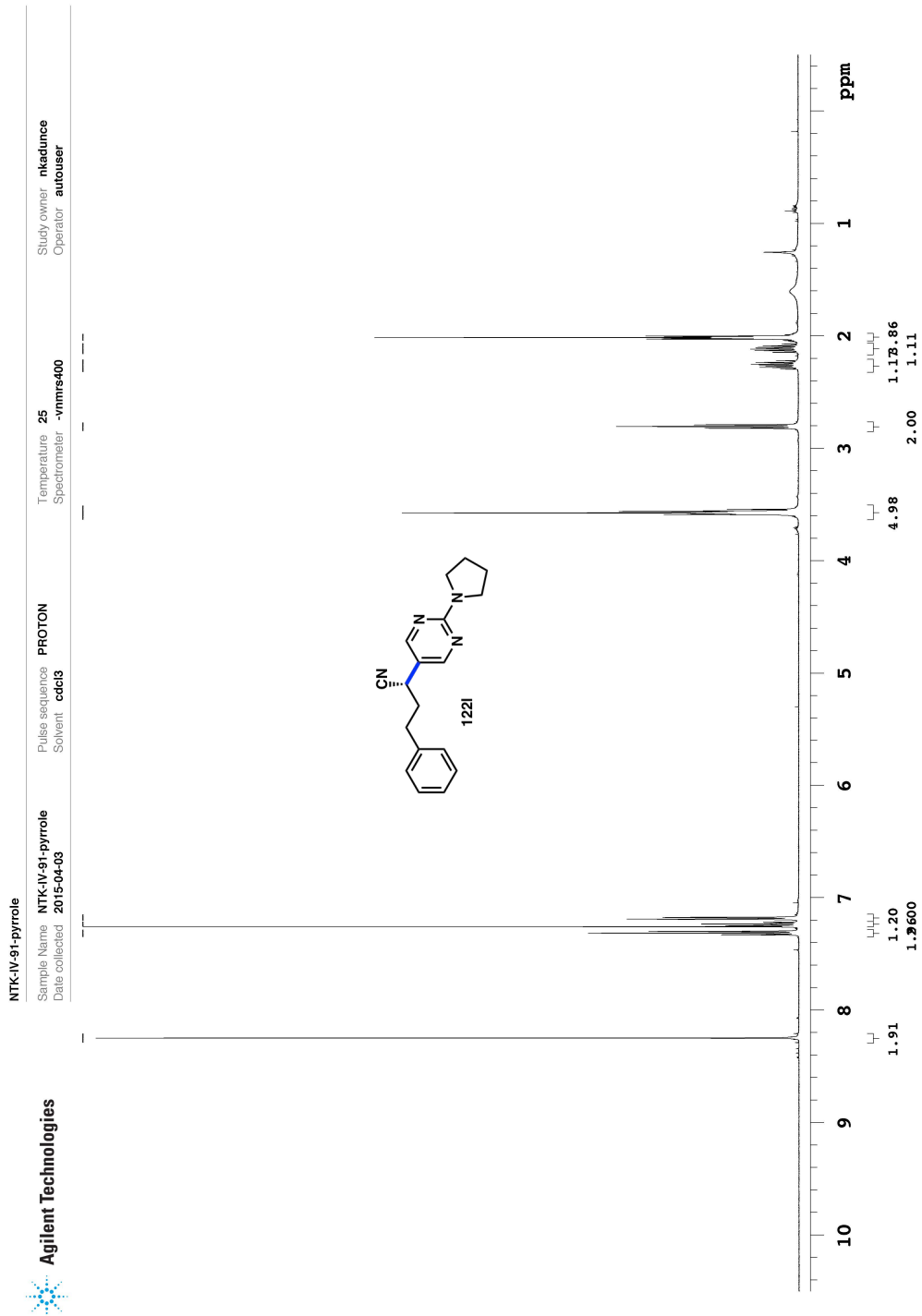
Plot date 2015-05-29

Data file: /ind/nkaadunce/vnmrsys\data/NTK-IV-91-piperidine/PROTON01.fid

NTK-IV-91-piperidine  
 Sample Name NTK-IV-91-piperidine  
 Date collected 2015-04-03  
 Pulse sequence CARBON  
 Solvent cdc13  
 Temperature 25  
 Spectrometer -vnmrs400  
 Study owner nkaclunce  
 Operator autouser



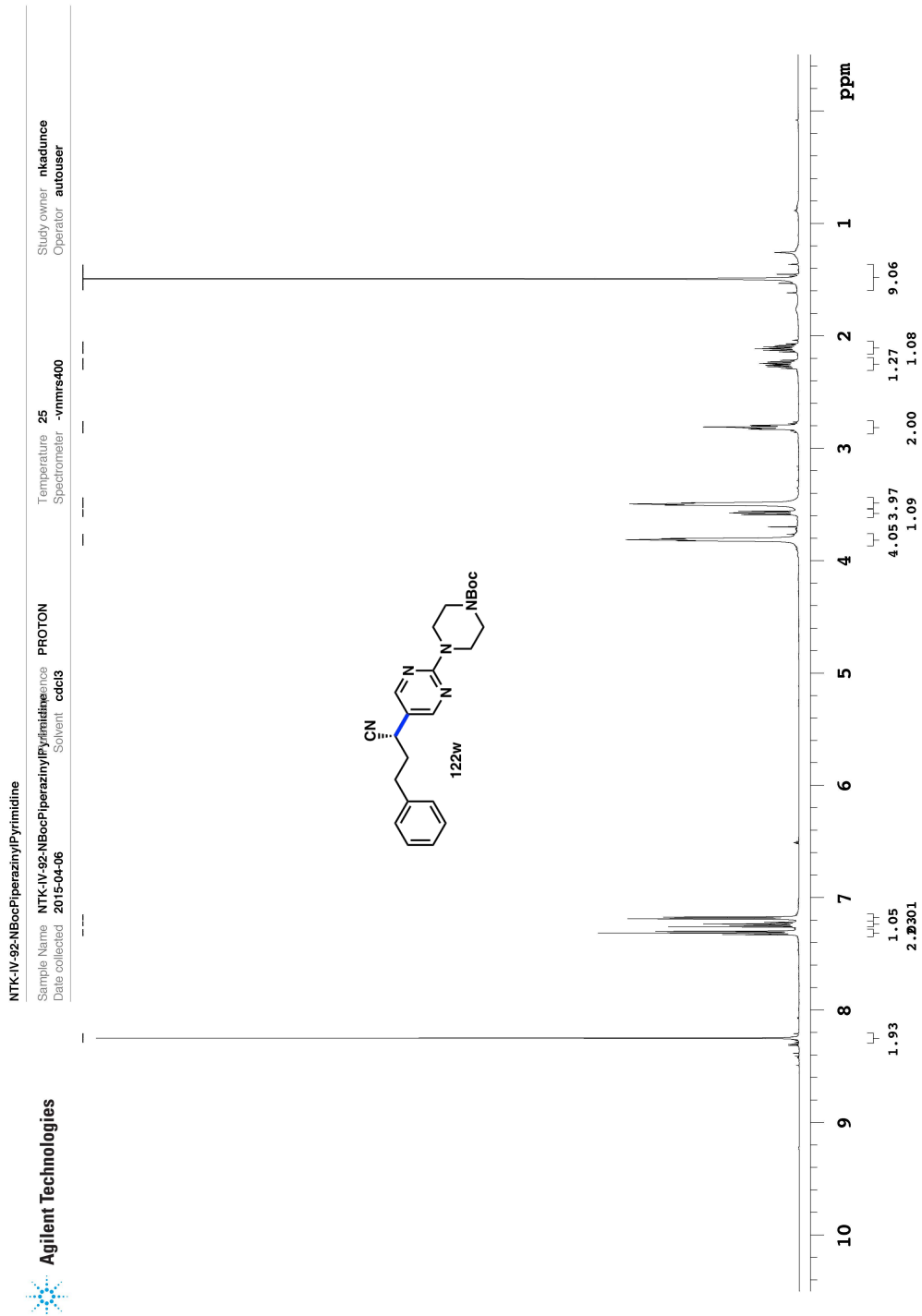
Data file f:\ndy\nkaclunce\vnmsys\data\NTK-IV-91-piperidine\CARBON01.fid  
 Plot date 2015-05-29



Plot date 2015-05-29

Data file: /ind/nkaadunce/vnmrsys\data/NTK-IV-91-pyrrole/PROTON01.fid

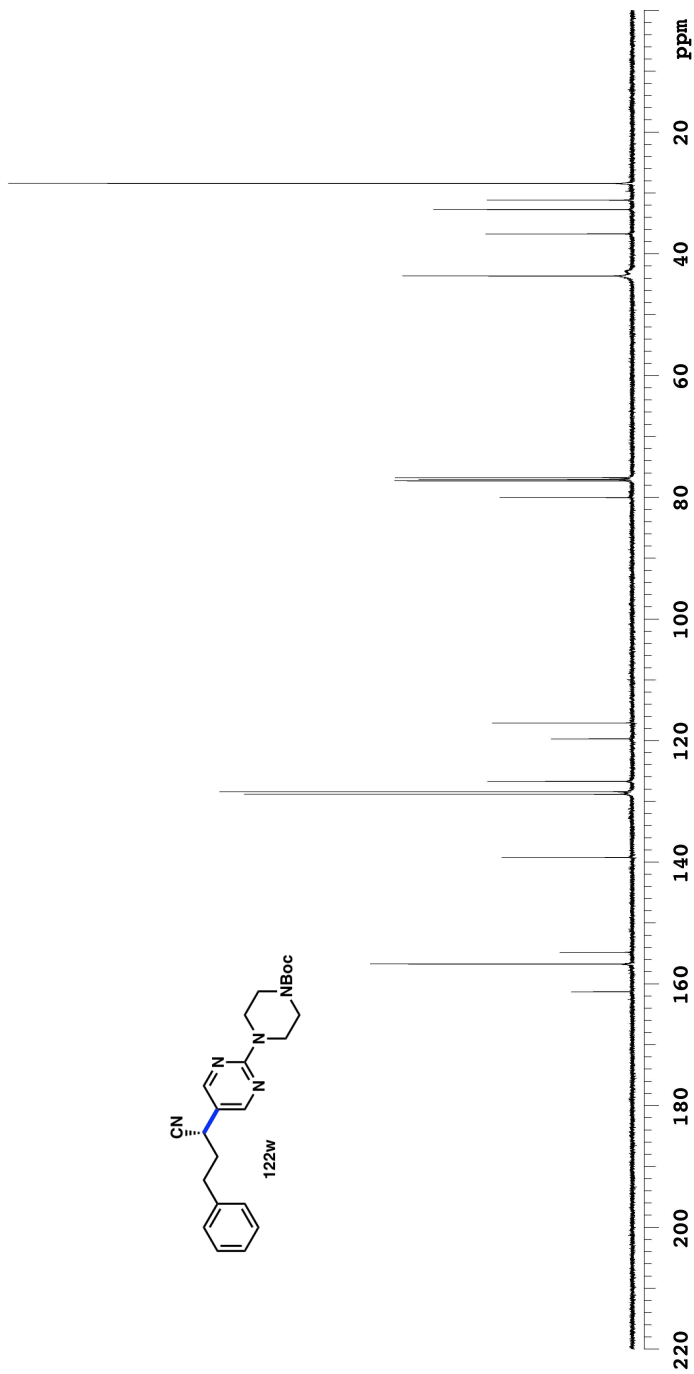
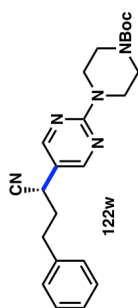




Plot date 2015-05-29

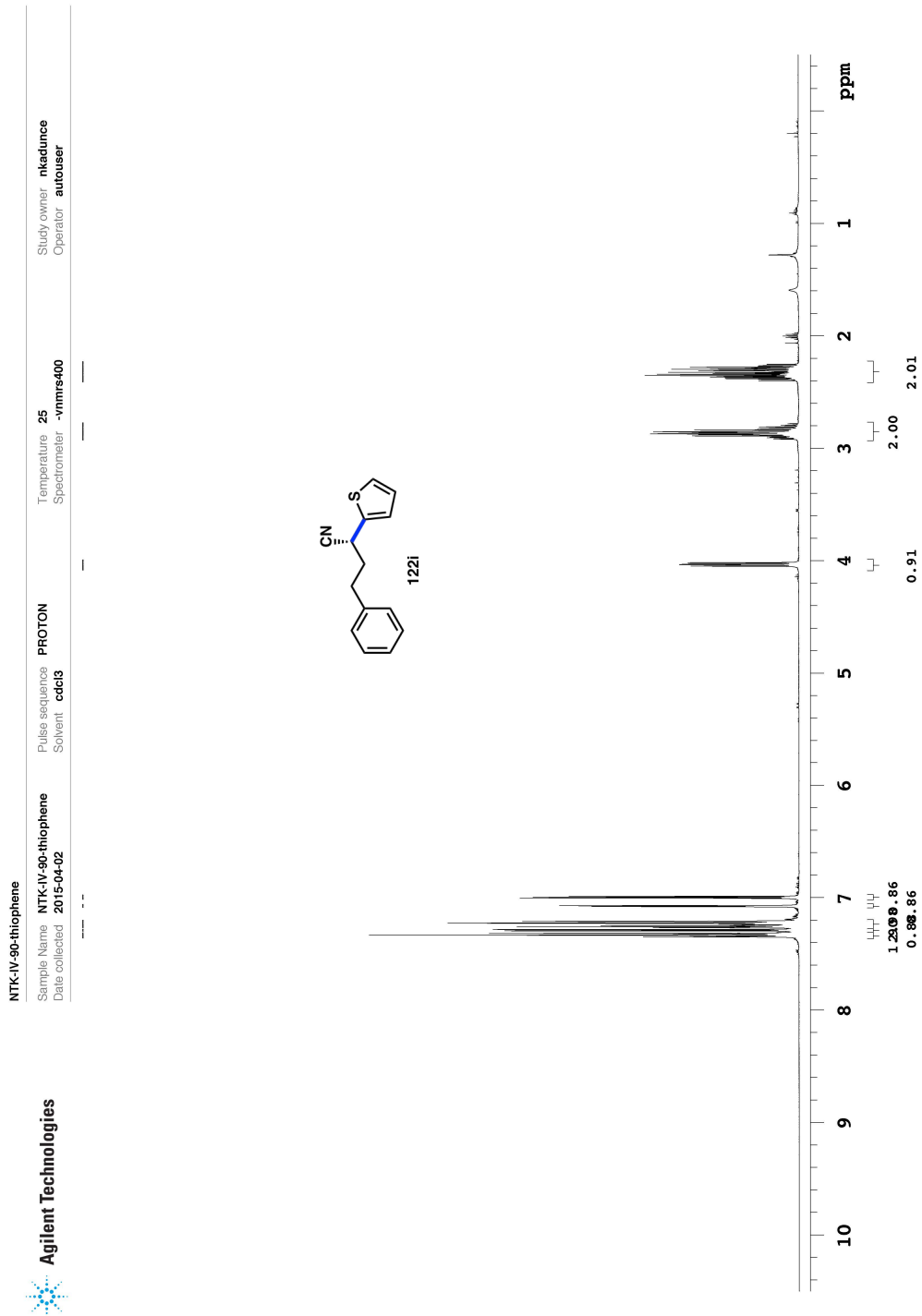
Data file: /ind/nkaadunce/vrmsys/data/NTK-IV-92-NBocPiperazinyPyrimidine/PROTON01.tid

NTK-IV-92-NBocPiperazinyPyrimidine  
 Sample Name NTK-IV-92-NBocPiperazinyPyrimidine  
 Date collected 2015-04-06  
 Temperature Spectrometer 25 -vrms400  
 Solvent cdc13  
 Study owner nkaadunce  
 Operator autouser



Plot date 2015-05-29

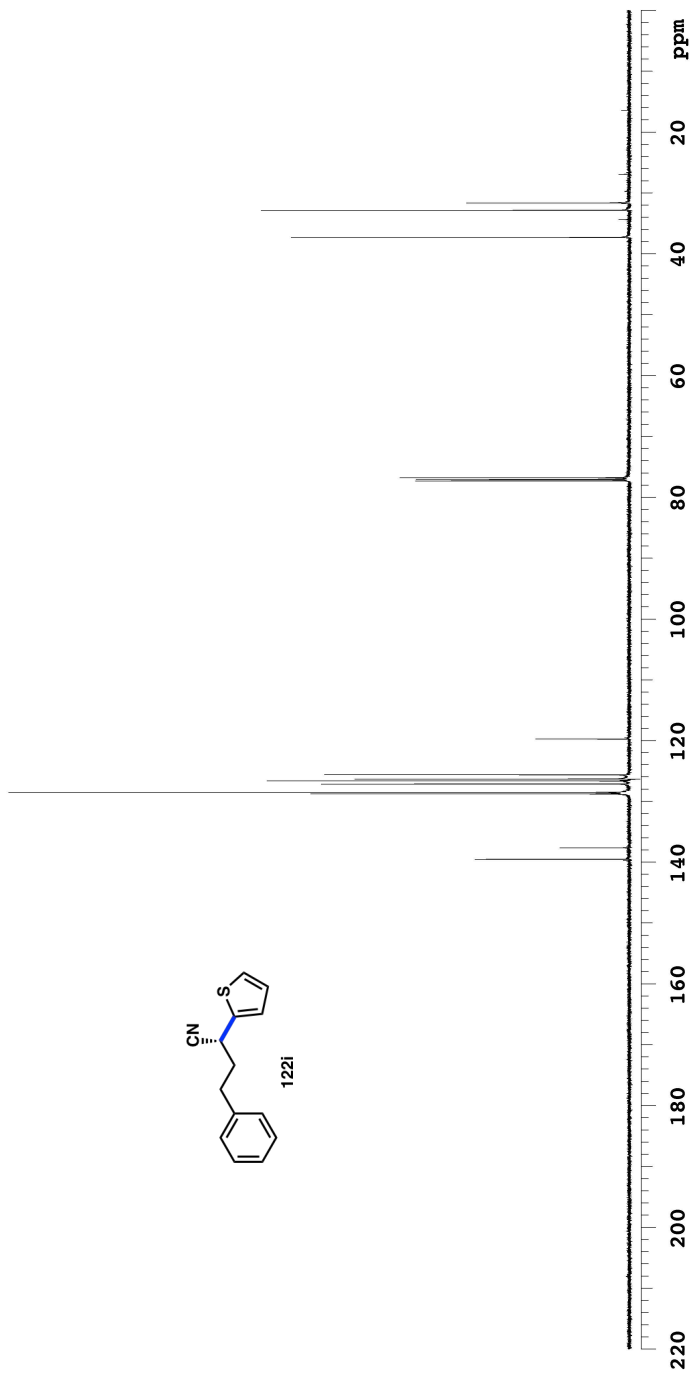
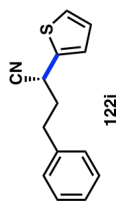
Data file /find/nkaadunce/vrmsys\data/NTK-IV-92-NBocPiperazinyPyrimidine/CARBON01.tid



Plot date 2015-05-29

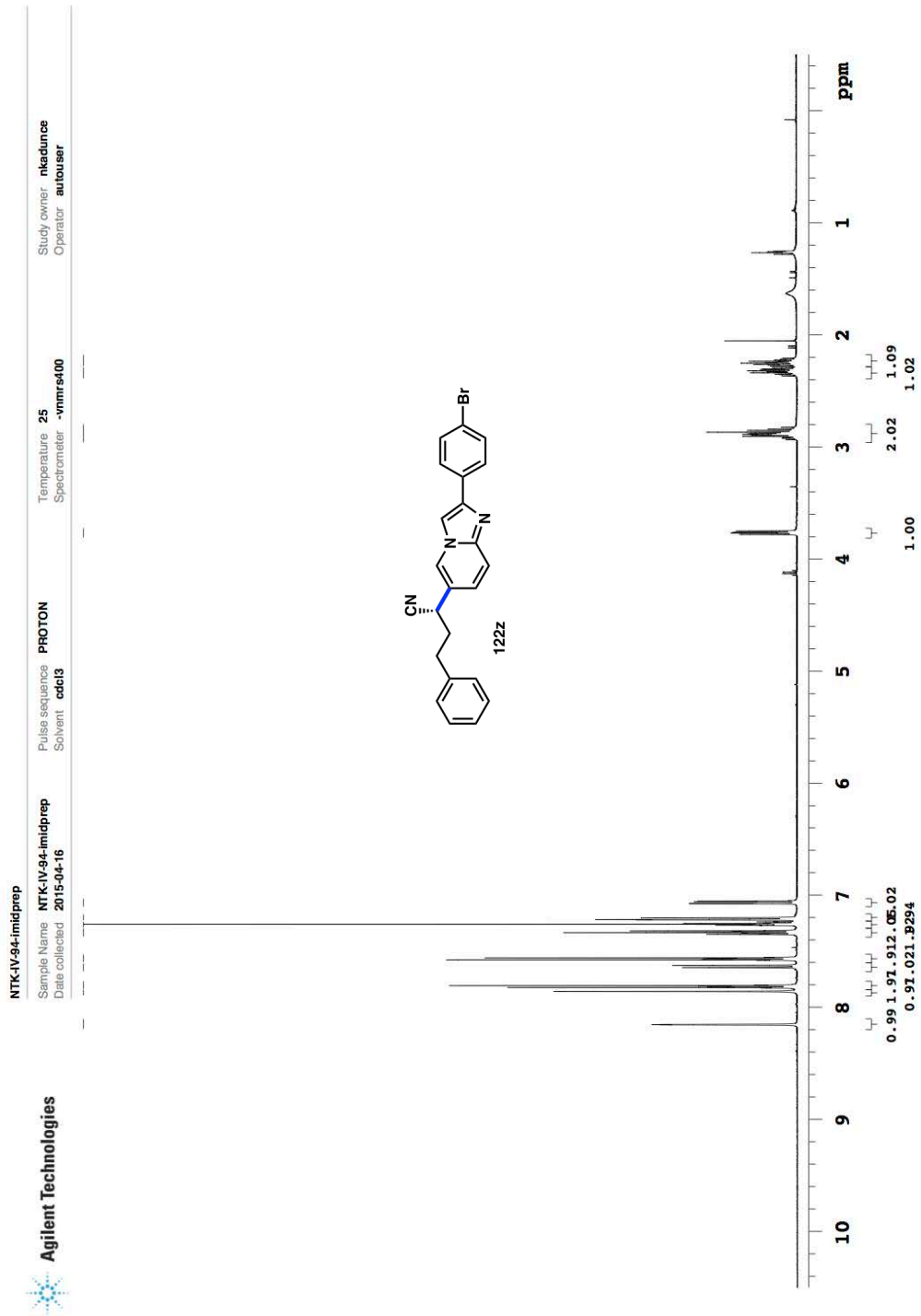
Data file: /ind/nkaadunce/vnmrsys/data/NTK-IV-90-thiophene/PROTON01.fid

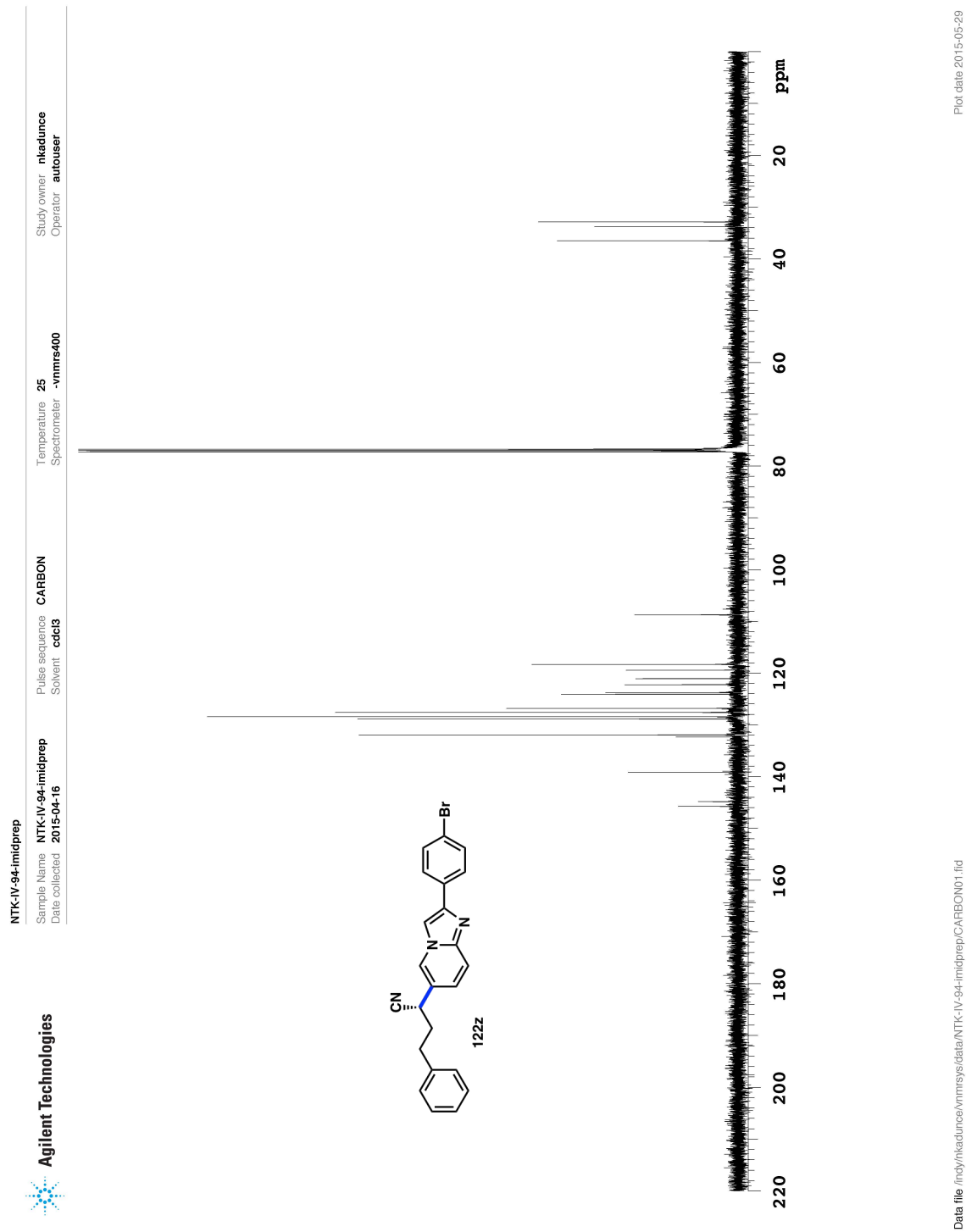
NTK-IV-90-thiophene  
 Sample Name NTK-IV-90-thiophene  
 Date collected 2015-04-02  
 Pulse sequence CARBON  
 Solvent cdc13  
 Temperature 25  
 Spectrometer -vnmrs400  
 Study owner nkaclunce  
 Operator autouser

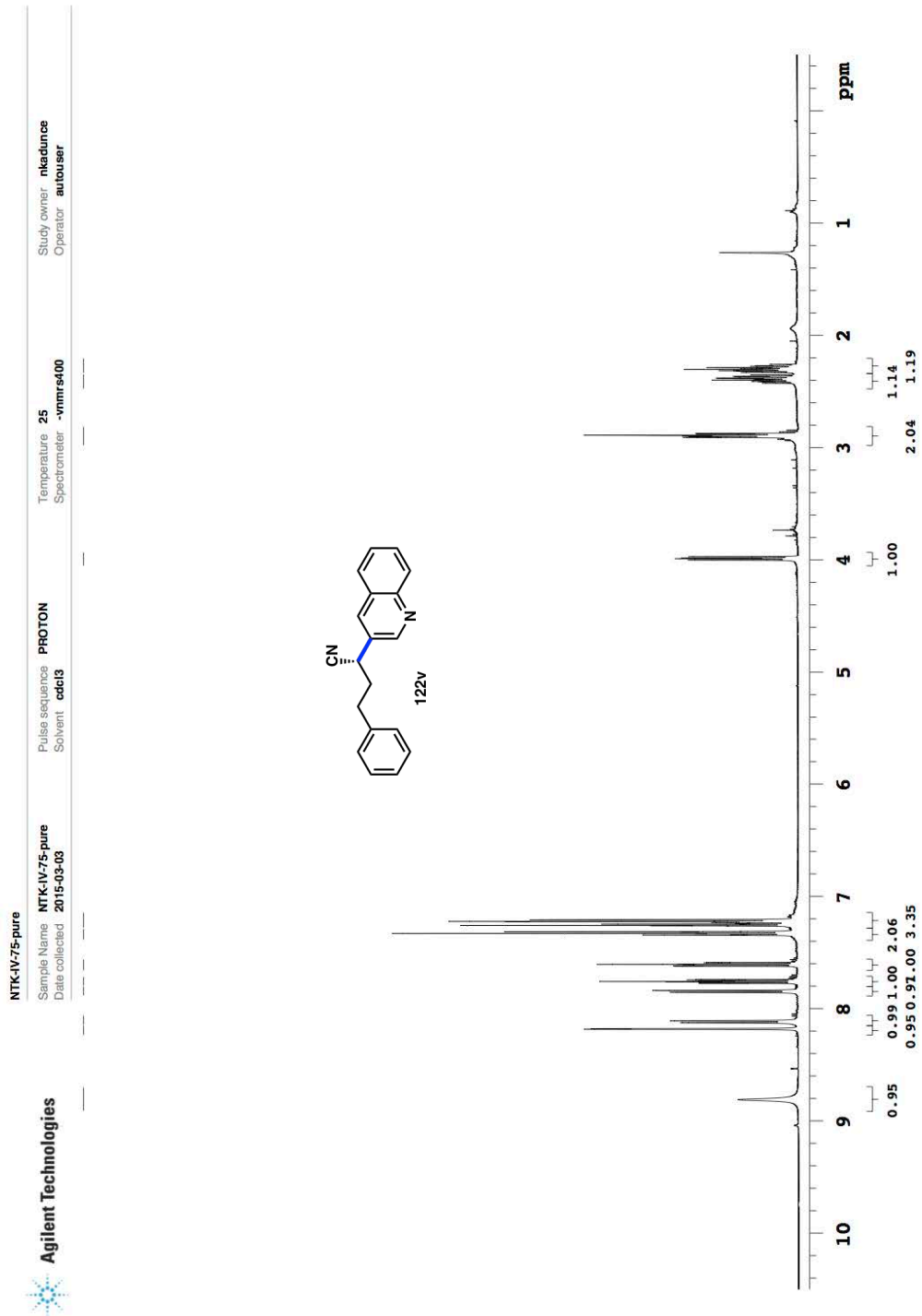


Plot date 2015-05-29

Data file f:\ndy\nkaclunce\vnmsys\data\NTK-IV-90-thiophene\CARBON01.fid



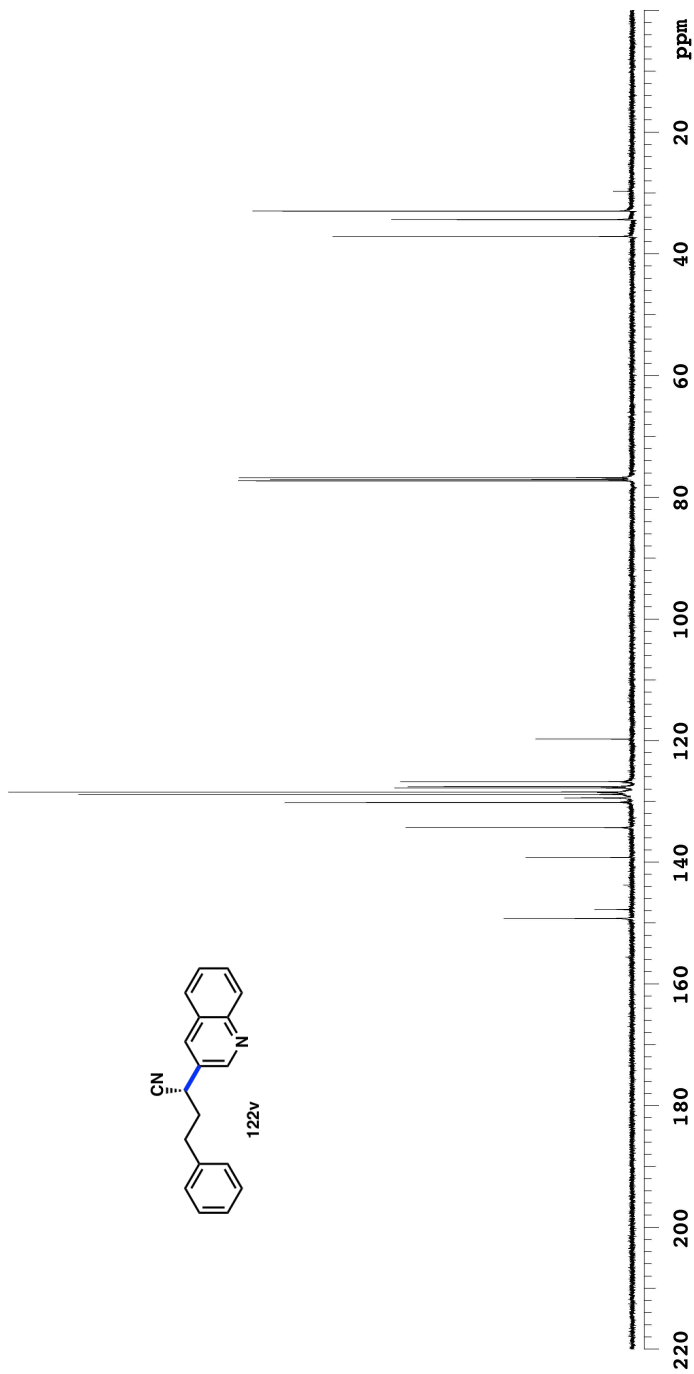
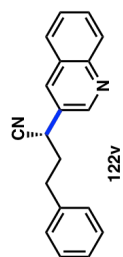




Data file /data/ndy/hadunce/vnmrsys/data/NTK-IV-75-pure/PROTON1.fid

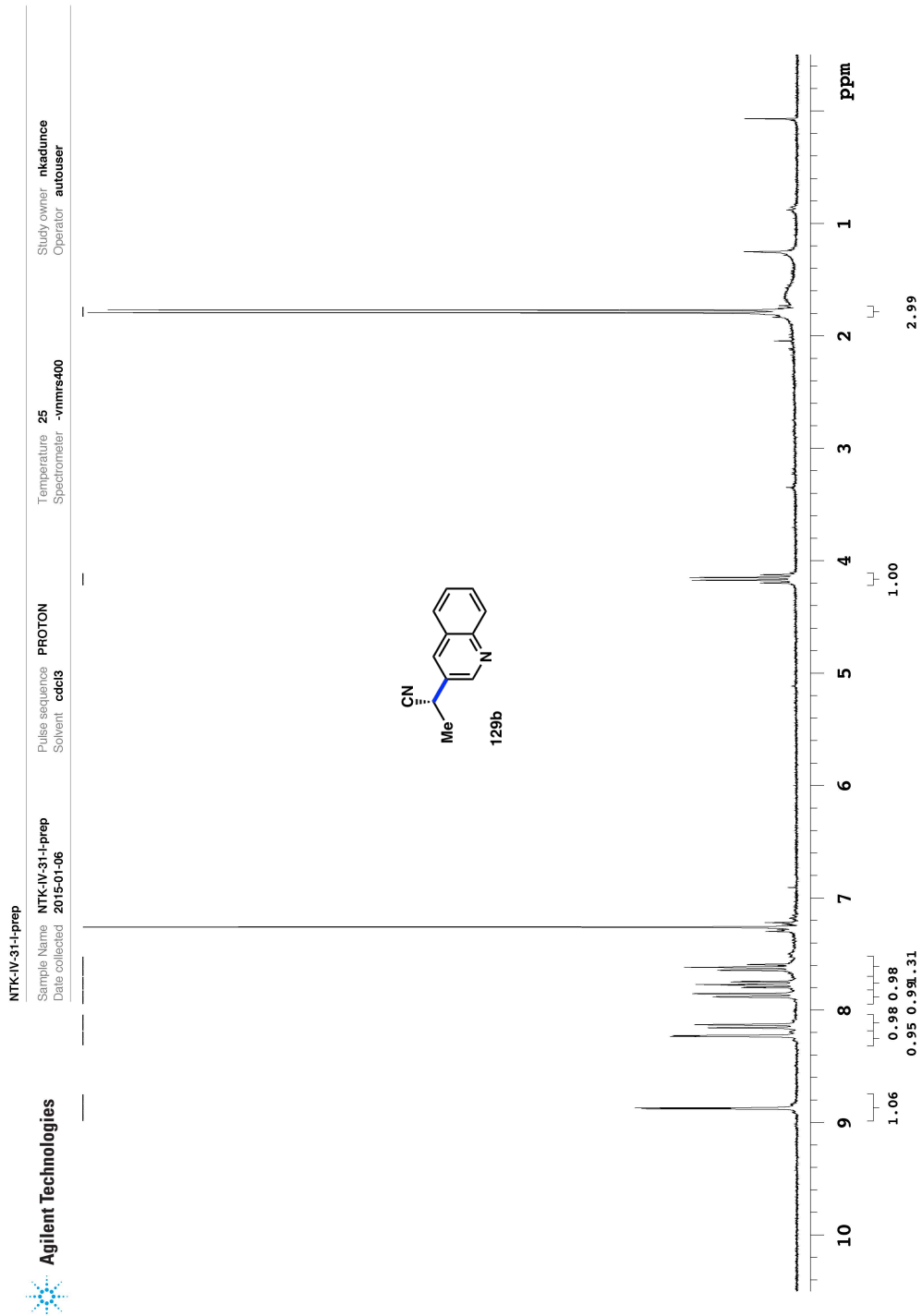
Plot date 2015-06-18

NTK-IV-75-pure  
 Sample Name NTK-IV-75-pure  
 Date collected 2015-03-03  
 Pulse sequence CARBON  
 Solvent cdc13  
 Temperature 25  
 Spectrometer -vnmr400  
 Study owner nkaadunce  
 Operator autouser



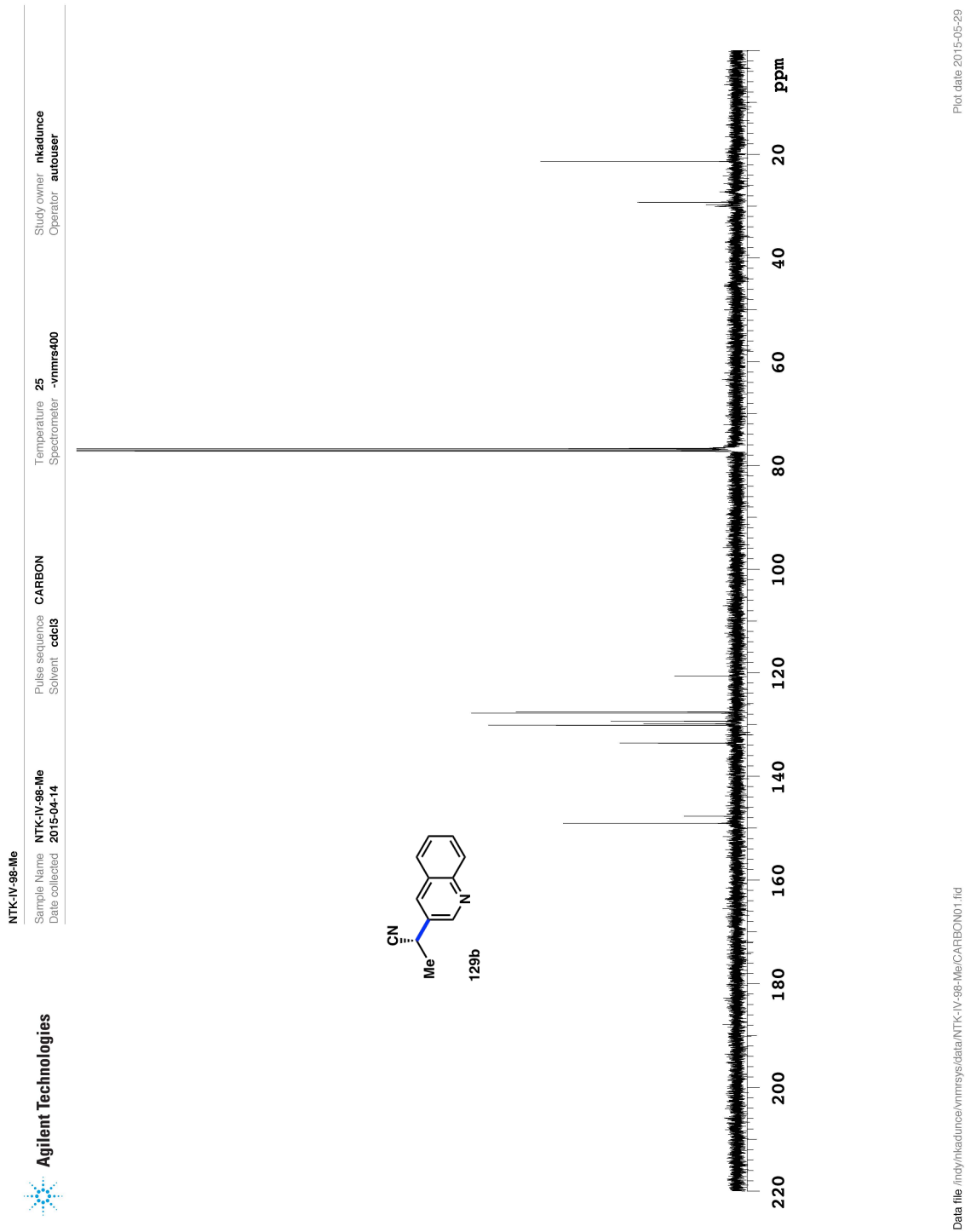
Plot date 2015-05-29

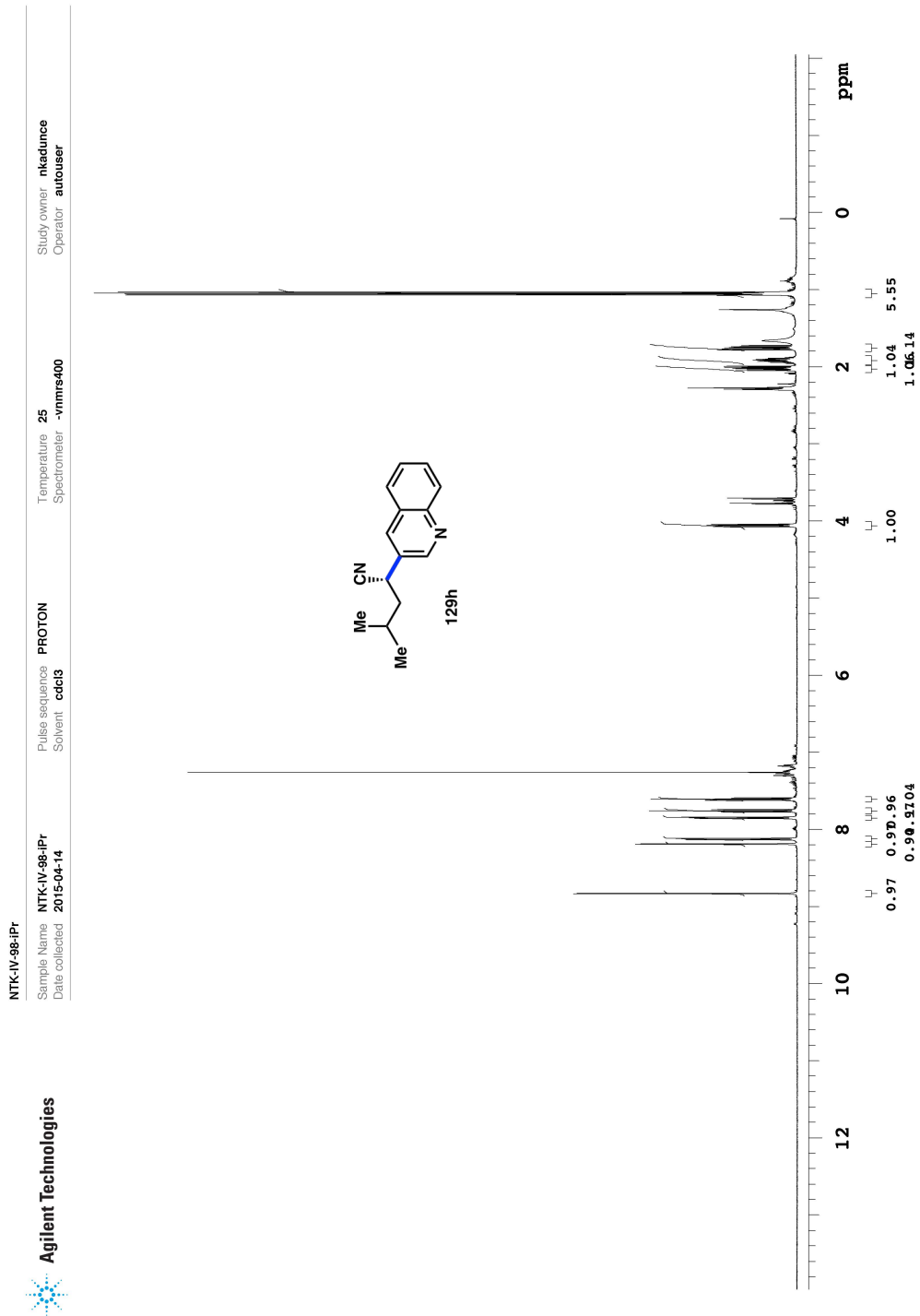
Data file f:\ndy\nkaadunce\vnmr\data\NTK-IV-75-pure\CARBON01.fid



Plot date 2015-06-04

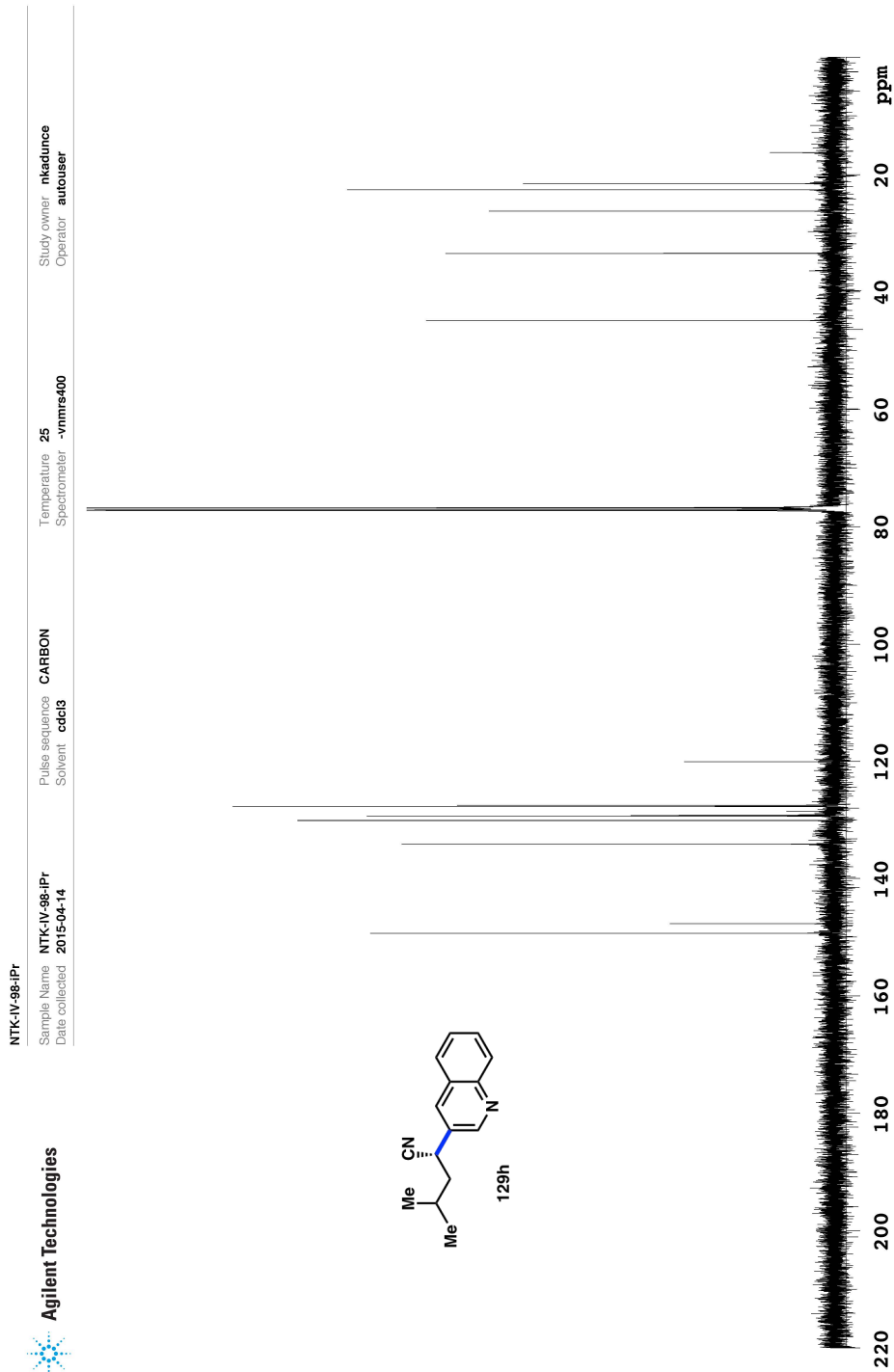
Data file: /jg3/nkaadunce/vnmrsys/data/NTK-IV-31-1-prep/PROTON01.fid





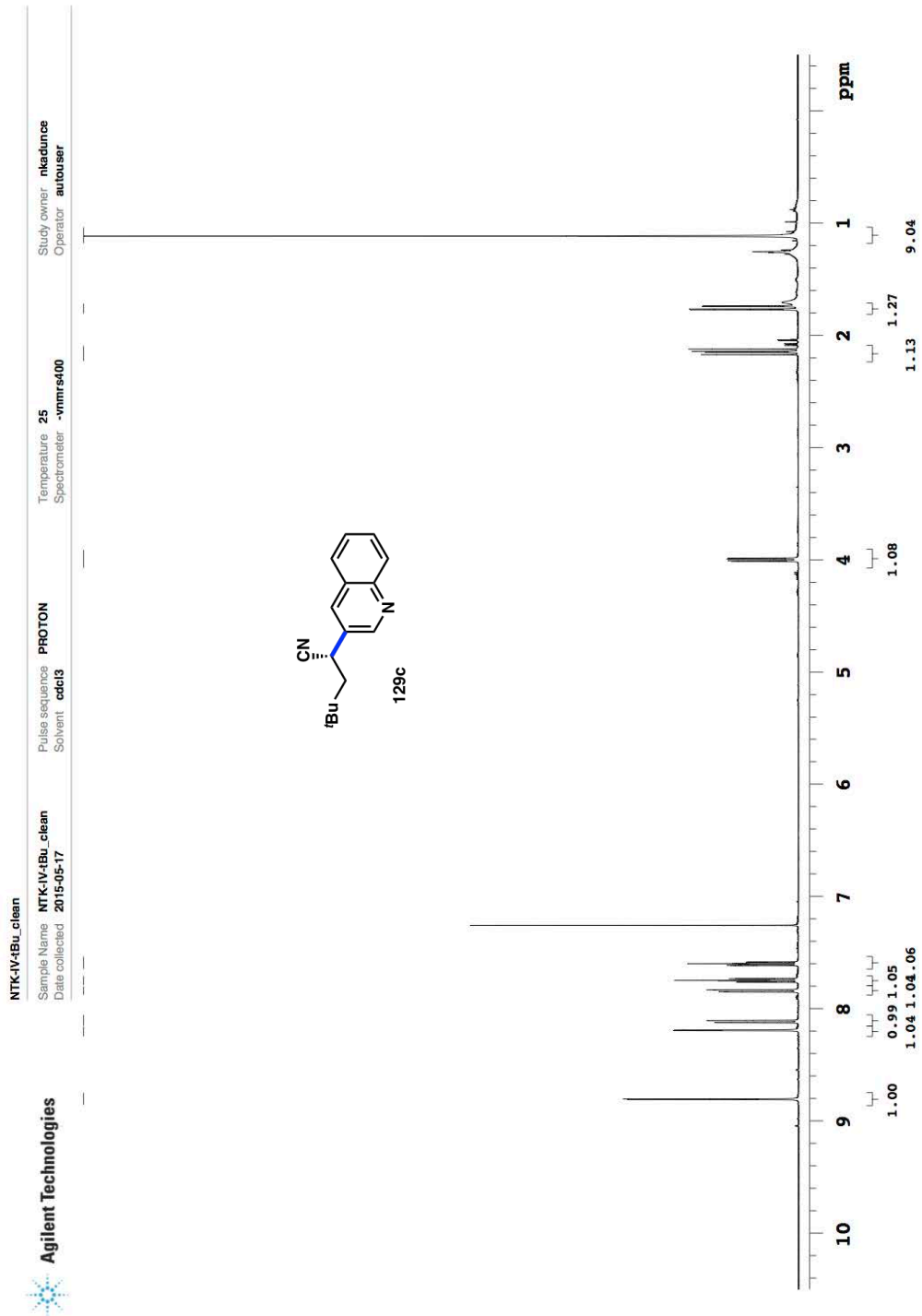
Plot date 2015-05-29

Data file: /ind/nkaadunce/vnmrsys\data/NTK-IV-98-IPr/PROTON01.fid

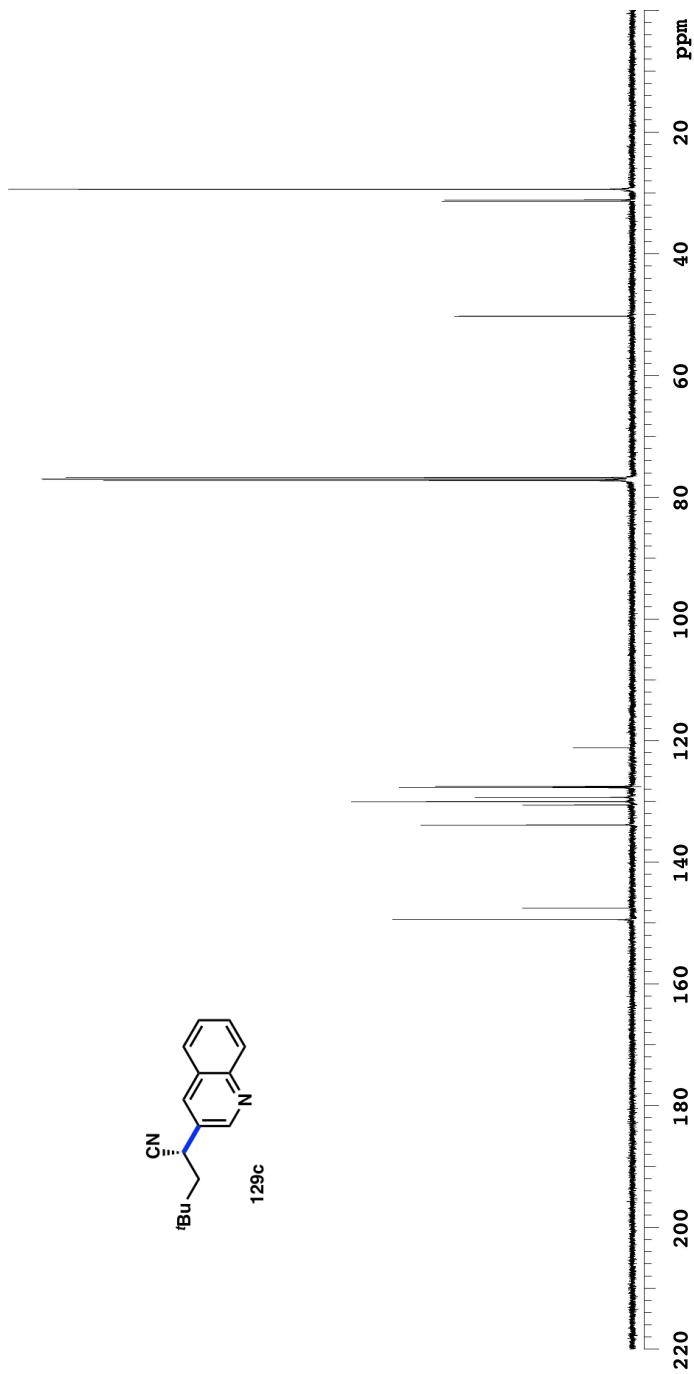
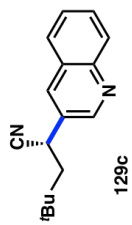


Plot date 2015-05-29

Data file: /ind/nkaclunice/vnmr/ntk-iv-98-IPr/CARBON01.fid

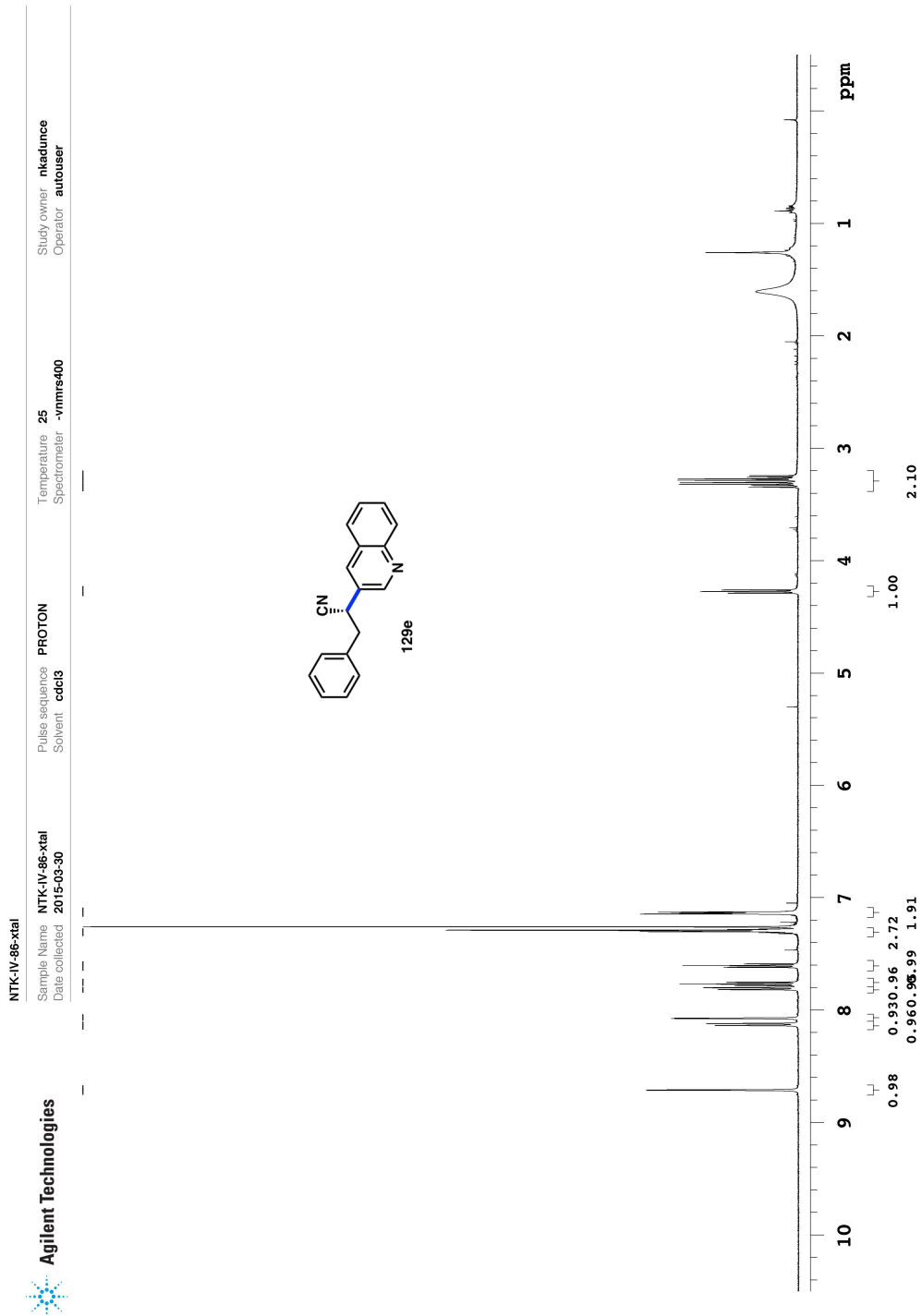


NTK-IV-tBu\_clean  
 Sample Name NTK-IV-tBu\_clean  
 Date collected 2015-05-17  
 Pulse sequence CARBON  
 Solvent cdc13  
 Temperature 25  
 Spectrometer vnmr400  
 Study owner nkaadunce  
 Operator autouser



Plot date 2015-05-29

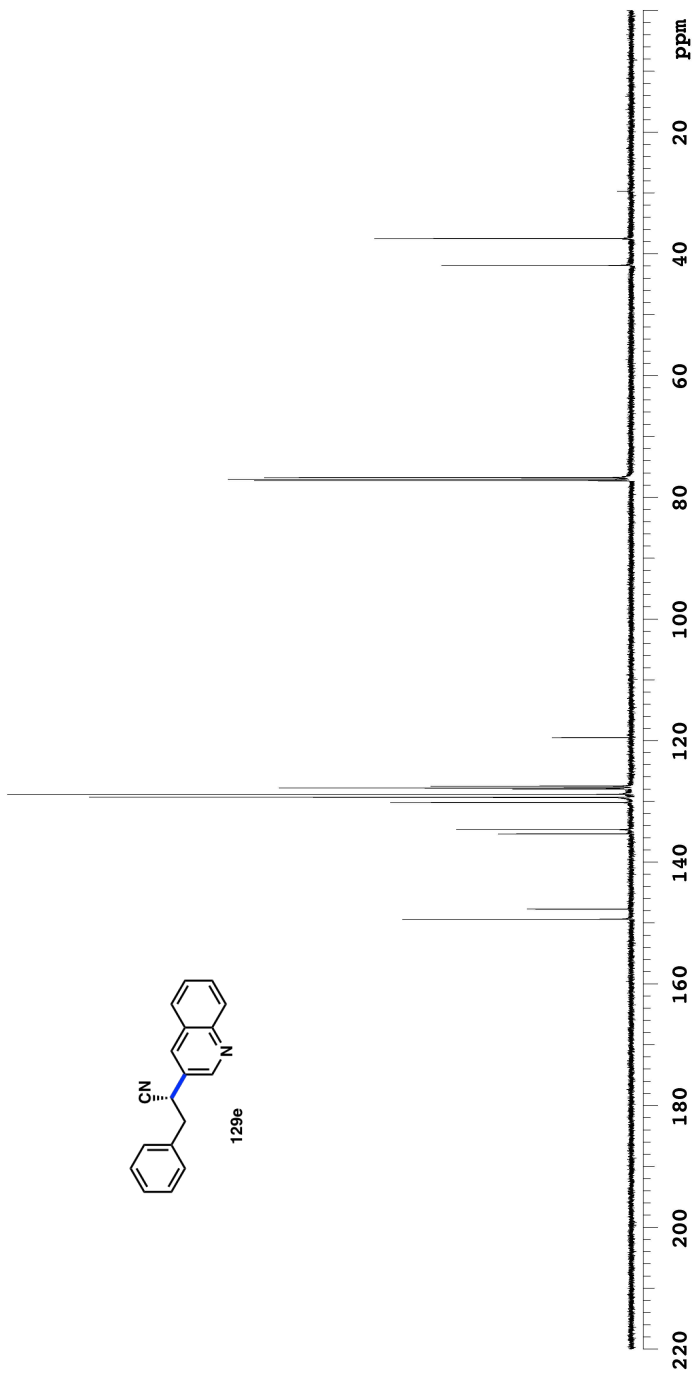
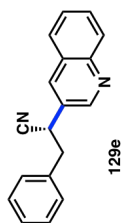
Data file f:\ndy\nkaadunce\vnmr4\data\NTK-IV-tBu\_clean\CARBON01.fid



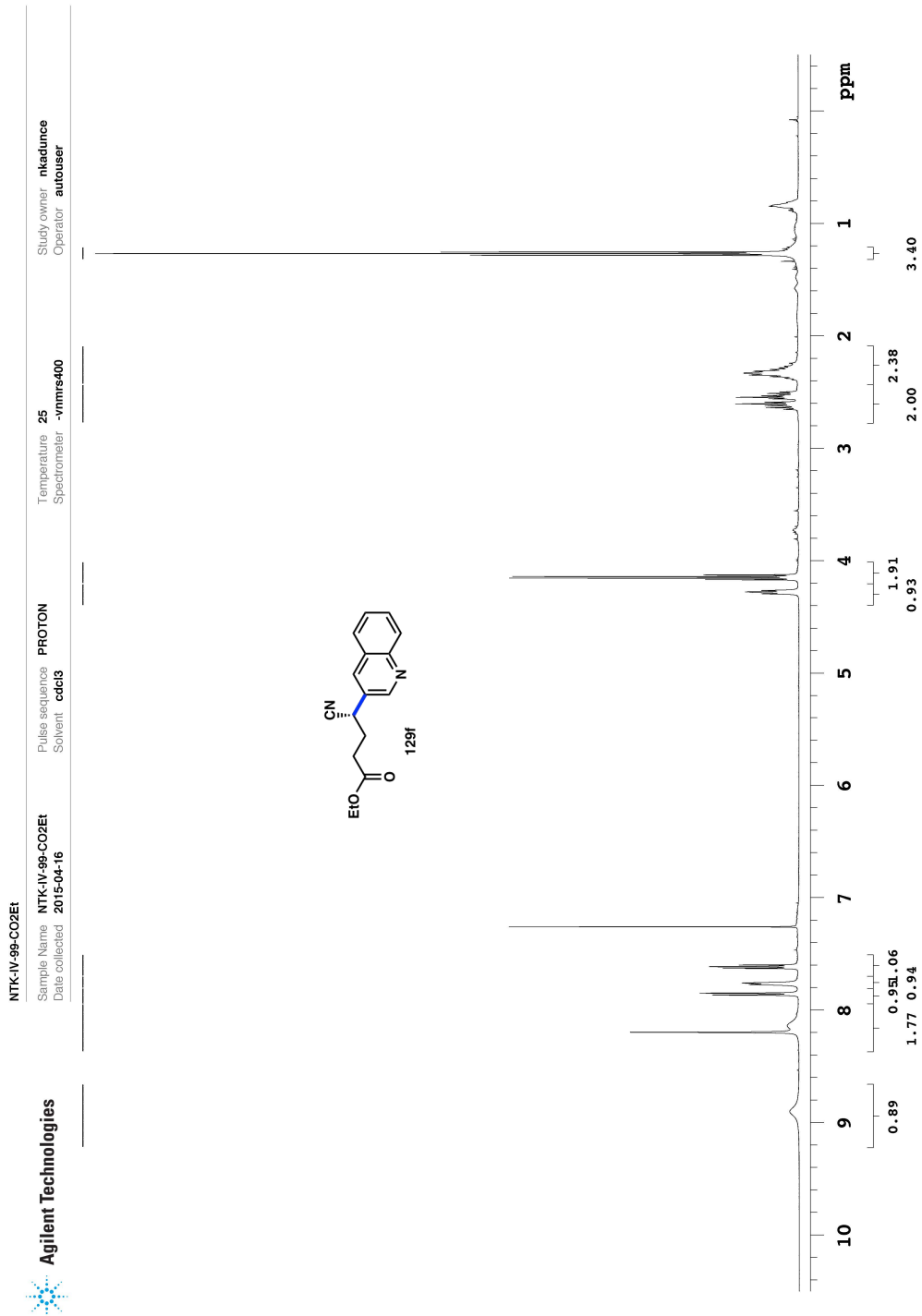
Plot date 2015-05-29

Data file: /ind/nkaadunce/vnmrs/data/NTK-IV-86-xtal/PPROT001.fid

NTK-IV-Bn\_13C  
 Sample Name NTK-IV-Bn\_13C  
 Date collected 2015-06-03  
 Pulse sequence CARBON  
 Solvent cdc13  
 Temperature 25  
 Spectrometer -vnmrs400  
 Study owner nkaadunce  
 Operator autouser

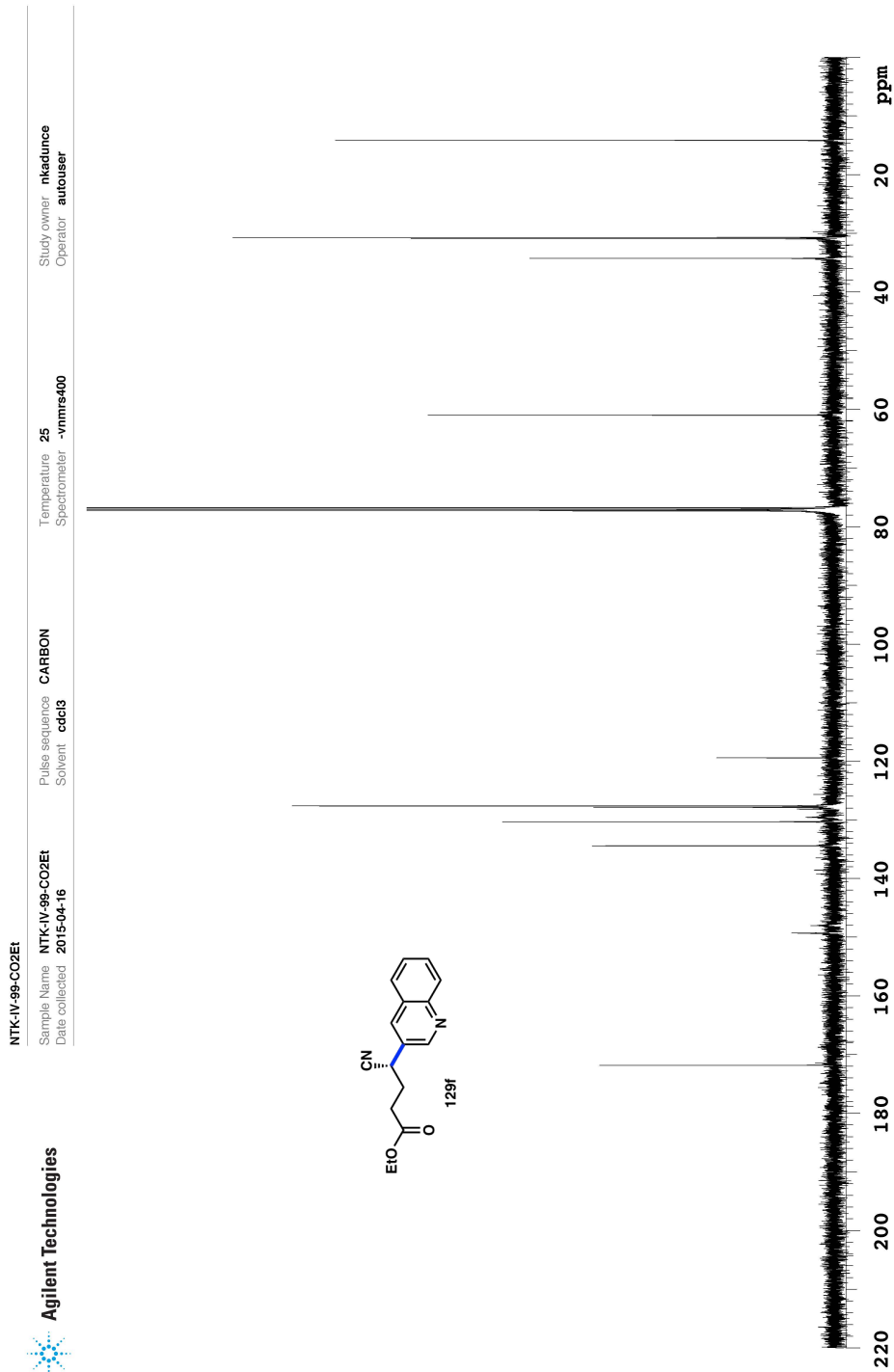


Data file f:\ndy\nkaadunce\vnmsys\data\NTK-IV-Bn\_13C\CARBON01.tid  
 Plot date 2015-06-04

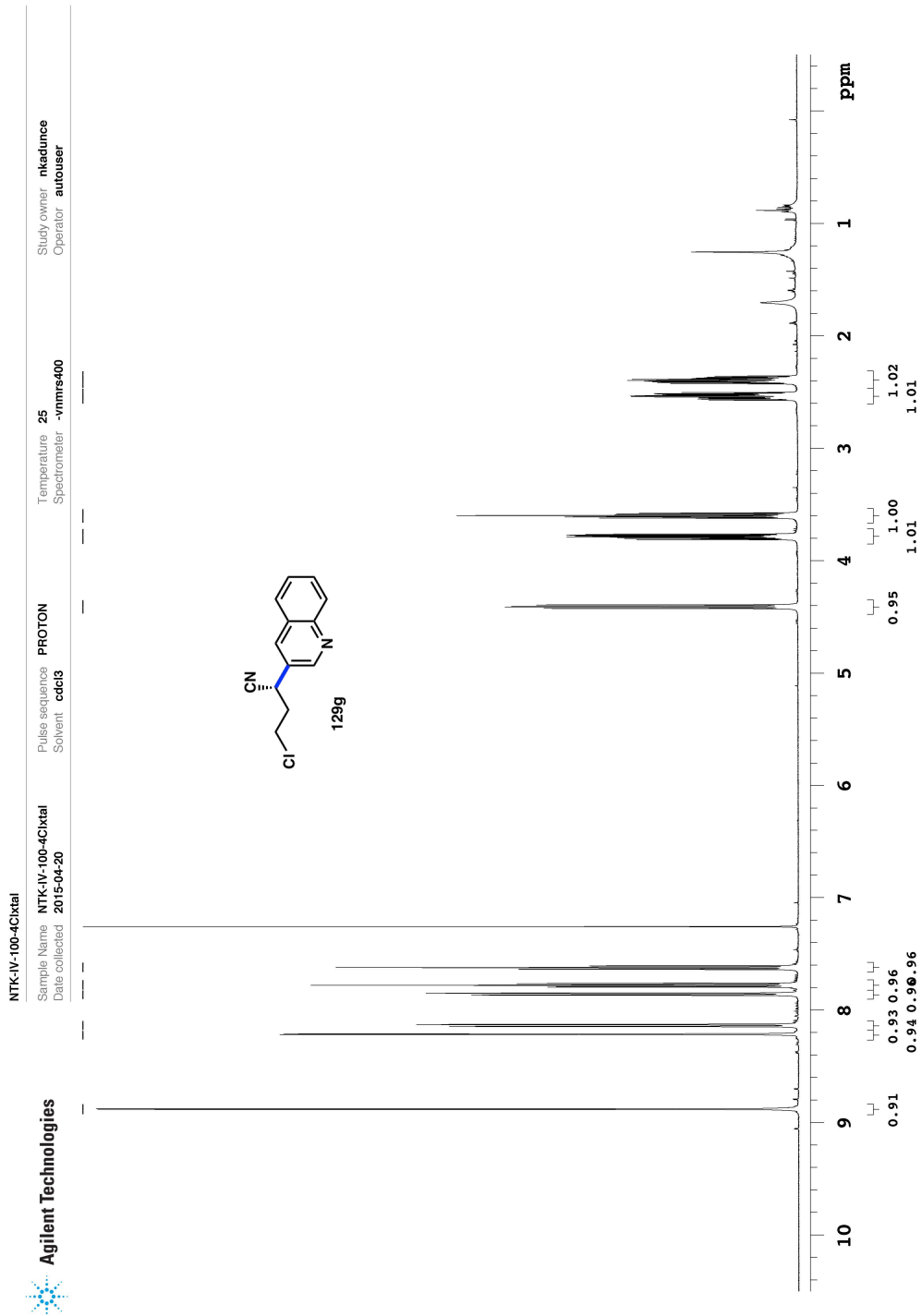


Data file: /ind/nkaadunce/vnmrsys\data/NTK-IV-99-CO2E1/PROTON02.fid

Plot date: 2015-05-29

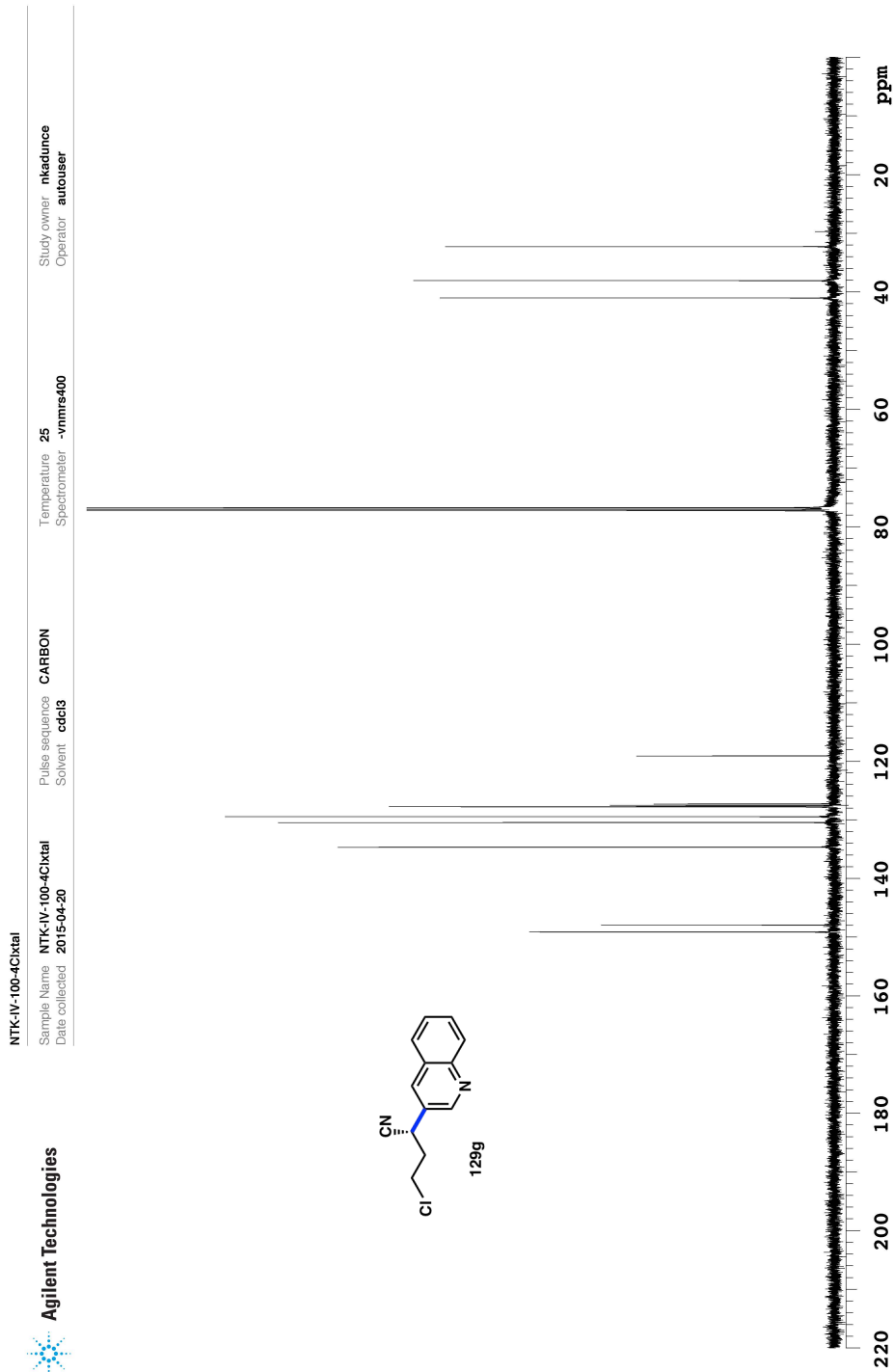


Data file: /ind/nkaudince/vnmrsys/data/NTK-IV-99-CO2Et/CARBON01.fid  
Plot date: 2015-05-29



Plot date 2015-05-29

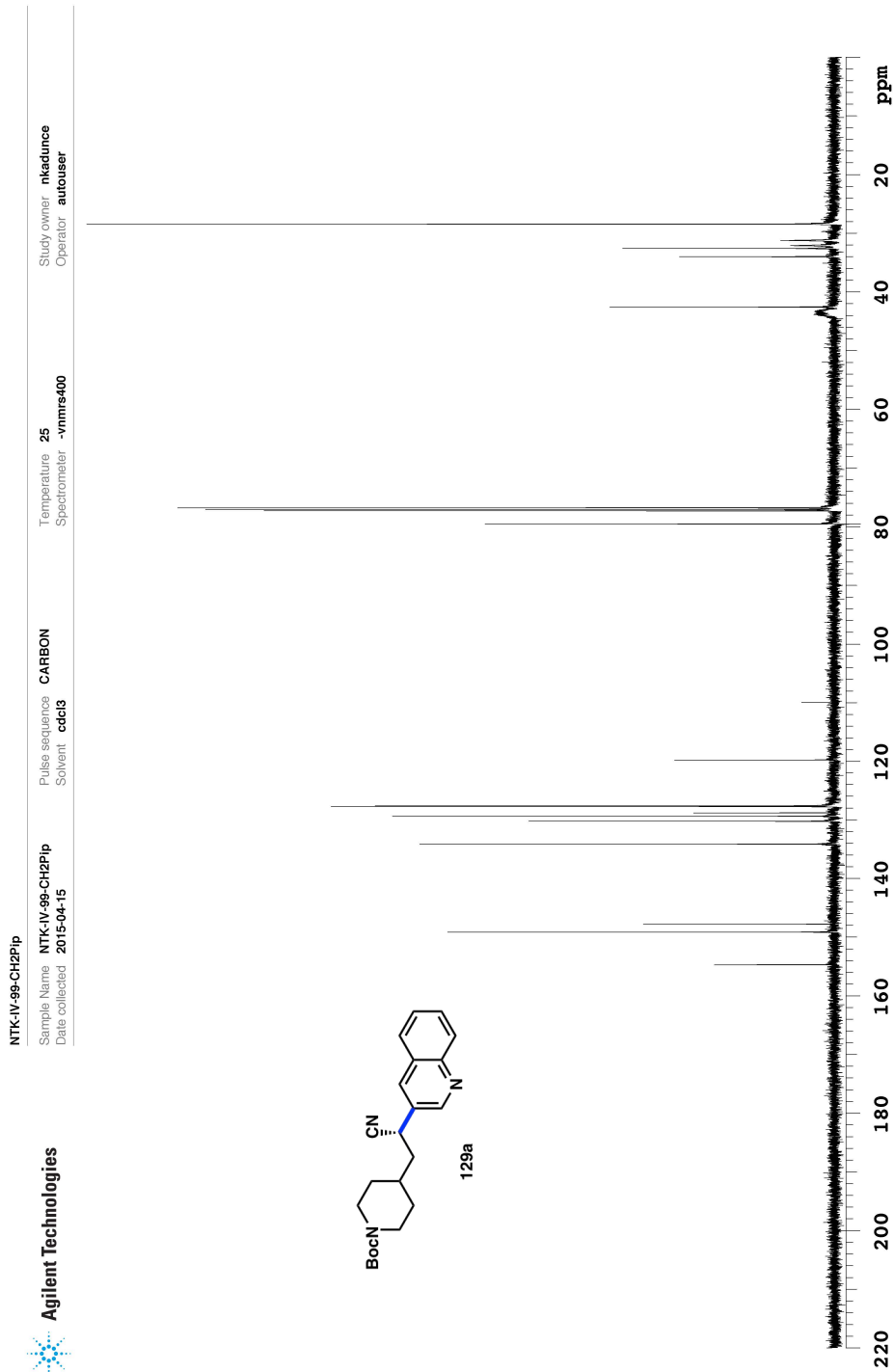
Data file: /ind/nkaadunce/vnmrs/data/NTK-IV-100-4Clxial/PROTON01.fid



Plot date 2015-05-29

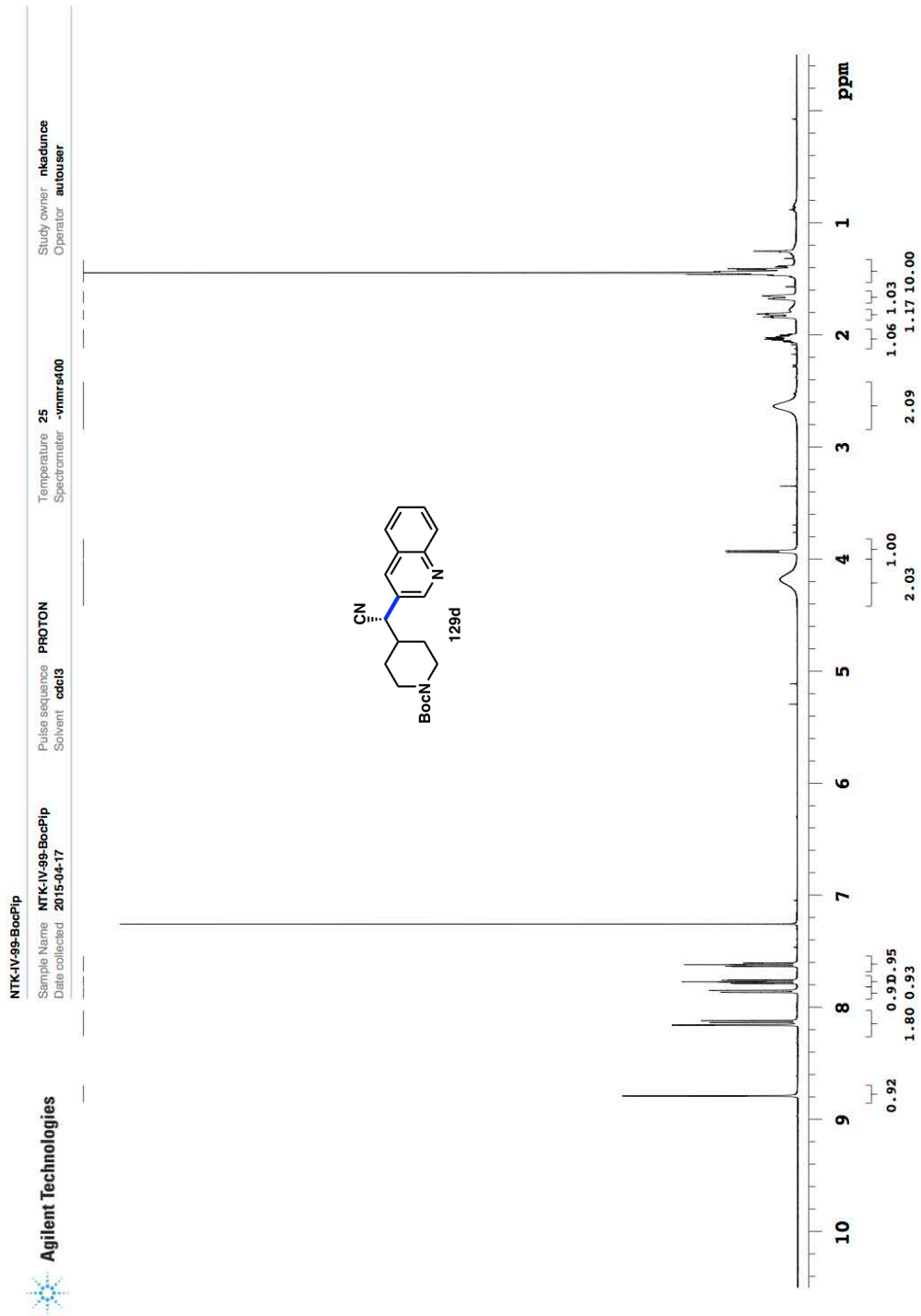
Data file: /ind/nkaadunce/vnmrsys/data/NTK-IV-100-4Clx1al/CARBON01.fid

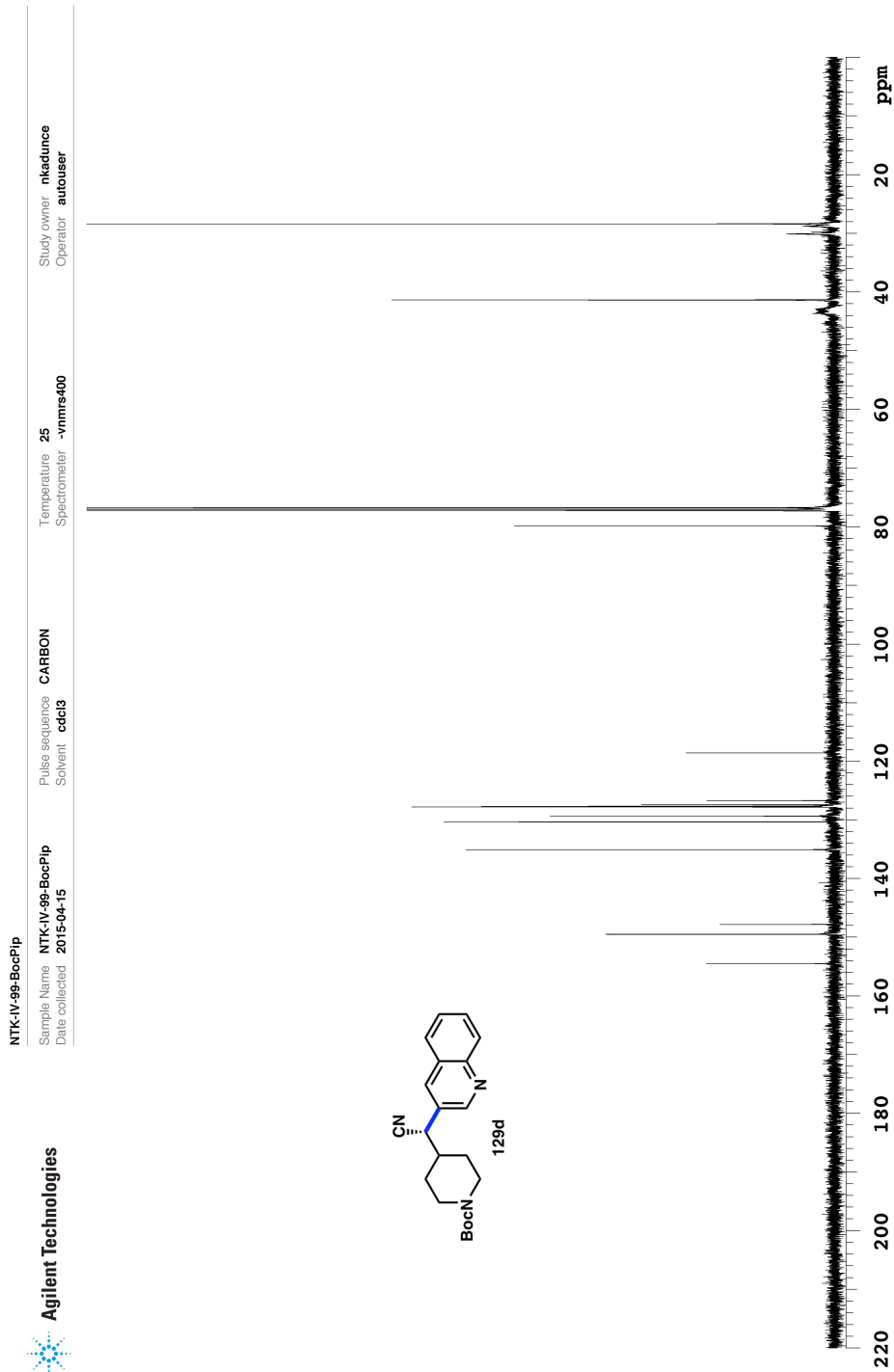




Plot date 2015-05-29

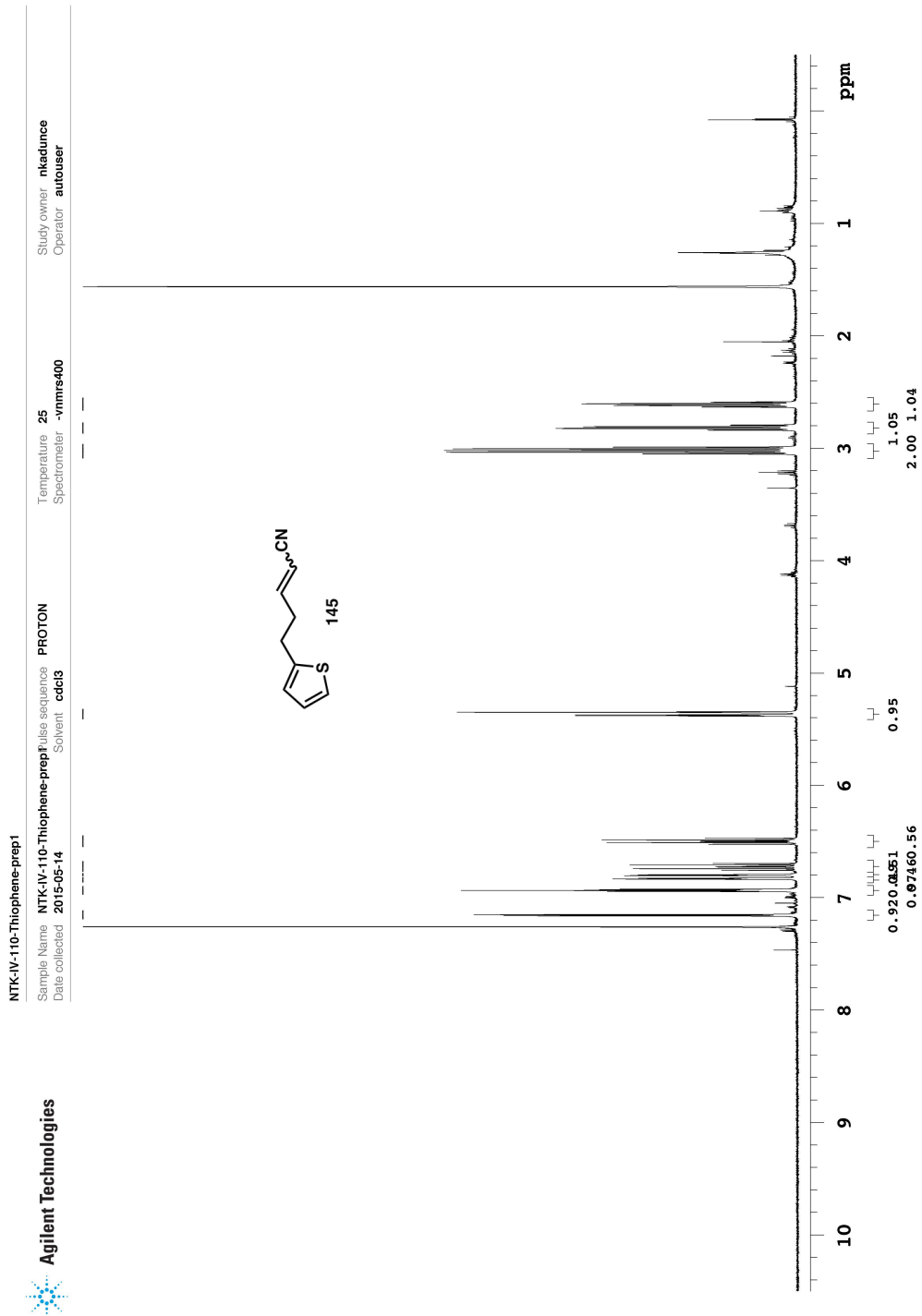
Data file: /ind/nkaclunce/vnmrsys/data/NTK-IV-99-CH2Pip/CARBON01.tid





Plot date: 2015-05-29

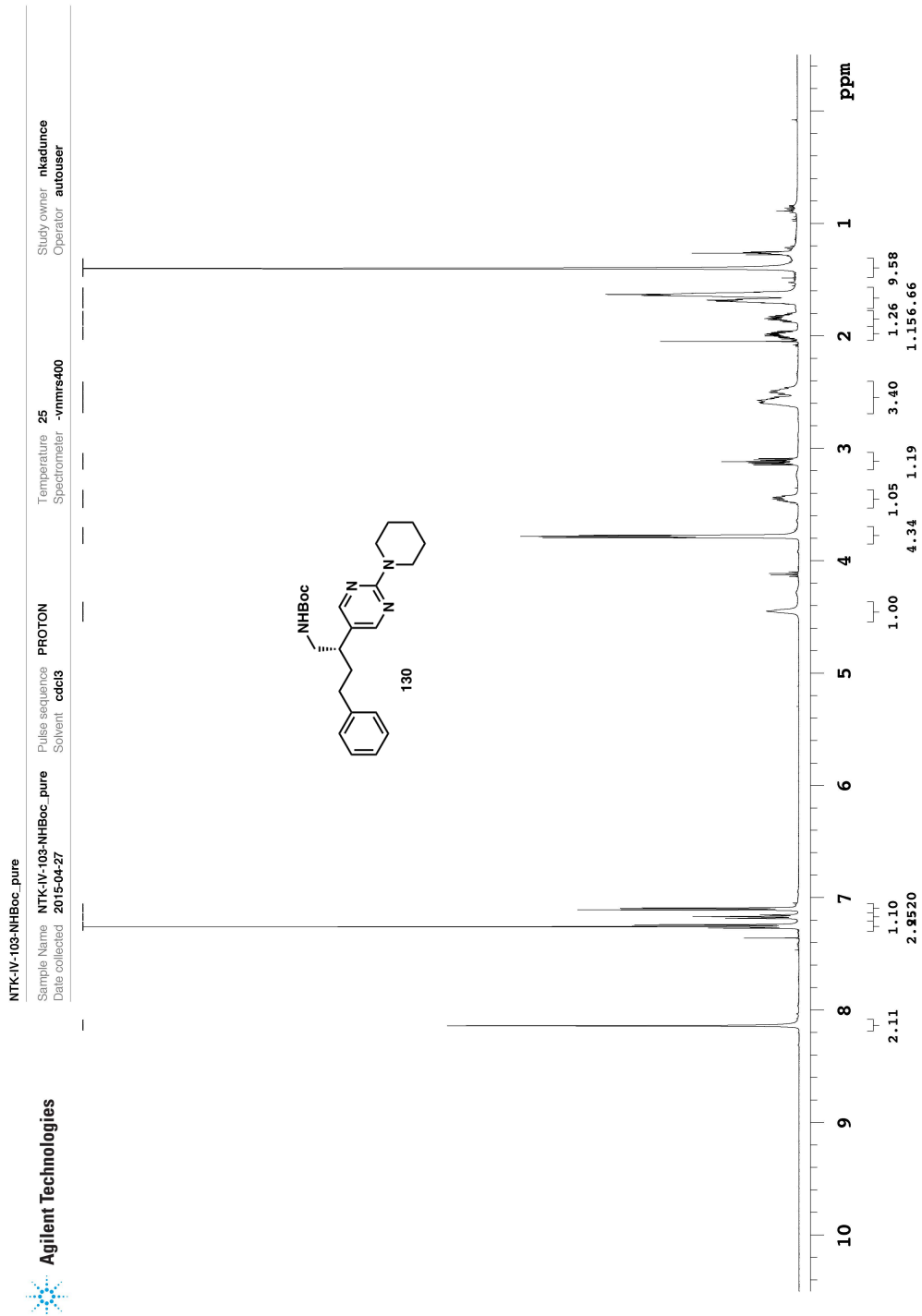
Data file: /ind/nkaadunce/vnmr/ntk-iv-99-bocpip/carbon01.fid



Plot date 2015-05-29

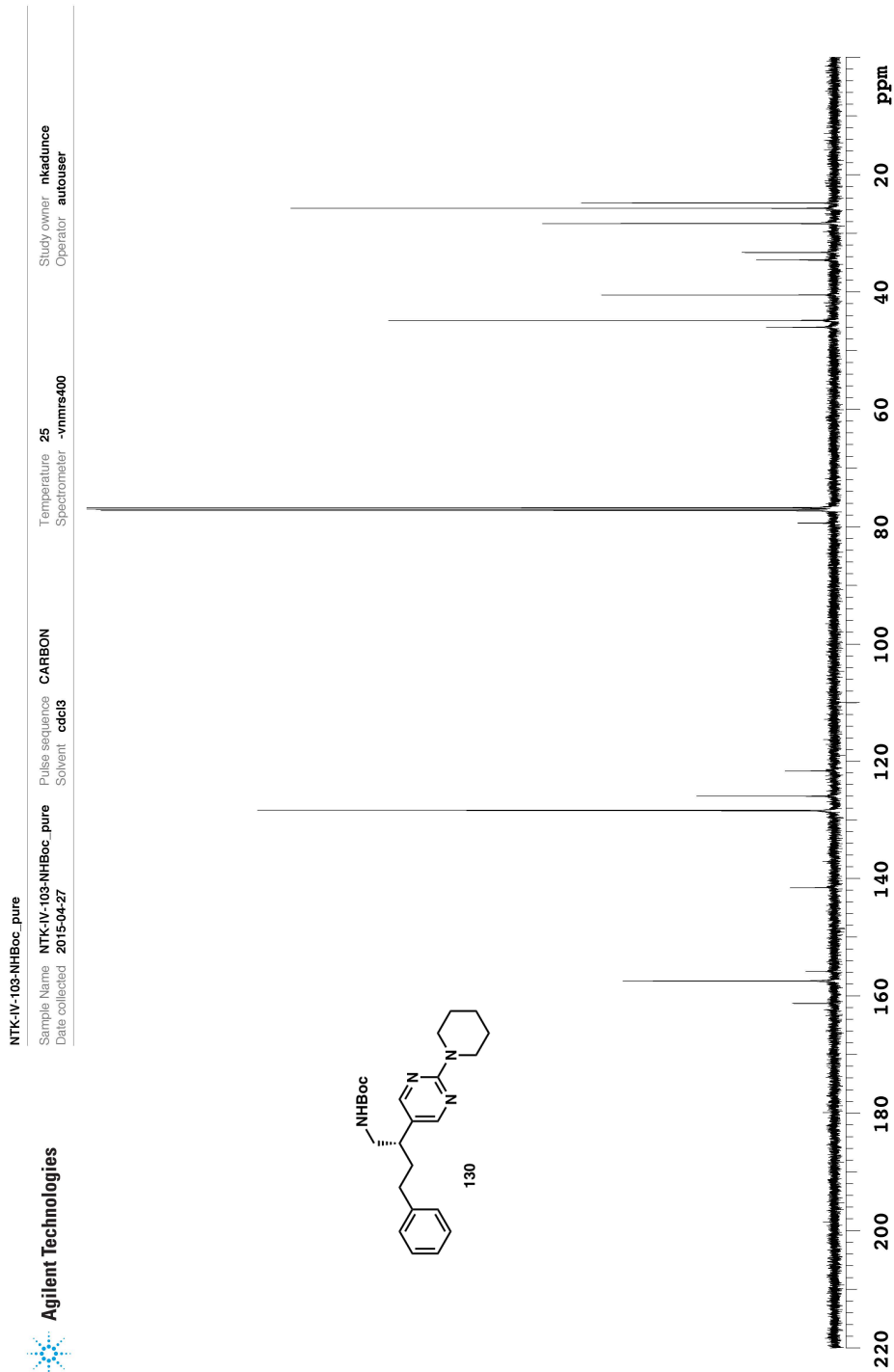
Data file f:\ndy\nkaadance\vmmsys\data\NTK-IV-110-Thiophene-prep1\PROTON01.fid





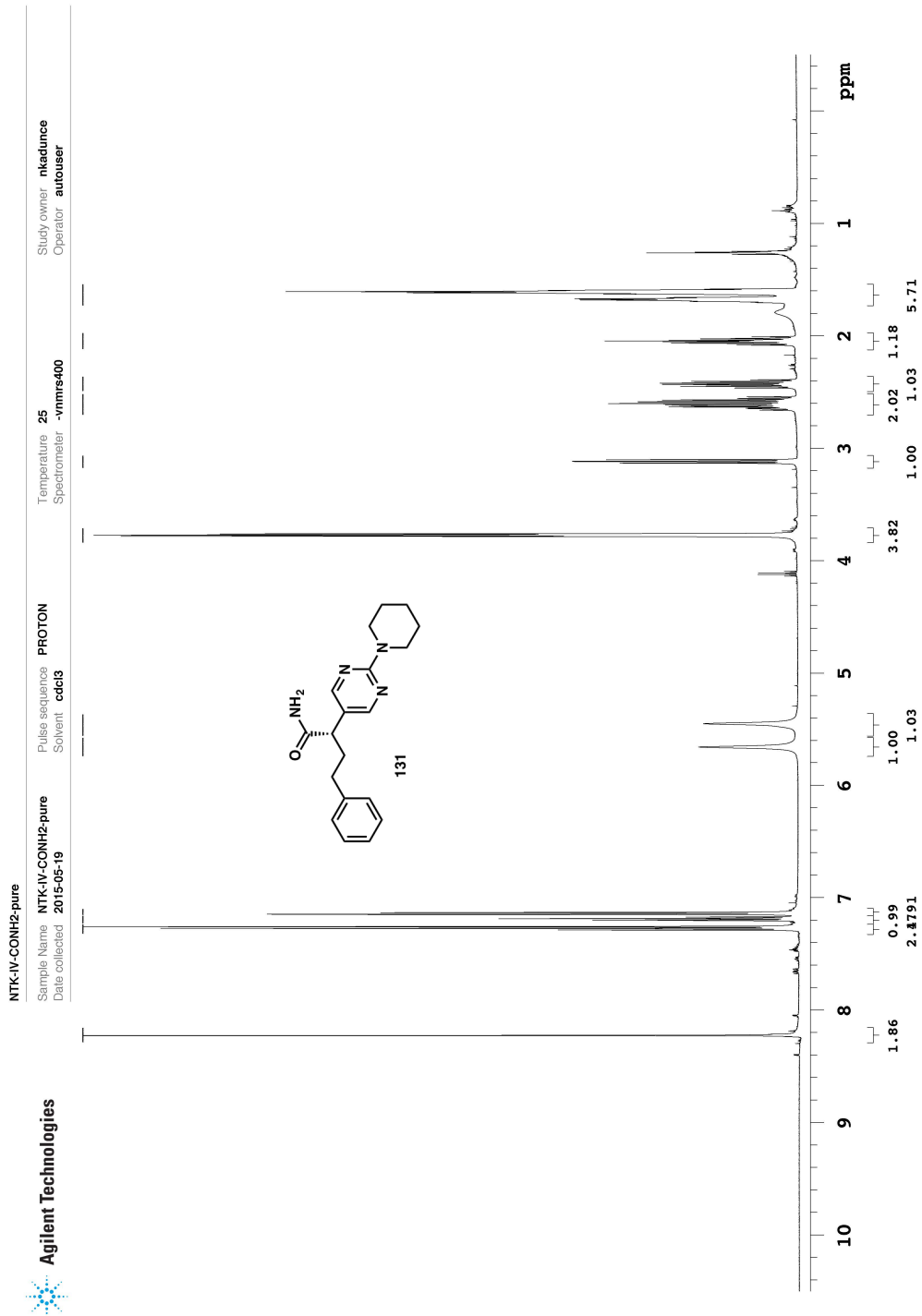
Plot date 2015-05-29

Data file: /ind/nkaadunce/vnmrs/data/NTK-IV-103-NHBoc\_pure/PROTON01.fid



Plot date 2015-05-29

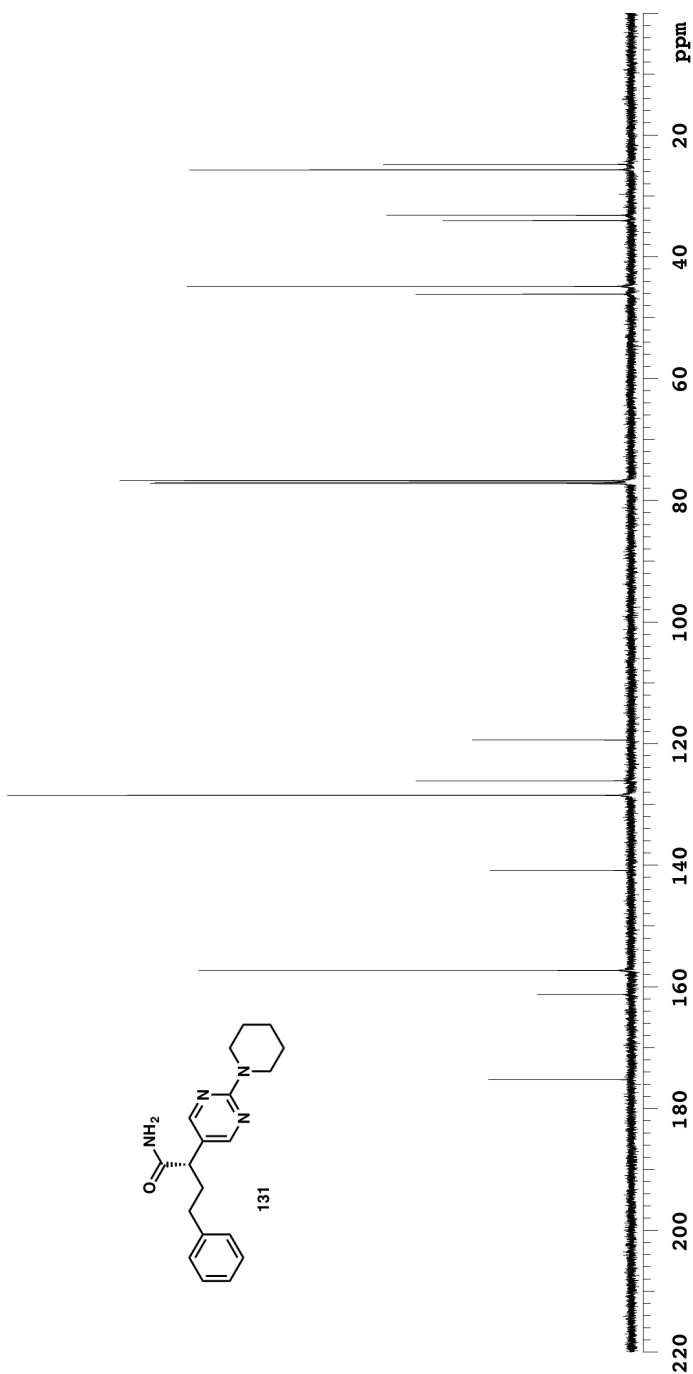
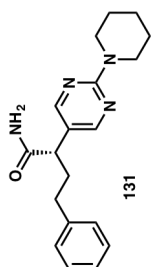
Data file: /ind/nkaadunce/vnmrsys/data/NTK-IV-103-NHBoc\_pure/CARBON01.fid



Plot date 2015-05-29

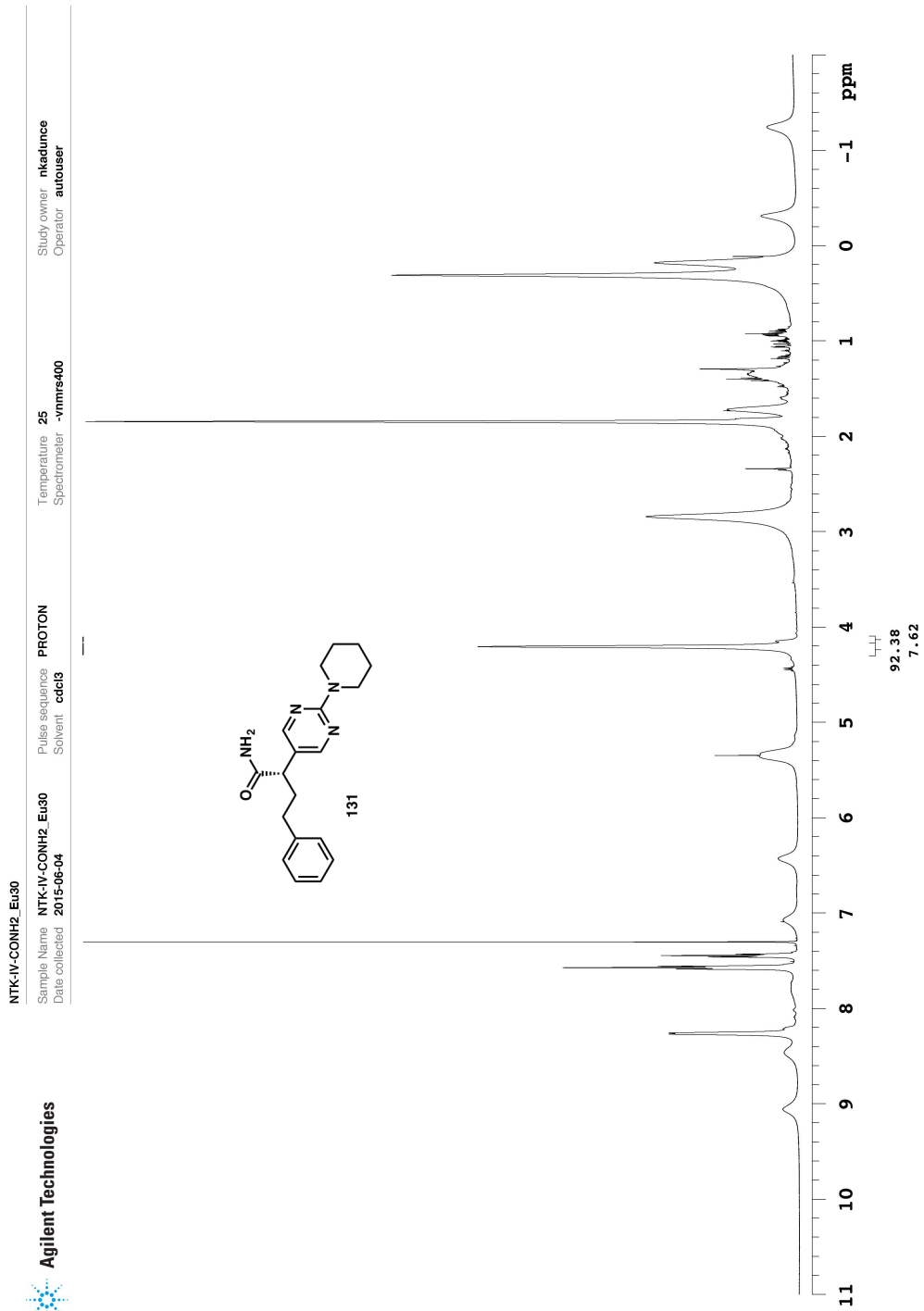
Data file: /ind/nkaadunce/vnmrsys\data/NTK-IV-CONH2-pure/PROTON01.fid

NTK-IV-CONH2-pure  
 Sample Name NTK-IV-CONH2-pure  
 Date collected 2015-05-19  
 Pulse sequence CARBON  
 Solvent cdc13  
 Temperature 25  
 Spectrometer -vnmr400  
 Study owner nkaclunce  
 Operator autouser



Plot date 2015-05-29

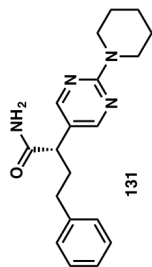
Data file f:\ndy\nkaclunce\vnmr4\data\NTK-IV-CONH2-pure\CARBON01.fid



Plot date 2015-06-04

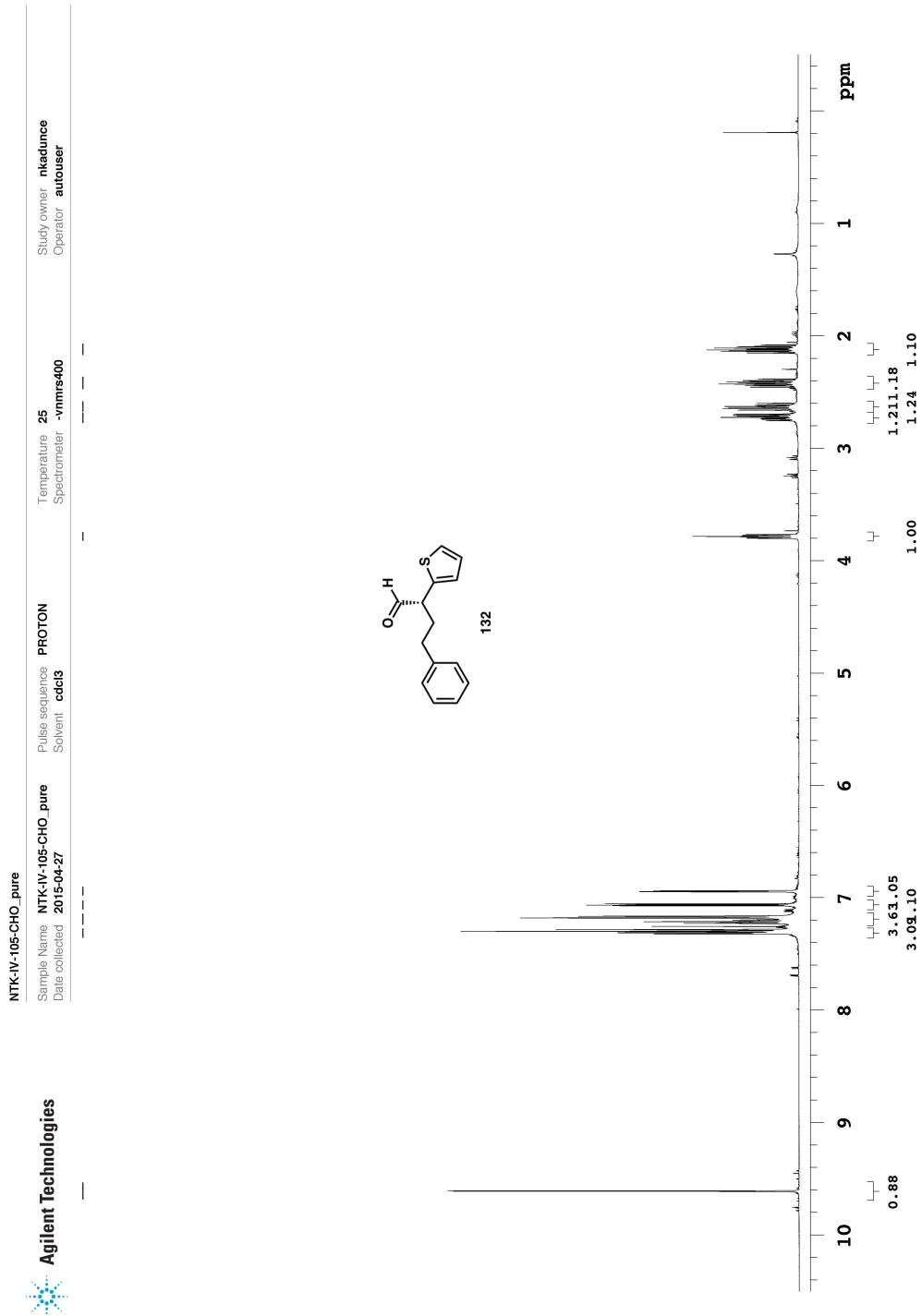
Data file f:\ndy\nkauduce\vnmr\data\NTK-IV-CONH2\_Eu30\PROTON01.fid

NTK-IV-CONH2\_Eu30  
 Sample Name NTK-IV-CONH2\_Eu30  
 Date collected 2015-06-04  
 Pulse sequence PROTON  
 Solvent cdc13  
 Temperature Spectrometer 25 -vrms400  
 Study owner nkaeunce  
 Operator autouser



92.38 7.62

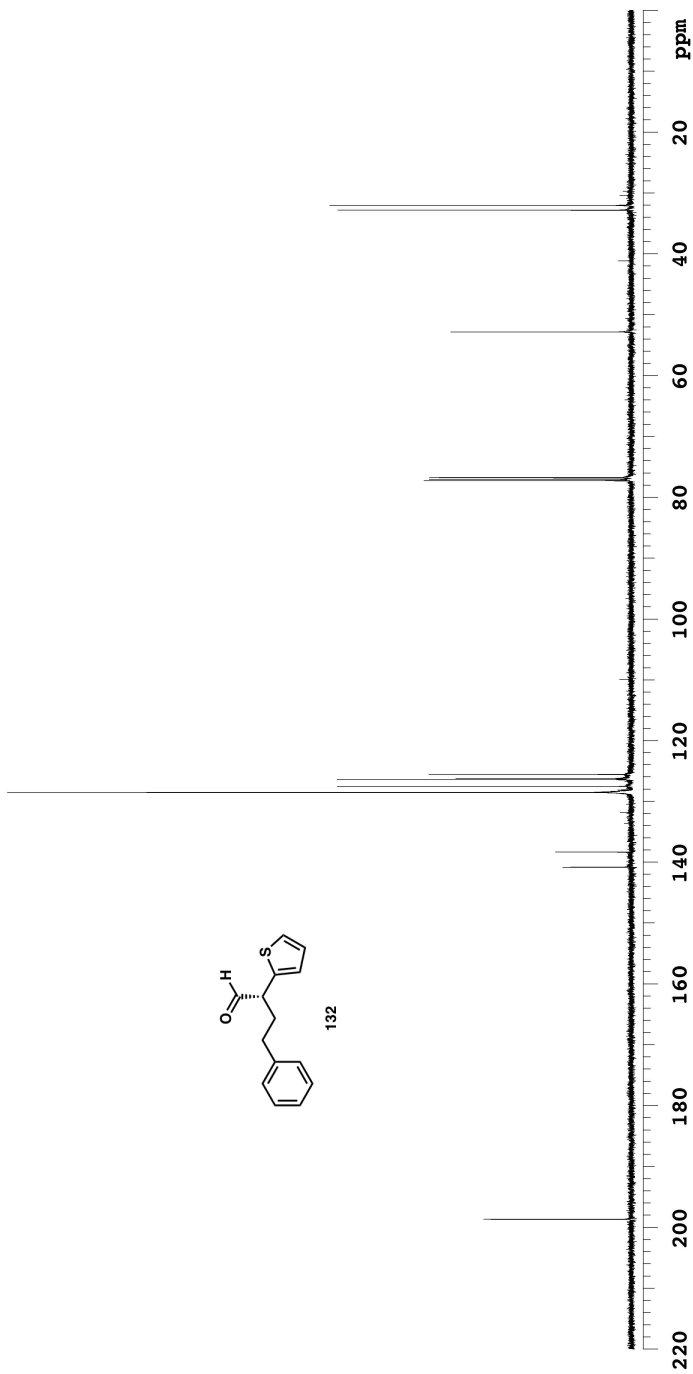
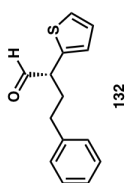
Data file: /ind/nkaeunce/vrmsys/data/NTK-IV-CONH2\_Eu30/PROTON01.fid  
 Plot date: 2015-06-04



Plot date 2015-05-29

Data file f:\ndy\nkaadunce\vnmsys\data\NTK-IV-105-CHO\_pure\PROTON01.fid

NTK-IV-105-CHO\_pure  
 Sample Name NTK-IV-105-CHO\_pure  
 Date collected 2015-04-27  
 Pulse sequence CARBON  
 Solvent cdcl3  
 Temperature 25  
 Spectrometer -vnmrs400  
 Study owner nkaclunice  
 Operator autouser



Data file f:\ndy\nkaclunice\vnmsys\data\NTK-IV-105-CHO\_pure\CARBON01.fid  
 Plot date 2015-05-29

## Chapter 4

### *Nickel-Catalyzed Asymmetric Reductive Cross-Coupling to Access 1,1-Di(hetero)arylalkanes<sup>o</sup>*

#### 4.1 INTRODUCTION

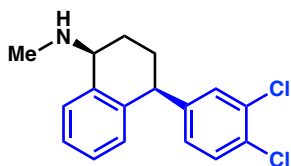
##### 4.1.1 Background and catalytic asymmetric approaches

1,1-Diarylalkanes are a common pharmacophore, present in biologically active natural products as well as marketed drugs for a diverse range of indications (**Figure 1**). In many cases, these bioactive molecules exhibit a substantial eudysmic ratio, in which one enantiomer is significantly more potent than the other.<sup>1</sup> As such, methods for the enantioselective preparation of diarylalkanes have become a proving ground in asymmetric catalysis, with methods to afford these products being reported by many synthetic laboratories.<sup>2</sup>

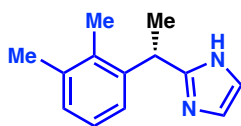
---

<sup>o</sup> Portions of this chapter have been reproduced from a manuscript in preparation and the supporting information found therein. This work was conducted with Kelsey Poremba, a graduate student in the Reisman lab. Preliminary investigations discussed herein were conducted by Dr. Alan H. Cherney, then a graduate student in the Reisman lab.

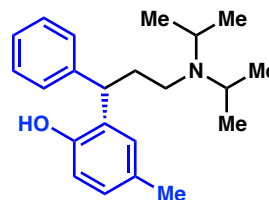
**Figure 4.1.** Selected bioactive chiral 1,1-diarylalkanes.



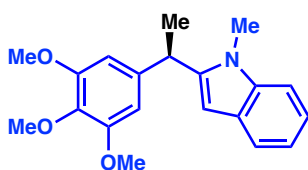
**Sertraline or Zoloft®**  
serotonin reuptake inhibitor used as antidepressant and anti-anxiety



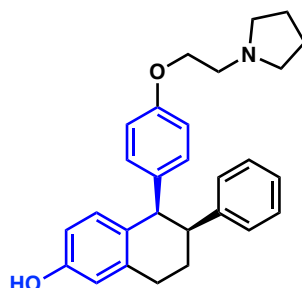
**Demiditraz**  
pesticide, used in veterinary topical antiparasitic treatments



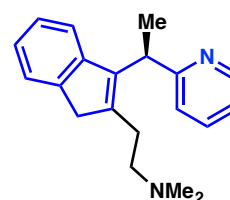
**Tolterodine or Detrol®**  
antimuscarinic drug used to treat urinary incontinence



**Indoleisocombretistatin**  
tubulin polymerization inhibitor with potent cytotoxicity against multiple human cancer cell lines



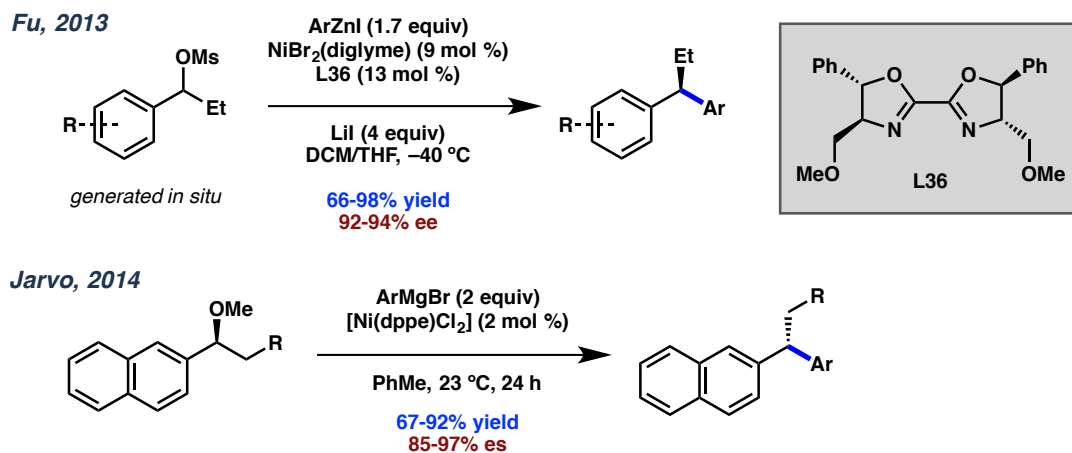
**Lasofoxifene**  
non-steroidal selective estrogen receptor modulator (SERM) used for treatment of osteoporosis



**R-Dimethindene or Fenistil®**  
 $H_1$ -antihistamine for treatment of allergic reactions and insomnia

The pseudosymmetry of these molecules makes them particularly appealing targets for cross-coupling. Many methods employing asymmetric hydrogenation of 1,1-diarylethenes have been reported, affording the corresponding diarylalkanes in excellent ee.<sup>3</sup> However, these require a proximal desymmetrizing or directing group on one of the aryl rings to enable facial differentiation by the catalyst, greatly limiting the accessible product scope of these technologies. A cross-coupling disconnection circumvents this issue, accessing the product convergently from a C(sp<sup>3</sup>) benzyl fragment and a C(sp<sup>2</sup>) aryl partner. In redox-neutral couplings, one of these is a halide electrophile, while the other is some organometallic nucleophile, with both stereoconvergent<sup>2d</sup> and stereospecific<sup>4</sup> methods having been reported (**Scheme 4.1**).<sup>2j</sup> This disconnection also lends itself to reductive cross-coupling logic, with the two electrophilic fragments being differentiable by hybridization.

**Scheme 4.1.** Selected recent asymmetric cross-couplings to access 1,1-diarylalkanes.

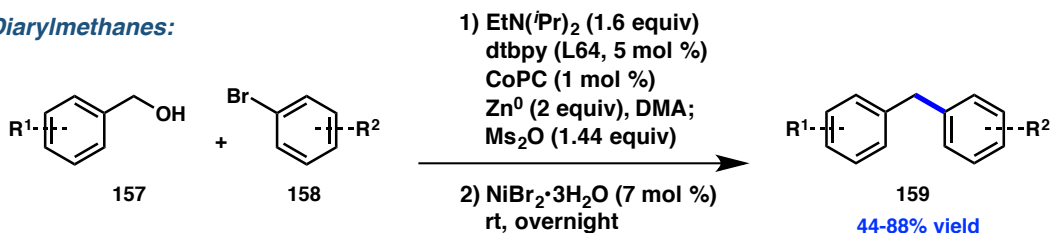


#### 4.1.2 Reductive cross-coupling approaches and preliminary investigations

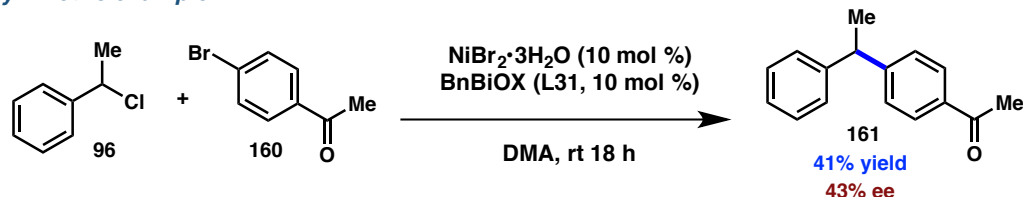
A racemic reductive cross-coupling strategy to access 1,1-diarylalkanes was first reported by Weix and coworkers in 2015, with the majority of the products disclosed being achiral diarylmethanes.<sup>5</sup> Employing benzylic alcohols, *in situ* mesylate formation generates the active C(sp<sup>3</sup>) electrophile, which undergoes chemoselective Ni-catalyzed reductive coupling with aryl halide partners (**Scheme 4.2**). Interestingly, the authors report a single example of an asymmetric coupling, which requires the benzylic chloride substrate **96** to achieve modest enantioinduction, employing BnBiOX (**L31**) as the chiral ligand.<sup>2k</sup>

**Scheme 4.2.** Weix's reductive cross-couplings to access 1,1-diarylalkanes.

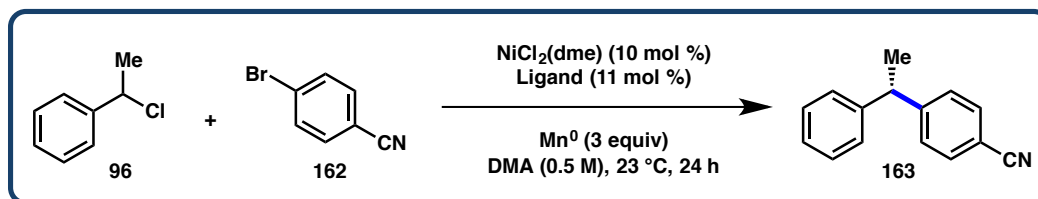
**Diarylmethanes:**



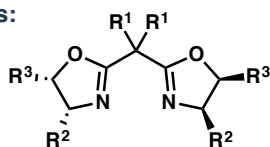
**Asymmetric example:**



Concurrent with these efforts by the Weix group, our laboratory also investigated formation of these products as a platform for asymmetric catalysis development.<sup>6</sup> The earliest of these efforts employed conditions derived from the racemic couplings reported in the literature, similar to those described in **Chapter 2**. Employing amide solvents and an array of chiral ligands, the cross-coupling of 4-bromobenzonitrile (**162**) and 1-(chloroethyl)benzene (**96**) was targeted (**Table 4.1**). Unfortunately, these reactions were plagued with poor chemoselectivity, delivering homocoupled dimers of both substrates; however modest enantioselectivities were observed with both BOX and BiOX ligand scaffolds, suggesting promise for this enantioconvergent transformation. Further optimization identified NMP as an improved solvent at this stage, which afforded **163** in 62% yield and 37% ee when employing BnBiOX (**L31**), the best result achieved with this system.

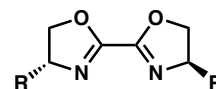
**Table 4.1.** Initial ligand investigation with 4-bromobenzonitrile (**162**).

BOX Ligands:



Entry	R <sup>1</sup>	R <sup>2</sup>	R <sup>3</sup>	% ee <b>163</b>
L62	Me	<sup>i</sup> Pr	H	19
L61	Me	<sup>t</sup> Bu	H	0
L63	Me	Bn	H	1
L32	Me	Ph	H	49
L59	Me	Ph	Ph	14
L57	H	Ph	Ph	11
L56	H	Ph	H	1
L107	H	<sup>t</sup> Bu	H	1
L108	H	indanyl		1
L46	Me	indanyl		3
L109	-CH <sub>2</sub> CH <sub>2</sub> -	indanyl		7

BiOX Ligands:

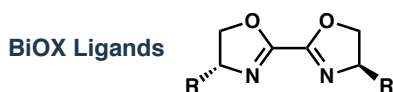
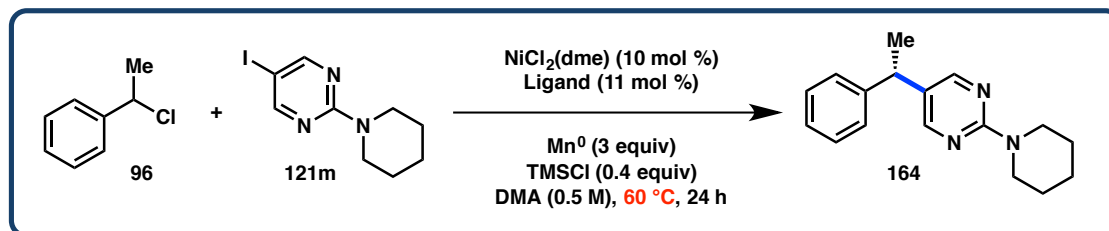


Entry	R	% ee <b>163</b>
L67	<sup>i</sup> Pr	24
L66	<sup>t</sup> Bu	8
L31	Bn	33
L68	Ph	1
L110	Cy	25
L111	<sup>s</sup> Bu	23
L112	CHPh <sub>2</sub>	3
L113	CH <sub>2</sub> (1-naph)	20
L114	CH <sub>2</sub> (2-naph)	29

These initial efforts were suspended until the discovery of the conditions described in **Chapter 3**. Following the development of the cross-coupling described therein, we returned to this reaction and applied these new conditions in a follow-up ligand screen, now employing heteroaryl iodide **121m** (**Table 4.2**). We were pleased to observe tolerance for the heteroaryl partner, as well as improved enantioselectivity. Unfortunately, only modest yields were only obtained with heating to 60 °C. Exploring a range of different ligands for this transformation, including a PHOX series, did not afford improved results or enable the lowering of the reaction temperature. Nonetheless, we felt

that this initial investigation held promise, providing proof-of-concept that the proposed reductive cross-coupling disconnection was amenable to asymmetric catalysis.

**Table 4.2.** Initial ligand investigation with 5-iodo-2-(*N*-piperidinyl)pyrimidine.



Entry	R	Yield 164 (%)	ee 164 (%)
L67	<sup>i</sup> Pr	2	26
L66	<sup>t</sup> Bu	12	7
L31	Bn	43	53
L68	Ph	11	40
L110	Cy	30	55

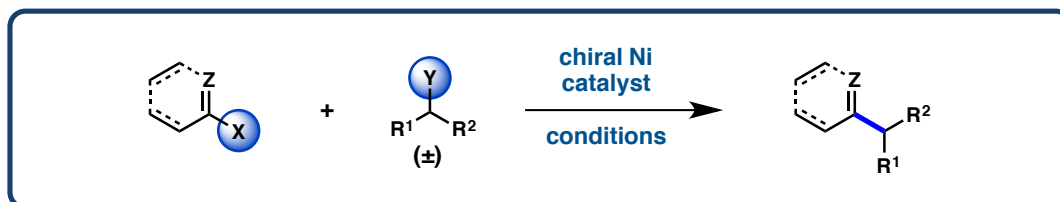
Entry	R	Yield 164 (%)	ee 164 (%)
L111	<sup>s</sup> Bu	36	65
L112	CHPh <sub>2</sub>	57	57
L115	<sup>i</sup> Bu	44	58
L113	CH <sub>2</sub> (1-naph)	58	47
L114	CH <sub>2</sub> (2-naph)	46	55

#### 4.1.3 Reaction design: substrate and condition considerations

The cross-coupling of C(sp<sup>3</sup>) benzylic halides with C(sp<sup>2</sup>) (hetero)aryl halides represents an opportunity to consider the logic of asymmetric cross-coupling and substrate selection. We have demonstrated that each of the substrate classes in **Figure 4.2** is competent in asymmetric cross-electrophile coupling (see Chapters 2 and 3).<sup>7</sup> Therefore, it stands to reason that the stereoconvergent coupling between them should be achievable, as these partners should also be differentiable based on their hybridization.<sup>8</sup> Knowing that the substrates should be amenable and that the coupling was feasible, we imagined the development of this reaction as a venue to survey conditions for their generality: to build on the understanding gained in our previous efforts and to facilitate streamlined optimization in the future. The need for more general asymmetric reductive

coupling conditions is illustrated by **Figure 4.2**. None of our previously optimized conditions were high-performing in any of the other couplings, highlighting the difficulty of extending these conditions to new reaction development between novel electrophiles.

**Figure 4.2.** Cross-reactions of previously developed electrophile pairs and conditions.



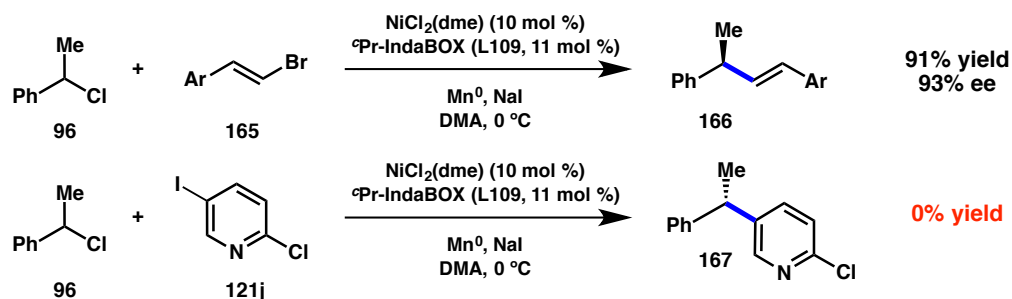
Products Conditions			
NiCl <sub>2</sub> (dme), BOX L32 Mn <sup>0</sup> , DMBA, 3Å MS DMA/THF, rt	Control 79% yield, 93% ee	41% yield, 2% ee	22% yield, 24% ee
NiCl <sub>2</sub> (dme), BOX L109 Mn <sup>0</sup> , NaI DMA, 0 °C	0% yield	Control 91% yield, 93% ee	0% yield
NiCl <sub>2</sub> (dme), PHOX L89 Mn <sup>0</sup> , TMSCl Dioxane, rt, 18 h	0% yield	0% yield	Control 78% yield, 85% ee

As an initial entrée to this campaign, we selected 2-chloro-5-iodopyridine **121j** as a model heteroaryl partner in the cross-coupling with benzyl chloride **96**. As anticipated based on the results in **Figure 4.2** and the difficulties encountered in our prior efforts, the conditions developed for couplings of these substrates in previous reactions did not afford product in the attempted cross-coupling between them (**Scheme 4.3**). These results serve to illustrate the two-part goal of this new reaction development: a) to develop an asymmetric cross-coupling to access valuable enantioenriched 1,1-diarylalkane products,

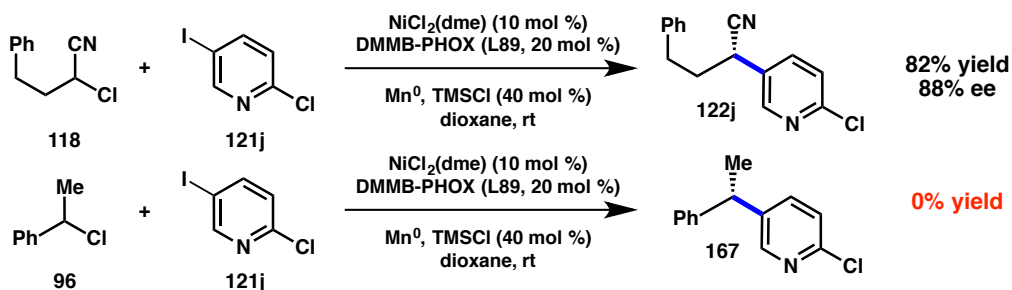
and b) to arrive at a more general set of conditions as an entry point for future asymmetric cross-couplings, in the hope of reducing optimization for each new substrate class. Herein we report the successful realization of these goals, with preliminary results toward future couplings being reported in Chapter 5.

**Scheme 4.3.** Application of previously developed conditions.

**a) Benzyl chloride + vinyl halide conditions (same C(sp<sup>3</sup>) electrophile)**



**b) Chloronitrile + heteroaryl halide conditions (same C(sp<sup>2</sup>) electrophile)**



## 4.2 REACTION DEVELOPMENT

### 4.2.1 Ligand exploration and condition optimization

We began our optimization by considering the results in **Table 4.2**. The reaction conditions employing dioxane as solvent with TMSCl as a surface activator (as in **Chapter 3**) with BiOX ligands gave promising results, but only at elevated temperature. This was surprising, given that both electrophiles have been shown to be reactive under

similar conditions at room temperature. Therefore, we targeted a room temperature reaction, in order to improve enantioselectivity as well as chemoselectivity and yield. Employing the model system described above (**Scheme 4.3**), we conducted parallel ligand screens at 60 °C, 40 °C, and room temperature to assess the effect of temperature on this reaction (**Table 4.3**).

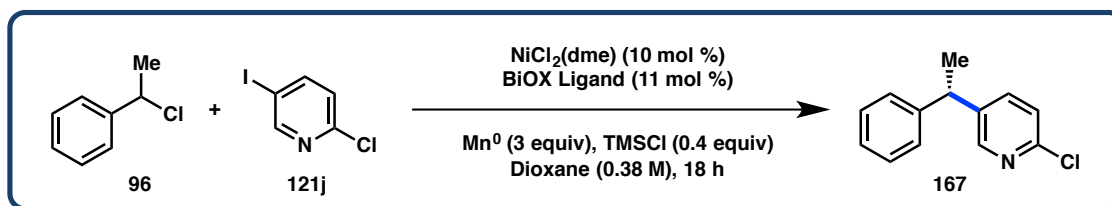
**Table 4.3.** Screening temperature versus BiOX ligands.

a) Temperature= 60 °C				b) Temperature= 40 °C				c) Temperature= 23 °C			
Entry	R	Yield (%)	ee (%)	Entry	R	Yield (%)	ee (%)	Entry	R	Yield (%)	ee (%)
L31	Bn	70	39	L31	Bn	61	43	L31	Bn	39	44
L112	CHPh <sub>2</sub>	53	54	L112	CHPh <sub>2</sub>	69	66	L112	CHPh <sub>2</sub>	37	67
L111	<sup>s</sup> Bu	31	53	L111	<sup>s</sup> Bu	70	54	L111	<sup>s</sup> Bu	71	71
L115	<sup>t</sup> Bu	68	45	L115	<sup>t</sup> Bu	69	62	L115	<sup>t</sup> Bu	68	56
L110	Cy	56	55	L110	Cy	65	62	L110	Cy	74	70

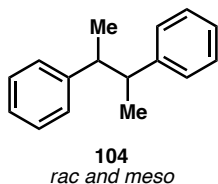
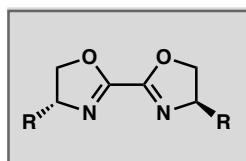
We were pleased to observe improvement with decreasing temperature among several of the ligands screened. Specifically, BiOX ligands bearing branched alkyl substituents (**L110**, **L111**, and **L115**) behaved favorably, giving significantly improved yields and enantioselectivities at room temperature. These ligands afforded a cleaner reaction profile at lower temperature (**Table 4.3c**), giving diminished amounts of homocoupled side products and favoring the desired reaction chemoselectively. Interestingly, BnBiOX **L31** (the ligand employed by Weix and coworkers, **Scheme 4.2**)

showed the opposite trend, affording **167** in the highest yield at elevated temperature, with only slight variation in ee across temperatures.

**Table 4.4.** Evaluation of BiOX ligand scaffolds at room temperature.



#### BiOX Ligands

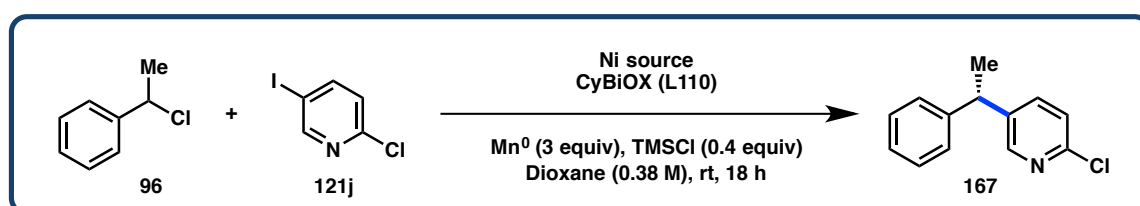


Entry	R	Yield BiBn 104 (%)	Yield <b>167</b> (%)	ee <b>167</b> (%)
L68	Ph	0	0	-
L113	CH <sub>2</sub> -1-Nap	3	17	44
L114	CH <sub>2</sub> -2-Nap	5	32	50
L116	<i>c</i> -Pentyl	15	81	75
L110	Cy	32	68	69
L117	<i>c</i> -Heptyl	28	72	75
L118	3-Pentyl	23	65	75
L119	4-Heptyl	16	81	80

We explored these trends further by conducting a wider BiOX ligand screen at room temperature, incorporating branched alkyl ligands, as well as arene-containing R-groups. All of the ligands bearing aryl substituents (**L68**, **L113**, and **L114**) afforded poor yields of product in moderate ee, reaffirming the result obtained with BnBiOX **L31**. Fortunately, the branched alkyl ligands tested all furnished **167** in good ee and high yield. We were particularly delighted to find that 4-HeptylBiOX **L119** gave 81% yield of **167** in 80% ee and with lower levels of homocoupling, the best result obtained by far. The role of these longer alkyl groups remains unclear at this stage. One can imagine the hydrophobic chains simply providing bulkier blocking of the quadrants, providing increased enantioinduction. However, the origin of the effect on chemoselectivity and

yield is less straightforward. Further studies are required to determine if these groups are significantly altering the solvent cage about the catalyst, changing ligand bite angles, or influencing some other mechanistic parameter to produce for the observed effects.

**Table 4.5.** Evaluation of Ni precatalysts, metal/ligand ratio, and catalyst loading.

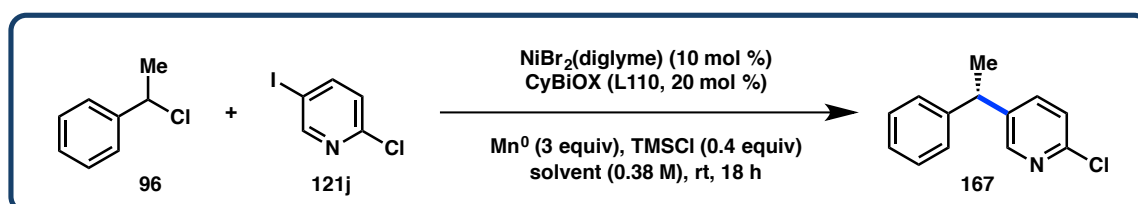


with 11 mol % CyBiOX (L110):				with NiBr <sub>2</sub> (diglyme):				
Ni Source (10 mol %)	Yield BiBn 104 (%)	Yield 167 (%)	ee 167 (%)	% Ni	M:L	Yield BiBn 104 (%)	Yield 167 (%)	ee 167 (%)
NiCl <sub>2</sub> (dme)	30	69	69	5%	1:1	15	71	75
Ni(OAc) <sub>2</sub> ·4H <sub>2</sub> O	0	22	72	5%	1:2	22	77	75
Ni(BF <sub>4</sub> ) <sub>2</sub> ·6H <sub>2</sub> O	5	0	-	10%	1:1	16	68	74
Ni(acac) <sub>2</sub>	30	69	69	10%	1:1.5	23	77	72
NiBr <sub>2</sub> (dme)	25	74	72	10%	1:2	25	75	74
NiBr <sub>2</sub> (diglyme)	20	81	74	10%	1:3	27	78	74
				15%	1:1	29	71	71
				15%	1:2	29	71	74

With these promising ligand results in hand, we turned our attention to the optimization of the remaining reaction parameters. Because of the synthetic challenge posed by the noncommercial amino acid-derived branched ligands (such as **L119**), we conducted these studies employing CyBiOX **L110**, anticipating that this more easily accessible branched-alkyl ligand would show analogous responses to varying reaction conditions. Beginning with a screen of Ni precatalysts, we were surprised and pleased to see a significant improvement in yield and selectivity upon switching to NiBr<sub>2</sub>(diglyme), the first time that a Ni source other than NiCl<sub>2</sub>(dme) has been optimal in our hands (**Table 4.5**). Employing this Ni salt, we conducted a screen of metal/ligand ratios and

catalyst loading. This survey revealed a remarkable tolerance for variability in these parameters. However a catalyst loading of 10 mol % with a 2:1 ligand: metal ratio gave the most reproducible results and was chosen as the standard condition for further studies.

**Table 4.6.** Evaluation of solvents and reaction concentration.

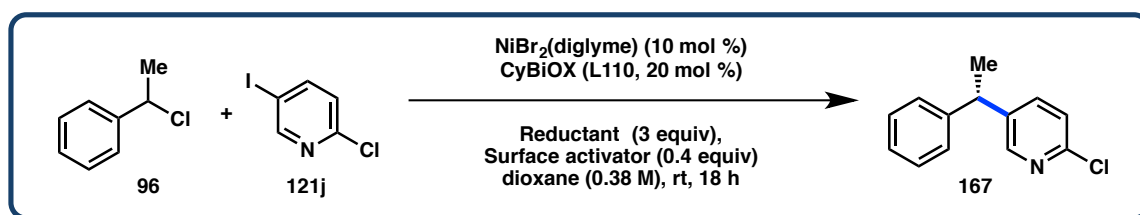


				<i>with 1,4-dioxane:</i>			
Solvent	Yield BiBn 104 (%)	Yield 167 (%)	ee 167 (%)	Concentration [M]	Conv 96 (%)	Yield 167 (%)	ee 167 (%)
1,4-Dioxane	26	74	74	0.05	54	37	69
1,3-Dioxane	0	0	-	0.1	61	42	66
THF	51	49	43	0.2	91	76	74
DME	41	54	55	0.36	77	69	75
DMPU	33	60	49	1.0	35	30	70
DMA	72	25	31				
MeCN	47	44	6				
DCM	50	10	44				
MeOH	77	13	73				

Next, we screened a range of solvents to ensure that 1,4-dioxane remained optimal in this transformation (**Table 4.6**). As before, acyclic ethereal solvents such as TBME and Et<sub>2</sub>O failed to suspend the Mn<sup>0</sup> dust, leading to no conversion (not shown). Other cyclic ethereal solvents proved to be inferior to 1,4-dioxane. A marked increase in homocoupling was observed with more polar solvents, such as DMA and MeOH. Therefore, we concluded that 1,4-dioxane was the best solvent for this reaction and proceeded to evaluate concentration as a parameter. Gratifyingly, some range of tolerance was identified, with the 0.2 M and 0.36 M conditions being identical within error. More

or less concentrated conditions led to lower conversions and yields. Attempts at lowering the reaction temperature through the use of mixed solvent systems containing 1,4-dioxane did not prove fruitful, affording only decreased yields with no significant improvement in selectivity. Therefore 0.36 M dioxane at room temperature was selected as the optimal solvent condition.

**Table 4.7.** Evaluation of reductants and activating reagents.



*with TMSCl:*

Entry	Reductant	Yield (%)	ee (%)
1	Mn <sup>0</sup>	83	72
2	Zn <sup>0</sup>	20	30
3	Zn <sup>0</sup> + MgCl <sub>2</sub>	6	0
4	In <sup>0</sup>	0	-
5	TDAE	6	31
6	TDAE (-TMSCl)	6	43

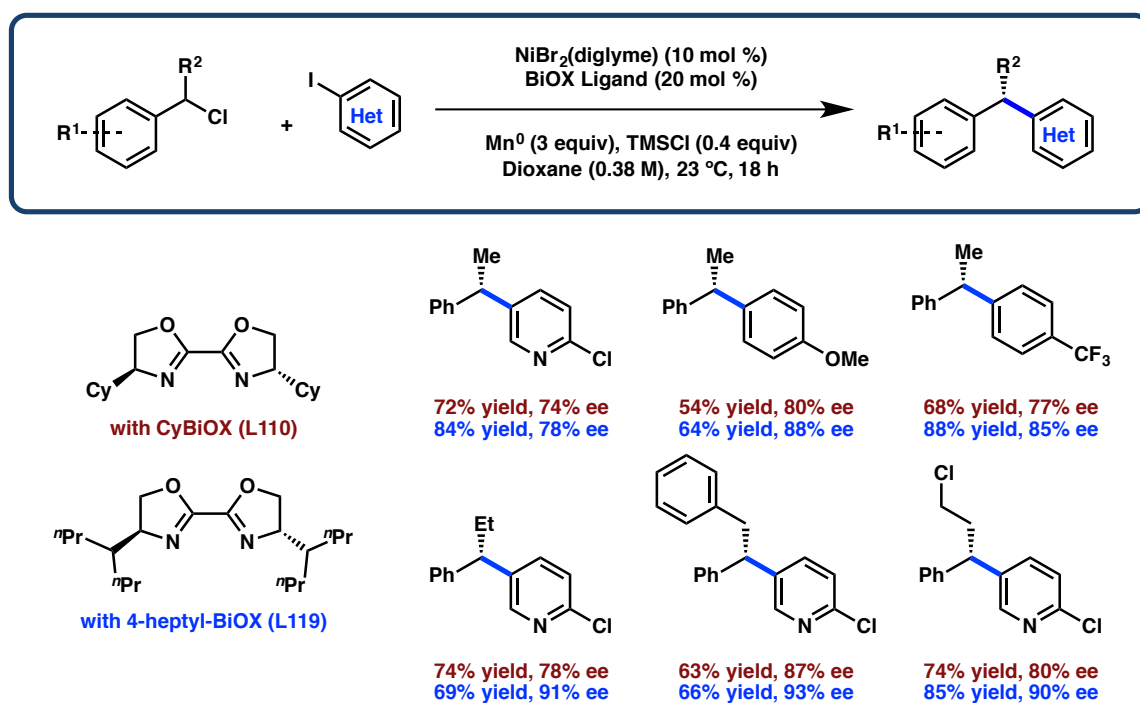
*with Mn<sup>0</sup>:*

Entry	Surface activator	Yield (%)	ee (%)
1	TMSCl	74	74
2	TFA	3	0
3	TMSOTf	18	64
4	TfOH	1	3
5	4 M HCl/dioxane	4	60

Finally, with temperature and solvent conditions identified, we revisited the stoichiometric reductant and surface-activating reagent. In a survey of reductants, Mn<sup>0</sup> emerged as the most efficacious in this series, with Zn<sup>0</sup> giving lower yield and selectivity. The difference in reactivity may be attributable to the difference in reduction potential between the metals. However, the change in enantioselectivity is harder to rationalize. It is possible that the reductants favor different mechanisms, or one can imagine that the Lewis-acidic stoichiometric salt byproducts may exert significant influence over the course of the reaction. Poor yields were achieved employing the soluble organic

reductant TDAE, with lower selectivity. However these entries demonstrate the feasibility of the reaction in the absence of stoichiometric metal, suggesting that improvement of the organic reductant scaffold may be a useful line of inquiry.

**Scheme 4.4.** Comparison of CyBiOX (**L110**) with 4-HeptylBiOX (**L119**).

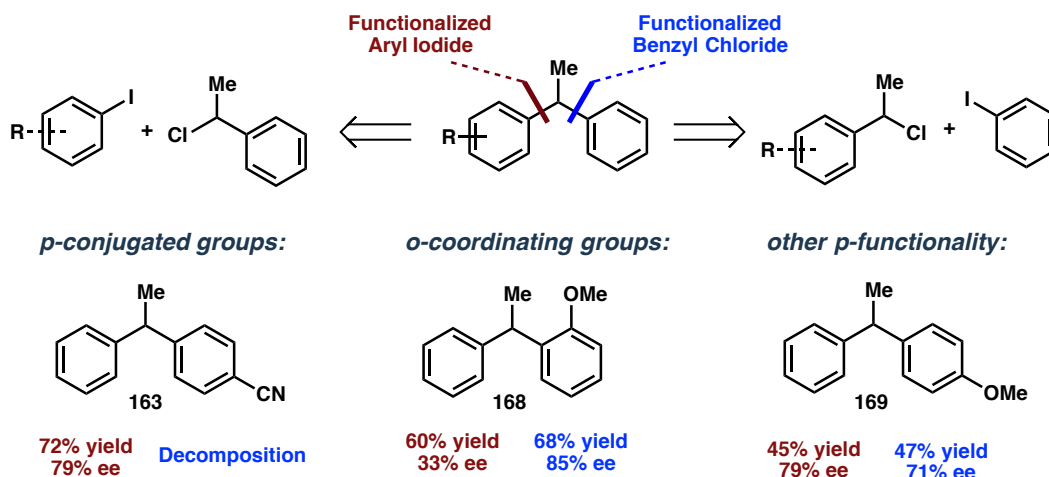


At this stage, we had succeeded in optimizing all of the reaction parameters and components, arriving at the conditions in **Scheme 4.4**. We returned our focus then to the BiOX ligand scaffold, to evaluate the performance and necessity of 4-HeptylBiOX **L119** with multiple test substrates. We were gratified to find that the optimization carried out with CyBiOX **L110** indeed led to improved results in all cases with **L119**, affording the best results to date for a series of products (**Scheme 4.4**). Confident now that these composed the final set of reaction conditions, we sought to prepare 4-HeptylBiOX (**L119**) on large scale and set out to evaluate the substrate scope of this transformation more thoroughly.

### 4.2.2 Substrate scope and disconnection strategy

Before investigating a wide range of substrates, we first wanted to assess the strategy of substrate selection to access these pseudosymmetric products. That is, to prepare any desired mono-substituted 1,1-diarylalkane, substitution may be placed on either the benzyl component or the aryl partner. If various classes of functional groups perform better on one partner than the other, this knowledge is critical in designing an ideal disconnection of the target. This versatility, in which any product can be disconnected in two ways, is a significant advantage of this cross-coupling methodology. Therefore, we initially explored a small series of simply substituted electrophiles to compare their performance in the reaction. Selected examples are shown in **Figure 4.3** to illustrate the trends we observed.

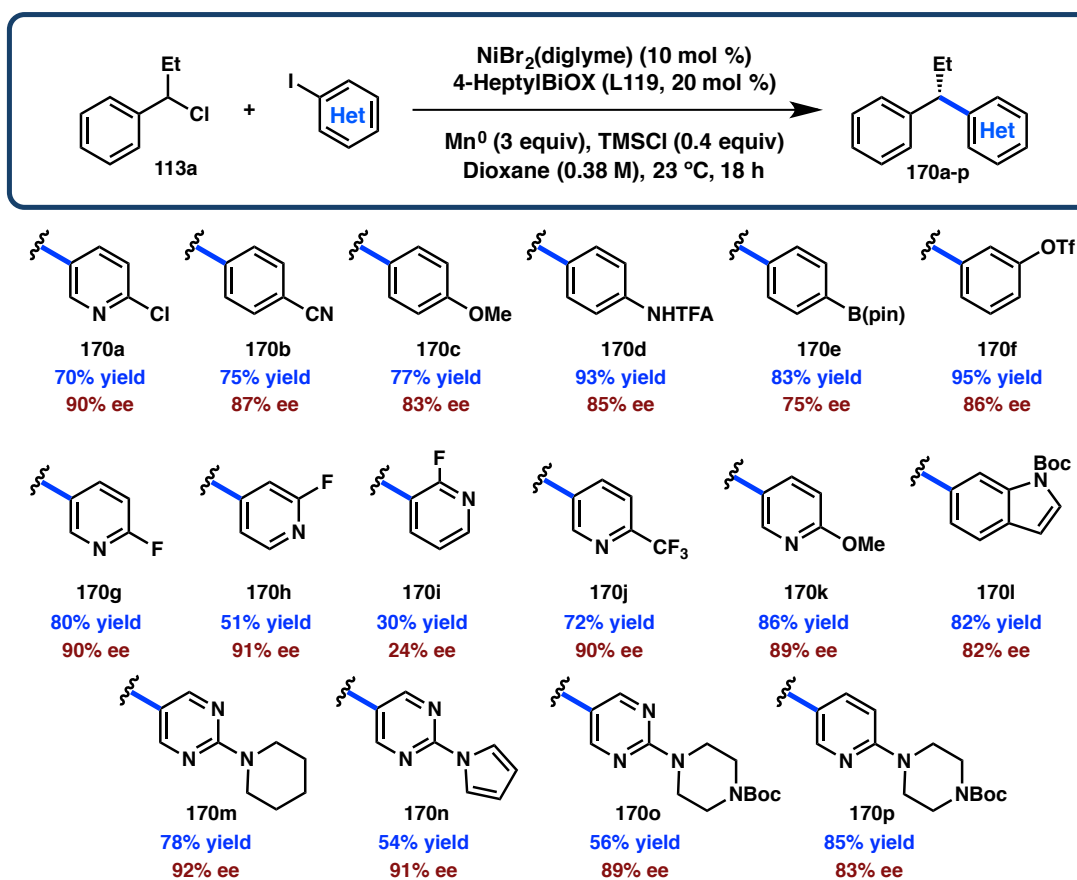
**Figure 4.3.** Possible disconnections of pseudosymmetric 1,1-diarylalkanes.



Benzyl chlorides bearing conjugated electron-withdrawing groups such as nitriles (**163**) underwent rampant decomposition, affording low yields and messy reaction profiles. We hypothesize that this may be attributable to the delocalization of benzylic radical intermediates, affording a complicated mixture of products. Fortunately, these

groups behaved well when incorporated via the aryl iodide partner. The opposite trend was observed with *ortho*-coordinating groups, such as *o*-methoxy **168**. These groups afforded good yields and very high ee's when brought in on the benzyl chloride partner, but gave low enantioselectivity when placed on the aryl iodide. Non-conjugated groups at the *para* and *meta* positions gave only slight and unpredictable variability between the two partners, as exemplified by *para*-methoxy **169**. Finally, non-coordinating *ortho*-substituents such as methyl performed very poorly on both substrates (not shown).

**Scheme 4.5.** (Hetero)aryl iodide scope.<sup>a</sup>



<sup>a</sup> Yields determined by <sup>1</sup>H NMR with an internal standard, reactions conducted on 0.2 or 0.05 mmol scale under an N<sub>2</sub> atmosphere in a glovebox. % ee determined by SFC using a chiral stationary phase.

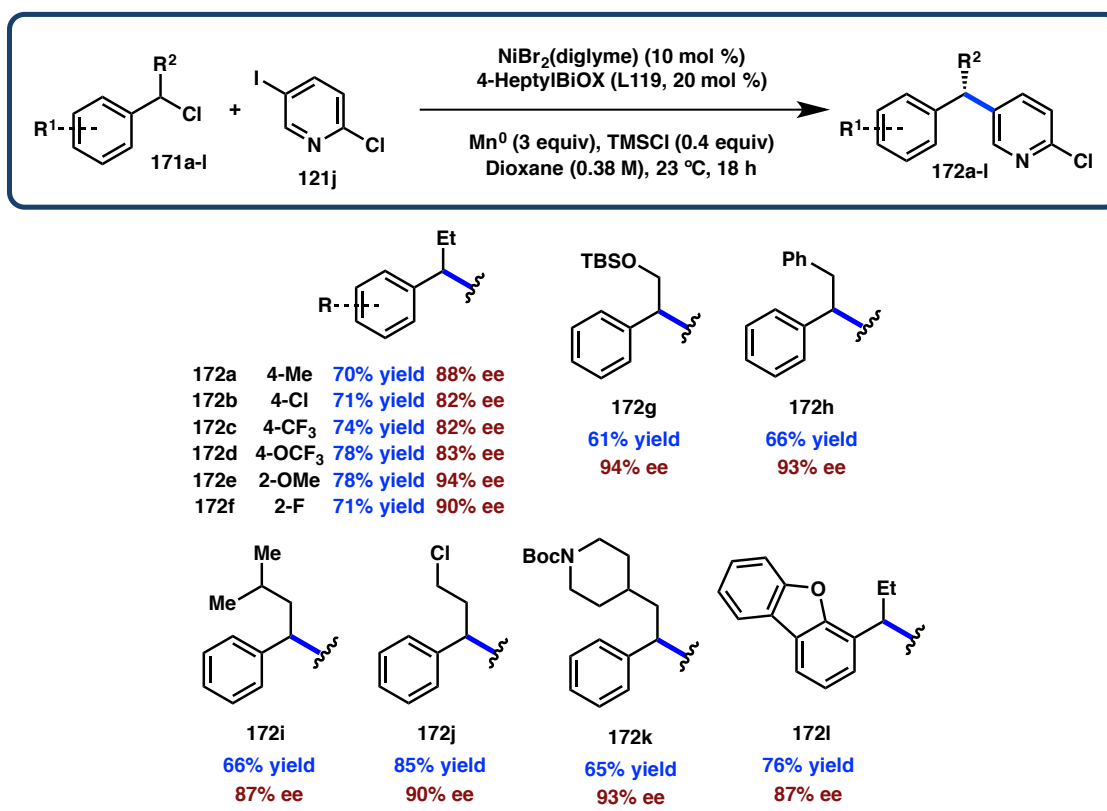
With an understanding of the basic reactivity trends and functional group tolerance for each reaction partner, we focused our attention on the (hetero)aryl iodide

scope. Based on the above results, we selected 1-(chloropropyl)benzene (**113a**) as a representative model benzyl chloride substrate for these studies. Beginning with phenyl-based arenes, we were very pleased to see that electron-withdrawing (**170b**) as well as electron-donating (**170c**) substituents afforded products in high yield and ee (**Scheme 4.5**). Acidic protons were tolerated, as shown by trifluoroacetanilide **170d**, with no protodehalogenated side-products observed. The reaction was also orthogonal to nucleophilic boronates (**170e**) as well electrophilic triflates (**170f**), providing useful handles for further functionalization or elaboration via cross-coupling.<sup>9</sup>

At this point, we moved on to explore heteroaryl iodides, beginning with substituted pyridines. 2-Chloro- and 2-fluoropyridines afforded the cross-coupled products (**170a, g–i**) in excellent ee and moderate to high yields, with the exception of 2-fluoro-3-iodopyridine, highlighting the difficulty of introducing *ortho*-substituents via the aryl iodide partner. Notably, these substrates coupled with complete chemoselectivity, reacting exclusively at the iodo position.<sup>10</sup> Electron withdrawing (**170j**) as well as donating (**170k**) groups performed well, including 2-(N-Boc-piperazinyl)pyridine **170p**. Gratifyingly, pyrimidine substrates also behaved well in the reaction, generating 2-aminopyrimidine derivatives **170m–o** with excellent enantioselectivity, including 2-(N-pyrrolo)pyrimidine **170n**, which had not been successful in the cross-coupling with chloronitriles (**Chapter 4.3**). We also noted that 4-iodo-2-(N-piperidinyl)pyrimidine **121m** cross-coupled in high yield and excellent ee at room temperature, in contrast to the initial studies shown in **Table 4.2**. This result suggests that **L119** is critical to the success of these mild conditions with heteroaromatics. Finally, we were pleased to find that N-Boc-6-iodoindole cross-coupled in very high yield and ee. Importantly, no condition

modification was necessary between substrates. This is in contrast to our previous work in asymmetric reductive cross-coupling, as well as the work of other groups studying the cross-coupling of heteroaromatic electrophiles.<sup>11</sup>

**Scheme 4.6.** Benzyl chloride substrate scope.<sup>a</sup>



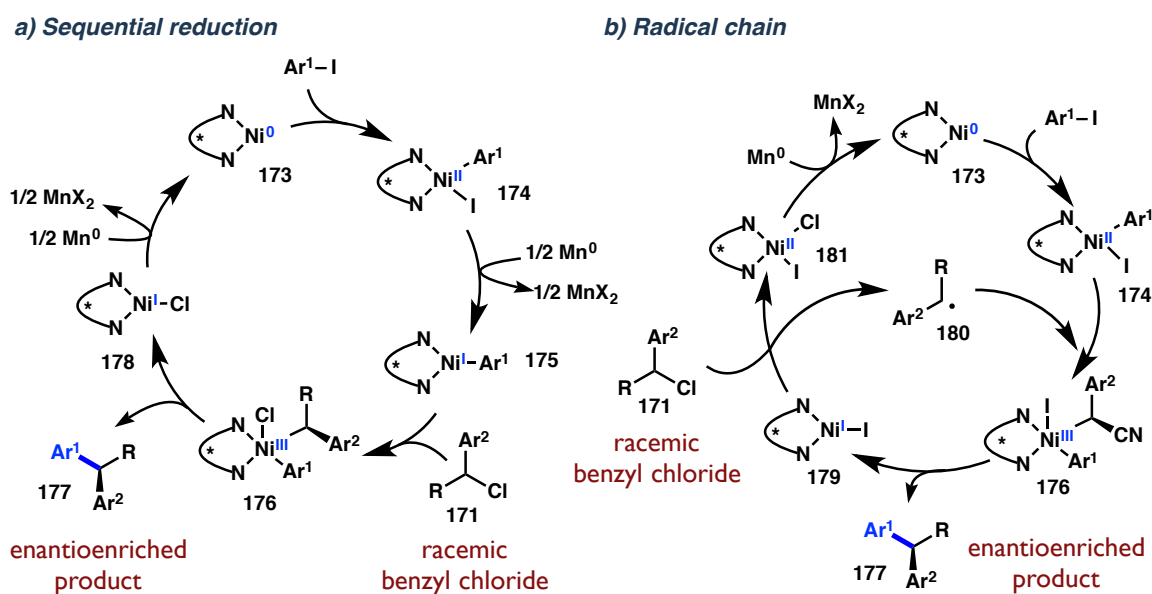
<sup>a</sup> Yields determined by <sup>1</sup>H NMR with an internal standard, reactions conducted on 0.2 or 0.05 mmol scale under an N<sub>2</sub> atmosphere in a glovebox. % ee determined by SFC using a chiral stationary phase.

We then shifted our focus to investigating the scope of the benzyl chloride partner. As shown in **Figure 4.3**, this electrophile scope unfortunately does not include conjugated electron-withdrawing substituents. However a synthetically useful range of other substituents on the aryl ring was well-tolerated, including electron-rich (**172a**) and electron-withdrawing groups (**172c** and **172d**), as well as an electrophilic chloride handle (**172b**) for further cross-coupling (**Scheme 4.6**). Most interestingly, *ortho*-substituted partners bearing functional groups capable of forming an attractive interaction with Ni

performed best in this reaction. *Ortho*-methoxy **172e** and *ortho*-fluoro **172f** were formed in high yields and excellent ee's. This is especially notable in contrast with the scope of the aryl iodide partner, where these groups performed very poorly (**Figure 4.3 168** and **Scheme 4.5 170i**). Inspired by these results, we also prepared 4-(1-chloropropyl)dibenzofuran, a bulkier substrate maintaining the *ortho* oxygen motif of **171l**. Gratifyingly, this substrate also performed very well, coupling to give **172l** in 76% yield and 87% ee. Finally, we explored a series of benzyl chlorides bearing substitution at the  $\alpha$ -position, in order to access a more diverse range of diarylalkane products. We were very pleased to see that this series behaved well in the reaction, coupling in high yields and even better ee's than many of the simpler previous substrates. Importantly, the functional group tolerance at this position was excellent, allowing for the incorporation of silyl ether **172g**, primary alkyl chloride **172j**, and Boc-protected piperidine **172k**.

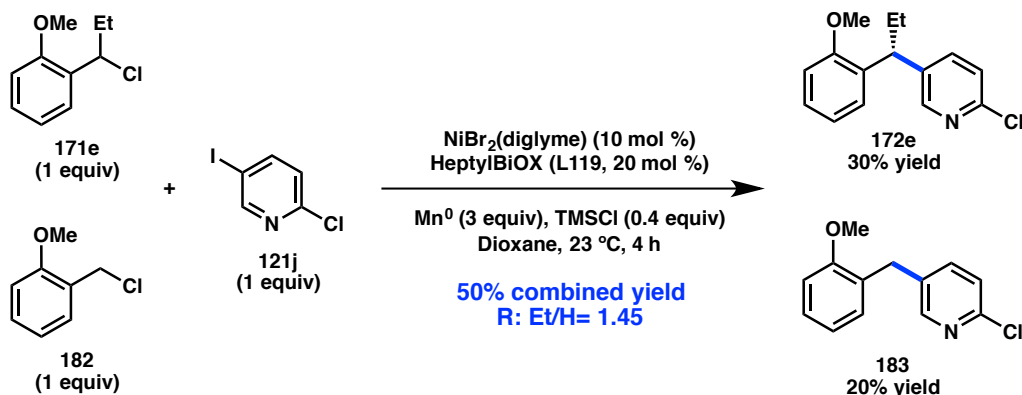
### 4.3 MECHANISTIC INVESTIGATIONS

**Figure 4.4.** Potential mechanisms for the asymmetric reductive cross-coupling.



Having evaluated a wide range of coupling partners for both substrate classes, we turned our attention to the mechanism of the asymmetric cross-coupling transformation. The two mechanistic hypotheses that guided our reaction development are shown in **Figure 4.4**. For a detailed consideration of the elementary steps, see **Chapter 1 and 3**, in which the mechanisms are discussed generally and for  $\alpha$ -chloronitrile  $C(sp^3)$  electrophiles. As in our previous mechanistic explorations, we focused our efforts on elucidating the presence and nature of radical intermediates derived from the  $C(sp^3)$  electrophilic component, the benzyl chloride, in the proposed reaction with  $Ni^I$  **175** or **179**. This putative prochiral radical species (**180**) is expected to be critical to the success of the reaction, enabling differentiation of the electrophiles via sequential oxidative addition, and facilitating stereoconvergence of the racemic halide precursor.

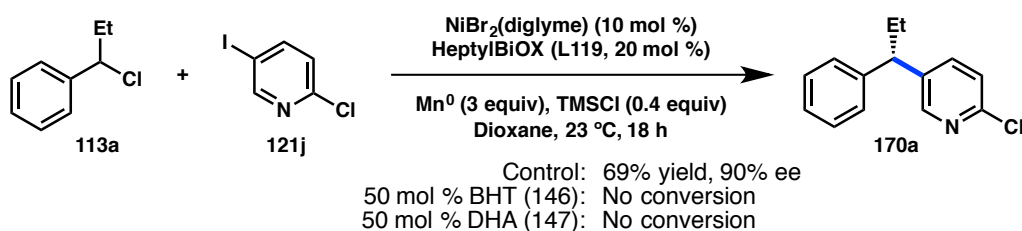
**Scheme 4.7.** Competition experiment between 1° and 2° benzyl chlorides.



As an initial probe to determine if the benzylic partner is reacting via a stabilized radical intermediate, we conducted a competition experiment between primary benzyl chloride **182** and secondary benzyl chloride **171e** (**Scheme 4.7**). While both partners could conceivably react via either an  $S_N2$  oxidative addition or a halide abstraction radical oxidative addition, we anticipated that these substrates would undergo such

transformations at markedly different rates. That is, if the mechanism of benzylic oxidative addition were  $S_N2$ -like, then the less hindered primary chloride would be expected to react faster, favoring **183** in the reaction. On the other hand, if the oxidative addition step proceeds via halide abstraction to form a benzylic radical, then the more stabilized secondary chloride should react faster, forming more **172e**. Indeed, upon workup after 4 hours, the ratio of products favors the secondary cross-coupled **172e** by 1.45 to 1, suggesting that a radical mechanism may be at play.

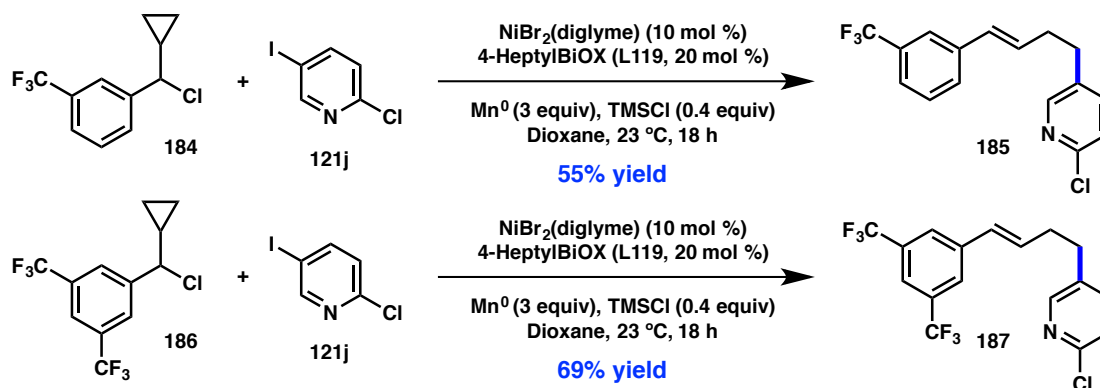
**Scheme 4.8.** Radical inhibitor studies.



As a follow-up to this experiment, we explored the effect of radical inhibitors on the course of the reaction (**Scheme 4.8**). Employing 50 mol % of either BHT (**146**) or DHA (**147**), no conversion of either coupling partner was observed. This led us to conduct one final set of experiments, utilizing a radical clock substrate, to probe the presence of the radical intermediates (**Scheme 4.9**). Unfortunately, no reaction was observed employing benzylic electrophiles with tethered olefins, making cyclization clocks untenable. However, cyclopropylcarbonyl radical clocks proved more helpful.<sup>12</sup> While unsubstituted  $\alpha$ -cyclopropyl benzyl chlorides are too unstable to be handled under the reaction conditions, trifluoromethylated versions **184** and **186** allowed for synthesis and isolation of the radical clock substrates.<sup>13</sup> Presumably, this is due to the destabilizing effect of the trifluoromethyl substituents on a benzylic carbocation intermediate, thus suppressing spontaneous heterolysis and decomposition. Subjecting these radical clocks

to the reaction conditions afforded only the rearranged cross-coupled products **185** and **187**, supporting the intermediacy of a cyclopropylcarbinyl radical derived from the benzyl chloride.

**Scheme 4.9.** Radical clock experiments.



The combined results of the inhibitor studies and the radical clock experiments are interesting when compared with previous studies of similar reactions. When employing  $\alpha$ -chloronitriles as the  $\text{C}(\text{sp}^3)$  partner under very similar conditions, complete rearrangement of a cyclopropyl radical clock was observed. However no inhibition by BHT or DHA was noted (see **Chapter 3**). This is in contrast to our results here, where both rearrangement and complete inhibition were seen. This may suggest a divergence of mechanism between these two substrate classes. The cyanomethyl radical is less stable than the benzyl radical by 19 kJ/mol,<sup>14</sup> perhaps limiting its half-life and favoring a rapid recombination with Ni, leading to a sequential reduction mechanism. Under these conditions, the fleeting radical would not diffuse into the solvent, preventing inhibition by BHT or DHA. On the other hand, the more stable benzylic radicals may persist long enough to escape the solvent cage, favoring a radical chain mechanism and leading to poisoning by radical inhibitors. However, more research is needed to elucidate the

mechanisms of these transformations and the differences between them. These results suggest an interesting divergence that may serve as an entry point to these studies.

## 4.4 CONCLUSION

We have successfully developed a highly enantioselective reductive cross-coupling between secondary benzylic chlorides and (hetero)aryl iodides to afford a diverse range of 1,1-di(hetero)arylalkanes. This marks the conclusion of a longstanding effort in our laboratory and presents a novel approach to these valuable chiral molecules with unprecedented substrate scope. In so doing, we have demonstrated the second application of a dioxane/TMSCl solvent system in asymmetric reductive cross-coupling. The extension of these conditions to other substrate classes will be discussed in **Chapter 5**. It is our hope that these conditions will provide a useful starting point in the discovery of other transformations, facilitating methodology development and streamlining optimization for new substrate classes.

## 4.5 EXPERIMENTAL SECTION

### 4.5.1 *Materials and methods*

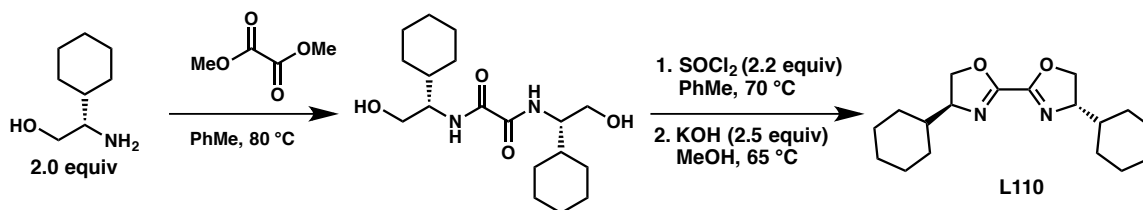
Unless otherwise stated, reactions were performed under a nitrogen atmosphere using freshly dried solvents. Methylene chloride ( $\text{CH}_2\text{Cl}_2$ ), diethyl ether ( $\text{Et}_2\text{O}$ ), tetrahydrofuran (THF), and toluene (PhMe) were dried by passing through activated alumina columns. All other commercially obtained reagents were used as received unless specifically indicated. Aryl iodides were purchased from Sigma Aldrich, Combi-Blocks, or Astatech. Manganese powder (>99.9%) was purchased from Sigma Aldrich.

NiBr<sub>2</sub>(diglyme) was purchased from Strem. All reactions were monitored by thin-layer chromatography using EMD/Merck silica gel 60 F254 pre-coated plates (0.25 mm). Silica gel column chromatography was performed as described by Still et al. (W. C. Still, M. Kahn, A. Mitra, *J. Org. Chem.* **1978**, *43*, 2923) using silica gel (particle size 0.032-0.063) purchased from Silicycle. <sup>1</sup>H and <sup>13</sup>C NMR were recorded on a Varian Inova 500 (at 500 MHz and 125 MHz respectively) or a Varian Inova 600 (at 600 MHz and 150 MHz respectively), and are reported relative to internal chloroform (<sup>1</sup>H, δ = 7.26, <sup>13</sup>C, δ = 77.0). Data for <sup>1</sup>H NMR spectra are reported as follows: chemical shift (δ ppm) (multiplicity, coupling constant (Hz), integration). Multiplicity and qualifier abbreviations are as follows: s = singlet, d = doublet, t = triplet, q = quartet, m = multiplet, br = broad. IR spectra were recorded on a Perkin Elmer Paragon 1000 spectrometer and are reported in frequency of absorption (cm<sup>-1</sup>). Analytical SFC was performed with a Mettler SFC supercritical CO<sub>2</sub> analytical chromatography system with Chiralcel AD-H, OD-H, AS-H, OB-H, and IA columns (4.6 mm x 25 cm). HRMS were acquired using either an Agilent 6200 Series TOF with an Agilent G1978A Multimode source in electrospray ionization (ESI), atmospheric pressure chemical ionization (APCI), or mixed (MM) ionization mode. Low-temperature X-ray diffraction data ( $\phi$ - and  $\omega$ -scans) were collected on a Bruker AXS D8 VENTURE KAPPA diffractometer coupled to a PHOTON 100 CMOS detector with Cu-K $\alpha$  radiation ( $\lambda = 1.54178 \text{ \AA}$ ) from an I $\mu$ S micro-source.

## 4.5.2 Ligand preparation

### A. Preparation of (4*S*,4'*S*)-4,4'-dicyclohexyl-4,4',5,5'-tetrahydro-2,2'-bioxazole

#### (L110, (*S*)-CyBiOX)

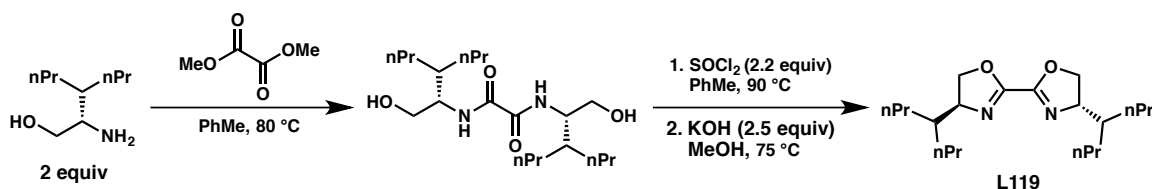


(*S*)-2-Amino-2-cyclohexylethan-1-ol (2 equiv, 1.00 g, 6.98 mmol) and dimethyl oxalate (1 equiv, 0.438 g, 3.7 mmol) were dissolved in PhMe (75 mL) and heated to 80 °C. The reaction was allowed to stir overnight with the diamide precipitating out of solution as a white solid. Reaction was cooled to room temperature and concentrated *in vacuo* to afford the crude diol (1.260 g, 3.70 mmol). The crude diol was dissolved in PhMe (30 mL) and heated to 70 °C whereupon the thionyl chloride (2.2 equiv, 0.6 mL, 8.22 mmol) was added. Reaction was stirred at 70 °C for 30 minutes then heated to 90 °C for 90 minutes. Reaction was cooled to room temperature and poured into 20% KOH solution cooled to 0 °C. The aqueous layer was separated and extracted (x3) with DCM and the combined organic layers were washed with 20% KOH solution, NaHCO<sub>3</sub> and brine. The organic layer was dried with Na<sub>2</sub>SO<sub>4</sub>, filtered through a pad of Celite, and concentrated under reduced pressure. The crude dichloride (1.40 g, 3.71 mmol) was then dissolved in MeOH (35 mL) and KOH (0.52 g, 9.27 mmol) was added. Reaction was heated to reflux for 14 hours. Reaction was cooled to room temperature and concentrated to remove the MeOH. Crude mixture was loaded directly onto a silica gel column and eluted in 30% EtOAc/Hex to 40% EtOAc/Hex. The pure **L110** was obtained as a white solid (0.556 g, 49% over 3 steps). <sup>1</sup>H NMR (400 MHz, CD<sub>3</sub>CN) δ 4.40 (dd, *J*

= 9.7, 8.2 Hz, 1H), 4.15–4.00 (m, 2H), 1.93– 1.85 (m, 1H), 1.77 (ddt,  $J = 9.4, 5.4, 1.4$  Hz, 2H), 1.69 (dtd,  $J = 9.2, 3.1, 1.5$  Hz, 1H), 1.58 (ddt,  $J = 12.4, 3.4, 1.8$  Hz, 1H), 1.45 (tdt,  $J = 11.6, 6.7, 3.4$  Hz, 1H), 1.35–1.15 (m, 3H), 1.15–0.94 (m, 2H).  $^{13}\text{C}$  NMR (101 MHz,  $\text{CD}_3\text{CN}$ )  $\delta$  154.2, 71.9, 70.7, 42.3, 28.9, 28.8, 26.2, 25.7, 25.6; FTIR (NaCl, thin film): 2922, 2850, 1614, 1450, 1130, 1103  $\text{cm}^{-1}$ ; HRMS (MM) calc'd for  $[\text{M} + \text{H}_3\text{O}]^+$  323.2329, found 323.2319.

## B. Preparation of (4*S*,4'*S*)-4,4'-diheptan-4-yl)-4,4',5,5'-tetrahydro-2,2'-bioxazole

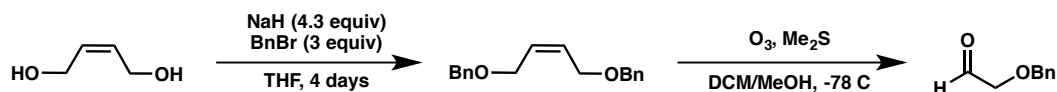
### (L119, (S)-4-HeptylBiOX)



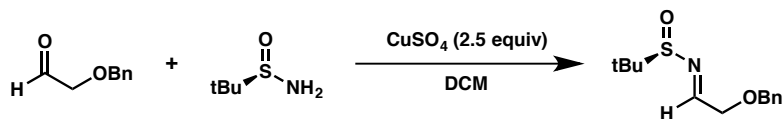
(*S*)-2-Amino-3-propylhexan-1-ol (2 equiv, 2.8 g, 17.6 mmol) and dimethyl oxalate (1 equiv, 1.038 g, 8.8 mmol) were dissolved in PhMe (200 mL) and heated to 80 °C. The reaction was allowed to stir overnight with the diamide precipitating out of solution as a white solid. Reaction was cooled to room temperature and concentrated *in vacuo* to afford the crude diol (3.3 g, 8.86 mmol). The crude diol was dissolved in PhMe (60 mL) and heated to 70 °C whereupon the thionyl chloride (1.4 mL, 19.2 mmol) was added. Reaction was stirred at 70 °C for 30 minutes then heated to 90 °C for 90 minutes. Reaction was cooled to room temperature and poured into 20% KOH solution cooled to 0 °C. The aqueous layer was separated and extracted (x3) with DCM and the combined organic layers were washed with 20% KOH solution,  $\text{NaHCO}_3$  and brine. The organic layer was dried with  $\text{Na}_2\text{SO}_4$ , filtered through a pad of Celite, and concentrated under

reduced pressure. The crude dichloride (3.6 g, 8.8 mmol) was then dissolved in MeOH (90 mL) and KOH (1.23 g, 21.9 mmol) was added. Reaction was heated to reflux for 14 hours. Reaction was cooled to room temperature and concentrated to remove the MeOH. Crude mixture was loaded directly onto a silica gel column and eluted in 10% EtOAc/Hex. The pure **L119** was obtained as a white solid (1.55 g, 53% over 3 steps).  $R_f = 0.58$  (50% EtOAc/Hex);  $^1\text{H NMR}$  (500 MHz, Acetonitrile- $d_3$ )  $\delta$  4.43 (dd,  $J = 10.1, 8.3$  Hz, 1H), 4.33 (ddd,  $J = 10.1, 8.5, 5.9$  Hz, 1H), 4.11 (t,  $J = 8.4$  Hz, 1H), 1.65 – 1.54 (m, 1H), 1.50 – 1.17 (m, 7H), 0.93 (td,  $J = 7.1, 2.6$  Hz, 6H).

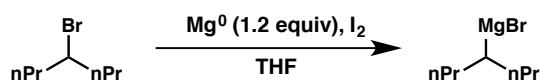
### C. Preparation of (S)-2-amino-3-propylhexan-1-ol



(Z)-But-2-ene-1,4-diol was benzyl protected under known literature procedure. (Z)-1,4-bis(benzyloxy)but-2-ene (1 equiv, 15 g, 56 mmol) was dissolved in 3:1 solution of DCM/MeOH (150 mL) and cooled to  $-78$  °C. Ozone was bubbled through the reaction until the solution turned blue, signaling  $\text{O}_3$  saturation. Reaction sparged with  $\text{O}_2$ , then  $\text{N}_2$  for 15 minutes. Dimethyl sulfide (12 equiv, 50 mL, 676 mmol) was added and the reaction was allowed to warm to room temperature and stir for 14 hours. Reaction was concentrated under reduced pressure and purified by column chromatography (30% EtOAc/Hex) to afford the aldehyde (16.6 g, 99% yield).

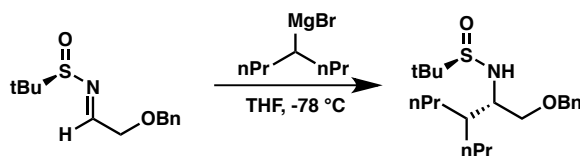


2-(benzyloxy)acetaldehyde (1 equiv, 16.6 g, 111 mmol) was dissolved in DCM (225 mL) at room temperature. (R)-(+)-*tert*-butylsulfonamide (1.1 equiv, 14.9 g, 123 mmol) and copper (II) sulfate (2.5 equiv, 44.1 g, 276 mmol) were added and the reaction was allowed to stir at room temperature for 36 hours. Reaction was filtered through a plug of Celite with DCM. Solution concentrated and purified by column chromatography (20% EtOAc/Hex) to afford imine product (17 g, 61% yield).



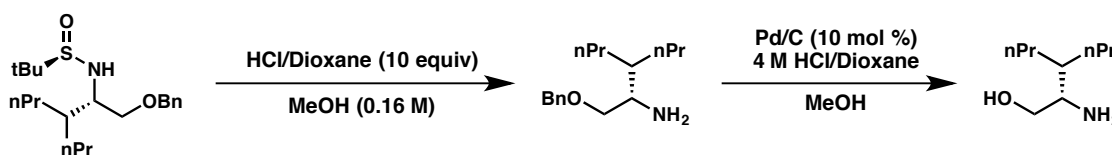
### Grignard formation:

Magnesium (1.3 equiv, 4.00 g, 172 mmol) was activated with 1 M HCl, then washed with water, ethanol, and ether before transfer to a flame dried, 500 mL 3-neck flask equipped with a reflux condenser and stir bar. The  $\text{Mg}^0$  was stirred under vacuum overnight. THF (170 mL) and a fleck of  $\text{I}_2$  was added and the stirring mixture was heated to reflux with a heat gun periodically over 20 minutes until the brown solution turned dark, translucent gray. 4-bromoheptane (1 equiv, 21 mL, 134 mmol) was added slowly, portion-wise, with heating to reflux in the intervals between additions. After addition of alkyl bromide, reaction was heated to 80 °C for 1 hour, then cooled to room temperature and titrated (0.36 M, 49% yield).



Sulfonamide (1 equiv, 7.33 g, 28.9 mmol) was dissolved in THF (260 mL) and cooled to -78 °C. Freshly prepared, heptan-4-ylmagnesium bromide (1.6 equiv, 9.4 g,

46.2 mmol) was added via cannula. Reaction was stirred at  $-78\text{ }^{\circ}\text{C}$  for 8 hours then allowed to stir overnight while the bath warmed slowly. The reaction mixture was quenched with water and  $\text{Na}_2\text{SO}_4$  was added. Mixture was filtered through a plug of Celite and concentrated. Product was purified by silica gel chromatography (10% EtOAc/Hex to 30% EtOAc/Hex) to afford product (9.9 g, 97% yield, 97:3 d.r.).  $^1\text{H}$  NMR (500 MHz, Benzene- $d_6$ )  $\delta$  7.28 (dd,  $J = 8.1, 1.4$  Hz, 2H), 7.20 – 7.14 (m, 2H), 7.09 – 7.02 (m, 1H), 4.39 (d,  $J = 11.9$  Hz, 1H), 4.26 (d,  $J = 11.8$  Hz, 1H), 3.64 – 3.56 (m, 2H), 3.52 (dd,  $J = 9.5, 4.7$  Hz, 1H), 3.40 (dq,  $J = 8.4, 4.9$  Hz, 1H), 1.72 (dt,  $J = 10.0, 6.3, 3.6$  Hz, 1H), 1.38 – 1.05 (m, 6H), 1.03 (s, 9H), 0.91 – 0.80 (m, 7H).



To a pale yellow solution of sulfonamide (1 equiv, 9.9 g, 28 mmol) in MeOH (175 mL) at room temperature, 4 M HCl/Dioxane (10 equiv, 70 mL) was added. Reaction was stirred for 1 hour and turned light amber. Reaction mixture was concentrated *in vacuo*. Crude oil was dissolved in minimal 50% EtOAc/Hex and loaded onto a silica gel column. 1 L of 50% EtOAc/Hex was eluted to remove sulfur impurities, then solvent system was switched to 10% MeOH/DCM to elute brown product band from the top of the silica (6.2g, 89% yield).  $^1\text{H}$  NMR (500 MHz, Chloroform- $d$ )  $\delta$  8.50 (s, 3H), 7.42 – 7.22 (m, 5H), 4.59 (d,  $J = 12.2$  Hz, 1H), 4.52 (d,  $J = 12.1$  Hz, 1H), 3.66 (d,  $J = 5.5$  Hz, 2H), 3.34 (s, 1H), 1.91 – 1.80 (m, 1H), 1.61 – 1.50 (m, 1H), 1.45 – 1.12 (m, 6H), 0.88 (td,  $J = 7.2, 4.0$  Hz, 6H).

Pd/C (5.9 g) was added to flask and dissolved in minimal EtOAc and put under  $\text{N}_2$ . Amine (1 equiv, 6.0 g, 24.1 mmol) was dissolved in MeOH (50 mL) and added to the

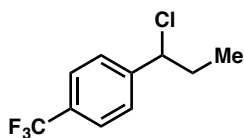
reaction flask via cannula. 4 M HCl/Dioxane (50 mL) was added and the N<sub>2</sub> atmosphere was exchanged with H<sub>2</sub> and the reaction was allowed to stir 14 h under H<sub>2</sub>. Upon completion, the reaction was sparged with argon and filtered through a pad of Celite with EtOAc. The filtrate was concentrated then dissolved in 250 mL EtOAc and added to 250 mL of 4 M NaOH. The organic layer was separated and extracted with 3x 200 mL EtOAc. The combined organic layers were dried, filtered, and concentrated under reduced pressure to afford pure amino alcohol (2.8 g, 74% yield). <sup>1</sup>H NMR (500 MHz, Chloroform-*d*) δ 3.58 (dd, *J* = 10.4, 4.0 Hz, 1H), 3.30 (dd, *J* = 10.4, 9.3 Hz, 1H), 2.81 (dt, *J* = 8.7, 4.0 Hz, 1H), 1.74 (s, 4H), 1.42 – 1.12 (m, 7H), 0.90 (td, *J* = 6.9, 2.0 Hz, 7H).

### 4.5.3 Substrate preparation

#### General procedure 1: Benzyl Chloride Synthesis from Benzylic Alcohols

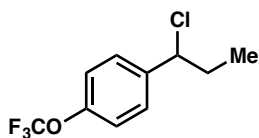
A flame-dried flask was charged with the benzylic alcohol substrate (1 equiv) and chloroform (0.30 M) and sealed with a rubber septum. This solution was cooled to 0 °C in an ice bath and placed under a positive pressure of nitrogen. The flask was vented via a Teflon cannula into a saturated solution of NaHCO<sub>3</sub> to quench evolved SO<sub>2</sub> gas. To the cooled solution was slowly added thionyl chloride (1.05 equiv) via syringe. The reaction was allowed to stir overnight and the ice bath allowed to melt, unless otherwise noted. Reactions were then concentrated to typically afford the crude substrates as yellow oils containing a mixture of benzylic chloride and the styrenyl elimination product. Substrates were purified by column chromatography on silica gel in 100% hexanes to elute first the elimination product (strong staining by KMnO<sub>4</sub> and brightly fluorescent) followed by the desired chloride product (dimly fluorescent, no staining).

### 1-(1-chloropropyl)-4-(trifluoromethyl)benzene (**171c**)



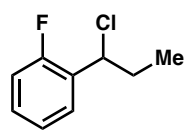
Prepared from 1-(4-(trifluoromethyl)phenyl)propan-1-ol (5.0 mmol, 1.02 g) following General Procedure 1 to yield 350 mg (31% yield, 1.57 mmol) of **171c** as a mobile clear liquid. <sup>1</sup>H NMR (300 MHz, Chloroform-*d*)  $\delta$  7.62 (dt,  $J = 8.1, 0.7$  Hz, 2H), 7.53 – 7.47 (m, 2H), 4.81 (dd,  $J = 7.8, 6.4$  Hz, 1H), 2.23 – 1.96 (m, 2H), 1.01 (t,  $J = 7.3$  Hz, 3H).

### 1-(1-chloropropyl)-4-(trifluoromethoxy)benzene (**171d**)

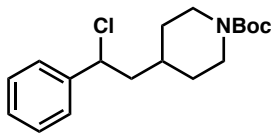


Prepared from 1-(4-(trifluoromethoxy)phenyl)propan-1-ol (13.1 mmol, 2.88 g) following General Procedure 1 to yield 2.51 g (80% yield, 10.48 mmol) of **171d** as a mobile clear liquid. <sup>1</sup>H NMR (300 MHz, Chloroform-*d*)  $\delta$  7.54 – 7.29 (m, 2H), 7.24 – 7.15 (m, 2H), 4.78 (dd,  $J = 7.9, 6.5$  Hz, 1H), 2.24 – 1.95 (m, 2H), 1.00 (t,  $J = 7.3$  Hz, 3H).

### 1-(1-chloropropyl)-2-fluorobenzene (**171f**)

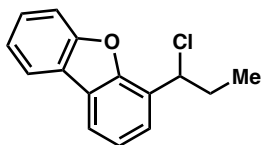


Prepared from 1-(2-fluorophenyl)propan-1-ol (19.7 mmol, 3.03 g) following General Procedure 1 to yield 2.63 g (77% yield, 15.2 mmol) of **171f** as a mobile clear liquid. <sup>1</sup>H NMR (300 MHz, Chloroform-*d*)  $\delta$  7.51 (td,  $J = 7.6, 1.9$  Hz, 1H), 7.35 – 7.21 (m, 1H), 7.16 (ddd,  $J = 8.3, 7.4, 1.1$  Hz, 1H), 7.11 – 6.97 (m, 1H), 5.24 – 5.11 (m, 1H), 2.27 – 1.98 (m, 2H), 1.02 (t,  $J = 7.3$  Hz, 3H).

***tert*-butyl 4-(2-chloro-2-phenylethyl)piperidine-1-carboxylate (**171k**)**

Prepared from *tert*-butyl 4-(2-hydroxy-2-phenylethyl)piperidine-1-carboxylate (6.2 mmol, 1.89 g) following General Procedure 1.

The reaction was concentrated and loaded onto a silica plug. Elution with  $\text{CHCl}_3$  delivered degradation products. Subsequent elution with 10% MeOH/DCM afforded the deprotected HCl salt of **171k** as a tan solid in 68% yield (4.22 mmol, 1.02 g). This product was not competent in the cross-coupling reaction. Reprotection with  $\text{Boc}_2\text{O}$  (1.05 equiv) in DCM with  $\text{Et}_3\text{N}$  (4 equiv) afforded the desired product cleanly.  $^1\text{H}$  NMR (300 MHz, Chloroform-*d*)  $\delta$  7.47 – 7.27 (m, 5H), 4.95 (dd,  $J = 9.2, 5.9$  Hz, 1H), 4.09 (s, 2H), 2.67 (t,  $J = 12.9$  Hz, 2H), 2.12 (ddd,  $J = 14.4, 9.2, 5.5$  Hz, 1H), 1.88 (ddd,  $J = 14.0, 7.5, 5.9$  Hz, 1H), 1.81 – 1.56 (m, 2H), 1.45 (s, 9H), 1.30 – 1.00 (m, 3H).

**4-(1-chloropropyl)dibenzo[*b,d*]furan (**171l**)**

Prepared from 1-(dibenzo[*b,d*]furan-4-yl)propan-1-ol (9.2 mmol, 2.08 g) following General Procedure 1 to yield 1.74 g (84% yield, 7.7 mmol) of **171l** as a mobile clear liquid.  $^1\text{H}$  NMR (300 MHz,

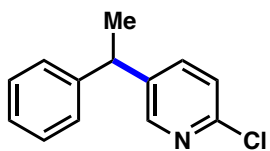
Chloroform-*d*)  $\delta$  7.96 (ddd,  $J = 7.7, 1.4, 0.7$  Hz, 1H), 7.90 (dd,  $J = 7.7, 1.3$  Hz, 1H), 7.61 (ddd,  $J = 8.3, 0.7$  Hz, 1H), 7.57 (ddd,  $J = 7.7, 1.3, 0.5$  Hz, 1H), 7.51 – 7.45 (m, 1H), 7.40 – 7.37 (m, 1H), 7.37 – 7.34 (m, 1H), 2.50 – 2.20 (m, 2H), 1.08 (t,  $J = 7.3$  Hz, 3H).

#### 4.5.4 *Enantioselective reductive cross-coupling*

##### **General Procedure 2: Enantioselective reductive coupling of benzyl chlorides and (hetero)aryl iodides**

On the bench-top, a 20 mL scintillation vial was charged with a cross stirbar, Mn<sup>0</sup> powder (3 equiv, 33 mg, 0.6 mmol), aryl iodide (*if solid*, 1 equiv, 0.2 mmol), and **L119** (0.2 equiv, 13.5 mg, 0.04 mmol). The vial was transferred into a N<sub>2</sub>-filled glovebox and charged with NiBr<sub>2</sub> (diglyme) (10 mol %, 7.1 mg, 0.02 mmol), aryl iodide (*if liquid*, 1 equiv, 0.2 mmol) and 1,4-dioxane (0.56 mL, 0.36 M). Reaction was allowed to stir at 100 rpm for several seconds before addition of TMSCl (20 uL, 0.8 equiv). After a short period of stirring, benzyl chloride (1 equiv, 0.2 mmol) was added. The vial was sealed with a Teflon cap and removed from the glovebox. The mixture was stirred at 480 rpm over a period of 14 hours, over which time the heterogeneous solution turned from dark gray to a light green, deep red or light gray color. The reaction was quenched by loading directly onto a short plug of silica, using 20% ethyl acetate/hexane eluent. The solution was concentrated to afford a clear oil which was then diluted in toluene and loaded onto a silica gel column and eluted in a hexane/EtOAc gradient. Remaining benzyl chloride could be recovered in the first couple fractions, with biaryl homocoupled product being the most polar component. Reaction success is critically dependent on stirring. A stirbar too small for the reaction vessel will fail to suspend the Mn powder and lead to low conversions. The reaction vessel should be sufficiently large (solvent height should be sufficiently low) to allow even distribution of Mn powder with vigorous stirring.

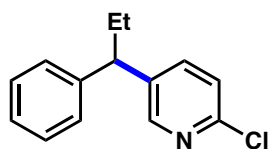
### 2-chloro-5-(1-phenylethyl)pyridine (167)



Prepared from 2-chloro-5-iodopyridine (1 equiv, 48.0 mg, 0.2 mmol) and 1-(chloroethyl)benzene (1 equiv, 28 mg, 0.2 mmol) following General Procedure 2. The crude residue was analyzed

by NMR to give a 84% yield. The enantiomeric excess was determined to be 78% by chiral SFC analysis (AD-H, 2.5 mL/min, 7% IPA in CO<sub>2</sub>,  $\lambda = 254$  nm):  $t_R(\text{minor}) = 6.5$  min,  $t_R(\text{major}) = 7.6$  min. <sup>1</sup>H NMR (300 MHz, Chloroform-*d*)  $\delta$  8.29 (dt,  $J = 2.6, 0.7$  Hz, 1H), 7.44 (ddd,  $J = 8.2, 2.6, 0.6$  Hz, 1H), 7.38 – 7.27 (m, 2H), 7.25 – 7.14 (m, 5H), 4.16 (q,  $J = 7.2$  Hz, 1H), 1.65 (d,  $J = 7.2$  Hz, 4H).

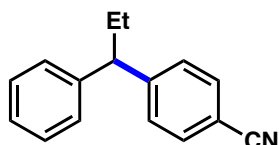
### 2-chloro-5-(1-phenylpropyl)pyridine (170a)



Prepared from 2-chloro-5-iodopyridine (1 equiv, 48.0 mg, 0.2 mmol) and 1-(chloropropyl)benzene (1 equiv, 31 mg, 0.2 mmol) following General Procedure 2. The crude residue was analyzed

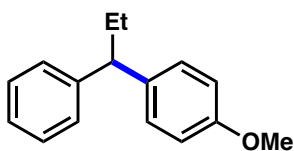
by NMR to give a 70% yield. The enantiomeric excess was determined to be 90% by chiral SFC analysis (AD-H, 2.5 mL/min, 8% IPA in CO<sub>2</sub>,  $\lambda = 254$  nm):  $t_R(\text{major}) = 6.4$  min,  $t_R(\text{minor}) = 7.6$  min. <sup>1</sup>H NMR (500 MHz, Chloroform-*d*)  $\delta$  8.30 (d,  $J = 2.5$  Hz, 1H), 7.47 (dd,  $J = 8.3, 2.5$  Hz, 1H), 7.30 (dd,  $J = 8.2, 6.9$  Hz, 2H), 7.25 – 7.16 (m, 3H), 3.80 (t,  $J = 7.8$  Hz, 1H), 2.16 – 1.97 (m, 2H), 0.91 (t,  $J = 7.3$  Hz, 3H). <sup>13</sup>C NMR (126 MHz, cdcl<sub>3</sub>)  $\delta$  149.37, 149.30, 143.37, 139.57, 138.24, 128.84, 127.86, 126.80, 124.17, 50.10, 28.37, 12.67.

#### 4-(1-phenylpropyl)benzonitrile (170b)



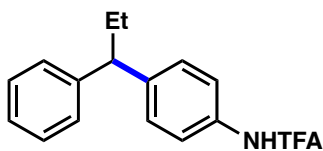
Prepared from 4-iodobenzonitrile (1 equiv, 46.0 mg, 0.2 mmol) and 1-(chloropropyl)benzene (1 equiv, 31 mg, 0.2 mmol) following General Procedure 2. The crude residue was analyzed by NMR to give a 75% yield. The enantiomeric excess was determined to be 87% by chiral SFC analysis (OB-H, 2.5 mL/min, 10% IPA in CO<sub>2</sub>, λ = 254 nm):  $t_R(\text{major}) = 5.3$  min,  $t_R(\text{minor}) = 7.2$  min. <sup>1</sup>H NMR (500 MHz, Chloroform-*d*) δ 7.59 – 7.54 (m, 2H), 7.36 – 7.32 (m, 2H), 7.32 – 7.27 (m, 2H), 7.24 – 7.17 (m, 3H), 3.84 (t,  $J = 7.8$  Hz, 1H), 2.15 – 2.01 (m, 2H), 0.90 (t,  $J = 7.3$  Hz, 3H).

#### 1-methoxy-4-(1-phenylpropyl)benzene (170c)



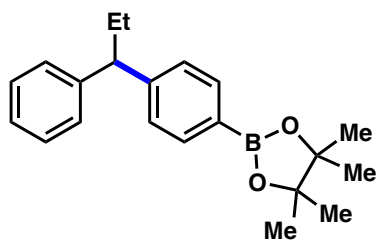
Prepared from 4-iodoanisole (1 equiv, 47.0 mg, 0.2 mmol) and 1-(chloropropyl)benzene (1 equiv, 31 mg, 0.2 mmol) following General Procedure 2. The crude residue was analyzed by NMR to give a 77% yield. The enantiomeric excess was determined to be 83% by chiral SFC analysis (OJ-H, 2.5 mL/min, 8% IPA in CO<sub>2</sub>, λ = 210 nm):  $t_R(\text{minor}) = 8.8$  min,  $t_R(\text{major}) = 10.9$  min. <sup>1</sup>H NMR (500 MHz, Chloroform-*d*) δ 7.30 – 7.23 (m, 3H), 7.23 – 7.19 (m, 2H), 7.17 – 7.12 (m, 2H), 6.84 – 6.80 (m, 2H), 3.77 (s, 4H), 3.74 (t,  $J = 7.8$  Hz, 1H), 2.09 – 1.98 (m, 2H), 0.89 (t,  $J = 7.3$  Hz, 3H).

**2,2,2-trifluoro-*N*-(4-(1-phenylpropyl)phenyl)acetamide (170d)**

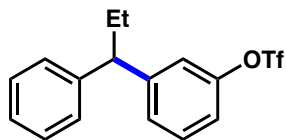


Prepared from 2,2,2-trifluoro-*N*-(4-iodophenyl)acetamide (1 equiv, 63.0 mg, 0.2 mmol) and 1-(chloropropyl)benzene (1 equiv, 31 mg, 0.2 mmol) following General Procedure 2. The crude residue was analyzed by NMR to give a 93% yield. The enantiomeric excess was determined to be 85% by chiral SFC analysis (OD-H, 2.5 mL/min, 10% IPA in CO<sub>2</sub>, λ = 254 nm): *t*<sub>R</sub>(minor) = 6.5 min, *t*<sub>R</sub>(major) = 9.7 min. <sup>1</sup>H NMR (500 MHz, Chloroform-*d*) δ 7.49 – 7.45 (m, 2H), 7.26 (s, 4H), 7.23 – 7.16 (m, 3H), 3.79 (t, *J* = 7.8 Hz, 1H), 2.06 (pd, *J* = 7.4, 2.4 Hz, 2H), 0.89 (t, *J* = 7.3 Hz, 3H).

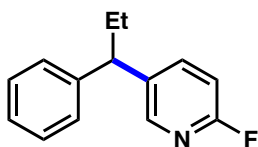
**4,4,5,5-tetramethyl-2-(4-(1-phenylpropyl)phenyl)-1,3,2-dioxaborolane (170e)**



Prepared from 2-(4-iodophenyl)-4,4,5,5-tetramethyl-1,3,2-dioxaborolane (1 equiv, 66.0 mg, 0.2 mmol) and 1-(chloropropyl)benzene (1 equiv, 31 mg, 0.2 mmol) following General Procedure 2. The crude residue was analyzed by NMR to give a 83% yield. The enantiomeric excess was determined to be 75% by chiral SFC analysis (AD-H, 2.5 mL/min, 7% IPA in CO<sub>2</sub>, λ = 254 nm): *t*<sub>R</sub>(minor) = 5.9 min, *t*<sub>R</sub>(major) = 6.5 min. <sup>1</sup>H NMR (500 MHz, Chloroform-*d*) δ 7.77 – 7.69 (m, 2H), 7.29 – 7.19 (m, 6H), 7.19 – 7.13 (m, 1H), 3.80 (t, *J* = 7.8 Hz, 1H), 2.12 – 2.04 (m, 2H), 1.32 (s, 12H), 0.89 (t, *J* = 7.3 Hz, 3H).

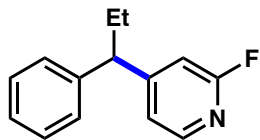
**3-(1-phenylpropyl)phenyl trifluoromethanesulfonate (170f)**

Prepared from 3-iodophenyl trifluoromethanesulfonate (1 equiv, 70.0 mg, 0.2 mmol) and 1-(chloropropyl)benzene (1 equiv, 31 mg, 0.2 mmol) following General Procedure 2. The crude residue was analyzed by NMR to give a 95% yield. The enantiomeric excess was determined to be 86% by chiral SFC analysis (OJ-H, 2.5 mL/min, 1% IPA in CO<sub>2</sub>,  $\lambda$  = 210 nm):  $t_R$ (major) = 5.7 min,  $t_R$ (minor) = 6.4 min. <sup>1</sup>H NMR (500 MHz, Chloroform-*d*)  $\delta$  7.37 – 7.27 (m, 2H), 7.26 – 7.17 (m, 4H), 7.14 (t,  $J$  = 2.1 Hz, 1H), 7.09 (ddd,  $J$  = 8.2, 2.5, 1.0 Hz, 1H), 3.83 (t,  $J$  = 7.8 Hz, 1H), 2.17 – 1.97 (m, 2H), 0.90 (t,  $J$  = 7.3 Hz, 3H); <sup>13</sup>C NMR (126 MHz, cdcl<sub>3</sub>)  $\delta$  149.69, 148.34, 143.67, 130.06, 128.62, 128.05, 127.81, 126.55, 120.64, 118.81, 77.28, 77.02, 76.77, 52.78, 28.42, 12.57; <sup>19</sup>F NMR (282 MHz, cdcl<sub>3</sub>)  $\delta$  -72.76.

**2-fluoro-5-(1-phenylpropyl)pyridine (170g)**

Prepared from 2-fluoro-5-iodopyridine (1 equiv, 45.0 mg, 0.2 mmol) and 1-(chloropropyl)benzene (1 equiv, 31 mg, 0.2 mmol) following General Procedure 2. The crude residue was analyzed by NMR to give a 80% yield. The enantiomeric excess was determined to be 90% by chiral SFC analysis (AD-H, 2.5 mL/min, 5% IPA in CO<sub>2</sub>,  $\lambda$  = 254 nm):  $t_R$ (major) = 5.5 min,  $t_R$ (minor) = 6.0 min. <sup>1</sup>H NMR (500 MHz, Chloroform-*d*)  $\delta$  8.11 (ddt,  $J$  = 2.5, 1.2, 0.6 Hz, 1H), 7.59 (dddd,  $J$  = 8.3, 7.7, 2.6, 0.5 Hz, 1H), 7.35 – 7.28 (m, 2H), 7.24 – 7.17 (m, 3H), 6.87 – 6.80 (m, 1H), 3.82 (t,  $J$  = 7.8 Hz, 1H), 2.15 – 2.00 (m, 2H), 0.91 (t,  $J$  = 7.3 Hz, 3H).

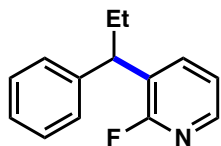
### 2-fluoro-4-(1-phenylpropyl)pyridine (170h)



Prepared from 2-fluoro-4-iodopyridine (1 equiv, 45.0 mg, 0.2 mmol) and 1-(chloropropyl)benzene (1 equiv, 31 mg, 0.2 mmol) following General Procedure 2. The crude residue was analyzed by

NMR to give a 51% yield. The enantiomeric excess was determined to be 91% by chiral SFC analysis (OJ-H, 2.5 mL/min, 5% IPA in CO<sub>2</sub>,  $\lambda = 254$  nm):  $t_R(\text{minor}) = 4.1$  min,  $t_R(\text{major}) = 4.6$  min. <sup>1</sup>H NMR (500 MHz, Chloroform-*d*)  $\delta$  8.09 (dt,  $J = 5.2, 0.7$  Hz, 1H), 7.34 – 7.29 (m, 2H), 7.27 – 7.17 (m, 3H), 7.03 (dddd,  $J = 5.3, 2.0, 1.4, 0.5$  Hz, 1H), 6.79 (td,  $J = 1.4, 0.6$  Hz, 1H), 3.81 (t,  $J = 7.8$  Hz, 1H), 2.12 – 2.02 (m, 2H), 0.91 (t,  $J = 7.3$  Hz, 3H).

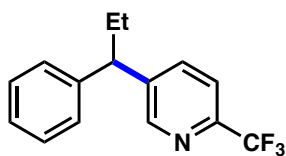
### 2-fluoro-3-(1-phenylpropyl)pyridine (170i)



Prepared from 2-fluoro-3-iodopyridine (1 equiv, 45.0 mg, 0.2 mmol) and 1-(chloropropyl)benzene (1 equiv, 31 mg, 0.2 mmol) following General Procedure 2. The crude residue was analyzed by NMR to

give a 30% yield. The enantiomeric excess was determined to be 24% by chiral SFC analysis (AD-H, 2.5 mL/min, 5% IPA in CO<sub>2</sub>,  $\lambda = 254$  nm):  $t_R(\text{major}) = 4.2$  min,  $t_R(\text{minor}) = 4.6$  min. <sup>1</sup>H NMR (500 MHz, Chloroform-*d*)  $\delta$  8.04 (ddd,  $J = 4.8, 1.9, 1.2$  Hz, 1H), 7.66 (dddd,  $J = 9.6, 7.5, 2.0, 0.6$  Hz, 1H), 7.34 – 7.27 (m, 2H), 7.25 – 7.18 (m, 3H), 7.13 (ddd,  $J = 7.5, 4.8, 1.7$  Hz, 1H), 4.08 (t,  $J = 7.9$  Hz, 1H), 2.13 – 2.02 (m, 2H), 0.93 (t,  $J = 7.3$  Hz, 3H).

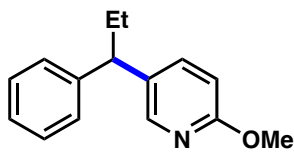
### 5-(1-phenylpropyl)-2-(trifluoromethyl)pyridine (170j)



Prepared from 5-iodo-2-(trifluoromethyl)pyridine (1 equiv, 55.0 mg, 0.2 mmol) and 1-(chloropropyl)benzene (1 equiv, 31 mg, 0.2 mmol) following General Procedure 2. The crude residue was

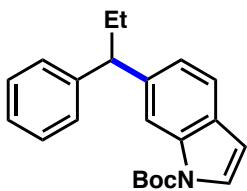
analyzed by NMR to give a 72% yield. The enantiomeric excess was determined to be 90% by chiral SFC analysis (AD-H, 2.5 mL/min, 5% IPA in CO<sub>2</sub>, λ = 254 nm): *t*<sub>R</sub>(major) = 3.7 min, *t*<sub>R</sub>(minor) = 4.1 min. <sup>1</sup>H NMR (500 MHz, Chloroform-*d*) δ 8.63 (d, *J* = 2.1 Hz, 1H), 7.68 (dd, *J* = 8.2, 2.2 Hz, 1H), 7.59 (dd, *J* = 8.0, 0.8 Hz, 1H), 7.35 – 7.29 (m, 2H), 7.25 – 7.18 (m, 3H), 3.90 (t, *J* = 7.8 Hz, 1H), 2.20 – 2.06 (m, 2H), 0.93 (t, *J* = 7.3 Hz, 3H).

### 2-methoxy-5-(1-phenylpropyl)pyridine (170k)

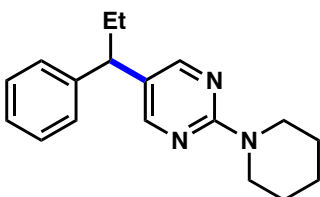


Prepared from 5-iodo-2-methoxypyridine (1 equiv, 47.0 mg, 0.2 mmol) and 1-(chloropropyl)benzene (1 equiv, 31 mg, 0.2 mmol) following General Procedure 2. The crude residue was analyzed

by NMR to give a 86% yield. The enantiomeric excess was determined to be 89% by chiral SFC analysis (OJ-H, 2.5 mL/min, 4% IPA in CO<sub>2</sub>, λ = 210 nm): *t*<sub>R</sub>(minor) = 5.9 min, *t*<sub>R</sub>(major) = 6.4 min. <sup>1</sup>H NMR (500 MHz, Chloroform-*d*) δ 8.06 (d, *J* = 2.6 Hz, 1H), 7.40 (dd, *J* = 8.6, 2.5 Hz, 1H), 7.28 (dd, *J* = 8.1, 7.1 Hz, 2H), 7.23 – 7.15 (m, 3H), 6.66 (d, *J* = 8.5 Hz, 1H), 3.90 (s, 3H), 3.74 (t, *J* = 7.8 Hz, 1H), 2.12 – 1.97 (m, 2H), 0.90 (t, *J* = 7.3 Hz, 3H).

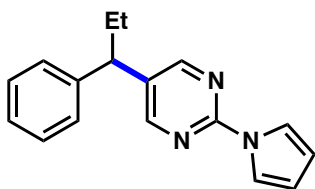
***tert*-butyl-6-(1-phenylpropyl)-1*H*-indole-1-carboxylate (170l)**

Prepared from *tert*-butyl 6-iodo-1*H*-indole-1-carboxylate (1 equiv, 69.0 mg, 0.2 mmol) and 1-(chloropropyl)benzene (1 equiv, 31 mg, 0.2 mmol) following General Procedure 2. The crude residue was analyzed by NMR to give a 82% yield. The enantiomeric excess was determined to be 82% by chiral SFC analysis (AD-H, 2.5 mL/min, 8% IPA in CO<sub>2</sub>, λ = 254 nm): *t*<sub>R</sub>(minor) = 7.5 min, *t*<sub>R</sub>(major) = 8.7 min. <sup>1</sup>H NMR (500 MHz, Chloroform-*d*) δ 7.33 – 7.26 (m, 6H), 6.90 – 6.82 (m, 1H), 6.51 (ddd, *J* = 13.3, 3.7, 0.8 Hz, 3H), 3.92 (t, *J* = 7.8 Hz, 1H), 2.15 (pd, *J* = 7.3, 1.3 Hz, 2H), 1.66 (s, 9H), 0.93 (t, *J* = 7.3 Hz, 3H).

**5-(1-phenylpropyl)-2-(piperidin-1-yl)pyrimidine (170m)**

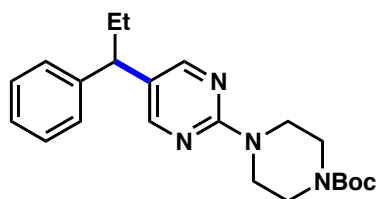
Prepared from 5-iodo-2-(piperidin-1-yl)pyrimidine (1 equiv, 58.0 mg, 0.2 mmol) and 1-(chloropropyl)benzene (1 equiv, 31 mg, 0.2 mmol) following General Procedure 2. The crude residue was analyzed by NMR to give a 78% yield. The enantiomeric excess was determined to be 98% by chiral SFC analysis (OB-H, 2.5 mL/min, 15% IPA in CO<sub>2</sub>, λ = 254 nm): *t*<sub>R</sub>(minor) = 5.8 min, *t*<sub>R</sub>(major) = 7.5 min. <sup>1</sup>H NMR (500 MHz, Chloroform-*d*) δ 8.17 (d, *J* = 0.5 Hz, 2H), 7.31 – 7.26 (m, 2H), 7.22 – 7.14 (m, 3H), 3.78 – 3.68 (m, 4H), 3.59 (t, *J* = 7.8 Hz, 1H), 2.11 – 1.92 (m, 2H), 1.71 – 1.62 (m, 2H), 1.62 – 1.52 (m, 4H), 0.90 (t, *J* = 7.3 Hz, 3H).

**5-(1-phenylpropyl)-2-(1*H*-pyrrol-1-yl)pyrimidine (170n)**



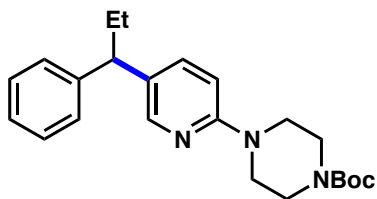
Prepared from 5-iodo-2-(1*H*-pyrrol-1-yl)pyrimidine (1 equiv, 54.0 mg, 0.2 mmol) and 1-(chloropropyl)benzene (1 equiv, 31 mg, 0.2 mmol) following General Procedure 2. The crude residue was analyzed by NMR to give a 54% yield. The enantiomeric excess was determined to be 91% by chiral SFC analysis (OB-H, 2.5 mL/min, 15% IPA in CO<sub>2</sub>, λ = 254 nm): *t<sub>R</sub>*(minor) = 9.3 min, *t<sub>R</sub>*(major) = 11.2 min. <sup>1</sup>H NMR (500 MHz, Chloroform-*d*) δ 8.47 (d, *J* = 0.5 Hz, 2H), 7.75 – 7.70 (m, 2H), 7.32 (tq, *J* = 7.7, 1.0 Hz, 2H), 7.25 – 7.18 (m, 3H), 6.33 – 6.29 (m, 2H), 3.79 (t, *J* = 7.8 Hz, 1H), 2.20 – 2.06 (m, 2H), 0.95 (t, *J* = 7.3 Hz, 3H).

***tert*-butyl-4-(5-(1-phenylpropyl)pyrimidin-2-yl)piperazine-1-carboxylate (170o)**



Prepared from *tert*-butyl 4-(5-iodopyrimidin-2-yl)piperazine-1-carboxylate (1 equiv, 78.0 mg, 0.2 mmol) and 1-(chloropropyl)benzene (1 equiv, 31 mg, 0.2 mmol) following General Procedure 2. The crude residue was analyzed by NMR to give a 56% yield. The enantiomeric excess was determined to be 89% by chiral SFC analysis (AD-H, 2.5 mL/min, 10% IPA in CO<sub>2</sub>, λ = 254 nm): *t<sub>R</sub>*(major) = 10.3 min, *t<sub>R</sub>*(minor) = 11.7 min. <sup>1</sup>H NMR (500 MHz, Chloroform-*d*) δ 8.20 (s, 2H), 7.29 (dd, *J* = 8.4, 6.9 Hz, 2H), 7.19 (d, *J* = 7.5 Hz, 3H), 3.75 (t, *J* = 5.2 Hz, 4H), 3.62 (t, *J* = 7.8 Hz, 1H), 3.47 (t, *J* = 5.3 Hz, 4H), 2.10 – 1.95 (m, 3H), 1.48 (s, 9H), 0.91 (t, *J* = 7.3 Hz, 3H).

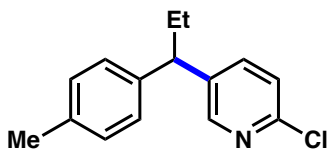
***tert*-butyl-4-(5-(1-phenylpropyl)pyridin-2-yl)piperazine-1-carboxylate (170p)**



Prepared from *tert*-butyl 4-(5-iodopyridin-2-yl)piperazine-1-carboxylate (1 equiv, 78.0 mg, 0.2 mmol) and 1-(chloropropyl)benzene (1 equiv, 31 mg, 0.2 mmol) following General Procedure 2. The crude residue was

analyzed by NMR to give an 85% yield. The enantiomeric excess was determined to be 83% by chiral SFC analysis (OJ-H, 2.5 mL/min, 15% IPA in CO<sub>2</sub>, λ = 254 nm): *t*<sub>R</sub>(major) = 6.9 min, *t*<sub>R</sub>(minor) = 7.7 min. <sup>1</sup>H NMR (500 MHz, Chloroform-*d*) δ 8.11 (d, *J* = 2.4 Hz, 1H), 7.33 (dd, *J* = 8.8, 2.5 Hz, 1H), 7.31 – 7.23 (m, 2H), 7.23 – 7.13 (m, 3H), 6.58 (dd, *J* = 8.7, 0.8 Hz, 1H), 3.69 (t, *J* = 7.8 Hz, 1H), 3.52 (q, *J* = 3.9, 3.1 Hz, 4H), 3.49 – 3.44 (m, 4H), 2.10 – 1.95 (m, 2H), 1.48 (s, 9H), 0.89 (t, *J* = 7.2 Hz, 3H).

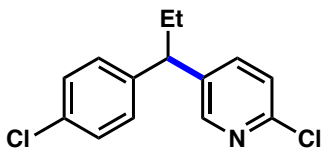
**2-chloro-5-(1-(*p*-tolyl)propyl)pyridine (172a)**



Prepared from 2-chloro-5-iodopyridine (1 equiv, 48.0 mg, 0.2 mmol) and 1-(1-chloropropyl)-4-methylbenzene (1 equiv, 34 mg, 0.2 mmol) following General Procedure 2. The crude

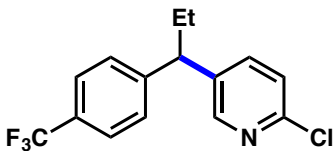
residue was analyzed by NMR to give a 70% yield. The enantiomeric excess was determined to be 88% by chiral SFC analysis (AD-H, 2.5 mL/min, 8% IPA in CO<sub>2</sub>, λ = 254 nm): *t*<sub>R</sub>(major) = 6.8 min, *t*<sub>R</sub>(minor) = 8.5 min. <sup>1</sup>H NMR (400 MHz, Chloroform-*d*) δ 8.29 (d, *J* = 2.6 Hz, 1H), 7.46 (dd, *J* = 8.2, 2.5 Hz, 1H), 7.21 (d, *J* = 8.2 Hz, 1H), 7.15 – 7.04 (m, 4H), 3.76 (t, *J* = 7.8 Hz, 1H), 2.31 (s, 3H), 2.05 (qt, *J* = 13.6, 7.5 Hz, 2H), 0.90 (t, *J* = 7.3 Hz, 3H). <sup>13</sup>C NMR (101 MHz, CDCl<sub>3</sub>) δ 149.22, 149.11, 140.27, 139.72, 138.09, 136.27, 129.40, 127.60, 124.02, 49.61, 28.30, 20.98, 12.57.

### 2-chloro-5-(1-(4-chlorophenyl)propyl)pyridine (172b)



Prepared from 2-chloro-5-iodopyridine (1 equiv, 48.0 mg, 0.2 mmol) and 1-chloro-4-(1-chloropropyl)benzene (1 equiv, 38 mg, 0.2 mmol) following General Procedure 2. The crude residue was analyzed by NMR to give a 71% yield. The enantiomeric excess was determined to be 82% by chiral SFC analysis (AD-H, 2.5 mL/min, 12% IPA in CO<sub>2</sub>, λ = 210 nm): *t<sub>R</sub>*(minor) = 6.1 min, *t<sub>R</sub>*(major) = 6.5 min. <sup>1</sup>H NMR (500 MHz, Chloroform-*d*) δ 8.27 (dt, *J* = 2.6, 0.7 Hz, 1H), 7.43 (ddd, *J* = 8.3, 2.6, 0.5 Hz, 1H), 7.31 – 7.26 (m, 2H), 7.25 – 7.21 (m, 1H), 7.16 – 7.09 (m, 2H), 3.78 (t, *J* = 7.8 Hz, 1H), 2.10 – 1.97 (m, 2H), 0.90 (t, *J* = 7.3 Hz, 3H); <sup>13</sup>C NMR (126 MHz, cdcl<sub>3</sub>) δ 149.61, 149.31, 141.87, 139.05, 138.13, 132.64, 129.24, 129.01, 125.60, 124.29, 49.48, 28.35, 12.60.

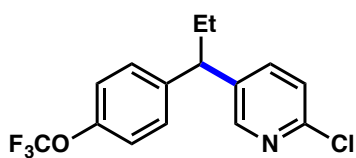
### 2-chloro-5-(1-(4-(trifluoromethyl)phenyl)propyl)pyridine (172c)



Prepared from 2-chloro-5-iodopyridine (1 equiv, 48.0 mg, 0.2 mmol) and 1-(1-chloropropyl)-4-(trifluoromethyl)benzene (1 equiv, 45 mg, 0.2 mmol) following General Procedure 2. The crude residue was analyzed by NMR to give a 74% yield. The enantiomeric excess was determined to be 82% by chiral SFC analysis (AD-H, 2.5 mL/min, 2% IPA in CO<sub>2</sub>, λ = 210 nm): *t<sub>R</sub>*(minor) = 14.7 min, *t<sub>R</sub>*(major) = 15.3 min. <sup>1</sup>H NMR (500 MHz, Chloroform-*d*) δ 8.29 (dt, *J* = 2.6, 0.6 Hz, 1H), 7.56 (dt, *J* = 7.9, 0.7 Hz, 2H), 7.45 (ddd, *J* = 8.3, 2.6, 0.5 Hz, 1H), 7.34 – 7.28 (m, 2H), 3.87 (t, *J* = 7.8 Hz, 1H), 2.17 – 2.01 (m, 2H), 0.92 (t, *J* = 7.3 Hz, 3H); <sup>13</sup>C NMR (126 MHz, cdcl<sub>3</sub>)

149.82, 149.35, 147.43, 138.53, 138.14, 136.99, 128.27, 125.86 (q,  $J = 3.7$  Hz), 124.39, 119.02, 110.14, 49.95, 28.25, 12.59.

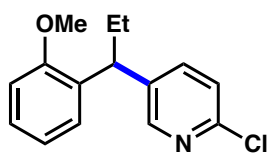
### 2-chloro-5-(1-(4-(trifluoromethoxy)phenyl)propyl)pyridine (172d)



Prepared from 2-chloro-5-iodopyridine (1 equiv, 48.0 mg, 0.2 mmol) and 1-(1-chloropropyl)-4-(trifluoromethoxy)benzene (1 equiv, 48 mg, 0.2 mmol)

following General Procedure 2. The crude residue was analyzed by NMR to give a 78% yield. The enantiomeric excess was determined to be 83% by chiral SFC analysis (AD-H, 2.5 mL/min, 15% IPA in CO<sub>2</sub>,  $\lambda = 210$  nm):  $t_R(\text{minor}) = 9.8$  min,  $t_R(\text{major}) = 10.2$  min. <sup>1</sup>H NMR (500 MHz, Chloroform-*d*)  $\delta$  8.28 (d,  $J = 2.4$  Hz, 1H), 7.45 (ddd,  $J = 8.3, 2.5, 0.5$  Hz, 1H), 7.25 – 7.18 (m, 3H), 7.18 – 7.12 (m, 2H), 3.82 (t,  $J = 7.8$  Hz, 1H), 2.14 – 1.99 (m, 2H), 0.91 (t,  $J = 7.3$  Hz, 3H); <sup>13</sup>C NMR (126 MHz, cdcl<sub>3</sub>)  $\delta$  149.66, 149.34, 148.00 (q,  $J = 2.1$  Hz), 142.11, 138.93, 138.15, 129.17, 124.34, 121.59, 121.37, 119.55, 49.46, 28.43, 12.62.

### 2-chloro-5-(1-(2-methoxyphenyl)propyl)pyridine (172e)

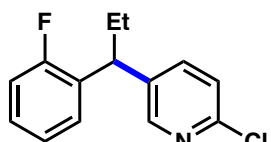


Prepared from 2-chloro-5-iodopyridine (1 equiv, 48.0 mg, 0.2 mmol) and 1-(1-chloropropyl)-2-methoxybenzene (1 equiv, 37 mg, 0.2 mmol) following General Procedure 2. The crude residue

was analyzed by NMR to give a 78% yield. The enantiomeric excess was determined to be 94% by chiral SFC analysis (OJ-H, 2.5 mL/min, 7% IPA in CO<sub>2</sub>,  $\lambda = 210$  nm):  $t_R(\text{minor}) = 4.0$  min,  $t_R(\text{major}) = 4.4$  min. <sup>1</sup>H NMR (500 MHz, Chloroform-*d*)  $\delta$  8.30 (d,  $J$

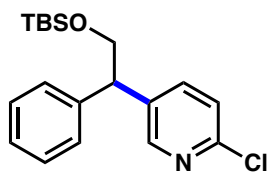
= 2.5 Hz, 1H), 7.46 (dd,  $J = 8.3, 2.5$  Hz, 1H), 7.25 – 7.15 (m, 3H), 6.95 (td,  $J = 7.5, 1.2$  Hz, 1H), 6.82 (dd,  $J = 8.2, 1.1$  Hz, 1H), 4.20 (t,  $J = 7.9$  Hz, 1H), 3.74 (s, 3H), 2.14 – 1.92 (m, 2H), 0.90 (t,  $J = 7.3$  Hz, 3H);  $^{13}\text{C}$  NMR (126 MHz,  $\text{cdCl}_3$ )  $\delta$  156.92, 149.83, 148.63, 139.47, 138.18, 131.65, 127.71, 127.04, 123.70, 120.60, 110.63, 55.27, 42.49, 27.17, 12.53.

### 2-chloro-5-(1-(2-fluorophenyl)propyl)pyridine (172f)



Prepared from 2-chloro-5-iodopyridine (1 equiv, 48.0 mg, 0.2 mmol) and 1-(1-chloropropyl)-2-fluorobenzene (1 equiv, 35 mg, 0.2 mmol) following General Procedure 3. The crude residue was analyzed by NMR to give a 71% yield. The enantiomeric excess was determined to be 90% by chiral SFC analysis (AD-H, 2.5 mL/min, 7% IPA in  $\text{CO}_2$ ,  $\lambda = 254$  nm):  $t_{\text{R}}$ (minor) = 5.7 min,  $t_{\text{R}}$ (major) = 6.6 min.  $^1\text{H}$  NMR (500 MHz, Chloroform- $d$ )  $\delta$  8.35 – 8.27 (m, 1H), 7.53 – 7.45 (m, 1H), 7.25 – 7.17 (m, 2H), 7.11 (td,  $J = 7.5, 1.3$  Hz, 1H), 7.00 (ddt,  $J = 11.4, 8.2, 1.7$  Hz, 1H), 4.15 – 4.10 (m, 1H), 2.19 – 1.97 (m, 2H), 0.97 – 0.88 (m, 3H).

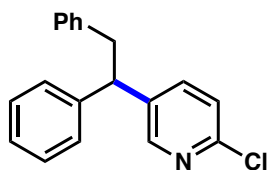
### 5-(2-((*tert*-butyldimethylsilyloxy)-1-phenylethyl)-2-chloropyridine (172g)



Prepared from 2-chloro-5-iodopyridine (1 equiv, 48.0 mg, 0.2 mmol) and *tert*-butyl(2-chloro-2-phenylethoxy)dimethylsilane (1 equiv, 54.0 mg, 0.2 mmol) following General Procedure 2. The crude residue was analyzed by NMR to give a 61% yield. The enantiomeric excess was determined to be 94% by chiral SFC analysis (AD-H, 2.5 mL/min, 5% IPA in  $\text{CO}_2$ ,  $\lambda = 210$  nm):  $t_{\text{R}}$ (minor) = 4.5 min,  $t_{\text{R}}$ (major) = 5.3 min.  $^1\text{H}$  NMR (500 MHz, Chloroform- $d$ )  $\delta$

8.33 (dt,  $J = 2.5, 0.6$  Hz, 1H), 7.52 (ddd,  $J = 8.3, 2.5, 0.5$  Hz, 1H), 7.34 – 7.27 (m, 2H), 7.26 – 7.21 (m, 2H), 7.20 – 7.15 (m, 2H), 4.22 – 4.03 (m, 3H), 0.82 (s, 9H), -0.04 (d,  $J = 5.0$  Hz, 6H).

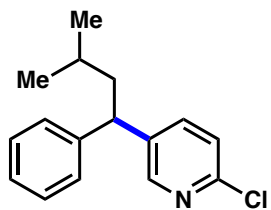
### 2-chloro-5-(1,2-diphenylethyl)pyridine (172h)



Prepared from 2-chloro-5-iodopyridine (1 equiv, 48.0 mg, 0.2 mmol) and (1-chloroethane-1,2-diyl)dibenzene (1 equiv, 43.0 mg, 0.2 mmol) following General Procedure 2. The crude residue was

analyzed by NMR to give a 66% yield. The enantiomeric excess was determined to be 93% by chiral SFC analysis (AD-H, 2.5 mL/min, 12% IPA in CO<sub>2</sub>,  $\lambda = 210$  nm):  $t_R(\text{minor}) = 6.3$  min,  $t_R(\text{major}) = 9.7$  min. <sup>1</sup>H NMR (500 MHz, Chloroform-*d*)  $\delta$  8.16 (dt,  $J = 2.6, 0.6$  Hz, 1H), 7.42 (ddd,  $J = 8.3, 2.6, 0.5$  Hz, 1H), 7.33 – 7.27 (m, 2H), 7.24 – 7.11 (m, 7H), 7.03 – 6.95 (m, 2H), 4.24 (dd,  $J = 8.9, 7.0$  Hz, 1H), 3.41 (dd,  $J = 13.7, 7.0$  Hz, 1H), 3.28 (dd,  $J = 13.6, 8.9$  Hz, 1H).

### 2-chloro-5-(3-methyl-1-phenylbutyl)pyridine (172i)

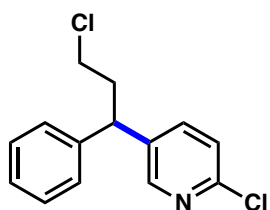


Prepared from 2-chloro-5-iodopyridine (1 equiv, 48.0 mg, 0.2 mmol) and (1-chloro-3-methylbutyl)benzene (1 equiv, 37.0 mg, 0.2 mmol) following General Procedure 2. The crude residue was analyzed by NMR to give a 66% yield. The enantiomeric excess

was determined to be 87% by chiral SFC analysis (AD-H, 2.5 mL/min, 6% IPA in CO<sub>2</sub>,  $\lambda = 210$  nm):  $t_R(\text{minor}) = 7.3$  min,  $t_R(\text{major}) = 8.3$  min. <sup>1</sup>H NMR (500 MHz, Chloroform-*d*)  $\delta$  8.30 (dt,  $J = 2.6, 0.6$  Hz, 1H), 7.48 (ddd,  $J = 8.3, 2.6, 0.5$  Hz, 1H), 7.30 (ddd,  $J = 8.6,$

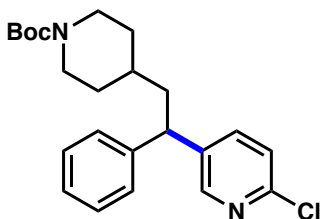
6.7, 0.6 Hz, 2H), 7.24 – 7.17 (m, 4H), 4.02 (t,  $J = 8.0$  Hz, 1H), 1.90 (dddd,  $J = 41.4$ , 13.7, 8.0, 7.0 Hz, 2H), 1.42 (hept,  $J = 6.7$  Hz, 1H), 0.92 (dd,  $J = 6.6$ , 1.6 Hz, 6H).

### 2-chloro-5-(3-chloro-1-phenylpropyl)pyridine (172j)



Prepared from 2-chloro-5-iodopyridine (1 equiv, 48.0 mg, 0.2 mmol) and (1,3-dichloropropyl)benzene (1 equiv, 38.0 mg, 0.2 mmol) following General Procedure 2. The crude residue was analyzed by NMR to give a 85% yield. The enantiomeric excess was determined to be 90% by chiral SFC analysis (AD-H, 2.5 mL/min, 8% IPA in CO<sub>2</sub>,  $\lambda = 210$  nm):  $t_R$ (minor) = 9.7 min,  $t_R$ (major) = 11.1 min. <sup>1</sup>H NMR (500 MHz, Chloroform-*d*)  $\delta$  8.36 – 8.29 (m, 1H), 7.50 (ddd,  $J = 8.2$ , 2.6, 0.6 Hz, 1H), 7.37 – 7.30 (m, 2H), 7.29 – 7.18 (m, 4H), 4.27 (t,  $J = 7.8$  Hz, 1H), 3.50 – 3.41 (m, 2H), 2.58 – 2.40 (m, 2H).

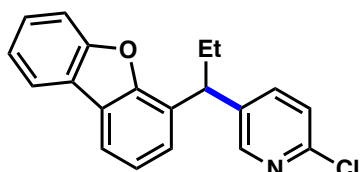
### tert-butyl-4-(2-(6-chloropyridin-3-yl)-2-phenylethyl)piperidine-1-carboxylate (172k)



Prepared from 2-chloro-5-iodopyridine (1 equiv, 48.0 mg, 0.2 mmol) and *tert*-butyl 4-(2-chloro-2-phenylethyl)piperidine-1-carboxylate (1 equiv, 65.0 mg, 0.2 mmol) following General Procedure 2. The crude residue was analyzed by NMR to give a 65% yield. The enantiomeric excess was determined to be 93% by chiral SFC analysis (OJ-H, 2.5 mL/min, 15% IPA in CO<sub>2</sub>,  $\lambda = 210$  nm):  $t_R$ (minor) = 5.3 min,  $t_R$ (major) = 10.9 min. <sup>1</sup>H NMR (500 MHz, Chloroform-*d*)  $\delta$  8.29 (dt,  $J = 2.6$ , 0.6 Hz, 1H), 7.47 (ddd,  $J = 8.3$ , 2.6, 0.5 Hz, 1H), 7.34 – 7.28 (m, 2H), 7.25 – 7.17 (m, 4H), 4.05 (t,  $J = 8.0$  Hz, 3H), 2.56 (s,

2H), 2.04 – 1.84 (m, 2H), 1.67 (t,  $J = 12.4$  Hz, 2H), 1.44 (s, 9H), 1.32 – 1.22 (m, 1H), 1.16 (dd,  $J = 13.1, 9.2$  Hz, 2H).

**2-chloro-5-(1-(dibenzo[*b,d*]furan-4-yl)propyl)pyridine (172l)**

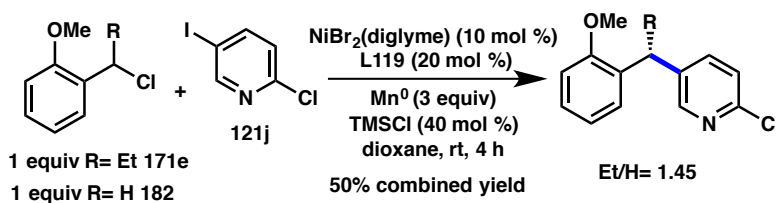


Prepared from 2-chloro-5-iodopyridine (1 equiv, 48.0 mg, 0.2 mmol) and 4-(1-chloropropyl)dibenzo[*b,d*]furan (1 equiv, 49.0 mg, 0.2 mmol) following General Procedure 2.

The crude residue was analyzed by NMR to give a 76% yield. The enantiomeric excess was determined to be 87% by chiral SFC analysis (OB-H, 2.5 mL/min, 10% IPA in CO<sub>2</sub>,  $\lambda = 254$  nm):  $t_{R(\text{minor})} = 9.9$  min,  $t_{R(\text{major})} = 11.7$  min. <sup>1</sup>H NMR (500 MHz, Chloroform-*d*)  $\delta$  8.49 (dt,  $J = 2.5, 0.6$  Hz, 1H), 7.93 (ddd,  $J = 7.7, 1.3, 0.7$  Hz, 1H), 7.86 – 7.80 (m, 1H), 7.64 (ddd,  $J = 8.3, 2.6, 0.5$  Hz, 1H), 7.56 (dt,  $J = 8.2, 0.8$  Hz, 1H), 7.45 (ddd,  $J = 8.4, 7.3, 1.4$  Hz, 1H), 7.37 – 7.29 (m, 3H), 7.23 – 7.18 (m, 1H), 4.46 (t,  $J = 7.9$  Hz, 1H), 2.43 – 2.28 (m, 1H), 2.28 – 2.12 (m, 1H), 0.98 (t,  $J = 7.3$  Hz, 3H).

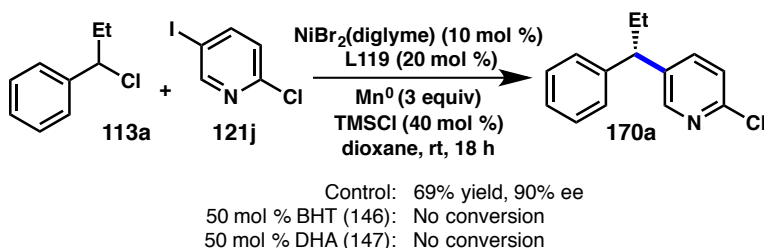
### 4.5.5 Mechanistic experiments

#### a. Competition Experiment



The experiment was conducted according to general procedure 2 for cross-coupling, except that 1-(1-chloropropyl)-2-methoxybenzene (**171e**, 0.05 mmol, 9.2 mg, 1 equiv) was added, followed by 2-methoxybenzyl chloride (**182**, 0.05 mmol, 7.8 mg, 1 equiv, Aldrich). After 4 h, the reaction was a cardinal red with some cloudy precipitate. The vial was opened and the reaction diluted with 20% EtOAc/hexanes and filtered through a short silica plug. Analysis of the crude reaction mixture by <sup>1</sup>H NMR showed a product ratio of Et/H = 1.45 by integration of the 2-pyridyl protons ( $\delta^{\text{Et}}$  8.31,  $\delta^{\text{H}}$  8.28) in a combined yield of 50%.

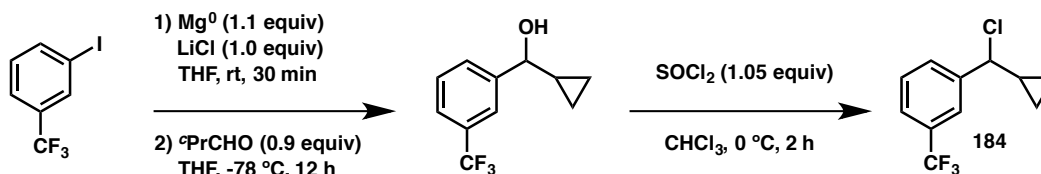
#### b. Inhibitor Studies



The experiment was conducted according to general procedure 2 for cross-coupling, except that either BHT (0.025 mmol, 4.5 mg, 0.5 equiv) or DHA (0.025 mmol, 5.5 mg, 0.5 equiv) were added prior to pumping into the glovebox. After 18 h, the reactions were light grey with minimal precipitate. The vials were opened and the

reactions diluted with 20% EtOAc/hexanes and filtered through short silica plugs. Analysis of the crude reaction mixture by  $^1\text{H}$  NMR showed no consumption of either coupling partner.

### c. Radical Clock Experiment



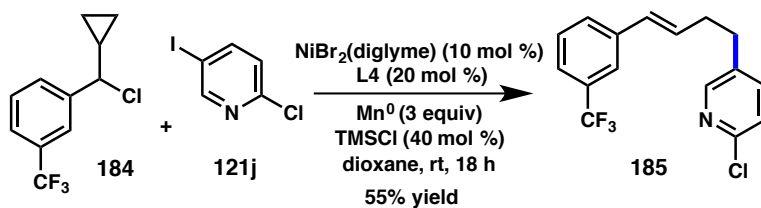
In a glovebox, a flame-dried scintillation vial was charged with a cross-shaped stirbar,  $\text{Mg}^0$  turnings (15.3 mmol, 371 mg, 1.1 equiv),  $\text{LiCl}$  (13.9 mmol, 589 mg, 1 equiv), and THF (10 mL) and sealed with a septum cap pierced with a vent needle. 3-Iodobenzotrifluoride (13.9 mmol, 2 mL, 1 equiv) was added in four portions with stirring. After each addition of 0.5 mL, the reaction was allowed to stir until a small exotherm was noted. After the final addition, the reaction was allowed to stir for 30 min until a muddy brown suspension was achieved with visible consumption of the  $\text{Mg}$  turnings. The vent needle was then removed and the vial was taken out of the glovebox. A separate flame-dried flask was charged with cyclopropylcarboxaldehyde (12 mmol, 0.9 mL, 0.9 equiv) and THF (33 mL), placed under  $\text{N}_2$ , and cooled to  $-78\text{ }^\circ\text{C}$ . The Grignard solution was then added dropwise via syringe. The vial was rinsed with additional THF (2 mL) and this was also added to the flask. The reaction was stirred overnight while the dry ice bath was allowed to warm to room temperature. The reaction was then quenched with 50% sat. aqueous  $\text{NH}_4\text{Cl}$  (30 mL). The layers were separated and the aqueous phase was extracted with  $\text{Et}_2\text{O}$  (2x 20 mL). Organics were combined, dried over  $\text{Na}_2\text{SO}_4$ , and concentrated to

afford the known benzylic alcohol as a yellow oil pure by  $^1\text{H}$  NMR (97% yield, 11.7 mmol, 2.52 g).<sup>1</sup>  $^1\text{H}$  NMR (500 MHz, Chloroform-*d*)  $\delta$  7.71 (tq,  $J = 1.9, 0.7$  Hz, 1H), 7.62 (dddt,  $J = 7.7, 1.9, 1.3, 0.6$  Hz, 1H), 7.55 (ddt,  $J = 7.8, 1.8, 0.9$  Hz, 1H), 7.47 (tt,  $J = 7.7, 0.8$  Hz, 1H), 4.06 (dd,  $J = 8.5, 3.0$  Hz, 1H), 1.33 – 1.12 (m, 1H), 0.68 (dddd,  $J = 9.4, 7.9, 5.5, 4.1$  Hz, 1H), 0.65 – 0.58 (m, 1H), 0.54 – 0.47 (m, 1H), 0.43 (dtd,  $J = 9.6, 5.3, 4.4$  Hz, 1H).

This material was subjected immediately to the chlorination procedure ( $\text{SOCl}_2$  (1.05 equiv, 1.0 mL, 12.6 mmol) in  $\text{CHCl}_3$  (40 mL)) and maintained at 0 °C for 2 h until workup (according to known procedure except for shorter reaction time with monitoring by TLC). Care was taken to minimize exposure to light or heat during reaction, concentration, and handling. The material was stored at -20 °C wrapped in foil. The product was isolated as a 4:1 inseparable mixture of the desired benzylic chloride **184** and the protodehalogenated, rearranged styrene product. This mixture was used as is according to literature procedure.<sup>2</sup>  $^1\text{H}$  NMR (500 MHz, Chloroform-*d*)  $\delta$  7.70 (dtt,  $J = 1.8, 1.2, 0.7$  Hz, 1H), 7.64 (dddt,  $J = 7.7, 1.8, 1.1, 0.6$  Hz, 1H), 7.58 (ddd,  $J = 7.9, 2.3, 1.0$  Hz, 1H), 7.49 (tt,  $J = 7.9, 0.8$  Hz, 1H), 4.32 (d,  $J = 9.3$  Hz, 1H), 1.55 (dtt,  $J = 9.6, 8.0, 4.9$  Hz, 1H), 0.86 (dddd,  $J = 9.0, 7.9, 6.0, 4.9$  Hz, 1H), 0.73 (dddd,  $J = 8.9, 8.0, 6.1, 4.9$  Hz, 1H), 0.62 (ddt,  $J = 9.7, 6.1, 4.9$  Hz, 1H), 0.45 (ddt,  $J = 9.6, 6.0, 4.9$  Hz, 1H).

<sup>1</sup> Neckers, D. C., Schaap, A. P., and Hardy J. *J. Am. Chem. Soc.*, **1966**, 88 (6), 1265.

<sup>2</sup> Hitchcock, S., Amegadzie, A., Qian, W., Xia, X., and Harried. S. S. Glycine transporter-1 inhibitors. WO2008002583 (A1) Jan. 3, 2008.



The cross coupling of radical clock substrate **184** was performed according to general procedure 2 employing 2-chloro-5-iodopyridine (1 equiv, 12.0 mg, 0.05 mmol) and 1-(chloro(cyclopropyl)methyl)-3-(trifluoromethyl)benzene (1 equiv, 16.0 mg, 0.05 mmol). The crude reaction mixture contained the rearranged product **185** as the only cross-coupled product. No cyclopropyl peaks were remaining in the crude  $^1\text{H}$  NMR. **185** was isolated (55% yield, 8.6 mg, 0.028 mmol) by preparative TLC (5%  $\text{Et}_2\text{O}$ , 10%  $\text{PhMe}$ , 85% hexanes,  $\text{RF} = 0.15$ ).  $^1\text{H}$  NMR (500 MHz,  $\text{Chloroform-}d$ )  $\delta$  8.21 (dd,  $J = 2.6, 0.7$  Hz, 1H), 7.51 (q,  $J = 1.4$  Hz, 1H), 7.48 – 7.39 (m, 4H), 7.37 (d,  $J = 7.6$  Hz, 1H), 7.22 (dd,  $J = 8.2, 0.7$  Hz, 1H), 6.40 – 6.35 (m, 1H), 6.22 (dt,  $J = 15.8, 6.9$  Hz, 1H), 2.76 (dd,  $J = 8.4, 6.9$  Hz, 2H), 2.51 (dtd,  $J = 8.6, 6.9, 1.4$  Hz, 2H).  $^{13}\text{C}$  NMR (126 MHz,  $\text{cdCl}_3$ )  $\delta$  149.62, 149.26, 138.83, 137.93, 135.50, 130.41, 130.17, 129.17, 128.99, 123.96, 123.79 (q,  $J = 3.8$  Hz), 122.68, 122.65, 34.23, 31.92.  $^{19}\text{F}$  NMR (282 MHz,  $\text{cdCl}_3$ )  $\delta$  -62.79.

## 4.6 NOTES AND REFERENCES

- (1) Moree, W. J.; Li, B. F.; Jovic, F.; Coon, T.; Yu, J.; Gross, R. S.; Tucci, F.; Marinkovic, D.; Zamani-Kord, S.; Malany, S.; Bradbury, M. J.; Hernandez, L. M.; O'Brien, Z.; Wen, J.; Wang, H.; Hoare, S. R.; Petroski, R. E.; Saccaan, A.; Madan, A.; Crowe, P. D.; Beaton, G. *J. Med. Chem.* **2009**, *52*, 5307.
- (2) (a) Imao, D.; Glasspoole, B. W.; Laberge, V. S.; Crudden, C. M. *J. Am. Chem. Soc.* **2009**, *131*, 5024; (b) Taylor, B. L.; Swift, E. C.; Waetzig, J. D.; Jarvo, E. R. *J. Am. Chem. Soc.* **2011**, *133*, 389; (c) Maity, P.; Shacklady-McAtee, D. M.; Yap, G. P.; Sirianni, E. R.; Watson, M. P. *J. Am. Chem. Soc.* **2013**, *135*, 280; (d) Do, H. Q.; Chandrashekar, E. R.; Fu, G. C. *J. Am. Chem. Soc.* **2013**, *135*, 16288; (e) Harris, M. R.; Hanna, L. E.; Greene, M. A.; Moore, C. E.; Jarvo, E. R. *J. Am. Chem. Soc.* **2013**, *135*, 3303; (f) Zhou, Q.; Srinivas, H. D.; Dasgupta, S.; Watson, M. P. *J. Am. Chem. Soc.* **2013**, *135*, 3307; (g) Wisniewska, H. M.; Swift, E. C.; Jarvo, E. R. *J. Am. Chem. Soc.* **2013**, *135*, 9083; (h) Crudden, C.; Glasspoole, B.; Oderinde, M.; Moore, B.; Antoft-Finch, A. *Synthesis* **2013**, *45*, 1759; (i) Shacklady-McAtee, D. M.; Roberts, K. M.; Basch, C. H.; Song, Y. G.; Watson, M. P. *Tetrahedron* **2014**, *70*, 4257; (j) Cherney, A. H.; Kadunce, N. T.; Reisman, S. E. *Chem. Rev.* **2015**, *115*, 9587; (k) Gutierrez, O.; Tellis, J. C.; Primer, D. N.; Molander, G. A.; Kozlowski, M. C. *J. Am. Chem. Soc.* **2015**, *137*, 4896.
- (3) (a) Wang, Z.; Ai, F.; Wang, Z.; Zhao, W.; Zhu, G.; Lin, Z.; Sun, J. *J. Am. Chem. Soc.* **2015**, *137*, 383; (b) Chen, J.; Chen, C.; Ji, C.; Lu, Z. *Org. Lett.* **2016**, *18*, 1594.
- (4) (a) Yonova, I. M.; Johnson, A. G.; Osborne, C. A.; Moore, C. E.; Morrisette, N. S.; Jarvo, E. R. *Angew. Chem. Int. Ed. Engl.* **2014**, *53*, 2422; (b) Tollefson, E. J.; Hanna, L. E.; Jarvo, E. R. *Acc. Chem. Res.* **2015**, *48*, 2344.
- (5) Ackerman, L. K.; Anka-Lufford, L. L.; Naodovic, M.; Weix, D. J. *Chem Sci* **2015**, *6*, 1115.
- (6) For full details of these preliminary investigations, see Chapter 5 Dr. Alan H. Cherney's Ph.D. thesis.
- (7) (a) Cherney, A. H.; Kadunce, N. T.; Reisman, S. E. *J. Am. Chem. Soc.* **2013**, *135*, 7442; (b) Cherney, A. H.; Reisman, S. E. *J. Am. Chem. Soc.* **2014**, *136*, 14365; (c) Kadunce, N. T.; Reisman, S. E. *J. Am. Chem. Soc.* **2015**, *137*, 10480.
- (8) Everson, D. A.; Weix, D. J. *J. Org. Chem.* **2014**, *79*, 4793.
- (9) Ackerman, L. K.; Lovell, M. M.; Weix, D. J. *Nature* **2015**, *524*, 454.
- (10) Everson, D. A.; Buonomo, J. A.; Weix, D. J. *Synlett* **2014**, *25*, 233.

- (11) Molander, G. A.; Traister, K. M.; O'Neill, B. T. *J. Org. Chem.* **2014**, *79*, 5771.
- (12) Nonhebel, D. C. *Chem. Soc. Rev.* **1993**, *22*, 347.
- (13) Hitchcock, S. A. S. D., CA, US), Amegadzie, Albert (Moorpark, CA, US), Qian, Wenyan (Newbury Park, CA, US), Xia, Xiaoyang (Thousand Oaks, CA, US), Harried, Scott S. (Pittsburgh, PA, US); AMGEN INC. (Thousand Oaks, CA, US): United States, 2015.
- (14) Henry, D. J.; Parkinson, C. J.; Mayer, P. M.; Radom, L. *J. Phys. Chem. A* **2001**, *105*, 6750.

## **APPENDIX 3**

*Spectra Relevant to Chapter 4:*

*Nickel-Catalyzed Asymmetric Reductive Cross-Coupling to Access*

*1,1-Di(hetero)arylalkanes*

NTK-IV-205-CF3\_flashed

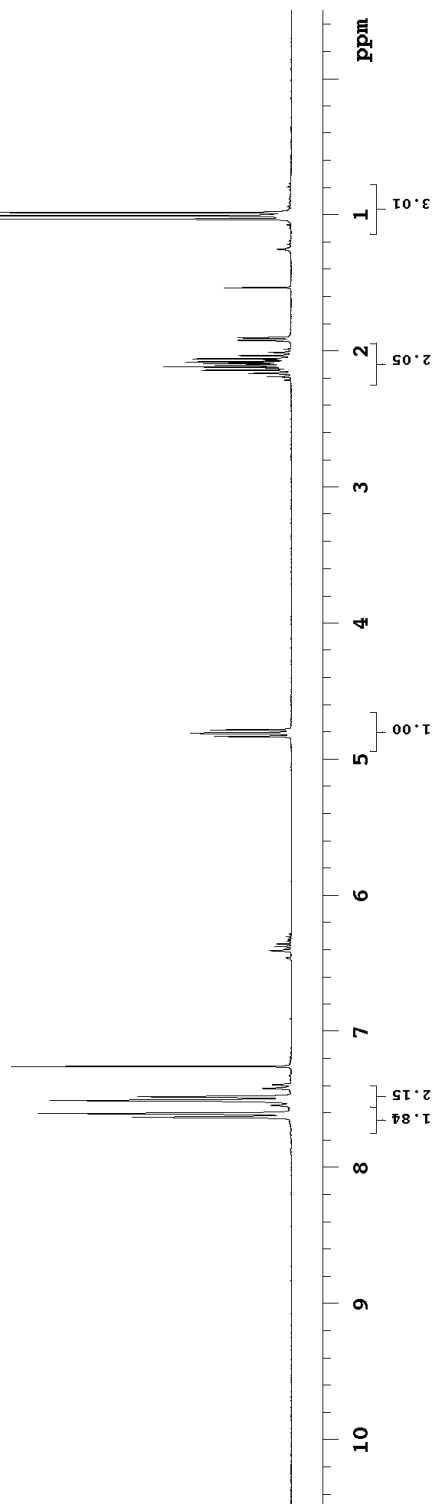
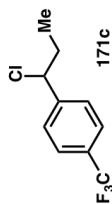
Sample Name:  
 NTK-IV-205-CF3\_flashed  
 Data Collected on:  
 hg3.caltech.edu-mercury300  
 Archive directory:  
 /home/nkadance/vnmrsys/data  
 Sample directory:  
 NTK-IV-205-CF3\_flashed  
 Fidfile: PROTON01

Pulse Sequence: PROTON (s2pul)  
 Solvent: cdcl3  
 Data collected on: Nov 20 2015

sample #16, Operator: nkadance

Relax. delay 2.000 sec  
 Pulse 45.0 degrees  
 Acq. time 2.500 sec  
 Width 4796.2 Hz  
 32 repetitions

OBSERVE H1, 300.0901675 MHZ  
 DATA PROCESSING  
 Line broadening 0.2 Hz  
 F1 size 32768  
 Total time 2 min 29 sec

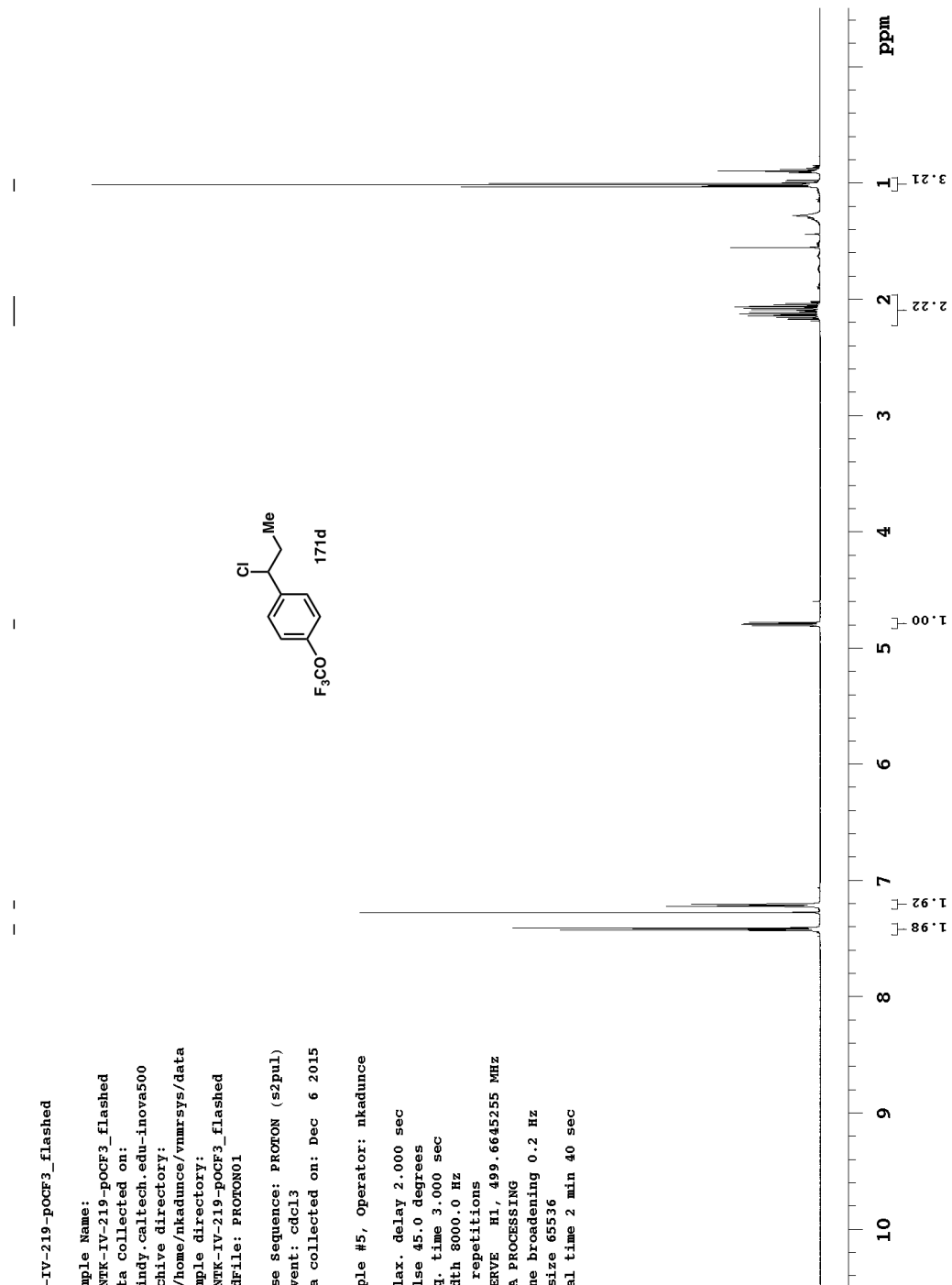
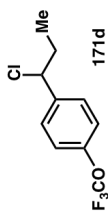


NTK-IV-219-pOCF3\_flashed

Sample Name:  
 NTK-IV-219-pOCF3\_flashed  
 Data Collected on:  
 indy.caltech.edu-inova500  
 Archive directory:  
 /home/nkadunce/vnmrsys/data  
 Sample directory:  
 NTK-IV-219-pOCF3\_flashed  
 FIDfile: PROTON01

Pulse Sequence: PROTON (s2pul)  
 solvent: cdcl3  
 Data collected on: Dec 6 2015

Sample #5, Operator: nkadunce  
 Relax. delay 2.000 sec  
 Pulse 45.0 degrees  
 Acq. time 3.000 sec  
 Width 8000.0 Hz  
 32 repetitions  
 OBSERVE H1, 499.6645255 MHz  
 DATA PROCESSING  
 Line broadening 0.2 Hz  
 FT size 65536  
 Total time 2 min 40 sec

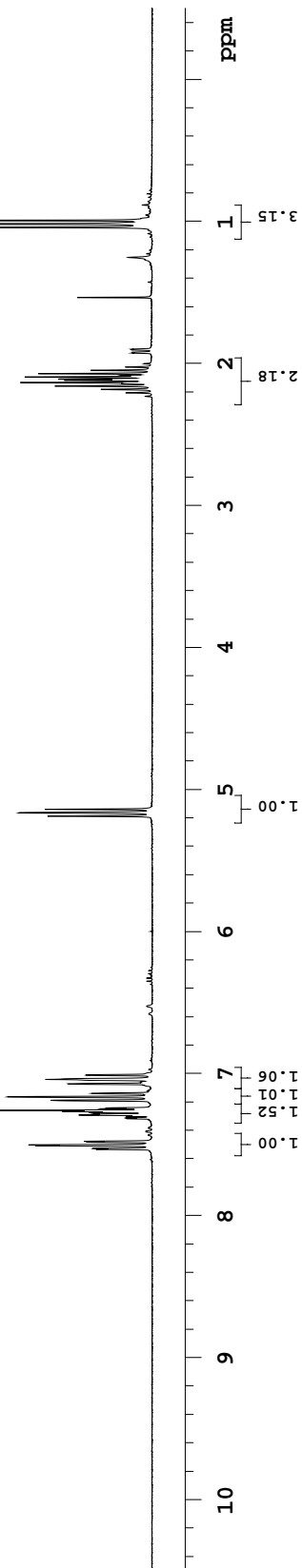
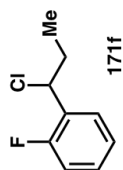


NTK-IV-205-OF-flashed

Sample Name:  
 NTK-IV-205-OF-flashed  
 Data Collected on:  
 hg3.caltech.edu-mercury300  
 Archive directory:  
 /home/nkadunce/vnmrSYS/data  
 Sample directory:  
 NTK-IV-205-OF-flashed  
 Fidfile: PROTON01

Pulse Sequence: PROTON (s2pul)  
 Solvent: cdc13  
 Data collected on: Nov 22 2015

Sample #15, Operator: nkadunce  
 Relax. delay 2.000 sec  
 Pulse 45.0 degrees  
 Acq. time 2.500 sec  
 Width 4796.2 Hz  
 32 repetitions  
 OBSERVE HL, 300.0901675 MHz  
 DATA PROCESSING  
 Line broadening 0.2 Hz  
 FT size 32768  
 Total time 2 min 29 sec

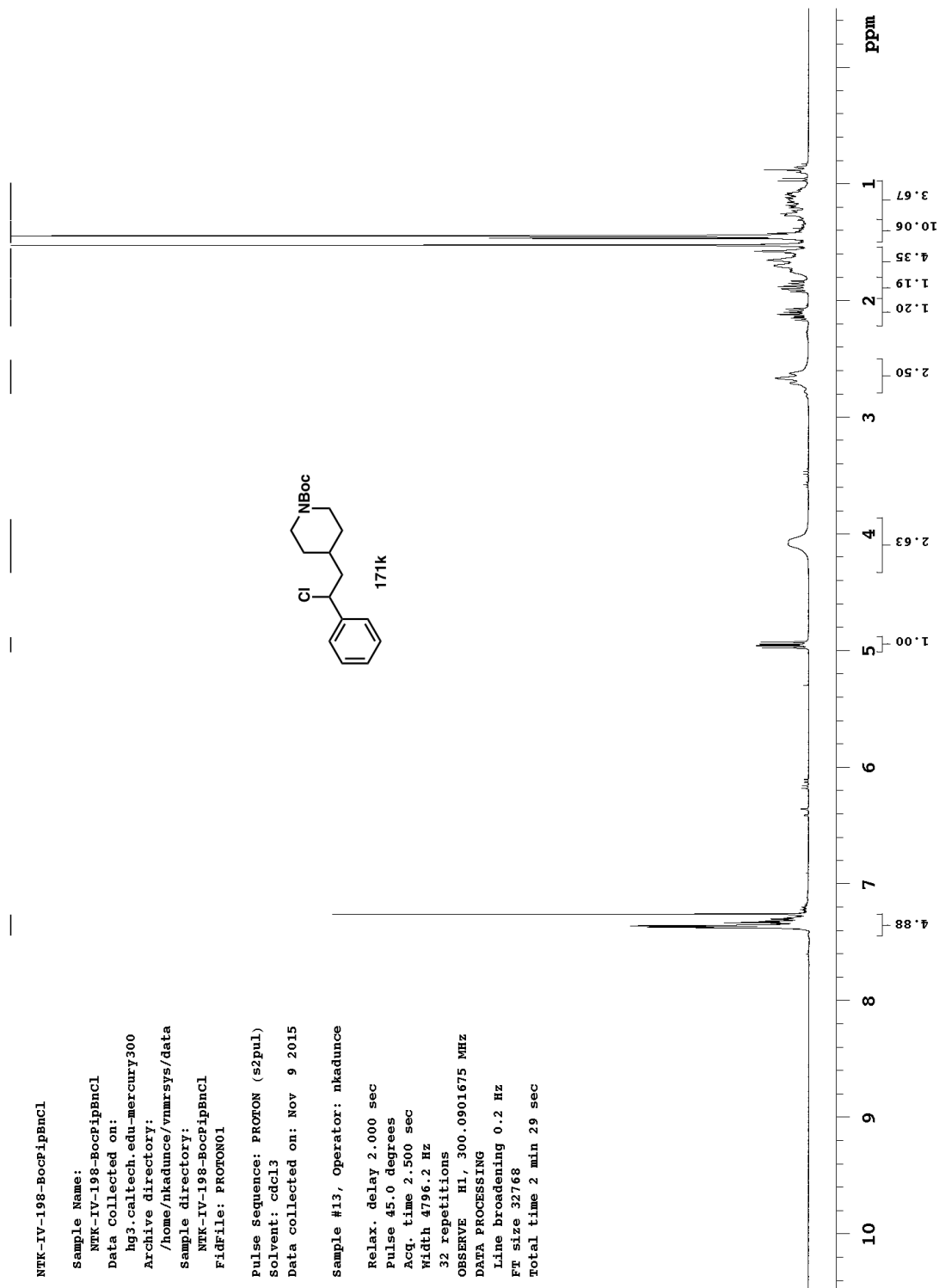
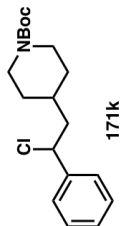


NTK-IV-198-BocPipBnCl

Sample Name:  
 NTK-IV-198-BocPipBnCl  
 Data Collected on:  
 hg3.caltech.edu-mercury300  
 Archive directory:  
 /home/nkadunce/vnmrsys/data  
 Sample directory:  
 NTK-IV-198-BocPipBnCl  
 FIDfile: PROTON01

Pulse Sequence: PROTON (s2pul)  
 solvent: cdcl3  
 Data collected on: Nov 9 2015

Sample #13, Operator: nkadunce  
 Relax. delay 2.000 sec  
 Pulse 45.0 degrees  
 Acq. time 2.500 sec  
 Width 4796.2 Hz  
 32 repetitions  
 OBSERVE H1, 300.0901675 MHz  
 DATA PROCESSING  
 Line broadening 0.2 Hz  
 FT size 32768  
 Total time 2 min 29 sec



NTK-IV-BnClPyr\_F1

Sample Name:

NTK-IV-BnClPyr\_F1

Data Collected on:

hg3.caltech.edu-mercury300

Archive directory:

/home/nkadance/vnmrsys/data

Sample directory:

NTK-IV-BnClPyr\_F1

FidFile: PROTON01

Pulse sequence: PROTON (s2pul)

Solvent: cdcl3

Data collected on: Jun 29 2015

Sample #16, Operator: nkadance

Relax. delay 2.000 sec

Pulse 45.0 degrees

Acq. time 2.500 sec

Width 4796.2 Hz

32 repetitions

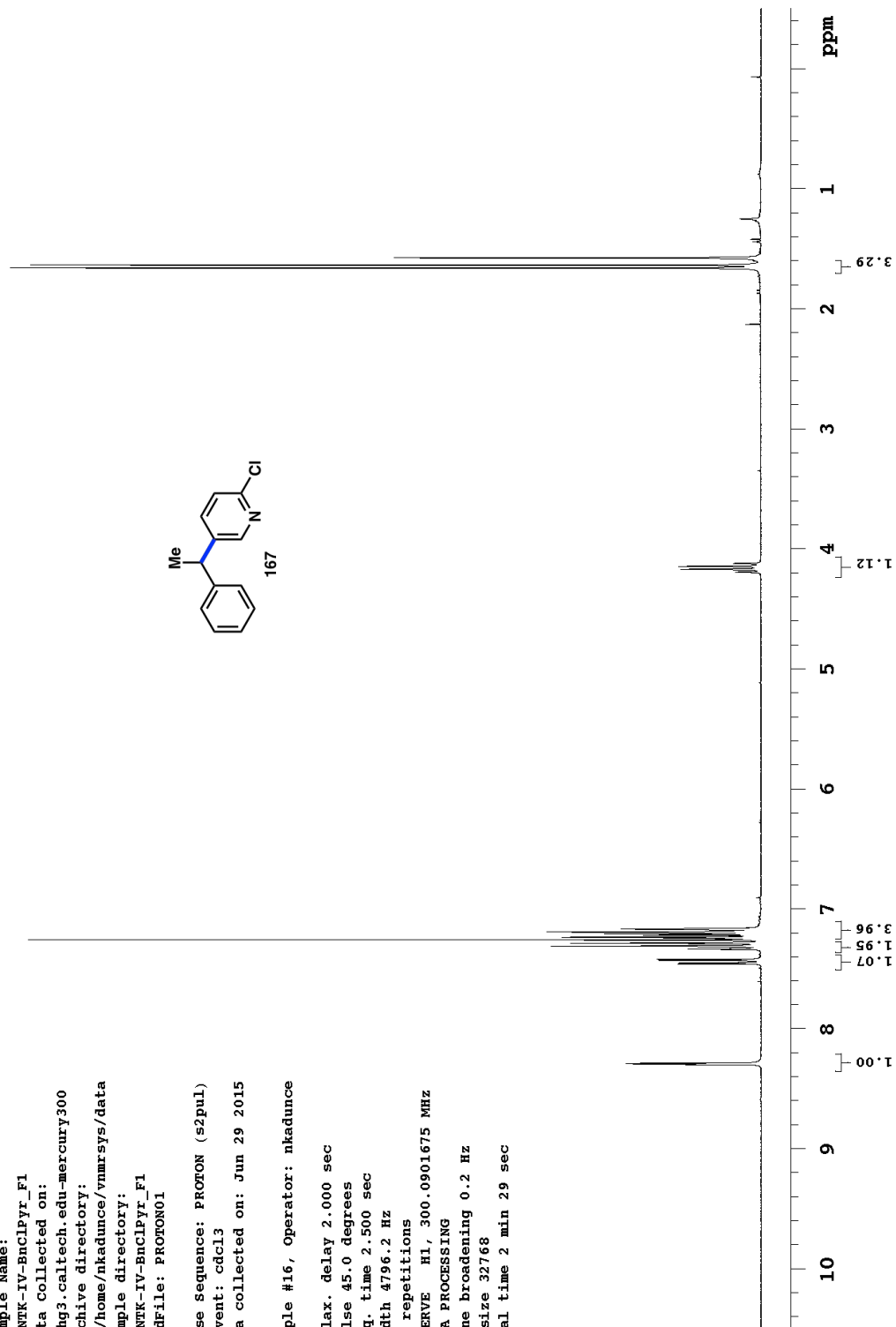
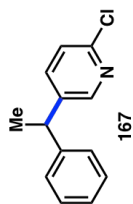
OBSERVE H1, 300.0901675 MHz

DATA PROCESSING

Line broadening 0.2 Hz

FT size 32768

Total time 2 min 29 sec

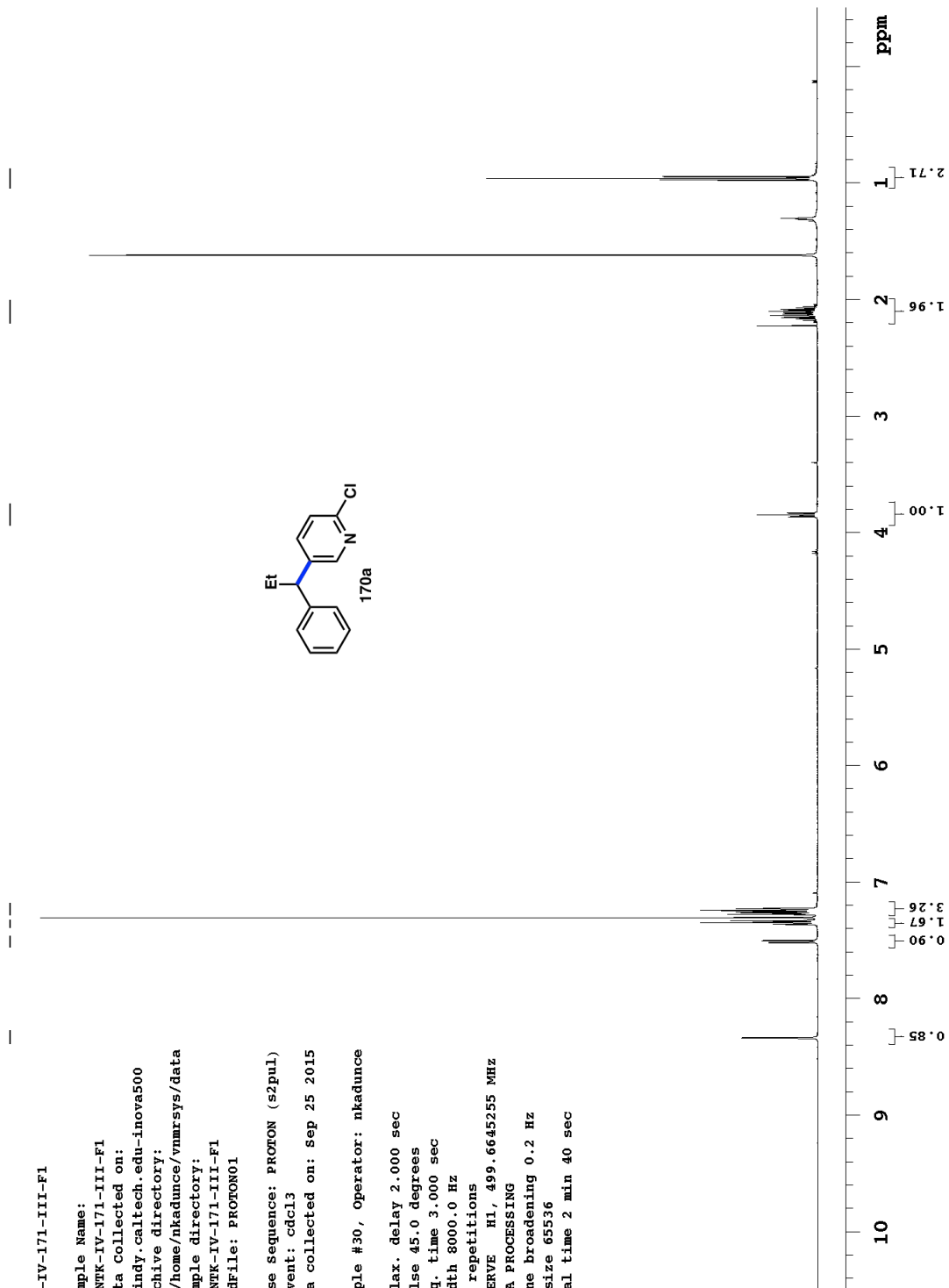
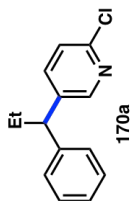


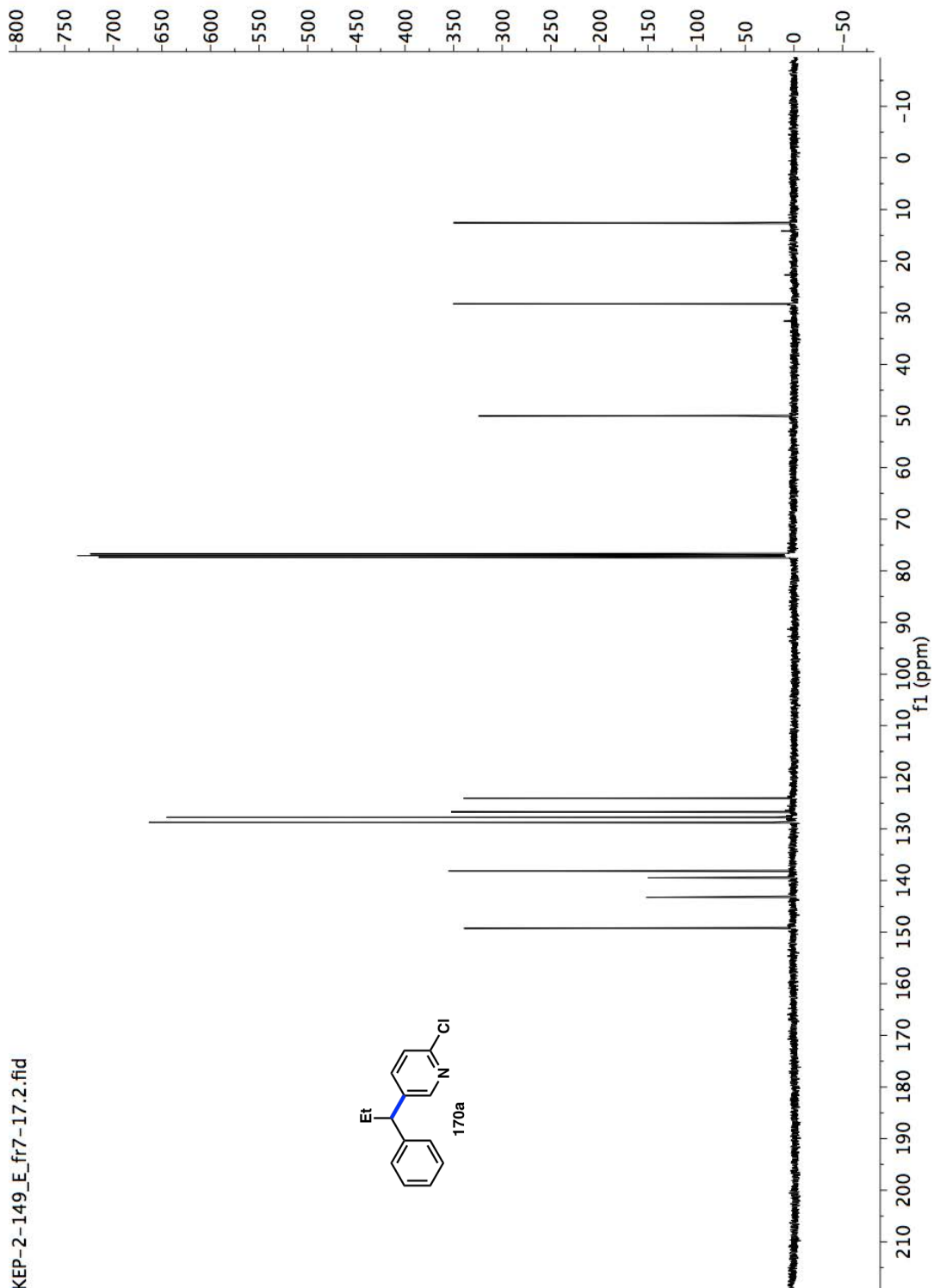
NTK-IV-171-III-F1

Sample Name:  
 NTK-IV-171-III-F1  
 Data Collected on:  
 indy.caltech.edu-inova500  
 Archive directory:  
 /home/nkadance/vnmrsys/data  
 Sample directory:  
 NTK-IV-171-III-F1  
 Fidfile: PROTON01

Pulse sequence: PROTON (s2pul)  
 Solvent: cdcl3  
 Data collected on: Sep 25 2015

sample #30, Operator: nkadance  
 Relax. delay 2.000 sec  
 Pulse 45.0 degrees  
 Acq. time 3.000 sec  
 Width 3000.0 Hz  
 32 repetitions  
 OBSERVE H1, 499.6645255 MHZ  
 DATA PROCESSING  
 Line broadening 0.2 Hz  
 FT size 65536  
 Total time 2 min 40 sec



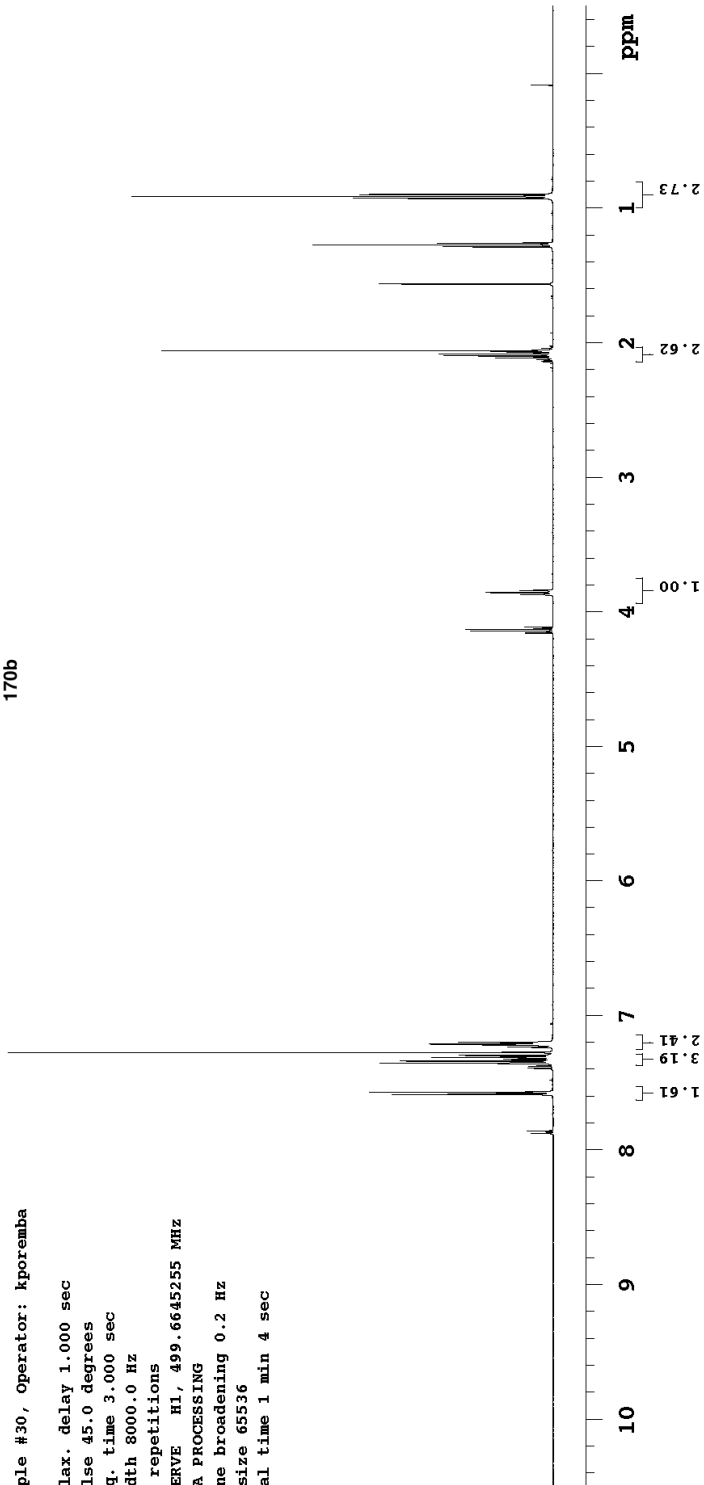
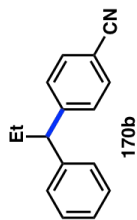


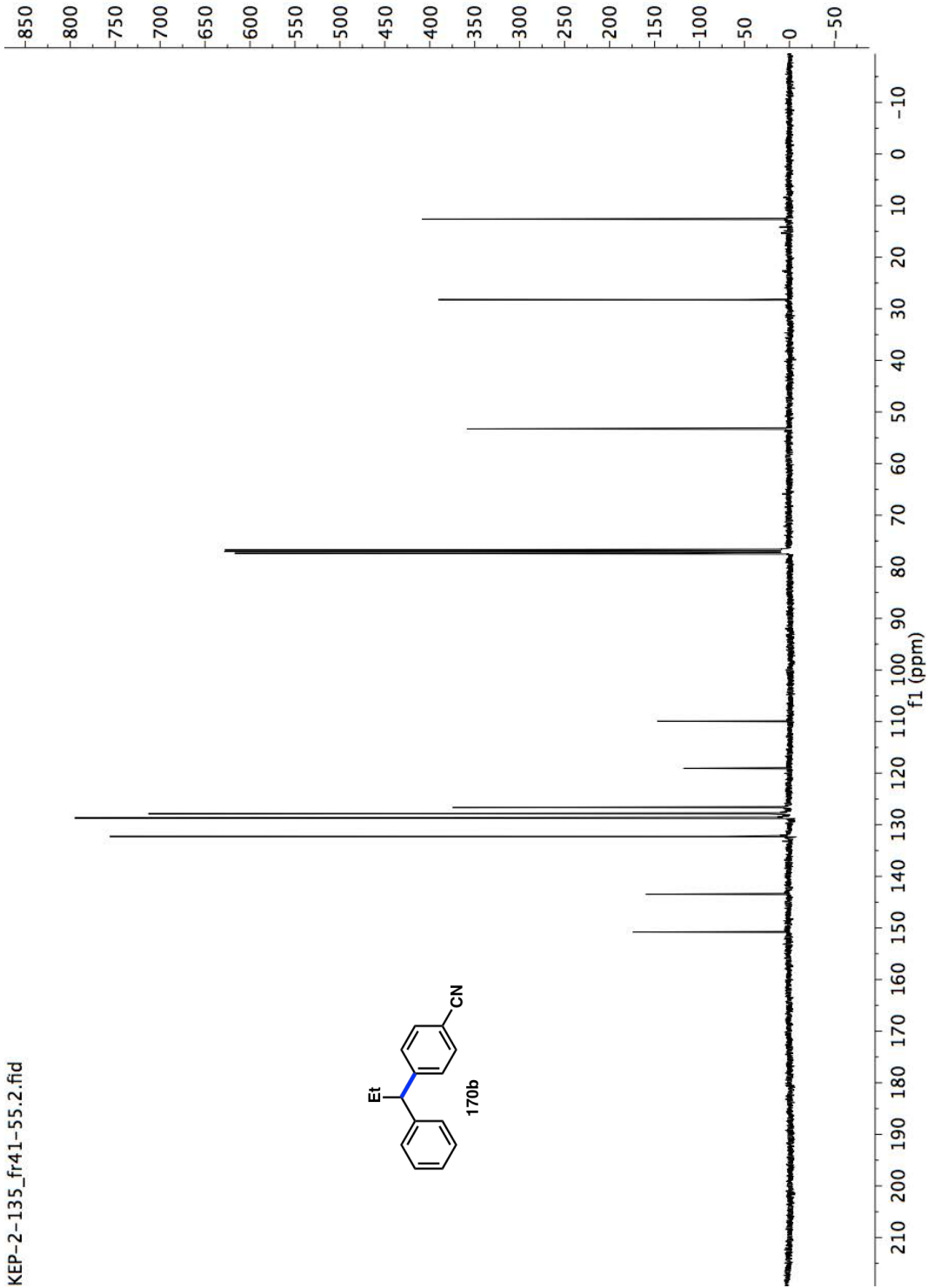
KEP-2-62\_B\_prep1

Sample Name:  
 KEP-2-62\_B\_prep1  
 Data Collected on:  
 indy.caltech.edu-inova500  
 Archive directory:  
 /home/kporemba/vnmrsys/data  
 Sample directory:  
 KEP-2-62\_B\_prep1  
 File: PROTON01

Pulse Sequence: PROTON (s2pul)  
 Solvent: cdcl3  
 Data collected on: Nov 22 2015

Sample #30, Operator: kporemba  
 Relax. delay 1.000 sec  
 Pulse 45.0 degrees  
 Acq. time 3.000 sec  
 Width 8000.0 Hz  
 16 repetitions  
 OBSERVE H1, 499.6645255 MHz  
 DATA PROCESSING  
 Line broadening 0.2 Hz  
 FT size 65536  
 Total time 1 min 4 sec



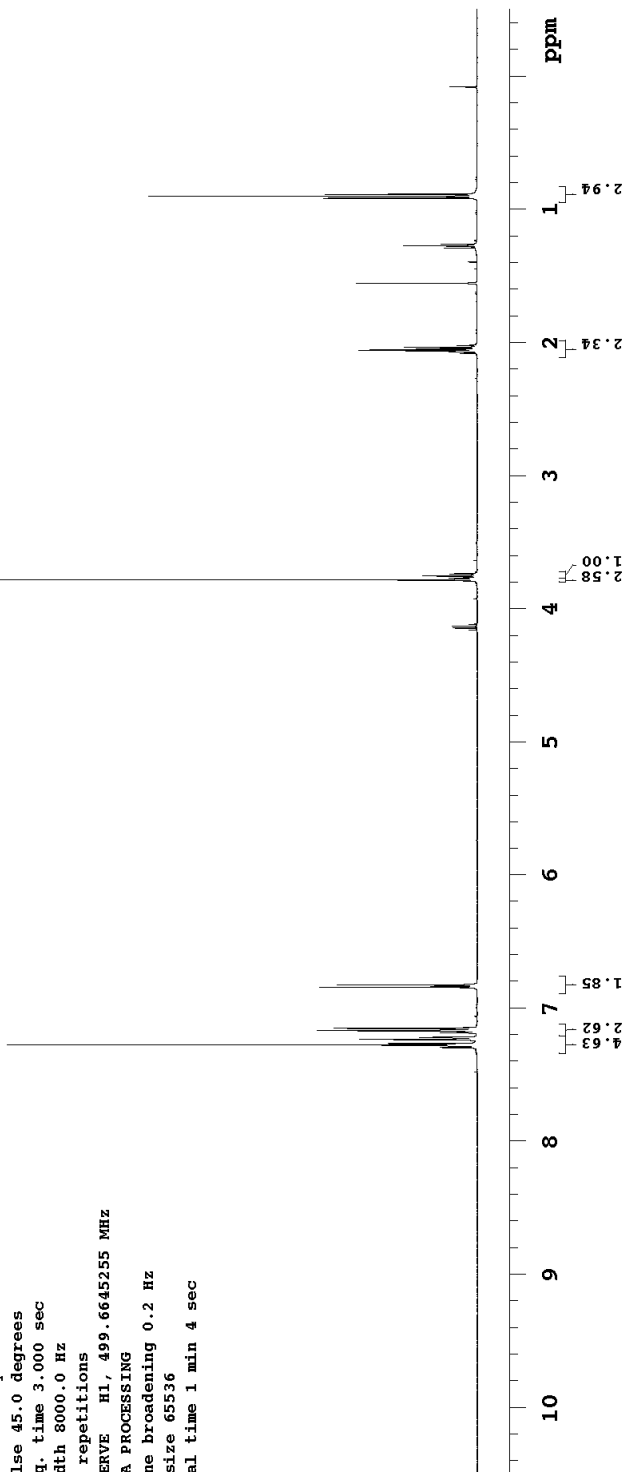
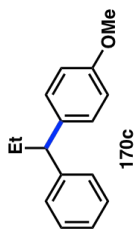


KEP-2-62\_A\_prep1

Sample Name:  
 KEP-2-62\_A\_prep1  
 Data collected on:  
 indy.caltech.edu-inova500  
 Archive directory:  
 /home/kporemba/vnmrSYS/data  
 sample directory:  
 KEP-2-62\_A\_prep1  
 FIDFile: PROTON01

Pulse Sequence: PROTON (s2pul)  
 Solvent: cdcl3  
 Data collected on: Nov 22 2015

Sample #29, Operator: kporemba  
 Relax. delay 1.000 sec  
 Pulse 45.0 degrees  
 Acq. time 3.000 sec  
 Width 8000.0 Hz  
 16 repetitions  
 OBSERVE H1, 499.6645255 MHZ  
 DATA PROCESSING  
 Line broadening 0.2 Hz  
 FT size 65536  
 Total time 1 min 4 sec



KEP-2-136\_fr24-33

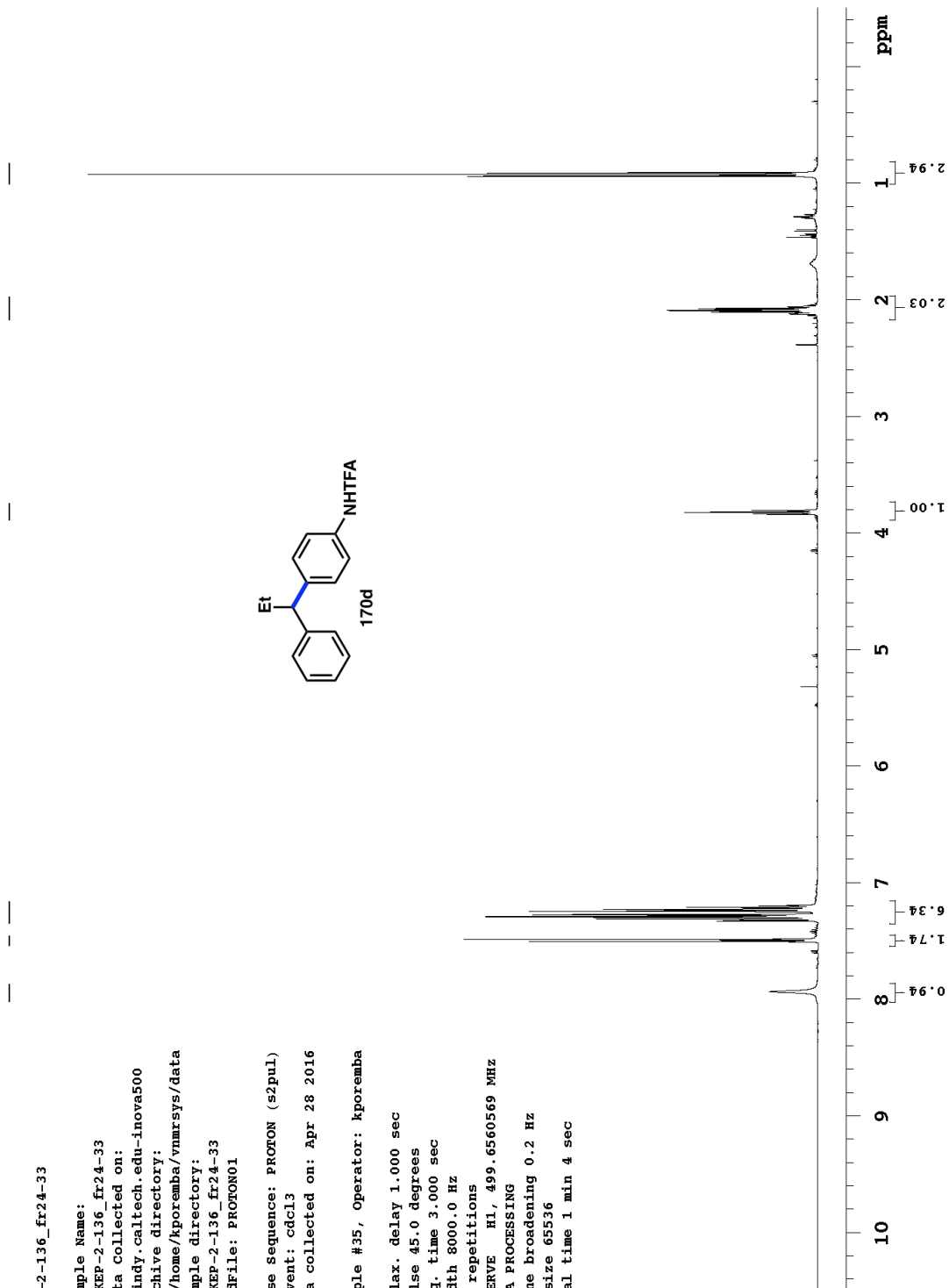
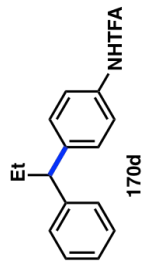
Sample Name:  
 KEP-2-136\_fr24-33  
 Data Collected on:  
 indy.caltech.edu-inova500  
 Archive directory:  
 /home/kporemba/vnmrSYS/data  
 Sample directory:  
 KEP-2-136\_fr24-33  
 FIDfile: PROTON01

Pulse Sequence: PROTON (s2pul)  
 Solvent: cdcl3  
 Data collected on: Apr 28 2016

Sample #35, Operator: kporemba

Relax. delay 1.000 sec  
 Pulse 45.0 degrees  
 Acq. time 3.000 sec  
 Width 8000.0 Hz  
 16 repetitions

OBSERVE H1, 499.6560569 MHz  
 DATA PROCESSING  
 Line broadening 0.2 Hz  
 FT size 65536  
 Total time 1 min 4 sec



KEP-2-136\_fr24-33

Sample Name:

KEP-2-136\_fr24-33

Data Collected on:

hg3.caltech.edu-mercury300

Archive directory:

/home/kporemba/vnmrsys/data

Sample directory:

KEP-2-136\_fr24-33

Fidfile: FLUORINE01

Pulse Sequence: FLUORINE (s2pul)

Solvent: cdcl3

Data collected on: May 3 2016

Sample #12, Operator: kporemba

Relax. delay 1.000 sec

Pulse 30.0 degrees

Acq. time 0.986 sec

Width 64935.1 Hz

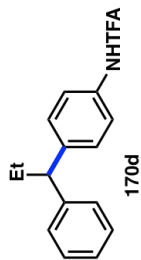
16 repetitions

OBSERVE F19, 282.3668752 MHz

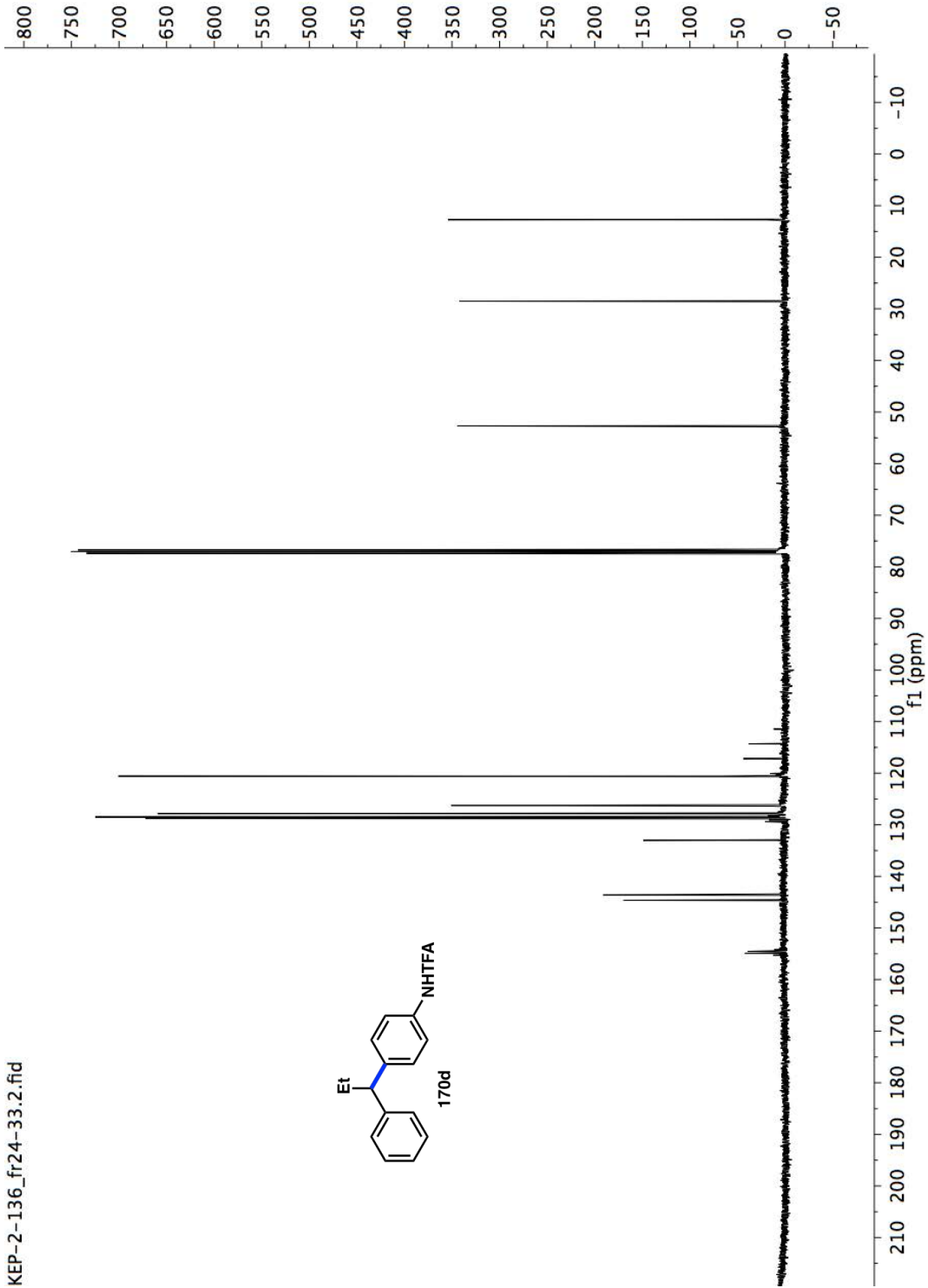
DATA PROCESSING

FT size 131072

Total time 0 min 36 sec



20 0 -20 -40 -60 -80 -100 -120 -140 -160 -180 ppm



KEP-2-151\_fr35-42

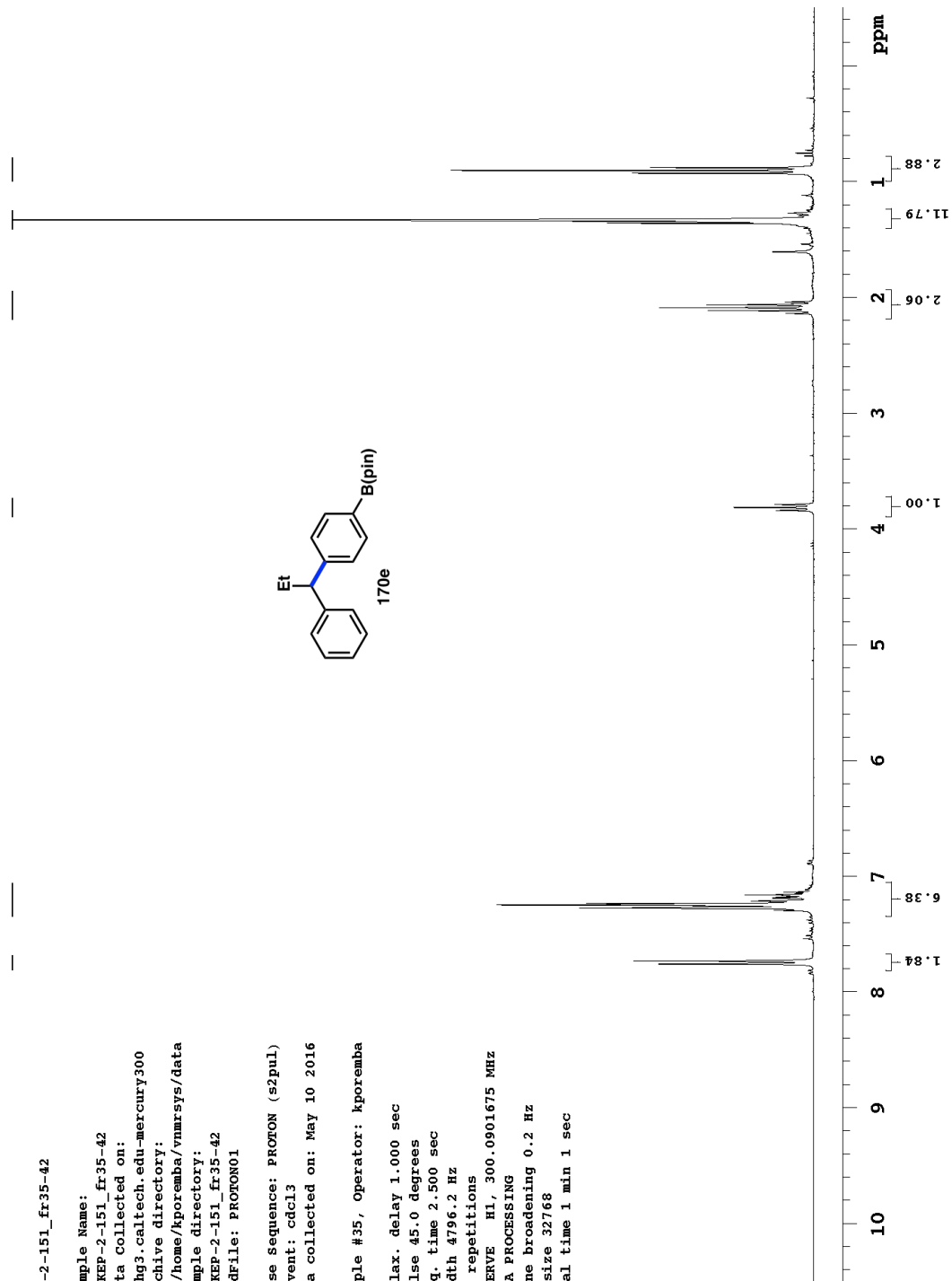
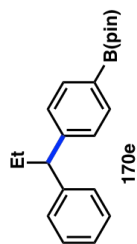
Sample Name:  
 KEP-2-151\_fr35-42  
 Data Collected on:  
 hg3.caltech.edu-mercury300  
 Archive directory:  
 /home/kporemba/vnmrsys/data  
 Sample directory:  
 KEP-2-151\_fr35-42  
 Fidfile: PROTON01

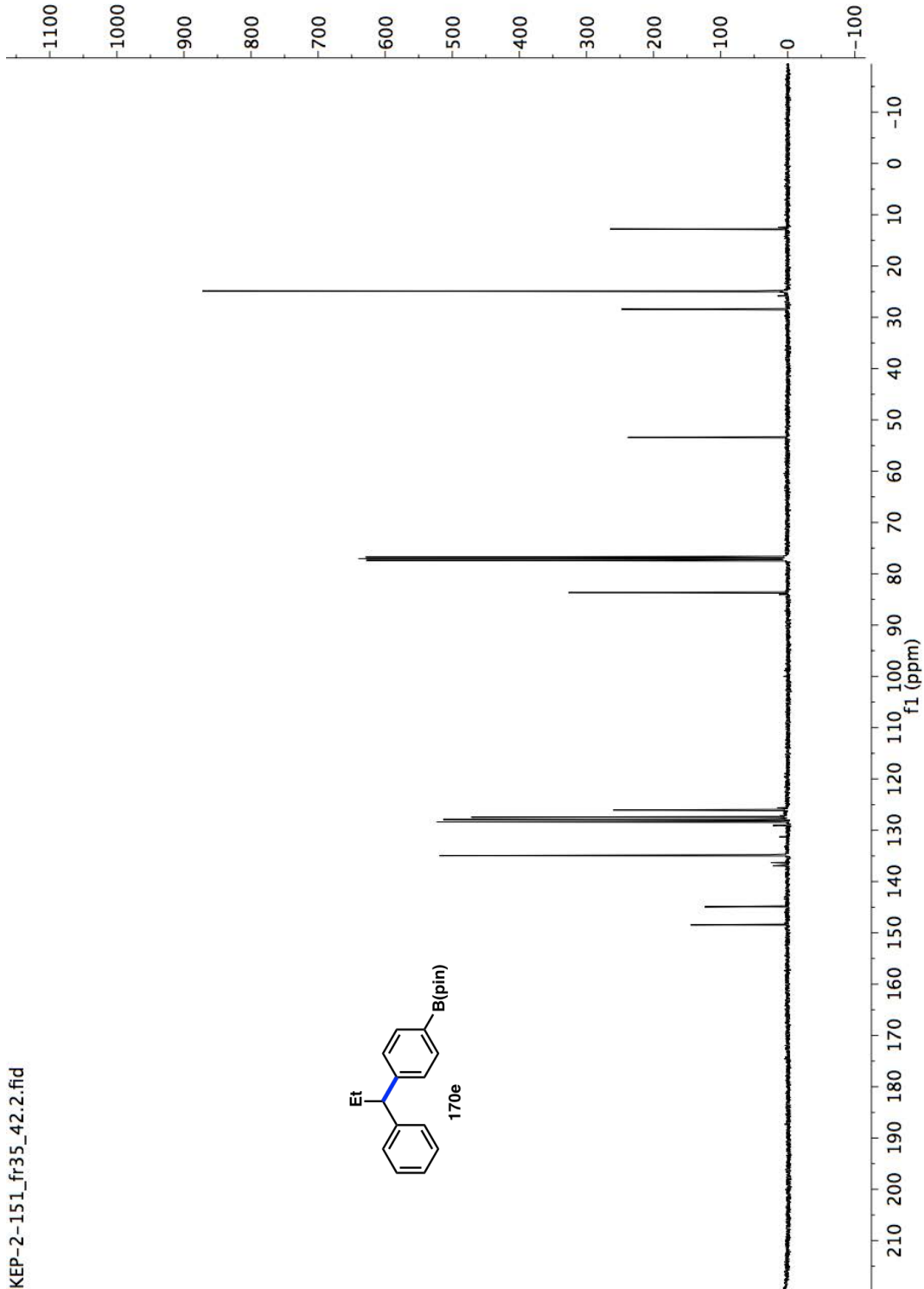
Pulse Sequence: PROTON (s2pul)  
 Solvent: cdcl3  
 Data collected on: May 10 2016

sample #35, Operator: kporemba

Relax. delay 1.000 sec  
 Pulse 45.0 degrees  
 Acq. time 2.500 sec  
 Width 4796.2 Hz

16 repetitions  
 OBSERVE H1, 300.0901675 MHZ  
 DATA PROCESSING  
 Line broadening 0.2 Hz  
 Ft size 32768  
 Total time 1 min 1 sec





KEP-2-151\_fr35\_42.2.fid



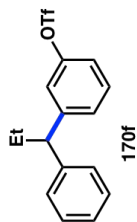
STANDARD FLUORINE PARAMETERS

Sample Name: NTK-IV-233-III-MOTf\_F2  
 Data Collected on: hg3.caltech.edu-mercury300 Archive  
 directory: ~~ntk-iv-233-iii-motf\_f2~~pkadunce/vmrsys/data Sample  
 NTK-IV-233-III-MOTf\_F2 FIDFile: FLUORINE01

Pulse Sequence: FLUORINE (s2pul) Solvent: cdcl3  
 Data collected on: Jan 13 2016

Sample #4, Operator: nkadunce  
 Relax. delay 1.000 sec Pulse 30.0 degrees  
 Acq. time 0.986 sec Width 64935.1 Hz  
 16 repetitions

OBSERVE F19, 282.3668752  
 MHZ DATA PROCESSING  
 FT size 131072  
 Total time 0 min 36 sec



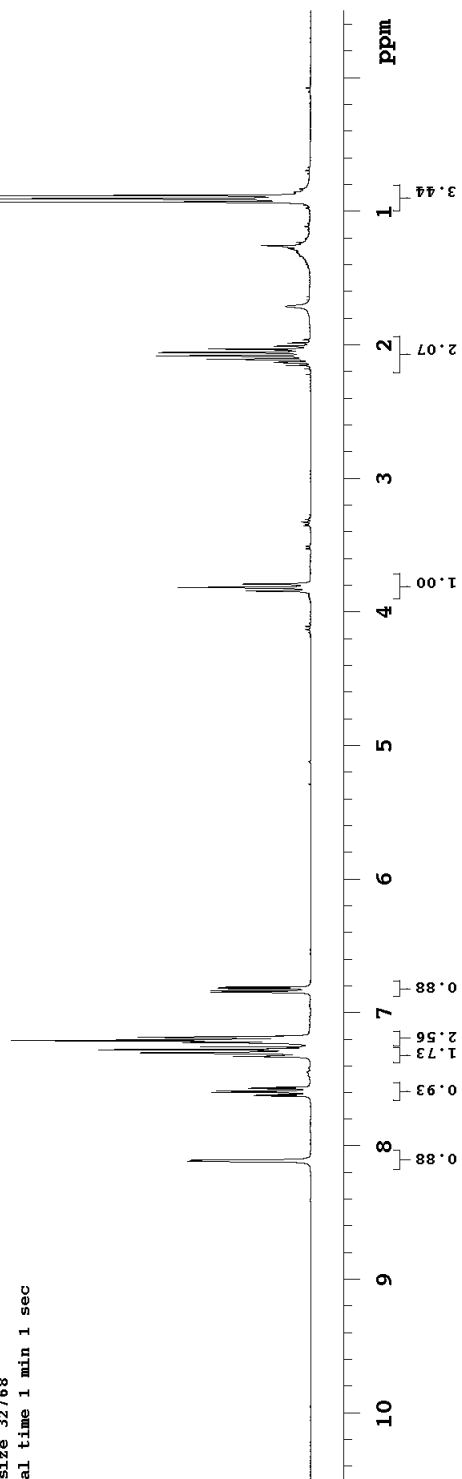
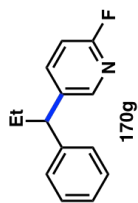


KEP-2-144\_13-24

Sample Name:  
 KEP-2-144\_13-24  
 Data Collected on:  
 hg3.caltech.edu-mercury300  
 Archive directory:  
 /home/kporemba/vnmrsys/data  
 sample directory:  
 KEP-2-144\_13-24  
 FIDfile: PROTON01

Pulse sequence: PROTON (s2pul)  
 Solvent: cdcl3  
 Data collected on: May 3 2016

Sample #9, Operator: kporemba  
 Relax. delay 1.000 sec  
 Pulse 45.0 degrees  
 Acq. time 2.500 sec  
 Width 4796.2 Hz  
 16 repetitions  
 OBSERVE H1, 300.0901675 MHZ  
 DATA PROCESSING  
 Line broadening 0.2 Hz  
 FT size 32768  
 Total time 1 min 1 sec

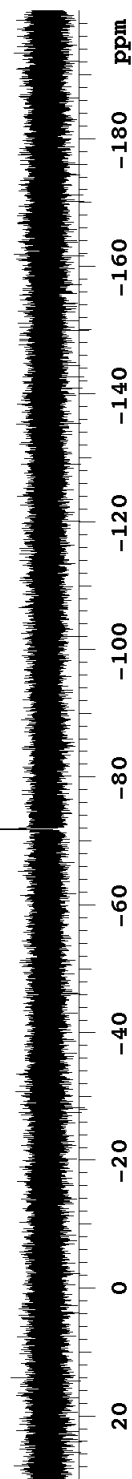
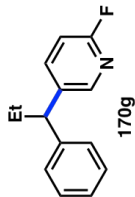


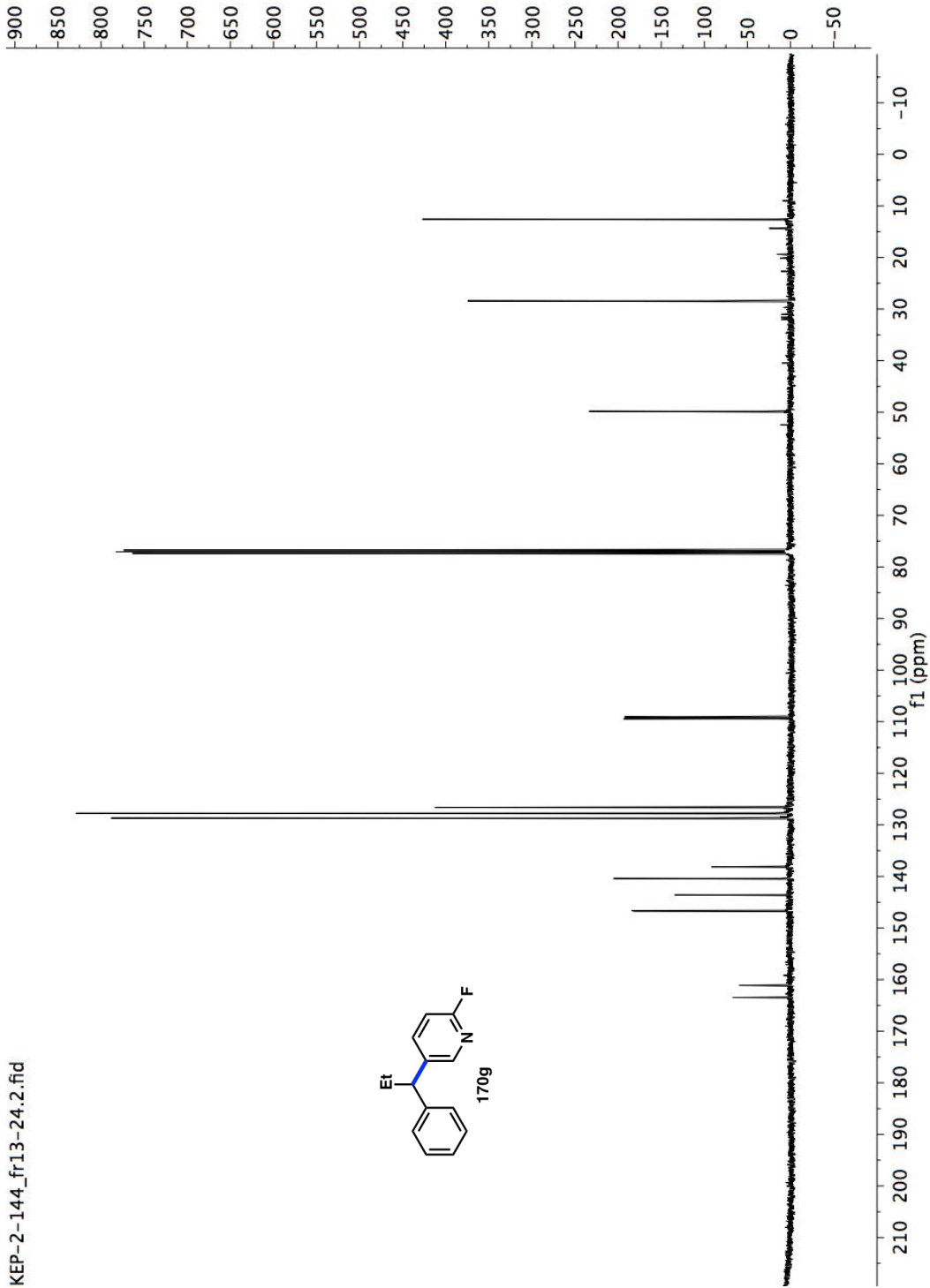
KEP-2-144\_13-24

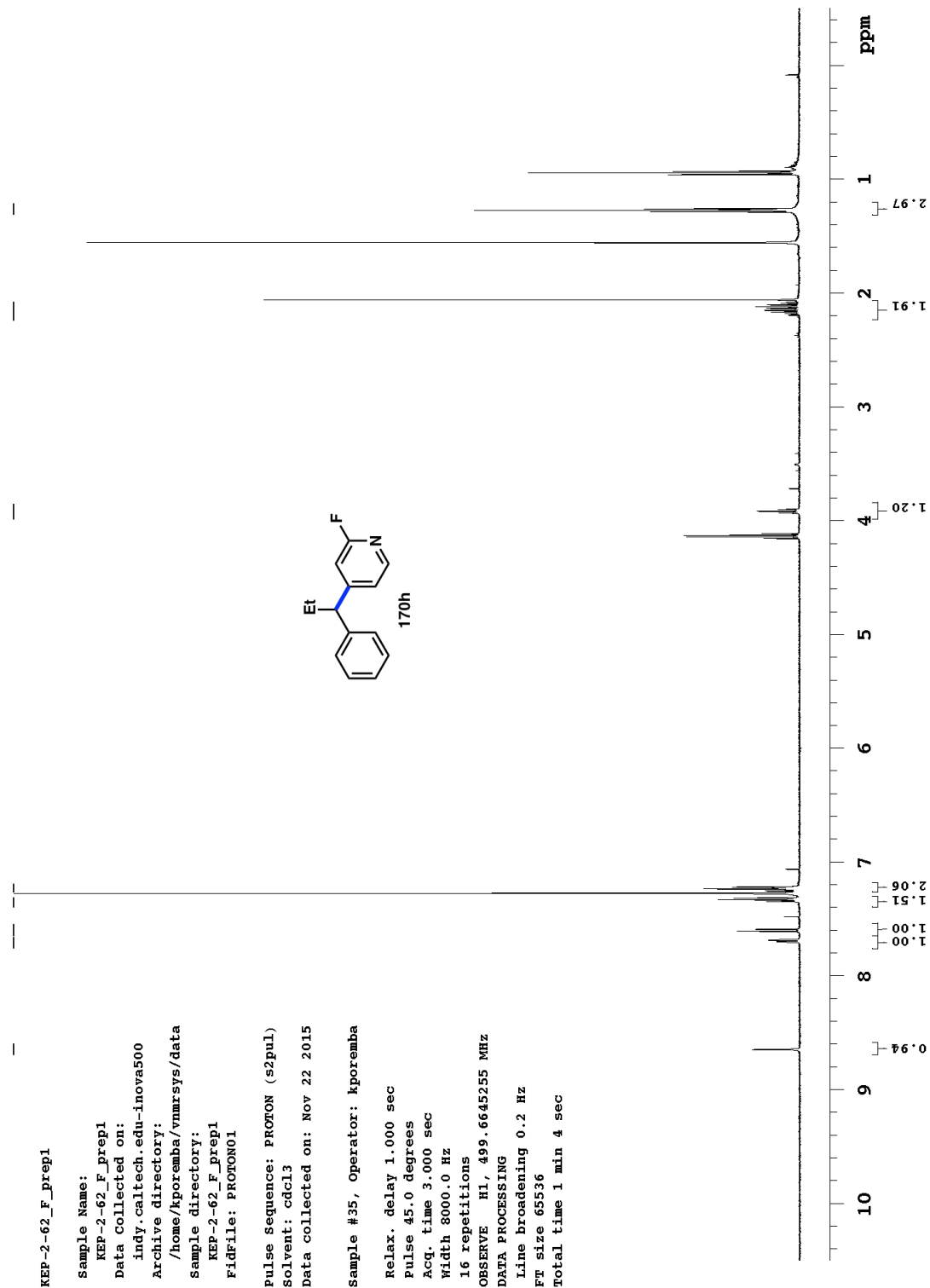
Sample Name:  
KEP-2-144\_13-24  
Data Collected on:  
hg3.caltech.edu-mercury300  
Archive directory:  
/home/kporemba/vnmrSYS/data  
sample directory:  
KEP-2-144\_13-24  
FIDfile: FLUORINE01

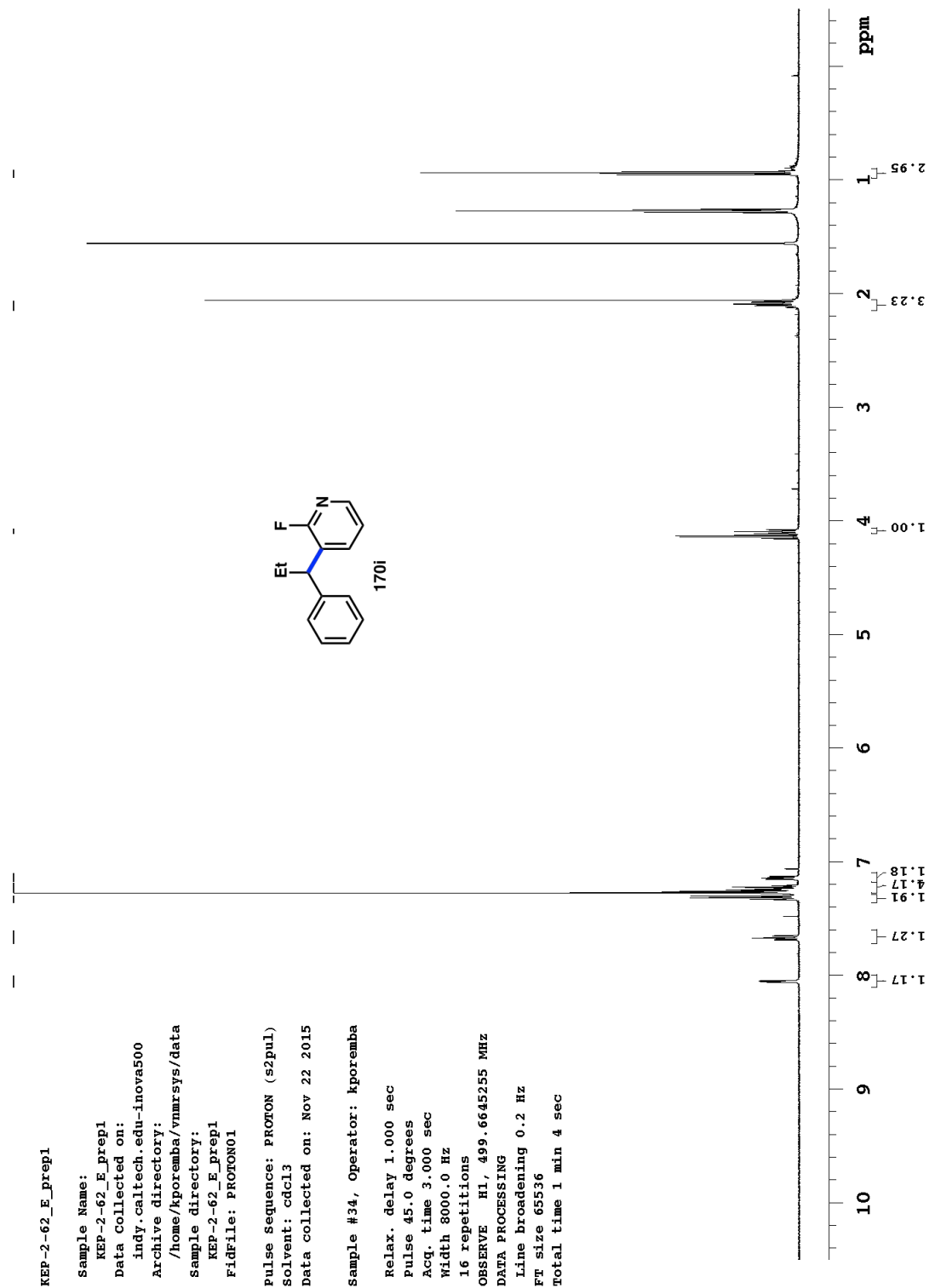
Pulse Sequence: FLUORINE (s2pul)  
Solvent: cdcl3  
Data collected on: May 3 2016

Sample #9, Operator: kporemba  
Relax. delay 1.000 sec  
Pulse 30.0 degrees  
Acq. time 0.986 sec  
Width 64935.1 Hz  
16 repetitions  
OBSERVE F19, 282.3668752 MHZ  
DATA PROCESSING  
FT size 131072  
Total time 0 min 36 sec







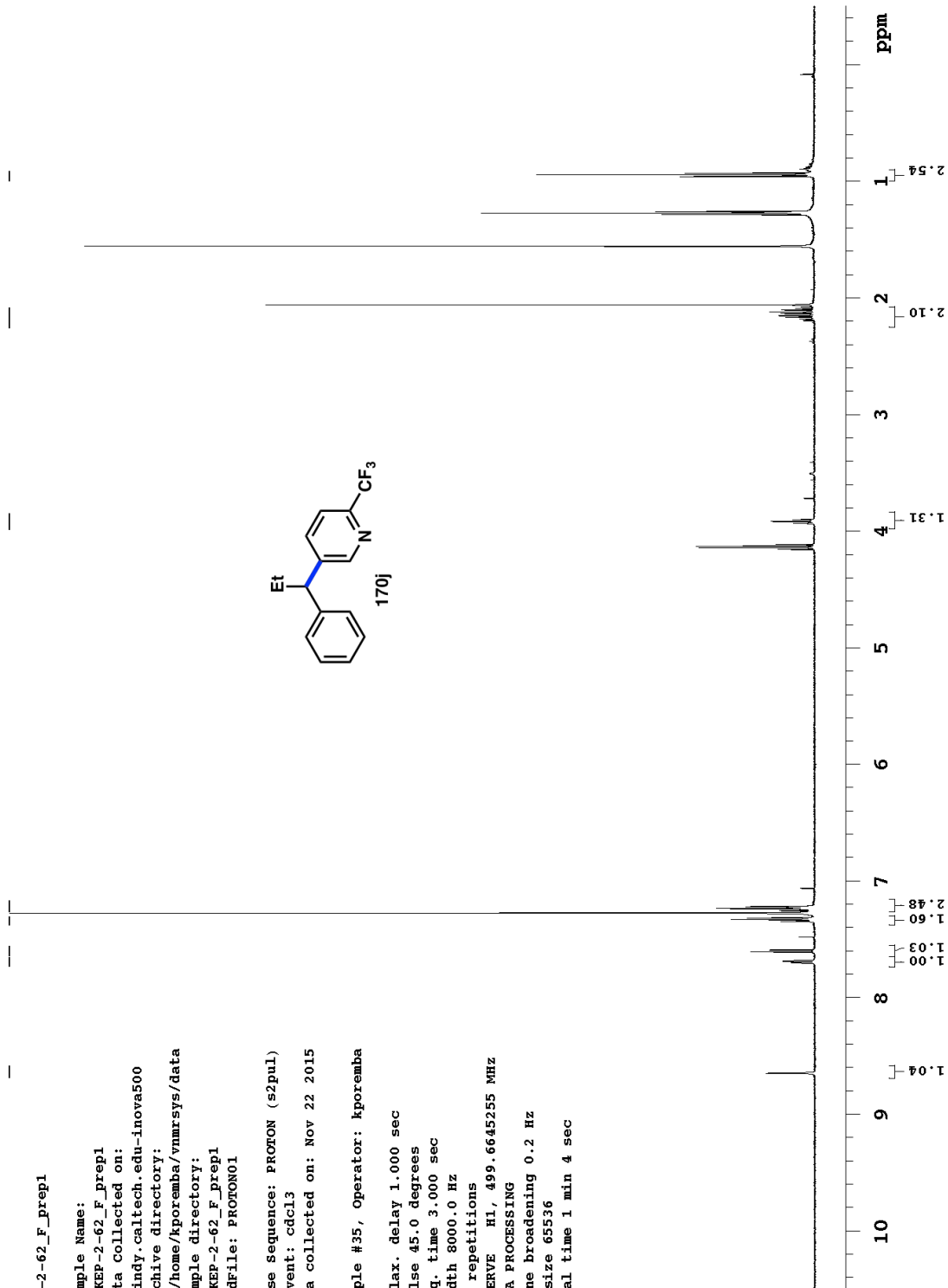
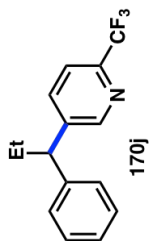


KEP-2-62\_F\_prep1

Sample Name:  
 KEP-2-62\_F\_prep1  
 Data collected on:  
 indy.caltech.edu-inova500  
 Archive directory:  
 /home/kporemba/vnmrsys/data  
 sample directory:  
 KEP-2-62\_F\_prep1  
 File: PROTON01

Pulse sequence: PROTON (s2pul)  
 Solvent: cdcl3  
 Data collected on: Nov 22 2015

Sample #35, Operator: kporemba  
 Relax. delay 1.000 sec  
 Pulse 45.0 degrees  
 Acq. time 3.000 sec  
 Width 8000.0 Hz  
 16 repetitions  
 OBSERVE H1, 499.6645255 MHZ  
 DATA PROCESSING  
 Line broadening 0.2 Hz  
 FT size 65536  
 Total time 1 min 4 sec



KEP-2-78\_B\_prep3

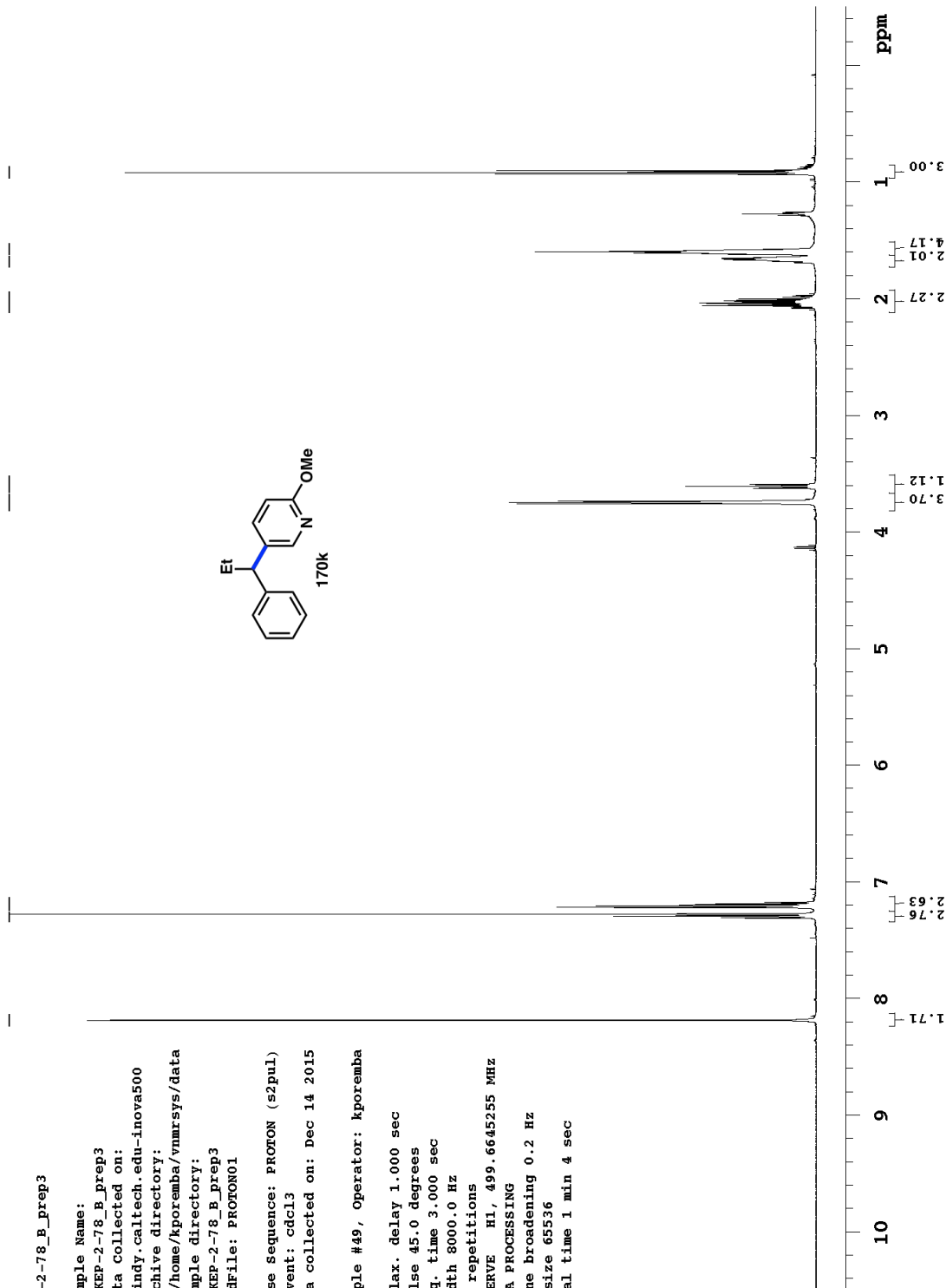
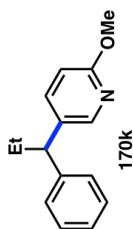
Sample Name:

KEP-2-78\_B\_prep3  
 Data Collected on:  
 indy.caltech.edu-inova500  
 Archive directory:  
 /home/kporemba/vnmrsys/data  
 Sample directory:  
 KEP-2-78\_B\_prep3  
 FidFile: PROTON01

Pulse Sequence: PROTON (s2pul)  
 Solvent: cdcl3  
 Data collected on: Dec 14 2015

Sample #49, Operator: kporemba

Relax. delay 1.000 sec  
 Pulse 45.0 degrees  
 Acq. time 3.000 sec  
 Width 8000.0 Hz  
 16 repetitions  
 OBSERVE H1, 499.6645255 MHZ  
 DATA PROCESSING  
 Line broadening 0.2 Hz  
 FT size 65536  
 Total time 1 min 4 sec



KEP-2-78\_D\_prep2

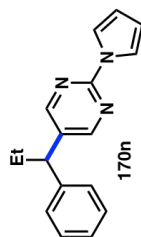
Sample Name:  
 KEP-2-78\_D\_prep2  
 Data Collected on:  
 indy.caltech.edu-inova500  
 Archive directory:  
 /home/kporemba/vnmrsys/data  
 Sample directory:  
 KEP-2-78\_D\_prep2  
 FIDFile: PROTON01

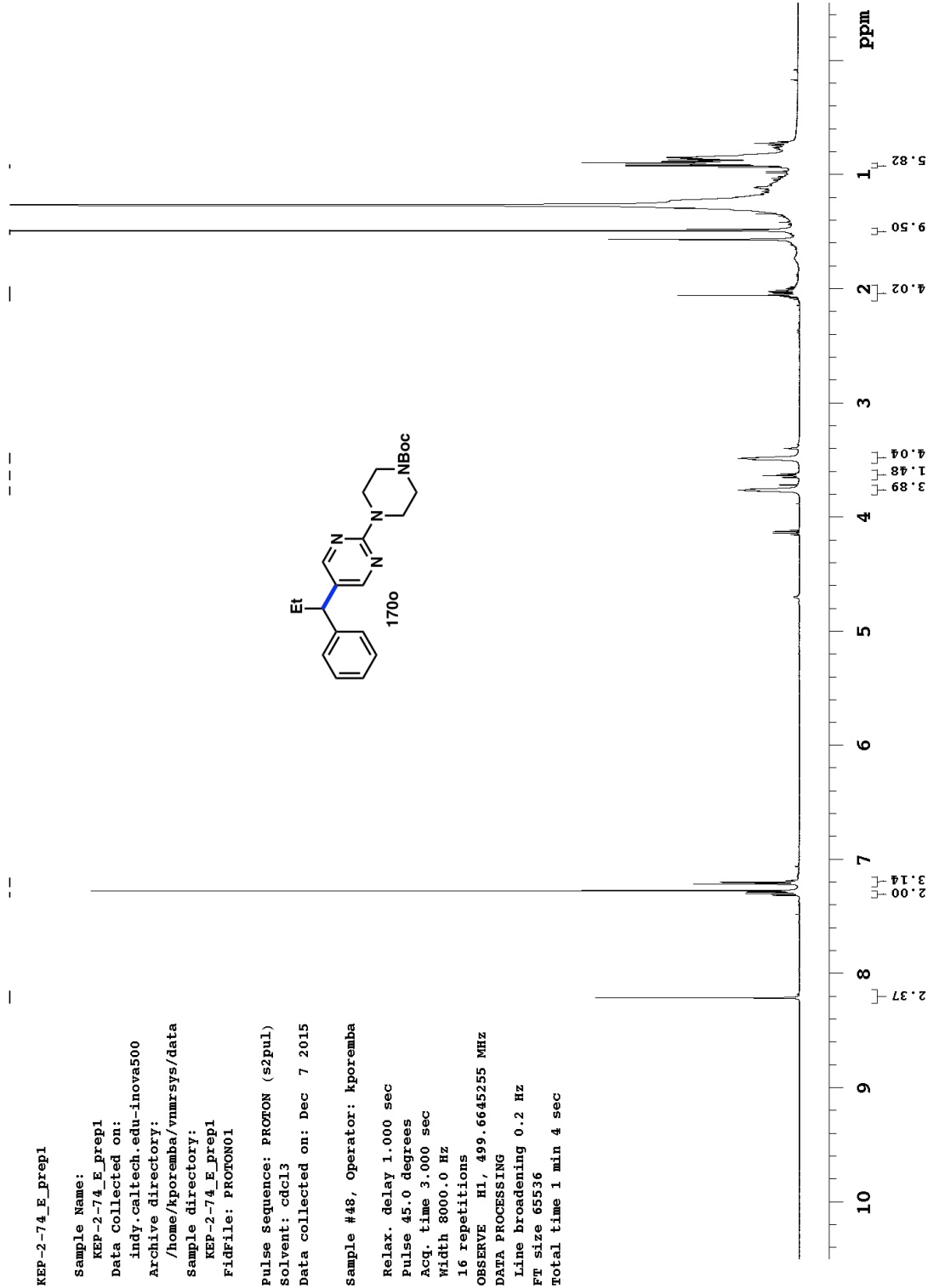
Pulse Sequence: PROTON (s2pul)  
 Solvent: cdcl3  
 Data collected on: Dec 14 2015

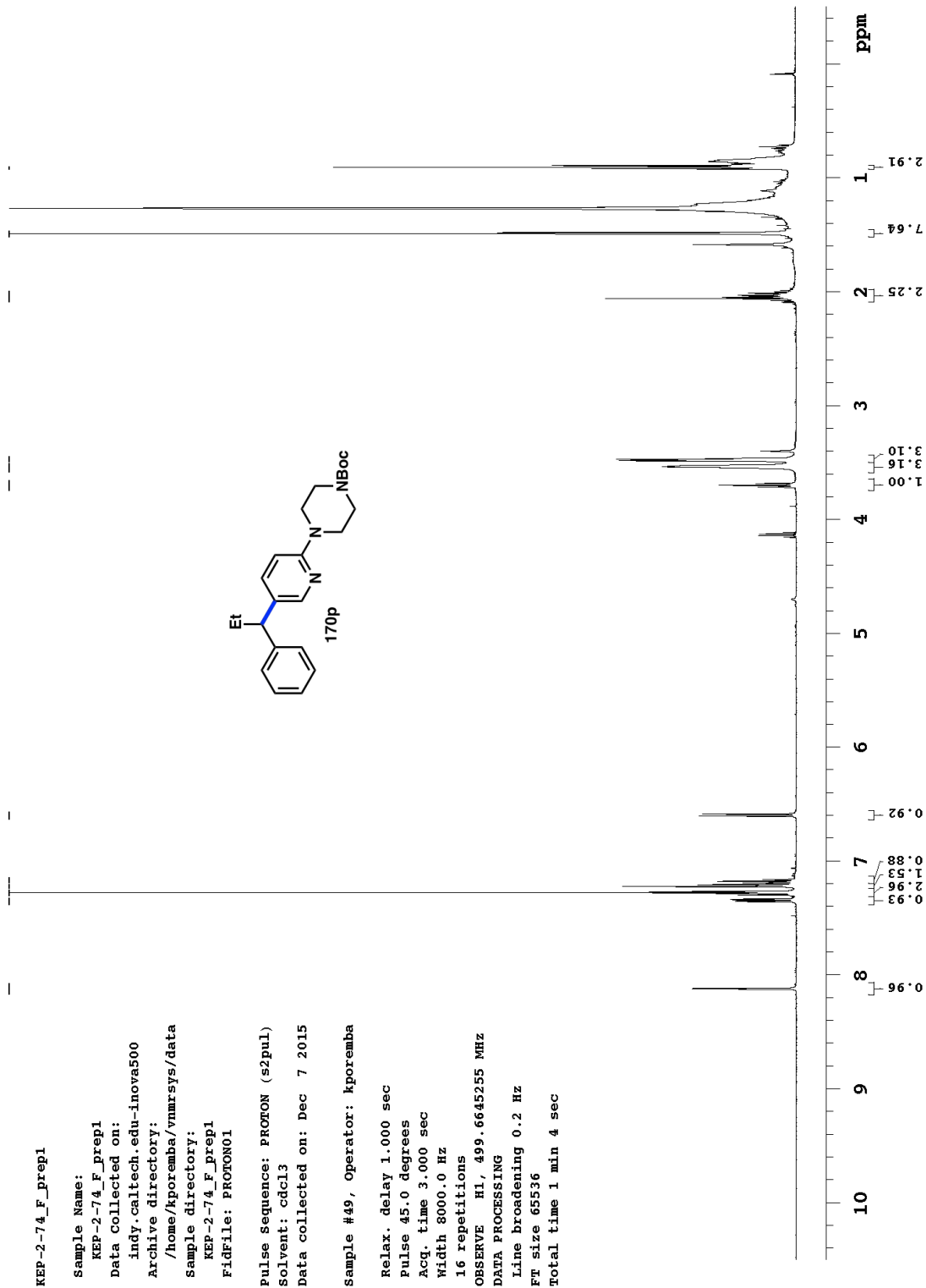
Sample #1, Operator: kporemba

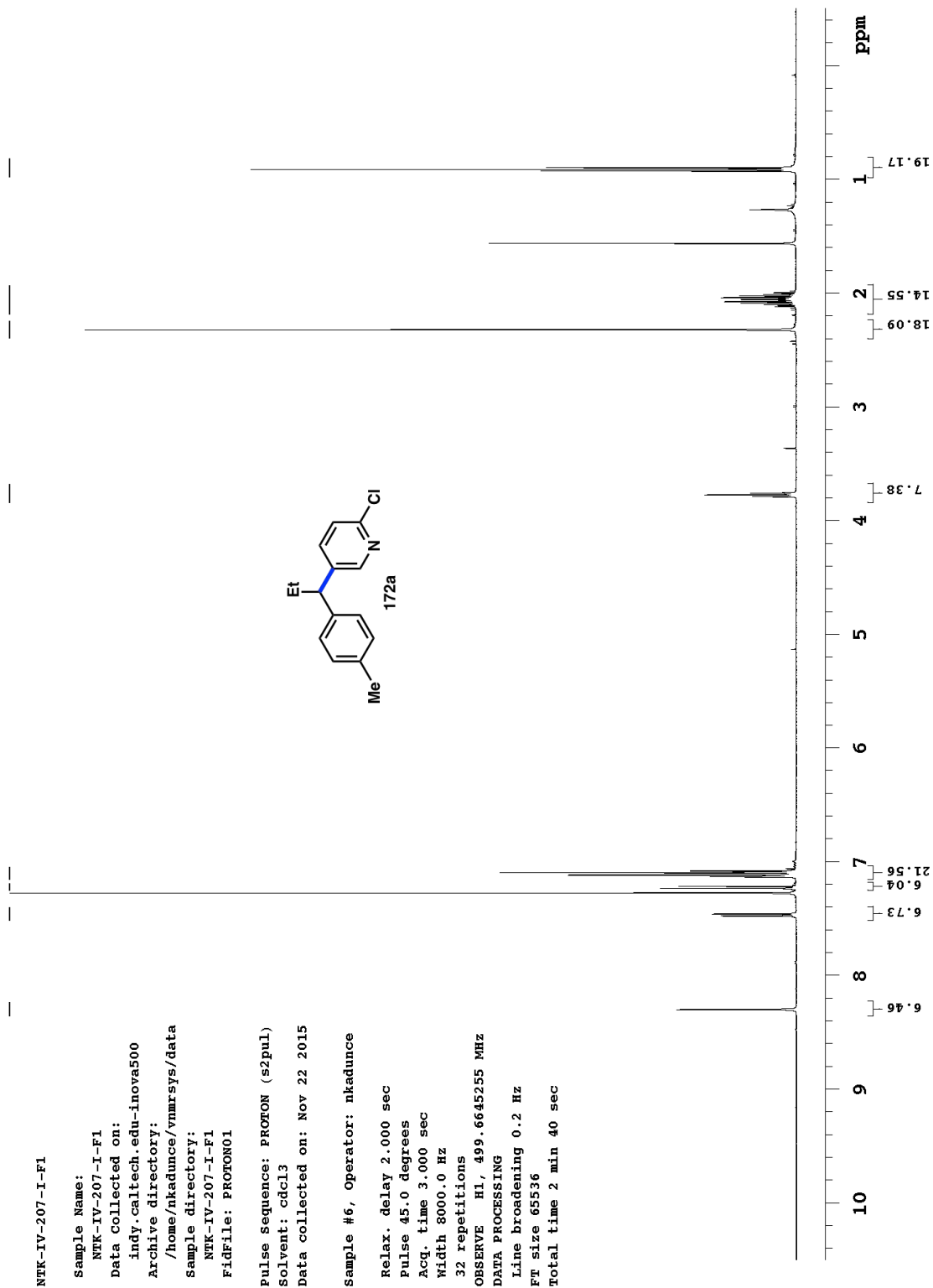
Relax. delay 1.000 sec  
 Pulse 45.0 degrees  
 Acq. time 3.000 sec  
 Width 8000.0 Hz  
 16 repetitions

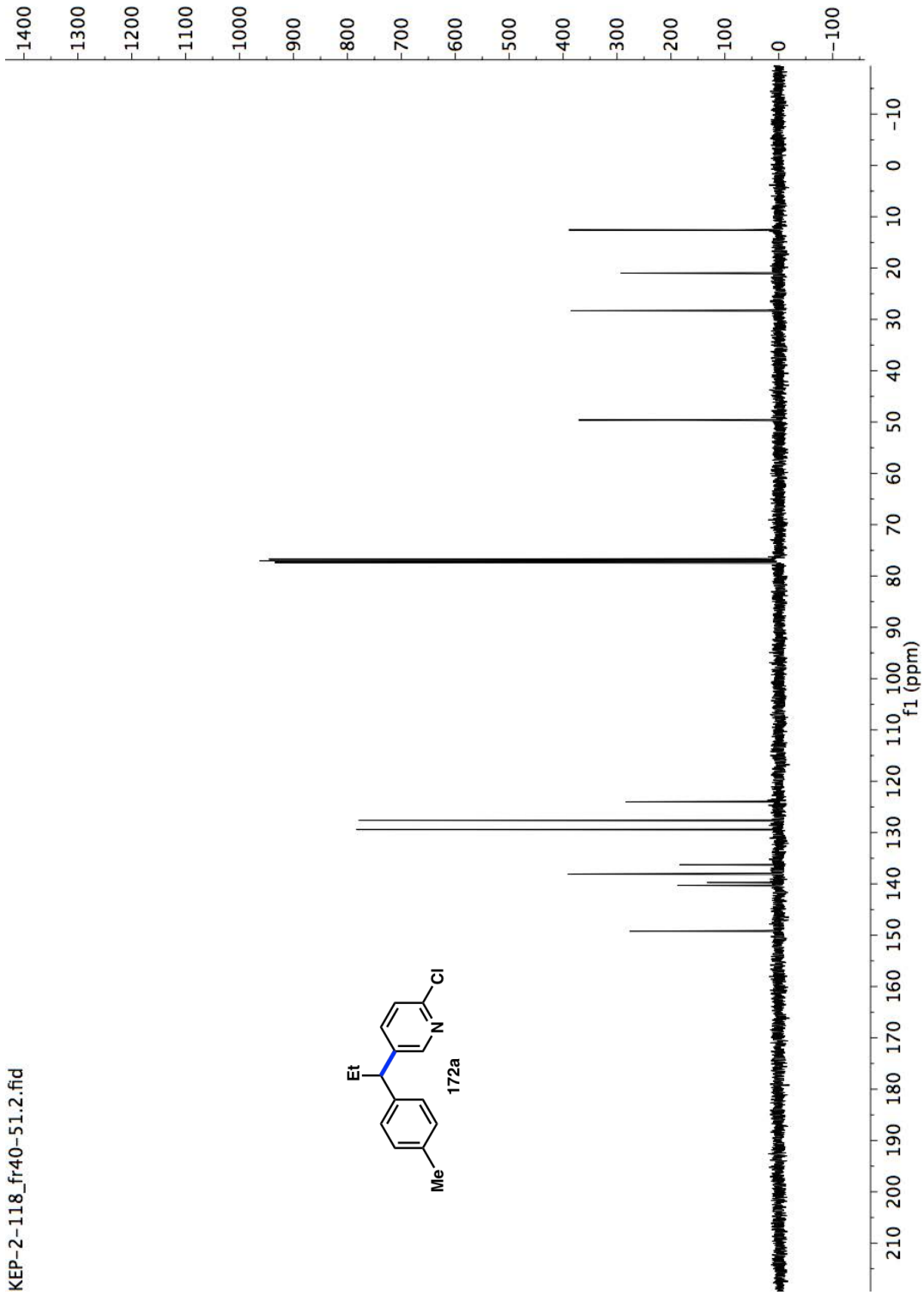
OBSERVE H1, 499.6645255 MHZ  
 DATA PROCESSING  
 Line broadening 0.2 Hz  
 FT size 65536  
 Total time 1 min 4 sec











NTK-IV-207-II-F1

Sample Name:

NTK-IV-207-II-F1

Data Collected on:

indy.caltech.edu-inova500

Archive directory:

/home/nkadunce/vnmrSYS/data

Sample directory:

NTK-IV-207-II-F1

FidFile: PROTON01

Pulse Sequence: PROTON (s2pul)

Solvent: cdcl3

Data collected on: Nov 22 2015

Sample #7, Operator: nkadunce

Relax. delay 2.000 sec

Pulse 45.0 degrees

Acq. time 3.000 sec

Width 8000.0 Hz

32 repetitions

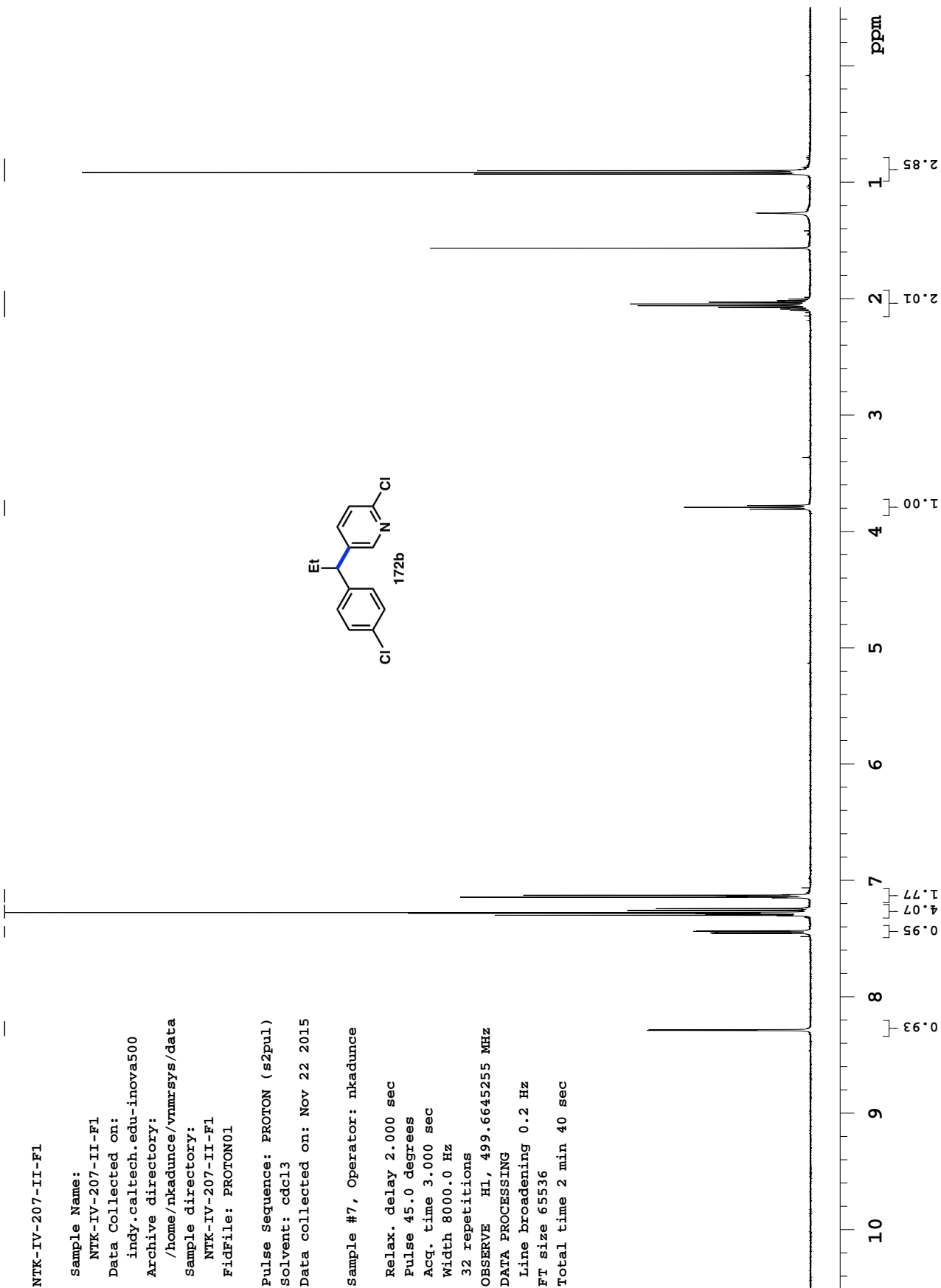
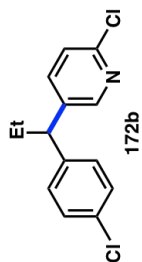
OBSERVE H1, 499.6645255 MHz

DATA PROCESSING

Line broadening 0.2 Hz

FT size 65536

Total time 2 min 40 sec



NTK-IV-207-II-F1

Sample Name:

NTK-IV-207-II-F1

Data Collected on:

indy.caltech.edu-inova500

Archive directory:

/home/nkadunce/vnmrsys/data

sample directory:

NTK-IV-207-II-F1

FIGfile: CARBON01

Pulse sequence: CARBON (s2pul)

Solvent: cdcl3

Data collected on: Nov 22 2015

Sample #17, Operator: nkadunce

Relax. delay 1.000 sec

Pulse 45.0 degrees

Acq. time 1.042 sec

Width 31446.5 Hz

512 repetitions

OBSERVE C13, 125.6407449 MHZ

DECOUPLE H1, 499.6670239 MHZ

Power 36 dB

continuously on

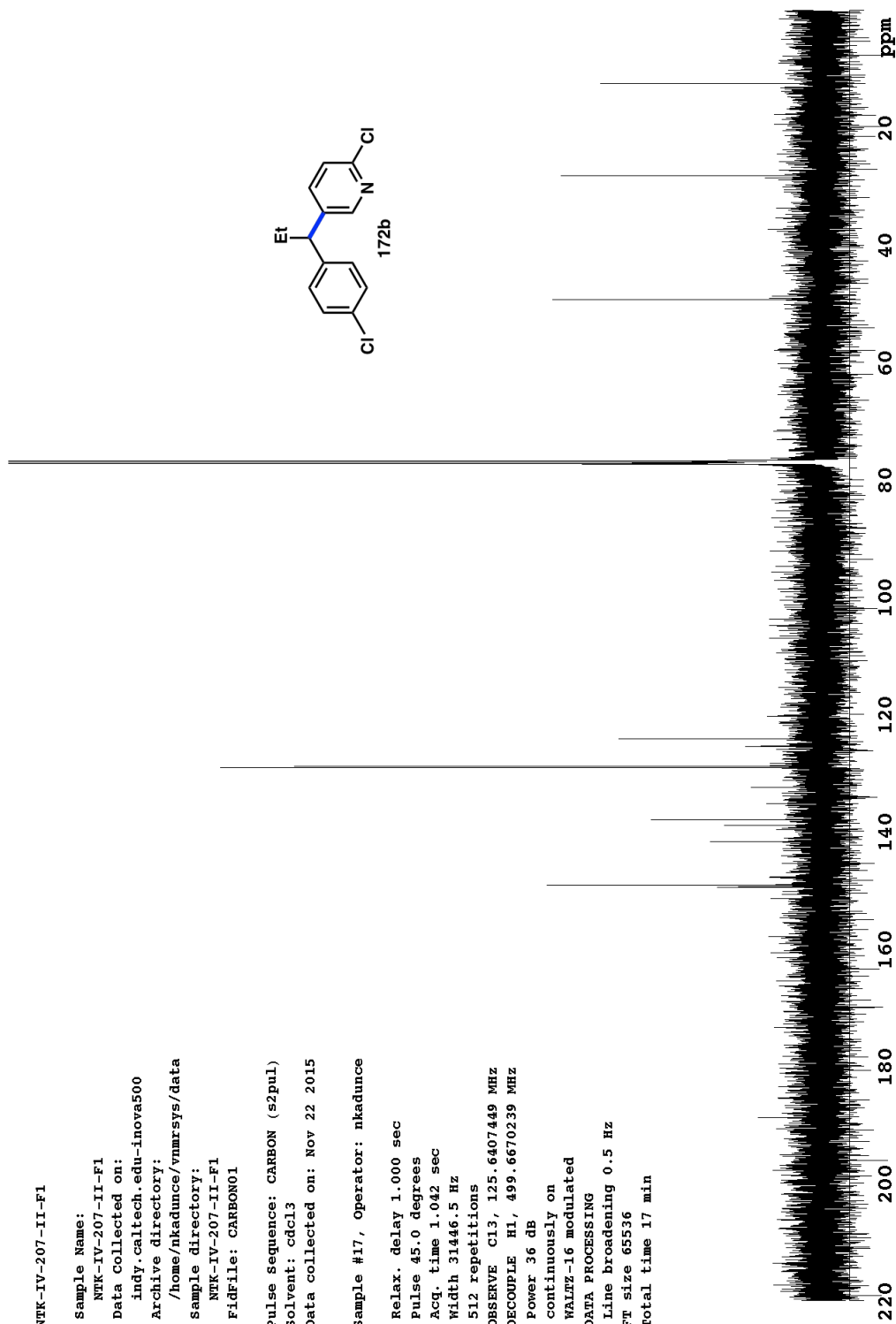
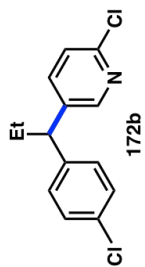
WALTZ-16 modulated

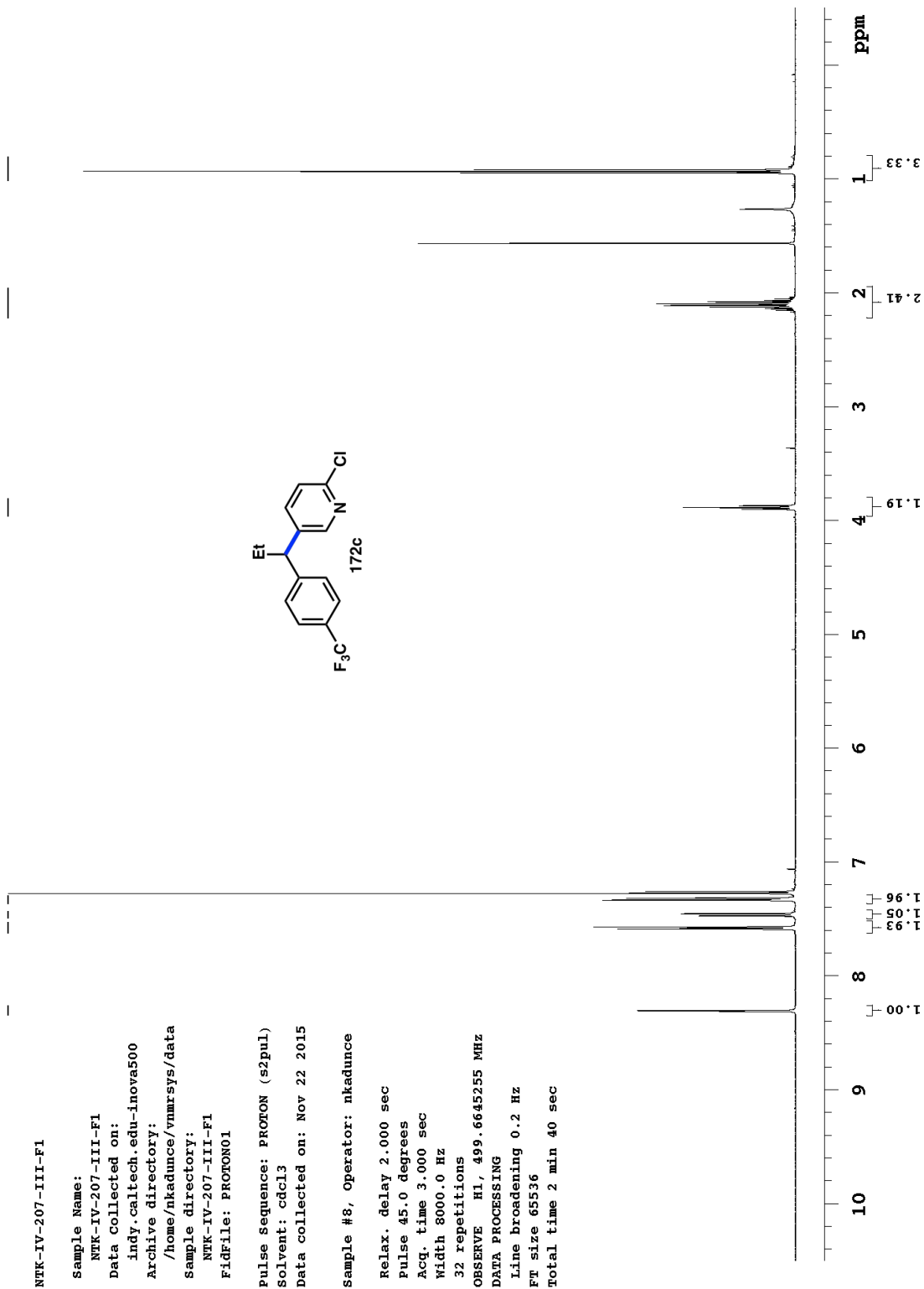
DATA PROCESSING

Line broadening 0.5 Hz

FT size 65536

Total time 17 min





NTK-IV-207-III-F1

Sample Name:

NTK-IV-207-III-F1

Data Collected on:

indy.caltech.edu-inova500

Archive directory:

/home/nkadance/vnmrSYS/data

Sample directory:

NTK-IV-207-III-F1

File: CARBON02

Pulse sequence: CARBON (s2pul)

Solvent: cdcl3

Data collected on: Nov 22 2015

Sample #27, Operator: nkadance

Relax. delay 1.000 sec

Pulse 45.0 degrees

Acq. time 1.042 sec

Width 31446.5 Hz

1000 repetitions

OBSERVE C13, 125.6407449 MHz

DECOUPLE H1, 499.6670239 MHz

power 36 dB

continuously on

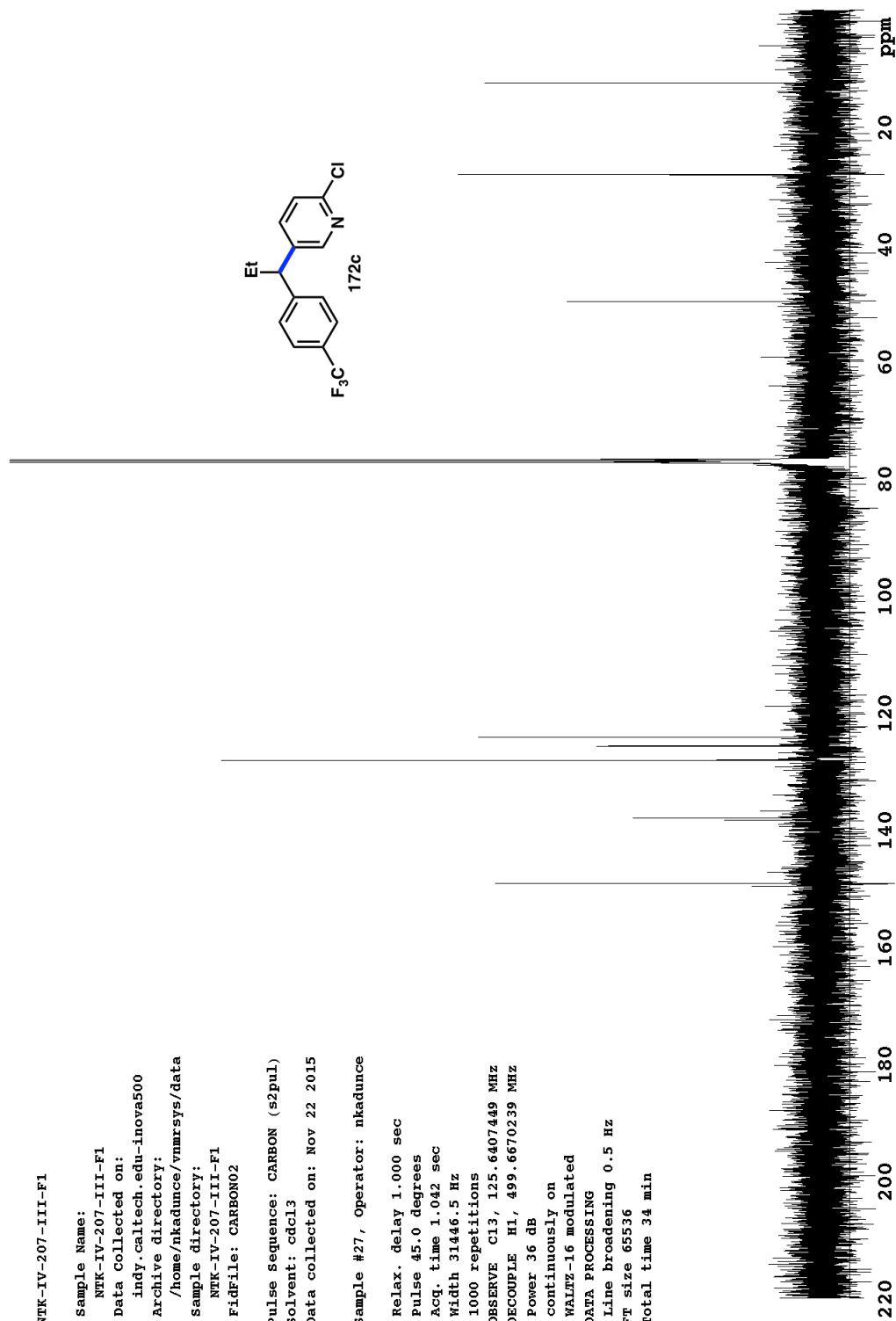
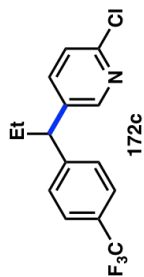
WALTZ-16 modulated

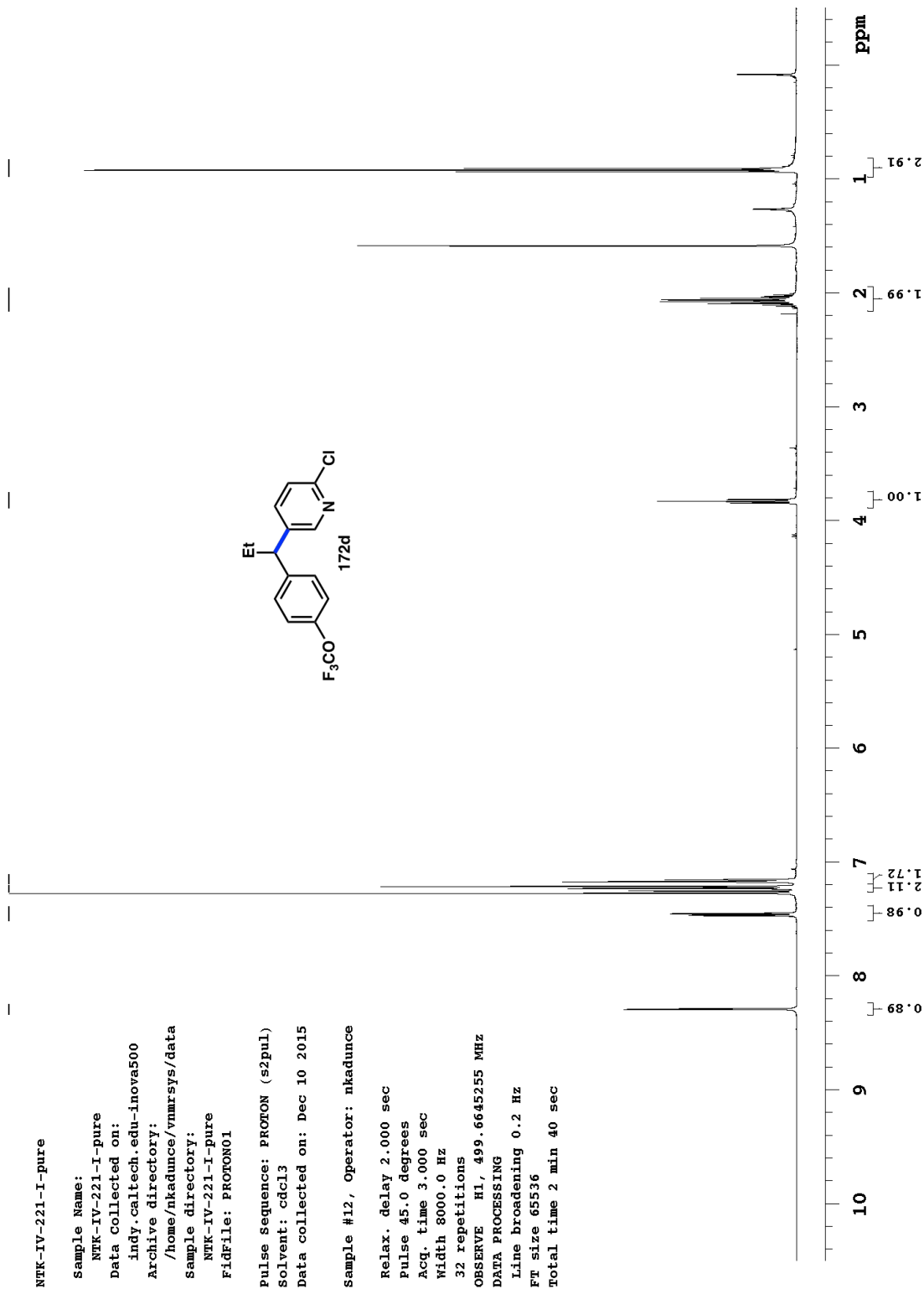
DATA PROCESSING

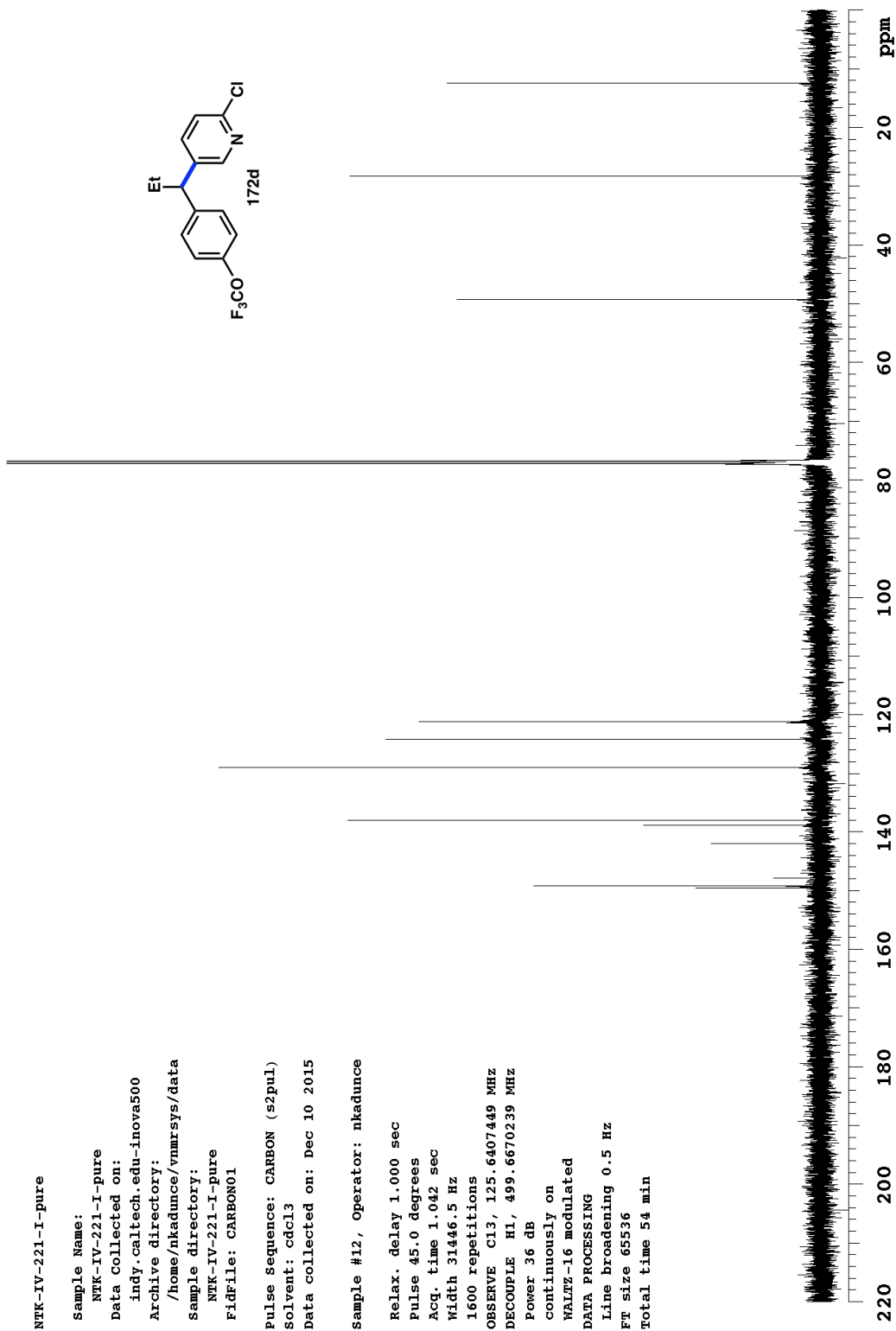
Line broadening 0.5 Hz

FT size 65536

Total time 34 min







NFK-IV-212-II-pure

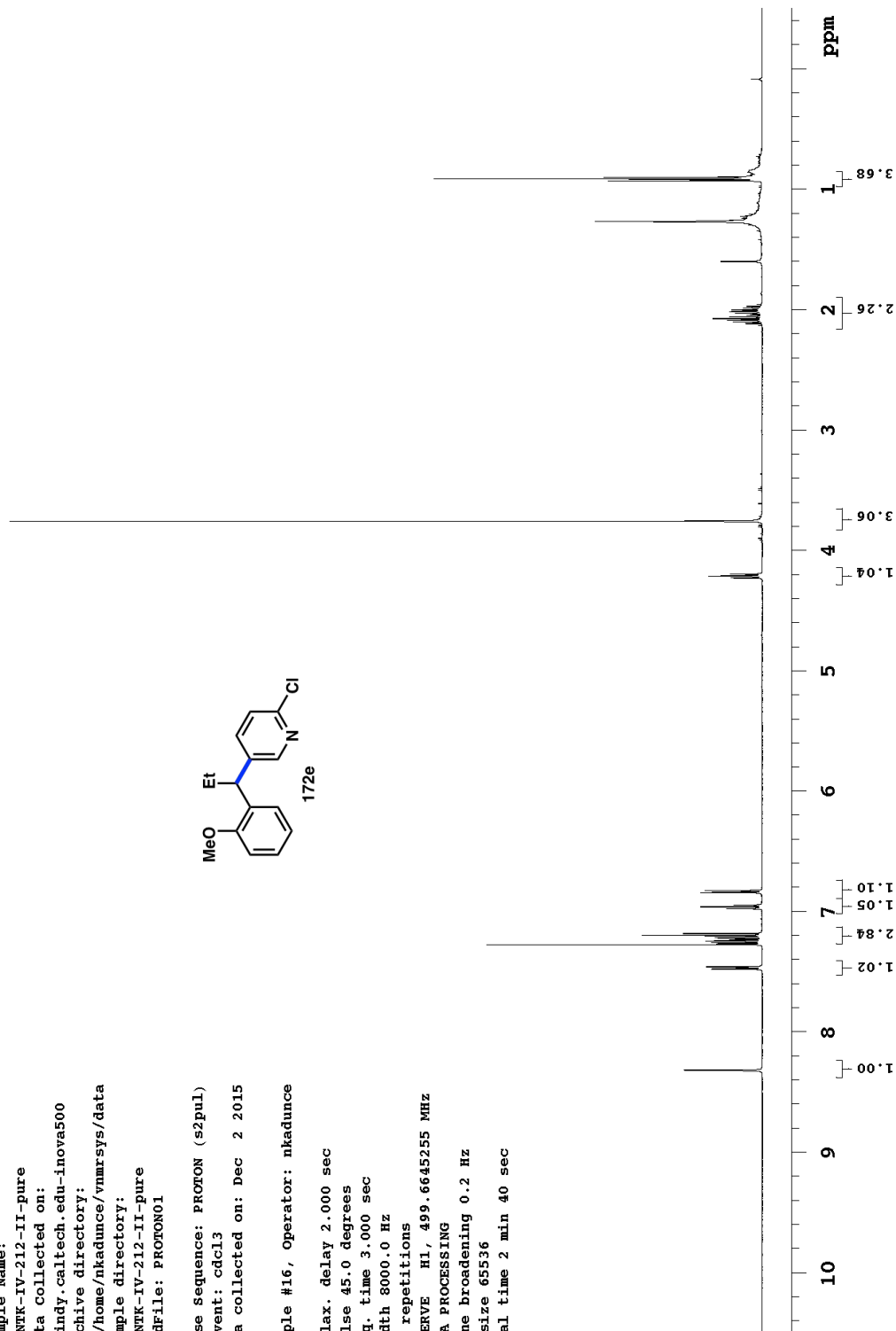
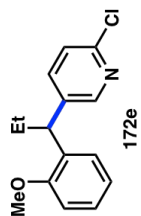
Sample Name:

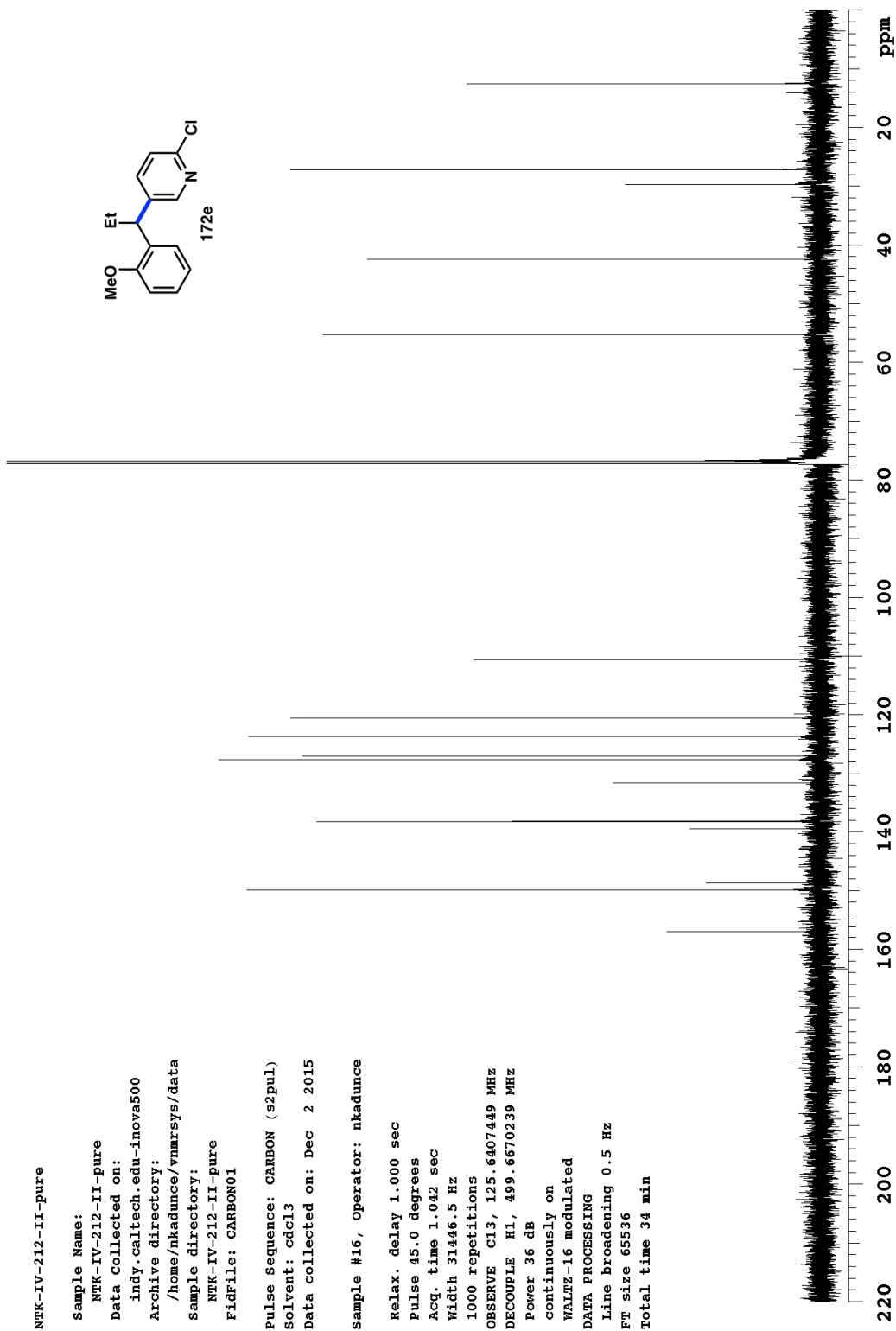
NFK-IV-212-II-pure  
 Data Collected on:  
 indy.caltech.edu-inova500  
 Archive directory:  
 /home/nkadance/vnmrsys/data  
 Sample directory:  
 NFK-IV-212-II-pure  
 Fidfile: PROTON01

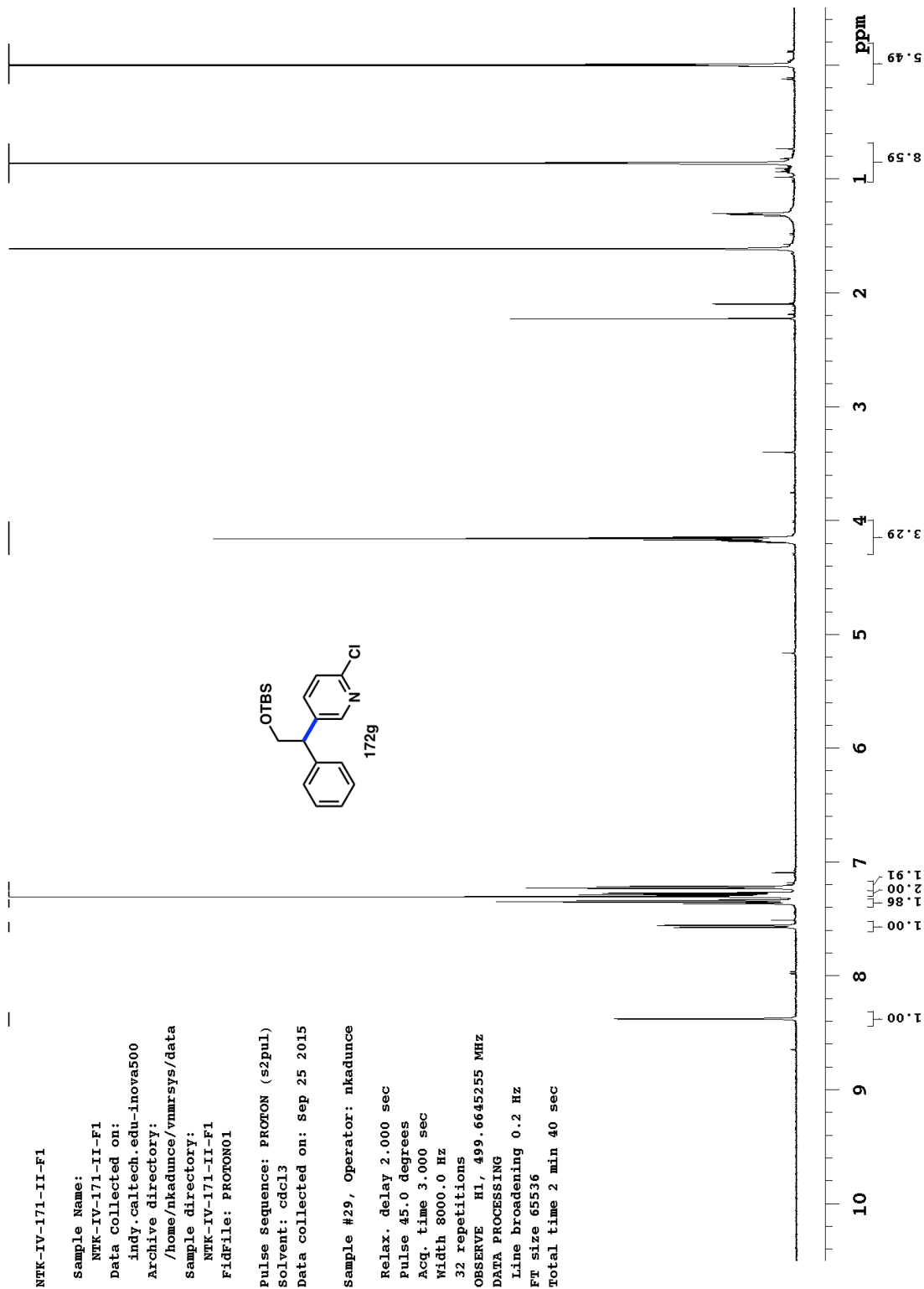
Pulse sequence: PROTON (s2pul)  
 Solvent: cdcl3  
 Data collected on: Dec 2 2015

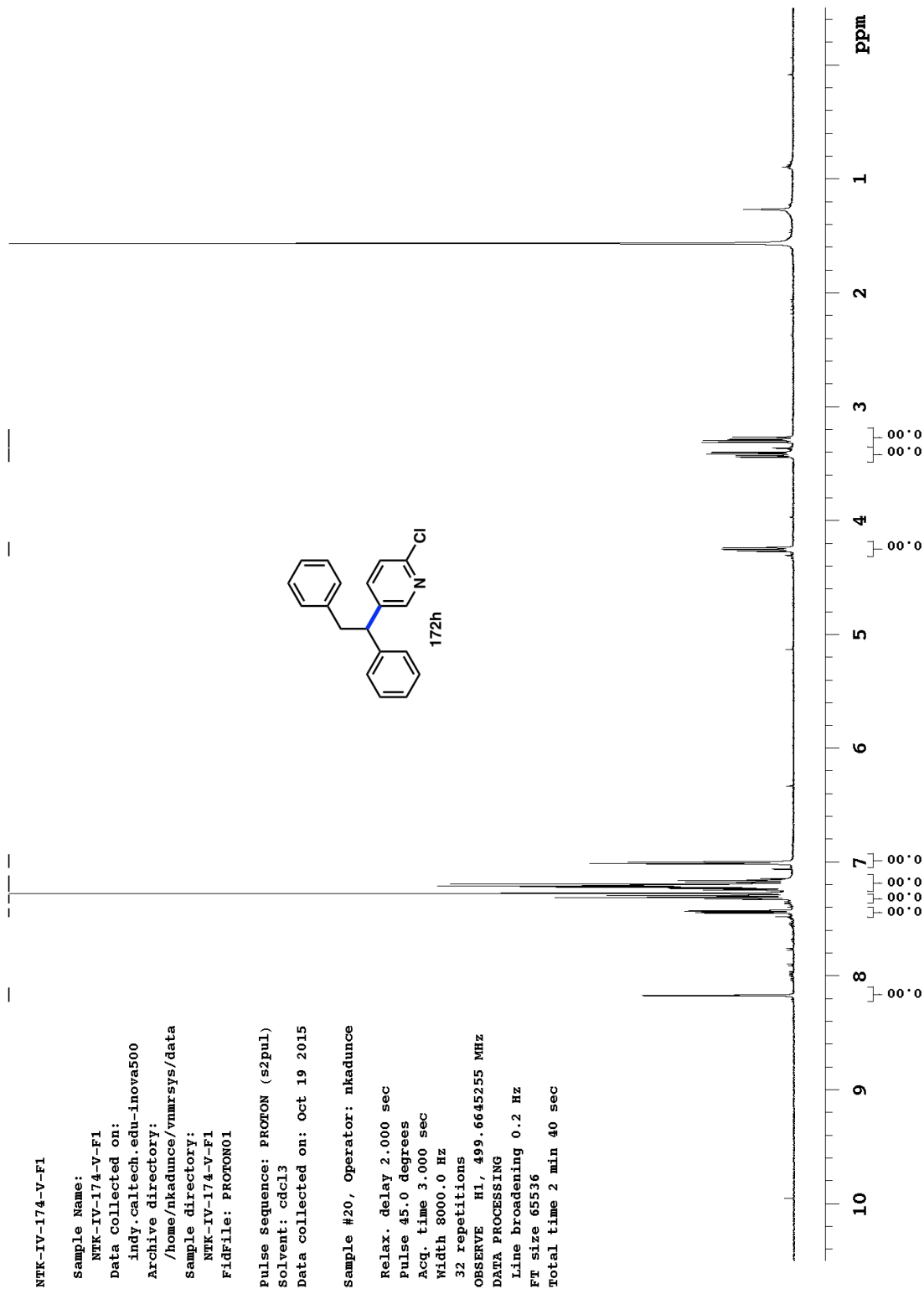
Sample #16, Operator: nkadance

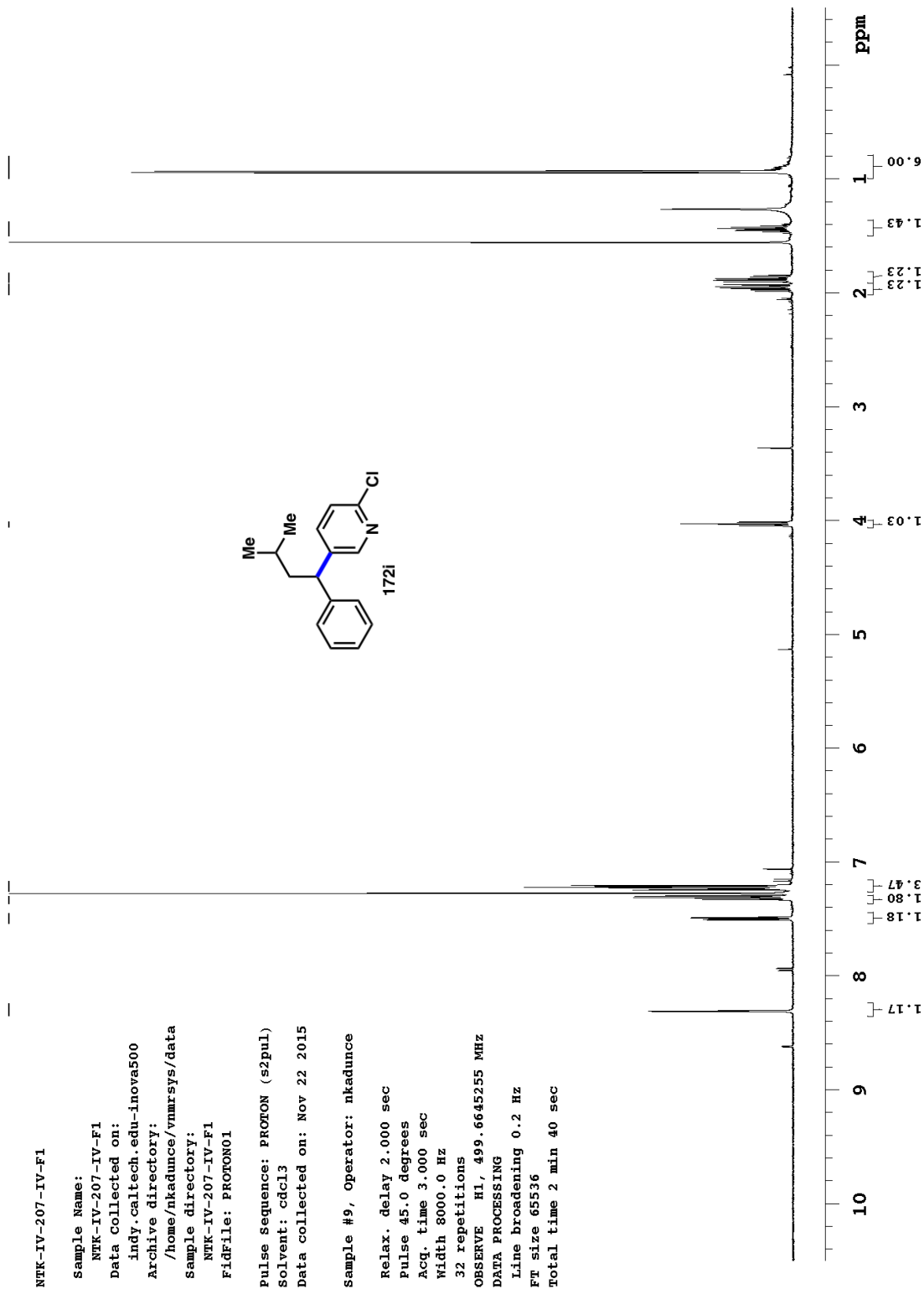
Relax. delay 2.000 sec  
 Pulse 45.0 degrees  
 Acq. time 3.000 sec  
 Width 8000.0 Hz  
 32 repetitions  
 OBSERVE H1, 499.6645255 MHz  
 DATA PROCESSING  
 Line broadening 0.2 Hz  
 FT size 65536  
 Total time 2 min 40 sec

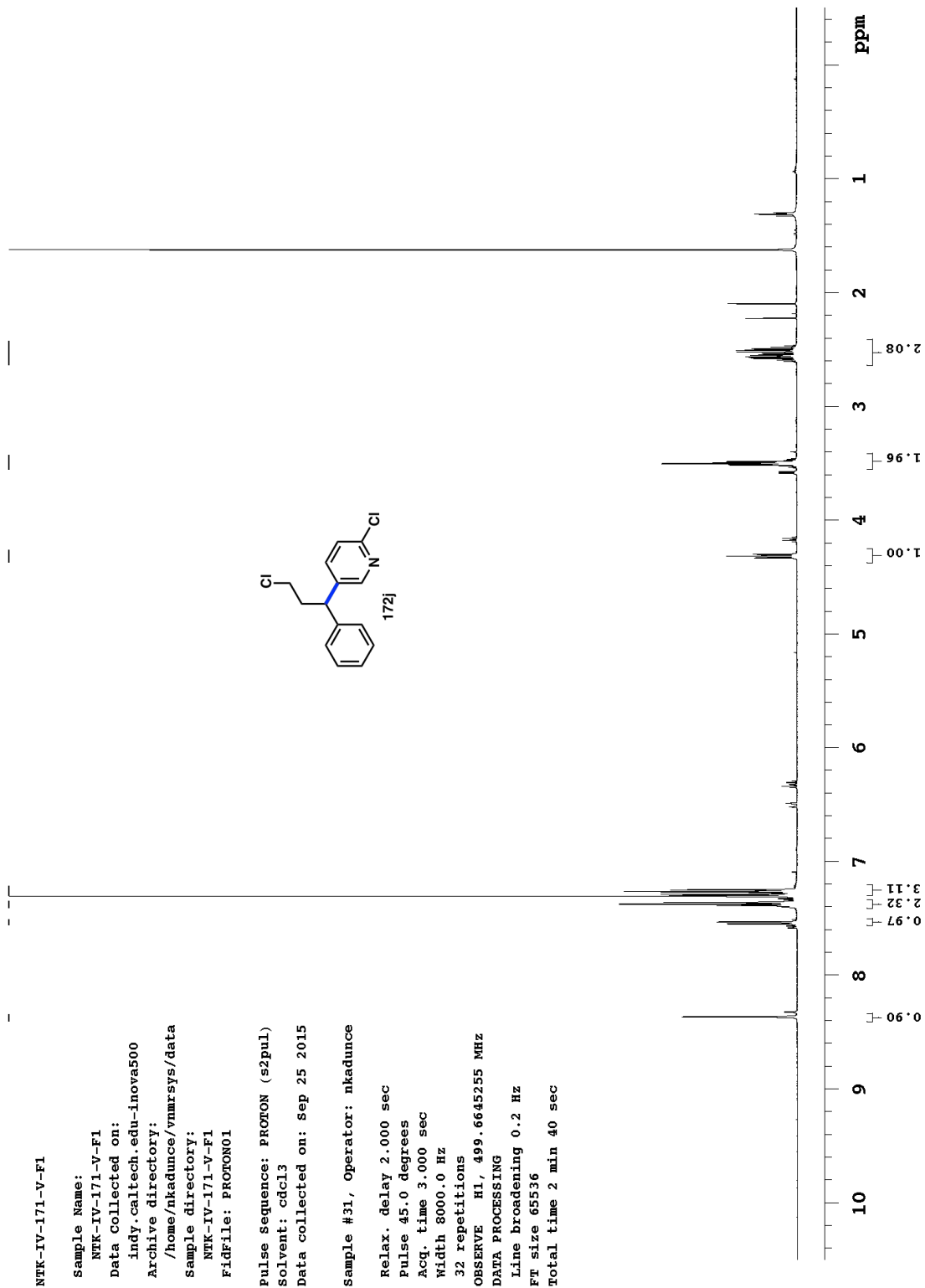


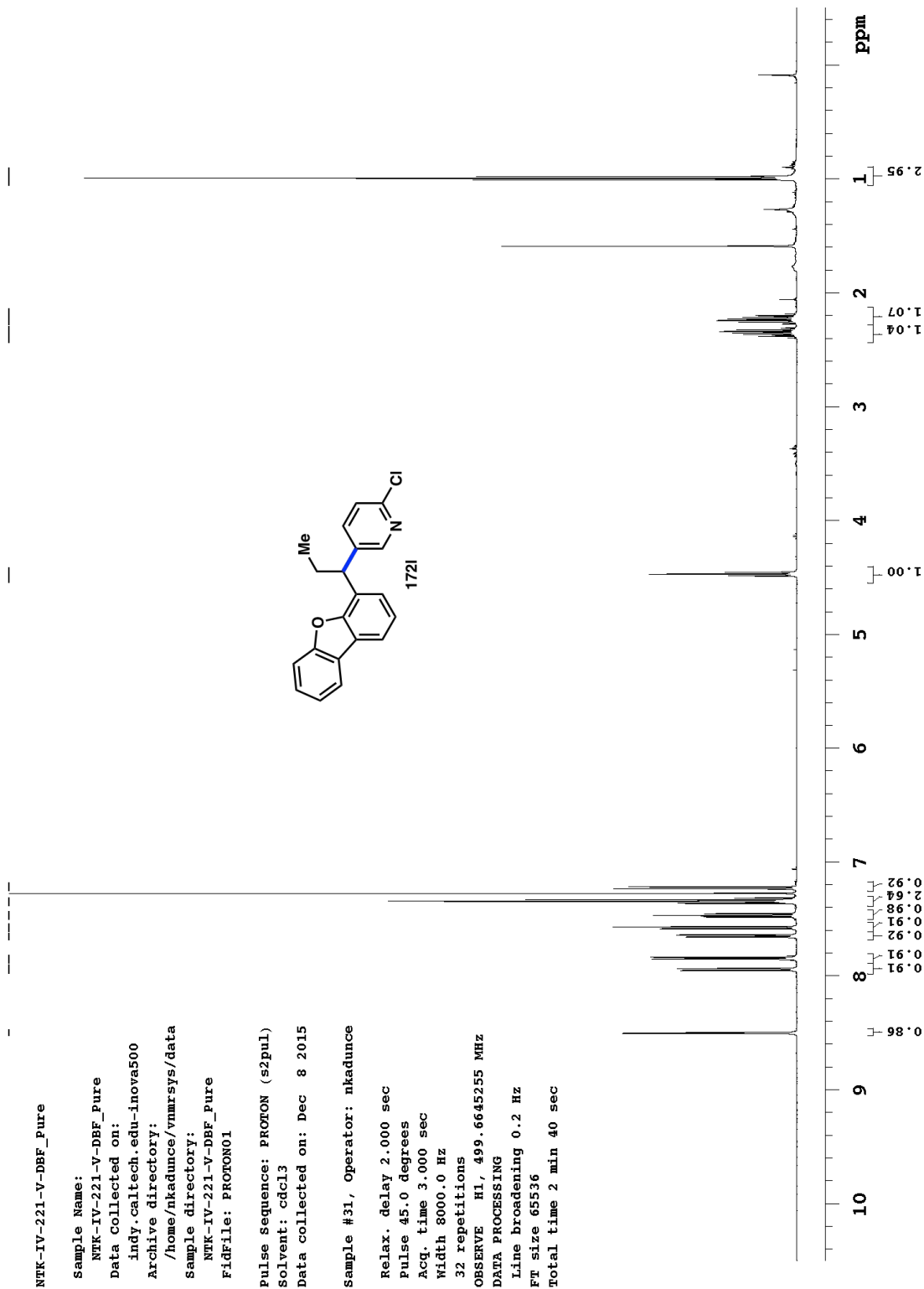


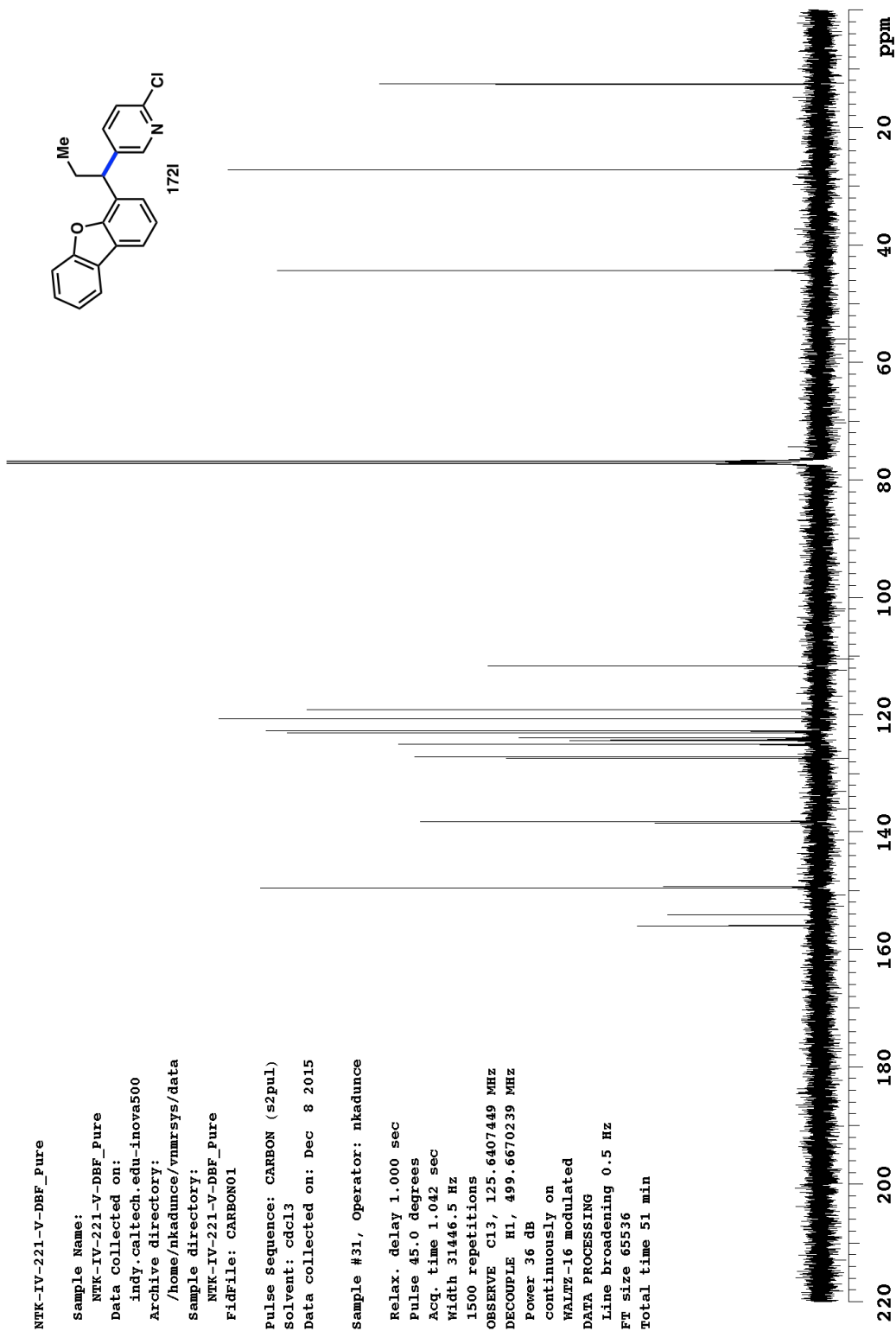










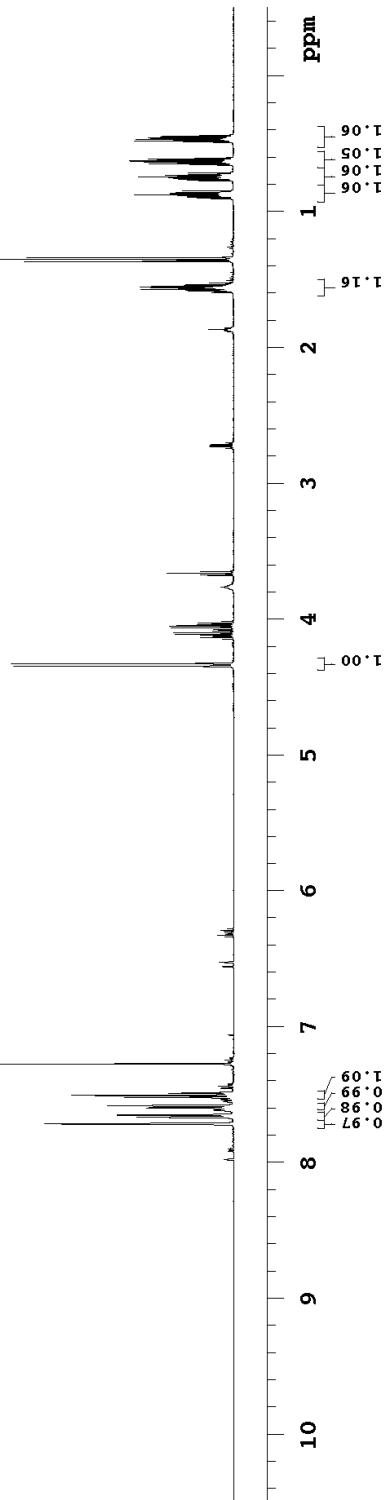
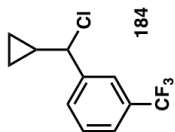


NFK-IV-251-Cl\_crude

Sample Name:  
 NFK-IV-251-Cl\_crude  
 Data Collected on:  
 indy.caltech.edu-inova500  
 Archive directory:  
 /home/nkadance/vnmrsys/data  
 Sample directory:  
 NFK-IV-251-Cl\_crude  
 FidFile: PROTON01

Pulse sequence: PROTON (s2pul)  
 Solvent: cdcl3  
 Data collected on: Feb 3 2016

Sample #10, Operator: nkadance  
 Relax. delay 5.000 sec  
 Pulse 45.0 degrees  
 Acq. time 3.000 sec  
 Width 8000.0 Hz  
 8 repetitions  
 OBSERVE H1, 499.6645255 MHz  
 DATA PROCESSING  
 Line broadening 0.2 Hz  
 FT size 65536  
 Total time 1 min 4 sec

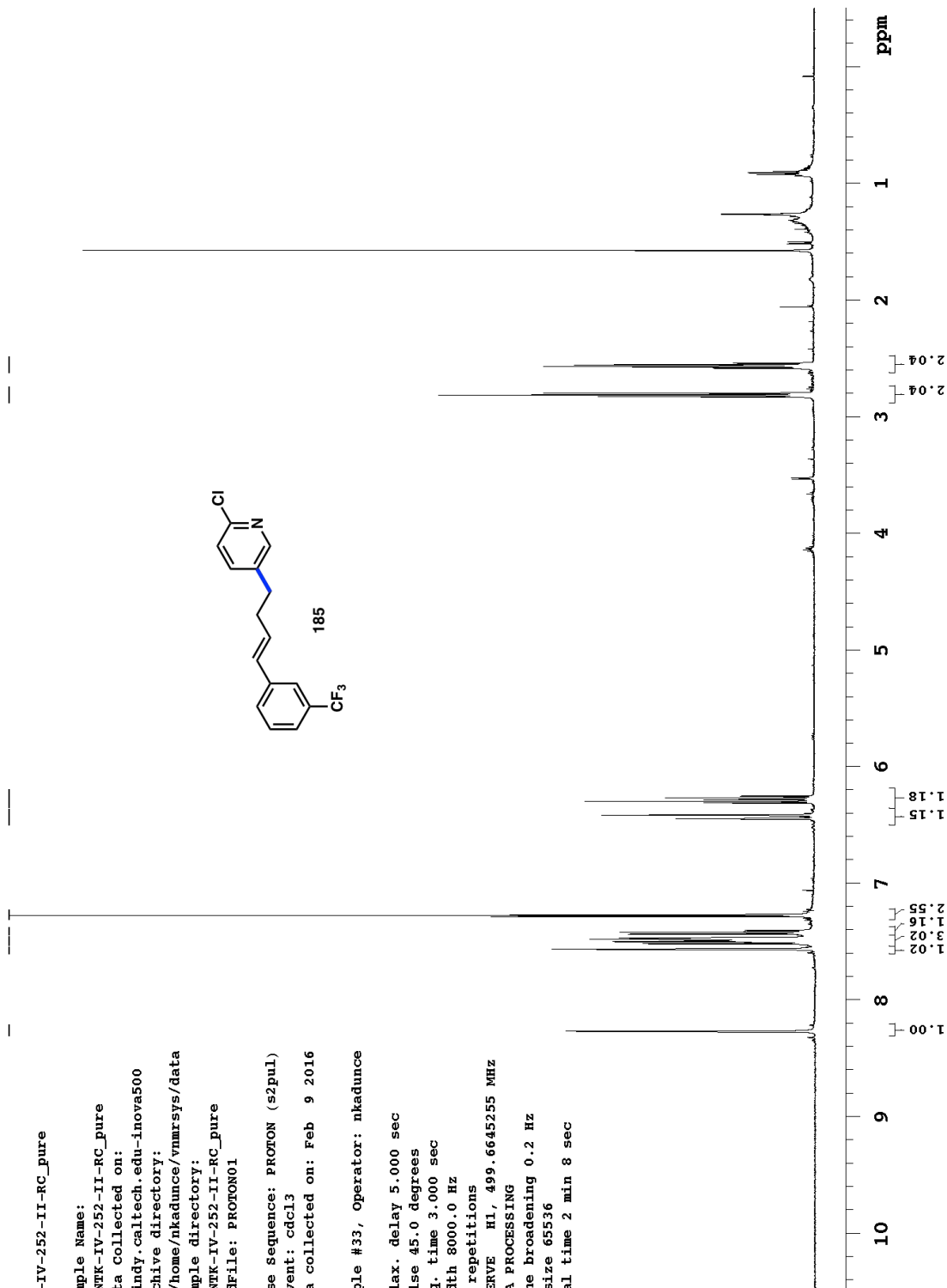
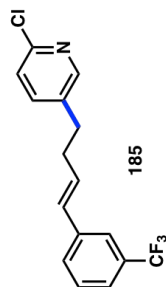


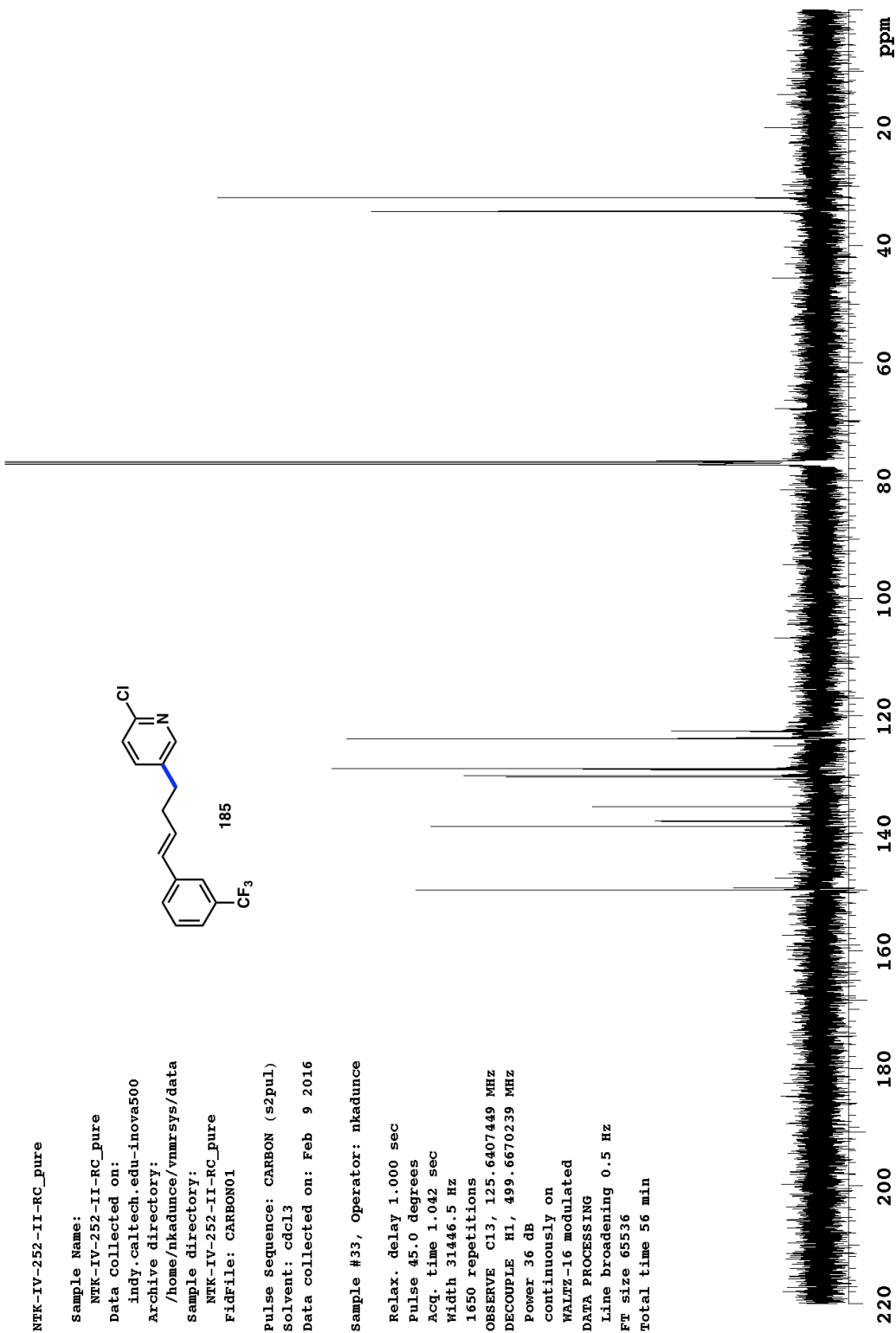
NFK-IV-252-II-RC\_pure

Sample Name:  
 NFK-IV-252-II-RC\_pure  
 Data Collected on:  
 indy.caltech.edu-inova500  
 Archive directory:  
 /home/nkadance/vnmrsys/data  
 Sample directory:  
 NFK-IV-252-II-RC\_pure  
 FidFile: PROTON01

Pulse sequence: PROTON (s2pul)  
 Solvent: cdcl3  
 Data collected on: Feb 9 2016

Sample #33, Operator: nkadance  
 Relax. delay 5.000 sec  
 Pulse 45.0 degrees  
 Acq. time 3.000 sec  
 Width 8000.0 Hz  
 16 repetitions  
 OBSERVE H1, 499.6645255 MHz  
 DATA PROCESSING  
 Line broadening 0.2 Hz  
 FT size 65536  
 Total time 2 min 8 sec



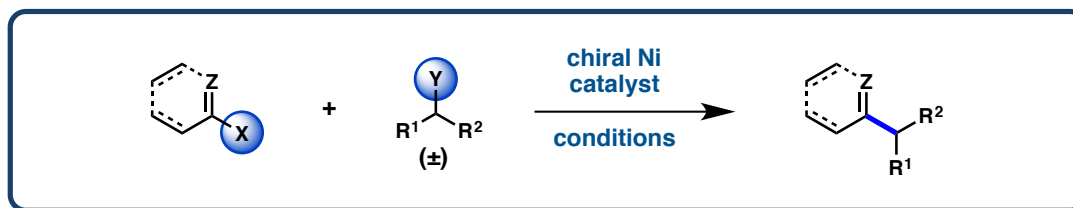


## **Chapter 5**

### *Preliminary Results Toward Novel Ni-Catalyzed Asymmetric Reductive Cross-Couplings*

#### **5.1 INTRODUCTION**

As discussed in the previous chapters, the development of Ni-catalyzed asymmetric reductive cross-coupling has been a primary focus of research in our group for several years. This work has led to the successful development and publication of several such methods and opened the door to a new avenue of asymmetric catalysis. However, the pace of reaction development has suffered from significant difficulty in optimizing these transformations. Each new coupling requires a fresh assessment of reaction conditions and catalyst parameters, especially ligand structure. While some amount of this empirical evaluation is inevitable, a more general and reliable starting point for optimization would be advantageous, hastening the key later aspects of ligand design.

**Table 5.1.** Cross-coupling substrates versus optimal conditions.

Products Conditions	 109	 166	 122j	 167
<b>NiCl<sub>2</sub>(dme), L32</b> <b>Mn<sup>0</sup>, DMBA, 3Å MS</b> <b>DMA/THF, rt</b>	<b>Control</b> <b>79% yield, 93% ee</b>	41% yield, 2% ee	22% yield, 24% ee	0% yield
<b>NiCl<sub>2</sub>(dme), L109</b> <b>Mn<sup>0</sup>, NaI</b> <b>DMA, 0 °C</b>	0% yield	<b>Control</b> <b>91% yield, 93% ee</b>	0% yield	0% yield
<b>NiCl<sub>2</sub>(dme), L89</b> <b>Mn<sup>0</sup>, TMSCI</b> <b>Dioxane, rt, 18 h</b>	0% yield	0% yield	<b>Control</b> <b>78% yield, 85% ee</b>	0% yield
<b>NiBr<sub>2</sub>(diglyme), L119</b> <b>Mn<sup>0</sup>, TMSCI</b> <b>Dioxane, rt, 18 h</b>	0% yield	50% yield, 72% ee	7% yield, 80% ee	<b>Control</b> <b>85% yield, 79% ee</b>

Recognizing this challenge, we were pleased to find that the cross-coupling of benzylic chlorides with (hetero)aryl iodides proceeded in high yield and ee under conditions very similar to those developed for the reductive (hetero)arylation of  $\alpha$ -chloronitriles, differing only in ligand scaffold (see Chapters 3 and 4). This marked the greatest overlap in optimal reaction conditions we had developed and signaled a potential advance in generality. As shown in **Table 1**, a full survey of the reaction conditions developed in our group versus the substrate pairs for which they were optimal demonstrates the highly specific nature of our transformations. While the reaction parameters employed for reductive coupling of acyl chlorides provided modest yields of

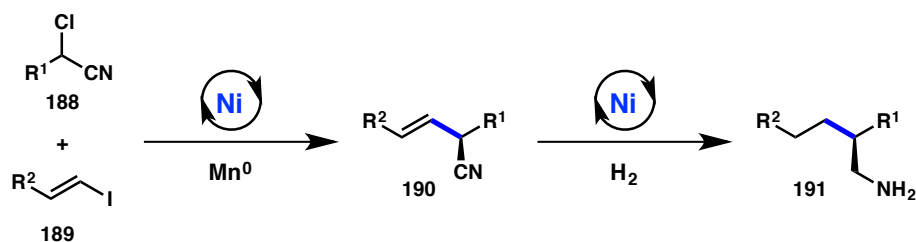
three of the products, only the model system gave promising enantioselectivity (Table 5.1, row 1). Conditions developed for the reductive coupling of vinyl bromides and benzylic chlorides were not tolerated in any other combination of electrophiles (Table 1, row 2). On the other hand, the conditions developed in Chapter 4 to afford diarylalkanes also furnished product in three of the reactions, and all above 70% ee (Table 1, row 4). Curiously, these were the only reaction conditions to succeed in the coupling to form diarylalkanes, suggesting that this transformation is perhaps uniquely challenging. While the conditions developed in Chapter 3 for the reductive coupling of  $\alpha$ -chloronitriles and (hetero)aryl iodides were not tolerated by any other combination of electrophiles (Table 1, row 3), the similarity to the conditions for the formation of diarylalkanes, and the promising application of those conditions to other systems, suggests that dioxane/TMSCl may constitute a privileged solvent system for these reactions.

With these conditions in hand, we have launched preliminary explorations with a series of novel coupling partners. While none of the reactions described here have been optimized to any extent, they represent the ease with which new product scaffolds can be accessed under these conditions. While previous couplings have required significant effort simply to obtain even racemic product prior to parameter optimization, we anticipate that these reactions will yield to ligand and condition evaluation and enable faster successful development and publication.

## 5.2 VINYLATION OF $\alpha$ -CHLORONITRILES

Contemporaneously with the efforts described in Chapter 3 toward the heteroarylation of  $\alpha$ -chloronitriles, we also conducted preliminary screens on the vinylation of these C(sp<sup>3</sup>) electrophiles.<sup>1</sup> As with the corresponding arylation reaction, this reductive cross-coupling has not been reported in the literature, even in the racemic sense. These products (**190**) are particularly interesting targets for further development because of the opportunities for their derivatization. Simultaneous reduction of the nitrile and olefin functionalities under simple Raney Ni conditions should enable access to  $\beta$ -amino tertiary alkyl stereocenters (**191**) difficult to access convergently by other means (Scheme 5.1).

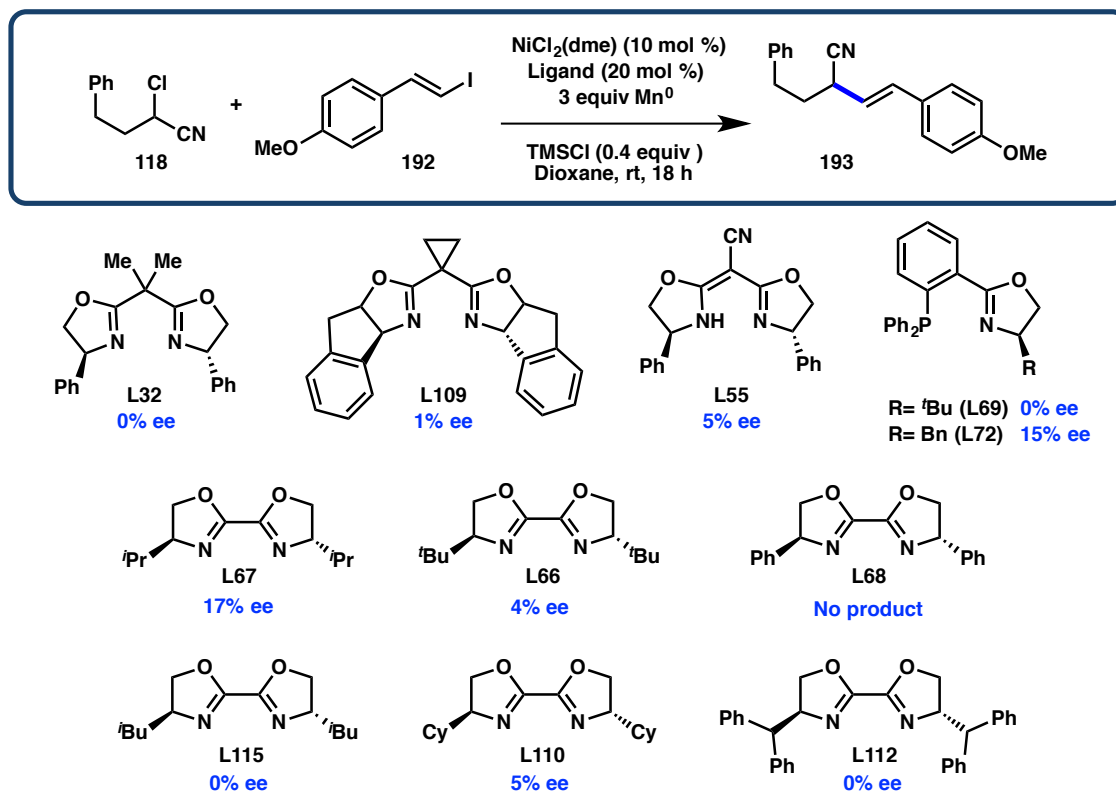
**Scheme 5.1.** Reductive cross-coupling of chloronitriles with vinyl iodides.



Iodostyrene **192** was chosen as the initial model vinyl halide for this transformation, cross-coupling with standard chloronitrile **118** (Scheme 5.2). Employing the room temperature dioxane/TMSCl conditions, we were delighted to find modest to good conversions and yields that were not quantified in these initial screens (10-50% yields estimated). As in many of the reactions in Table 5.1, BiOx ligands (in particular **L67**) were found to be optimal for both conversion and ee, although only poor enantioselectivity was achieved. However, promising results were also obtained

employing BnPHOX **L72**, suggesting that either of these ligand classes may prove to be successful upon further optimization.

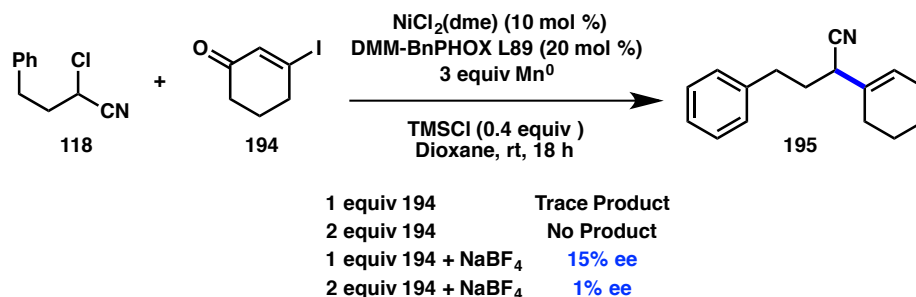
**Scheme 5.2.** Ligand screen for the vinylation of chloronitriles.



Later in this development of the arylation chemistry discussed in Chapter 3, a second vinylation reaction was attempted, this time with  $\beta$ -iodocyclohexenone (**194**) (**Scheme 5.3**). This haloenone substrate was selected because of its resemblance to the best-performing heteroaryl iodides in the analogous cross-coupling. In that reaction, electron-deficient heteroaryl iodides were optimal substrates. Therefore we identified **194** as also being an electron-poor, cyclic,  $\text{C}(\text{sp}^2)$  electrophile. Unfortunately for the reaction at the time, this substrate behaves more like iodostyrene **192** than the heteroaryl halide series, affording **195** in only 15% ee when using optimal DMM-BnPHOX **L89**. It is

interesting to note that this coupling required  $\text{NaBF}_4$  as an additive to observe modest yield, suggesting that this may be a crucial parameter to investigate moving forward.<sup>2</sup>

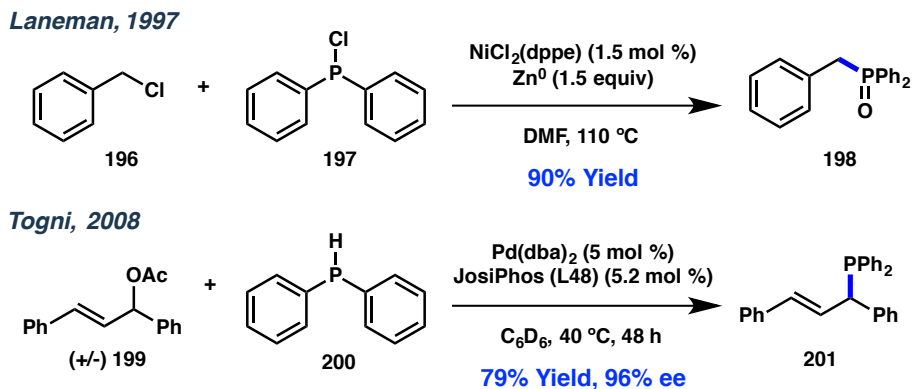
**Scheme 5.3.** Condition screen for the coupling of chloronitriles with a haloenone.



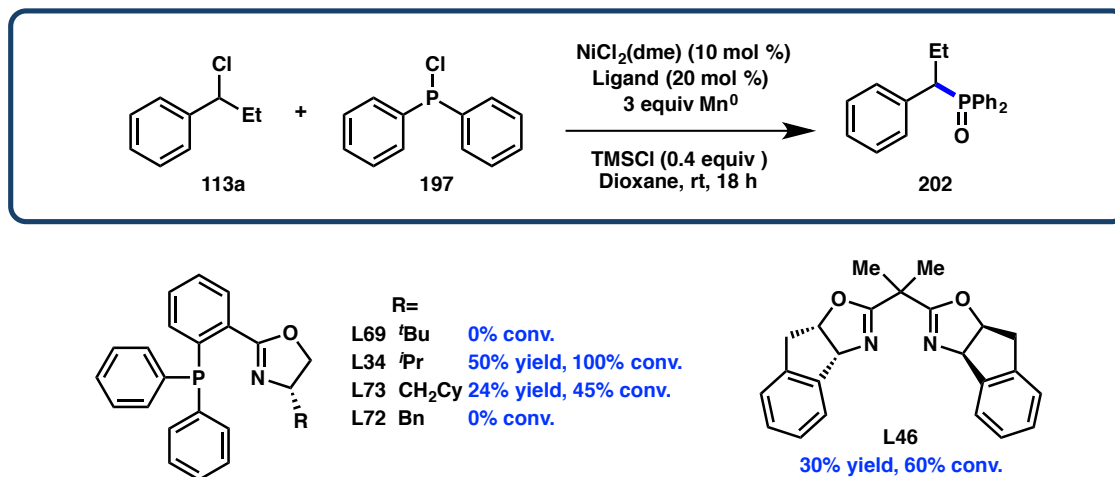
There are many important avenues of exploration remaining in the development of this vinyl cross-coupling. Some of these can be anticipated by looking to related cross-couplings in the literature. Firstly, it is likely that lower temperatures will be advantageous in this reaction. The asymmetric reductive vinylation of benzylic chlorides reported by Reisman and coworkers is the only such reaction to perform best at low temperature (0 °C), while the asymmetric Negishi coupling of bromonitriles developed by Fu and coworkers proceeds at -60 °C, the lowest they have observed.<sup>3</sup> Additives are also likely to be important, as shown by the effect of  $\text{NaBF}_4$  in **Scheme 5.3** and the beneficial effect of NaI in Reisman's vinylation. Finally, based on our experiences in other methodology development campaigns, extensive exploration of ligand scaffolds is likely to be the most important variable. Interestingly, both BiOX and PHOX ligands perform adequately and similarly at this stage, providing ample space for optimization.

### 5.3 COUPLING OF BENZYL CHLORIDES WITH CHLOROPHOSPHINES

In the recent surge of reports on reductive cross-coupling (see **Chapter 1**), the focus has been exclusively on reactions to form C–C bonds. Indeed while Pd catalysis has been developed extensively to facilitate carbon–heteroatom bond formation, Ni has been employed much less often to this end. It is surprising then to note that some of the earliest work in Ni-catalyzed reductive cross-coupling employing chemical reductants (as opposed to electrochemical studies) is actually in the field of carbon–heteroatom bond formation, namely C–P coupling.<sup>4</sup> In 1997, Laneman and coworkers from Monsanto published a wide-ranging report on the cross-coupling of chloro(diphenyl)phosphine **197** with various C(sp<sup>2</sup>) electrophiles, as well as C(sp<sup>3</sup>) benzyl bromide **196** (**Scheme 5.4**).<sup>5</sup> Remarkably, the phosphine products are obtained in good yields when employing aryl, vinyl, or benzyl halides, including both bromides and triflates. No secondary alkyl halides are explored in this paper, and the benzyl product is reported to oxidize on work-up to phosphine oxide **198**. This report was followed by an electrochemical version in 1999 (suggesting that organo/phosphinozinc intermediates are unlikely)<sup>6</sup> and an expansion of the aryl halide scope in 2003.<sup>7</sup> While this reaction takes place under harsh conditions and no chiral products are reported, this presents an interesting entry to an unprecedented class of targets for asymmetric cross-electrophile coupling.

**Scheme 5.4.** Selected cross-couplings to afford alkyl(diaryl)phosphines.

Therefore, we set out to explore the potential of these chlorophosphines as electrophiles in asymmetric reductive cross-coupling. Importantly, some interesting difficulties can be imagined in this proposed disconnection. For one, the desired products are chiral alkyl phosphines, strongly  $\sigma$ -donating ligands which may compete with the intended chiral ligand for binding to Ni, perturbing reactivity and selectivity. We were tentatively encouraged in this regard by a single report from Togni and coworkers, in which enantioenriched alkyl(diaryl)phosphines (**201**) are formed via asymmetric Pd catalysis using a JosiPhos ligand (**Scheme 5.4**).<sup>8</sup> While some mixed catalysis or even autocatalysis cannot be ruled out conclusively, this example at least suggests that highly enantioenriched phosphines can be obtained under such conditions. Second, Laneman and coworkers observed facile oxidation of their phosphine products upon workup. If observed, this may be avoidable by a rigorously air-free workup procedure, or perhaps the free phosphine can be complexed to a Lewis-acid such as borane, or protonated prior to workup, stabilizing it. Indeed, alkyl phosphine tetrafluoroborate salts can frequently be employed directly in catalysis with the addition of co-catalytic base, suggesting this is an approach worthy of consideration.<sup>9</sup>

**Scheme 5.5.** Ligand screen for coupling chlorophosphines and benzylic chlorides.

As a preliminary exploration then, we subjected model benzylic chloride **113a** and chloro(diphenyl)phosphine **197** to the reductive cross-coupling conditions developed in Chapters 3 and 4 employing dioxane/TMSCl at room temperature, with a range of chiral ligands (**Scheme 5.5**). We were once again pleased to find moderate yields of the desired product in this first attempt, and with both PHOX and BOX ligand families. These results constitute the lowest-temperature Ni-catalyzed reductive C–P couplings by over 100 °C, and are the first such reactions to employ 2° alkyl electrophiles. While these reactions still require substantial optimization to mitigate homocoupling and improve conversion, the potential impact of these transformations is clear even racemically. As we anticipated, the products are obtained as the phosphine oxides (distinguishable by polarity and  $^{31}\text{P}$  NMR). However, further exploration of workup (as described above) is expected to enable isolation of the free phosphines or stable complexes thereof. Unfortunately, no attempts at this coupling employing achiral ligands (including bipyridines, diphosphines, and phenanthrolines) have been successful, precluding the development of separation

conditions to assay the ee of these products. At worst, this may be solved by employing scalemic chiral ligands, or preferably by identifying a compatible achiral ligand.

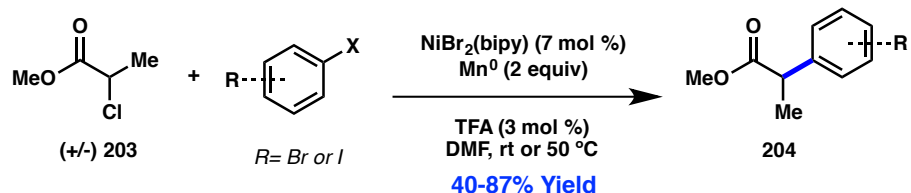
Moving forward, there are clearly many promising lines of inquiry with regard to this reaction. The usual reaction parameters of solvent, Ni source, and temperature should be examined. However, given the success observed under the initial conditions, a significant ligand screen of both BOX and PHOX classes should be conducted quickly to gauge the impact of ligand scaffold and substitution (especially once a suitable ee assay is developed). The more exciting aspect, however, is likely the substrate scope of this transformation. A wide range of diaryl- and dialkylchlorophosphines are commercially available (as well as chlorophosphites and diaminochlorophosphines), while the benzyl chloride partners are well-precedented in our laboratory. This disconnection would open the door to simple and convergent modular chiral phosphine synthesis. We anticipate that these products may prove useful as monodentate chiral ligands in transition metal catalysis, as well as in the field of nucleophilic catalysis where phosphines and NHCs find ample use.<sup>10</sup>

## 5.4 COUPLING OF (HETERO)ARYL IODIDES AND $\alpha$ -CHLOROESTERS

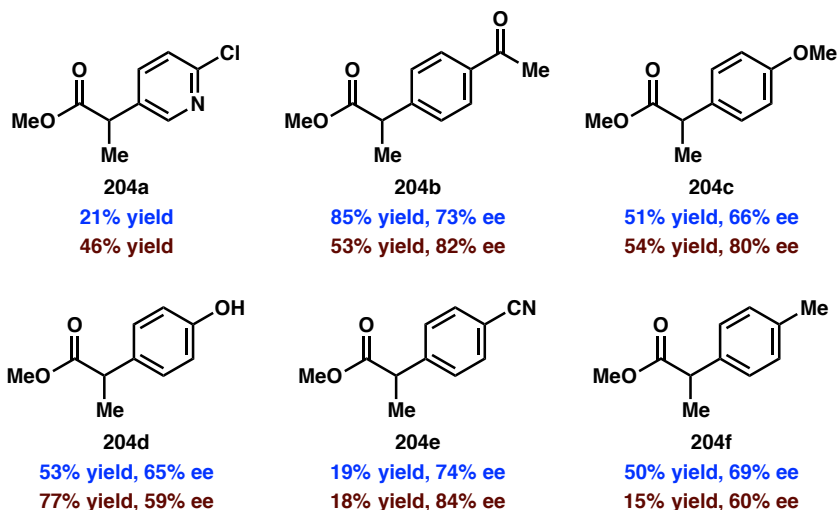
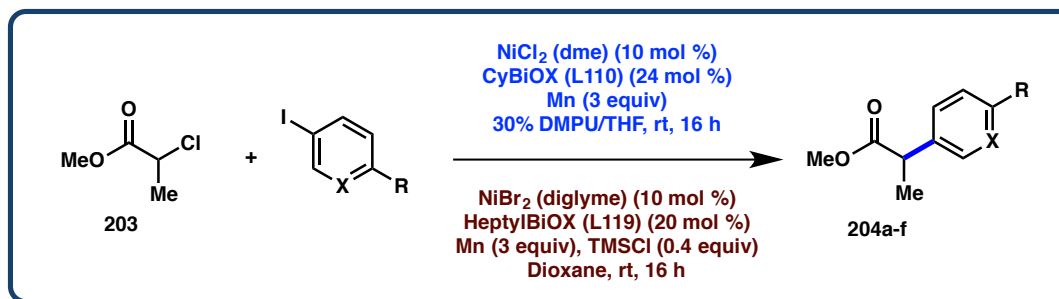
As a final example of the successful employment of these TMSCl/dioxane conditions on difficult asymmetric reductive cross-couplings, we include this entry. It is critical to note that all early work described in this section was carried out by Dr. Leah Cleary, while the new preliminary results were obtained by Kelsey Poremba. These results are included simply to further illustrate the robustness of dioxane/TMSCl as a solvent condition for the development of these reactions.

**Scheme 5.6.** Durandetti's reductive cross-coupling of  $\alpha$ -chloroesters.

Durandetti, 2007



Also contemporaneously with the reaction development described in Chapter 3, significant work was conducted by our laboratory on the asymmetric reductive cross-coupling of  $\alpha$ -haloesters with aryl iodides. As discussed in Chapter 1, this reaction was the first racemic reductive C–C bond-forming cross-coupling to be disclosed employing a chemical reductant (**Scheme 5.6**).<sup>11</sup> Therefore we imagined it may be amenable to asymmetric catalysis, expanding the scope of C(sp<sup>3</sup>) electrophiles employable in this chemistry. To explore this reaction, we chose to study the coupling of commercially available methyl 2-chloropropionate (**203**) with various aryl iodides (**Scheme 5.7**). Importantly, the products of these couplings are chiral arylpropionates (**204**), a valuable pharmacophore present in a large family of nonsteroidal anti-inflammatory drugs such as Naproxen.<sup>12</sup> Extensive optimization was carried out on this system, including thorough evaluation of solvent, catalyst, additives, and ligands. Branched alkyl BiOx ligands were identified as providing optimal yield and ee. While moderate to good yields could be obtained for some substrates, synthetically useful ee's were never obtained during this effort and research on this project was temporarily suspended.

**Scheme 5.7.** Asymmetric reductive cross-couplings of  $\alpha$ -chloroesters.

Recognizing the unique reactivity and selectivity, as well as generality afforded by the dioxane/TMSCl solvent system developed in Chapters 3 and 4, we decided to return to this reaction and assess the impact of these parameters. We were pleased to find that improved yields and ee's were obtainable for several substrates with no optimization whatsoever. Employing dioxane as solvent with TMSCl as an activator was successful in delivering several improved results over the previous conditions that had required more than a year to develop. This serves to illustrate the impact of highly general reaction parameters on optimization campaigns. We anticipate that beginning from this new result, a survey of BiOX ligand scaffolds and simple reaction parameters such as

concentration, Ni source, temperature, and substrate ratios may afford a high yielding and enantioselective transformation in comparatively short order.

## 5.5 CONCLUDING REMARKS

We have begun to evaluate the application of the reaction conditions developed in Chapters 3 and 4 to novel reductive cross-coupling transformations. This solvent system consisting of dioxane and substoichiometric TMSCl has been shown to be remarkably general in these reactions, enabling the generation of cross-coupled products with no optimization. First, the coupling of vinyl iodides with  $\alpha$ -chloronitriles proceeds with modest yields and poor enantioselectivity, but with multiple ligand classes. Development of this reaction should enable the synthesis of chiral  $\beta$ -tertiary primary amines via short, convergent sequence. Second, the mildest reductive C–P bond-forming reductive cross-coupling to date was demonstrated. This is also the first such transformation to employ 2° alkyl electrophiles. We hope that development of this asymmetric reaction will enable the convergent preparation of chiral monodentate phosphines useful as ligands or nucleophilic catalysts. Finally, recent work from our group was discussed involving the coupling of  $\alpha$ -chloroesters with (hetero)aryl iodides. Reaction conditions employing a dioxane/TMSCl solvent system gave comparable and frequently improved results to previous reaction conditions that had been extensively optimized. Further ligand screening based on these results is expected to enable a highly asymmetric cross-coupling. These results suggest an unprecedented generality under these conditions that should facilitate more rapid method development as we seek to expand the scope of Ni-

catalyzed asymmetric reductive cross-coupling. Work on these reactions and more is ongoing in our laboratory.

## 5.6 EXPERIMENTAL SECTION

### 5.6.1 *Materials and Methods*

Unless otherwise stated, reactions were performed under a nitrogen atmosphere using freshly dried solvents. Tetrahydrofuran (THF), methylene chloride ( $\text{CH}_2\text{Cl}_2$ ), and diethyl ether ( $\text{Et}_2\text{O}$ ) were dried by passing through activated alumina columns. Anhydrous dimethylacetamide (DMA) and 1,4-dioxane were purchased from Aldrich and stored under inert atmosphere. Manganese powder (– 325 mesh, 99.3%) was purchased from Alfa Aesar.  $\text{NiCl}_2(\text{dme})$  was purchased from Strem and stored in a glovebox under  $\text{N}_2$ .  $\text{NiBr}_2(\text{diglyme})$  was purchased from Sigma Aldrich and stored in a glovebox under  $\text{N}_2$ . Unless otherwise stated, chemicals and reagents were used as received. All reactions were monitored by thin-layer chromatography using EMD/Merck silica gel 60 F254 pre-coated plates (0.25 mm) and were visualized by UV, CAM, or  $\text{KMnO}_4$  staining. Flash column chromatography was performed as described by Still et al. using silica gel (particle size 0.032-0.063) purchased from Silicycle. Optical rotations were measured on a Jasco P-2000 polarimeter using a 100 mm path-length cell at 589 nm.  $^1\text{H}$  and  $^{13}\text{C}$  NMR spectra were recorded on a Varian Inova 500 (at 500 MHz and 126 MHz, respectively), and are reported relative to internal  $\text{CHCl}_3$  ( $^1\text{H}$ ,  $\delta = 7.26$ ) and  $\text{CDCl}_3$  ( $^{13}\text{C}$ ,  $\delta = 77.0$ ). Data for  $^1\text{H}$  NMR spectra are reported as follows: chemical shift ( $\delta$  ppm) (multiplicity, coupling constant (Hz), integration). Multiplicity and qualifier abbreviations are as follows: s = singlet, d = doublet, t = triplet, q = quartet, m = multiplet, br = broad, app =

apparent. Analytical SFC was performed with a Mettler SFC supercritical CO<sub>2</sub> analytical chromatography system with Chiralcel AD-H, OD-H, AS-H, OB-H, and OJ-H columns (4.6 mm x 25 cm) with visualization at 210, 254, and 280 nm.

### 5.6.2 Vinyl iodide/ $\alpha$ -chloronitrile cross-coupling (Schemes 5.2, 5.3)

In a glovebox, to a 1 dram vial was added the appropriate ligand (0.01 mmol, 20 mol %), reductant (0.3 mmol, 3 equiv), NiCl<sub>2</sub>(dme) (0.005 mmol, 10 mol %), and vinyl iodide substrate (if solid, 0.05 mmol, 1 equiv). The vial was charged with the 1,4-dioxane (0.14 mL, 0.37 M) followed by vinyl iodide substrate (if liquid, 0.05 mmol, 1 equiv), benzyl chloride substrate (0.05 mmol, 1.0 equiv), TMSCl (0.02 mmol, 0.4 equiv), and benzyl ether (internal standard). The vial was sealed and removed from the glovebox. The mixture was stirred vigorously at 500 rpm, ensuring that the reductant was uniformly suspended, at 23 °C for 24 h. The reaction mixture was diluted with 10% ethyl acetate/hexane and passed through a plug of silica, using 20% ethyl acetate/hexane eluent. The solution was concentrated, and the crude reaction mixture was analyzed by <sup>1</sup>H NMR.

### 5.6.3 Chlorophosphine/benzyl chloride cross-coupling (Scheme 5.5)

In a glovebox, to a 1 dram vial was added the appropriate ligand (0.01 mmol, 20 mol %), reductant (0.3 mmol, 3 equiv), and NiCl<sub>2</sub>(dme) (0.005 mmol, 10 mol %). The vial was charged with the 1,4-dioxane (0.14 mL, 0.37 M) followed by chlorophosphine substrate (0.05 mmol, 1 equiv), benzyl chloride substrate (0.05 mmol, 1.0 equiv), TMSCl (0.02 mmol, 0.4 equiv), and benzyl ether (internal standard). The vial was sealed and

removed from the glovebox. The mixture was stirred vigorously at 500 rpm, ensuring that the reductant was uniformly suspended, at 23 °C for 24 h. The reaction mixture was diluted with 10% ethyl acetate/hexane and passed through a plug of silica, using 40% ethyl acetate/hexane eluent. The solution was concentrated, and the crude reaction mixture was analyzed by <sup>1</sup>H and <sup>31</sup>P NMR.

#### 5.6.4 (Hetero)aryl iodide/ $\alpha$ -chloroester cross-coupling (Scheme 5.7)

In a glovebox, to a 1 dram vial was added the appropriate ligand (0.01 mmol, 20 mol %), reductant (0.3 mmol, 3 equiv), and NiBr<sub>2</sub>(diglyme) (0.005 mmol, 10 mol %). The vial was charged with the 1,4-dioxane (0.14 mL, 0.37 M) followed by  $\alpha$ -chloroester substrate (0.05 mmol, 1 equiv), aryl iodide substrate (0.05 mmol, 1.0 equiv), TMSCl (0.02 mmol, 0.4 equiv), and benzyl ether (internal standard). The vial was sealed and removed from the glovebox. The mixture was stirred vigorously at 500 rpm, ensuring that the reductant was uniformly suspended, at 23 °C for 24 h. The reaction mixture was diluted with 10% ethyl acetate/hexane and passed through a plug of silica, using 20% ethyl acetate/hexane eluent. The solution was concentrated, and the crude reaction mixture was analyzed by <sup>1</sup>H NMR.

## 5.7 NOTES AND REFERENCES

- (1) Kadunce, N. T.; Reisman, S. E. *J. Am. Chem. Soc.* **2015**, *137*, 10480.
- (2) Molander, G. A.; Traister, K. M.; O'Neill, B. T. *J. Org. Chem.* **2014**, *79*, 5771.
- (3) Cherney, A. H.; Reisman, S. E. *J. Am. Chem. Soc.* **2014**, *136*, 14365.
- (4) Wauters, I.; Debrouwer, W.; Stevens, C. V. *Beilstein J. Org. Chem.* **2014**, *10*, 1064.
- (5) J. Ager, D.; A. Laneman, S. *Chem. Commun.* **1997**, 2359.
- (6) Budnikova, Y.; Kargin, Y.; Nédélec, J.-Y.; Périchon, J. *J. Organomet. Chem.* **1999**, *575*, 63.
- (7) Le Gall, E.; Troupel, M.; Nédélec, J.-Y. *Tetrahedron* **2003**, *59*, 7497.
- (8) Butti, P.; Rochat, R.; Sadow, A. D.; Togni, A. *Angew. Chem. Int. Ed. Engl.* **2008**, *47*, 4878.
- (9) Netherton, M. R.; Fu, G. C. *Org. Lett.* **2001**, *3*, 4295.
- (10) (a) Xiao, Y.; Sun, Z.; Guo, H.; Kwon, O. *Beilstein J. Org. Chem.* **2014**, *10*, 2089;  
(b) Lagasse, F.; Kagan, H. B. *Chem. Pharm. Bull.* **2000**, *48*, 315.
- (11) Durandetti, M.; Gosmini, C.; Périchon, J. *Tetrahedron* **2007**, *63*, 1146.
- (12) Landoni, M. F.; Soraci, A. *Curr. Drug Metab.* **2001**, *2*, 37.

## ABOUT THE AUTHOR

Nathaniel Thomas Kadunce was born on October 28, 1988 to Dr. Beverly A. Carl, M.D. and Dr. William M. Kadunce in Pittsburgh, PA. He grew up in nearby Beaver, PA, graduating from Beaver Area High School in 2007. Following that, he made his first westward move, attending Oberlin College in Oberlin, OH. His interest in chemistry, particularly organic chemistry, was fostered there by valuable courses, but more importantly by research. Joining the laboratory of Prof. Jason Belitsky gave Nat his first experience doing hands-on research in a lab, developing a C–H borylation/Suzuki coupling approach to the iterative synthesis of eumelanin analogues. After receiving his B.A. degree in Chemistry and Biochemistry in 2011, Nat was committed to a future in synthetic organic chemistry, with a particular interest in transition metal catalysis.

Following this passion, Nat and Julia drove to the west coast in 2011, where he enrolled at the California Institute of Technology in sunny Pasadena. He commenced his doctoral studies under the supervision of Prof. Sarah Reisman and focused his research on the development of asymmetric Ni-catalyzed reductive cross-coupling reactions. 2014 saw the happy marriage of Nat and Julia, and 2016 saw the successful conclusion of Nat's Ph. D. studies. In the summer of 2016, they will make a much shorter move to the Bay area, where Nat will begin his industrial career within the process chemistry group at Gilead Sciences in Foster City.